frontiers | Research Topics

Advances in detection and control of post-harvest pathogens

Edited by
Khamis Youssef, Sergio Ruffo Roberto, Antonio Ippolito and Kamal A. M. Abo-Elyousr

Published in
Frontiers in Microbiology

ISSN 1664-8714
ISBN 978-2-8325-2472-5
DOI 10.3389/978-2-8325-2472-5

About Frontiers

Frontiers is more than just an open access publisher of scholarly articles: it is a pioneering approach to the world of academia, radically improving the way scholarly research is managed. The grand vision of Frontiers is a world where all people have an equal opportunity to seek, share and generate knowledge. Frontiers provides immediate and permanent online open access to all its publications, but this alone is not enough to realize our grand goals.

Frontiers journal series

The Frontiers journal series is a multi-tier and interdisciplinary set of open-access, online journals, promising a paradigm shift from the current review, selection and dissemination processes in academic publishing. All Frontiers journals are driven by researchers for researchers; therefore, they constitute a service to the scholarly community. At the same time, the *Frontiers journal series* operates on a revolutionary invention, the tiered publishing system, initially addressing specific communities of scholars, and gradually climbing up to broader public understanding, thus serving the interests of the lay society, too.

Dedication to quality

Each Frontiers article is a landmark of the highest quality, thanks to genuinely collaborative interactions between authors and review editors, who include some of the world's best academicians. Research must be certified by peers before entering a stream of knowledge that may eventually reach the public - and shape society; therefore, Frontiers only applies the most rigorous and unbiased reviews. Frontiers revolutionizes research publishing by freely delivering the most outstanding research, evaluated with no bias from both the academic and social point of view. By applying the most advanced information technologies, Frontiers is catapulting scholarly publishing into a new generation.

What are Frontiers Research Topics?

Frontiers Research Topics are very popular trademarks of the *Frontiers journals series*: they are collections of at least ten articles, all centered on a particular subject. With their unique mix of varied contributions from Original Research to Review Articles, Frontiers Research Topics unify the most influential researchers, the latest key findings and historical advances in a hot research area.

Find out more on how to host your own Frontiers Research Topic or contribute to one as an author by contacting the Frontiers editorial office: frontiersin.org/about/contact

Advances in detection and control of post-harvest pathogens

Topic editors

Khamis Youssef — Agricultural Research Center, Egypt
Sergio Ruffo Roberto — State University of Londrina, Brazil
Antonio Ippolito — University of Bari Aldo Moro, Italy
Kamal A. M. Abo-Elyousr — Assiut University, Egypt

Citation

Youssef, K., Roberto, S. R., Ippolito, A., Abo-Elyousr, K. A. M., eds. (2023). *Advances in detection and control of post-harvest pathogens*. Lausanne: Frontiers Media SA. doi: 10.3389/978-2-8325-2472-5

Table of contents

frontiers | Frontiers in Microbiology

TYPE Editorial
PUBLISHED 28 March 2023
DOI 10.3389/fmicb.2023.1184039

OPEN ACCESS

EDITED AND REVIEWED BY
Giovanna Suzzi,
University of Teramo, Italy

*CORRESPONDENCE
Khamis Youssef
youssefeladawy@arc.sci.eg
Antonio Ippolito
antonio.ippolito@uniba.it
Sergio Ruffo Roberto
sroberto@uel.br
Kamal A. M. Abo-Elyousr
kaaboelyousr@agr.au.edu.eg

SPECIALTY SECTION
This article was submitted to Food Microbiology, a section of the journal Frontiers in Microbiology

RECEIVED 10 March 2023
ACCEPTED 16 March 2023
PUBLISHED 28 March 2023

CITATION
Youssef K, Roberto SR, Ippolito A and Abo-Elyousr KAM (2023) Editorial: Advances in detection and control of post-harvest pathogens. *Front. Microbiol.* 14:1184039. doi: 10.3389/fmicb.2023.1184039

Editorial: Advances in detection and control of post-harvest pathogens

Khamis Youssef[1,2]*, Sergio Ruffo Roberto[3]*, Antonio Ippolito[4]* and Kamal A. M. Abo-Elyousr[5,6]*

[1]Agricultural Research Center, Plant Pathology Research Institute, Giza, Egypt, [2]Agricultural and Food Research Council, Academy of Scientific Research and Technology (ASRT), Cairo, Egypt, [3]Agricultural Research Center, State University of Londrina, Londrina, PR, Brazil, [4]Department of Soil, Plant and Food Science, University of Bari "Aldo Moro", Bari, Italy, [5]Department of Arid Land Agriculture, Faculty of Meteorology, Environment and Arid Land Agriculture, King Abdulaziz University, Jeddah, Saudi Arabia, [6]Department of Plant Pathology, Faculty of Agriculture, University of Assiut, Assiut, Egypt

KEYWORDS

foodborne pathogens, fungal pathogens, bacterial pathogens, post-harvest disease, detection, contamination

Editorial on the Research Topic
Advances in detection and control of post-harvest pathogens

Introduction

Post-harvest pathogens can cause disease in harvested products during transportation, handling, packaging, and storage. Such pathogens can cause serious damage in the fresh produce supply chain, with post-harvest losses of fresh fruit and vegetables estimated to be up to 50%. Rotting is a major issue in such losses, being caused mainly by fungal pathogens after fruit ripening (Junior et al., 2019). For fresh produce, heat-based treatments are difficult to apply during the post-harvest packing process. Current processes usually rely on washing, which can enhance contamination or leave the produce vulnerable to contamination. Inadequate storage of fresh produce may also provide ideal conditions for pathogens to grow. However, advances in detection and control methods have greatly improved our ability to manage these pathogens (Teixeira et al., 2021). Further research is needed to develop more sustainable and environmentally friendly methods for controlling these pathogens (Salem et al., 2016). Traditional testing methods for post-harvest pathogens can take days to produce results, which can lead to significant losses. However, rapid testing methods such as PCR and ELISA can detect pathogens in just a few hours, allowing for quicker identification and control (Law et al., 2015).

The aim of this Research Topic was to further understanding of bacteria and fungi causing post-harvest disease, and present future directions to improve the detection and control of such pathogens. Thirteen articles were accepted for this Research Topic dealing with grapes, blueberries, apples, Jerusalem artichoke, wolfberries, Shengzhou nane, and goji fruit. In this context, Ji et al. investigated the effects of ethanol vapor on the inhibition of *Alternaria alternata* and *Botrytis cinerea* in post-harvest blueberry and the induction of defense-related enzymes (DREs) activities in fungi-inoculated blueberries stored at 0 ± 0.5°C for 16 days. The authors found that ethanol vapor markedly inhibited the mycelial

growth of all pathogens. Also, ethanol vapor enhanced the activities of DREs in fungi-inoculated blueberries, including β-1,3-glucanase (GLU), chitinase (CHI), phenylalnine ammonialyase (PAL), peroxidase (POD), and polyphenol oxidase (PPO). The findings of this study suggest that ethanol could be used as an activator of defense responses in blueberry against Alternaria and Botrytis rots, by activating DREs, having practical application value in the preservation of quality of fruits and vegetables during post-harvest phase. Guan et al. in their review discussed the regulatory requirements on gaseous interventions as well as organic production and handling of apples that could contribute to future industrial application and benefit the apple processors. Maluleke et al. tested 31 yeast strains from 21 species using different agar media and liquid mixed cultures. *Pichia kudriavzevii* was the most potent against *B. cinerea*, but with a narrow activity spectrum. Twelve other strains had broad antagonistic activity against multiple fungi. Most antagonistic strains produced chitinases and glucanases when exposed to *B. cinerea*. Analysis of volatile and non-volatile compounds produced by antagonistic yeast strains in the presence of *B. cinerea* revealed higher amount of alcohols, esters, organosulfur compounds, monoterpenes, cyclic peptides, and diketopiperazine. This study is the first to demonstrate the inhibitory effect of non-volatile compounds produced by various yeast species. Ling et al. investigated the inhibitory effect of *Bacillus velezensis* L1 on post-harvest disease of wolfberry. *B. velezensis* L1 and its volatiles (2,3-butanedione) effectively reduced the decay caused by pathogenic fungi and prolonged storage time. These results provide favorable evidence for the biocontrol activity of strain L1 against *Alternaria iridiaustralis* and other important fungal pathogens, and also provide insights to develop storage systems for fresh fruits and vegetables after harvest. Charlermroj et al. investigated a new lateral flow test strip assay that uses phage from microarray screening to distinguish live from dead *Salmonella enteritidi*s cells. The assay only takes 15 min, much shorter than culture-based methods that typically need 24 h. This screening method can be adapted for phage-based binder selection against other pathogen targets, eliminating the need for animal immunization. The phage-based lateral flow test strip assay is not limited to foodborne pathogens and could be used to test other targets, such as viruses. Guo T.-R. et al. isolated and identified *Aspergillus niger* as the pathogen causing fruit rot in Shengzhou nane fruit. Optimal growth conditions were determined, and a combined treatment of sodium bicarbonate (SBC) and natamycin (NT) showed high antifungal efficacy against *A. niger*, damaging cell and mitochondrial membrane integrity and disrupting energy metabolism. *In vivo* experiments showed a reduction in rot lesion diameter and decay rate in Shengzhou nane fruit with the combined treatment of SBC and NT. The study suggests that this combined treatment could be a viable alternative to synthetic fungicides for controlling post-harvest fruit decay caused by *A. niger*. Du et al. conducted a study on Jerusalem artichoke to determine the dynamics of the microbiome during storage in relation to varieties and various other factors. They found that *Flavobacterium*, *Sphingobacterium*, *Staphylococcus*, *Dysgonomonas*, *Acinetobacter*, and *Serratia* played important roles. The bacterial community was affected by crop genotype and carbohydrate structure. Wang et al. found that the main pathogens causing post-harvest decay of bagging-free apples were *Botryosphaeria dothidea* and *Colletotrichum gloeosporioides*, and that cinnamon and clove essential oils (EOs) were effective in limiting fungal growth and reducing rot in both *in vitro* and *in vivo* trials. The study also noted that the two identified organisms had different levels of resistance to the tested EOs, and that further research would be conducted on the synergistic effects of cinnamon and clove EOs for controlling post-harvest spoilage in bagging-free apples. Zhao et al. conducted a study on the effect of carvacrol (CVR) on *Alternaria alternata* demonstrating its damaging effect on pathogen by altering the integrity of the mycelial cell wall. Meanwhile, both the contents of cell wall polycarbohydrates containing chitin and β-1,3-glucan and the activities of the enzymes related to the biosynthesis of these polycarbohydrates were significantly decreased by CVR treatment, while the activities of chitinase and β-1,3-glucanase response of degrading the two polycarbohydrates were increased by CVR treatment. Sun et al. suggested that *Pseudomonas syringae* strain B-1 may be a promising candidate for the biological control of post-harvest apple ring rot, potentially reducing the need for chemical fungicides and improving the sustainability of apple production. Also, Esteves et al. confirmed the potential of wine yeasts as biocontrol agents, while highlighting the need for the establishment of fit-for-purpose selection programs depending on the mold target, the timing, and the mode of application. Ou et al. concluded that formation of the viable but non-culturable (VBNC) state in methicillin-resistant *Staphylococcus aureus* (MRSA) strains was verified, then two propidium monoazide-crossing priming amplification assays were developed and applied to detect MRSA in the VBNC state from pure culture and food samples.

Author contributions

KY, SR, AI, and KA-E: writing—review and editing. All authors contributed to the article and approved the submitted version.

Conflict of interest

The authors declare that the research was conducted in the absence of any commercial or financial relationships that could be construed as a potential conflict of interest.

Publisher's note

References

Junior, O. J. C., Youssef, K., Koyama, R., Ahmed, S., Dominguez, A. R., Mühlbeier, D. T., et al. (2019). Control of gray mold on clamshell-packaged 'benitaka' table grapes using sulphur dioxide pads and perforated liners. *Pathogens* 8, 271. doi: 10.3390/pathogens8040271

Law, J. W.-F., Ab Mutalib, N.-S., Chan, K.-G., and Lee, L.-H. (2015). Rapid methods for the detection of foodborne bacterial pathogens: principles, applications, advantages and limitations. *Front. Microbiol.* 5, 770. doi: 10.3389/fmicb.2014.00770

Salem, E. A., Youssef, K., and Sanzani, S. M. (2016). Evaluation of alternative means to control postharvest Rhizopus rot of peaches. *Sci. Horticult.* 198, 86–90. doi: 10.1016/j.scienta.2015.11.013

Teixeira, G. M., Mosela, M., Nicoletto, M. L. A., Ribeiro, R. A., Hungria, M., Youssef, K., et al. (2021). Genomic insights into the antifungal activity and plant growth-promoting ability in *Bacillus velezensis* CMRP 4490. *Front. Microbiol.* 11, 618415. doi: 10.3389/fmicb.2020.618415

frontiers in Microbiology

ORIGINAL RESEARCH
published: 26 January 2021
doi: 10.3389/fmicb.2021.618252

Effect of Ethanol Vapor Treatment on the Growth of *Alternaria alternata* and *Botrytis cinerea* and Defense-Related Enzymes of Fungi-Inoculated Blueberry During Storage

Yaru Ji[1,2], Wenzhong Hu[2,3], Jia Liao[2,3], Zhilong Xiu[1], Aili Jiang[2,3], Xiaozhe Yang[1,2], Yuge Guan[1,2], Ke Feng[2,3] and Gaowa Saren[1,2]*

[1]School of Bioengineering, Dalian University of Technology, Dalian, China, [2]Key Laboratory of Biotechnology and Bioresources Utilization, Ministry of Education, Dalian, China, [3]College of Life Science, Dalian Minzu University, Dalian, China

OPEN ACCESS

Edited by:
Haifeng Zhao,
South China University of Technology, China

Reviewed by:
Xingfeng Shao,
Ningbo University, China
Hongyin Zhang,
Jiangsu University, China
Yonghong Ge,
Bohai University, China

***Correspondence:**
Wenzhong Hu
wenzhongh@sina.com

Specialty section:
This article was submitted to Food Microbiology, a section of the journal Frontiers in Microbiology

Received: 16 October 2020
Accepted: 04 January 2021
Published: 26 January 2021

Citation:
Ji Y, Hu W, Liao J, Xiu Z, Jiang A, Yang X, Guan Y, Feng K and Saren G (2021) Effect of Ethanol Vapor Treatment on the Growth of Alternaria alternata and Botrytis cinerea and Defense-Related Enzymes of Fungi-Inoculated Blueberry During Storage. Front. Microbiol. 12:618252. doi: 10.3389/fmicb.2021.618252

The aim of the present study was to investigate the effects of ethanol vapor on the inhibition of *Alternaria alternata* and *Botrytis cinerea* in postharvest blueberry and the induction of defense-related enzymes (DREs) activities in fungi-inoculated blueberries stored at 0 ± 0.5°C for 16 days. Results indicated that ethanol vapor markedly inhibited the mycelial growth of *A. alternata* and *B. cinerea* in a dose-dependent manner, with inhibition rates of 9.1% (250 μl L^{-1}), 36.4% (500 μl L^{-1}), and 5.5% (1,000 μl L^{-1}) on *A. alternata* and 14.2% (250 μl L^{-1}), 44.7% (500 μl L^{-1}), and 76.6% (1,000 μl L^{-1}) on *B. cinerea*, respectively. Meanwhile, ethanol vapor also enhanced the activities of DREs in fungi-inoculated blueberries, including β-1,3-glucanase (GLU), chitinase (CHI), phenylalnine ammonialyase (PAL), peroxidase (POD), and polyphenol oxidase (PPO). In particular, 500 μl L^{-1} ethanol vapor increased the activities of DREs by 84.7% (GLU), 88.0% (CHI), 37.9% (PAL), 85.5% (POD), and 247.0% (PPO) in *A. alternata*-inoculated blueberries and 103.8% (GLU), 271.1% (CHI), 41.1% (PAL), 148.3% (POD), and 74.4% (PPO) in *B. cinerea*-inoculated blueberries, respectively. But, the activity of PPO was decreased by 55.2 and 31.9% in 500 μl L^{-1} ethanol-treated blueberries inoculated with *A. alternata* and *B. cinerea*, respectively, after 8 days of storage. Moreover, the surface structure and ultrastructure of 500 μl L^{-1} ethanol-treated blueberry fruit cells were more integrated than those of other treatments. The findings of the present study suggest that ethanol could be used as an activator of defense responses in blueberry against *Alternaria* and *Botrytis* rots, by activating DREs, having practical application value in the preservation of postharvest fruit and vegetables.

Keywords: blueberry, ethanol vapor, *Alternaria alternata*, *Botrytis cinerea*, defense-related enzymes

INTRODUCTION

Blueberries (*Vaccinium* spp., Ericaceae) are native to North America, but are cultivated worldwide, and are an increasingly popular functional fruit, with production increasing by 60.7% between 2010 and 2019 (FAO, 2020). The nutritional value of the fruit can be attributed to its remarkably high levels of health-promoting components, including anthocyanins, vitamins, flavonols, and dietary fiber (Wang et al., 2012; Chen et al., 2017). However, fresh blueberries are highly perishable, owing to senescence caused by physiological metabolism, physical damage (e.g., mechanical damage and temperature effects), and decay caused by microbial pathogens (Ji et al., 2019), and microbial infection is the main factor that limits blueberry storage, transportation, and marketing. Furthermore, the aging and softening of blueberries during storage weaken the fruit's resistance to pathogens that lurk on the fruit surface and in the environment. The fungal pathogens that cause blueberry rot differ by area, but the principal pathogenic fungi include *Alternaria alternata* (Alternaria rot), *Botrytis cinerea* (Botrytis rot), and *Colletotrichum acutatum* (Anthracnose rot; Wang et al., 2010).

Botrytis cinerea (*B. cinerea*), one of the main rotting fungi, generally colonizes and infects senescent flower remnants of blueberries directly by secreting cell wall degrading enzymes (pectin lyase, polygalacturonase, etc.) and virulence factors (organic acids, botrydial, etc.) before harvest (Huang et al., 2012; Zhang et al., 2014), but can also infect blueberry fruit through stem scar and mechanical wounds, especially when the fruits' resistance mechanisms are reduced after harvest. Furthermore, even though the optimum temperature for *B. cinerea* spore germination is 15–25°C, the pathogen can also grow at very low temperatures (e.g., −2°C), which enables it to affect fruit during cold storage (Sommer, 1985). During initial infection, the skin of *B. cinerea*-infected fruit is gray-white, and as soft rot occurs, numerous gray mycelia, which are rich in conidia, emerge on the surface of the diseased portion of the fruit, accompanied by slight fruit wilting. After air drying, the fruit is shriveled and stiff.

Meanwhile, *Alternaria* spp. are major pathogenic fungi of many fruit and vegetables, such as grapefruit, strawberry, grape, tomato, pepper, and onion, with *A. alternata* being the most damaging to blueberry fruit (Barkai, 2001; Wang et al., 2021). The optimum temperature for *A. alternata* spore germination is about 28°C. However, the pathogen can also maintain growth at −3°C, which enables it to maintain growth during cold chain transportation and refrigeration (Sommer, 1985). During infection, the mycelia of *A. alternata* penetrate the epidermis of blueberry fruit and then remain dormant in the fruit, only reactivating when the concentration of antifungal substances in the fruit decreases. Indeed, studies have shown that *A. alternata* is latent on blueberry fruit before harvest, and *A. alternata*-infected blueberry fruit is usually harvested together with healthy fruit, thereby spreading the disease throughout the postharvest chain, including picking, transportation, packaging, and storing. During initial infection, the pericarp of *A. alternata*-infected fruit exhibits sunken, dark-brown spots, and then numerous white mycelia grow on the diseased portion of the fruit (Caruso and Ramsdell, 1995).

Ethanol has long been used as a disinfectant, owing to its antimicrobial property, and, as a plant secondary metabolite, has low toxicity to fruit and vegetables. As such, ethanol is a FDA-certified generally recognized safe substance (GRAS) in the United States and a food industrial additive with unrestricted residues prescribed by GB 2760-2014 in China. Many studies have investigated the use of ethanol dip or vapor as non-biological control agent for reducing fruit decay and for extending the shelf-life of fruit and vegetables, such as sweet cherry (Karabulut et al., 2004a), Chinese bayberries (Wang et al., 2011), and table grapes (Lichter et al., 2002; Candir et al., 2012). In fact, ethanol can directly kill or inhibit the growth of rot microorganisms and may also be absorbed by the treated fruit or vegetables, thereby enhancing their disease resistance. Studies have reported that 30–40% ethanol dips can kill *B. cinerea* conidia isolated from table grapes *in vitro* (Lichter et al., 2002; Karabulut et al., 2004b), and that ethanol vapor can effectively reduce the postharvest decay rate of blueberry fruit (Ji et al., 2019). However, little information is available regarding the effects of ethanol treatment at a method of fumigation on the germination of *B. cinerea* and *A. alternata* spores or on the disease resistance of blueberry fruit.

Accordingly, the objectives of the present study were to investigate (1) the antifungal activities of ethanol vapor against *A. alternata* and *B. cinerea in vitro* and (2) the effect of ethanol treatment on the activities of defense-related enzymes in blueberry fruit. This research will contribute to the practical application of ethanol for preserving the postharvest fruit and vegetables.

MATERIALS AND METHODS

Blueberry and Fungal Materials

Southern highbush blueberries (*Vaccinium corymbosum* L. "O'Neal") used in this trial, were hand-harvested from the blueberry plantation at the Dalian Blueberry Technology Development Co., Ltd. facility in Zhuanghe City (Dalian, Liaoning, China) during the summer (June) of 2017 and 2018 (two repetitions). The fruits were consistent in maturity (100% blue) and transported to the laboratory within 3 h of harvest using a refrigerated vehicle (10°C, S.F. Express, Dalian, Liaoning, China). In the laboratory, the fruits were cooled for 24 h at 0 ± 0.5°C and 90% RH, and then undamaged fruits that were uniform in size and color were selected (0 ± 0.5°C and 90% RH) for use.

Alternaria alternata and *B. cinerea* were obtained from School of Bioengineering, Dalian University of Technology, China, and were maintained at 4°C in the dark in Petri dishes containing Potato Dextrose Agar (PDA; Hopebio, Qingdao, China).

Spores Suspension Pretreatment

Both *A. alternata* and *B. cinerea* were cultured on PDA slants at 28°C, and after 5 days, 5 ml septic NaCl solution (0.9%, v/v) was added to each slant and slowly scraped off the agar surface. The aseptic NaCl solutions containing pathogen spores

were each transferred to a sterile triangle bottle and then dispersed with glass beads. After shaking, the spore solutions were filtered using absorbent cotton to remove mycelial fragments and were then washed 2–3 times with aseptic NaCl solution. Finally, 1×10^6 CFU ml^{-1} spore suspensions were prepared as needed using a blood cell counting board.

Ethanol Vapor Treatment of *A. alternata* and *B. cinerea* on PDA

Melted PDA (15–20 ml) was poured into a disposable plastic culture dish (90 mm × 20 mm), and after coagulation, a 6-mm-diameter hole was dug in the medium in the center of each culture dish and inoculated with 20 µl spore suspension. Sterile filter paper was trimmed to fit inside Petri dish covers, and according to the remaining space volume, absolute ethanol was dropped onto each filter paper-lined Petri dish cover, which was then placed quickly on its corresponding dish. Ethanol volumes were calculated to achieve concentrations of 0 (Control), 250, 500, or 1,000 µl L^{-1} (ratio of liquid ethanol to container volume). The inoculated and treated plates were then sealed with preservative film, inverted, and incubated at 28°C. After 7 days, the vertical diameters (mm) of the colonies were measured using a caliper, and inhibition rate was calculated as follows:

$$\text{Inhibition rate} = (C - T) / C \times 100\%.$$

where C is the mean ($n = 3$) colony diameter of the control group and T is the mean ($n = 3$) colony diameter of the treatment group. Each treatment included three replicates, and the experiment was repeated three times.

Ethanol Vapor Treatment of Blueberries Inoculated With *A. alternata* and *B. cinerea*

Inoculation

Groups of 50 individual fruit (400 fruit total) were superficially sterilized by a 2-min immersion in 2% (v/v) sodium hypochlorite solution, washed for 2 min in sterile distilled, and then dried on sterile filter paper. The fruits were then wounded (2 mm diameter × 3 mm deep) at the equator of each fruit with a sterilized nail and inoculated with 10 µl either *A. alternata* (50 fruit × 4) or *B. cinerea* (50 fruit × 4) spore suspension (1.0×10^6 CFU ml^{-1}).

Ethanol Vapor Treatment

All inoculated blueberries were left to air-dry and then divided into eight groups: *A*-Control, *A*-250, *A*-500, *A*-1000, *B*-Control, *B*-250, *B*-500, and *B*-1000 (*A*-Control, inoculated with *A. alternata* and treated with 0 µl L^{-1} ethanol; *A*-250, inoculated with *A. alternata* and treated with 250 µl L^{-1} ethanol; *A*-500, inoculated with *A. alternata* and treated with 500 µl L^{-1} ethanol; *A*-1000, inoculated with *A. alternata* and treated with 1,000 µl L^{-1} ethanol; *B*-Control, inoculated with *B. cinerea* and treated with 0 µl L^{-1} ethanol; *B*-250, inoculated with *B. cinerea* and treated with 250 µl L^{-1} ethanol; *B*-500, inoculated with *B. cinerea* and treated with 500 µl L^{-1} ethanol; and *B*-1000, inoculated with *B. cinerea* and treated with 1,000 µl L^{-1} ethanol). More specifically, six disposable Petri dishes without cover that contained qualitative filter paper (to allow gradual diffusion of the ethanol), were placed in the bottom of each photosynthetic modified atmosphere preservation container (dimensions: 46.3 cm × 27.3 cm × 26.6 cm; Beijing Hengqingyuan Technology Co. Ltd., Beijing, China), and the blueberries (with the inoculation wound facing up) were put on the hollowed-out interlayer of each container. Then, the blueberries in each group were subjected to ethanol vapor treatments with corresponding amount of ethanol (99.7%; 0, 250, 500, or 1,000 µl L^{-1}) dripped on the qualitative filter papers for 18 h (0 ± 0.5°C, 90% RH). Three containers were prepared for each treatment. After ethanol treatment, the blueberries were ventilated (0 ± 0.5°C, 90% RH) for 24 h, transferred to commercial PET plastic boxes (10.5 cm × 10.5 cm × 3 cm), and then stored at 0 ± 0.5°C and 90% RH. The treated and cold-stored blueberries were randomly sampled at different storage time points (0, 4, 8, 12, and 16 days), frozen in liquid nitrogen, and then stored at −80°C until analysis. All the analyses were performed in triplicate, and this is a split-plot experimental design, with a 4 × 5 (doses × days) factorial design.

Determination of DREs Activities

The activities of β-1,3-glucanase (GLU), chitinase (CHI), phenylalnine ammonialyase (PAL), peroxidase (POD), and polyphenol oxidase (PPO) were determined using assay kits (Suzhou Keming Biotechnology Co., Ltd., Suzhou, Jiangsu, China).

Extraction of crude enzyme solution: according to the instructions of the kits, 0.15–0.2 g of fruit sample was homogenized with 1 ml of corresponding extraction solution in ice bath. After centrifugation at 10000 × g for 20 min at 4°C, the supernatants were collected and placed on ice for enzyme activity determination.

Then, the reagents were added in accordance with the instructions, and the absorbance values at 550 (GLU), 585 (CHI), 290 (PAL), 470 (POD), and 525 (PPO) nm were measured, respectively. Both the GLU and CHI activities were expressed as mg h^{-1} g^{-1}. The activities of PAL, POD, and PPO were expressed as U g^{-1}, where U represented a 0.1 change in absorbance (290 nm), 0.005 change in absorbance (470 nm), and 0.005 change in absorbance (525 nm), respectively, per minute per gram of tissue per ml of the reaction system.

Production and Observation of Electron Microscope Sections

Each group (*A*-Control, *A*-500, *A*-1000, *B*-Control, *B*-500, and *B*-1000) was randomly sampled at day 8 of the storage for scanning electron microscope (SEM) and transmission electron microscope (TEM) observation. Fresh picked blueberries were taken and treated with the same wound (2 mm diameter × 3 mm deep), as the control without inoculation with rotting fungi (Wound-Control).

For SEM, the selected blueberry samples were finely cut into transparent slices using a surgical blade, immediately immersed in 2.5% (v/v) glutaraldehyde solution, and fixed overnight at 4°C. The following day, they were washed three times (5–10 min each) using sterile distilled water, dehydrated

using an ethanol gradient (15 min each in 50, 70, 90, and 95% ethanol, v/v, and twice for 10–15 min in 100% ethanol), soaked in isoamyl acetate (15 min), and then dried at room temperature (~25°C). The dried samples were then adhered to aluminum discs using double-sided carbon tape, sputter-coated using gold, and then scanned and photographed using a Hitachi S-4800 SEM (Hitachi High-Technologies Co., Tokyo, Japan).

For TEM, an appropriate section (about 1 mm × 1 mm × 3 mm) of flesh with peel was cut from each selected blueberry, immediately immersed in 2.5% (v/v) glutaraldehyde solution, and fixed overnight at 4°C. The following day, the fixed samples were soaked in 1% osmium tetroxide solution for 2 h, washed three times in phosphate buffer solution (0.1 M), dehydrated using an ethanol gradient solution (15 min each in 30, 50, 70, 90, and 95% ethanol, v/v) and acetone (15 min; 100%, v/v), embedded in epoxy resin (60°C for 72 h), and then cut into ~70-nm slices using a Leica EM UC7 Ultramicrotome (Leica, Germany). The ultrathin sections were finally double-stained using uranyl acetate (25–30 min) and lead citrate (5–10 min) and then observed and filmed using a Hitachi JEM-2100 transmission electron microscope.

Statistical Analysis

All the experiments were performed in triplicate. The bar charts were generated using Origin Software 8.0, and all data were analyzed using SPSS 14.0. One-way ANOVA and least significant difference (LSD) tests were used to differentiate mean values, and differences at the $p < 0.05$ level were considered significant.

RESULTS

Effect of Ethanol Vapor on Fungal Growth

The colony diameters of both *A. alternata* and *B. cinerea* on PDA medium were significantly reduced by ethanol vapor treatment (**Figure 1A**), and the mycelial growth of *A. alternata* and *B. cinerea* was inhibited by 9.1 and 14.2% (250 μl L^{-1}), 36.4 and 44.7% (500 μl L^{-1}), and 5.5 and 76.6% (1,000 μl L^{-1}; **Figure 1B**). Although the inhibition rates of ethanol against the pathogens generally increased with increasing ethanol concentration, the ethanol treatments had a significantly greater inhibition effect on *B. cinerea* than on *A. alternata* ($p < 0.05$), and the inhibition of *A. alternata* reached a maximum at 500 μl L^{-1}.

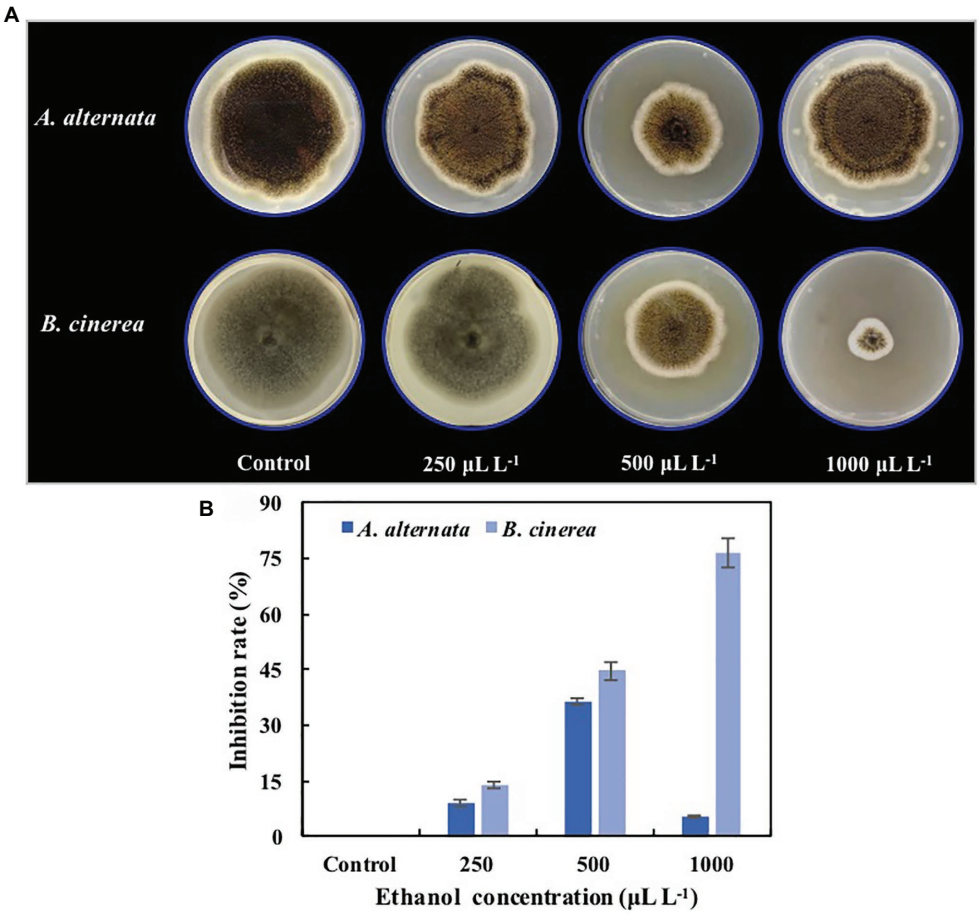

FIGURE 1 | Inhibition effects of ethanol vapor on the growth of *Alternaria alternata* and *Botrytis cinerea*. **(A)** Visual effects of ethanol vapor treatments. **(B)** Inhibition rates of ethanol vapor treatments. Error bars represent the standard deviation of the means ($n = 3$).

Effect of Ethanol Vapor on DREs Activities in Blueberry

The results of the present study demonstrate that both the GLU and CHI activities of *A. alternata*- or *B. cinerea*-inoculated blueberry fruit can be increased by treatment with appropriate concentrations of ethanol vapor (**Figures 2, 3**).

β-1,3-glucanase activity of the control inoculated blueberries was relatively constant during the 16-day storage period and was consistently lower than those of the ethanol vapor-treated inoculated blueberries (**Figure 2**). Furthermore, GLU activity of the *A. alternata*-inoculated blueberries that was treated with 500 μl L^{-1} ethanol was significantly greater than those of the other treatment groups and reached a maximum of 66.83 mg h^{-1} g^{-1} at day 4 of storage, which was 1.85, 1.78, and 1.34 times that of the *A. alternata*-inoculated blueberries treated with 0, 250, or 1,000 μl L^{-1} ethanol, respectively (**Figure 2A**). However, a different pattern was observed for the blueberries inoculated with *B. cinerea* (**Figure 2B**). During the first 12 days of storage, GLU activity of the 500 and 1,000 μl L^{-1} ethanol-treated *B. cinerea*-inoculated blueberries was significantly greater than those of the control, and GLU activity of the 1,000 μl L^{-1} ethanol-treated blueberries was better than that of the 500 μl L^{-1} ethanol-treated blueberries. Similar to measurements of GLU activity in the *A. alternata*-inoculated blueberries, GLU activity of the *B. cinerea*-inoculated blueberries treated with 500 and 1,000 μl L^{-1} ethanol reached maximum values (72.05 and 83.31 mg h^{-1} g^{-1}, respectively) at day 4 of storage, which were 1.73 and 2.00 times greater than that of the control, respectively.

Meanwhile, 250, 500, and 1,000 μl L^{-1} ethanol treatment increased CHI activity of *A. alternata*-inoculated blueberries by 3–32, 55–88, and −3–7%, respectively, and increased those of *B. cinerea*-inoculated blueberries by −30–97, 85–271, and 159–337%, respectively (**Figure 3**). The maximum CHI activity (8.69 mg h^{-1} g^{-1}) of the *A. alternata*-inoculated blueberries was observed at day 8 after treatment with 500 μl L^{-1} ethanol, which was later than that of the other groups (day 4), and the maximum activity of the 500 μl L^{-1} ethanol-treated blueberries was 1.83, 1.50, and 1.75 times greater than that of the 0, 250, and 1,000 μl L^{-1} ethanol-treated blueberries, respectively (**Figure 3A**). However, the maximum CHI activity (2.72 mg h^{-1} g^{-1}) of the

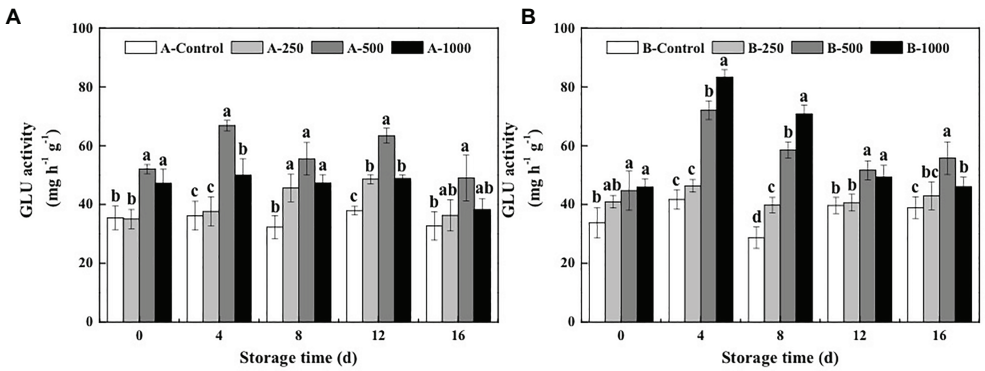

FIGURE 2 | Effect of ethanol vapor on the β-1,3-glucanase (GLU) activity of blueberries inoculated with **A** (*A. alternata*, A) and **B** (*B. cinerea*, B). Two-hundred and fifty, 500, and 1,000 are the amount of ethanol used (μl L^{-1}). Error bars represent the standard deviation of the means ($n = 3$). Different letters on the same column represent significant differences ($p < 0.05$).

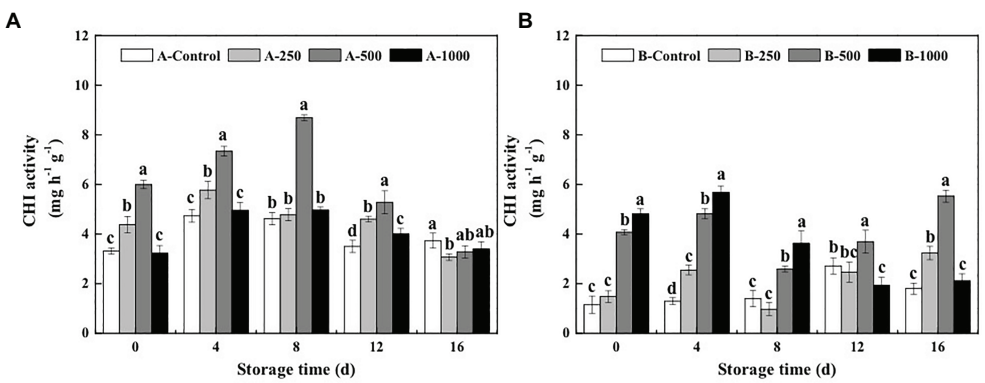

FIGURE 3 | Effect of ethanol vapor on the chitinase (CHI) activity of blueberries inoculated with **A** (*A. alternata*, A) and **B** (*B. cinerea*, B). Two-hundred and fifty, 500, and 1,000 are the amount of ethanol used (μl L^{-1}). Error bars represent the standard deviation of the means ($n = 3$). Different letters on the same column represent significant differences ($p < 0.05$).

B. cinerea-inoculated blueberries without ethanol treatment (B-Control) was observed on the 12th day of storage (**Figure 3B**). At the same time, the activity of 500 μl L^{-1} ethanol-treated blueberries was 3.70 mg h^{-1} g^{-1}, which was 1.36 times higher than that in the B-Control.

Appropriate concentrations of ethanol vapor treatment had an immediate effect on PAL activity of blueberries inoculated with *A. alternata* and *B. cinerea* (**Figure 4**). PAL activity was activated quickly, and even at day 0 after treatment, the 500 μl L^{-1} ethanol treatment increased PAL activity of the *A. alternata*- and *B. cinerea*-inoculated blueberries to 1.14 and 1.41 times higher than those of their control, respectively. Moreover, the 500 μl L^{-1} ethanol treatment consistently induced the greatest activity level over the 16-day storage period, whereas the 1,000 μl L^{-1} ethanol treatment had little effect. After 8 days of storage, PAL activity of *A. alternata*- and *B. cinerea*-inoculated blueberries treated with 500 μl L^{-1} ethanol was 1.12 and 1.24 times higher than those of the control, respectively.

As shown in **Figure 5A**, POD activity of all the *A. alternata*-inoculated blueberries exhibited the same trend, throughout the 16-day storage period, first increasing and then decreasing, and only the 500 μl L^{-1} ethanol treatment significantly improved the POD activity of the *A. alternata*-inoculated blueberries, whereas treatments with lower (250 μl L^{-1}) and higher (1,000 μl L^{-1}) concentrations had no significant effect compared with the control ($p > 0.05$). For all treatment groups, POD activities of blueberries reached a maximum on the 4th day of storage, at which point the POD activity of the *A. alternata*-inoculated blueberries treated with 500 μl L^{-1} was 1.83, 1.93, and 1.66 times the activities of the other *A. alternata*-inoculated blueberries treated with 0, 250, and 1,000 μl L^{-1}, respectively. The POD activity of *B. cinerea*-inoculated blueberries was also increased significantly by the 500 μl L^{-1} ethanol treatment but peaked on the 8th day of storage (**Figure 5B**), at which point the POD activity of the *B. cinerea*-inoculated blueberries treated with 500 μl L^{-1} ethanol was 2.48, 1.81, and 3.43 times the activity of *B. cinerea*-inoculated blueberries treated with 0, 250, and 1,000 μl L^{-1} ethanol, respectively. However, the POD activity of *B. cinerea*-inoculated blueberries treated with 1,000 μl L^{-1} ethanol was greater than that of the other groups on day 0 (0.39 U g^{-1})

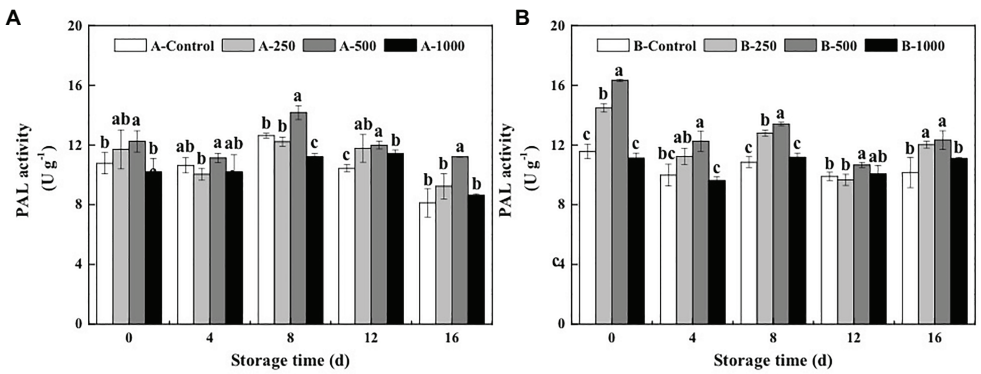

FIGURE 4 | Effect of ethanol vapor on the phenylalnine ammonialyase (PAL) activity of blueberries inoculated with **A** (*A. alternata*, A) and **B** (*B. cinerea*, B). Two-hundred and fifty, 500, and 1,000 are the amount of ethanol used (μl L^{-1}). Error bars represent the standard deviation of the means ($n = 3$). Different letters on the same column represent significant differences ($p < 0.05$).

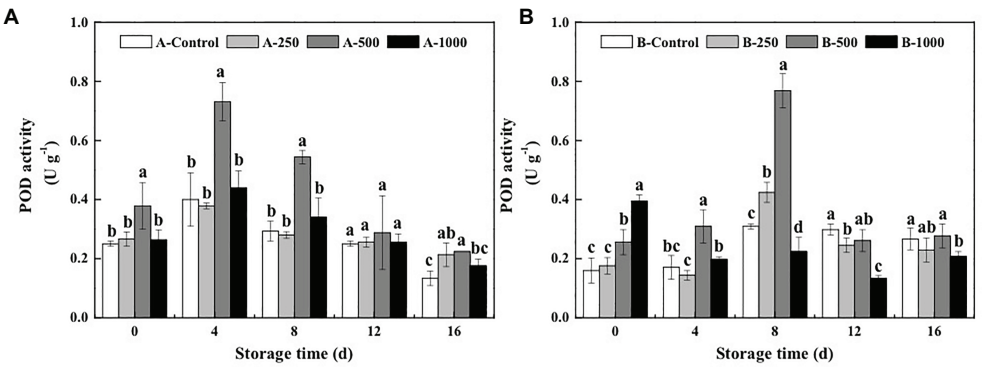

FIGURE 5 | Effect of ethanol vapor on the peroxidase (POD) activity of blueberries inoculated with **A** (*A. alternata*, A) and **B** (*B. cinerea*, B). Two-hundred and fifty, 500, and 1,000 are the amount of ethanol used (μl L^{-1}). Error bars represent the standard deviation of the means ($n = 3$). Different letters on the same column represent significant differences ($p < 0.05$).

but decreased rapidly and was significantly lower than that of *B. cinerea*-inoculated control group after 8 days.

Polyphenol oxidase activity of blueberries inoculated with *A. alternata* and *B. cinerea* first decreased during storage and then increased (**Figure 6**). On day 0, PPO activity of the *A. alternata*- and *B. cinerea*-inoculated blueberries was significantly increased by the 500 μl L^{-1} (3.47 and 1.55 times, respectively) and 1,000 μl L^{-1} (2.50 and 1.61 times, respectively) ethanol treatments and then decreased rapidly. On the 4th day of storage, ethanol had no effect on PPO activity of the *A. alternata*-inoculated blueberries, whereas PPO activity of the *B. cinerea*-inoculated blueberries treated with 250, 500, and 1,000 μl L^{-1} ethanol was 1.16, 1.74, and 2.88 times of the control, respectively. Furthermore, the PPO activity of the control blueberries increased rapidly after 4 days of storage, whereas that of the blueberries treated with 500 μl L^{-1} ethanol increased slowly but remained the lowest, with activities that were 33.5–55.2 and 8.7–31.9% lower than the control for the *A. alternata*- and *B. cinerea*-inoculated blueberries, respectively.

Effect of Ethanol Vapor on Blueberry Cell Microstructure

Scanning electron microscope revealed that the pericarp cells of all inoculated blueberries were damaged to varying degrees (**Figure 7**). The 1,000 μl L^{-1} ethanol-treated blueberry exhibited the greatest damage, whereas the pericarp cells of the 500 μl L^{-1} ethanol-treated blueberry were the most similar to those of the Wound-Control, uniform, and intact.

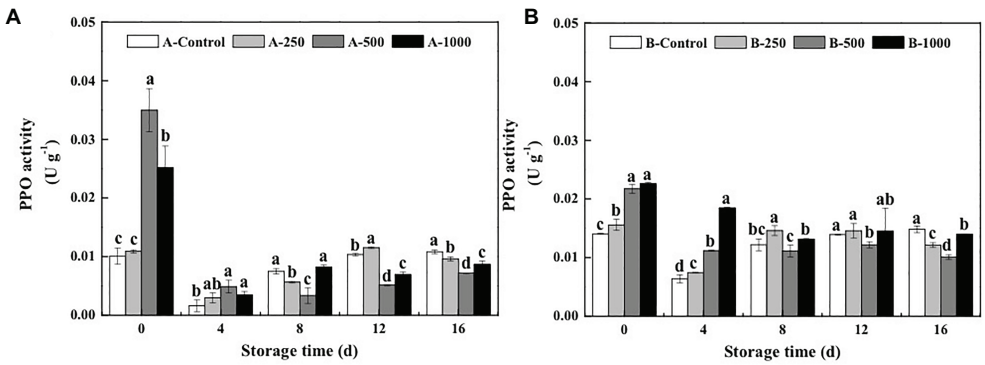

FIGURE 6 | Effect of ethanol vapor on the polyphenol oxidase (PPO) activity of blueberries inoculated with **A** (*A. alternata*, A) and **B** (*B. cinerea*, B). Two-hundred and fifty, 500, and 1,000 are the amount of ethanol used (μl L^{-1}). Error bars represent the standard deviation of the means ($n = 3$). Different letters on the same column represent significant differences ($p < 0.05$).

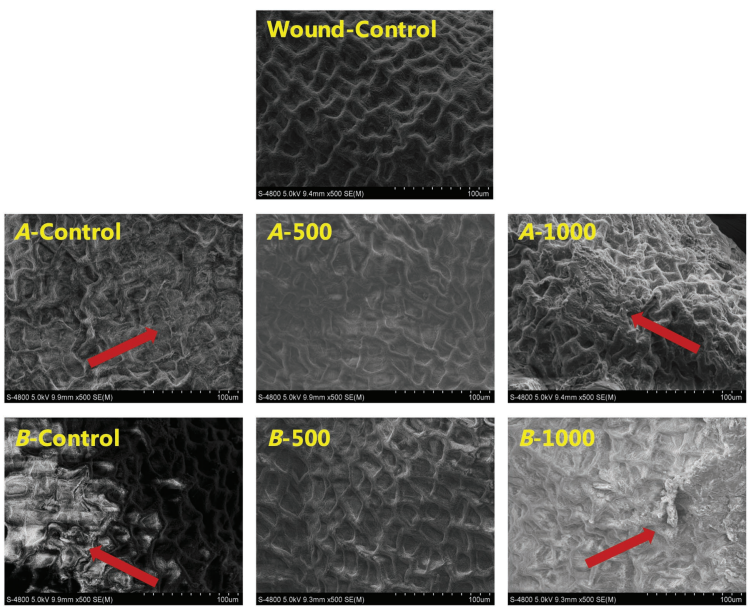

FIGURE 7 | Scanning electron microscope (SEM) images of fruit cells of *A. alternata*- and *B. cinerea*-inoculated blueberry after treatment with ethanol on the 8th day of storage at 0 ± 0.5°C. The scale bars represent 100 μm.

Meanwhile, TEM revealed that pathogen inoculation induced conspicuous plasmolysis, and obscure membrane structure and broken intracellular compartmentalization (**Figures 8B,E**). However, the 500 μl L^{-1} ethanol treatment appeared to protect cell structure and prevent plasmolysis (**Figures 8C,F**), with the complete nucleus, numerous complete mitochondria with typically closely arranged cristae, and osmiophilic granules dispersed in plastid matrix. However, numerous vacuoles were produced in cells of the 1,000 μl L^{-1} ethanol-treated blueberries, and the vacuoles degraded the organelles (e.g., mitochondria and chloroplasts), thereby causing serious plasmolysis (**Figures 8D,G**).

DISCUSSION

Blueberries are vulnerable to microbial infection and rot throughout their production chain, from harvest to transportation, storage, and sale, thereby affecting their market value. However, the secondary plant metabolite ethanol exhibits strong and broad-spectrum antimicrobial activity and has been widely used for controlling fruit and vegetables diseases, owing to its safety, environmental friendliness, lack of residue, low cost, and widespread availability. Previous studies have reported that low levels of ethanol can be used to inhibit the growth of *Verticicladiella abietina*, *Penicillium citrinum*, *Trichoderma viride*, and *C. acutatum in vitro* (Wang et al., 2011, 2015), and Lichter et al. (2002) even reported that proved that ethanol liquid treatment could inhibit the spore germination and growth of *B. cinerea*. In the present study, the inhibition effect of ethanol vapor on the growth of fungal blueberry pathogens was assessed. Ethanol vapor treatment markedly reduced the growth of *A. alternata* and *B. cinerea* mycelia in a dose-dependent manner (**Figure 1**), which confirmed its effectiveness as a fungal growth inhibitor and may explain the previously reported effects of ethanol vapor on the decay

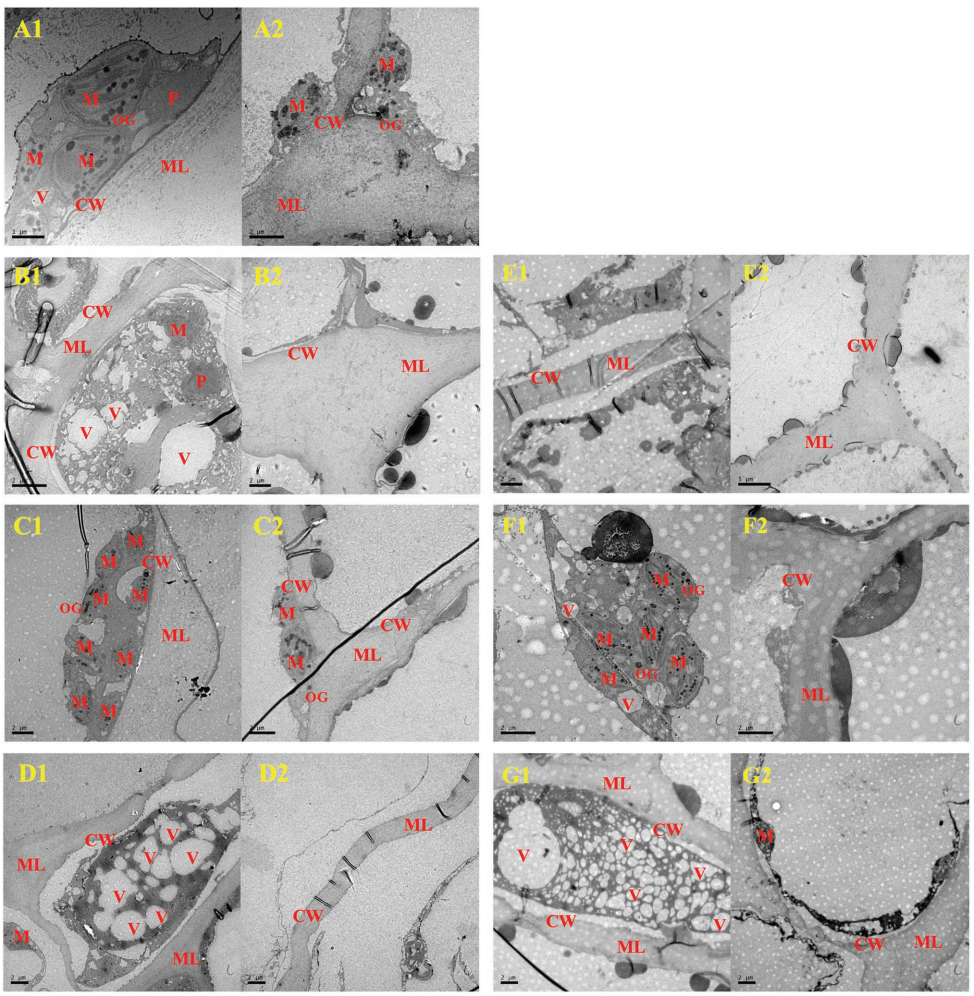

FIGURE 8 | The cellular ultrastructure of *A. alternata*- **(B–D)** and *B. cinerea*- **(E–G)** inoculated blueberry fruit after treatment with ethanol on the 8th day of storage at 0 ± 0.5°C. **A1** and **A2**, Wound-Control; **B1** and **B2**, *A*-Control; **C1** and **C2**, *A*-500; **D1** and **D2**, *A*-1000; **E1** and **E2**, *B*-Control; **F1** and **F2**, *B*-500; **G1** and **G2**, *B*-1000. CW, cell wall; M, mitochondria; ML, middle lamella; P, plastid; V, vacuole. The scale bars for **A1** represents 1 μm, for **(A2,B1,B2,C1,C2,E1,F1,F2,G1,G2)** represent 2 μm, and for **E2** represents 5 μm.

of postharvest blueberries (Ji et al., 2019). Interestingly, *A. alternata* and *B. cinerea* differed in their sensitivity to ethanol. For example, *B. cinerea* was inhibited in a dose-dependent manner (1,000 μl L^{-1} >500 μl L^{-1} >250 μl L^{-1}), whereas *A. alternata* was most inhibited by the 500 μl L^{-1} ethanol treatment, in contrast to previous reports – the higher the ethanol concentration, the stronger the ability of killing *B. cinerea* spores (Lichter et al., 2002; Karabulut et al., 2004a,b). The difference for *A. alternata* with previous studies could be due to differences in ethanol treatment methods (e.g., liquid treatment vs. vapor treatment), which could have different modes of action or cause different damage to microbial cells. Ethanol vapor is reportedly useful for controlling the postharvest decay of fruit and vegetables, such as sweet cherries (Karabulut et al., 2004a), table grapes (Lichter et al., 2002; Karabulut et al., 2004b), loquats (Wang et al., 2015), and blueberries (Ji et al., 2019), which can be explained by the inhibitory activity of ethanol against the growth of rot fungi of many fruit and vegetables.

However, it was found that the disease control effect of ethanol on postharvest fruit and vegetables relies both on its direct antimicrobial properties, as well as on the mechanism of "priming," which induces and improves the resistance of fruit and vegetables to postharvest diseases (Tzortzakis, 2010). The activation of defense-related enzymes, such as GLU, CHI, PAL, POD, and PPO, in fruit and vegetables is considered to be an important factor in the diseases resistance of postharvest horticultural crops (Tian et al., 2006; Wang et al., 2014; Shao et al., 2015). In the present study, the activity of both CHI and GLU, which can degrade chitin and β-1,3-glucan in fungal cell walls and effectively prevent the infection of fruits and vegetables, was significantly greater in ethanol-treated blueberries than in control blueberries (Souza et al., 2017; **Figures 2, 3**). Meanwhile, PAL and POD are important resistant substance synthetases in fruit and vegetables and can catalyze the synthesis of lignin, flavonoids, and phenols. This is important because phenols can be transformed into quinones, which are more toxic to pathogens, and because lignin is valuable for strengthening fruit cell walls and, thereby, inhibiting pathogenesis (Farkas and Stahmann, 1996). In the present study, both PAL and POD activities were significantly enhanced by the 500 μl L^{-1} ethanol treatment (**Figures 4, 5**). PPO is a copper enzyme that also contributes to the lignification of host cells and catalyzes the oxidation of phenolic compounds into toxic quinones with strong antifungal activity against pathogens (Cindi et al., 2016). In the present study, the PPO activity of blueberry increased immediately after the ethanol vapor treatment, potentially enhancing resistance of blueberries against pathogens. Therefore, these effects could collectively contribute to the development of disease resistance in blueberries against *A. alternata* and *B. cinerea*. Similarly, many studies also have been reported on enhancing disease resistance of fruit and vegetables by inducing the activities of DREs, such as in pear fruit (GLU, CHI, PAL, POD, and PPO) with *L*-glutamate treatment against *Penicillium expansum* (Jin et al., 2019), in pear fruit (GLU, CHI, PAL, POD, and PPO) with γ-aminobutyric acid treatment against *P. expansum* (Yu et al., 2014), in tomato fruit (PAL, PPO, CHI, and GLU) with *L*-arginine treatment against *B. cinerea* (Zheng et al., 2011), and in strawberry (CHI and GLU) with tea tree oil and hot air treatment against *B. cinerea* (Wei et al., 2018). Therefore, the induction of disease resistance by enhancing DREs (CHI, GLU, PAL, POD, and PPO) activities might be an important mechanism by which ethanol vapor is able to reduce the postharvest decay of blueberries. Ethanol vapor can induce the disease resistance of blueberries infected by *A. alternata* and *B. cinerea*, but the disease resistance of blueberry infected by *B. cinerea* is stronger than that of blueberry infected by *A. alternata*.

Correlation analysis indicated that there were different correlations among the DREs (GLU, CHI, PAL, POD, and PPO) in *A. alternata*- and *B. cinerea*-inoculated blueberries with ethanol treatment (**Figure 9**), which indicated that different pathways were involved in the disease resistance-promoting effects of ethanol against different pathogens. For example, PPO activity was negatively or not correlated with GLU, CHI, and POD activity in blueberries affected with either pathogen, possibly because the production of quinones or the other defense-related substances catalyzed by PPO is not one of the main mechanism underlying such ethanol-induced disease resistance. The PAL, the key enzyme of phenylpropanoid pathway, its activity in *A. alternata*-inoculated blueberries with ethanol treatment was significantly positively correlated with CHI and GLU, which indicated that ethanol vapor inducers could stimulate defense mechanisms, such as phenylpropanoid pathway activation, helping to protect the blueberries against *A. alternate*. Similar result was confirmed on strawberries treated by terpinen-4-ol (Li et al., 2020).

In addition, the cells microstructure of the 500 μl L^{-1} ethanol-treated blueberries was the most similar to that of the control (Wound-control) in the present study, being uniform and intact (surface structure; **Figure 7**), and exhibited the relatively abundant inclusions (ultrastructure; **Figure 8**). These findings indicated that the senescence of blueberry cells could be delayed by appropriate ethanol vapor treatment. The 500 μl L^{-1} ethanol treatment also resulted in the attachment of rough substances to the closely arranged fiber microfibrils on the cell walls, and those substances could be phenolic substances and lignin that was induced by the ethanol treatment, thereby improving the firmness of the cell wall and the barrier defense capability,

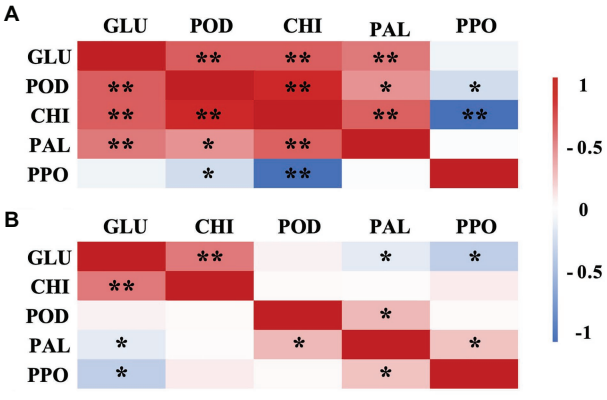

FIGURE 9 | Pearson correlation matrix of the disease resistance-related enzyme activities (GLU, CHI, PAL, POD, and PPO) in ethanol-treated blueberries inoculated with *A. alternata* **(A)** and *B. cinerea* **(B)**. *Significance at the $p < 0.05$ probability level. **Significance at the $p < 0.01$ probability level.

thus, the pathogen resistance. However, further study on ethanol vapor inducing disease resistance of blueberries is needed.

DATA AVAILABILITY STATEMENT

The original contributions presented in the study are included in the article/supplementary material, further inquiries can be directed to the corresponding author.

AUTHOR CONTRIBUTIONS

YJ, WH, ZX, and AJ: conceptualization. WH: methodology, project administration, and funding acquisition. YJ: validation, formal analysis, data curation, and writing-original draft preparation. YJ and JL: investigation. YJ, WH, JL, ZX, AJ, XY, YG, KF, and GS: writing-review and editing. WH and ZX: supervision. All authors contributed to the article and approved the submitted version.

FUNDING

This study was supported by "Thirteenth Five-Year Plan" for National Key Research and Development Program (grant no. 2016YFD0400903), National Natural Science Foundation (grant no. 31471923), and "Twelfth Five-Year Plan" for National Science and Technology Support Program (grant no. 2012BAD38B05).

REFERENCES

Barkai, G. R. (2001). *Postharvest diseases of fruits and vegetables*. Amsterdam: Elsevier.

Candir, E., Ozdemir, A. E., Kamiloglu, O., Soylu, E. M., Dilbaz, R., and Ustun, D. (2012). Modified atmosphere packaging and ethanol vapor to control decay of 'red globe' table grapes during storage. *Postharvest Biol. Technol.* 63, 98–106. doi: 10.1016/j.postharvbio.2011.09.008

Caruso, F. L., and Ramsdell, D. C. (1995). Compendium of blueberry and cranberry diseases. Disease Compendium.

Chen, Y., Hung, Y., Chen, M., and Lin, H. (2017). Effects of acidic electrolyzed oxidizing water on retarding cell wall degradation and delaying softening of blueberries during postharvest storage. *LWT-Food Sci. Technol.* 84, 650–657. doi: 10.1016/j.lwt.2017.06.011

Cindi, M. D., Soundy, P., Romanazzi, G., and Sivakumar, D. (2016). Different defense responses and brown rot control in two *Prunus persica* cultivars to essential oil vapours after storage. *Postharvest Biol. Technol.* 119, 9–17. doi: 10.1016/j.postharvbio.2016.04.007

FAO (2020). FAOSTAT statistics database. Available at: http://www.fao.org/faostat/en/#data/QC/

Farkas, G. L., and Stahmann, A. (1996). On the nature of changes in peroxidase isoenzymes in bean leaves infected by southern bean mosaic virus. *Phytopathology* 56, 669–677.

Huang, R., Che, H. J., Zhang, J., Yang, L., Jiang, D. H., and Li, G. Q. (2012). Evaluation of Sporidiobolus pararoseus strain YCXT3 as biocontrol agent of *Botrytis cinerea* on postharvest strawberry fruits. *Biol. Control* 62, 53–63. doi: 10.1016/j.biocontrol.2012.02.010

Ji, Y., Hu, W., Jiang, A., Xiu, Z., Liao, J., Yang, X., et al. (2019). Effect of ethanol treatment on the quality and volatiles production of blueberries after harvest. *J. Sci. Food Agric.* 99, 6296–6306. doi: 10.1002/jsfa.9904

Jin, L., Cai, Y., Sun, C., Huang, Y., and Yu, T. (2019). Exogenous *L*-glutamate treatment could induce resistance against *Penicillium expansum* in pear fruit by activating defense-related proteins and amino acids metabolism. *Postharvest Biol. Technol.* 150, 148–157. doi: 10.1016/j.postharvbio.2018.11.009

Karabulut, O. A., Arslan, U., Kuruoglu, G., and Ozgenc, T. (2004a). Control of postharvest diseases of sweet cherry with ethanol and hot water. *J. Phytopathol.* 152, 298–303. doi: 10.1111/j.1439-0434.2004.00844.x

Karabulut, O. A., Gabler, F. M., Mansour, M., and Smilanick, J. L. (2004b). Postharvest ethanol and hot water treatments of table grapes to control gray mold. *Postharvest Biol. Technol.* 34, 169–177. doi: 10.1016/j.postharvbio.2004.05.003

Li, Z., Wang, N., Wei, Y., Zou, X., Jiang, S., Xu, F., et al. (2020). Terpinen-4-ol enhances disease resistance of postharvest strawberry fruit more effectively than tea tree oil by activating the phenylpropanoid metabolism pathway. *J. Agric. Food Chem.* 68, 6739–6747. doi: 10.1021/acs.jafc.0c01840

Lichter, A., Zutkhy, Y., Sonego, L., Dvir, O., Kaplunov, T., Sarig, P., et al. (2002). Ethanol controls postharvest decay of table grapes. *Postharvest Biol. Technol.* 24, 301–308. doi: 10.1016/s0925-5214(01)00141-7

Shao, X., Cao, B., Xu, F., Xie, S., Yu, D., and Wang, H. (2015). Effect of postharvest application of chitosan combined with clove oil against citrus green mold. *Postharvest Biol. Technol.* 99, 37–43. doi: 10.1016/j.postharvbio.2014.07.014

Sommer, N. F. (1985). Role of controlled environments in suppression of postharvest diseases. *Can. J. Plant Pathol.* 7, 331–339. doi: 10.1080/07060668509501700

Souza, T. P., Dias, R. O., and Silvafilho, M. C. (2017). Defense-related proteins involved in sugarcane responses to biotic stress. *Genet. Mol. Biol.* 40, 360–372. doi: 10.1590/1678-4685-gmb-2016-0057

Tian, S. P., Wan, Y. K., Qin, G. Z., and Xu, Y. (2006). Induction of defense responses against *Alternaria* rot by different elicitors in harvested pear fruit. *Appl. Microbiol. Biotechnol.* 70, 729–734. doi: 10.1007/s00253-005-0125-4

Tzortzakis, N. G. (2010). Ethanol, vinegar and *Origanum vulgare* oil vapour suppress the development of anthracnose rot in tomato fruit. *Int. J. Food Microbiol.* 142, 14–18. doi: 10.1016/j.ijfoodmicro.2010.05.005

Wang, S. Y., Camp, M. J., and Ehlenfeldt, M. K. (2012). Antioxidant capacity and α-glucosidase inhibitory activity in peel and flesh of blueberry (*Vaccinium* spp.) cultivars. *Food Chem.* 132, 1759–1768. doi: 10.1016/j.foodchem.2011.11.134

Wang, K., Cao, S., Di, Y., Liao, Y., and Zheng, Y. (2015). Effect of ethanol treatment on disease resistance against *anthracnose* rot in postharvest loquat fruit. *Sci. Hortic.* 188, 115–121. doi: 10.1016/j.scienta.2015.03.014

Wang, C. Y., Chen, C. T., and Yin, J. J. (2010). Effect of allyl isothiocyanate on antioxidants and fruit decay of blueberries. *Food Chem.* 120, 199–204. doi: 10.1016/j.foodchem.2009.10.007

Wang, K. T., Jin, P., Han, L., Shang, H. T., Tang, S. S., and Rui, H. J. (2014). Methyl jasmonate induces resistance against *Penicillium citrinum* in Chinese bayberry by priming of defense responses. *Postharvest Biol. Technol.* 98, 90–97. doi: 10.1016/j.postharvbio.2014.07.009

Wang, K. T., Jin, P., Tang, S. S., Shang, H. T., Rui, H. J., Di, H. T., et al. (2011). Improved control of postharvest decay in Chinese bayberries by a combination treatment of ethanol vapor with hot air. *Food Control* 22, 82–87. doi: 10.1016/j.foodcont.2010.05.011

Wang, F., Saito, S., Michailides, T. J., and Xiao, C. L. (2021). Postharvest use of natamycin to control Alternaria rot on blueberry fruit caused by Alternaria alternata and *A. arborescens*. *Postharvest Biol. Technol.* 172:111383. doi: 10.1016/j.postharvbio.2020.111383

Wei, Y., Wei, Y., Xu, F., and Shao, X. (2018). The combined effects of tea tree oil and hot air treatment on the quality and sensory characteristics and decay of strawberry. *Postharvest Biol. Technol.* 136, 139–144. doi: 10.1016/j.postharvbio.2017.11.008

Yu, C., Zeng, L., Sheng, K., Chen, F., Zhou, T., Zheng, X., et al. (2014). γ-Aminobutyric acid induces resistance against *Penicillium expansum* by priming of defence responses in pear fruit. *Food Chem.* 159, 29–37. doi: 10.1016/j.foodchem.2014.03.011

Zhang, Z., Qin, G., Li, B., and Tian, S. (2014). Knocking out bcsas1 in *Botrytis cinerea* impacts growth, development, and secretion of extracellular proteins, which decreases virulence. *Mol. Plant-Microbe Interact.* 27, 590–600. doi: 10.1094/MPMI-10-13-0314-R

Zheng, Y., Sheng, J., Zhao, R., Zhang, J., Lv, S., Liu, L., et al. (2011). Preharvest *L*-arginine treatment induced postharvest disease resistance to *Botrysis cinerea* in tomato fruits. *J. Agric. Food Chem.* 59, 6543–6549. doi: 10.1021/jf2000053

Conflict of Interest: The authors declare that the research was conducted in the absence of any commercial or financial relationships that could be construed as a potential conflict of interest.

frontiers in Microbiology

REVIEW
published: 09 December 2021
doi: 10.3389/fmicb.2021.782934

A Review: Gaseous Interventions for *Listeria monocytogenes* Control in Fresh Apple Cold Storage

*Jiewen Guan[1,2], Alison Lacombe[1], Bhargavi Rane[1,2], Juming Tang[2], Shyam Sablani[2] and Vivian C. H. Wu[1]**

[1] Produce Safety and Microbiology Research Unit, Western Regional Research Center, Agricultural Research Service, United States Department of Agriculture, Albany, CA, United States, [2] Department of Biological Systems Engineering, Washington State University, Pullman, WA, United States

Listeria monocytogenes (*L. monocytogenes*) causes an estimated 1600 foodborne illnesses and 260 deaths annually in the U.S. These outbreaks are a major concern for the apple industry since fresh produce cannot be treated with thermal technologies for pathogen control before human consumption. Recent caramel apple outbreaks indicate that the current non-thermal sanitizing protocol may not be sufficient for pathogen decontamination. Federal regulations provide guidance to apple processors on sanitizer residue limits, organic production, and good manufacturing practices (GMPs). However, optimal methods to control *L. monocytogenes* on fresh apples still need to be determined. This review discusses *L. monocytogenes* outbreaks associated with caramel apples and the pathogen's persistence in the environment. In addition, this review identifies and analyzes possible sources of contaminant for apples during cold storage and packing. Gaseous interventions are evaluated for their feasibility for *L. monocytogenes* decontamination on apples. For example, apple cold storage, which requires waterless interventions, may benefit from gaseous antimicrobials like chlorine dioxide (ClO_2) and ozone (O_3). In order to reduce the contamination risk during cold storage, significant research is still needed to develop effective methods to reduce microbial loads on fresh apples. This requires commercial-scale validation of gaseous interventions and intervention integration to the current existing apple cold storage. Additionally, the impact of the interventions on final apple quality should be taken into consideration. Therefore, this review intends to provide the apple industry suggestions to minimize the contamination risk of *L. monocytogenes* during cold storage and hence prevent outbreaks and reduce economic losses.

Keywords: *Listeria monocytogenes*, food safety, fresh apples, cold storage, gaseous interventions

OPEN ACCESS

Edited by:
Arun K. Bhunia,
Purdue University, United States

Reviewed by:
Sujata Sirsat,
University of Houston, United States
Joelle K. Salazar,
U.S. Food and Drug Administration, United States

****Correspondence:***
Vivian C. H. Wu
vivian.wu@usda.gov

Specialty section:
This article was submitted to Food Microbiology, a section of the journal Frontiers in Microbiology

Received: *25 September 2021*
Accepted: *25 October 2021*
Published: *09 December 2021*

Citation:
Guan J, Lacombe A, Rane B, Tang J, Sablani S and Wu VCH (2021) A Review: Gaseous Interventions for Listeria monocytogenes Control in Fresh Apple Cold Storage. Front. Microbiol. 12:782934. doi: 10.3389/fmicb.2021.782934

INTRODUCTION

Apples are one of the most valuable fruit crops in the United States (U.S.). The apple industry brings 5 billion dollars of revenue to the economy annually (U.S. Apple Association [USApple], 2021). In 2014, caramel apples contaminated with *L. monocytogenes* were linked to a foodborne illness outbreak in which 35 people across 12 U.S. states contracted listeriosis, 7 (20%) of which

died (U.S. Centers for Disease Control and Prevention [CDC], 2014). Apples are commonly consumed raw or minimally processed (Du et al., 2002). There is no "kill step" included in the fresh produce postharvest packing process to eliminate pathogenic bacteria. The current fresh apple industry relies heavily on postharvest washing to control foodborne pathogens. However, the most commonly used sanitizer, chlorine (hypochlorite), has been reported to react with organic matters to form carcinogenic compounds, raising health and environmental hazards (Artés et al., 2009).

During harvest, apples are picked by hand in the orchards and transported in bins to the packinghouse, where they are either cold-stored or washed, sized, sorted, and packed for the retail market. Unwashed apples are moved into refrigerated storage – either short-term conventional refrigeration or long-term controlled atmosphere (CA) (Pietrysiak et al., 2019). *L. monocytogenes* has the ability to grow at refrigeration temperatures and is persistent in a cold environment (Walker et al., 1990). The environmental testing of the caramel apple outbreak showed that the contamination was introduced on the apples at the firm's packing facility. Since then, several voluntary recalls have been reported for potential *Listeria* contaminations on fresh apples (U.S. Food and Drug Administration [FDA], 2017a, 2019a). These incidents show the need to improve current food safety systems in the apple packing industry. In particular, there is a need for developing and validating effective interventions to reduce contamination.

Several European countries such as Germany, Belgium, Denmark, Switzerland, and the Netherlands have banned chlorine in commercial produce washing (Artés et al., 2009; Shen et al., 2016). The efficacy of chlorine disinfection is highly dependent on the pH of the solution (Connell, 1996; Sun et al., 2019). Various environmentally friendly alternative sanitizers like chlorine dioxide, peracetic acid (PAA), and ozone have been suggested to replace chlorine (Rodgers et al., 2004; Hua et al., 2019; Guan et al., 2021). However, there has been limited information on the feasibility of those and other potential interventions for the apple industry.

Food safety interventions that minimize contamination risks are of critical importance. Therefore, the objective of this review is to identify the safety gaps during apple packing process and analyze the potential application of gaseous interventions in apple cold storage. An integrated approach to the existing apple packing facility is urgently needed. Currently, the federal agencies, the fresh apple industry, and researchers have switched their focus to gaseous interventions that decontaminate *L. monocytogenes* on fresh apples. This review will consider the regulatory requirements on gaseous interventions as well as organic production and handling of apples that could contribute to future industrial application and benefit the apple processors.

LISTERIA MONOCYTOGENES

Listeria monocytogenes Outbreaks

Listeriosis is a serious infection caused by the consumption of *L. monocytogenes* contaminated food. U.S. Centers for Disease Control and Prevention [CDC] (2021) reports that an estimated 1,600 people have been diagnosed with listeriosis yearly, and the death rate is about 16% in the U.S. *Listeria monocytogenes* is a gram-positive, facultative anaerobic pathogenic bacterium. It has the ability to replicate at refrigeration temperatures. These characteristics help *L. monocytogenes* adapt to produce-associated environments (e.g., cold storage) where other bacteria might be prohibited to grow (Du et al., 2002). For example, in the caramel apple outbreak in 2014, all fresh Granny Smith and Gala apples were voluntarily recalled because environmental testing revealed contamination with *L. monocytogenes* at the firm's apple-packing facility in California (U.S. Centers for Disease Control and Prevention [CDC], 2014). In January 2015, the U.S. Food and Drug Administration (FDA) conducted a traceback investigation. Six of the seven environmental samples positive for *L. monocytogenes* indistinguishable from the outbreak strains were isolated from food contact surfaces (FCS), including polishing brush, drying brushes, conveyor, and inside a wooden bin.

FDA investigation found the cross-contamination between FCS and apples likely played a role in the consecutive apple contamination in the outbreak. Thus, it has been hypothesized that *L. monocytogenes* contamination could happen throughout the packing process and the distribution chain. Once the pathogen is introduced to the environment, it is difficult to eliminate if appropriate good manufacturing practices (GMPs) are not applied. The *Listeria*-contaminated fresh produce caused foodborne illness and increased the food and economic loss for the produce industry, heightening awareness of food safety and implementing the Food Safety Modernization Act (FSMA). Fresh fruit growers, packers, and processors are required to adopt validated and effective preventive controls by the Produce Rule of the FSMA (U.S. Food and Drug Administration [FDA], 2011).

Persistence in Environment

There are many opportunities for *L. monocytogenes* to attach to the produce surface in a typical apple packing house. In the investigation of the cantaloupe and caramel apple outbreaks, environmental contamination at packing houses and equipment FCS were likely the source of listeriosis outbreaks (U.S. Centers for Disease Control and Prevention [CDC], 2011, 2014). These include cross-contamination during washing, the wax coating unit operation, cold storage, and FCS like polishing brushes and dryer rollers (Ruiz-Llacsahuanga et al., 2021). Cooling and packing operations may also be responsible for bacterial contamination of the produce due to the significant amount of water utilized during the packing process. Wet surface areas in packing facilities are favorable for bacterial growth (Pietrysiak et al., 2019). Water may facilitate biofilm development as one of the main locations, which enhances the persistence of *L. monocytogenes* in the environment (Galié et al., 2018). *L. monocytogenes* may spread in the environment and lead to food contamination, which emphasizes the importance of good agriculture practices (GAPs), good manufacturing practices (GMPs), and HACCP for the produce postharvest handling and processing (Farber et al., 2003). Therefore, it is critical to identify the safety gaps during the packing lines and implement preventive interventions to avoid contamination.

Listeria monocytogenes has been isolated from soil, water, animal manure, and decaying vegetation (Farber and Peterkin, 1991; U.S. Food and Drug Administration [FDA], 2019b). Unlike other foodborne pathogens, *L. monocytogenes* can survive between a wide range of temperature (−0.4 to 50°C) and pH values (4.3 to 9.4) (Farber and Peterkin, 1991; Pietrysiak et al., 2019), and is resistant to adverse environmental conditions, such as low temperature, water activity or oxygen, and high acidity or salt (Buchanan and Phillips, 1990; Walker et al., 1990). The unique ability of *L. monocytogenes* to survive or even grow at low temperatures makes it a primary pathogen to contaminate fresh produce in refrigerated packing. *L. monocytogenes* persists in a produce packing environment from months to years, resulting in recontamination of the produce passing through that environment (Leong et al., 2017) and posing a high safety risk to the prolonged storage of fresh apples. The expression of cold shock proteins has been reported to help *L. monocytogenes* with the adaptation of low temperatures (Matereke and Okoh, 2020). Neunlist et al. (2005) concluded that the membrane lipids alteration of *L. monocytogenes* protects it from cold stress. In addition, whole-genome sequencing (WGS) showed that *Listeria* isolates from the voluntarily recalled whole apples, collected along the distribution chain, were highly related to the outbreak strains (U.S. Centers for Disease Control and Prevention [CDC], 2014; Angelo et al., 2017).

Biofilm Formation

Biofilms are complex structures composed of multiple cells embedded in an extracellular matrix that is mainly formed by polysaccharides, proteins, or extracellular DNA. This matrix can adhere to hard surfaces in a food processing environment, such as FCS (equipment, transport, storage surfaces, etc.) or food surfaces (vegetables, fruits, meat, etc.), responsible for the strong persistence of biofilm in the food industry. Biofilm formation offers the microbial cells higher physical resistance against desiccation, mechanical resistance against removal by liquid streams, and chemical resistance against antimicrobials and disinfectants (Galié et al., 2018). The presence of biofilm in food industry environments puts human health at risk. Thus, the food industry is seeking biofilm prevention and disruption methods.

Listeria monocytogenes biofilms are generally formed by teichoic acids. They can grow on major food contact surfaces, including stainless steel, low-density polyethylene (LDPE), polyvinyl chloride (PVC), polyester (PET), rubber, and glass surfaces throughout the food industry (Hua et al., 2019). Dygico et al. (2020) stated that factors like time, temperature, surface type, nutrient availability, and origin could affect the biofilm formation of *L. monocytogenes*. Then this pathogen can contaminate the food batches from the surfaces. With the replication ability at low temperatures, *L. monocytogenes* reinforces its hydrophilicity and induces biofilm formation as a response to cold temperatures, enhancing its attachment to surfaces and its resistance to sanitation procedures in food manufacturing plants. These characteristics highlight the great importance of inspecting and controlling *L. monocytogenes* biofilms in the food industry (Galié et al., 2018).

FRESH APPLE PACKING PROCESS

After Harvest

After being picked and transported from the orchard to the packing house, fresh apples are either directly washed and packed for shipment or stored in cold storage for future packing (**Figure 1**). Postharvest fungicide treatment (drenching or fogging) is often applied to fresh apples to avoid mold spoilage for extended storage time. However, the reuse of fungicide solutions in the drenching step may cause cross-contamination with pathogens like *L. monocytogenes*. Additionally, there is no elimination step to remove damaged apples (caused during harvest or transportation) before cold storage. The injured apples might promote the survival, growth, and spread of bacteria and fungus during storage (Ruiz-Llacsahuanga et al., 2021). Thus the preventive controls to reduce the microbial load on apples would be necessary to integrate into the cold storage before washing.

Postharvest Washing

Postharvest washing is a typical step to reduce contamination for most fresh produce, including processed (i.e., fresh-cut) produce. The aim of most produce washing sanitization on the commercial scale is a 3-log reduction of pathogens on foods and food contact surfaces (Gombas et al., 2017). Various washing steps are used for different apple varieties and fruit quality. Fresh apples in wooden/plastic harvest bins are dumped into flume tanks to remove soil and debris in packing lines. Sanitizers are usually added to the washing water, and the water quality is monitored to avoid cross-contamination. To prevent produce contamination, suitable antimicrobial agents are used, and several runs of freshwater wash are applied (**Figure 1**). The widely used antimicrobial agents are chlorine, peracetic acid (PAA), aqueous chlorine dioxide (ClO_2), aqueous ozone (O_3) and electrolyzed water (EW) (Murray et al., 2017; Sheng et al., 2020). The second flume wash is followed by a soap wash to further remove the dirt and disinfectant remaining on the surfaces. Spray washing intends to use higher pressure to wash off any chemicals or bacteria further.

The industry's gold-standard sanitizer is sodium hypochlorite for apple postharvest washing. However, the free chlorine reacts with the organic matter in the wash water, reducing efficacy before reaching its target pathogen. U.S. Food and Drug Administration [FDA] (2014) indicated that the commonly used concentrations of hypochlorite (50-200 ppm) maximumly achieve 1 to 2 log reductions on many produce commodities. For example, washing at a 200-ppm concentration of chlorine for 5 min resulted in a 0.6 log reduction for *L. monocytogenes* on whole apples (Beuchat et al., 1998). Recently, potential *Listeria* contamination on fresh apples resulted in voluntary recalls in several states (U.S. Food and Drug Administration [FDA], 2017a, 2019a), suggesting the current washing protocols may not be sufficient for pathogen reduction.

Apples are dried after washing. A typical drying process often includes mild heat with blowing fans. Then, the apples are waxed with an edible coating to improve their appearance and slow down the decay of fresh apples. Before

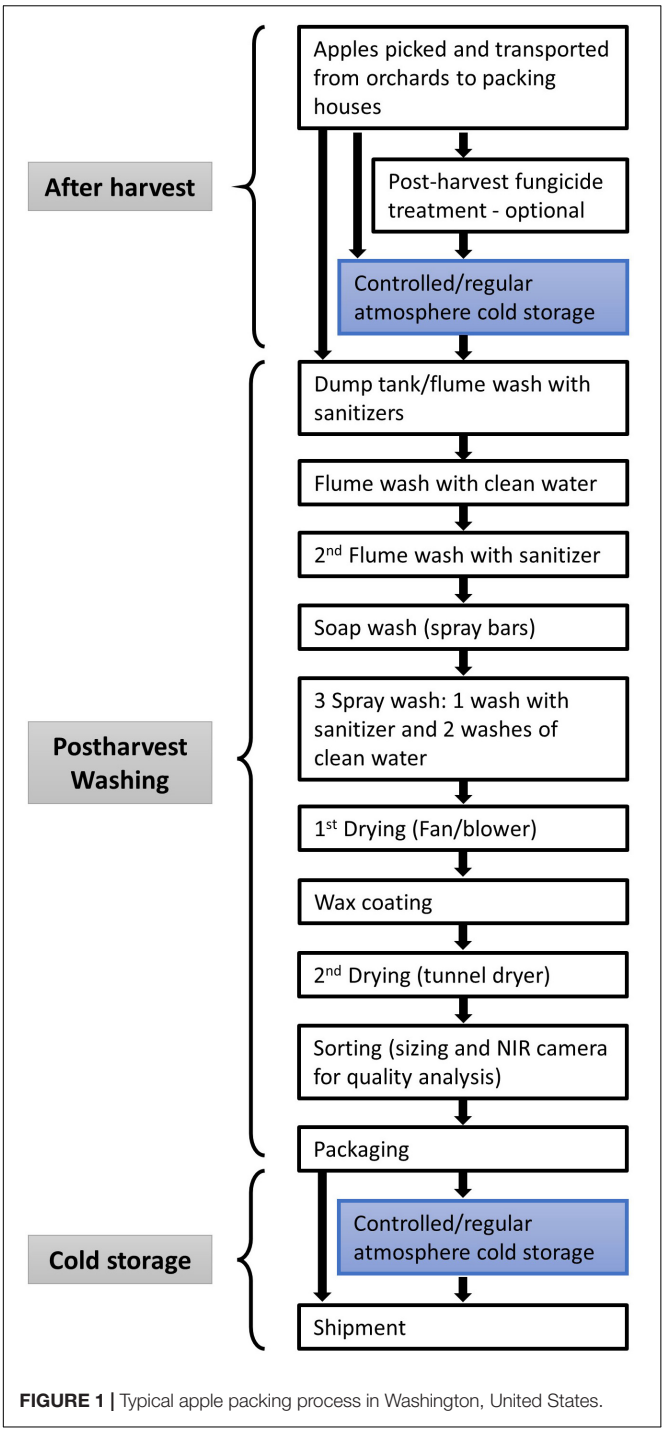

FIGURE 1 | Typical apple packing process in Washington, United States.

packaging, sizing, and near-infrared (NIR) cameras are used for quality analysis to reject the "bad" apples. After automatic packaging, apples are shipped to the retail markets with minimum storage during the distribution (Pietrysiak et al., 2019; Ruiz-Llacsahuanga et al., 2021).

The challenges on apple decontamination may be due to the naturally irregular shape and microstructures like lenticels (**Figure 2**), which shield bacteria from the sanitizing interventions (Pietrysiak and Ganjyal, 2018). Gaseous interventions like ClO_2 have the ability to reach the bacteria harbored inside the lenticels, which could improve sanitation efficacy (Rane et al., 2021). Some lab-scale studies have shown effective log reductions of *Listeria* on apples (Du et al., 2002; Park and Kang, 2017). However, scaling up the methods to fit in the industrial processing line may be challenging due to the line setup and production scale.

Cold Storage

Two steps of cold storage may take place during the apple packing process (**Figure 1**). Firstly, the freshly picked apples may be stored in cold storage before they are washed and packaged where cross-contamination may be caused by the damaged apples or happen in environmental conditions (i.e., the facility and the environment). The second storage may happen after packaging before reaching the market. Even if sanitized by washing, the packed apples would contact with bacteria from the environment inside the storage room. The CA cold storage room provides refrigerated temperature, high relative humidity, low oxygen content, circulated air that can facilitate the survival of *L. monocytogenes*.

Controlled atmosphere (CA) was developed to provide an optimum environment (typically 1-2% O_2, 1-3% CO_2, and N_2) for keeping the freshness of fresh produce and increasing the length of storage by adjustment of normal air composition (78% N_2, 21% O_2, 0.03% CO_2 and other gases). A typical CA cold storage room setup is shown in **Figure 3**. Optimal CA cold storage reduces the respiration rate and ripening of fresh apples, resulting in maintaining the quality of fruit for up to 11 or 12 months (Farber et al., 2003; Sheng et al., 2018). However, regular atmosphere (RA) or CA cold storage has been designed mainly to extend the shelf-life of fresh apples. *L. monocytogenes* may survive those storage conditions, which becomes a food safety concern. For example, from a previous study (Sheng et al., 2017), *L. monocytogenes* on Fuji apples were decreased by 0.8–1.8 Log_{10} CFU/apple after 3 months of refrigerated atmosphere (RA) storage (1, 4, and 10°C). Sheng et al. (2018) has reported that 30-week of CA cold storage led to 2.5–3.0 Log_{10} CFU/apple reduction of *L. innocua* (surrogate bacteria of *L. monocytogenes*) on Fuji apples. Limited reductions of *Listeria* were observed in both studies. Therefore, RA or CA storage alone is ineffective at controlling *Listeria* on fresh apples, and additional antimicrobial interventions are needed during long-term storage.

SAFETY GAPS DURING APPLE PACKING PROCESS

Barrera et al. (2012) reported that the actual log reduction of the target pathogen was limited to 1-2 log CFU regardless of the sanitizer or washing time applied, which indicates that the efficacy of postharvest washing is minimal. Various studies showed that the factors that limited efficacy might include pathogen attachment, biofilm formation, and internalization into the plant. Another factor is the dynamics of organic

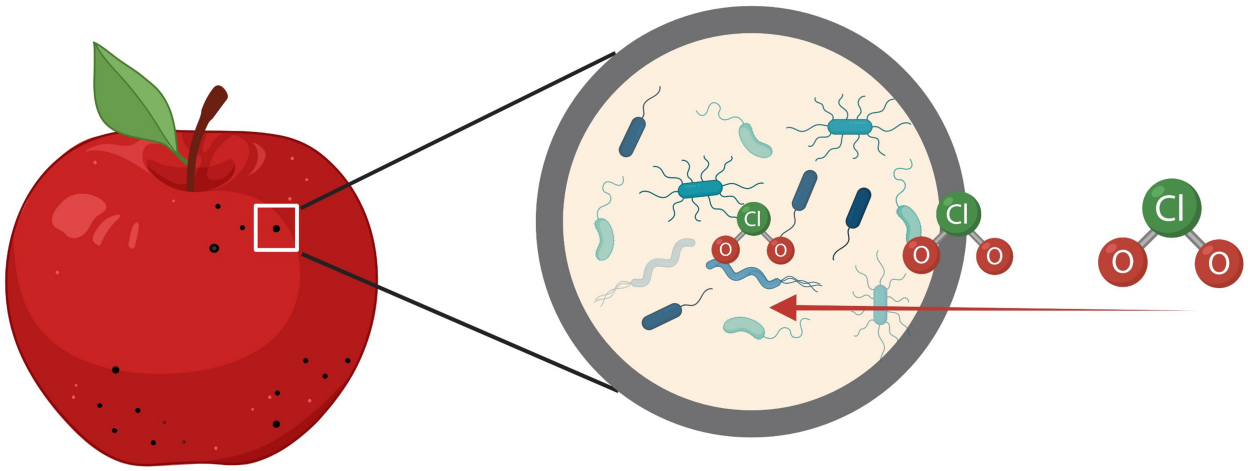

FIGURE 2 | Gaseous chlorine dioxide reaches the bacteria harbored inside the lenticels on apple surfaces.

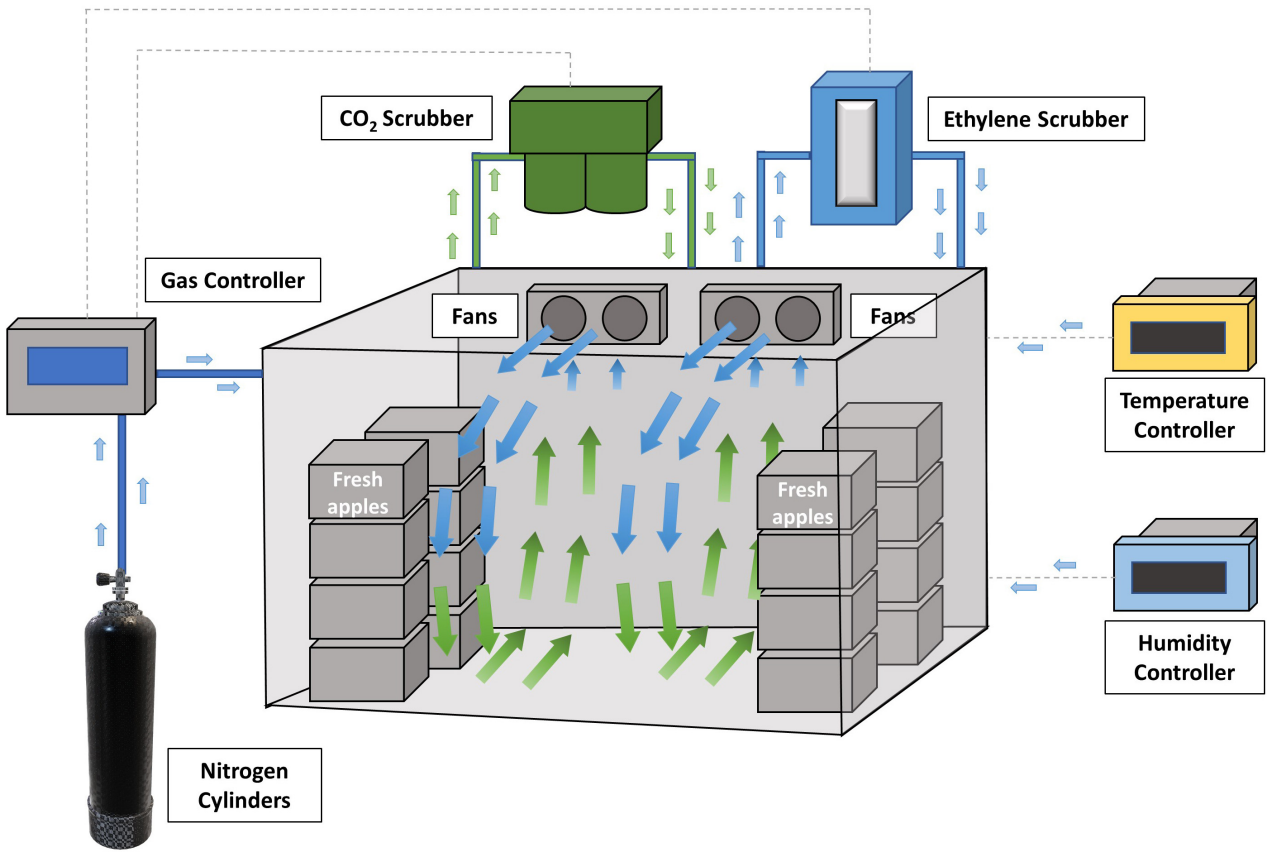

FIGURE 3 | Fresh apples are stored in a controlled atmosphere (CA) cold storage room (adopted from http://www.agroripe.com/controlled-atmosphere-storage/).

load in the washing flume, which harbors the pathogens from sanitizers and neutralizes part of the antimicrobials, especially relevant in chlorine wash (Shen et al., 2016). The research focus has transitioned from fresh produce decontamination to the prevention of cross-contamination. The concentration of active sanitizer in the wash flume, the quality of water, and organic load have been studied to improve the efficacy of washing, which is challenging in commercial validation (Gombas et al., 2017). Thus, washing itself is insufficient as part of a risk control and prevention approach. Additional or alternative interventions

need to be explored and applied to control *L. monocytogenes* in the apple packing process.

Every year, about 4.2 billion pounds of fresh apples are stored in CA cold storage (33-38°F) for up to 12 months, where apples are vulnerable to contamination with *L. monocytogenes* and spoilage microorganisms (Tree Top, 2019). Once contaminated, the apple surface is difficult to decontaminate because of its irregular shape, hydrophobic property, and presence of lenticels (Pietrysiak and Ganjyal, 2018). It is desirable to implement interventions during cold storage as preventive controls. The current existing gas systems in the CA cold storage provide an ideal environment to integrate gaseous interventions to reduce the microbial load on fresh apples. However, there are limited safety interventions implemented during CA cold storage. Furthermore, there is a knowledge gap on integrating current interventions into the CA storage system to ensure safety.

1-Methylcyclopropene (1-MCP) is a widely used inhibitor of ethylene receptors, which delays the ripening of fresh produce products. Commercial application of 1-MCP helps to reduce the ripening process, maintain quality, extend the shelf life of perishable fruits and vegetables (Menniti et al., 2006). 1-MCP can serve as a complementary strategy to CA cold storage to maintain a better quality of the fruit. Lum et al. (2017) reported that 1-MCP in combination with CA cold storage effectively controlled physiologically disordered (senescent scald and internal breakdown) in certain cultivar pear fruits. Mattheis et al. (2017) studied the impacts of 1-MCP and CA storage on the development of bitter pit (physiological disorder) in 'Honeycrisp' apples. The results indicated that the use of 1-MCP and/or CA storage can potentially manage the development of bitter pit in 'Honeycrisp' apples. Even though 1-MCP fumigation has been combined with CA storage in the apple industry, both methods are applied to preserve food quality. The control of food safety during storage is still missing. Therefore, the integration of an antimicrobial gas to the CA storage can be a potential food safety intervention during the prolonged storage of fresh apples.

POTENTIAL GASEOUS INTERVENTIONS DURING COLD STORAGE

In the fresh produce packing industry, different applications of antimicrobial interventions exist throughout the process. Several review papers have summarized various decontamination methods presented in lab-scale studies and used in the fresh produce industry (Deng et al., 2019; Gurtler et al., 2019; Pietrysiak et al., 2019; Marik et al., 2020; Singh et al., 2021; Zhang et al., 2021). Most interventions are still focused on water treatment based on chlorine or alternatives. As water itself can become a pathogen carrier and provide favorable growth conditions for the pathogen, it is well worth outlining the waterless options for the inactivation of *L. monocytogenes* on fresh produce. As one of the waterless methods, gaseous interventions have the advantages to be integrated into the CA cold storage. Potential gaseous interventions include (1) gaseous ClO_2; (2) gaseous O_3; and (3) hurdle technology that combines multiple methods. Limited studies have been conducted on gaseous interventions during CA cold storage. Potential interventions that have been applied to fresh apples are summarized in **Table 1**.

Gaseous Chlorine Dioxide (ClO_2)

Gaseous ClO_2 is a non-thermal and dry antimicrobial process that can be integrated into controlled atmosphere (CA) processes in order to extend shelf life and inactivate foodborne pathogens. There are several advantages of ClO_2 over traditional chlorine wash (current industry practice), including a higher oxidative capacity (2.5x), enhanced antimicrobial efficacy on porous surfaces, no formation of carcinogenic trichloramine, and reduced corrosion of stainless-steel processing equipment (Wu and Rioux, 2010). Moreover, its higher penetration into the harboring sites of microorganisms or irregular shape of the produce also contributes to the inactivation efficacy (Praeger et al., 2018; Deng et al., 2019).

Gaseous ClO_2 has been reported to effectively decontaminate foodborne pathogens on various fresh produce (Bridges et al., 2018; Chai et al., 2020; Lacombe et al., 2020; Guan et al., 2021). Gaseous ClO_2 has been utilized to disinfect *L. monocytogenes* and spoilage microorganisms on fresh apples on a lab scale by Du et al. (2002). This study achieved a reduction of 6.5-log CFU/spotted site *L. monocytogenes* on fresh apples (Du et al., 2002). The survival of *L. monocytogenes* on different spots, including the calyx, stem cavity, and pulp surface of apples, was also studied. *L. monocytogenes* attached to the pulp skin were concluded to be further inactivated by gaseous ClO_2. Park and Kang (2017) reported that gaseous ClO_2 could achieve a 3.5 log CFU/cm^2 reduction of *L. monocytogenes* under 20 parts per million by volume (ppmv) for 15 min. Lee et al. (2006) demonstrated that *Alicyclobacillus acidoterrestis* spores were reduced by 4.5 log CFU/apple by low release gaseous ClO_2 sachet for 3 h. Treatment with low-release ClO_2 gas sachets did not affect the visual quality of apples, whereas medium and high release sachets helped with the development of small black spots on apple skin. Sy et al. (2005) studied the decay microorganisms' survival at 4.1 mg/L gaseous ClO_2 treatment for 25 min. A 1.68-log CFU/piece reduction of total yeasts and molds was achieved. The treated apples were consistently judged slightly but significantly ($\alpha = 0.05$) poorer in appearance, color, and overall quality. But the ratings from the sensory panel did not fall below "neither like nor dislike." These findings agree with the conclusion that gaseous ClO_2 would effectively inactivate *L. monocytogenes* on fresh apples. However, it is not clear whether the apple quality was sacrificed and what ClO_2 concentrations may damage the quality.

Decay microorganisms are one of the biggest industry concerns as they cause food waste and economic losses. Gaseous ClO_2 has been reported to inactivate yeasts and molds, which may help to extend the shelf-life of apples. Application of gaseous ClO_2 on reducing decay microorganisms of jujube fruit and kiwifruit in cold storage was studied by Park et al. (2019, 2020). An obvious increase in the quality of jujube fruit was observed with a reduction of 1.1-log CFU/g of total bacteria under 50 mg/L gaseous ClO_2 at 2 ± 1°C (Park et al., 2020). Similarly, Park et al. (2019) indicated that decay incidence and growth of microorganisms were reduced, and the ripening

TABLE 1 | Gaseous food safety interventions for bacteria decontamination on fresh apples.

Interventions	Cold storage highlighted	Food commodity	Pathogen of concern	Conditions	Generation method	Sample mass	Log reduction	Impact on produce quality	References
Gaseous									
Chlorine dioxide (ClO_2)		Fresh apples	*Listeria monocytogenes*	1–8 mg/L, 10–30 min, 21°C, RH = 90–95%	ClO_2 generator	4 apples	Calyx cavity: 2.8–5.3 log CFU/spotted site; Stem catity: 2.2–5.0 log CFU/spotted site; Pulp surface: 3.5–6.5 log CFU/spotted site.	NM*	Du et al., 2002
		Fresh apples	*Escherichia coli* O157:H7	1.1–18.0mg/L, 10–30 min, 21°C, RH = 90–95%	ClO_2 generator	4 apples	Calyx cavity: 2.1–6.5 log CFU/site; Stem catity: 1.6–4.1 log CFU/site; Pulp skin: 2.8–7.3 log CFU/site.	NM	Du et al., 2003
		Fresh apples	*Salmonella*	1.4–4.1 mg/L, 6–25 min, 22 ± 1°C, RH = 35–68%	ClO_2 gas sachets	3 apples	3.21–4.21 log CFU/piece	Subjective evaluation revealed that treatment of apples with 4.1 mg/L ClO_2 gas for 25 min at 58% relative humidity caused the formation of small brown spots on the skin. The appearance of apples treated with 1.4 and 2.7 mg/L ClO_2 at 65 to 68% relative humidity was unaffected.	Sy et al., 2005
			Total yeasts and molds				1.09–1.68 log CFU/piece		
		Fresh apples	*Alicyclobacillus acidoterrestis*	0.39–6.55 mg/L peak concentration, 30 min–3 hrs, 22 ± 2°C	ClO_2 gas sachets	1 apple	2.7–5 log CFU/piece	Treatment with low-release ClO_2 gas sachets did not affect the visual quality of apples, whereas medium and high-release sachets helped develop small black spots on apple skin.	Lee et al., 2006
		Fresh apples	*Listeria monocytogenes*	20 ppmv, 5–15 min, 22 ± 2°C, RH = 90 ± 2%	ClO_2 generator	5 × 2 cm pieces	1.47–3.50 log CFU/cm^2	NM	Park and Kang, 2017
			Escherichia coli O157:H7				1.39–4.72 log CFU/cm^2		
			Salmonella Typhimurium				1.25–3.95 log CFU/cm^2		
Ozone (O_3)	Cold storage (4–6°C)	Fresh apples	Fungi	1 μl/L for 1 min every 12 hr, 84 days, 4–6°C	O_3 generator	5 kg	A larger portion of infected apples within the group of ozonated fruits.	Ozone at 1 ppm was unsuccessful in terms of inhibition of fungal disease. However, utilization of ozone slowed down the ripening of apples.	Antos et al., 2018

(Continued)

TABLE 1 | (Continued)

Interventions	Cold storage highlighted	Food commodity	Pathogen of concern	Conditions	Generation method	Sample mass	Log reduction	Impact on produce quality	References
	Cold storage (sample conditioned at 4°C)	Fresh apples	*Listeria monocytogenes*	23 ppm. 20 min, > 4°C, RH > 85% condensation on the apple surfaces	Forced air ozone reactor	NM	4.26–5.21 log CFU/apple	NM	Murray et al., 2018
	Controlled atmosphere (CA) cold storage (2% O_2, 1% CO_2, 0.6°C)	Fresh apples	*Listeria innocua*	50.0–87.0 ppb, 30 weeks, 0.6°C, RH was not actively controlled and expected to be 95% or higher	O_3 generator	120 apples	2.5–3.0 Log_{10} CFU/apple	Application of gaseous ozone in CA storage did not cause ozone burn or any other unintended side effect on apple fruit quality.	Sheng et al., 2018
			Total bacteria				~1 Log_{10} CFU/apple		
			Total yeasts & molds				~0.6 Log_{10} CFU/apple		
		Fresh apples	*Listeria monocytogenes*	77 ppm ± 2 ppm, 15min	O_3 generator	10 apples	~3 log CFU/apple	NM	Arévalo Camargo et al., 2019
	Cold storage (12–13°C)		*Lactobacillus*	5 ppm, 40 min, 12–13°C, RH = 55–57%	Forced air ozone reactor	540 kg apples	> 1.5 log CFU/apple		

**NM: not mentioned.*

process was retarded under 30 mg/L gaseous ClO_2 treatment for 30 min. Reductions of 1 log CFU/g, 1.4 log CFU/g, and 0.6 log CFU/g were achieved on total bacteria, total yeasts, and total molds of kiwifruit, respectively. These results demonstrated that gaseous ClO_2 treatment during cold storage could be a promising decontamination method to reduce microbial load on fruits and maintain the quality.

However, there is a knowledge gap between lab-scale experiments and commercial-scale applications. Predictive models can be a useful tool to bridge the gap. The target reduction of 3-log of pathogens on foods and food contact surfaces and the lab-scale experimental data can be collected to establish the models (Gombas et al., 2017). By modeling the inactivation response of *L. innocua* under different doses, the amount of gaseous ClO_2 needed in the scale-up study can be calculated via the models. The final step is to integrate gaseous ClO_2 into the commercial CA cold storage for the decontamination of the *Listeria*-inoculated apples with the predicted conditions. As a result, the fresh apple industry can use the validated models and the engineering setup to apply gaseous ClO_2 disinfection during their long-term CA storage.

Gaseous Ozone (O_3)

Gaseous O_3 is one of the most powerful oxidizers among food industrial-use sanitizers. The main advantages of O_3 are the higher efficacy at low concentration over other antimicrobial agents and no residue formation because of decomposition to oxygen. Due to its high reactive and explosive character, O_3 is unstable and can only be generated right before use. Numerous studies have demonstrated the efficacy of O_3 inactivation on *L. monocytogenes* (Murray et al., 2018; Sheng et al., 2018).

Several studies integrated gaseous O_3 into the RA or CA cold storage of fresh apples for bacteria inactivation. Murray et al. (2018) reported that 23 ppm of forced air ozone treatment for 20 min could result in 3.07 log CFU/apple reductions of *L. monocytogenes* on fresh apples taken out of the fridge at 4°C. A commercial-scale ozone treatment on fresh apples was conducted to inactivate *L. innocua* and total bacteria, yeasts, and molds during CA cold storage. *L. innocua* was reduced by 3.0 log CFU/apple under 50-87 ppb ozone treatment at 0.6°C for 30 weeks. Under the same condition, total bacteria and yeasts and molds were reduced approx. 1 and 0.6 log CFU/apple, respectively. Application of gaseous ozone in CA storage did not cause ozone burn or any other unintended side effect on apple fruit quality (Sheng et al., 2018). Another commercial-scale research was conducted by Arévalo Camargo et al. (2019). A forced-air ozone reactor was used during the cold storage of fresh apples to decontaminate *Lactobacillus*, which was selected and validated as the surrogate of *L. monocytogenes* in the same study. Two plastic vented bins containing 540 kg of apples were treated with 5 ppm ozone for 40 min, resulting in more than 1.5 log CFU/apple reductions.

Even though gaseous ozone has been applied under semi-commercial scale CA cold storage, ozone was found unstable since it decomposes fast after generation (Brodowska et al., 2018). In addition, a higher investment in equipment (generator and gas tanks) is required to set up the ozone system. As a strong oxidizer,

ozone is more corrosive, particularly on rubber, plastics, and steel (Smilanick, 2003). In the past, gaseous ozone treatments have "burned" overexposed apples during long-term storage (Antos et al., 2018). Therefore, future studies are needed to overcome the difficulties and apply gaseous ozone to control *L. monocytogenes* in CA cold storage.

Hurdle Technology

Hurdle technology combines different methods to preserve a higher quality of fresh produce for extended shelf-life or to achieve higher efficacy of bacterial decontamination to enhance food safety. Studies on the effectiveness of hurdle technology (gaseous intervention involved) against bacteria on produce are summarized in **Table 2**. Gaseous ClO_2 (50 mg/L) and sodium diacetate (200 mg/kg) were combined with CA cold storage ($0 \pm 1°C$) of fresh walnuts to control mold during 135 d of storage. CA cold storage plus ClO_2 was the optimal treatment and kept the quality of fresh walnuts for 135 d at $0 \pm 1°C$, with the lowest mold incidence (5%), the highest firmness and contents of fat and melatonin, as well as the maximum peroxidase activity (Ma et al., 2020). Park et al. (2018) reported a hurdle technology of ClO_2 with UV-C radiation to inactivate *L. monocytogenes* on spinach leaves and tomato surfaces. The combination of UVC and 10 ppmv ClO_2 were applied on 5×2 cm of samples (spinach leaves and tomatoes) for 20 min, which resulted in 4.32 log CFU/g reductions on spinach leaves and undetectable on tomato surfaces after treatment. In this study, the treatments did not significantly ($p > 0.05$) affect the color and texture of samples during storage at 7°C for 7 days. Therefore, the hurdle technology of multiple decontamination methods could potentially reduce *L. monocytogenes* in the apple packing process.

FEDERAL REGULATIONS

Food Safety Modernization Act

Ready-To-Eat (RTE) foods represent foods that are eaten without any further processing to reduce the microbiological hazards. RTE foods that have intrinsic characteristics (such as pH and water activity) can be natural or processed to prevent the growth of *L. monocytogenes*. As one of the RTE foods, apples are naturally preventing the growth of *L. monocytogenes* since the pH is less than 4.4 (U.S. Food and Drug Administration [FDA], 2017b). U.S. Food and Drug Administration [FDA] (2008) considers the adulteration of *L. monocytogenes* on a food product that contains more than 100 colony forming units (CFU) per gram of food when an RTE product does not support the growth of *L. monocytogenes* (Smith et al., 2018). Additionally, there is a zero-tolerance of *L. monocytogenes* if the RTE food supports *L. monocytogenes* growth.

Since fresh apples are considered both produce and Raw Agricultural Commodity (RAC), fresh apple packing house falls under the FDA Food Safety Modernization Act (FSMA) Final Produce Safety Rule (PSR). RAC means any food in its raw or natural state. All fruits, including fresh apples that are washed, colored, or treated in their unpeeled natural state prior to marketing, is considered as RAC (U.S. Food and Drug Administration [FDA], 2008). When a particular RAC is made into processed food, for example, irradiated papayas, the PSR applies only when the fresh papaya is a RAC before irradiation. When signed into law in 2011, FSMA highlighted the importance of preventive controls to reduce the incidence of food contamination that can lead to foodborne illness and outbreaks (U.S. Food and Drug Administration [FDA], 2011).

As a part of FSMA, PSR demonstrates the science-based requirements throughout the safe growing, harvesting, packing, and holding of produce grown for human consumption. The final rule went into effect in 2016. The rule requires the covered farms to take appropriate actions to minimize the risk of severe health consequences or death from the exposure to covered produce. It also requires the necessary prevention of the introduction of known or reasonably foreseeable hazards into the produce and providing suitable controls that save the produce from being adulterated. A Food Safety Plan (FSP), required by the FSMA Preventive Controls for Human Food (PCHF), documents a systematic approach to identify the food safety hazards that must be controlled to prevent or minimize the risk of foodborne illness. It is challenging for the produce industry to comply with the requirements since there is no "kill" step to eliminate pathogens. Therefore, identification of safety hazards and implementation of sufficient cleaning and sanitation preventive controls (i.e., safety interventions) draws great attention (U.S. Food and Drug Administration [FDA], 2016).

Residue Limits

The major ClO_2 disinfectant by-products (DBPs) of concern are chlorite (ClO^{2-}) and chlorate (ClO_3^-) ions, with no direct formation of organohalogen DBPs. Unlike the other disinfectants, the major ClO_2 DBPs are derived from the decomposition of the disinfectant as opposed to reaction with precursors (World Health Organization [WHO], 2000). The maximum contaminant level (MCL) of chlorite in drinking water, is 1.0 mg/L (U.S. Environmental Protection Agency [EPA], 2011).

In a recent study, the European Food Safety Authority investigated the presence of residues of chlorate in food and drinking water. The data showed that the chlorate exposure exceeded the tolerable daily intake has negatively impacted the iodine uptake, especially among infants and young children. In order to reduce the chlorate levels, the European Commission published new regulations of maximum residue levels for chlorate and perchlorate in foods in the summer of 2020. The maximum allowed level of chlorate on apples is 0.05 mg/kg. Perchlorate mainly affects fruits and vegetables. The maximum allowed level is 0.05 mg/kg. These new regulations highlighted the importance of monitoring chlorate and perchlorate residues after chlorine-based sanitation and reducing the concentration of disinfectant used in or on food products (European Commission [EC], 2020a,b).

Environmental Protection Agency Final Rule (EPA–HQ–OPP–2017–0063) was effective on December 26, 2018. 40 CFR Part 180 (Federal Register Number: 2018-27908) stated that "Residues of chlorate in or on tomato and cantaloupe are exempt

TABLE 2 | Hurdle technologies (gaseous intervention involved) for bacteria decontamination on produce.

Interventions	Cold storage highlighted	Food commodity	Pathogen of concern	Conditions	Generation method	Sample mass	Log reduction	Impact on produce quality	References
Hurdle technology									
Gaseous ozone (O_3) and hot water		Cantaloupe melon	Mesophilic bacteria	Water (75°C) + air dry (15 min) + O_3 (10,000 ppm, 30 min, 11°C, RH = 90–95%)	O_3 generator	6 whole melons	3.8 log CFU/g	No evidence of damage in melons treated with hot water, ozone, or their combination and they maintained initial texture and aroma.	Selma et al., 2008
			Psychrotrophic bacteria				5.1 log CFU/g		
			Molds				2.2 log CFU/g		
			Coliforms				2.3 log CFU/g		
Chlorine dioxide gas (ClO_2) and aerosolized peracetic acid (PAA)		Spinach leaves	*Escherichia coli* O157:H7	80 ppm PAA + 5/10 ppmv ClO_2, 5–20 min, 22 ± 2°C, RH = 90 ± 2%	ClO_2 generator + a commercial ultrasonic nebulizer	5 × 3 cm in size	0.9–5.4 log CFU/g	Combined treatment of ClO_2 gas (10 ppmv) and aerosolized PAA (80 ppm) did not significantly ($p > 0.05$) affect the color and texture of samples during 7 days of storage.	Park and Kang, 2015
			Salmonella Typhimurium				0.8–5.1 log CFU/g		
			Listeria monocytogenes				0.3–4.1 log CFU/g		
		Tomatoes	*Escherichia coli* O157:H7			5 × 2 cm pieces	1.0–5.1 log CFU/g		
			Salmonella Typhimurium				0.9–5.2 log CFU/g		
			Listeria monocytogenes				0.4–4.5 log CFU/g		
ClO_2 gas and freezing		Blueberry	Mesophilic aerobic bacteria (MAB)	ClO_2 gas (4 mg/L, 12 h, 12–14°C) + processing + freezing (-20°C quick, intermediate, slow)	ClO_2 sachet	16 lugs of blueberries (~9.1 kg/lug)	2 log CFU/g	ClO_2 gassing followed by quick freezing effectively meets the current microbiological standards being imposed by buyers of frozen blueberries.	Zhang et al., 2015
			Yeasts and molds				1 log CFU/g		
ClO_2 gas, ultraviolet-C (UV-C) light, and fumaric acid		Plum	*Escherichia coli* O157:H7	15–30 ppmv ClO_2 gas, 0.5% fumaric acid, and 10 kJ/m^2 UV-C, 5–20 min, RH = 80%	ClO_2 gas generator + UV germicidal lamps	20 ± 0.3 g	4.37–5.48 log CFU/g	The optimal treatment condition does not affect the quality of plum samples.	Kim and Song, 2017
			Listeria monocytogenes				5.36–6.26 log CFU/g		

(Continued)

TABLE 2 | (Continued)

Interventions	Cold storage highlighted	Food commodity	Pathogen of concern	Conditions	Generation method	Sample mass	Log reduction	Impact on produce quality	References
ClO_2 gas with UV-C radiation		Spinach leaves	*Listeria monocytogenes*	UVC + 10 ppmv ClO_2 gas, 20 min, 22 ± 1°C, RH = 90 ± 2%	ClO_2 generator + UV lamp	5 × 2 cm in size	4.32 ± 0.52 log CFU/g	Did not significantly ($p > 0.05$) affect the color and texture of samples during storage at 7°C for 7 days.	Park et al., 2018
		Tomato surfaces				5 × 2 cm pieces	Not Detectable (ND)		
UV + gaseous O_3 + hydrogen peroxide		Fresh apples	*Listeria monocytogenes*	UV-C light (54-mJ cm^2 dose), 6% (v/v) hydrogen peroxide, 2 g/h ozone, 30–120 s, 48°C, RH > 85%	UV-C lamps + ozone-emitting lamps + vaporizimg unit	3 apples	3 log CFU/apple	NM*	Murray et al., 2018
Gaseous ClO_2 + an edible coating	Cold storage (6°C)	Cantaloupe	*Salmonella*	Gaseous ClO_2 (5 mg/L, 4.5 h, 6°C, RH = 75%) + NatureSeal edible coating (NS) + cold storage (4°C)	ClO_2 generator	10 whole cantaloupes	Negative for *Salmonella* after 21 days of storage (detection limit = 2 CFU/g)	For the sensory quality parameters analyzed (color, water loss, and texture), the samples treated with NatureSeal had significantly better quality ($p > 0.05$) than did the control samples.	Alicea et al., 2018
Gaseous ClO_2 + cold storage	Cold storage (2°C)	Kiwifruit	Total bacteria	ClO_2 (30 mg/L, 30 min, RH = 75–80%) + 2 ± 1°C	ClO_2 generator	270 fruits	1 log CFU/g	Decay incidence and growth of microorganisms reduced, and the ripening process retarded.	Park et al., 2019
			Total yeasts				1.4 log CFU/g		
			Total molds				0.6 log CFU/g		
Gaseous O_3 + UV-C		Persimmon fruits	Fungi	O_3 (9.81 mg/m^3, 1–24) + UV-C (24 cm, 0.5 h)	Activated oxygen generator	6 fruits	99.58–100% killing rate	This non-thermal sterilization could alleviate astringency but hadn't significant effects on other properties, including color, moisture content, water activity, and protopectin.	Chen et al., 2020
Gaseous ClO_2 + cold storage	Cold storage (2°C)	Jujube fruit	Total bacteria	10, 30, 50 mg/L, 2 ± 1°C, RH = 80%	ClO_2 generator	5 kg (35 fruits per sample)	1.1 log CFU/g	An obvious increase in quality.	Park et al., 2020
			Total yeasts and molds				Significantly reduced		

(Continued)

TABLE 2 | (Continued)

Interventions	Cold storage highlighted	Food commodity	Pathogen of concern	Conditions	Generation method	Sample mass	Log reduction	Impact on produce quality	References
Gaseous ClO_2 and sodium diacetate (SDA)	Controlled atmosphere (CA) cold storage (2% O_2 + 25% CO_2, 0°C)	Fresh walnuts	Mold	CA + 50 mg/L ClO_2, 0 ± 1°C, 135 d, RH = 70–80%	ClO_2 powder + water	200 fresh nuts	Mold in the CA + SDA, and CA + ClO_2 treatments were not detected until day 135	CA + ClO_2 was the optimal treatment and kept the quality of fresh walnuts for 135 d at 0 ± 1°C, with the lowest mold incidence (5%), the highest firmness, and contents of fat and melatonin, as well as the maximum POD activity.	Ma et al., 2020
				CA + 200 mg/kg SDA, 0 ± 1°C, 135 d, RH = 70–80%	Directly purchased				
Gaseous ClO_2 + moisture + mild heat		Almond	*Salmonella*	ClO_2 (20-g precursor dose) + moisture content (7%) + mild heat (40 ± 1.5°C), 1–4 h	ClO_2 sachet	400 g	2.0 log CFU/g	No visual damages were observed on almonds post-treatment	Rane et al., 2021
			Enterococcus faecium NRRL B-2354				1.6 log CFU/g		
Gaseous O_3 + ultrasonic-assisted aerosolization sanitizer		Lettuce	*Escherichia coli* O157:H7	Gaseous O_3 (4 and 8 ppm, 3 min) + sodium hypochlorite (SH, 100 and 200 ppm)/acetic acid (AA, 1% and 2%)/lactic acid (LA, 1% and 2%)	Ozone generator + ultrasonic-assisted nebulizer	10 g	0.7 log CFU/g	Quality analysis indicates that LA + 8 ppm ozone and SH + 8 ppm ozone did not negatively affect color, polyphenolic content, weight loss, and sensory properties; however, the levels of two individual phenolic responsible for phenylpropanoid synthesis were significantly increased after treatment with 2% LA + 8 ppm ozone.	Wang et al., 2021
			Salmonella Typhimurium				0.75–1.28 log CFU/g		
			Listeria monocytogenes				0.58 log CFU/g		
Gaseous ClO_2 + 1-methylcicloropropene (1-MCP)	Cold storage (4°C)	Sweet cherry	Fungi	ClO_2 (30 μL/L) + 1-MCP (1 μL/L), 24 h, 4°C	Release from solid ClO_2 + release from 1-MCP powder formulation	4 kg	11.7% decay incidence (more than 38.9% decrease)	Better improve the postharvest quality of sweet cherry fruit.	Zhao et al., 2021

**NM: not mentioned.*

from the requirement of a tolerance when resulting from the application of gaseous chlorine dioxide as a fungicide, bactericide, and antimicrobial pesticide," which allows for the expanded use of gaseous ClO_2 on fresh produce. Other food commodities might be exempted with more data and scientific support in the future (U.S. Environmental Protection Agency [EPA], 2018).

Organic Production and Handling

The U.S. Department of Agriculture (USDA) has established a National Organic Program (NOP) rule to enforce organic production and handling requirements. The NOP provides the guidance of "The Use of Chlorine Materials in Organic Production and Handling" to state that approved chlorine materials may be utilized in direct contact with organic production according to label directions. Allowed chlorine materials in organic production are calcium hypochlorite, ClO_2, and sodium hypochlorite. Chlorine use must be immediately followed by a rinse sufficient to reduce chlorine levels on the product to potable water levels at the maximum residual disinfectant level of 4 mg/L for chlorine (as Cl_2) and 0.8 mg/L for ClO_2, which is currently established by the Environmental Protection Agency (EPA) at 40 CFR § § 141.2, 141.65 (U.S. Department of Agriculture [USDA], 2011; U.S. Environmental Protection Agency [EPA], 2011).

However, ClO_2 is currently allowed for use in liquid solution in crop production as a preharvest algicide, disinfectant, and sanitizer, including in irrigation system cleaning systems (7 CFR § 205.601(a)(2)(ii)); in organic livestock production for use in disinfecting and sanitizing facilities and equipment (7 CFR § 205.603 (a)(7)(ii)); and in organic handling for disinfecting and sanitizing food contact surfaces (7 CFR § 205.605(b)). For these uses, residual chlorine levels in the water cannot exceed the maximum residual disinfectant limit under the Safe Water Drinking Act. A petition was submitted to NOP to extend the use of ClO_2 in gaseous form for the antimicrobial treatment of products labeled "organic" or "made with organic [specified ingredients or food group(s)]" in 2015. This petition was transmitted to National Organic Standards Board (NOSB) in U.S. Department of Agriculture [USDA] (2018).

The current regulation status indicates that ClO_2 in its liquid form under the guidance has been considered organic production, whereas in its gaseous form has not yet been approved. More studies on gaseous ClO_2 and the demand for higher efficacy sanitation from the food industry may facilitate the approval of the petition.

O_3, as one of the approved chemicals for use in organic postharvest systems, is considered GRAS (Generally Recognized as Safe) for produce and equipment disinfection. Exposure limits for worker safety apply (U.S. Department of Agriculture [USDA], 2011). The Occupational Safety and Health Administration (OSHA) regulates employee exposure to O_3 gas through its Air Contaminants Standard, 29 CFR 1910.1000. The permissible exposure limit (PEL) is an 8-h, time-weighted average value of 0.1 part of O_3 per million parts of air (ppm) (Occupational Safety and Health Administration [OSHA], 1994).

CONCLUSION

During the postharvest packing process, a heat-based lethal treatment cannot be applied to fresh produce like apples. As a persistent and pathogenic microorganism, *L. monocytogenes* has caused high risk contamination in fresh produce packing facilities in previous outbreaks. The current packing process mostly relies on postharvest washing has been reported to be insufficient for produce decontamination. Additionally, the long-term CA cold storage of fresh apples provides optimal conditions for *Listeria* growth and persistence. Therefore, potential safety interventions to inactivate *L. monocytogenes* during cold storage are in great need.

Waterless safety intervention and hurdle technology can be future directions to help improve the apple decontamination efficiency. Water treatment has brought numerous problems like reacting with organic loads, cross-contamination, and abundant water usage. In comparison, waterless treatments may avoid the problems and increase the effectiveness of the antimicrobials. However, waterless interventions might have different problems like residue allowance, workers' safety concerns, etc. The related regulations are still undergoing review. Both water and waterless treatments lack methodological standards, making it hard to compare data from different studies.

The integration of gaseous ClO_2 into industrial CA cold storage offers critical food safety benefits for fresh apples by reducing the risk of pathogen contamination during storage. But it is necessary to ensure that ClO_2 does not induce any lenticel breakdown nor bitter pit symptoms. Since the lenticels can harbor bacteria, thus protecting them from antimicrobial interventions, the gas interventions should inactivate pathogens without causing tissue damage. The overall fruit quality after gaseous ClO_2 treatment needs to be inspected for any negative impact. Dry media generation of ClO_2 avoids overdosing through control-released technology. However, there is a lack of knowledge with regards to the optimum initial dose to prevent any damage to the fruits. In addition, recent studies have concluded that a slow controlled release of ClO_2 using dry precursors resulted in undetectable amounts of chlorate and chlorite residues (Smith and Scapanski, 2020). The lack of chemical residue is very important in order to maintain industry standards. The new commercial-scale integration system could augment GMP safety plans by reinforcing critical control points that rely heavily on postharvest washing. Apple growers and processors can use this in a storage decontamination step as part of the hurdle technology safety plans, helping to secure food safety and reduce food waste and economic losses. Therefore, gaseous ClO_2 integrated into CA cold storage of fresh apples can potentially control *L. monocytogenes*.

Significant research is still greatly needed to develop effective methods to reduce microbial loads on fresh apples. Critical aspects, including surface characteristics of apples, commercial-scale validation of the intervention, intervention implementation/integration to the current existing apple packing process, and the impact of the interventions on final apple quality, should be taken into consideration.

AUTHOR CONTRIBUTIONS

JG contributed to the conceptualization and design, reviewed the literature, prepared the figures and tables, and wrote the original draft of the manuscript. AL contributed to the conceptualization and design, and wrote, reviewed, and edited the manuscript. BR and SS wrote, reviewed, and edited the manuscript. JT supervised the data and wrote, reviewed, and edited the manuscript. VW contributed to the conceptualization, supervised the data, carried out the project administration, funding acquisition, and resources, and wrote, reviewed, and edited the manuscript. All authors contributed to the article and approved the submitted version.

FUNDING

This work was supported by the United States Department of Agriculture National Institute of Food and Agriculture (USDA NIFA) Grant (grant number 2015-69003-32075).

REFERENCES

Alicea, C., Annous, B. A., Mendez, D. P., Burke, A., and Orellana, L. E. (2018). Evaluation of hot water, gaseous chlorine dioxide, and chlorine treatments in combination with an edible coating for enhancing safety, quality, and shelf life of fresh-cut cantaloupes. *J. Food Protect.* 81, 534–541. doi: 10.4315/0362-028X.JFP-17-392

Angelo, K. M., Conrad, A. R., Saupe, A., Dragoo, H., West, N., Sorenson, A., et al. (2017). Multistate outbreak of *Listeria monocytogenes* infections linked to whole apples used in commercially produced, prepackaged caramel apples: United States, 2014-2015. *Epidemiol. Infect.* 145, 848–856. doi: 10.1017/S0950268816003083

Antos, P., Piechowicz, B., Gorzelany, J., Matłok, N., Migut, D., Józefczyk, R., et al. (2018). Effect of ozone on fruit quality and fungicide residue degradation in apples during cold storage. *Ozone Sci. Eng.* 40, 482–486. doi: 10.1080/01919512.2018.1471389

Arévalo Camargo, J., Murray, K., Warriner, K., and Lubitz, W. (2019). Characterization of efficacy and flow in a commercial scale forced air ozone reactor for decontamination of apples. *Lwt* 113:108325. doi: 10.1016/j.lwt.2019.108325

Artés, F., Gómez, P., Aguayo, E., Escalona, V., and Artés-Hernández, F. (2009). Sustainable sanitation techniques for keeping quality and safety of fresh-cut plant commodities. *Post. Biol. Technol.* 51, 287–296. doi: 10.1016/j.postharvbio.2008.10.003

Barrera, M. J., Blenkinsop, R., and Warriner, K. (2012). The effect of different processing parameters on the efficacy of commercial postharvest washing of minimally processed spinach and shredded lettuce. *Food Control* 25, 745–751. doi: 10.1016/j.foodcont.2011.12.013

Beuchat, L. R., Nail, B. V., Adler, B. B., and Clavero, M. R. S. (1998). Efficacy of spray application of chlorinated water in killing pathogenic bacteria on raw apples, tomatoes, and lettuce. *J. Food Protect.* 61, 1305–1311. doi: 10.4315/0362-028X-61.10.1305

Bridges, D. F., Rane, B., and Wu, V. C. H. (2018). The effectiveness of closed-circulation gaseous chlorine dioxide or ozone treatment against bacterial pathogens on produce. *Food Control* 91, 261–267. doi: 10.1016/j.foodcont.2018.04.004

Brodowska, A. J., Nowak, A., and Śmigielski, K. (2018). Ozone in the food industry: principles of ozone treatment, mechanisms of action, and applications: an overview. *Crit. Rev. Food Sci. Nutr.* 58, 2176–2201. doi: 10.1080/10408398.2017.1308313

Buchanan, R. L., and Phillips, J. G. (1990). Response surface model for predicting the effects of temperature pH, sodium chloride content, sodium nitrite concentration and atmosphere on the growth of *Listeria monocytogenes*. *J. Food Protect.* 53, 370–376. doi: 10.4315/0362-028x-53.5.370

Chai, H. E., Hwang, C. A., Huang, L., Wu, V. C. H., and Sheen, L. Y. (2020). Feasibility and efficacy of using gaseous chlorine dioxide generated by sodium chlorite-acid reaction for decontamination of foodborne pathogens on produce. *Food Control* 108:106839. doi: 10.1016/j.foodcont.2019.106839

Chen, X., Liu, B., Chen, Q., Liu, Y., and Duan, X. (2020). Application of combining ozone and UV-C sterilizations in the artificial drying of persimmon fruits. *Lwt* 134:110205. doi: 10.1016/j.lwt.2020.110205

Connell, G. (1996). *The Chlorination/Chloramination Handbook*. Denver, CO: American Water Works Association.

Deng, L. Z., Mujumdar, A. S., Pan, Z., Vidyarthi, S. K., Xu, J., Zielinska, M., et al. (2019). Emerging chemical and physical disinfection technologies of fruits and vegetables: a comprehensive review. *Crit. Rev. Food Sci. Nutr.* 60, 2481–2508. doi: 10.1080/10408398.2019.1649633

Du, J., Han, Y., and Linton, R. H. (2002). Inactivation by chlorine dioxide gas (ClO_2) of *Listeria monocytogenes* spotted onto different apple surfaces. *Food Microbiol.* 19, 481–490. doi: 10.1006/fmic.2002.0501

Du, J., Han, Y., and Linton, R. H. (2003). Efficacy of chlorine dioxide gas in reducing *Escherichia coli* O157:H7 on apple surfaces. *Food Microbiol.* 20, 583–591. doi: 10.1016/S0740-0020(02)00129-6

Dygico, L. K., Gahan, C. G. M., Grogan, H., and Burgess, C. M. (2020). The ability of *Listeria monocytogenes* to form biofilm on surfaces relevant to the mushroom production environment. *Int. J. Food Microbiol.* 317:108385. doi: 10.1016/j.ijfoodmicro.2019.108385

European Commission [EC] (2020a). *Maximum Levels of Perchlorate in Certain Foods*. Available online at: https://eur-lex.europa.eu/legal-content/EN/TXT/PDF/?uri=CELEX:32020R0685&qid=1591624227155&from=EN (accessed 24 July 2021).

European Commission [EC] (2020b). *Maximum Residue Levels for Chlorate in or on Certain Products*. Available online at: https://eur-lex.europa.eu/legal-content/EN/TXT/PDF/?uri=CELEX:32020R0749&rid=1 (accessed 24 July 2021).

Farber, J. M., and Peterkin, P. I. (1991). *Listeria monocytogenes*, a foodborne pathogen. *Microbiol. Rev.* 55, 476–511.

Farber, J. N., Harris, L. J., Parish, M. E., Beuchat, L. R., Suslow, T. V., Gorney, J. R., et al. (2003). Microbiological safety of controlled and modified atmosphere packaging of fresh and fresh-cut produce. *Compreh. Rev. Food Sci. Food Safety* 2, 142–160. doi: 10.1111/j.1541-4337.2003.tb00032.x

Galié, S., García-Gutiérrez, C., Miguélez, E. M., Villar, C. J., and Lombó, F. (2018). Biofilms in the food industry: health aspects and control methods. *Front. Microbiol.* 9:898. doi: 10.3389/fmicb.2018.00898

Gombas, D., Luo, Y., Brennan, J., Shergill, G., Petran, R., Walsh, R., et al. (2017). Guidelines to validate control of cross-contamination during washing of fresh-cut leafy vegetables. *J. Food Protect.* 80, 312–330. doi: 10.4315/0362-028X.JFP-16-258

Guan, J., Lacombe, A., Tang, J., Bridges, D. F., Sablani, S., Rane, B., et al. (2021). Use of mathematic models to describe the microbial inactivation on baby carrots by gaseous chlorine dioxide. *Food Control* 123:107832. doi: 10.1016/j.foodcont.2020.107832

Gurtler, J. B., Fan, X., Jin, T., and Niemira, B. A. (2019). Influence of antimicrobial agents on the thermal sensitivity of foodborne pathogens: a review. *J. Food Protect.* 82, 628–644. doi: 10.4315/0362-028X.JFP-18-441

Hua, Z., Korany, A. M., El-Shinawy, S. H., and Zhu, M.-J. (2019). Comparative evaluation of different sanitizers against *Listeria monocytogenes* biofilms on major food-contact surfaces. *Front. Microbiol.* 10:2462. doi: 10.3389/fmicb.2019.02462

Kim, H. G., and Song, K. (2017). Combined treatment with chlorine dioxide gas, fumaric acid, and ultraviolet-C light for inactivating *Escherichia coli* O157:H7 and *Listeria monocytogenes* inoculated on plums. *Food Control* 71, 371–375. doi: 10.1016/j.foodcont.2016.07.022

Lacombe, A., Antosch, J. G., and Wu, V. C. H. (2020). Scale-up model of forced air-integrated gaseous chlorine dioxide for the decontamination of lowbush blueberries. *J. Food Safety* 40:e12793. doi: 10.1111/jfs.12793

Lee, S. Y., Dancer, G. I, Chang, S., Rhee, M. S., and Kang, D. H. (2006). Efficacy of chlorine dioxide gas against *Alicyclobacillus acidoterrestris* spores on apple surfaces. *Int. J. Food Microbiol.* 108, 364–368. doi: 10.1016/j.ijfoodmicro.2005.11.023

Leong, D., NicAogáin, K., Luque-Sastre, L., McManamon, O., Hunt, K., Alvarez-Ordóñez, A., et al. (2017). A 3-year multi-food study of the presence and persistence of *Listeria monocytogenes* in 54 small food businesses in Ireland. *Int. J. Food Microbiol.* 249, 18–26. doi: 10.1016/j.ijfoodmicro.2017.02.015

Lum, G. B., DeEll, J. R., Hoover, G. J., Subedi, S., Shelp, B. J., and Bozzo, G. G. (2017). 1-Methylcylopropene and controlled atmosphere modulate oxidative stress metabolism and reduce senescence-related disorders in stored pear fruit. *Postharvest Biol. Technol.* 129, 52–63. doi: 10.1016/j.postharvbio.2017.03.008

Ma, Y., Li, P., Watkins, C. B., Ye, N., Jing, N., Ma, H., et al. (2020). Chlorine dioxide and sodium diacetate treatments in controlled atmospheres retard mold incidence and maintain quality of fresh walnuts during cold storage. *Postharvest Biol. Technol.* 161:11063. doi: 10.1016/j.postharvbio.2019.111063

Marik, C. M., Zuchel, J., Schaffner, D. W., and Strawn, L. K. (2020). Growth and survival of *Listeria monocytogenes* on intact fruit and vegetable surfaces during postharvest handling: a systematic literature review. *J. Food Protect.* 83, 108–128. doi: 10.4315/0362-028X.JFP-19-283

Matereke, L. T., and Okoh, A. I. (2020). *Listeria monocytogenes* virulence, antimicrobial resistance and environmental persistence: a review. *Pathogens* 9:528. doi: 10.3390/pathogens9070528

Mattheis, J. P., Rudell, D. R., and Hanrahan, I. (2017). Impacts of 1-methylcyclopropene and controlled atmosphere established during conditioning on development of bitter pit in 'Honeycrisp' apples. *HortScience* 52, 132–137. doi: 10.21273/HORTSCI11368-16

Menniti, A. M., Donati, I., and Gregori, R. (2006). Responses of 1-MCP application in plums stored under air and controlled atmospheres. *Postharvest Biol. Technol.* 39, 243–246. doi: 10.1016/j.postharvbio.2005.11.007

Murray, K., Moyer, P., Wu, F., Goyette, J. B., and Warriner, K. (2018). Inactivation of *Listeria monocytogenes* on and within apples destined for caramel apple production by using sequential forced air ozone gas followed by a continuous advanced oxidative process treatment. *J. Food Protect.* 81, 357–364. doi: 10.4315/0362-028X.JFP-17-306

Murray, K., Wu, F., Shi, J., Jun Xue, S., and Warriner, K. (2017). Challenges in the microbiological food safety of fresh produce: limitations of postharvest washing and the need for alternative interventions. *Food Qual. Safety* 1, 289–301. doi: 10.1093/fqsafe/fyx027

Neunlist, M. R., Federighi, M., Laroche, M., Sohier, D., Delattre, G., Jacquet, C., et al. (2005). Cellular lipid fatty acid pattern heterogeneity between reference and recent food isolates of *Listeria monocytogenes* as a response to cold stress. *Antonie Leeuwenhoek* 88, 199–206. doi: 10.1007/s10482-005-5412-7

Occupational Safety and Health Administration [OSHA]. (1994). *Occupational Safety and Health Administration's (OSHA) Regulations for Ozone*. Available online at: https://www.osha.gov/laws-regs/standardinterpretations/1994-09-29-0 (accessed 25 July 2021).

Park, H., Han, N., Kim, C. W., and Lee, U. (2019). Chlorine dioxide gas treatment improves the quality of hardy kiwifruit (*Actinidia arguta*) during storage. *For. Sci. Technol.* 15, 159–164. doi: 10.1080/21580103.2019.1636414

Park, H., Kim, C. W., Han, N., Jeong, M., and Lee, U. (2020). Gaseous chlorine dioxide treatment suppresses decay and microbial growth in cold-stored jujube fruit. *Hortic. Sci. Technol.* 38, 860–869. doi: 10.7235/HORT.20200078

Park, S. H., and Kang, D. H. (2015). Combination treatment of chlorine dioxide gas and aerosolized sanitizer for inactivating foodborne pathogens on spinach leaves and tomatoes. *Int. J. Food Microbiol.* 207, 103–108. doi: 10.1016/j.ijfoodmicro.2015.04.044

Park, S. H., and Kang, D. H. (2017). Influence of surface properties of produce and food contact surfaces on the efficacy of chlorine dioxide gas for the inactivation of foodborne pathogens. *Food Control* 81, 88–95. doi: 10.1016/j.foodcont.2017.05.015

Park, S. H., Kang, J. W., and Kang, D. H. (2018). Inactivation of foodborne pathogens on fresh produce by combined treatment with UV-C radiation and chlorine dioxide gas, and mechanisms of synergistic inactivation. *Food Control* 92, 331–340. doi: 10.1016/j.foodcont.2018.04.059

Pietrysiak, E., and Ganjyal, G. M. (2018). Apple peel morphology and attachment of *Listeria innocua* through aqueous environment as shown by scanning electron microscopy. *Food Control* 92, 362–369. doi: 10.1016/j.foodcont.2018.04.049

Pietrysiak, E., Smith, S., and Ganjyal, G. M. (2019). Food safety interventions to control *Listeria monocytogenes* in the fresh apple packing industry: a review. *Compreh. Rev. Food Sci. Food Safety* 18, 1705–1726. doi: 10.1111/1541-4337.12496

Praeger, U., Herppich, W. B., and Hassenberg, K. (2018). Aqueous chlorine dioxide treatment of horticultural produce: effects on microbial safety and produce quality–A review. *Crit. Rev. Food Sci. Nutr.* 58, 318–333. doi: 10.1080/10408398.2016.1169157

Rane, B., Lacombe, A., Sablani, S., Bridges, D. F., Tang, J., Guan, J., et al. (2021). Effects of moisture content and mild heat on the ability of gaseous chlorine dioxide against *Salmonella* and *Enterococcus faecium* NRRL B-2354 on almonds. *Food Control* 123:107732. doi: 10.1016/j.foodcont.2020.107732

Rodgers, S. L., Cash, J. N., Siddiq, M., and Ryser, E. T. (2004). A comparison of different chemical sanitizers for inactivating *Escherichia coli* O157:H7 and *Listeria monocytogenes* in solution and on apples, lettuce, strawberries, and cantaloupe. *J. Food Protect.* 67, 721–731. doi: 10.4315/0362-028X-67.4.721

Ruiz-Llacsahuanga, B., Hamilton, A., Zaches, R., Hanrahan, I., and Critzera, F. (2021). Prevalence of *Listeria* species on food contact surfaces in Washington State Apple Packinghouses. *Appl. Environ. Microbiol.* 87:e02932-20. doi: 10.1128/AEM.02932-20

Selma, M. V., Ibáñez, A. M., Allende, A., Cantwell, M., and Suslow, T. (2008). Effect of gaseous ozone and hot water on microbial and sensory quality of cantaloupe and potential transference of *Escherichia coli* O157:H7 during cutting. *Food Microbiol.* 25, 162–168. doi: 10.1016/j.fm.2007.06.003

Shen, C., Norris, P., Williams, O., Hagan, S., and Li, K. W. (2016). Generation of chlorine by-products in simulated wash water. *Food Chem.* 190, 97–102. doi: 10.1016/j.foodchem.2015.04.146

Sheng, L., Edwards, K., Tsai, H. C., Hanrahan, I., and Zhu, M. J. (2017). Fate of *Listeria monocytogenes* on fresh apples under different storage temperatures. *Front. Microbiol.* 8:1396. doi: 10.3389/fmicb.2017.01396

Sheng, L., Hanrahan, I., Sun, X., Taylor, M. H., Mendoza, M., and Zhu, M. J. (2018). Survival of *Listeria innocua* on Fuji apples under commercial cold storage with or without low dose continuous ozone gaseous. *Food Microbiol.* 76, 21–28. doi: 10.1016/j.fm.2018.04.006

Sheng, L., Shen, X., and Zhu, M. J. (2020). Screening of non-pathogenic surrogates of *Listeria monocytogenes* applicable for chemical antimicrobial interventions of fresh apples. *Food Control* 110:106977. doi: 10.1016/j.foodcont.2019.106977

Singh, S., Maji, P. K., Lee, Y. S., and Gaikwad, K. K. (2021). Applications of gaseous chlorine dioxide for antimicrobial food packaging: a review. *Environ. Chem. Lett.* 19, 253–270. doi: 10.1007/s10311-020-01085-8

Smilanick, J. L. (2003). "Use of ozone in storage and packing facilities," in *Proceedings of the Washington Tree Fruit Postharvest Conference*, Wenatche, WA, 1–10.

Smith, A., Moorhouse, E., Monaghan, J., Taylor, C., and Singleton, I. (2018). Sources and survival of *Listeria monocytogenes* on fresh, leafy produce. *J. Appl. Microbiol.* 125, 930–942. doi: 10.1111/jam.14025

Smith, D. J., and Scapanski, A. (2020). Distribution and chemical Fate of [36Cl]chlorine dioxide gas on avocados, eggs, onions, and sweet potatoes. *J. Agric. Food Chem.* 68, 5000–5008. doi: 10.1021/acs.jafc.0c01466

Sun, X., Baldwin, E., and Bai, J. (2019). Applications of gaseous chlorine dioxide on postharvest handling and storage of fruits and vegetables–A review. *Food Control* 95, 18–26.

Sy, K. V., McWatters, K. H., and Beuchat, L. R. (2005). Efficacy of gaseous chlorine dioxide as a sanitizer for killing *Salmonella*, yeasts, and molds on blueberries, strawberries, and raspberries. *J. Food Protect.* 68, 1165–1175. doi: 10.4315/0362-028X-68.6.1165

Tree Top (2019). *U.S. Apple Crop Forecast 2019/20*. Available online at: https://foodingredients.treetop.com/fruit-ingredients-blog/Post/U.S.-Apple-Crop-Forecast-2019-2020/ (accessed 25 July 2021).

U.S. Apple Association [USApple] (2021). *Industry at A Glance*. Available online at: https://usapple.org/industry-at-a-glance (accessed August 05, 2021).

U.S. Centers for Disease Control and Prevention [CDC] (2011). *Multistate Outbreak of Listeriosis Linked to Whole Cantaloupes from Jensen Farms, Colorado (FINAL UPDATE)*. Available online at: https://www.cdc.gov/listeria/outbreaks/cantaloupes-jensen-farms/index.html (accessed 25 July 2021).

U.S. Centers for Disease Control and Prevention [CDC] (2014). *Multistate Outbreak of Listeriosis Linked to Commercially Produced, Prepackaged Caramel Apples Made from Bidart Bros. Apples (Final Update)*. Available online at: https://www.cdc.gov/listeria/outbreaks/caramel-apples-12-14/index.html (accessed 11 July 2021).

U.S. Centers for Disease Control and Prevention [CDC] (2021). *Listeria* (Listeriosis). Available online at: https://www.cdc.gov/listeria/index.html (accessed 25 July 2021).

U.S. Department of Agriculture [USDA] (2011). *National Organic Program (NOP) Guidance: The Use of Chlorine in Organic Production and Handling*. Available online at: https://www.ams.usda.gov/sites/default/files/media/5026.pdf (accessed 24 July 2021).

U.S. Department of Agriculture [USDA], (2018). *National Organic Standards Board Handling Subcommittee Petitioned Material Proposal Sodium Chlorite, for the Generation of Chlorine Dioxide Gas*. Available online at: https://www.ams.usda.gov/sites/default/files/media/HSSodiumChloriteChlorineDioxideGasPropOct2018Web.pdf (accessed 24 July 2021).

U.S. Environmental Protection Agency [EPA] (2011). *40 CFR part 141 National Primary Drinking Water Regulations*. Available online at: https://www.epa.gov/sites/default/files/2015-11/documents/howepargulates_cfr-2003-title40-vol20-part141_0.pdf (accessed 24 July 2021).

U.S. Environmental Protection Agency [EPA] (2018). *Chlorate; Pesticide Exemptions From Tolerance*. Available online at: https://www.federalregister.gov/documents/2018/12/26/2018-27908/chlorate-pesticide-exemptions-from-tolerance (accessed 25 July 2021).

U.S. Food and Drug Administration [FDA] (2008). *COMPLIANCE POLICY GUIDE (CPG) Sec 555.320 Listeria monocytogenes*. Available online at: https://www.fda.gov/regulatory-information/search-fda-guidance-documents/cpg-sec-555320-listeria-monocytogenes#III_B (accessed 25 July 2021).

U.S. Food and Drug Administration [FDA] (2011). *Food Safety Modernization Act (FSMA)*. Available online at: https://www.fda.gov/food/guidance-regulation-food-and-dietary-supplements/food-safety-modernization-act-fsma (accessed 25 July 2021).

U.S. Food and Drug Administration [FDA] (2014). *Chapter V. Methods to Reduce/Eliminate Pathogens from Produce and Fresh-Cut Produce*. Available online at: http://wayback.archive-it.org/7993/20170111183954/http://www.fda.gov/Food/FoodScienceResearch/SafePracticesforFoodProcesses/ucm091363.htm (accessed 19 October 2020).

U.S. Food and Drug Administration [FDA] (2016). *FSMA Final Rule on Produce Safety*. Available online at: https://www.fda.gov/food/food-safety-modernization-act-fsma/fsma-final-rule-produce-safety (accessed 25 July 2021).

U.S. Food and Drug Administration [FDA] (2017a). *Jack Brown Produce, Inc. Recalls Gala, Fuji, Honeycrisp and Golden Delicious Apples Due to Possible Health Risk*. Available online at: https://www.fda.gov/safety/recalls-market-withdrawals-safety-alerts/jack-brown-produce-inc-recalls-gala-fuji-honeycrisp-and-golden-delicious-apples-due-possible-health (accessed 25 July 2021).

U.S. Food and Drug Administration [FDA] (2017b). *Control of Listeria monocytogenes* in Ready-To-Eat Foods: Guidance for Industry Draft Guidance. Available online at: https://www.fda.gov/files/food/published/Draft-Guidance-for-Industry--Control-of-Listeria-monocytogenes-in-Ready-To-Eat-Foods-%28PDF%29.pdf (accessed 25 July 2021).

U.S. Food and Drug Administration [FDA] (2019a). *North Bay Produce Voluntarily Recalls Fresh Apples Because of Possible Health Risk*. Available online at: https://www.fda.gov/safety/recalls-market-withdrawals-safety-alerts/north-bay-produce-voluntarily-recalls-fresh-apples-because-possible-health-risk (accessed 25 July 2021).

U.S. Food and Drug Administration [FDA] (2019b). *Listeria* (Listeriosis). Available online at: https://www.fda.gov/food/foodborne-pathogens/listeria-listeriosis (accessed 25 July 2021).

Walker, S. J., Archer, P., and Banks, J. G. (1990). Growth of *Listeria monocytogenes* at refrigeration temperatures. *J. Appl. Bacteriol.* 68, 157–162.

Wang, J., Zhang, Y., Yu, Y., Wu, Z., and Wang, H. (2021). Combination of ozone and ultrasonic-assisted aerosolization sanitizer as a sanitizing process to disinfect fresh-cut lettuce. *Ultrason. Sonochem.* 76:105622. doi: 10.1016/j.ultsonch.2021.105622

World Health Organization [WHO] (2000). *Environmental Health Criteria 216 Disinfectants and Disinfectant By-Products*. Available online at: http://apps.who.int/iris/bitstream/handle/10665/42274/WHO_EHC_216.pdf;jsessionid=B9CAC5ACDD3E141BC4A84A6FD48E9464?sequence=1 (accessed July 25, 2021).

Wu, V. C. H., and Rioux, A. (2010). A simple instrument-free gaseous chlorine dioxide method for microbial decontamination of potatoes during storage. *Food Microbiol.* 27, 179–184.

Zhang, L., Yan, Z., Hanson, E. J., and Ryser, E. T. (2015). Efficacy of chlorine dioxide gas and freezing rate on the microbiological quality of frozen blueberries. *Food Control* 47, 114–119. doi: 10.1016/j.foodcont.2014.06.008

Zhang, W., Cao, J., and Jiang, W. (2021). Application of electrolyzed water in postharvest fruits and vegetables storage: a review. *Trends Food Sci. Technol.* 114, 599–607. doi: 10.1016/j.tifs.2021.06.005

Zhao, H., Fu, M., Du, Y., Sun, F., Chen, Q., Jin, T., et al. (2021). Improvement of fruit quality and pedicel color of cold stored sweet cherry in response to pre-storage 1-methylcyclopropene and chlorine dioxide treatments: combination treatment of 1-MCP plus ClO_2 improves postharvest quality of sweet cherry fruit. *Sci. Hortic.* 277:109806. doi: 10.1016/j.scienta.2020.109806

Conflict of Interest: The authors declare that the research was conducted in the absence of any commercial or financial relationships that could be construed as a potential conflict of interest.

Publisher's Note: All claims expressed in this article are solely those of the authors and do not necessarily represent those of their affiliated organizations, or those of the publisher, the editors and the reviewers. Any product that may be evaluated in this article, or claim that may be made by its manufacturer, is not guaranteed or endorsed by the publisher.

frontiers | Frontiers in Microbiology

TYPE Original Research
PUBLISHED 23 August 2022
DOI 10.3389/fmicb.2022.986229

OPEN ACCESS

EDITED BY
Antonio Ippolito,
University of Bari Aldo Moro, Italy

REVIEWED BY
Giacomo Zara,
University of Sassari,
Italy
Francesco Fancello,
University of Sassari,
Italy

*CORRESPONDENCE
Mathabatha Evodia Setati
setati@sun.ac.za

SPECIALTY SECTION
This article was submitted to Food Microbiology, a section of the journal Frontiers in Microbiology

RECEIVED 04 July 2022
ACCEPTED 29 July 2022
PUBLISHED 23 August 2022

CITATION
Maluleke E, Jolly NP, Patterton HG and Setati ME (2022) Antifungal activity of non-conventional yeasts against *Botrytis cinerea* and non-*Botrytis* grape bunch rot fungi.
Front. Microbiol. 13:986229.
doi: 10.3389/fmicb.2022.986229

Antifungal activity of non-conventional yeasts against *Botrytis cinerea* and non-*Botrytis* grape bunch rot fungi

Evelyn Maluleke[1], Neil Paul Jolly[2], Hugh George Patterton[3] and Mathabatha Evodia Setati[1]*

[1]Department of Viticulture and Oenology, South African Grape and Wine Research Institute, Stellenbosch University, Matieland, South Africa, [2]Post Harvest and Agro-Processing Technologies, ARC Infruitec-Nietvoorbij (The Fruit, Vine and Wine Institute of the Agricultural Research Council), Stellenbosch, South Africa, [3]Centre for Bioinformatics and Computational Biology, Stellenbosch University, Matieland, South Africa

Grapes harbour a plethora of non-conventional yeast species. Over the past two decades, several of the species have been extensively characterised and their contribution to wine quality is better understood. Beyond fermentation, some of the species have been investigated for their potential as alternative biological tools to reduce grape and wine spoilage. However, such studies remain limited to a few genera. This work aimed to evaluate the antagonistic activity of grape must-derived non-conventional yeasts against *Botrytis cinerea* and *non-Botrytis* bunch-rotting moulds and to further elucidate mechanisms conferring antifungal activity. A total of 31 yeast strains representing 21 species were screened on different agar media using a dual culture technique and liquid mixed cultures, respectively. *Pichia kudriavzevii* was the most potent with a minimum inhibitory concentration of 10^2 cells/mL against *B. cinerea* but it had a narrow activity spectrum. Twelve of the yeast strains displayed broad antagonistic activity, inhibiting three strains of *B. cinerea* (B05. 10, IWBT FF1 and IWBT FF2), a strain of *Aspergillus niger* and *Alternaria alternata.* Production of chitinases and glucanases in the presence of *B. cinerea* was a common feature in most of the antagonists. Volatile and non-volatile compounds produced by antagonistic yeast strains in the presence of *B. cinerea* were analysed and identified using gas and liquid chromatography mass spectrometry, respectively. The volatile compounds identified belonged mainly to higher alcohols, esters, organosulfur compounds and monoterpenes while the non-volatile compounds were cyclic peptides and diketopiperazine. To our knowledge, this is the first report to demonstrate inhibitory effect of the non-volatile compounds produced by various yeast species.

KEYWORDS

***Wickerhamomyces anomalus*, antagonistic yeasts, biological control, cell wall lytic enzymes, volatile organic compounds**

Introduction

Grape berries harbour a complex microbial community comprising myriads of yeast, bacterial and mould species, that play pivotal roles in grape quality and wine production (Varela and Borneman, 2017; Liu et al., 2020; Griggs et al., 2021). Within this community, some environmental bacteria as well as moulds are known to flourish on grape berries (Barata et al., 2012). Moulds may exist on grapes either as saprophytes and opportunistic pathogens or as obligate parasites. For instance, *Botrytis cinerea*, *Rhizopus* spp., *Penicillium* spp., *Aspergillus* spp., as well as *Alternaria alternata* are associated with grape rot. *B. cinerea* is a widely described causative agent of grey rot while *Aspergillus niger* and *A. alternata* are associated with black rot (Steel et al., 2013). Yeasts, lactic acid bacteria as well as acetic acid bacteria influence wine aroma and flavour. In particular, yeasts are key drivers of the alcoholic fermentation process, however, some basidiomycetous yeasts such as species of the genera *Rhodotorula*, *Cryptococcus*, *Filobasidium*, *Sporobolomyces* as well as ascomycetous yeasts of the genera *Candida*, *Metschnikowia*, *Zygoascus* and *Pichia* which are oxidative or weakly fermentative do not thrive in a wine fermentation environment (Barata et al., 2012).

Grape and grape must-associated yeasts have widely been studied to decipher their role in wine fermentation and their contribution to wine organoleptic properties. Such studies have resulted in commercialisation of non-*Saccharomyces* yeasts including *Lachancea thermotolerans*, *Torulaspora delbrueckii*, *Metschnikowia pulcherrima* and *Pichia kluyveri* to name a few (Vejarano and Gil-Calderón, 2021). However, more than 40 yeast species have been isolated from grape and wine fermentation environments (Jolly et al., 2014) and recent studies show that some of these have great potential as bioprotectants and biocontrol agents against spoilage organisms (Kuchen et al., 2019; Mewa-Ngongang et al., 2019a) and phytopathogens (Bleve et al., 2006; Nally et al., 2015; Cordero-Bueso et al., 2017; Mewa-Ngongang et al., 2019b; Marsico et al., 2021; Sabaghian et al., 2021). The most frequently reported yeast antagonists include mainly strains belonging to the *Metschnikowia pulcherrima*, *Hanseniaspora* spp., *Pichia* spp. e.g., teleomorph *Meyerozyma* (*Pichia*) *guilliermondii*, as well as strains of *Wickerhamomyces anomalus*, *Aureobasidium pullulans* (yeast-like fungus) and *Meyerozyma guilliermondii* (Parafati et al., 2015; di Francesco et al., 2016; Cordero-Bueso et al., 2017; Chen et al., 2018; Pereyra et al., 2021).

Yeasts have been shown to express various mechanisms in antagonistic interactions. These include competition for space and nutrient (Parafati et al., 2015), secretion of extracellular lytic enzymes such as protease, glucanase and chitinase (Cordero-Bueso et al., 2017; Agarbati et al., 2022) and volatile organic compounds (Fredlund et al., 2004; Cordero-Bueso et al., 2017; Mewa-Ngongang et al., 2019b). Amongst the VOCs esters and higher alcohols such as ethyl acetate, phenyl acetate, isoamyl alcohol, benzyl alcohol, isoamyl octanoate, 2-methyl-1-propanol and 2-phenylethanol, have been implicated in inhibitory activities. These compounds are reported to suppress conidia germination and mycelium growth of *B. cinerea* and most of *Penicillium* spp. under both *in vitro* and *in vivo* conditions (Chen et al., 2018; Oro et al., 2018; Choińska et al., 2020; Piasecka-jo and Choin, 2020; Yalage Don et al., 2020). Antifungal activity is however strain dependent and therefore necessitates a screening of a myriad of isolates and strains of different origins in order to find strains with broad specificity.

Several biocontrol agents or products such as Aspire® (*Candida oleophila*), Candifruit® (*Candida sake*), Shemer® (*Metschnikowia fructicola*) and BoniProtect® (*Aureobasidium pullulans*) consisting of yeast or yeast-like fungi as active ingredients have been registered and made it to the market (Pretscher et al., 2018; Freimoser et al., 2019; Zhang et al., 2020). However, sustainable production and application of some of these were not realised and they were ultimately withdrawn from the market (Zhang et al., 2020). Some of the key limitations for wide use of biocontrol agents include narrow spectrum of activity, reduced efficacy in commercial and field conditions (Zhang et al., 2020). Traditionally, grey rot and other grapevine pathogens are controlled with the use of synthetic fungicides which have preventive and curative effects. While these fungicides have sustained grape and wine production for centuries, their application in vineyards may result in environmentally harmful residues (Ons et al., 2020; Schusterova et al., 2021). Moreover, application of such fungicides is not permissible within a 30-day period prior to harvest (Abbey et al., 2019; Ons et al., 2020; Zhang et al., 2020). Consequently, integrating grape and must derived yeasts with antifungal activity against several phytopathogens, to complement routine vineyard spray programs remains an attractive alternative that deserves in-depth exploration (di Canito et al., 2021; Lahlali et al., 2022).

Over the past decade, a wide range of oxidative and weakly fermentative non-conventional yeasts have been isolated and identified from South African vineyards (Setati et al., 2012; Bagheri et al., 2015; Ghosh et al., 2015; Shekhawat et al., 2018). While some of the isolates have been evaluated for their oenological traits (Rossouw and Bauer, 2016; Rollero et al., 2018; Porter et al., 2019), their biotechnological potential remains largely untapped. This study aimed to unravel the antifungal traits of non-conventional yeasts derived from wine grapes and must. The expression of antifungal activity *in vitro* and on grape berries was assessed.

Materials and methods

Microbial strains and culture media

Yeast strains isolated from grape must were obtained from the culture collection of the South African Grape and Wine Research Institute (SAGWRI), Stellenbosch University. Thirty-one strains (Supplementary Table S1) were routinely grown and maintained on Wallerstein Nutrient (WLN) agar (Merck Millipore,

South Africa). For long-term storage, the strains were stored at −80°C in 25% (*v*/*v*) glycerol in cryogenic tubes. Three strains of *B. cinerea*, laboratory strain (B05. 10), grape strains (IWBT FF1 and IWBT FF2) isolated from Cabernet Sauvignon grapes obtained from Thelema Mountain vineyard, South Africa (33°54′46.1′S 18°56′30.7′E), one strain of *Aspergillus niger* and *Alternaria alternata* isolated from soil collected from Stellenbosch University's Welgevallen experimental farm (33°57′03.0′S 18°52′05.6′E), were used in this study. Filamentous fungal cultures were revived on Malt Extract agar (MEA; Merck Millipore, South Africa) containing 2% (*w*/*v*) bacteriological agar. Yeast inoculums were prepared from overnight cultures grown in 5 ml YPD broth containing per litre (10 g yeast extract, 20 g peptone and 20 g glucose). Fresh yeast cultures were collected by centrifugation at 10,625 *g* for 5 min and washed twice with sterile 0.9% (*w*/*v*) NaCl solution. The yeast suspensions were adjusted to OD_{600} 0.1 (≈ 10^6 CFU/ml) using 0.9% (*w*/*v*) NaCl.

In vitro screening for yeast antagonistic activity

Dual culture plate assay

Antifungal activity of 31 yeast strains (Supplementary Table S1) was tested against three strains of *B. cinerea* (B05. 10, IWBT FF1) and IWBT FF2, *A. niger* (IWBT FF3) and *A. alternata* (IWBT FF4) by *in vitro* assay on MEA and low glucose (0.2% *w*/*v*) YPD agar referred to as YPD-L from hereon. Three replicate plates were prepared for each yeast. For the screening, 6 × 6 mm^2 agar plugs of the filamentous fungi were obtained from the margins (active growth zone) of young mycelia grown on MEA and inoculated face-down onto fresh agar at a distance of 27 mm away from the Petri dish edge (Standard 90 mm Petri dishes, Sigma-Aldrich, South Africa). Twenty microliter of yeast suspension (≈ 10^6 cells/ml) was inoculated 30 mm away from the fungal plug on the opposite side of the plate. Negative control plates were only inoculated with the filamentous fungi. A strain of the yeast-like fungus *Aureobasidium pullulans* W32 was used as a positive control as multiple strains of this fungus have been shown to inhibit *B. cinerea* (Yalage Don et al., 2020). The plates were incubated for 5 days at 25°C in the dark for *B. cinerea* strains experiments and under standard light conditions for *A. niger* and *A. alternata*. Mycelial growth was observed and images were captured to record the growth. The inhibition percentage was calculated as $[(R_c - R_{exp})/R_c] \times 100\%$, where R_c represents the longest distance of fungal mycelium from the inoculated fungal plug and R_{exp} is the horizontal distance from the inoculated fungal plug towards the yeast colony, which shows the inhibitory effect (Chen et al., 2018; Figure 1).

Liquid co-culture assay

To determine whether yeast antifungal activity varied between culture conditions, liquid co-culture assays were conducted. Ten microliter of yeast suspension (≈ 10^6 cells/mls) and of the spore suspension (≈ 10^6 spores/ml) of each pathogen (*B. cinerea*, *A. niger* and *A. alternata*) were inoculated into 24-well plates containing 2 ml of malt extract broth. The cultures were incubated at 25°C for 5 days. Microscopic observations of 20 µl wet mounts, were conducted to assess hyphal formation. Five fields on each slide were assessed and images were captured at 40, 100 and 400*x* magnification.

After the initial screening, yeast species with antifungal activity against the tested pathogens were selected and investigated for their Minimum inhibiting concentration (MIC) and production of cell wall lytic enzymes.

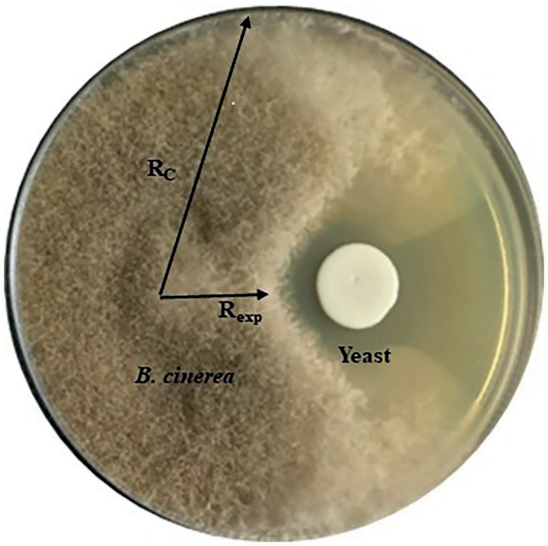

FIGURE 1
A representation of the dual culture assay showing yeast antifungal activity against *Botrytis cinerea* and how the inhibition was measured. R_c represents the longest distance of fungal mycelium growth from the inoculated fungal plug and R_{exp} is the horizontal distance from the inoculated fungal plug towards the yeast colony.

Determining modes of action

Evaluation of minimum inhibiting concentration

Minimum yeast cell concentration necessary to inhibit the growth of *B. cinerea* was investigated on yeast strains that displayed inhibition on plates and in liquid co-culture conditions against all the pathogens tested in this study. Fresh yeast cultures were inoculated in YPD broth and grown overnight at 25°C. For each yeast strain tested, malt extract broth and YPD agar plates were inoculated with cell suspensions from 10^2 to 10^6 cells/ml. Ten microliter of *B. cinerea* IWBT FF1 spore suspensions (~ 10^6 spores/ml) were inoculated on the centre of the Petri dish and into 2 ml malt extract broth in 24-well plates. A negative control with *B. cinerea* spore suspension was also prepared. The plates were incubated at 25°C for 5 days. The results were considered positive

when no or limited *B. cinerea* mycelial formation was observed. The experiment was conducted in three replicates. The MIC was recorded as the lowest yeast cell concentration required to inhibit *B. cinerea* mycelial growth.

Screening yeasts for chitinase and glucanase production

Preparation of colloidal chitin

Colloidal chitin was prepared according to the method described by Agrawal and Kotasthane (2012). Briefly, 20 g of chitin (chitin from shrimp cells-Sigma-Aldrich, South Africa) was dissolved in 350 ml cold 12 M HCl overnight at 4°C with continuous mixing on a magnetic stirrer plate, followed by extraction with 2,000 ml of ice-cold 95% ethanol and an overnight incubation at 25°C. The precipitate was centrifuged at 1,479 *g* for 20 min at 4°C. The pellet was washed with sterile distilled water three times and centrifuged at 1,479 *g* for 5 min at 4°C till the acid and ethanol were completely washed-off. The colloidal chitin obtained had a soft, pasty consistency with 90–95% moisture and was stored at 4°C until further use.

Hydrolytic enzyme production

In order to determine if the yeasts in the current study produced chitinases and β-1,3-glucanases as part of their antagonistic activity, dual culture plate assay were performed on agar supplemented with appropriate substrates. The protocol was adopted from Chen et al. (2018) and was adjusted by excluding the mineral salts from the media composition. Chitinase production was determined on YPD-L agar supplemented with 0.45% (*w*/*v*) colloidal chitin and 0.15 g/l bromocresol purple. The medium was adjusted to pH 4.7 with 1 M HCl and autoclaved. Glucanase activity was screened on a medium containing 0.5% (*w*/*v*) yeast extract, 1% (*w*/*v*) peptone and 0.2% (*w*/*v*) laminarin (Merck Millipore, South Africa), medium was adjusted to pH 4 with HCl (1 M) and mixed with bacteriological agar to a final concentration of 2% (*w*/*v*) after autoclaving (Ghosh et al., 2015). The plates were inoculated and incubated as described in the *in vitro* dual assay. Chitinase activity was detected by the formation of a purple zone around the yeast colony, while glucanase activity was visualised by staining the laminarin plates with 0.1% (*w*/*v*) Congo red for 1 h, followed by de-staining with 1 M NaCl till a clear zone around the yeast colony was observed (Ghosh et al., 2015; Chen et al., 2018). The inhibition percentage was measured using $[(R_c - R_{exp})/R_c] \times 100\%$. All the measurements were done on triplicate plates. Enzyme production was recorded as either weak or strong depending on the inhibition percentage (Table 1).

Hyphal structure phenotype of *Botrytis cinerea*

Botrytis cinerea and yeasts co-cultured for 5 days at 25°C on YPD-L agar were directly used for confocal microscopy analysis. After incubation, all the mycelium directly next to the inhibition zone were collected into an Eppendorf tube and washed with 1 ml phosphate-buffered saline (PBS; pH 7.4; Na_2HPO_4; Merck Millipore, South Africa). To measure chitin level, the hyphae were stained with 10 µl calcofluor white (Merck Millipore, South Africa) after the addition of 10 µl of 10% KOH (Merck Millipore, South Africa). For glucan content, the hyphae were stained with trypan blue (Merck Millipore, South Africa). Z-sectioning image acquisition was performed on a Carl Zeiss confocal laser scanning microscope (LSM) 780 Elyra S1 with super resolution structured illumination microscopy (SR-SIM super resolution) platform. Z-series images were taken at 0.5 µm intervals through the specimens. The excitation laser used was the violet laser with 407-nm wavelength, and the emission filter used was the Pacific Blue channel with a 450/40 band-pass filter for calcofluor white and trypan blue stained cells. Images were processed and background subtracted using the Zeiss Zen lite 2011 software and presented in a maximum-intensity projection.

TABLE 1 Exemplar images of the chitinase and glucanase plate screening showing yeast and *Botrytis cinerea* growth, enzyme production and weak or strong inhibition zone.

Enzyme	
Chitinases	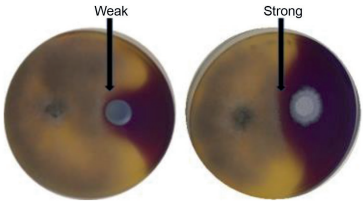
β-1,3-Glucanases	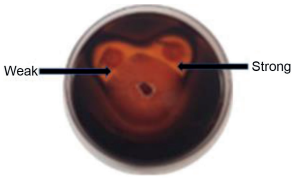

For further investigation, yeasts with broad spectrum activity were selected and analysed for the production of VOCs and non-volatile compounds.

Volatile organic compounds production

Experimental set up for SPME automated sampling of VOCs and analysis was done according to Yalage Don et al., 2020. Two layers of sterile YPD-L (1.5 ml) were prepared by pouring 1.5 ml of the agar on opposite sides of the vial as illustrated in Figure 2. For inoculation, *B. cinerea* IWBT FF1 spore suspension was prepared in sterile distilled water (10^6 spores/ml, 10 µl) and spread on one side of the vial using a 10 µl inoculation loop (LP ITAKIAN SPA, Milan, Italy) then incubated for 48 h at 25°C, after which the yeast cell suspension ($\approx 10^6$ cells/ml, 10 µl) prepared in 0.9% (*w*/*v*) NaCl was spread on the opposite side of the vial. The vials were incubated for a further 10 days. Control vials were inoculated with either *B. cinerea* spore suspension or a yeast cell suspension. Four replicates were performed for each antagonist-pathogen combination and controls.

Sample preparation for VOCs analysis (HS-SPME–GC–MS)

Prior to GC–MS analysis, 50 µl of a 10 ppm Anisole d8 solution was added to the centre of each vial as an internal

FIGURE 2
Headspace vial with YPD-L agar for automated sampling of volatile organic compounds produced by antagonistic yeasts in the presence of *Botrytis cinerea* IWBT FF1.

standard. The vials were incubated in the autosampler at 50°C for 5 min, after which a 50/30 µm divinylbenzene/carboxen/polydimethylsiloxane (DVB/CAR/PDMS) SPME fibre (Supelco, Bellafonte, PA, United States) was exposed to the headspace of the vial for 30 min at the same temperature. After equilibration, the fibre was injected onto the injector at 250°C, and 10 min were allowed for desorption of the compounds.

Chromatographic conditions

Analysis of VOCs was performed on an Agilent Gas Chromatography, model 6,890 N (Agilent, Palo Alto, CA, United States), coupled with an Agilent mass spectrometer detector (MS), model 5975B Inert XL EI/CI (Agilent, Palo Alto, CA, United States) equipped with a CTC Analytics PAL autosampler. The chromatographic separation of compounds was performed on a polar J&W DB-FFAP (60 m, 0.25 mm i.d., 0.5 µm film thickness) capillary column. The oven temperature program was set as follows: 40°C held for 1 min, then ramped up to 150°C at 25°C/min and held for 3 min, and again ramped up to 200°C at 5°C/min and held for 5 min, and finally up to 250°C at 5°C/min and held there for 2 min. The total run time was 30.54 min. Helium at a constant flow rate of 1.0 ml/min was used as a carrier gas. The injector operated in a split-less mode maintained at 250°C throughout the analysis. Both the purge flow and gas saver flow were activated at 50 ml/min for two and 5 min, respectively. The MS-detector was operated in single ion monitoring (SIM) mode. The ion source and quadrupole temperatures were maintained at 230°C and 150°C, respectively, with the transfer line set at 250°C. Compounds were identified using GC–MS retention times and cross-referencing their mass spectra with the NIST05 spectral library.

Extraction and analysis of non-volatile compounds

Non-volatile metabolites were extracted following a method described by Sasidharan et al. (2012). The antagonist yeast was co-cultured with *B. cinerea* IWBT FF1 in a 24-well plate containing 2 ml malt extract broth. Controls were prepared by growing *B. cinerea* and the yeasts in monocultures. Cultures were incubated at 25°C for 5 days. After incubation, 0.5 ml samples were collected and transferred into 0.5 ml of freshly prepared N-ethylmaleimide-methanol (NEM) solution (4 mM) kept in 1.5 ml screw cap tubes equilibrated using dry ice. The cultures were pelleted by flash centrifugation for 2 min (20,000 *g*; −9°C) and the supernatant containing the extracellular metabolites was transferred into new microcentrifuge tubes and stored at −80°C till analysis. Prior to analysis, samples were transferred to an LC vial, and all the vials were stored at −80°C for LC–MS analysis.

Liquid chromatography–mass spectrometry analysis

A Waters Synapt G2 Quadrupole time-of-flight (QTOF) mass spectrometer (MS) connected to a Waters Acquity ultra-performance liquid chromatograph (UPLC; Waters, Milford, MA, United States) was used for high-resolution UPLC-MS analysis. Column eluate first passed through a Photodiode Array (PDA) detector before going to the mass spectrometer, allowing simultaneous collection of UV and MS spectra. Electrospray ionisation was used in negative mode with a cone voltage of 15 V, desolvation temperature of 275°C, desolvation gas at 650 l/h, and the rest of the MS settings optimised for best resolution and sensitivity. Data were acquired by scanning from m/z 150 to 1,500 m/z in resolution mode as well as in MSE mode. In MSE mode two channels of MS data were acquired, one at a low collision energy (4 V) and the second using a collision energy ramp (40–100 V) to obtain fragmentation data as well. Leucine enkephalin was used as lock mass (reference mass) for accurate mass determination and the instrument was calibrated with sodium formate. Separation was achieved on a Waters HSS T3, 2.1 × 100 mm, 1.7 µm column. An injection volume of 2 µl was used and the mobile phase consisted of 0.1% formic acid (solvent A) and acetonitrile containing 0.1% formic acid as solvent B. The gradient started at 100% solvent A for 1 min and changed to 28% B over 22 min in a linear way. It then went to 40% B over 50 s and a wash step of 1.5 min at 100% B, followed by re-equilibration to initial conditions for 4 min. The flow rate was 0.3 ml/min and the column temperature was maintained at 55°C. Compounds were quantified in a relative manner against a calibration curve established by injecting a range of catechin standards from 0.5 to 100 mg/l catechin. Data was processed using MSDIAL and MSFINDER (RIKEN Centre for Sustainable Resource Science: Metabolome Informatics Research Team, Kanagawa, Japan).

Grape bioassay

For the *in vivo* test, yeast strains that proved to be the most effective antagonists against all the pathogens investigated in this study were selected and assessed for their Inhibitory activity on

grapes. Early sweet seedless white grapes (*Vitis vinifera*) were obtained from a local supermarket (Stellenbosch). Grape berries surface was disinfected by soaking grapes in 1% (*v*/*v*) sodium hypochlorite solution for 5 min and rinsed three times with sterile distilled water. The water was allowed to dry prior to the next step. Grapes were uniformly wounded with a sterile needle (< 1 mm diameter per wound) and allowed to dry prior to yeast treatments. Yeast cell and spore suspensions were prepared as previously described. For preventive treatments, wounded grapes were inoculated with 20 µl (≈ 10^6 cells/ml) of various yeast suspension using a micropipette and incubated 24 h at 25°C. Subsequently, the berries were inoculated with 20 µl (≈ 10^6 spores/ml) of *B. cinerea* IWBT FF1. The berries were incubated at 25°C and to maximise the attainment of a higher level of humidity, a heavily wet piece of paper towels was placed in each closed airtight container (Dixie injection & Blow moulders, South Africa). Negative controls (six berries each) were prepared by inoculating the fungal spores on the wounded berries without yeast cells. The antagonistic properties of the selected yeast species were analysed visually by assessing the grape colour changes and fungal development on treated berries. The disease severity was evaluated by a visual score of 1-to-4 (1: no visible symptoms; 2: soft rot; 3: formation of mycelium; 4: sporulation of mould).

Statistical analysis

Data are expressed as mean ± standard deviation (SD). The significance of differences between each experiment and control was determined in XLSTAT software. $p \leq 0.05$ was considered statistically significant (Data analysis and Statistical Solution for Microsoft Excel, Addinsoft, Paris, France 2022).

Results

Mycelial growth inhibition and cell wall hydrolases

Thirty-one yeast strains isolated from grape must were obtained from the SAGWRI culture collection and screened for antifungal activity against *B. cinerea*, *A. niger* and *A. alternata*. Twenty-three strains representing 15 species displayed varying inhibitory activity against the fungal pathogens in dual plate assays (Table 2). All the antagonistic strains also inhibited growth of the filamentous fungi in liquid cultures. This was evidenced by absence or limited formation of hyphae in the cultures when visualised under the microscope (Supplementary Figure S1). Among the 23 strains, 12 exhibited broad antagonistic activity inhibiting three strains of *B. cinerea*, as well as the strain of *A. niger* and *A. alternata*, while 11 had narrow-spectrum activity. Higher inhibition percentages were mostly recorded against *B. cinerea* B05.10 than the two grape strains (Figure 3). Furthermore, within the species, different yeast strains exhibited varying inhibition capabilities. For instance, among the *Wickerhamomyces anomalus* strains, Y934 displayed similar inhibition levels for all *B. cinerea* strains, while Y517 and Y541 were more inhibitory against B05.10 and IWBT-FF2. Similarly, intraspecific variabilities were observed with *Candida oleophila* and *Zygoascus meyerae* (Figure 3). *Pichia kudriavzevii* Y508 exhibited the lowest MIC of 10^2 cells/ml followed by *W. anomalus* strains (Y541, Y517 and Y934) and *C. oleophila* Y964 at 10^3 cells/ml, while for most strains an MIC of 10^4 cells/ml was observed (Table 2).

Following the initial screening on agar plates and liquid media, yeasts that inhibited the growth of all the pathogens were selected and investigated for the production of cell wall hydrolytic enzymes, volatile and non-volatile compounds. Overall, inter- and intra-specific variations in chitinase and glucanase production was observed (Table 2). For instance, within the genus *Pichia*, strong chitinase-associated inhibition was evident in *Hyphopichia burtonii* (formerly *Pichia burtonii*) and *P. guilliermondii*, while in *P. kudriavzevii*, *P. manshurica* and *P. occidentalis* this activity was weak. Within the *W. anomalus* species, all strains exhibited strong chitinase activity but only strain Y541 exhibited strong glucanase activity. Similarly, with *Zygoascus meyerae*, two strains displayed weak chitinase while all three strains had strong glucanase activity.

Selected yeast strains were co-cultured with *B. cinerea* and the hyphal chitin and glucan levels were assessed using a confocal microscope following staining with calcofluor white and trypan blue. Overall, huge variations were observed in the hyphal chitin and glucan levels, but tendentially a decrease was evident in the hyphae from the mycelia exposed to the antagonistic yeast (Table 3). In particular, *B. cinerea* hyphae from the mycelia exposed to *W. anomalus* Y541 and *W. anomalus* Y934 showed significant reduction in chitin levels, while a significant reduction in glucan levels was observed in the mycelia exposed to *W. anomalus* Y541 and *W. anomalus* Y517.

Volatile organic compounds production

In order to determine whether the production of VOCs was involved in the inhibition of growth of *B. cinerea* IWBT FF1 by selected yeast strains (*W. anomalus* Y541, Y517, Y934, *L. elongisporus* Y929 and *H. pseudoburtonii* Y963), SPME-GC–MS was conducted after 10 days of incubation confrontation cultures. A total of 29 compounds were detected and identified, however, only 13 were consistent across replicates (Figure 4). These include higher alcohols, aldehydes, esters, organosulfur compounds, monoterpenes, ketones and aromatic hydrocarbons. Overall, 2-methylisoborneol, 2-methyl-2-bornene and n-butanol were enhanced when *B. cinerea* was challenged with either of the three yeasts. In addition, *W. anomalus* displayed enhanced production of dimethylpyrazine, isoamyl alcohol and benzaldehyde in the presence of *B. cinerea*. In contrast, the production of methyl-tiglate and methyl-2-phenylacetate was reduced in *W. anomalus*

10.3389/fmicb.2022.986229

TABLE 2 Antifungal activity phenotypes of yeast species and strains.

Yeasts strains	Inhibition spectrum	% Mycelial inhibition against B05.10	Inhibitory activity in liquid cultures	Minimum inhibiting concentration (MIC)	Chitinase	s
A. pullulans	+++	39.22	+	ND	Strong	Strong
C. azyma Y979	---	–	–	ND	ND	ND
C. apicola Y957	---	–	–	ND	ND	ND
C. lusitaniae Y833	---	–	–	ND	ND	ND
C. oleophila NOVA-CH	++–	–	+	10^4	Weak	Strong
C. oleophila Y964	++–	–	+	10^3	Strong	ND
C. oleophila Y994	+++	32.02	+	10^4	Weak	Weak
F. capsuleginum Y938	---	–	–	ND	ND	ND
H. pseudoburtonii Y963**	+++	32.94	+	10^5	Strong	Strong
K. mangrovensis Y535	++–	29.83	+	ND	ND	ND
L. elongisporus Y929**	+++	35.94	+	10^5	Weak	Strong
L. elongisporus Y996**	+++	43.27	+	10^5	Weak	Strong
M. chrysoperlae Y955	++–	–	+	ND	ND	ND
M. bicuspidata Y540	---	–	–	ND	ND	ND
M. geulakonigii Y848	+++	31.39	+	10^5	Weak	Strong
H. burtonii Y951	+++	47.17	+	10^4	Strong	Strong
P. fermentans Y995	++–	–	+	10^4	ND	ND
P. fermentans KLBG-SB	++–	–	+	10^4	ND	ND
P. guilliermondii Y993	+++	44.99	+	10^6	Strong	Strong
P. kluyveri FRU-1	---	–	–	ND	ND	ND
P. kluyveri NOVA-CH	---	–	–	ND	ND	ND
P. kluyveri SIL-1	---	–	–	ND	ND	ND
P. kudriavzevii Y508	++–	–	+	10^2	Weak	ND
P. manshurica Y510	++–	–	+	10^5	Weak	ND
P. occidentalis BGLD-CH	++–	–ss	+	10^4	Weak	ND
P. fusiformata Y871	+++	47.54	+	10^6	Weak	Weak
W. anomalus Y517 **	+++	35.98	+	10^3	Strong	Weak
W. anomalus Y541**	+++	32.95	+	10^3	Strong	Strong
W. anomalus Y934**	+++s	25.77	+	10^3	Strong	Weak
Z. meyerae Y830	++–	33.98	+	10^5	Weak	Strong
Z. meysserae Y834	++–	–	+	10^5	Strong	Strong
Z. meyerae Y854	++–	28.07	+	10^5	Weak	Strong

Key: (Inhibition spectrum) +++, ++– or --- denotes strains capable of inhibiting all the three pathogens, two pathogens and no activity, respectively. Chitinase and glucanase activity: Strong, Weak or ND denotes inhibition percentage > 50% and < 50% and not determined, respectively.
Yeast strains marked with ** were selected for further investigation.

and *L. elongisporus* in the presence of *B. cinerea* compared to their respective monocultures (Figure 4).

Analysis of non-volatile compounds

No information is available on the role of non-volatile compounds especial cyclic peptides secreted by antagonistic yeasts as mode of action, therefore only three strains (*W. anomalus* Y541, *H. pseudoburtonii* Y963 and *L. elongisporus* Y929) representing three species were evaluated. Non-volatile organic compounds produced by yeast in the presence of *B. cinerea* IWBT FF1 were analysed using UPLC-MS. The three selected yeasts and *B. cinerea* were co-cultured in ME broth and incubated for 5 days. Principal component analysis revealed some separation between the monocultures and mixed cultures. Although an overlap was clear between the *H. pseudoburtonii* and its mixed culture with *B. cinerea* (Figure 5). Several non-volatile compounds were identified, however, only a few cyclic peptides were differentially enhanced where the respective yeast strains were co-cultured with *B. cinerea* (Table 4). The rest of the compounds are not shown since they could not be confidently associated with fungi. The cyclic peptides were secreted by yeast strains (*W. anomalus* Y541, *H. pseudoburtonii* Y963 and *L. elongisporus* Y929). Based on the average peak

10.3389/fmicb.2022.986229

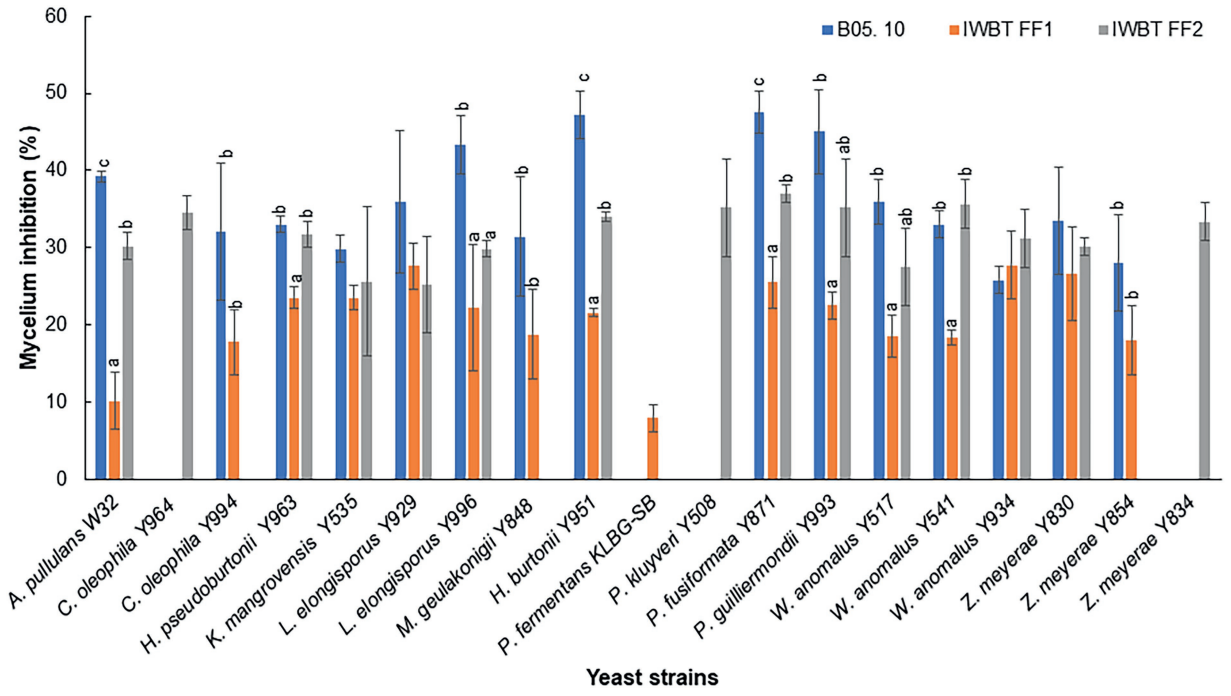

FIGURE 3
Yeast inhibition of *Botrytis cinerea* B05. 10, IWBT FF1 and IWBT FF2 mycelial growth. Bars represent average inhibitions of three replicates with standard deviation. Different superscript letters ($^{a, b, c}$) show significant differences according to Tukey and Dunnett test ($p < 0.05$) when comparing the mycelium inhibition of each *B. cinerea* strain by different yeasts. Strains with no superscript letters indicate those with no significant difference.

TABLE 3 Chitin and glucan content in *Botrytis cinerea* hyphae treated with various yeast strains capable of producing chitinase and glucanase.

Cultures	Chitin level	Glucan level
B. cinerea	25.22 ± 132	91.78 ± 30.21
B. cinerea + *W. anomalus* Y541	18.76 ± 6.03**	28.63 ± 9.11**
B. cinerea + *W. anomalus* Y517	18.26 ± 10.66	48.66 ± 27.29**
B. cinerea + *W. anomalus* Y934	43.02 ± 8.33**	44.12 ± 14.98
B. cinerea + *H. pseudoburtonii* Y963	19.18 ± 8.92	50.77 ± 36.31
B. cinerea + *L. elongisporus* Y929	12.63 ± 4.26	59.36 ± 49.46
B. cinerea + *L. elongisporus* Y996	28.17 ± 9.92	62.85 ± 41.13

Data expressed as mean ± SD.
**Show significant difference between yeast treatment and the control according to *t*-test ($p < 0.05$).

intensities, L-Cyclo(leucylprolyl) was found to be the most abundant compound in *L. elongisporus* Y929 however, its intensity was decreased in the presence of *B. cinerea*. In the presence of *B. cinerea*, *W. anomalus* Y541 showed an increase in the production of Leucylproline as compared to *W. anomalus* alone. *Hyphopichia pseudoburtonii* Y963 showed an enhanced production of L,L-Cyclo(leucylprolyl), Cyclo(D-Leu-L-Trp), cyclo(L-Pro-L-Val) and Leucylproline when co-cultured when *B. cinerea*.

To evaluate the effectiveness of the antagonistic yeasts on table grapes and to compare the outcomes of the *in vitro* assays, the grape bioassay in a closed airtight container was conducted. Measurements of grape deterioration are made per bunch rather than per berry. Therefore, no measures of radial inhibition were made. Efficacy of the selected yeast strains in reducing *B. cinerea* development moulds is reported in Table 5. *W. anomalus* strains *in vivo* (Table 5) showed a 90–100% reduction of *B. cinerea* growth. Soft mycelium developed in the presence of *H. pseudoburtonii* after 5 days of incubation. On grapes treated with *L. elongisporus* mycelial formation similar to that on grapes with only *B. cinerea* (control) was observed.

Discussion

Grapes and wine production worldwide suffer economic losses due to bunch rot. Mostly filamentous fungi are responsible for the decay of grapes, with *B. cinerea* (grey mould) being the most common; however, various other fungi, such as *Aspergillus* species and *Penicillium* species, can also cause the decay of grapes (Steel et al., 2013). These are widely controlled through the use of synthetic fungicides. However, growing concerns over undesirable chemical residues in the environment have spurred the exploration of non-conventional yeasts as biological alternatives (Freimoser et al., 2019; Zhang et al., 2020; Agarbati et al., 2022).

This study evaluated the antifungal activity of grape must associate yeasts against three strains of *B. cinerea*, one strain of *A. niger* and *A. alternata* and further demonstrated the possible

10.3389/fmicb.2022.986229

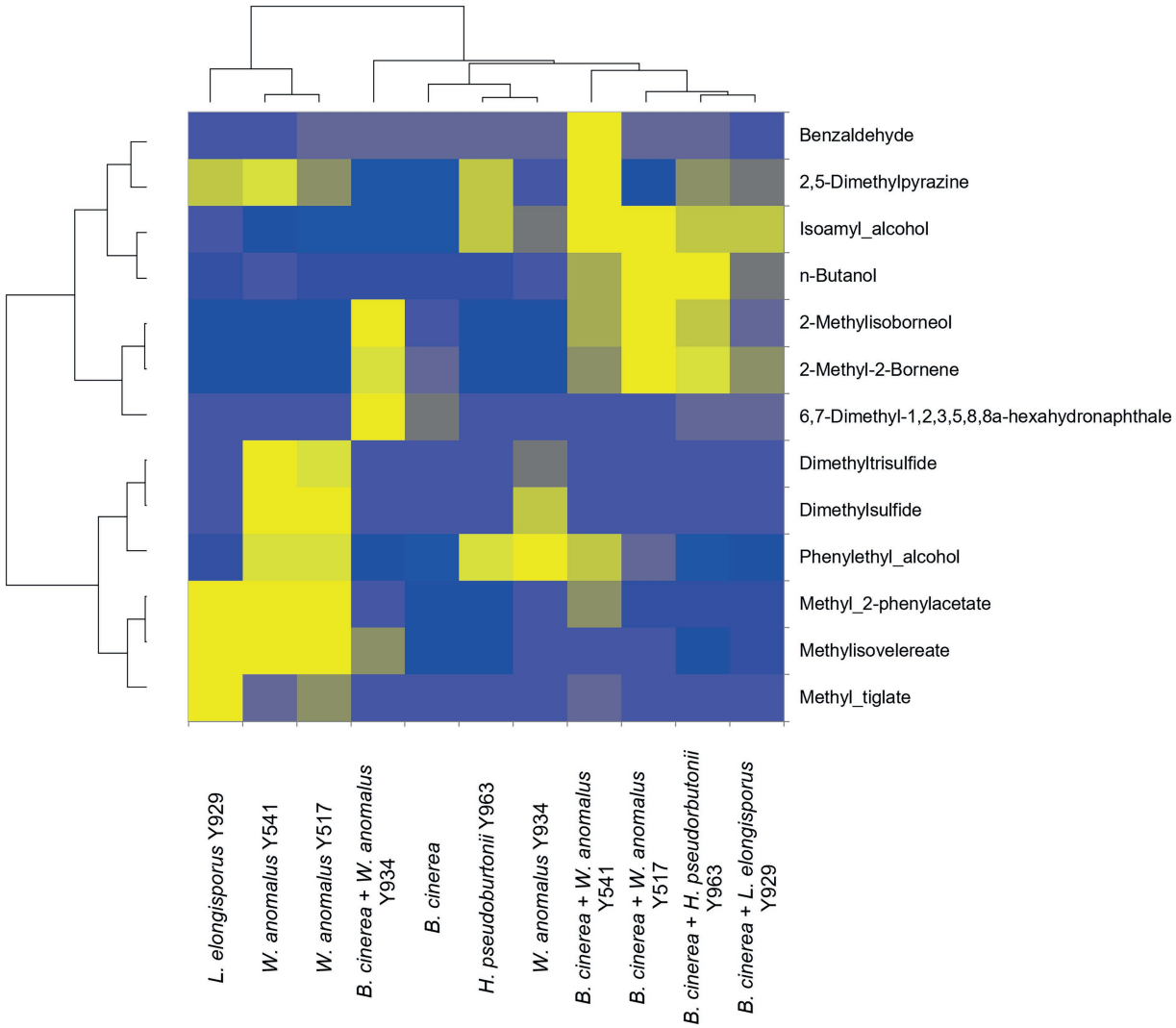

FIGURE 4
Relative fold changes coloured from blue (lowest) to yellow (highest) of volatile organic compounds produced by *Botrytis cinerea* (control) and yeast strains co-cultured with various yeasts strains. Compounds were identified using Anisole d8 (Std), comparison with mass spectra from MS NIST05 spectral library.

modes of action of the selected yeast strains against *B. cinerea*. Overall, our data show wide distribution of antifungal activity across different yeast species and strains. Intraspecific variability was observed in the form of differences in the presence and absence of activity, the spectrum as well as the strength of activity. For instance, within the species *Candida oleophila*, strain Y994 could inhibit all phytopathogens tested but displayed weak glucanase and chitinase activity, while Y964 and NOVA-CH inhibited two of the pathogens and expressed strong glucanase and chitinase activity. Conversely, within the *Wickerhamomyces anomalus* and *Zygoascus meyerae* strains, similar antifungal activity spectra as well as minimum inhibitory concentrations (MIC) were observed but these differed mainly in the levels of chitinase and glucanase displayed. Furthermore, yeast strains differed in their inhibition of *B. cinerea* strains. For instance, within the *W. anomalus* species, Y517 and Y541 displayed stronger inhibition against IWBT FF1 while Y934 displayed similar inhibition levels across different *B. cinerea* strains. Intraspecific variability is a common phenomenon in yeast antifungal activity and has been reported for many species (Bleve et al., 2006; Cordero-Bueso et al., 2017; Agarbati et al., 2022). In particular, intraspecific variability antagonistic activity was observed in several strains of *W. anomalus* against two strains of *B. cinerea* and *Curvularia lunata,* a fungal plant pathogen responsible for rice dirty panicle disease (Khunnamwong et al., 2020). Yeast species such as *C. oleophila*, *W. anomalus* and *P. kluyveri* have been reported several times as potential antagonists against different moulds for various pathogens infecting different fruits such as grapes, apples, sweet cherries and strawberries (Dlamini and Dube, 2008; Parafati et al., 2015; Wang et al., 2018; Comitini et al., 2021; Agarbati et al., 2022).

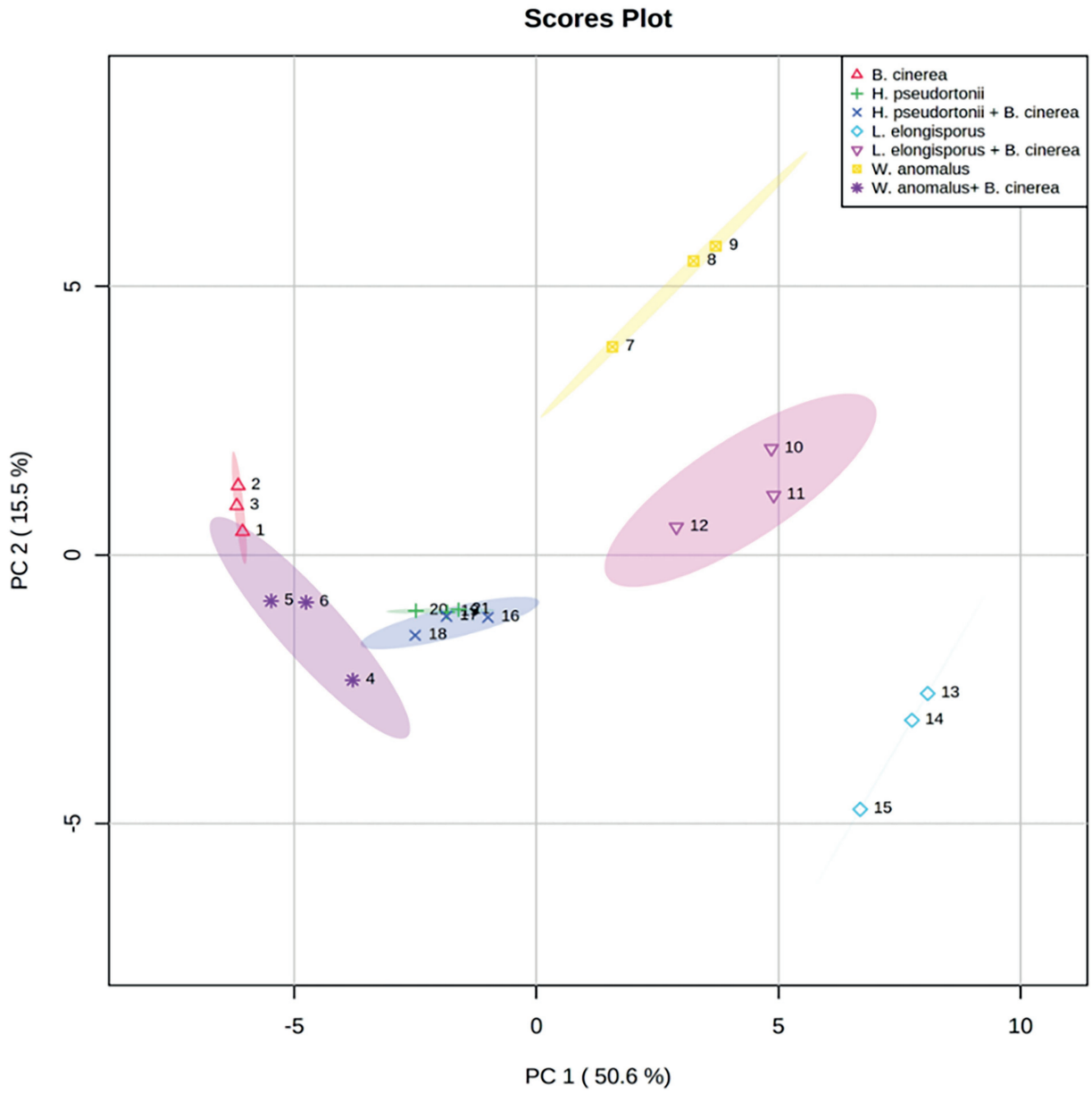

FIGURE 5
Principal component analysis score plots obtained from the non-volatile organic compounds profile of *Botrytis cinerea* and *Botrytis cinerea* co-cultured with various yeast species.

Antagonistic yeasts possess several mechanisms of action including competition for nutrients and space, production of cell wall degrading enzymes, VOCs and non-volatile compounds, as well as direct mycoparasitism (Freimoser et al., 2019). In the current study, yeast strains with antifungal activity against the tested pathogens secreted chitinases and β-1,3-glucanases in the presence of *B. cinerea* with variable concomitant reduction in chitin and glucan levels demonstrated in *B. cinerea* cell walls following exposure to *H. pseudoburtonii* as well as strains of *W. anomalus*, *L. elongisporus*. The reduction in these cell wall polysaccharides could partly be due to hydrolysis by the chitinases and glucanases. Indeed, a study by Tayel et al. (2013) observed a softening of the hyphal walls and an elastic texture in *Aspergillus flavus* hyphae exposed to chitinases and glucanases from *W. anomalus* (formerly *Pichia anomala*). This hyphal softening progressed into moderate hyphal lysis and finally complete hyphal degradation. Production of β-1,3 glucanases and chitinases by *W. anomalus* strains as part of its arsenal against different pathogens is well known (Lutz et al., 2013; Hong et al., 2017; Chen et al., 2018; Andrea et al., 2020; Cabañas et al., 2020). However, for *L. elongisporus* and *H. pseudoburtonii* this is the first report of

TABLE 4 Analysis of non-volatile organic compounds produced by *B. cinerea* (Bc), *H. pseudoburtonii* (Hp), *W. anomalus* (Wa) and *L. elongisporus* (Le).

RT (min)	[M+H]+	Compound name	Average peak height intensity						
			Bc	Hp	Le	Wa	Bc+Hp	Bc+Le	Bc+Wa
2.569	300.16891	cyclo(D-Leu-L-Trp)	17.33	63.33	476	24.33	69	99.33	20
3.335	229.15364	Leucylproline	304.66	273	287	356.33	648,33	305.66	400.33
3.965	197.12885	cyclo(L-Pro-L-Val)	298	372	633.33	366.66	467,33	326	322.33
4.624	211.14487	L,-Cyclo(leucylprolyl)	1341.33	1,224	3,388	1252.66	1,552,66	1377.33	1166.33

Compounds were analysed with UPLC-MS. Retention time (RT) and [M+H]+ of tentatively identified compounds by comparison with the NIST database.
Compounds were identified and confirmed by the retention time, structures and molecular weight by comparison with NIST database.

TABLE 5 *In vivo* test of the selected various yeast species against *Botrytis cinerea*.

Yeast strains	*B. cinerea* development
B. cinerea	4
L. elongisporus Y929	4
L. elongisporus Y996	4
H. pseudoburtonii Y963	3
W. anomalus Y934	2
W. anomalus Y541	2
W. anomalus Y517	2

The disease severity was evaluated by a visual score "1-to-4" (1, no visible symptoms; 2, soft rot; 3, formation of mycelium and 4, sporulation of mould).

their antifungal activity and the potential effect of their chitinase and glucanase activity on fungal cell wall composition.

Considering the negative effects of antagonistic yeast VOCs on fungal mycelial growth, spore germination and sporulation, selected yeast strains were evaluated for the production of VOCs in the presence of *B. cinerea*. The selected yeast strains released various VOCs in the presence of *B. cinerea*. The identified volatile compounds were grouped into different chemical families, such as higher alcohols, aldehydes, esters, organosulfur compounds, monoterpenes, ketones and aromatic hydrocarbons. In particular, phenylethyl alcohol, isoamyl alcohol, n-butanol, 2,5-dimethylpyrazine, seemingly originating from yeasts, remain moderately high in the challenge experiment. Furthermore, for some yeasts such as *W. anomalus* strains, dimethylsulfide and dimethyltrisulfide could still be detected in the challenge experiment albeit at lower levels compared to the yeast monoculture. Numerous studies on antagonistic yeast such as *A. pullulans*, *P. occidentalis*, *M. guilliermondii C. tropicalis*, *S. cerevisiae* and *P. kudriavzevii* revealed similar compounds as those found in this study. These compounds have been shown to effectively inhibit spore germination and mycelial growth of *B. cinerea*, *Aspergillus* and *Penicillium* species (Arrarte et al., 2017; Meshram et al., 2017; Choińska et al., 2020; Liu et al., 2020). Production of VOCs by antagonistic yeasts has been identified as a potential mode of action against a number of pathogens including *B. cinerea*, *Colletotrichum acutatum* and various *Penicillium* species such as *P. italicum*, *P. digitatum* and *P. expansum* under both *in vitro* and *in vivo* conditions. Compounds such as phenylethyl alcohol, n-butanol, isoamyl alcohol and 2-methyl-1-propanol have been shown to supress conidia germination and mycelium growth (di Francesco et al., 2016; Yalage Don et al., 2020; Zou et al., 2022). Furthermore, a compound like dimethyltrisulfide which is not frequently reported in yeast VOCs has been shown to suppress the expression of genes involved in the biosynthesis of β-1,3-D-glucan and chitin in another fruit rotting fungus, *Colletrichum gloeosporioides* (Tang et al., 2020). These data could suggest that to suppress the growth of phytopathogens a yeast like *W. anomalus* expresses various synergistic activities including production of cell wall degrading enzymes as well as VOCs that inhibit spore germination and biosynthesis of cell wall polysaccharides. The evaluation of the efficacy of yeasts in preventing *B. cinerea* development on table grapes showed a considerable decay reduction. *W. anomalus* revealed the highest efficacy in controlling the fungal development whereby only soft rots were recorded. Since the experiment was carried out in airtight containers, the suppression of *B. cinerea* growth in the presence of *W. anomalus* could confirm the production of diverse VOCs as a mode of action among others.

The selected antagonistic yeasts were found to produce in some cases slightly higher levels of cyclic peptides such as L,L-Cyclo(leucylprolyl), cyclo-(L-Phe-L-Pro) and cyclo-(L-Phe-L-Pro). In particular, cyclo(D-Leu-L-Trp) was abundant in *L. elongisporus* monoculture and remained high in the mixed culture with *B. cinerea*. Cyclic peptides inhibit fungal development by targeting fundamental features of the fungal cell wall constituents (Hur et al., 2012). Their production by bacteria has commonly been reported and several filamentous fungi have been shown to produce these compounds. In yeast, the most commonly encountered cyclic peptide is pulcherriminic acid produced by the yeast *Metschnikowia pulcherrima* (Gore-Lloyd et al., 2019). *Glaciozyma antarctica*, a psychrophilic yeast was also shown to produce a diversity of cyclic peptides (Rosandy et al., 2017). In the current study, the majority of the cyclic peptides were detected in both monocultures and mixed cultures, suggesting that their inhibitory activity may not play a role in these interactions, but this remains to be further unravelled.

Conclusion

Yeasts derived from grape must were found to be effective against the pathogens examined giving these yeasts potential to be developed and used as biocontrol agents. The efficacy of these yeast species can further be evaluated *in vivo* against various plant pathogens considering various environmental factors. This study

largely confirmed that various mechanisms including the pathogen cell wall degradation, inhibition of cell wall polysaccharide biosynthesis as well as inhibition of spore germination through the production of VOCs may be expressed in concert yeasts interacting with filamentous fungi. Moreover, our findings open a new area for further investigation into non-VOCs of yeast origin and their contribution to antifungal activity.

Data availability statement

The original contributions presented in the study are included in the article/Supplementary material, further inquiries can be directed to the corresponding author.

Author contributions

EM performed the experiments, analysed the data, and wrote the manuscript. NJ, HP, and MS conceived the experiments, supervised the experimental work, assisted in the interpretation of the data, and edited the manuscript. All authors contributed to the article and approved the submitted version.

Funding

This work is based on the research supported wholly by the National Research Foundation of South Africa (grant nos.: 118505 and 137960).

Acknowledgments

We thank Malcolm Taylor, Lucky Mokwena and Lindani Kotobe at the Central Analytical Facilities (CAF), Mass Spectrometry Unit, Stellenbosch University for analysis of VOCs and n-VOCs.

Conflict of interest

The authors declare that the research was conducted in the absence of any commercial or financial relationships that could be construed as a potential conflict of interest.

Publisher's note

All claims expressed in this article are solely those of the authors and do not necessarily represent those of their affiliated organizations, or those of the publisher, the editors and the reviewers. Any product that may be evaluated in this article, or claim that may be made by its manufacturer, is not guaranteed or endorsed by the publisher.

Supplementary material

The Supplementary material for this article can be found online at: https://www.frontiersin.org/articles/10.3389/fmicb.2022.986229/full#supplementary-material

References

Abbey, J. A., Percival, D., Abbey, L., Asiedu, S. K., Prithiviraj, B., and Schilder, A. (2019). Biofungicides as alternative to synthetic fungicide control of grey mould (*Botrytis cinerea*)–prospects and challenges. *Biocontrol Sci. Tech.* 29, 207–228. doi: 10.1080/09583157.2018.1548574

Agarbati, A., Canonico, L., Pecci, T., Romanazzi, G., Ciani, M., and Comitini, F. (2022). Biocontrol of non-*saccharomyces* yeasts in vineyard against the gray mold disease agent *Botrytis cinerea*. *Microorganisms* 10, 200. doi: 10.3390/microorganisms 10020200

Agrawal, T., and Kotasthane, A. S. (2012). Chitinolytic assay of indigenous *Trichoderma* isolates collected from different geographical locations of Chhattisgarh in Central India. *Springerplus* 1, 1–10. doi: 10.1186/2193-1801-1-73

Andrea, M., Mar, M., Pic, E., and Meinhardt, F. (2020). Killer yeasts for the biological control of postharvest fungal crop diseases. *Microorganisms* 8:11. doi: 10.3390/microorganisms8111680

Arrarte, E., Garmendia, G., Rossini, C., Wisniewski, M., and Vero, S. (2017). Volatile organic compounds produced by Antarctic strains of *Candida sake* play a role in the control of postharvest pathogens of apples. *Biol. Control* 109, 14–20. doi: 10.1016/j.biocontrol.2017.03.002

Bagheri, B., Bauer, F. F., and Setati, M. E. (2015). The diversity and dynamics of indigenous yeast communities in grape must from vineyards employing different agronomic practices and their influence on wine fermentation. *South African J. Enol. Vitic.* 36, 243–251. doi: 10.21548/36-2-957

Barata, A., Malfeito-Ferreira, M., and Loureiro, V. (2012). The microbial ecology of wine grape berries. *Int. J. Food Microbiol.* 153, 243–259. doi: 10.1016/j.ijfoodmicro.2011.11.025

Bleve, G., Grieco, F., Cozzi, G., Logrieco, A., and Visconti, A. (2006). Isolation of epiphytic yeasts with potential for biocontrol of *Aspergillus carbonarius* and *A. niger* on grape. *Int. J. Food Microbiol.* 108, 204–209. doi: 10.1016/j.ijfoodmicro.2005.12.004

Cabañas, C. M., Hernández, A., Martínez, A., Tejero, P., Vázquez-Hernández, M., Martín, A., et al. (2020). Control of *Penicillium glabrum* by indigenous antagonistic yeast from vineyards. *Foods* 9, 1–22. doi: 10.3390/foods9121864

Chen, P. H., Chen, R. Y., and Chou, J. Y. (2018). Screening and evaluation of yeast antagonists for biological control of *Botrytis cinerea* on strawberry fruits. *Mycobiology* 46, 33–46. doi: 10.1080/12298093.2018.1454013

Choińska, R., Piasecka-Jóźwiak, K., Chabłowska, B., Dumka, J., and Łukaszewicz, A. (2020). Biocontrol ability and volatile organic compounds production as a putative mode of action of yeast strains isolated from organic grapes and rye grains. *Antonie Van Leeuwenhoek* 113, 1135–1146. doi: 10.1007/s10482-020-01420-7

Comitini, F., Agarbati, A., Canonico, L., and Ciani, M. (2021). Yeast interactions and molecular mechanisms in wine fermentation. *Int. J. Mol. Sci.* 22:7754. doi: 10.3390/ijms22147754

Cordero-Bueso, G., Mangieri, N., Maghradze, D., Foschino, R., Valdetara, F., Cantoral, J. M., et al. (2017). Wild grape-associated yeasts as promising biocontrol agents against *Vitis vinifera* fungal pathogens. *Front. Microbiol.* 8:2025. doi: 10.3389/fmicb.2017.02025

di Canito, A., Mazzieri, M., Foschino, R., Cordero-bueso, G., and Vigentini, I. (2021). The role of yeasts as biocontrol agents for pathogenic fungi on postharvest grapes. *Foods* 10:1650. doi: 10.3390/foods10071650

di Francesco, A., Martini, C., and Mari, M. (2016). Biological control of postharvest diseases by microbial antagonists: how many mechanisms of action? *Eur. J. Plant Pathol.* 145, 711–717. doi: 10.1007/s10658-016-0867-0

Dlamini, N. R., and Dube, S. (2008). Studies on the physico-chemical, nutritional and microbiological changes during the traditional preparation of Marula wine in Gwanda, Zimbabwe. *Nutr. Food Sci.* 38, 61–69. doi: 10.1108/00346650810848025

Fredlund, E., Druvefors, U. Ä., Olstorpe, M. N., Passoth, V., and Schnürer, J. (2004). Influence of ethyl acetate production and ploidy on the anti-mould activity of Pichia anomala. *FEMS Microbiol. Lett.* 238, 33–137. doi: 10.1016/j.femsle.2004.07.027

Freimoser, F. M., Rueda-Mejia, M. P., Tilocca, B., and Migheli, Q. (2019). Biocontrol yeasts: mechanisms and applications. *World J. Microbiol. Biotechnol.* 35:154. doi: 10.1007/s11274-019-2728-4

Ghosh, S., Bagheri, B., Morgan, H. H., Divol, B., and Setati, M. E. (2015). Assessment of wine microbial diversity using ARISA and cultivation-based methods. *Ann. Microbiol.* 65, 1833–1840. doi: 10.1007/s13213-014-1021-x

Gore-Lloyd, D., Sumann, I., Brachmann, A. O., Schneeberger, K., Ortiz-Merino, R. A., Moreno-Beltrán, M., et al. (2019). Snf2 conttrol pulcherrimini acid biosynthesis and antifungal activity of the biocontrol yeast *Metschnikowia pulcherrima*. *Mol. Microbiol.* 112, 317–332. doi: 10.1111/mmi.14272

Griggs, R. G., Steenwerth, K. L., Mills, D. A., Cantu, D., and Bokulich, N. A. (2021). Sources and assembly of microbial communities in vineyards as a functional component of winegrowing. *Front. Microbiol.* 12:673810. doi: 10.3389/fmicb.2021.673810

Hong, S. H., Song, Y. S., Seo, D. J., Kim, K. Y., and Jung, W. J. (2017). Antifungal activity and expression patterns of extracellular chitinase and β-1,3-glucanase in *Wickerhamomyces anomalus* EG2 treated with chitin and glucan. *Microb. Pathog.* 110, 159–164. doi: 10.1016/j.micpath.2017.06.038

Hur, G. H., Vickery, C. R., and Burkart, M. D. (2012). Explorations of catalytic domains in non-ribosomal peptide synthetase enzymology. *Nat. Prod. Rep.* 29, 1074–1098. doi: 10.1039/c2np20025b

Jolly, N. P., Varela, C., and Pretorius, I. S. (2014). Not your ordinary yeast: non-*saccharomyces* yeasts in wine production uncovered. *FEMS Yeast Res.* 14, 215–237. doi: 10.1111/1567-1364.12111

Khunnamwong, P., Lertwattanasakul, N., Jindamorakot, S., Suwannarach, N., Matsui, K., and Limtong, S. (2020). Evaluation of antagonistic activity and mechanisms of endophytic yeasts against pathogenic fungi causing economic crop diseases. *Folia Microbiol.* 65, 573–590. doi: 10.1007/s12223-019-00764-6

Kuchen, B., Maturano, Y. P., Mestre, M. V., Combina, M., Toro, M. E., and Vazquez, F. (2019). Selection of native non-*saccharomyces* yeasts with biocontrol activity against spoilage yeasts in order to produce healthy regional wines. *Fermentation* 5:60. doi: 10.3390/fermentation5030060

Lahlali, R., Ezrari, S., Radouane, N., Kenfaoui, J., Esmaeel, Q., el Hamss, H., et al. (2022). Biological control of plant pathogens: a global perspective. *Microorganisms* 10:596. doi: 10.3390/microorganisms10030596

Liu, D., Chen, Q., Zhang, P., Chen, D., and Howell, K. S. (2020). The fungal microbiome is an important component of vineyard ecosystems and correlates with regional distinctiveness of wine. *mSphere* 5, e00534–e00520. doi: 10.1128/msphere.00534-20

Lutz, M. C., Lopes, C. A., Rodriguez, M. E., Sosa, M. C., and Sangorrín, M. P. (2013). Efficacy and putative mode of action of native and commercial antagonistic yeasts against postharvest pathogens of pear. *Int. J. Food Microbiol.* 164, 166–172. doi: 10.1016/j.ijfoodmicro.2013.04.005

Marsico, A. D., Velenosi, M., Perniola, R., Bergamini, C., Sinonin, S., David-vaizant, V., et al. (2021). Native vineyard non-*saccharomyces* yeasts used for biological control of botrytis cinerea in stored table grape. *Microorganisms* 9, 1–17. doi: 10.3390/microorganisms9020457

Meshram, V., Kapoor, N., Chopra, G., and Saxena, S. (2017). Muscodor camphora, a new endophytic species from Cinnamomum camphora. *Mycosphere* 8, 568–582. doi: 10.5943/mycosphere/8/4/6

Mewa-Ngongang, M., du Plessis, H. W., Hlangwani, E., Ntwampe, S. K. O., Chidi, B. S., Hutchinson, U. F., et al. (2019a). Activity interactions of crude biopreservatives against spoilage yeast consortia. *Fermentation* 5:53. doi: 10.3390/fermentation5030053

Mewa-Ngongang, M., du Plessis, H. W., Ntwampe, S. K. O., Chidi, B. S., Hutchinson, U. F., Mekuto, L., et al. (2019b). The use of *Candida pyralidae* and *Pichia kluyveri* to control spoilage microorganisms of raw fruits used for beverage production. *Foods* 8:454. doi: 10.3390/foods8100454

Nally, M. C., Pesce, V. M., Maturano, Y. P., Rodriguez Assaf, L. A., Toro, M. E., Castellanos de Figueroa, L. I., et al. (2015). Antifungal modes of action of *saccharomyces* and other biocontrol yeasts against fungi isolated from sour and grey rots. *Int. J. Food Microbiol.* 204, 91–100. doi: 10.1016/j.ijfoodmicro.2015.03.024

Ons, L., Bylemans, D., Thevissen, K., and Cammue, B. P. A. (2020). Combining biocontrol agents with chemical fungicides for integrated plant fungal disease control. *Microorganisms* 8, 1–19. doi: 10.3390/microorganisms8121930

Oro, L., Feliziani, E., Ciani, M., Romanazzi, G., and Comitini, F. (2018). Volatile organic compounds from *Wickerhamomyces anomalus*, *Metschnikowia pulcherrima* and *Saccharomyces cerevisiae* inhibit growth of decay causing fungi and control postharvest diseases of strawberries. *Int. J. Food Microbiol.* 265, 18–22. doi: 10.1016/j.ijfoodmicro.2017.10.027

Parafati, L., Vitale, A., Restuccia, C., and Cirvilleri, G. (2015). Biocontrol ability and action mechanism of food-isolated yeast strains against *Botrytis cinerea* causing post-harvest bunch rot of table grape. *Food Microbiol.* 47, 85–92. doi: 10.1016/j.fm.2014.11.013

Pereyra, M. M., Díaz, M. A., Soliz-Santander, F. F., Poehlein, A., Meinhardt, F., Daniel, R., et al. (2021). Screening methods for isolation of biocontrol epiphytic yeasts against *Penicillium digitatum* in lemons. *J. Fungi* 7, 1–13. doi: 10.3390/jof7030166

Piasecka-jo, K., and Choin, R. (2020). Biocontrol ability and volatile organic compounds production as a putative mode of action of yeast strains isolated from organic grapes and rye grains. *Antonie Leeuwenhoek* 113, 1135–1146. doi: 10.1007/s10482-020-01420-7

Porter, T. J., Divol, B., and Setati, M. E. (2019). Investigating the biochemical and fermentation attributes of *Lachancea* species and strains: deciphering the potential contribution to wine chemical composition. *Int. J. Food Microbiol.* 290, 273–287. doi: 10.1016/j.ijfoodmicro.2018.10.025

Pretscher, J., Fischkal, T., Branscheidt, S., Jäger, L., Kahl, S., Schlander, M., et al. (2018). Yeasts from different habitats and their potential as biocontrol agents. *Fermentation* 4:31. doi: 10.3390/fermentation4020031

Rollero, S., Bloem, A., Ortiz-Julien, A., Camarasa, C., and Divol, B. (2018). Fermentation performances and aroma production of non-conventional wine yeasts are influenced by nitrogen preferences. *FEMS Yeast Res.* 18:foy055. doi: 10.1093/femsyr/foy055

Rosandy, A. R., Abu Bakar, M., Abdul Rahman, N. N., Abdul Murad, A. M., Muhamad, A., and Khalid, R. M. (2017). Diketopiperazine produced by psychrophilic yeast *Glaciozyma antarctica* PI12. *Malaysian J. Anal. Sci.* 21, 1243–1249. doi: 10.17576/mjas-2017-2106-05

Rossouw, D., and Bauer, F. F. (2016). Exploring the phenotypic space of non-*saccharomyces* wine yeast biodiversity. *Food Microbiol.* 55, 32–46. doi: 10.1016/j.fm.2015.11.017

Sabaghian, S., Braschi, G., Vannini, L., Patrignani, F., Samsulrizal, N. H., and Lanciotti, R. (2021). Isolation and identification of wild yeast from Malaysian grapevine and evaluation of their potential antimicrobial activity against grapevine fungal pathogens. *Microorganisms* 9:2582. doi: 10.3390/microorganisms9122582

Sasidharan, K., Soga, T., Tomita, M., and Murray, D. B. (2012). A yeast metabolite extraction protocol optimised for time-series analyses. *PLoS One* 7, 1–10. doi: 10.1371/journal.pone.0044283

Schusterova, D., Hajslova, J., Kocourek, V., and Pulkrabova, J. (2021). Pesticide residues and their metabolites in grapes and wines from conventional and organic farming system. *Foods* 10:307. doi: 10.3390/foods10020307

Setati, M. E., Jacobson, D., Andongm, U.-C., and Bauer, F. (2012). The vineyard yeast microbiome, a mixed model microbial map. *PLoS One* 7:e52609. doi: 10.1371/journal.pone.0052609

Shekhawat, K., Porter, T. J., Bauer, F. F., and Setati, M. E. (2018). Employing oxygen pulses to modulate *Lachancea thermotolerans–Saccharomyces cerevisiae* chardonnay fermentations. *Ann. Microbiol.* 68, 93–102. doi: 10.1007/s13213-017-1319-6

Steel, C. C., Blackman, J. W., and Schmidtke, L. M. (2013). Grapevine bunch rots: impacts on wine composition, quality, and potential procedures for the removal of wine faults. *J. Agric. Food Chem.* 61, 5189–5206. doi: 10.1021/jf400641r

Tang, L., Mo, J., Guo, T., Huang, S., Li, Q., Ning, P., et al. (2020). In vitro antifungal activity of dimethyl trisulfide against Colletotrichum gloeosporioides from mango. *World J. Microbiol. Biotechnol.* 36, 1–15. doi: 10.1007/s11274-019-2781-z

Tayel, A. A., El-Tras, W. F., Moussa, S. H., and El-Agamy, M. A. (2013). Antifungal action of *Pichia anomala* against aflatoxigenic Aspergillus flavus and its application as a feed supplement. *J. Sci. Food Agr.* 93, 3259–3263. doi: 10.1002/jsfa.6169

Varela, C., and Borneman, A. R. (2017). Yeasts found in vineyards and wineries. *Yeast* 34, 111–128. doi: 10.1002/yea.3219

Vejarano, R., and Gil-Calderón, A. (2021). Commercially available non-*saccharomyces* yeasts for winemaking: current market, advantages over *saccharomyces*, biocompatibility, and safety. *Fermentation* 7:3. doi: 10.3390/fermentation7030171

Wang, X., Glawe, D. A., Kramer, E., Weller, D., and Okubara, P. A. (2018). Biological control of *Botrytis cinerea*: interactions with native vineyard yeasts from Washington state. *Phytopathology* 108, 691–701. doi: 10.1094/PHYTO-09-17-0306-R

Yalage Don, S. M., Schmidtke, L. M., Gambetta, J. M., and Steel, C. C. (2020). *Aureobasidium pullulans* volatilome identified by a novel, quantitative approach employing SPME-GC-MS, suppressed *Botrytis cinerea* and *Alternaria alternata in vitro*. *Sci. Rep.* 10:4498. doi: 10.1038/s41598-020-61471-8

Zhang, X., Li, B., Zhang, Z., and Chen, Y. (2020). Antagonistic yeasts: A promising alternative to chemical fungicides for controlling postharvest decay of fruit. *Journal of Fungi* 6:158. doi: 10.3390/jof6030158

Zou, X., Wei, Y., Jiang, S., Cao, Z., Xu, F., Wang, H., et al. (2022). Volatile organic compounds and rapid proliferation of *Candida pseudolambica* W16 are modes of action against gray mold in peach fruit. *Postharvest Biol. Technol.* 183:111751. doi: 10.1016/j.postharvbio.2021.111751

frontiers | Frontiers in Microbiology

TYPE Original Research
PUBLISHED 24 August 2022
DOI 10.3389/fmicb.2022.987844

OPEN ACCESS

EDITED BY
Khamis Youssef,
Agricultural Research Center,
Egypt

REVIEWED BY
Elsherbiny A. Elsherbiny,
Mansoura University,
Egypt
Sheng Qin,
Jiangsu Normal University,
China

*CORRESPONDENCE
Lijun Ling
13919343210@163.com

SPECIALTY SECTION
This article was submitted to Food Microbiology, a section of the journal Frontiers in Microbiology

RECEIVED 06 July 2022
ACCEPTED 03 August 2022
PUBLISHED 24 August 2022

CITATION
Ling L, Luo H, Yang C, Wang Y, Cheng W, Pang M and Jiang K (2022) Volatile organic compounds produced by *Bacillus velezensis* L1 as a potential biocontrol agent against postharvest diseases of wolfberry.
Front. Microbiol. 13:987844.
doi: 10.3389/fmicb.2022.987844

Volatile organic compounds produced by *Bacillus velezensis* L1 as a potential biocontrol agent against postharvest diseases of wolfberry

Lijun Ling[1,2,3]*, Hong Luo[1,2], Caiyun Yang[1,2], Yuanyuan Wang[1,2], Wenting Cheng[1,2], Mingmei Pang[1,2] and Kunling Jiang[1,2]

[1]College of Life Science, Northwest Normal University, Lanzhou, China, [2]Bioactive Products Engineering Research Center for Gansu Distinctive Plants, Northwest Normal University, Lanzhou, China, [3]New Rural Development Research Institute, Northwest Normal University, Lanzhou, China

Volatile organic compounds (VOCs) produced by antagonistic microorganisms have good biocontrol prospects against postharvest diseases. Infection caused by *Alternaria iridiaustralis* and 10 other significant fungal diseases can be successfully inhibited by VOCs produced by an identified and screened endophytic strain L1 (*Bacillus velezensis*). This study revealed the *in vivo* and *in vitro* biocontrol effects of VOCs released by *B. velezensis* L1 on *A. iridiaustralis*, a pathogenic fungus responsible for rot of wolfberry fruit. The inhibition rates of VOCs of *B. velezensis* L1 on the mycelial growth of *A. iridiaustralis in vitro* were 92.86 and 90.30%, respectively, when the initial inoculum concentration on the plate was 1×10^9 colony forming unit (CFU)/ml. Spore germination and sporulation were 66.89 and 87.96%, respectively. VOCs considerably decreased the wolfberry's disease index and decay incidence *in vivo*. Scanning electron microscopy revealed that the morphological and structural characteristics of *A. iridiaustralis* could be altered by VOCs. Ten VOCs were identified through headspace-gas chromatography-ion mobility spectrometry. Pure chemical tests revealed that 2.3-butanedione had the strongest antifungal effects, totally inhibiting *A. iridiaustralis* in wolfberry fruit at a 60 μl/L concentration. The theory underpinning the potential application of VOCs from *B. velezensis* is provided herein. This is also the first study to document the antifungal capabilities of the *B. velezensis* strain on postharvest wolfberry fruit.

KEYWORDS

volatile organic compounds, *Bacillus velezensis* L1, *Alternaria iridiaustralis*, wolfberry disease, biological control

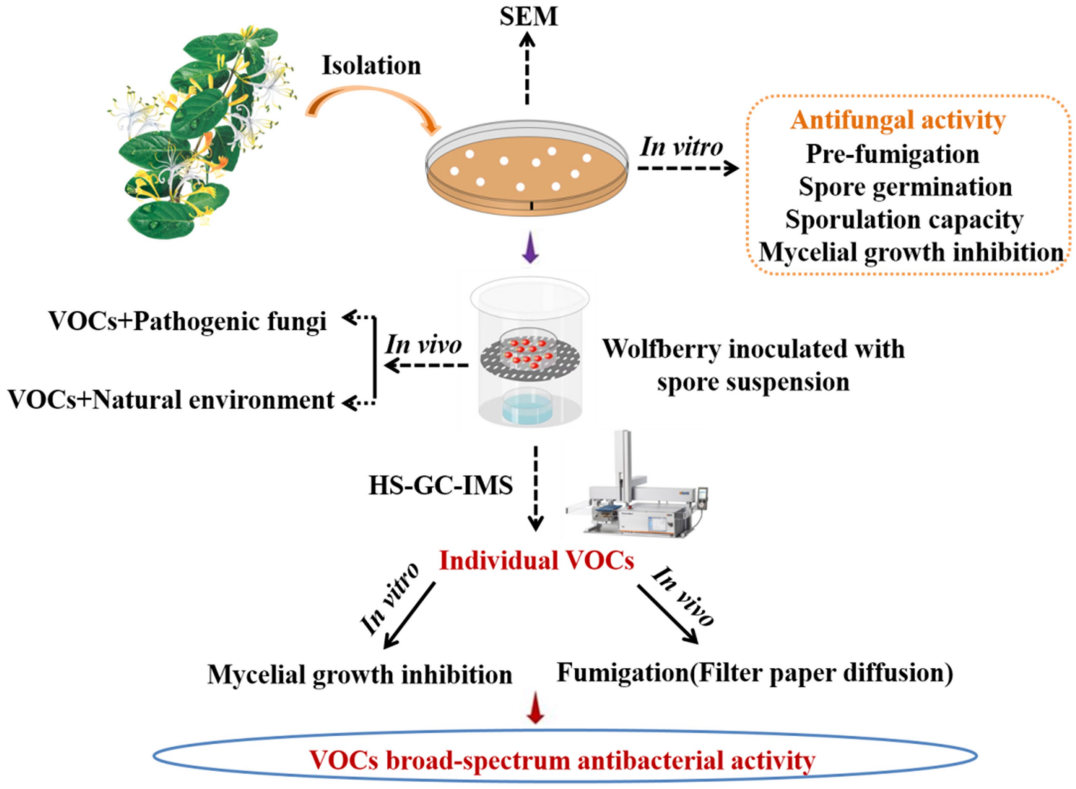

GRAPHICAL ABSTRACT

Introduction

Wolfberry (*Lycium barbarum* L) is gradually becoming one of the most popular functional fruits worldwide as it is rich in nutrients and phytochemicals (Wenli et al., 2021). Wolfberry has anticancer, antioxidant, antiaging, blood sugar control, and immune-enhancing properties. Therefore, this fruit is widely used in food and medicine fields (Zhou et al., 2017; Yajun et al., 2019). However, wolfberry fruit is highly perishable because of its susceptibility to various postharvest pathogenic diseases. Fungal diseases are the main cause of postharvest losses of wolfberry fruits. Particularly, *Alternaria* sp. are the most common postharvest pathogenic fungi of wolfberry fruits and can significantly reduce the fruit value and shelf life, causing severe economic losses (Yuan et al., 2012; Wei et al., 2017).

Regarding postharvest diseases of fruits, traditional physical methods can delay senescence but cannot completely prevent rot, which ultimately reduces fruit quality (Alijani et al., 2019). On the other hand, chemical fungicides have a substantial inhibitory effect on pathogenic fungi, but their long-term and large-scale use leads to deposition of residues in the environment and resistance of pathogenic fungi (Mari et al., 2016). Therefore, finding new, safe, efficient, and environmentally friendly methods for controlling these diseases is of great significance.

Increasing number of researchers have recently focused on biological control agents (BCAs; Do Kim et al., 2020). According to research, many bacteria can produce volatile organic compounds (VOCs) with antifungal function, which have shown strong inhibitory effects on fungal diseases (Di Francesco et al., 2020a). Gotor-Vila et al. (2017) reported that VOCs produced by *Bacillus amyloliquefaciens* CPA-8 significantly inhibited the mycelial growth of postharvest pathogens and reduced the rot of cherry fruits. Arrarte et al. (2017) revealed that VOCs released by *Candida sake* can control decay of apples caused by postharvest pathogens. Similarly, Oro et al. (2018) found that VOCs from *Wickerhamomyces anomalus*, *Metschnikowia pulcherrima*, and *Saccharomyces cerevisiae* can inhibit pathogenic fungi that cause rot in strawberries and control postharvest diseases. In this way, VOCs released by BCAs provide a new solution for the prevention and treatment of postharvest diseases.

VOCs have the characteristics of strong permeability and high diffusion efficiency, and are easy degradation, can greatly reduce residues. In a relatively closed environment, a full range of biological fumigation can be performed on items to achieve better results (Qin et al., 2017; Toffano et al., 2017). Therefore, compared with chemical fungicides, the mode of action of VOCs produced by BCAs is safer and more efficient. *B. velezensis* has been widely studied because of its highly effective inhibitory effect on pathogenic microorganisms.

Li et al. (2020) reported that VOCs from *B. velezensis* CT32 could inhibit strawberry vascular wilt pathogens *Verticillium dahliae* and *Fusarium oxysporum*. Gao et al. (2017) indicated that VOCs emitted by *B. velezensis* ZSY-1 could inhibit *A. solani* and *Botrytis cinerea*. Calvo et al. (2020) showed that VOCs produced by *B. velezensis* strains BUZ-14, I3 and I5 could inhibit postharvest fungal pathogens of fruits, thereby reducing the disease severity in grapes and apricots. *B. velezensis* is considered a promising BCA against postharvest fungal diseases.

Currently, research on postharvest preservation of wolfberry fresh fruit fruits is lacking. Therefore, this study evaluated the *in vivo* and *in vitro* effects of VOCs produced by *B. velezensis* L1 and individual pure substance against postharvest pathogenic fungi *A. iridiaustralis* in wolfberry fruit.

Materials and methods

Fruit and plants

The wolfberry fruit was purchased from Ningxia, Gansu. Fully ripe fruits of the same size and without any mechanical damage were sterilized with 1% sodium hypochlorite, rinsed three times with sterile distilled water (SDW), and air-dried naturally on an ultra-clean bench.

Lonicera maackii (Rupr.) Maxim is from Lanzhou Botanical Garden, Gansu, China. Picked stems and leaves were stored in airtight bags and kept at 4°C for later use.

Culture media and microorganisms

Tianqi Gene Biotechnology Co., Ltd. provided Luria–Bertani medium (LB) and potato dextrose agar medium (PDA; Lanzhuo, China). Agar was purchased from Niuniu Biochemical Co., Ltd. (Lanzhuo, China).

Wolfberry fungal pathogen *A. iridiaustralis* LB7 (MN 944921) was supplied by the College of Life Sciences, Northwest Normal University, China's Plant-Microbe Interactions Research Lab. This pathogen has been demonstrated to significantly worsen postharvest wolfberry deterioration in our previous study (Ling et al., 2021). *A. iridiaustralis* was inoculated on PDA at 28°C for 7 days, the fungal spores were resuspended in SDW, and the concentration of the spore suspension was adjusted to 1×10^5 spores/mL with a hemocytometer.

Pathogenic fungi *Phytophthora capsici* (ACCC 37132), *Colletotrichum capsici* (ACCC 36946), *F. oxysporum* (ACCC 39326), *B. cinerea* (ACCC 37347), *Rhizoctonia solani* (ACCC 38870), *F. graminearum* (ACCC 39334) were obtained from Agricultural Culture Collection of China, Beijing. *F. annulatum* (MT 434004), *Talaromyces tumuli* (MT 434003), *Colletotrichum fioriniae* (MN 944922), and *F. arcuatisporum* (MN 944920) were isolated from disease plants and all pathogenic strains were stored in the laboratory (Ling et al., 2021).

Isolation, screening and identification of a highly antifungal bacterial endophyte

Using our previous technique, we isolated and characterized endophytic bacteria from *L. maackii* (Rupr.) Maxim (Ling et al., 2019). Briefly, the fresh stems and leaves stored in the refrigerator were removed, rinsed under running water, air-dried naturally, sterilized, and rinsed three times with sterile water. Next, the stems and leaves were cut using a sterile scalpel and cultured in solid LB medium plates at 37°C. Each colony was transferred to new medium until a pure culture of the strain is obtained. Using the two sealed base plate approach, the strain with the greatest capacity to suppress the pathogenic fungus was selected for further investigation. In general, 80 µl of bacterial suspension was evenly distributed on LB solid medium. Subsequently, a 6 mm-diameter fungal disk was cut and placed in the center of a sterile PDA petri dish. The two plates were sealed to prevent the loss of VOCs. The bacteriostatic ability of endophytic bacteria against pathogenic fungi was evaluated on the basis of the diameter of the fungus.

The bacterial DNA template obtained by screening was extracted using of the bacterial genome extraction kit (Huada Gene Co., Ltd., Wuhan, China). The 16S rDNA fragment was amplified through PCR by using universal primers 27F (5′AGAGTTTGAT CCTGGCTCAG3′) and 1429R (5′GGTTACCTTGTTACGAC TT3′). The cycle parameters were as follows: predenaturation at 96°C for 5 min, followed by 30 cycles of denaturation at 96°C for 30 s, annealing at 62°C for 30 s, and a final extension at 72°C for 30 s. The extension was performed at 72°C for 10 min at the end of the cycle. PCR products were detected through 1% agarose gel electrophoresis and sequenced. The sequencing results of 16S rDNA were input into the nucleic acid database alignment system of the National Center for Biological Information (NCBI) website, and nucleic acid sequence alignment analysis was performed using the Blast program. A Phylogenetic tree was constructed using the neighbor-joining method with MEGA-X software to analyze the phylogenetic relationship.

In vitro inhibitory activity of VOCs from *Bacillus Velezensis* L1

Inhibitory activity of VOCs with different inoculation concentrations of *Bacillus Velezensis* L1

A dual culture method was used to evaluate the inhibitory effect of antagonistic bacteria produced VOCs on *A. iridiaustralis* mycelial growth and conidial germination (Ye et al., 2020; Di Francesco et al., 2020b). SDW was used to inoculate the control plates with the same amounts of bacteria as the test plates, which was 80 µl of bacterial suspension at a concentration of 10^6–10^9 colony forming units (CFU)/ml. The plate cover was then changed out by a PDA plate that had been injected with a 6 mm-diameter disk or 20 µl of *A. iridiaustralis* spore suspension. Both plates were immediately sealed with parafilm, and cultured for 7 days at 28°C. Each experiment was conducted three times.

Effect of VOCs from *Bacillus velezensis* L1 on the spore germination and sporulation capacity of *Alternaria iridiaustralis*

With a few minor adjustments, the preceding approach was used to measure spore germination and sporulation capacity (Bu et al., 2021; Wang et al., 2021b). LB plates were inoculated with strain L1 and PDA plates were covered with a fungal spore suspension (1×10^5 spores/mL), as indicated earlier. After 12 h incubation at 28°C, spore germination could be visualized under a light microscope. The sporulation capacity experiment was conducted according to instructions provided in Section 2.4.1. In general, a 6 mm fungal plug was removed from the cultivated PDA medium and vortexed in SDW. A hemocytometer was used to count the spores.

Effect of VOC prefumigation on mycelium growth

The LB plate coated with the 80 µl bacterial suspension and the PDA plate containing a 6 mm-diameter disk were snap-sealed. After 4 or 5 days of fumigation in the incubator, 6 mm-diameter disks were cut from the PDA plate by using a punching bear, transferred to a new PDA plate, and incubated at 28°C for 7 days. Then, mycelial growth of pathogenic fungi were measured.

Scanning electron microscopy analysis

The effect of VOCs produced by *B. velezensis* L1 on pathogenic fungi was observed using scanning electron microscopy (SEM). SEM analysis was performed as described previously (Wonglom et al., 2020).

In vivo biocontrol of *Alternaria iridiaustralis* on wolfberry fruit by VOCs from *Bacillus velezensis* L1

Inhibitory effects of VOCs on *Alternaria iridiaustralis in vivo*

The biocontrol effects of different initial amounts of VOCs *in vivo* were investigated using different numbers of plates. LB plates were treated with 80 µl bacterial suspension (1×10^8 CFU/ml), and these uncovered plates were then placed at the bottom of sterile glass containers in numbers of 2, 4, 6, and 8, respectively. Then, 5 µl of *A. iridiaustralis* spore suspension was inoculated into wolfberry fruits. After inoculation, the fruits were placed in sterile petri dishes and placed on top of glass containers. The container was sealed and incubated at room temperature for 7 days. The decay incidence and disease index of the wolfberry fruits were measured using previous methods (Xu et al., 2016).

Effect of VOCs on wolfberry fruit postharvest natural decay

Untreated wolfberry fruits were treated with different numbers of LB plates, and after fumigation for 7 days at room temperature, the decay incidence and disease index were measured.

Identification of VOCs

The method used for identifying VOC components of *B. velezensis* L1 is consistent with that described in our previous study (Ling et al., 2021). Then, 10 µl of the bacterial suspension of strain L1 was inoculated into a 20-mL headspace vial containing 5 ml of solid LB medium. The solid LB medium without the strain was used as a blank control, and each sample was repeated three times. After incubating the vials for 3 days in a 37°C incubator, the headspace-gas chromatography-ion mobility spectrometry (HS-GC-IMS) assay was performed. VOCs were collected and sent to the G.A.S. Department of Shandong HaiNeng Science Instrument Co., Ltd. (Shandong, China) for measurement using the HS-GC-IMS instrument (FlavourSpec®). The sample was incubated at 40°C for 15 min, and VOCs from the 500 µL headspace were injected into the testing instrument using a heated syringe (85°C). GC equipped with the MXT-5 column (15 m, ID: 0.53 mm df: 1 µm) was used for chromatographic separation at 60°C. Pure nitrogen (99.999% purity) was used as the carrier gas. The flow of drift gas (nitrogen) of the IMS was set to 150 ml/min, and a 9.8 cm drift tube was operated at a constant voltage at 45°C. The program was as follows: 2 ml/min for 2 min, 10 ml/min for 10 min, and 100 ml/min for 20 min. Data were acquired and processed using instrumental analysis software such as VOCal and Reporter, Gallery plot, Dynamic PCA, and GC × IMS Library. The GC-IMS Library Search software uses the National Institute of Standards and Technology database and IMS database for qualitative analysis of the components.

In vitro responses of *Alternaria iridiaustralis* to a single component of VOC

The pathogenic fungus *A. iridiaustralis* was grown on PDA medium at 28°C for 7 days. Using a punching bear, a 6 mm-diameter disks were removed from the PDA plate's edge and placed one by one in the center of each fresh petri plate. A sterile filter paper (diameter: 6 mm) was placed in the center of the petri dish lid. Then, equal volumes of each individual pure VOC (Table 1) were added to increase the air concentration from 20 µl/L to 100 µl/L. An identical volume of SDW was used for the control. A Vernier caliper was used to measure the plug diameter before the petri dishes were sealed and grown for 4 days at 28°C.

In vivo control of *Alternaria iridiaustralis* on wolfberry fruit by pure synthetic components of VOCs

A single VOC component was chosen for additional testing *in vivo* based on the outcomes of *in vitro* testing. Fruits were infected and placed in a sterile petri plate. Then, the decay incidence and disease index of wolfberry fruit was determined with various quantities of pure components.

Broad antagonistic activity of strain L1

We determined whether strain L1 has broad-spectrum antifungal activity against other significant fungal infections. Twelve pathogens were used in our test, namely *P. capsici*, *C. capsici*, *F. oxysporum*, *B. cinerea*, *R. solani*, *F. graminearum*, *F. annulatum*, *T. tumuli*, *C. fioriniae* and *F. arcuatisporum*. The following formula was used to compute the percentage of mycelial growth inhibition:

$$\text{Inhibition rate (\%)} = [(dc - dt)/dc] \times 100$$

Where the terms dc (cm) represent the average colony diameters of the control and treatment groups, respectively.

Statistical analysis

SPSS 20.0 software was used to perform statistical analyses. Followed by the Duncan's test, $p < 0.05$ was set to indicate a statistically significant difference. Drawn with the Origin 9.0 software, by measuring three independent replicates, all data were reported as the mean ± standard error.

TABLE 1 Pure components comprising the VOCs of *Bacillus velezensis* L1, these substances were purchased for further experiments.

Compound	CAS	Source	Purity
2,3-butanedione	C431038	Macklin	≥99.0%
1-Hydroxy-2-propanone	C116096	Macklin	≥95.0%
Acetoin	C513860	Macklin	≥97.0%
2-pentanone	C107879	Macklin	≥99.0%
2-heptanone	C110430	Macklin	≥99.7%
Cyclohexanone	C108941	Macklin	≥99.0%
methyl 2-methylbutanoate	C868575	Macklin	≥98.0%
2-Pentylfuran	C3777693	Macklin	≥98.0%
2-methylpropyl butanoate	C539902	Macklin	≥98.0%

Results

Identification of strain L1 using morphological and molecular markers

An endophyte (strain L1) was obtained from *L. maackii* (Rupr.) Maxim (Figure 1A). The strain L1 exhibited phenotypic similarity to the *Bacillus* spp. with respect to the biochemical, morphological, Gram staining, and cultural characteristics. Nucleotide blast on NCBI revealed that strain L1 shared extremely high similarity with *Bacillus velezensis* species (99%). On the basis of the strain L1 16S rRNA's sequence and blast alignment results, MEGA-X was employed to construct a phylogenetic neighbor connection tree that reflected the evolutionary relationship for L1 (Figure 1B). Combining all the resulting analyses, the isolate was identified to be *B. velezensis* (GenBank Accession No. ON340771).

In vitro antifungal activity of VOCs

Figure 2 presents the findings related to the antifungal activity of VOCs produced by *B. velezensis* L1. Mycelial development, spore germination, and sporulation ability of A. iridiaustralis were significantly ($p < 0.05$) inhibited by VOCs produced by strain L1. An increased inoculum concentration of *B. velezensis* L1 improved VOC-induced inhibition. Furthermore, increasing the concentration also enhanced the inhibitory effect of VOCs on pathogenic fungi.

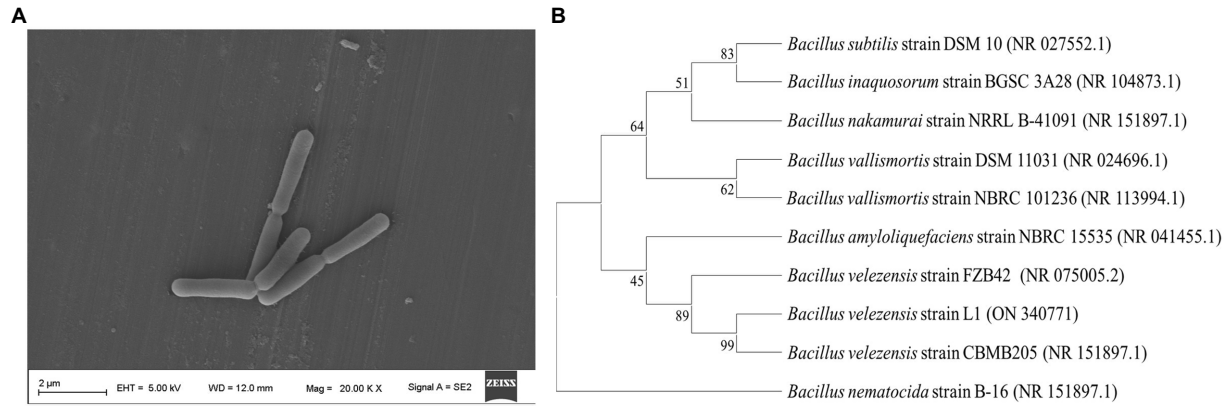

FIGURE 1
(A) Morphological characteristics of *B. velezensis* L1 detected by a scanning electron microscope. **(B)** Neighbor-joining tree of the *B. velezensis* L1 and its closely related species with the MEGA-X and 16S ribosomal RNA-sequencing data. The numbers at the nodes support the values derived from the MEGA-X bootstrap analysis.

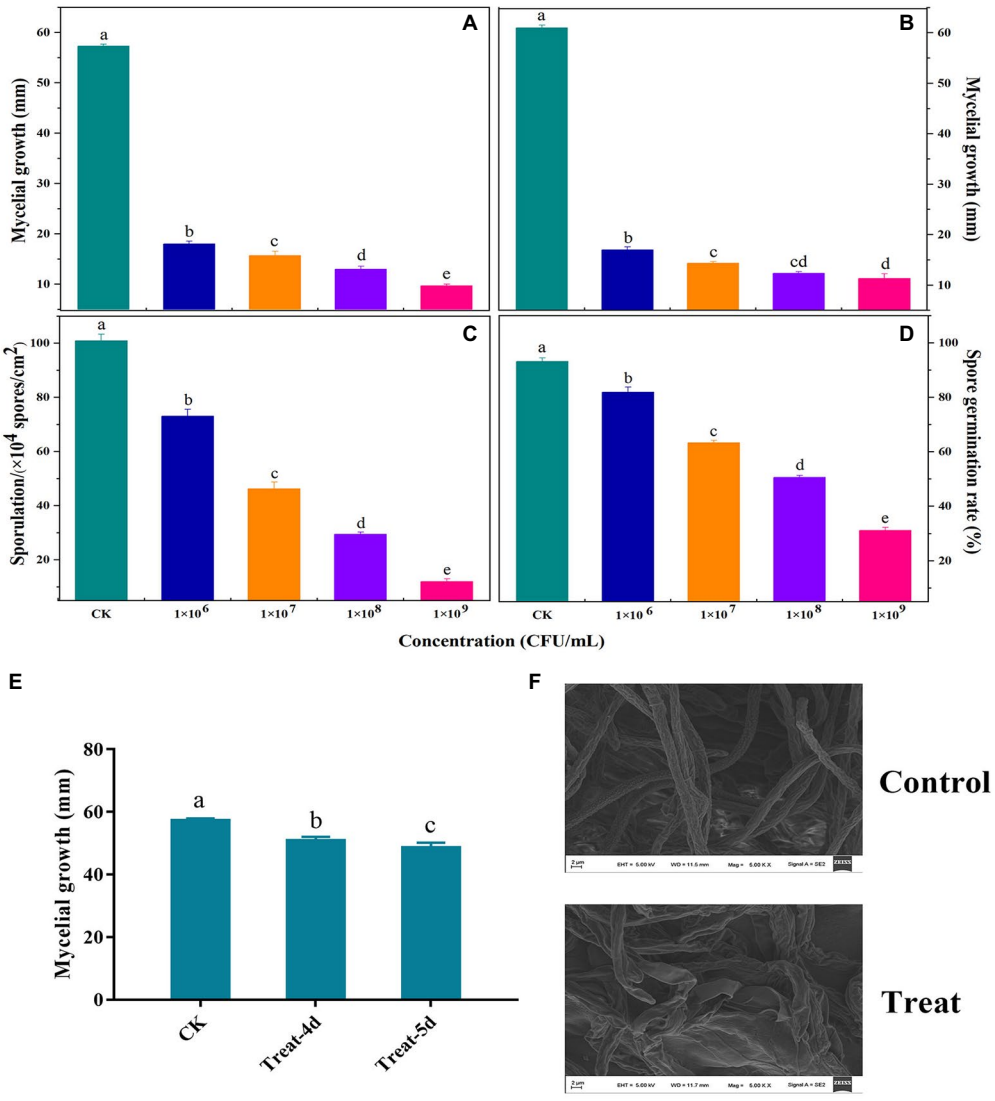

FIGURE 2
Antifungal activity of volatile organic compounds (VOCs) released by *B. velezensis* L1 against *A. iridiaustralis in vitro*. LB plates were coated with 80 μl of bacterial suspension at the concentration of 10^6, 10^7, 10^8, 10^9 colony forming units (CFU)/ml and then incubated at 37°C for 2 days. Their lids were subsequently replaced with PDA plates containing a 6 mm-diameter fungal disk or 20 μl of spore suspension of *A. iridiaustralis*. These plates were incubated at 28°C for 7 days. **(A)** Mycelial growth inhibition of a fungal disk of *A. iridiaustralis* on PDA plates exposed to VOCs at different concentrations. Different letters in represent differences ($p < 0.05$) among groups. **(B)** Mycelial growth inhibition 20 μl of spore suspension of *A. iridiaustralis* on PDA plates exposed to VOCs. Effect of VOCs produced by *B. velezensis* L1 suspension at different concentrations on sporulation **(C)** and spore germination **(D)** of *A. iridiaustralis*. Data are presented as means ± SE with three replicates. **(E)** Mycelial of *A. iridiaustralis* was fumigated with VOCs for 4 and 5 days, then a 6-mm-diameter fungal disk was inoculated on fresh PDA plates, after incubated at 28°C for 7 days, the diameter of the mycelium was measured. **(F)** Scanning electronic micrographs of *A. iridiaustralis* in the absence and presence of the VOCs produced by *B. velezensis* L1 strain.

The mycelial growth of plug and spore suspensions was inhibited by the bacterial suspension at 1×10^9 CFU/ml by approximately 92.86 and 90.30%, respectively (Figures 2A,B); the spore germination and sporulation processes were inhibited by 33.11 and 12.04%, respectively (Figures 2C,D). *A. iridiaustralis* fumigated with VOCs grew more slowly than usual, as observed in (Figure 2E). The hyphal morphology of pathogenic fungi are dramatically altered by VOCs, as observed through SEM. The treatment group's hyphae were twisted, flattened, enlarged, and lost their linearity compared with the control group (Figure 2F).

In vivo biocontrol effects of VOCs

To investigate the impact of VOC concentration on the effectiveness of biocontrol ability of VOC *in vivo*, various numbers of LB plates containing viable cells were used. VOCs considerably

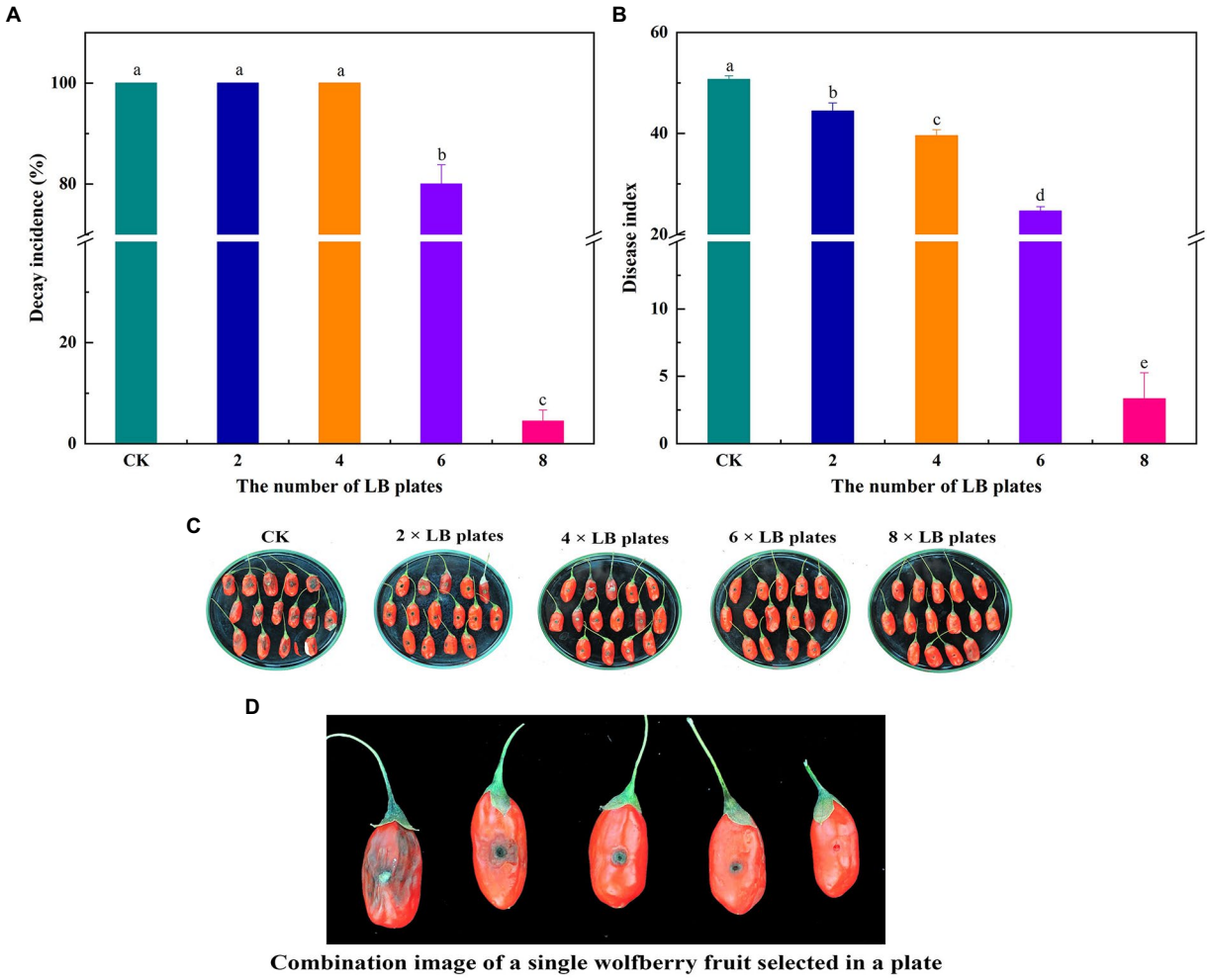

FIGURE 3
Fruits were fumigated with 2, 4, 6 and 8 LB plates, respectively, and the decay incidence **(A)** and disease index **(B)** were calculated according to the disease severity of the fruit infected with *A. iridiaustralis*. Biocontrol of wolfberry rot by biofumigation with different numbers of LB plates **(C)**. Combination image of a single wolfberry fruit selected in a plate **(D)**. Columns with different lower-case letters within the same panel are significantly different at $p<0.05$ level according to Duncan's multiple range test.

impeded the growth and spread of *A. iridiaustralis* (Figure 3). No mycelial was observed growth on the wolfberry fruits after exposure to the 8 LB plates. The decay incidence and disease index of the treatment group were 4.45 and 3.33%, respectively, which were considerably lower than those of the control group (100 and 50.67%, respectively). In general, biological control effects were better at higher VOC concentrations.

Effect of VOCs on postharvest natural decay

Figure 4 demonstrates the outcomes of the impact of VOCs on the fruit's natural decay after harvest. Under natural circumstances, the VOCs generated by *B. velezensis* L1 had a larger inhibitory effect on the decay incidence of postharvest wolfberry as the number of LB plates increased. The best inhibitory effect was observed when 8 LB plates were used, the wolfberry fruit was intact, and the lowest disease index was 3.33.

HS-GC-IMS identification of VOCs

From Figure 5, the whole VOC information of each sample as well as the variations in VOCs across samples can be observed when each row represents all signal peaks selected in a single sample and each column represents the signal peaks of the same VOC in numerous samples. The chemical's concentration is qualitatively represented by the hues of the peaks; the higher the red color, the higher the concentration. Table 2 lists a collection of specific details. Strain L1 produced the following recognized VOCs: 2-butanone, 2,3-butanedione, 1-hydroxy-2-propanone, 2-pentanone, acetoin, 2-heptanone, cyclohexanone, methyl 2-methylbutanoate, 2-pentylfuran, and 2-methylpropyl butanoate.

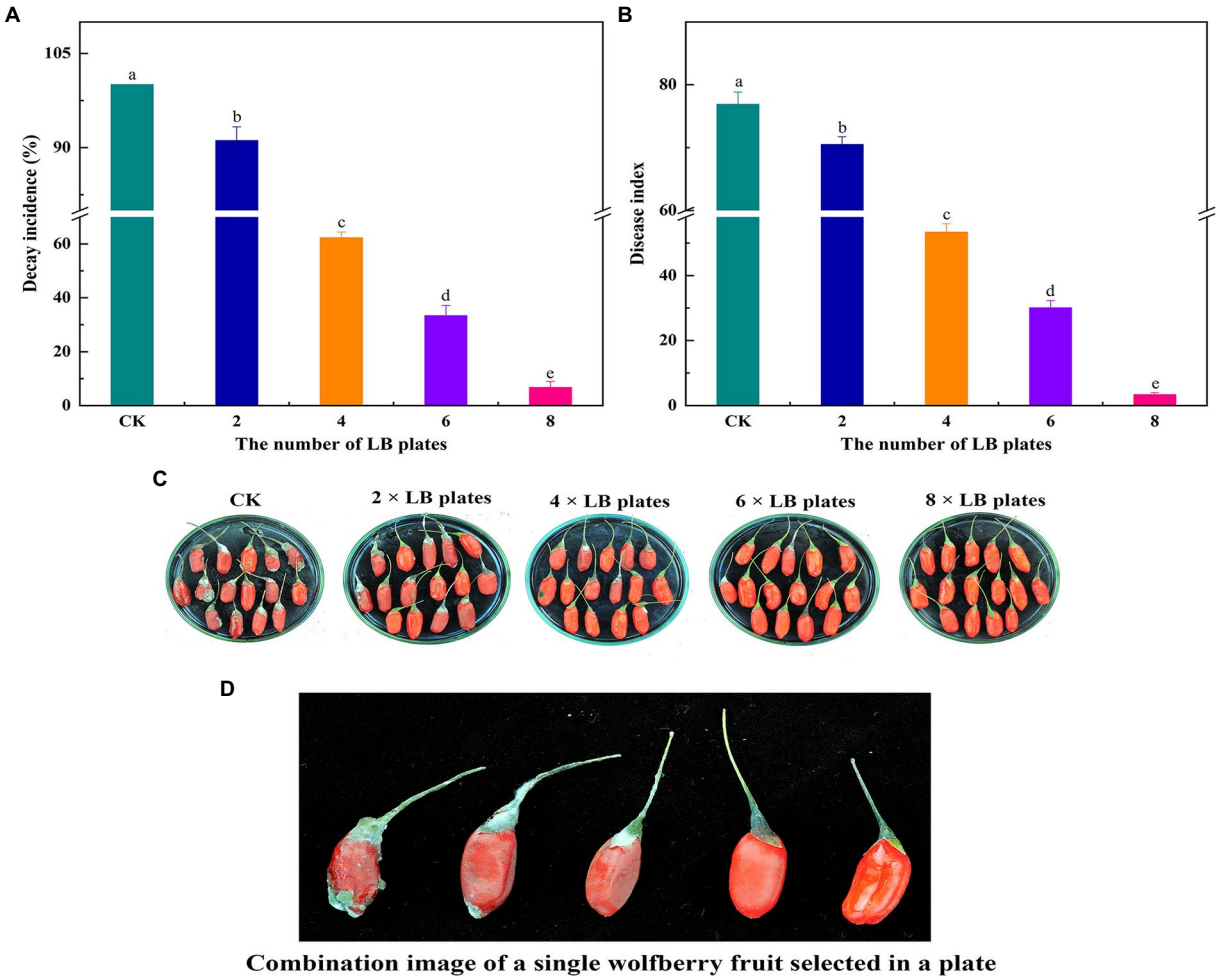

FIGURE 4
2, 4, 6 and 8 LB plates were used to fumigate untreated wolfberry fruit. The container were sealed and followed by incubation at room temperature for 7 days, the decay incidence **(A)** and disease index **(B)** were measured. Biocontrol of VOCs produced by *B. velezensis* L1 on postharvest natural decay of wolfberry fruit **(C)** and combination image of a single wolfberry fruit selected in a plate **(D)**. Columns with different lower-case letters within the same panel are significantly different at $p<0.05$ level according to Duncan's multiple range test.

Alternaria iridiaustralis is inhibited by a single known VOC

The effects of nine components on the growth of *A. iridiaustralis* mycelium were determined (Table 3). Among the nine tested pure substances, only 2,3-butanedione (40 μl/L) showed a strong effect, completely inhibiting the growth of the *A. iridiaustralis* mycelium. The remaining substances, including 1-hydroxy-2-propanone, 2-pentanone, acetoin, 2-heptanone, cyclohexanone, methyl 2-methylbutanoate, 2-pentylfuran and 2-methylpropyl butanoate, showed very weak or no antifungal activity on PDA plates.

Effects of pure VOC chemicals against *Alternaria iridiaustralis* on wolfberry

As shown in Table 4, 2,3-butanedione was found to be an effective BCA. At 60 μl/L, it completely inhibited the growth of *A. iridiaustralis*, and no obvious lesions were found on the wolfberry fruits. The decay incidence and disease index decreased significantly.

Broad spectrum antifungal activity of volatiles from *Bacillus velezensis* L1

Ten important pathogenic fungi including *P. capsici*, *C. capsici*, *F. oxysporum*, *B. cinerea*, *R. solani*, *F. graminearum*, *F. annulatum*, *T. tumuli*, *C. fioriniae* and *F. arcuatisporum*, were used to test the broad antifungal activity of *B. velezensis* L1. In the strain L1 treatment, the mycelial growth of the pathogenic fungi was greatly inhibited (Figure 6). The inhibition rate of L1 strain against the nine pathogenic strains was >80%. These results suggest that active volatiles produced by *B. velezensis* L1 have a broad antifungal activity against different genera of pathogenic fungi.

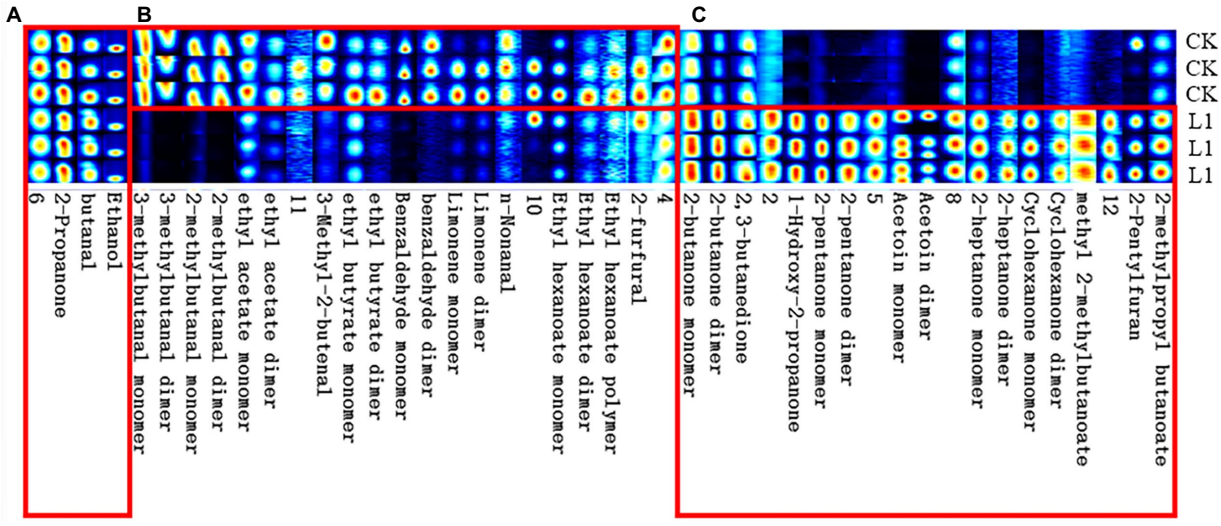

FIGURE 5
The Gallery plot of selected VOCs in the gas-phase ion mobility spectrum. Each row in the figure represents that all the signal peaks were selected in one sample, and each column represented the signal peaks of the same VOCs in different samples. Substances in area **(A)** were both identified in CK and *B. velezensis* L1. Substances in area **(B)** were identified in CK. Substances in area **(C)** were identified in *B. velezensis* L1.

TABLE 2 Qualitative information from HS-GC-IMS analysis of VOCs from tested *B. velezensis* L1.

Count	Compound	CAS#	Formula	MW	RI	Rt [sec]	Dt [RIPrel]
1	2-butanone monomer	C78933	C4H8O	72.1	608.5	139.894	1.0597
2	2-butanone dimer	C78933	C4H8O	72.1	601.6	136.916	1.24743
3	2,3-butanedione	C431038	C4H6O2	86.1	599	135.826	1.17873
4	1-Hydroxy-2-propanone	C116096	C3H6O2	74.1	638.4	152.575	1.22642
5	2-pentanone monomer	C107879	C5H10O	86.1	696	180.037	1.12034
6	2-pentanone dimer	C107879	C5H10O	86.1	697.7	181.4	1.37338
7	Acetoin monomer	C513860	C4H8O2	88.1	723.1	202.308	1.05484
8	Acetoin dimer	C513860	C4H8O2	88.1	720.3	200.04	1.32941
9	2-heptanone monomer	C110430	C7H14O	114.2	896.6	378.474	1.26411
10	2-heptanone dimer	C110430	C7H14O	114.2	895.7	376.962	1.62921
11	Cyclohexanone monomer	C108941	C6H10O	98.1	903	389.726	1.15422
12	Cyclohexanone dimer	C108941	C6H10O	98.1	902.6	389.001	1.45337
13	methyl 2-methylbutanoate	C868575	C6H12O2	116.2	775.6	245.523	1.18758
14	2-Pentylfuran	C3777693	C9H14O	138.2	1002.5	564.479	1.25597
15	2-methylpropyl butanoate	C539902	C8H16O2	144.2	960.2	489.067	1.32923

Dt, drift time; MW, molecular mass; RI, retention index; Rt, retention time; VOC, volatile organic compound.

Discussion

Postharvest regulation of fruits and vegetables can result in an incredibly high value (Lemos Junior et al., 2020). Recent VOCs control research has produced positive results and is regarded as a useful alternative strategy for reducing fungal infection (Raza et al., 2016; Syed-Ab-Rahman et al., 2019). In this study, we isolated and characterized a strain of *B. velezensis* L1 that suppresses *A. iridiaustralis* growth in wolfberry during the postharvest process and displayed the broad-spectrum antifungal activity of VOCs obtained from *B. velezensis* L1. Therefore, *B. velezensis* L1 is anticipated to be employed as an antagonistic microbe. To the best of our knowledge, this is the first known study exhibiting the antagonistic activity of *B. velezensis* VOCs against *A. iridiaustralis* on postharvest wolfberry.

In vitro antifungal experiments revealed that VOCs produced by *B. velezensis* L1 strongly inhibited the growth of *A. iridiaustralis* mycelium, spore germination, and sporulation. VOCs generated by *B. velezensis* C16 significantly suppress *A. solani* mycelium development and spore germination (Zhang et al., 2021).

TABLE 3 Effects different concentrations of tested compounds on the mycelial growth of *A. iridiaustralis* after an incubation at 28°C for 4 d.

Volatile compound	Different concentrations of volatiles				
	20 μl/L	40 μl/L	60 μl/L	80 μl/L	100 μl/L
Control	35.7 ± 0.4^{a}	35.7 ± 0.4^{a}	35.7 ± 0.4^{a}	35.7 ± 0.4^{a}	35.7 ± 0.4^{a}
2,3-butanedione	29.9 ± 0.5^{c}	19.1 ± 0.4^{b}	06.0 ± 0.0^{c}	06.0 ± 0.0^{c}	06.0 ± 0.0^{d}
1-Hydroxy-2-propanone	34.5 ± 0.4^{a}	34.1 ± 0.4^{a}	33.9 ± 0.4^{b}	33.6 ± 0.5^{b}	33.0 ± 0.3^{c}
Acetoin	35.5 ± 0.4^{a}	35.4 ± 0.4^{a}	35.9 ± 0.3^{a}	35.1 ± 0.2^{ab}	34.7 ± 0.4^{ab}
2-pentanone	35.5 ± 0.3^{a}	34.3 ± 0.4^{a}	34.5 ± 0.4^{ab}	34.2 ± 0.2^{b}	33.9 ± 0.3^{bc}
2-heptanone	31.4 ± 0.4^{b}	31.7 ± 0.3^{b}	32.9 ± 0.2^{b}	33.7 ± 0.3^{b}	32.6 ± 0.4^{c}
Cyclohexanone	35.9 ± 0.4^{a}	35.8 ± 0.5^{a}	35.6 ± 0.2^{a}	35.9 ± 0.3^{a}	36.1 ± 0.5^{a}
methyl 2-methylbutanoate	35.9 ± 0.4^{a}	34.1 ± 0.4^{a}	33.2 ± 0.2^{b}	34.5 ± 0.4^{ab}	32.6 ± 0.5^{c}
2-Pentylfuran	34.1 ± 0.2^{a}	35.3 ± 0.4^{a}	34.4 ± 0.4^{ab}	34.1 ± 0.4^{b}	34.1 ± 0.2^{bc}
2-methylpropyl butanoate	34.8 ± 0.2^{a}	34.1 ± 0.5^{a}	34.4 ± 0.4^{ab}	33.9 ± 0.3^{b}	34.2 ± 0.3^{bc}

Each value is the mean of three replicates ± standard error. Values in a column followed by a different letter are significantly different according to Duncan's multiple range test at $p < 0.05$ level.

TABLE 4 Effects different concentrations of 2,3-butanedione on the wolfberry fruit decay.

Concentrations (μL/L)	Decay incidence (%)	Disease index
0	100.00 ± 0.00^{a}	49.63 ± 1.96^{a}
20	92.59 ± 3.70^{b}	22.50 ± 1.44^{b}
40	48.15 ± 3.71^{c}	7.83 ± 1.17^{c}
60	0.00 ± 0.00^{d}	0.00 ± 0.00^{d}
80	0.00 ± 0.00^{d}	0.00 ± 0.00^{d}
100	0.00 ± 0.00^{d}	0.00 ± 0.00^{d}

Each value is the mean of three replicates ± standard error. Values in a column followed by a different letter are significantly different according to Duncan's multiple range test at $p < 0.05$ level.

According to Jiang et al. (2018), VOCs from the *B. velezensis* strain may prevent sporulation of *B. cinerea* in peppers. This agrees with the findings obtained for *B. velezensis* L1. Additionally, the regrowth of *A. iridiaustralis* was reduced by the VOCs from *B. velezensis* L1. The effects of VOCs on *B. cinerea* were comparable to those of *Pseudomonas fluorescens* ZX (Zhong et al., 2021). This might be because VOCs disrupt the pathogenic fungi's natural morphological structure and interfere with their normal proliferation. However, the damage appears to be lost with a reduction in VOC concentration, possibly because of the robust recovery and reproductive capacity of the fungi. According to SEM analysis, the VOCs from *B. velezensis* L1 can severely damage the morphology of *A. iridiaustralis*. Numerous studies have demonstrated that VOCs can harm pathogenic the walls and membrane systems of pathogenic fungi, impairing their ability to perform essential tasks (Zhao et al., 2019; Wang et al., 2021b). This might be one of the key ways through which VOCs prevent harmful the growth of fungi.

The effectiveness of VOCs *in vivo* was further investigated in light of the superior inhibitory capacity of *B. velezensis* L1 *in vitro*. The findings demonstrated that VOCs from *B. velezensis* L1 can greatly reduce disease severity in wolfberry. Although many descriptive studies have investigated the effectiveness of VOCs (Archana et al., 2021; Wang et al., 2021a), more research is focused on the screening of strains and the identification of volatiles produced, with most authors not choosing to explore the relationship between their concentrations and diseases, which may be due to difficulties associated with testing. Calvo et al. (2020) reported that the *B. velezensis* strain inhibits mycelial growth and sporulation and is not pathogenic to humans after use. However, the VOCs concentration was not considered in their study. Myo et al. (2019) found that *B. velezensis* NKG-2 adversely affected the growth of six pathogenic fungi, but they too did not consider the VOCs concentration. The effect of VOC concentrations on the prevention, occurrence, and severity of diseases is of great value for the postharvest preservation of fruits and vegetables (Sharifi and Ryu, 2016). These concentrations were influenced by different numbers of LB plates. With an increase in concentration, the disease status of wolfberry fruits inoculated with the pathogenic fungus *A. iridiaustralis* changed significantly. Wang et al. (2021c) also confirmed that a certain concentration of VOCs produced by *P. fluorescens* ZX can significantly control gray mold in citrus and inhibit decay development. When VOCs reach a certain concentration, the growth of pathogenic fungi in fruits is completely inhibited, resulting in the best control effect. This suggests that it is entirely feasible to utilize VOCs produced by antagonistic microorganisms as potential BCAs. More importantly, VOCs also have an excellent control effect on fruits that rot naturally after harvest, inhibited all pathogenic fungi that caused the disease, which greatly prolongs the storage time of wolfberry. Studies have confirmed that VOCs produced by some bacteria, yeast and fungi can induce resistance against pathogens in fruits and vegetables (Zheng et al., 2019). This may be related to another antifungal mechanism of VOCs. Zhou et al. (2019) reported that the VOCs of strain *CF*-3 could reduce the enzymatic activity involved in fruit decomposition, activate the antioxidant enzymes to prevent cell damage, and elevate the disease-resistant enzyme activity to prevent the invasion of pathogenic fungi,

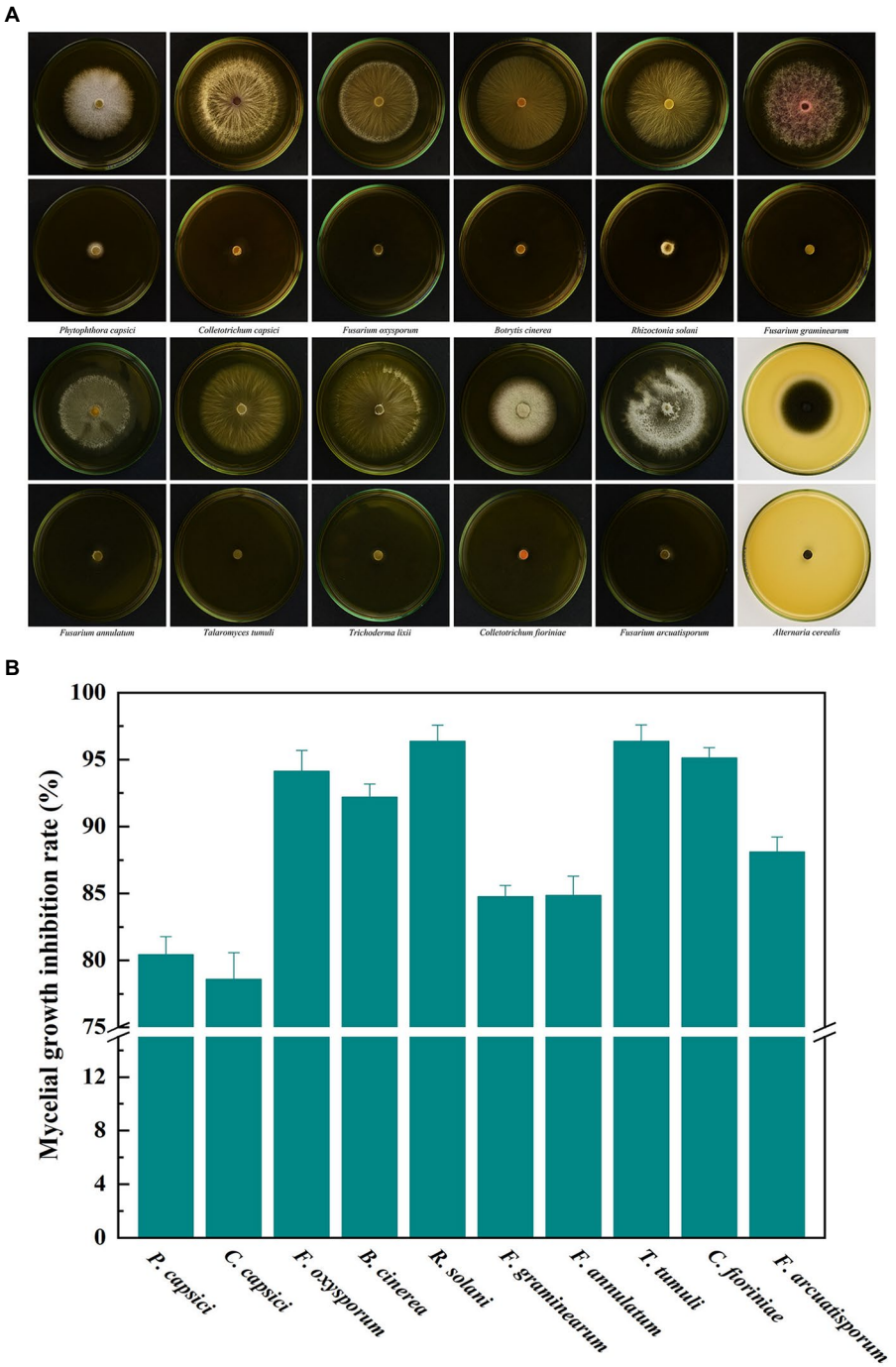

FIGURE 6
(A) Broad antifungal activity of *B. velezensis* L1 against ten fungal pathogens. **(B)** Corresponding histograms for statistical data on mycelial growth inhibition rate. Different fungal strains including *P. capsici*, *C. capsici*, *F. oxysporum*, *B. cinerea*, *R. solani*, *F. graminearum*, *F. annulatum*, *T. tumuli*, *C. fioriniae* and *F. arcuatisporum* were used in the tests.

thereby inducing resistance to fungi. Lee et al. (2019) showed that VOCs released by microorganisms induce self-resistance in the host to avoid the pathogen-induced harm. For the control of postharvest natural decay, strain L1 can be used as a new preservative with significant effect, which is of great value in commercial production.

In general, antagonistic microorganisms can produce VOCs such as ketones, alcohols, aldehydes, esters, and acidic and aromatic compounds with antifungal activity, and different strains released VOCs are specific (Raza et al., 2015; Kai, 2020). In addition, VOCs can be altered by changes in culture conditions. For example, *P. fluorescens* ZX produced different VOCs when

incubated on NB or NA (Wang et al., 2020). *B. amyloliquefaciens* PP19, *Exiguobacterium acetylicum* SI17, *B. pumilus* PI26 were reported to vary greatly in their VOCs with incubation time and between strains (L. Zheng et al., 2019). The FlavourSpec® Flavor Analyzer, which uses HS-GC-IMS technology, is mainly used for the research of food flavor (Wang et al., 2019; Yuan et al., 2019). Because of the high sensitivity and high resolution, the HS-GC-IMS technique is effective in identifying VOCs released by different strains. In this study, based on the complexity and diversity of VOCs, volatile gas chemicals emitted by *B. velezensis* L1 were identified using HS-GC-IMS, and 10 main components were found. The components identified varied from the volatile components discovered in other studies, which could be due to variations in the growth environment of the hostile bacteria (Wallace et al., 2017). On the other hand, the results obtained may vary because of the use of different types of equipment and materials in experiments to identify VOC components.

Nine pure compounds were commercially available and selected for further analysis. Among the components identified, 2,3-butanedione had the strongest inhibitory effect on pathogenic fungi both *in vitro* and *in vivo*. 2,3-Butanedione could reduce the rot disease index of wolfberry fruit. Compared with the complex VOCs components, pure compounds have clear structural characteristics and are easy to produce and synthesize and may have practical applications in future. Calvo et al. (2020) showed that 20 μl/L of 2,3-butanedione could completely control gray mold in grapes and reduce blue rot in mandarins to 60%. Gergolet Diaz et al. (2021) showed that 2,3-butanedione had the strongest inhibitory effect on the mycelial growth of *F. verticillioides*. 2,3-Butanedione is a naturally occurring, safe and edible volatile alpha-diketone often used in food additives and flavors because of its good flavor. Pathogenic fungi are very sensitive to even very low concentrations of VOC, and therefore, this VOC is considered a promising compound for postharvest preservation (Zheng et al., 2020). 2-Pentanone, 2-heptanone, and acetoin are the most common and abundant VOCs in many strains (Wu et al., 2015; Lazazzara et al., 2021). As observed in our study, they have little impact on the hyphal development of pathogenic fungi. However, VOCs are usually complex in composition, and their inhibitory effects often do not depend on a single active ingredient (Wang et al., 2021c). Few studies have investigated the optimal application and activity of the combination of VOC. Thus, whether the main components in these VOCs are synergistically involved in the antifungal effect deserves further investigation. 1-Hydroxy-2-propanone, cyclohexanone, methyl 2-methylbutanoate, 2-pentylfuran and 2-methylpropyl butan were found to be produced by the *B. velezensis* strain for the first time. However, they showed no antifungal activity against *A. iridiaustralis* in the tests. This could be related to the concentration chosen, some antifungal compounds showed weak activity or were ineffective at low concentrations (Vicentini et al., 2007). However, it is worth considering that high concentrations of antifungal substances can harm the human body, which is not in line with our original intention.

In addition, tests on pathogenic fungi that cause severe diseases in crops, fruits, vegetables and other foods have found that VOCs from *B. velezensis* L1 also significantly inhibit its growth. This provides more possibilities for the application of *B. velezensis* L1 and its VOCs as preservatives for controlling these diseases during storage. For different pathogenic fungi, the inhibitory effect of VOCs is also different. At present, the antifungal mechanisms discovered by VOCs mainly include inhibition of mycelial growth, damage to cell walls, regulation of enzyme activities, and induction of host resistance (Zhong et al., 2021). It is still important to explore the interactions and connections between VOCs, pathogenic fungi and hosts.

This work is the first to investigate the inhibitory effect of *B. velezensis* L1 on postharvest disease of wolfberry. In experiments, *B. velezensis* L1 and its volatiles (2,3-butanedione) can effectively reduce the decay caused by pathogenic fungi and prolong storage time. These results provide favorable evidence for the biocontrol activity of strain L1 against *A. iridiaustralis* and other important fungal pathogens, and also provides insights to develop storage systems for fresh fruits and vegetables after harvest.

Data availability statement

The original contributions presented in the study are included in the article/supplementary material, further inquiries can be directed to the corresponding author.

Author contributions

All authors contributed to the study conception and design. Material preparation, data collection, and analysis were performed by HL, CY, and LL. The first draft of the manuscript was written by HL. All authors contributed to the article and approved the submitted version.

Funding

The Lanzhou Science and Technology Plan Project 2018-1-104 is sincerely acknowledged by the authors; Special Fund Project for Guiding Science and Technology Innovation and Development in Gansu Province 2019ZX-05. Higher Education Industry Support Plan of Gansu Province (2020C-21).

Conflict of interest

The authors declare that the research was conducted in the absence of any commercial or financial relationships that could be construed as a potential conflict of interest.

Publisher's note

References

Alijani, Z., Amini, J., Ashengroph, M., and Bahramnejad, B. (2019). Antifungal activity of volatile compounds produced by Staphylococcus sciuri strain MarR44 and its potential for the biocontrol of *Colletotrichum nymphaeae*, causal agent strawberry anthracnose. *Int. J. Food Microbiol.* 307:108276. doi: 10.1016/j.ijfoodmicro.2019.108276

Archana, T. J., Gogoi, R., Kaur, C., Varghese, E., Sharma, R. R., Srivastav, M., et al. (2021). Bacterial volatile mediated suppression of postharvest anthracnose and quality enhancement in mango. *Postharvest Biol. Technol.* 177:111525. doi: 10.1016/j.postharvbio.2021.111525

Arrarte, E., Garmendia, G., Rossini, C., Wisniewski, M., and Vero, S. (2017). Volatile organic compounds produced by Antarctic strains of Candida sake play a role in the control of postharvest pathogens of apples. *Biol. Control* 109, 14–20. doi: 10.1016/j.biocontrol.2017.03.002

Bu, S., Munir, S., He, P., Li, Y., Wu, Y., Li, X., et al. (2021). *Bacillus subtilis* L1-21 as a biocontrol agent for postharvest gray mold of tomato caused by *Botrytis cinerea*. *Biol. Control* 157:104568. doi: 10.1016/j.biocontrol.2021.104568

Calvo, H., Mendiara, I., Arias, E., Gracia, A. P., Blanco, D., and Venturini, M. E. (2020). Antifungal activity of the volatile organic compounds produced by *Bacillus velezensis* strains against postharvest fungal pathogens. *Postharvest Biol. Technol.* 166:111208. doi: 10.1016/j.postharvbio.2020.111208

Di Francesco, A., Di Foggia, M., and Baraldi, E. (2020a). Aureobasidium pullulans volatile organic compounds as alternative postharvest method to control brown rot of stone fruits. *Food Microbiol.* 87:103395. doi: 10.1016/j.fm.2019.103395

Di Francesco, A., Di Foggia, M., and Baraldi, E. (2020b). Aureobasidium pullulans volatile organic compounds as alternative postharvest method to control brown rot of stone fruits. *Food Microbiol.* 87:103395. doi: 10.1016/j.fm.2019.103395

Do Kim, J., Kang, J. E., and Kim, B. S. (2020). Postharvest disease control efficacy of the polyene macrolide lucensomycin produced by Streptomyces plumbeus strain CA5 against gray mold on grapes. *Postharvest Biol. Technol.* 162:111115. doi: 10.1016/j.postharvbio.2019.111115

Gao, Z., Zhang, B., Liu, H., Han, J., and Zhang, Y. (2017). Identification of endophytic *Bacillus velezensis* ZSY-1 strain and antifungal activity of its volatile compounds against *Alternaria solani* and *Botrytis cinerea*. *Biol. Control* 105, 27–39. doi: 10.1016/j.biocontrol.2016.11.007

Gergolet Diaz, D. G., Pizzolitto, R. P., Vázquez, C., Usseglio, V. L., Zunino, M. P., Dambolena, J. S., et al. (2021). Effects of the volatile organic compounds produced by enterococcus spp. strains isolated from maize grain silos on *Fusarium verticillioides* growth and fumonisin B1 production. *J. Stored Prod. Res.* 93:101825. doi: 10.1016/j.jspr.2021.101825

Gotor-Vila, A., Teixidó, N., Di Francesco, A., Usall, J., Ugolini, L., Torres, R., et al. (2017). Antifungal effect of volatile organic compounds produced by *Bacillus* amyloliquefaciens CPA-8 against fruit pathogen decays of cherry. *Food Microbiol.* 64, 219–225. doi: 10.1016/j.fm.2017.01.006

Jiang, C. H., Liao, M. J., Wang, H. K., Zheng, M. Z., Xu, J. J., and Guo, J. H. (2018). *Bacillus velezensis*, a potential and efficient biocontrol agent in control of pepper gray mold caused by *Botrytis cinerea*. *Biol. Control* 126, 147–157. doi: 10.1016/j.biocontrol.2018.07.017

Kai, M. (2020). Diversity and distribution of volatile secondary metabolites throughout *Bacillus subtilis* isolates. *Front. Microbiol.* 11:559. doi: 10.3389/fmicb.2020.00559

Lazazzara, V., Vicelli, B., Bueschl, C., Parich, A., Pertot, I., Schuhmacher, R., et al. (2021). Trichoderma spp. volatile organic compounds protect grapevine plants by activating defense-related processes against downy mildew. *Physiol. Plant.* 172, 1950–1965. doi: 10.1111/ppl.13406

Lee, S., Behringer, G., Hung, R., and Bennett, J. (2019). Effects of fungal volatile organic compounds on *Arabidopsis thaliana* growth and gene expression. *Fungal Ecol.* 37, 1–9. doi: 10.1016/j.funeco.2018.08.004

Lemos Junior, W. J. F., Binati, R. L., Felis, G. E., Slaghenaufi, D., Ugliano, M., and Torriani, S. (2020). Volatile organic compounds from *Starmerella bacillaris* to control gray mold on apples and modulate cider aroma profile. *Food Microbiol.* 89:103446. doi: 10.1016/j.fm.2020.103446

Li, X., Wang, X., Shi, X., Wang, B., Li, M., Wang, Q., et al. (2020). Antifungal Effect of Volatile Organic Compounds from *Bacillus velezensis* CT32 against *Verticillium dahliae* and *Fusarium oxysporum*. *Processes* 8:1674. doi: 10.3390/pr8121674

Ling, L., Li, Z., Jiao, Z., Zhang, X., Ma, W., Feng, J., et al. (2019). Identification of novel endophytic yeast strains from tangerine Peel. *Curr. Microbiol.* 76, 1066–1072. doi: 10.1007/s00284-019-01721-9

Ling, L., Zhao, Y., Tu, Y., Yang, C., Ma, W., Feng, S., et al. (2021). The inhibitory effect of volatile organic compounds produced by *Bacillus subtilis* CL2 on pathogenic fungi of wolfberry. *J. Basic Microbiol.* 61, 110–121. doi: 10.1002/jobm.202000522

Mari, M., Bautista-Baños, S., and Sivakumar, D. (2016). Decay control in the postharvest system: role of microbial and plant volatile organic compounds. *Postharvest Biol. Technol.* 122, 70–81. doi: 10.1016/j.postharvbio.2016.04.014

Myo, E. M., Liu, B., Ma, J., Shi, L., Jiang, M., Zhang, K., et al. (2019). Evaluation of *Bacillus velezensis* NKG-2 for bio-control activities against fungal diseases and potential plant growth promotion. *Biol. Control* 134, 23–31. doi: 10.1016/j.biocontrol.2019.03.017

Oro, L., Feliziani, E., Ciani, M., Romanazzi, G., and Comitini, F. (2018). Volatile organic compounds from *Wickerhamomyces anomalus*, *Metschnikowia pulcherrima* and *Saccharomyces cerevisiae* inhibit growth of decay causing fungi and control postharvest diseases of strawberries. *Int. J. Food Microbiol.* 265, 18–22. doi: 10.1016/j.ijfoodmicro.2017.10.027

Qin, X., Xiao, H., Cheng, X., Zhou, H., and Si, L. (2017). Hanseniaspora uvarum prolongs shelf life of strawberry via volatile production. *Food Microbiol.* 63, 205–212. doi: 10.1016/j.fm.2016.11.005

Raza, W., Ling, N., Liu, D., Wei, Z., Huang, Q., and Shen, Q. (2016). Volatile organic compounds produced by *Pseudomonas fluorescens* WR-1 restrict the growth and virulence traits of Ralstonia solanacearum. *Microbiol. Res.* 192, 103–113. doi: 10.1016/j.micres.2016.05.014

Raza, W., Yuan, J., Ling, N., Huang, Q., and Shen, Q. (2015). Production of volatile organic compounds by an antagonistic strain *Paenibacillus polymyxa* WR-2 in the presence of root exudates and organic fertilizer and their antifungal activity against *Fusarium oxysporum* f. sp. niveum. *Biol. Control* 80, 89–95. doi: 10.1016/j.biocontrol.2014.09.004

Sharifi, R., and Ryu, C. M. (2016). Are bacterial volatile compounds poisonous odors to a fungal pathogen *Botrytis cinerea*, alarm signals to arabidopsis seedlings for eliciting induced resistance, or both? *Front. Microbiol.* 7:196. doi: 10.3389/fmicb.2016.00196

Syed-Ab-Rahman, S. F., Carvalhais, L. C., Chua, E. T., Chung, F. Y., Moyle, P. M., Eltanahy, E. G., et al. (2019). Soil bacterial diffusible and volatile organic compounds inhibit *Phytophthora capsici* and promote plant growth. *Sci. Total Environ.* 692, 267–280. doi: 10.1016/j.scitotenv.2019.07.061

Toffano, L., Fialho, M. B., and Pascholati, S. F. (2017). Potential of fumigation of orange fruits with volatile organic compounds produced by *Saccharomyces cerevisiae* to control citrus black spot disease at postharvest. *Biol. Control* 108, 77–82. doi: 10.1016/j.biocontrol.2017.02.009

Vicentini, C. B., Romagnoli, C., Andreotti, E., and Mares, D. (2007). Synthetic pyrazole derivatives as growth inhibitors of some phytopathogenic fungi. *J. Agric. Food Chem.* 55, 10331–10338. doi: 10.1021/jf072077d

Wallace, R. L., Hirkala, D. L., and Nelson, L. M. (2017). Postharvest biological control of blue mold of apple by *Pseudomonas fluorescens* during commercial storage and potential modes of action. *Postharvest Biol. Technol.* 133, 1–11. doi: 10.1016/j.postharvbio.2017.07.003

Wang, Z., Mei, X., Du, M., Chen, K., Jiang, M., Wang, K., et al. (2020). Potential modes of action of *Pseudomonas fluorescens* ZX during biocontrol of blue mold decay on postharvest citrus. *J. Sci. Food Agric.* 100, 744–754. doi: 10.1002/jsfa.10079

Wang, F., Xiao, J., Zhang, Y., Li, R., Liu, L., and Deng, J. (2021a). Biocontrol ability and action mechanism of *Bacillus halotolerans* against *Botrytis cinerea* causing grey mould in postharvest strawberry fruit. *Postharvest Biol. Technol.* 174:111456. doi: 10.1016/j.postharvbio.2020.111456

Wang, X., Yang, S., He, J., Chen, L., Zhang, J., Jin, Y., et al. (2019). A green triple-locked strategy based on volatile-compound imaging, chemometrics, and markers to discriminate winter honey and sapium honey using headspace gas chromatography-ion mobility spectrometry. *Food Res. Int.* 119, 960–967. doi: 10.1016/j.foodres.2019.01.004

Wang, Z., Zhong, T., Chen, K., Du, M., Chen, G., Chen, X., et al. (2021b). Antifungal activity of volatile organic compounds produced by *Pseudomonas*

fluorescens ZX and potential biocontrol of blue mold decay on postharvest citrus. *Food Control* 120:107499. doi: 10.1016/j.foodcont.2020.107499

Wang, Z., Zhong, T., Chen, X., Yang, B., Du, M., Wang, K., et al. (2021c). Potential of volatile organic compounds emitted by *pseudomonas fluorescens* ZX as biological fumigants to control citrus green mold decay at postharvest. *J. Agric. Food Chem.* 69, 2087–2098. doi: 10.1021/acs.jafc.0c07375

Wei, D., Wang, Y., Jiang, D., Feng, X., Li, J., and Wang, M. (2017). Survey of *Alternaria* toxins and other mycotoxins in dried fruits in China. *Toxins* 9, 1–12. doi: 10.3390/toxins9070200

Wenli, S., Shahrajabian, M. H., and Qi, C. (2021). Health benefits of wolfberry (Gou Qi Zi, *Fructus barbarum* L.) on the basis of ancient Chinese herbalism and Western modern medicine. *Avicenna J Phytomed.* 11, 109–119. doi: 10.22038/AJP.2020.17147

Wonglom, P., Shin-Ichi, I., and Sunpapao, A. (2020). Volatile organic compounds emitted from endophytic fungus *Trichoderma asperellum* T1 mediate antifungal activity, defense response and promote plant growth in lettuce (*Lactuca sativa*). *Fungal Ecol.* 43:100867. doi: 10.1016/j.funeco.2019.100867

Wu, Y., Yuan, J., Yaoyao, E., Raza, W., Shen, Q., and Huang, Q. (2015). Effects of volatile organic compounds from *Streptomyces albulus* NJZJSA2 on growth of two fungal pathogens. *J. Basic Microbiol.* 55, 1104–1117. doi: 10.1002/jobm.201400906

Xu, F., Wang, S., Xu, J., Liu, S., and Li, G. (2016). Effects of combined aqueous chlorine dioxide and UV-C on shelf-life quality of blueberries. *Postharvest Biol. Technol.* 117, 125–131. doi: 10.1016/j.postharvbio.2016.01.012

Yajun, W., Xiaojie, L., Sujuan, G., Yuekun, L., Bo, Z., Yue, Y., et al. (2019). Evaluation of nutrients and related environmental factors for wolfberry (*Lycium barbarum*) fruits grown in the different areas of China. *Biochem. Syst. Ecol.* 86:103916. doi: 10.1016/j.bse.2019.103916

Ye, X., Chen, Y., Ma, S., Yuan, T., Wu, Y., Li, Y., et al. (2020). Biocidal effects of volatile organic compounds produced by the myxobacterium *Corrallococcus* sp. EGB against fungal phytopathogens. *Food Microbiol.* 91:103502. doi: 10.1016/j.fm.2020.103502

Yuan, Z. Y., Qu, H. Y., Xie, M. Z., Zeng, G., Huang, H. Y., Ren, F., et al. (2019). Direct authentication of three Chinese materia medica species of the Lilii Bulbus family in terms of volatile components by headspace-gas chromatography-ion mobility spectrometry. *Anal. Methods* 11, 530–536. doi: 10.1039/c8ay02338g

Yuan, H. J., Yang, A. M., and Wu, G. F. (2012). Etiology of fruit rot of barbary wolfberry (*Lycium barbarum* L.) in the drying process with insolation method in green house. *Adv. Mater. Res.* 554-556, 1530–1533. doi: 10.4028/www.scientific.net/AMR.554-556.1530

Zhang, D., Yu, S., Zhao, D., Zhang, J., Pan, Y., Yang, Y., et al. (2021). Inhibitory effects of non-volatiles lipopeptides and volatiles ketones metabolites secreted by *Bacillus velezensis* C16 against *Alternaria solani*. *Biol. Control* 152:104421. doi: 10.1016/j.biocontrol.2020.104421

Zhao, P., Li, P., Wu, S., Zhou, M., Zhi, R., and Gao, H. (2019). Volatile organic compounds (VOCs) from *Bacillus subtilis* CF-3 reduce anthracnose and elicit active defense responses in harvested litchi fruits. *AMB Express* 9:119. doi: 10.1186/s13568-019-0841-2

Zheng, Y., Fei, Y., Yang, Y., Jin, Z., Yu, B., and Li, L. (2020). A potential flavor culture: lactobacillus harbinensis M1 improves the organoleptic quality of fermented soymilk by high production of 2,3-butanedione and acetoin. *Food Microbiol.* 91:103540. doi: 10.1016/j.fm.2020.103540

Zheng, L., Situ, J. J., Zhu, Q. F., Xi, P. G., Zheng, Y., Liu, H. X., et al. (2019). Identification of volatile organic compounds for the biocontrol of postharvest litchi fruit pathogen *Peronophythora litchii*. *Postharvest Biol. Technol.* 155, 37–46. doi: 10.1016/j.postharvbio.2019.05.009

Zhong, T., Wang, Z., Zhang, M., Wei, X., Kan, J., Zalán, Z., et al. (2021). Volatile organic compounds produced by *Pseudomonas fluorescens* ZX as potential biological fumigants against gray mold on postharvest grapes. *Biol. Control* 163:104754. doi: 10.1016/j.biocontrol.2021.104754

Zhou, M., Li, P., Wu, S., Zhao, P., and Gao, H. (2019). *Bacillus subtilis* CF-3 volatile organic compounds inhibit *Monilinia fructicola* growth in peach fruit. *Front. Microbiol.* 10:1804. doi: 10.3389/fmicb.2019.01804

Zhou, Z. Q., Xiao, J., Fan, H. X., Yu, Y., He, R. R., Feng, X. L., et al. (2017). Polyphenols from wolfberry and their bioactivities. *Food Chem.* 214, 644–654. doi: 10.1016/j.foodchem.2016.07.105

frontiers | Frontiers in Microbiology

TYPE Original Research
PUBLISHED 15 September 2022
DOI 10.3389/fmicb.2022.986659

OPEN ACCESS

EDITED BY
Khamis Youssef,
Agricultural Research Center,
Egypt

REVIEWED BY
Khaled A. El-Tarabily,
United Arab Emirates University,
United Arab Emirates
Mohamed A. Mohamed,
Agricultural Research Center,
Egypt

*CORRESPONDENCE
Qiwen Zhong
zhongqiwen@qhu.edu.cn
Shipeng Yang
qhyysp@163.com

SPECIALTY SECTION
This article was submitted to Food Microbiology, a section of the journal Frontiers in Microbiology

RECEIVED 05 July 2022
ACCEPTED 19 August 2022
PUBLISHED 15 September 2022

CITATION
Du G, Sun Z, Bao S, Zhong Q and Yang S (2022) Diversity of bacterial community in Jerusalem artichoke (*Helianthus tuberosus* L.) during storage is associated with the genotype and carbohydrates.
Front. Microbiol. 13:986659.
doi: 10.3389/fmicb.2022.986659

Diversity of bacterial community in Jerusalem artichoke (*Helianthus tuberosus* L.) during storage is associated with the genotype and carbohydrates

Guolian Du[1], Zhu Sun[1], Shanhua Bao[1], Qiwen Zhong[1,2]* and Shipeng Yang[1]*

[1]Qinghai Key Laboratory of Vegetable Genetics and Physiology, Agriculture and Forestry Sciences Institute of Qinghai University, Qinghai University, Xining, China, [2]Laboratory for Research and Utilization of Germplasm Resources in Qinghai Tibet Plateau, Qinghai University, Xining, China

Jerusalem artichoke (JA) is a fructan-accumulating crop that has gained popularity in recent years. The objective of the present study was to determine the dynamics of the JA-microbiome during storage. The microbial population on the surface of the JA tuber was determined by next-generation sequencing of 16S rRNA amplicons. Subsequently, the changes in carbohydrate and degree of polymerization of fructan in tubers during storage were measured. Among different genotypes of JA varieties, intergeneric differences were observed in the diversity and abundance of bacterial communities distributed on the surface of tubers. Additionally, bacterial diversity was significantly higher in storage-tolerant varieties relative to the storage-intolerant varieties. Redundancy analysis (RDA) and the correlation matrix indicated a relationship between changes in the carbohydrates and microbial community succession during tuber storage. The tuber decay rate correlated positively with the degree of polymerization of fructan. Moreover, *Dysgonomonas* and *Acinetobacter* in perishable varieties correlated significantly with the decay rate. Therefore, the bacteria associated with the decay rate may be involved in the degradation of the degree of polymerization of fructan. Furthermore, *Serratia* showed a significant positive correlation with inulin during storage but a negative correlation with the decay rate, suggesting its antagonistic role against pathogenic bacteria on the surface of JA tubers. However, the above correlation was not observed in the storage-tolerant varieties. Functional annotation analysis revealed that storage-tolerant JA varieties maintain tuber quality through enrichment of biocontrol bacteria, including *Flavobacterium*, *Sphingobacterium*, and *Staphylococcus* to resist pathogens. These results suggested that crop genotype and the structural composition of carbohydrates may result in differential selective enrichment effects of microbial communities on the surface of JA varieties. In this study, the relationship between microbial community succession and changes in tuber carbohydrates during JA storage was revealed for the first time through the combination of high-throughput sequencing, high-performance liquid chromatography (HPLC), and high-performance ion-exchange chromatography (HPIC). Overall, the findings of

this study are expected to provide new insights into the dynamics of microbial-crop interactions during storage.

KEYWORDS

Jerusalem artichoke, storage, microbiome, inulin, high-performance liquid chromatography, high-performance ion-exchange chromatography

Introduction

Complex carbohydrates, in the form of structural and storage polysaccharides, are products of primary metabolism. Biomass carbohydrates are a ubiquitous source of energy for microorganisms in different ecosystems (Gunina and Kuzyakov, 2015). Crop fruits and seeds are rich in carbohydrates, and their utilization by microorganisms is inextricably linked to different environmental factors and crop species. In the case of limited nutrient pools and changing temporal gradients, intense competitive relationships between microbial communities are found, which strongly influence the proliferation and survival of exogenous bacteria on agricultural products and changes with external conditions (Droby et al., 2016). Post-harvest fruit and vegetable loss accounts for nearly one-third of the total and majorly occurs during the processing and storage of agricultural products (Spang et al., 2019). Fruit decay crucially affects crop storage, processing, and merchantability (Wenneker and Thomma, 2020). Microbial communities on the surface of crop fruits are closely related to their decay. In addition, the equilibrium between microorganisms and their hosts is disrupted with increased storage time. The stability between the two is maintained through a complex molecular signaling system comprising microbial diversity and multiple factors. In addition, microbial diversity is associated with fruit quality (Zhang et al., 2021). Studies on bacterial diversity for varieties with different storage characteristics in the same environment can facilitate the understanding of fruit as an ecosystem, wherein bacterial communities play a crucial role in maintaining/regulating the health and physiology of fruits during the storage (Droby and Wisniewski, 2018).

Advances in next-generation sequencing (NGS) technologies have led to significant improvements in examining microbial communities. Several studies confirm that microorganisms identified by traditional isolated culture methods represent only 0.1–10% of the total environmental organisms (Amann et al., 1995; Tholozan et al., 1999). High-throughput sequencing allows for the extraction of DNA directly from different samples for the analyses of species composition and abundance without the need to isolate and culture them. Accumulating evidence from these techniques suggests that many microbial communities do not undergo spatial homogenization but display significant structures like many plant and animal communities. These findings are largely based on the analyses of bacteria (Morrison-Whittle and Goddard, 2015). Furthermore, these studies have focused on the following aspects: (1) specific microbial communities showing differential species composition and abundance among varieties of different crops (Zheng et al., 2015; Buchholz et al., 2021); (2) changes in microbial abundance over time during storage (Shen et al., 2018; Liu et al., 2020); (3) inhibitory effects of non-pathogenic microorganisms (Magerl et al., 2008), and (4) correlation with specific carbohydrates (Chatellard et al., 2016; Li et al., 2018). Although existing research extends to a wide range of crops, the diversity, function, and impact of specific communities of these communities on the overall community remain unknown. Consequently, strategies to prolong shelf life and avoid fruit diseases during storage should account for the indigenous microbiome and strategies should be implemented for a sustainable management (Kusstatscher et al., 2020).

Jerusalem artichoke (JA) is a perennial herb of the genus, *Helianthus* L., belonging to Asteraceae. Inulin, primarily stored in the tuber, accounts for 80% of the total dry weight of JA. Inulin-type fructans (ITFs), which are functional fructans and soluble dietary fibers, comprise a mixture of inulin, oligofructose, and fructooligosaccharide with β configuration. ITFs are mainly distributed in monocotyledonous and dicotyledonous plants, including JA, chicory, asparagus, wheat, garlic, banana, and onion (across Asteraceae, Gramineae, and Liliaceae). Inulin can regulate intestinal flora and is commonly used as a sugar substitute among patients with obesity, diabetes, and hyperlipidemia (Lovegrove et al., 2017; Man et al., 2020). ITF can be further classified into three subclasses of fructose units based on chain length or degree of polymerization (DP) as follows: small (3–5), medium (6–10), and long-chain (11–60). The length of DP is determined by genotype, environmental factors, harvest time, and storage processes. In general, DP determines the quality of the ITF and its commercial price. The type of carbohydrate determines to an extent the enrichment characteristics in microorganisms. Therefore, monitoring the development of bacterial communities during JA storage is crucial for understanding the primary pathogenic bacteria, improving the conservation of germplasm, and controlling fructan degradation.

In this study, we used high-throughput sequencing technology to analyze the bacterial community on the surface of tubers of jicama resources with different storage tolerance during storage. We focused on the following aspects: (1) decay-induced bacterial community changes between two different JA varieties with distinct storage-tolerant properties during storage to elucidate the correlation between microbial community structure and disease

occurrence; (2) cluster heatmap and radar chart analyses of highly abundant bacterial communities. Clustering analysis was performed for bacterial communities to assess the microbial enrichment in JA during storage, while the radar chart revealed dynamic changes among the common bacterial communities; (3) RDA and correlation analysis of fructans and bacterial communities to screen key microbial factors showing high correlation with disease occurrence and to elucidate the variability in pathogenicity and disease suppression exhibited at different storage periods. Furthermore, it provides theoretical support for deciphering the microbial mechanisms involved in JA tuber storage rot, as well as for preventing and controlling JA tuber storage rot.

Materials and methods

Sample sources

Test samples and storage conditions

The JA resources, including the storage-tolerant variety 'JA25' and the storage-intolerant variety 'JA187', were provided by the Institute of Horticulture, Qinghai Provincial Academy of Agriculture and Forestry Sciences. Microbial samples on the surface of tubers were collected from the JA storage base (at a constant temperature of 2°C and relative humidity of 40–60%) of the Institute. According to previous statistics, the peak of cellar storage-induced decay rate was 68% in 2020.

Grading storage-induced tuber decay

The decay rate was defined as the proportion of tubers with visible signs of decay and color changes on the surface relative to the total number of tubers in each treatment group. The incidence and condition index were used as indicators to investigate the decay rate of stored JA tubers. In addition, the storage-induced tuber decay was classified into four classes according to the criteria listed in Table 1.

TABLE 1 Grading criteria for rotting disease in stored Jerusalem artichoke tubers.

Grading	Tuber presentation
0	No significant changes in tubers, with the absence of pathogens.
1	Slight damage with white mycelium appearing on the epidermis, accounting for less than 5% of the total surface area of the tuber.
2	Moderate damage with mycelium accounting for less than 6–25% of the total surface area and initial decay on of the tuber epidermis.
3	Severe damage with mycelium accounts for less than 26–50% of the total surface area and initial decay of the tuber flesh.
4	Severe tuber decay with the white mycelium turning dark gray, accounting for more than 75% of the total surface area of the tuber.

Microbial sample collection from the tuber surface

Based on the results of the decay estimation, the first microbial sample collection on the surface of tubers was performed on December 31, 2019, for Grade 1. The time interval between two sample collections was set at 30 days. Four critical sampling periods were determined based on the disease incidence. Microbial samples of tubers were collected from the storage-tolerant variety, 'JA25', and the storage-intolerant variety, 'JA187', during storage (six replicates per storage period and six randomly selected tubers per replicate). In addition, the microbial samples from the five tubers were pooled and packed in sterile valve bags after removing soil and other impurities and frozen in liquid nitrogen until subsequent use.

Preservation and processing of microbial samples

First, the mycelium on tuber surfaces was gently scraped with a sterile blade and placed into sterile containers. Subsequently, phosphate belanced solution (PBS) buffer was added to each of the 48 bacterial samples, mixed by shaking for 20 min, and centrifuged at 12,000 rpm for 10 min to obtain the precipitate. Next, the samples were loaded into centrifuge tubes and frozen in liquid nitrogen. Subsequently, the frozen tissues were stored at-80°C for DNA extraction and bacterial community analyses. Samples were labeled as 'JA25'.1, 'JA25'.2, 'JA25'.3, 'JA25'.4, 'JA187'.1, 'JA187'.2, 'JA187'.3, and 'JA187'.4 (corresponding to the four collection periods of the two sampled varieties) and sent to Beijing Novogene Biotech for 16 s rRNA sequencing. In addition, the remaining JA tubers were sliced, oven-dried, and packed in sterile valve bags for the determination of physicochemical properties, including the fructan content and DP.

Determination of physicochemical properties of tuber carbohydrates

Fructan extraction and determination of its content

Distilled water (20 ml) was added to 0.5 g of dried JA powder and boiled in a water bath for 30 min, during which the samples were stirred several times using a glass rod. Next, the samples were allowed to cool at room temperature and poured into a centrifuge tube, and centrifuged for 10 min (12,000 r/min). Finally, the supernatant was poured into a 25 ml volumetric flask for determining the volume. Further,17.5 ml of distilled water and 1 ml of hydrochloric acid (3 mol L^{-1}) were added to an equal weight of the dried JA powder and boiled for 1 h; the samples were stirred several times using a glass rod. Next, the samples were allowed to cool at room temperature.

Subsequently, 1 ml of sodium hydroxide (3 mol L^{-1}) and 0.6 ml of aluminum sulfate (3 mol L^{-1}) were added to each sample, mixed well, poured into a centrifuge tube, and centrifuged for 10 min (12,000 r/min). Finally, the supernatant was poured into a 25 ml volumetric flask for determining the volume. Next, 1 ml of each solution from the reserve was added to 50 µl of sulfosalicylic acid (0.2 g L^{-1}) and filtered through a filter membrane (0.22 µm). In addition, the samples were analyzed by HPLC with the following parameters: detector: differential refractive index detector; analytical column: SUGAR KS-802 (8.0 mmId × 300 mml) special column for sugar analysis; mobile phase: ultrapure water; flow rate: 1 ml/min; column temperature: 80°C, and injection volume: 5 µl.

Glucose, sucrose, and fructose standards were prepared (0.1, 0.25, 0.5, 0.75, and 1 mg/ml standard solutions). Subsequently, the samples were analyzed by HPLC (Shimadzu RID-10A, Kyoto, Japan), and the appearance periods were 7.12, 8.23, and 9.75 min for sucrose, glucose, and fructose, respectively. Finally, a linear graph was plotted based on the peak areas and the concentrations of the standards, the results of their linear regression equations are shown in Supplementary Table S1.

DP determination for fructan

The DP of inulin extracts was analyzed by high-efficiency ion chromatography coupled with pulsed amperometric detection (Au, Ag/AgCl reference electrodes). The inulin extracts were diluted to an appropriate concentration with deionized water (900 µl of ultrapure water was added to 100 µl of fructan extract), and filtered through a 0.22 µm filter membrane before injection. The sample was injected using an AS50 autosampler with the column temperature set at 30°C, the injection volume set at 5 µl and the flow rate set at 1 ml/min. A high-capacity anion-exchange column compatible with gradient elution was used for a set time of 60 min. The peak periods were 3.5, 4.6, 8.2, 13.6, 16.6, 19.1, 21.3, and 23.3 for 1-kestose, nystose, 1F-fructofuranosyl nystose, 1,1,1,1-kestohexose, fructoheptasaccharide, fructo-oligosac charide DP8, fructo-oligosaccharide DP9, and fructo-oligosaccharide DP10, respectively. The relative percentage DP composition of inulin was calculated based on the peak area under the chromatogram, integrated with the Chromeleon™ software (version 6.2, Dionex).

Analyses of the bacterial communities

Total DNA extraction

Genomic DNA of the samples was extracted using cetyltriethylammnonium bromide (CTAB) lysis buffer. Subsequently, the purity and concentration of DNA were measured by agarose gel electrophoresis (0.8%). An appropriate amount of sample DNA was taken in a centrifuge tube and diluted to a final concentration of 1 ng/µl in sterile water.

PCR amplification of the 16S rDNA-V4 region of the bacterial genome

Using the diluted genomic DNA as a template, the specific primers, 515F (5'-GTTTCGGTGCCAGCMGCCGCGGTAA-3′) and 806R (5'-CAGATCGGACTVGGGTWTCTAAT-3′), with barcodes for the 16S rDNA-V4 region were used according to the selected sequencing region. The 20 µl reaction system used to identify bacterial diversity was as follows: 5xFastPfu Buffer: 4 µl, 2.5 mm dNTPs: 2 µl, 515F (5 µm): 0.8 µl, 806R (5 µm): 0.8 µl, FastPfu Polymerase: 0.4 µl, BSA: 0.2 µl, template DNA: 10 ng, and ddH2O: 20 µl. In addition, the polymerase chain reaction (PCR) reaction parameters were as follows: pre-denaturation at 95°C for 3 min, denaturation at 95°C for 30 s, annealing at 55°C for 30 s, extension at 72°C for 45 s (27 cycles in total), and final extension at 72°C for 10 min. Finally, PCR amplification was performed using a high-efficiency and high-fidelity enzyme (Phusion® High-Fidelity PCR Master Mix with GC Buffer, New England Biolabs) to ensure efficiency and accuracy of amplification.

Mixing and purification of PCR products

Mixing to equal concentration was performed according to the PCR product concentration, following which the PCR products were detected on 2% agarose gel at 120 V for approximately 30 min. Finally, the target bands were recovered using a gel recovery kit (Qiagen).

Library construction and sequencing

The purified PCR products were used to construct the library using the TruSeq® DNA PCR-Free Sample Preparation Kit. The constructed libraries were quantified by Qubit and qPCR. Subsequently, the qualified libraries were sequenced on the NovaSeq 6,000 on the Illumina HiSeq 2,500 sequencing platform of Novogene.

Processing of sequencing data

In general, some noise is present in the raw data obtained after sequencing. Consequently, splicing and filtering were performed to obtain valid data for accurate and reliable analyses. First, data for each sample was split from the data to be sequenced according to barcode sequences and PCR amplification primer sequences. Next, the barcode and primer sequences were truncated. Subsequently, the reads in each sample were spliced using the FLASH software package (FLASH v1.2.7[1]; Magoč and Salzberg, 2011), and the resulting spliced sequences were the raw tags. Further, the raw reads were filtered using Qiime (V1.9.1; Caporaso et al., 2010) to obtain high-quality reads. Following the tag quality control process, the final valid data (effective Tags) were obtained after removing chimeric sequences (Rognes et al., 2016).

1 http://ccb.jhu.edu/software/FLASH/

OTU clustering and species annotation

Operational Taxonomic Units (OTU) clustering was performed for the valid data at the 97% level using the Uparse software (Uparse v7.0.1001[2]; Haas et al., 2011). In addition, sequences with the highest frequency of occurrence of OTUs were screened as the representative sequences for those OTUs based on the ribosomal database project (RDP) classifier Bayesian algorithm using the Qiime (V1.9.1).[3] Subsequently, species annotation analysis (with a threshold of 0.8 to 1) was performed based on the Mothur method using the small-subunit rRNA (SSUrRNA) database (Wang et al., 2007) from SILVA132 (Edgar, 2013). The structural composition of microbial communities was detected by statistical analysis of OTUs for abundance, α-diversity, β-diversity, and community outcomes for the species at each taxonomic level (DeSantis et al., 2006; Wang et al., 2007). In addition, the optimal comparisons were selected to determine the taxonomic information and species-based distribution of bacterial sequence abundance. Finally, the least amount of data among the samples were standardized for homogenization.

Sample complexity analysis

Sample complexity analysis was performed by assessing the alpha diversity (within-habitat diversity) and sample diversity indices were calculated using the Qiime software (Version 1.9.1). The ACE and Chao1 indices were used to evaluate community richness. Subsequently, community diversity was calculated using Shannon and Simpson indices. The sequencing depth index was assessed by Good's coverage. Box plots between microbial community groups based on these diversity indices were drawn in R. Tukey's HSD was used to examine the differences in microorganisms between different JA varieties during the storage period. Furthermore, effective tags were visualized using Origin 2019. Finally, the variance test was performed using Duncan's new multiple range method using the SPSS software.

Multi-sample comparisons

Differences in bacterial species diversities between samples were compared using the ß-diversity index. Subsequently, Unifrac distances were calculated using the Qiime (Caporaso et al., 2010) software. Venn analysis was performed using the "VennDiagram" package in R software, which automatically generates highly-customizable, high-resolution Venn diagrams to assess common and unique microorganisms between JA varieties with differential storage characteristics across storage periods. In addition, ggplot2, reshape2, ggalluvial (Brunson, 2018), and vegan packages in R software were used to create collision diagrams of changes in microbial time series composition to visualize abundances of dominant bacterial and fungal taxa at phylum and genus levels. Subsequently, the top 35 bacterial genera in terms of abundance in each period were selected based on the abundance information for the bacterial communities, and clustering heatmaps were generated. Next, the common OTUs between the two varieties were selected to draw the radar chart. Finally, Linear discriminant analysis Effect Size (LEfSe) analysis was performed to identify changes in bacterial abundances between the two varieties during storage, and the screening value of the Linear discriminant analysis (LDA) score was set to 4 (Zhang et al., 2013).

Correlational analysis for carbohydrate factors

Redundancy analysis (RDA) plots were drawn to perform RDA between carbohydrates and specific bacterial species to obtain carbohydrate factors that significantly influenced the changes across bacterial communities. Spearman correlation coefficients were calculated using the R package, ggcor (Huang et al., 2020), based on the information for differential species abundance obtained from LEfSE analysis. Finally, a correlation analysis was performed between carbohydrates and specific bacterial communities.

Results

Richness and diversity analyses of bacterial communities

A total of 3,634,419 high-quality bacteria sequences were obtained from 48 samples (24 from 'JA25' and 24 from 'JA187'), with each having an average of 75,717 sequences. Good's coverage is an important metric for evaluating the sample coverage (i.e., the likelihood of sequencing the 16S rRNA PCR amplicons). As shown in Supplementary Table S1, the calculated Good's coverage values for bacterial community abundance ranged between 0.998 and 0.999, indicating that the samples had high coverage and that the sequencing results could truly characterize the bacterial diversity on the surface of JA tubers. In addition, the α-diversity index was calculated to assess the differences in bacterial community richness and diversity among different JA varieties during the storage period. As shown in Figure 1, the changing trend for OTU species between 'JA25' and 'JA187' was the same (decreasing–increasing–decreasing). Subsequently, bacterial abundance was evaluated using Chao and ACE indices. The number of bacterial OTUs detected in the storage-tolerant variety, 'JA25', was higher than that in the storage-intolerant variety, 'JA187'. Shannon and Simpson's indices are indicators of bacterial community diversity within the samples. It is generally accepted that a high Shannon index represents greater diversity, whereas a high Simpson index represents lower diversity. Herein, the diversity of bacteria in 'JA25' was higher than that in 'JA187'. Therefore, microorganisms may play a crucial role in the formation of microbial community diversity between the two varieties. Specifically, microbial community diversity was maintained in the 'JA25' variety. In contrast, dominant bacteria are more likely to develop in the 'JA187' variety, thus resulting in a reduction in diversity.

2 http://www.drive5.com/uparse/

3 http://qiime.org/scripts/split_libraries_fastq.html

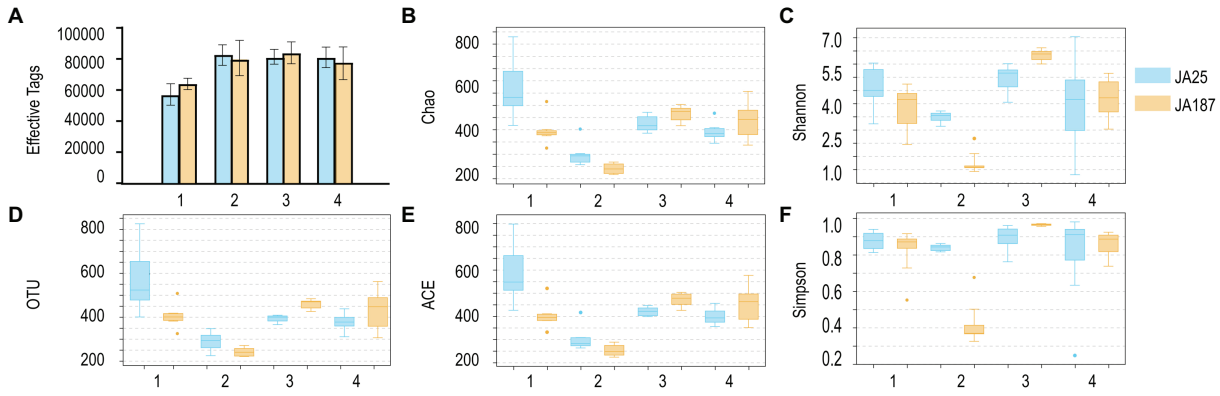

FIGURE 1
Results of the analysis of the number of effective sequences, operational taxonomic units and Alpha diversity index of bacteria on the surface of tubers of different Jerusalem artichoke resources during storage. **A**: Effective tags; **B**: Chao index; **C**: Shannon index; **D**: OTUs; **E**: ACE index; **F**: Simpson index. The numbers of replicated samples in this figure are as follows: 'JA25' (*n*=24), 'JA187' (*n*=24).

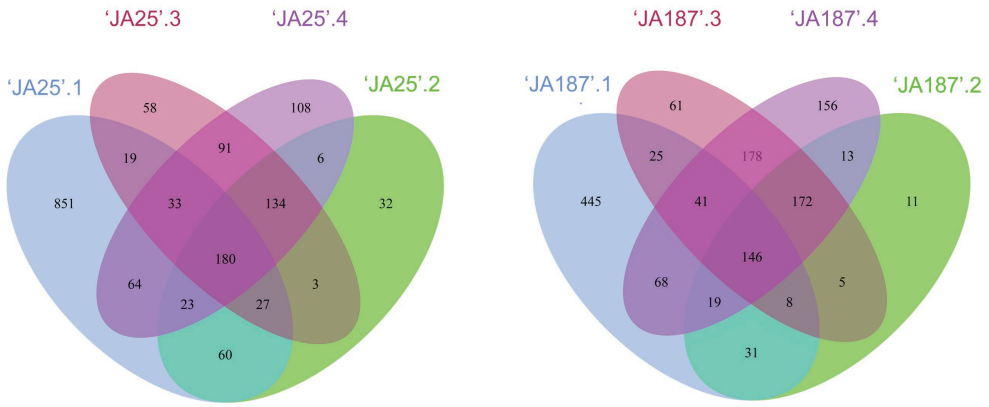

FIGURE 2
Bacterial taxa on the surface of tubers of different Jerusalem artichoke resources during storage. Venn diagram showing OTUs unique to and shared by 'JA25' (left) and 'JA187' (right) Jerusalem artichoke tuber surfaces. Each circle in the figure represents one sample. The number of overlapping areas represents the number of OTUs shared between the samples. The numbers without overlapping areas represented the number of unique OTUs in the sample.

In the Venn diagram, the circles denote different microbiomes, whereby their area of overlap represents the core. The common and unique bacteria between the two varieties were examined. A significant overlap in enriched OTUs was observed across different storage periods (Figure 2). The OTUs enriched during the fourth storage settled successfully throughout the enyire storage period. Of the 639/793 OTUs enriched in the fourth storage period, 531/637 were also enriched in the remaining three storage periods: (i.e., 531 and 637 OTUs were consistently present in the corresponding two JA varieties, during the four storage periods). Furthermore, there were differences in the number of core microbiomes, whereby 'JA25' had more core microbiomes in the most overlapping region than 'JA187', suggesting an important contribution to the enrichment of the whole microbial community.

Main members of the bacterial community on tuber surfaces during storage

The abundance of individual microbial species during storage was analyzed using the 16S rRNA sequences to elucidate the dominant bacterial composition in JA during storage. The top 10 most abundant phyla and genera are shown in Figure 3. The dominant phylum and relative abundance remained consistent between the two varieties. However, significant differences were observed in the proportion of bacteria at the genus level across the storage periods. Proteobacteria and Bacteroidetes were the dominant phyla, accounting for more than 80% of the entire community. The trend for Proteobacteria's relative abundance between 'JA25' and 'JA187' was the same (increasing and then decreasing), reaching its peak during the

second storage and then decreasing, and maintaining a constant level from the third to the fourth storage periods. The relative abundance of Bacteroidetes exhibited an overall decreasing trend during the storage of 'JA25', i.e., a decrease in the second period (lowest), followed by a marginal increase in the third and fourth storage periods. The pattern of variation in the relative abundance of this phylum during the storage of the 'JA187' variety was consistent with the observed pattern of microbial diversity from the beginning till the end of storage (Figure 3A). The abundance of unclassified fungal genera was significantly higher in the 'JA25' variety relative to the 'JA187' variety throughout the storage period. *Flavobacterium*, *Sphingobacterium*, and *Staphylococcus* were the most abundant genera at the beginning of storage in the 'JA25' variety, and their relative abundances decreased with the storage time. However, *Sphingobacterium* and *Staphylococcus* showed low abundances for most of the storage period in the 'JA187' variety. *Serratia* was the most dominant genus during storage and its relative abundance was higher than that in 'JA25' for the same period (Figure 3B).

Changes in bacterial diversity during JA storage

The top 35 genera were classified in a clustering heatmap to visualize the dynamic differences in the composition of the bacterial community (Figure 4). The changes in the abundance of bacterial communities on the tuber surfaces of the two varieties were similar across the four storage periods and could be divided into five clusters. The relative abundance of bacteria gradually increased with time in Cluster 1 but decreased in Cluster 5. Further functional analysis was performed on differential bacterial populations between the two varieties (Supplementary Table S3). Most of the genera with high relative abundances in the 'JA187' variety consisted of phytopathogens and carbohydrate-degrading endophytes. Phytopathogens were present in relatively low abundances in the 'JA25' variety and were mostly non-pathogenic. Subsequently, radar chart analysis was performed to examine the variations-in the abundances of 22 common bacteria on the surface of different JA varieties and the relative proportions of bacteria between the two varieties. The results suggested that three types of bacteria (*Acinetobacter*, Cyanobacteria, and *Staphylococcus*) were dominant among the six bacterial populations showing significant differences in their abundance. The relative abundance of *Staphylococcus,* having a biocontrol function, increased with time in the 'JA25' variety. In contrast, the relative abundance in the 'JA187' variety was low. Therefore, the differences in the function of unique bacteria and the abundances of common bacteria jointly influenced the storage process between the two JA varieties, thus proving that the differential storage characteristics between the two varieties were determined by microorganisms.

Lefse analysis of the bacterial communities

LEfSe was used to identify taxa that differed significantly in their abundance among different groups. The threshold for feature discrimination was a logarithmic LDA score of 4.0. In the LEfSe analysis, some bacterial community members exhibited a significant shift on the surface of tubers between the 'JA25' and 'JA187' varieties. At the genus level, the abundance of *Flavobacterium, Sphingobacterium*, and *Staphylococcus* increased significantly in the 'JA25' variety. However, six genera were present in the 'JA187' variety, including *Pseudomonas*, Cyanobacteria, *Serratia*, *Myroides*, *Dysgonomonas*, and *Acinetobacter*. Therefore, the storage-intolerant variety, 'JA187', comprised greater microorganisms during JA decay. Furthermore, the absence of 'JA25'0.4 in the figure indicates no significant differential taxa in this group (Figure 5).

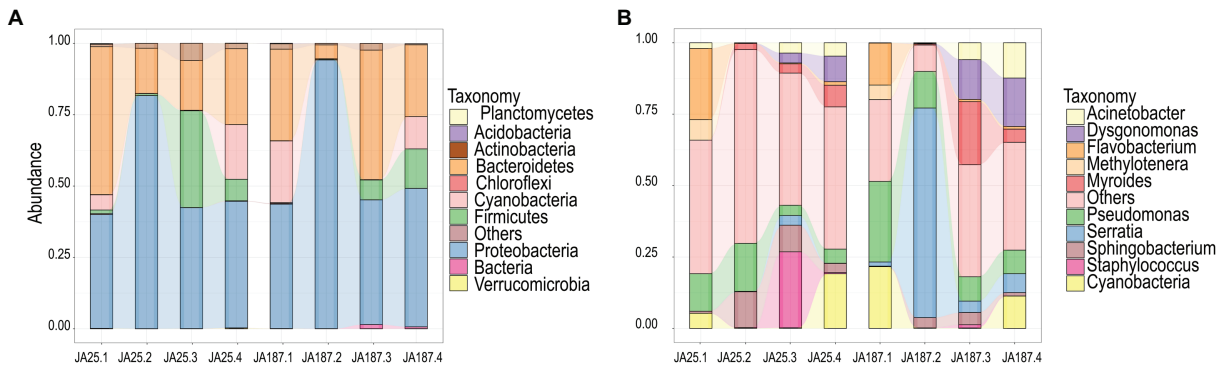

FIGURE 3
Demonstration of the composition of two Jerusalem artichoke resources at the phylum and genus level during storage. **(A)** phylum level **(B)** genus level. Each bar represents the relative abundance in each sample. Each color represents a particular phylum or genus.

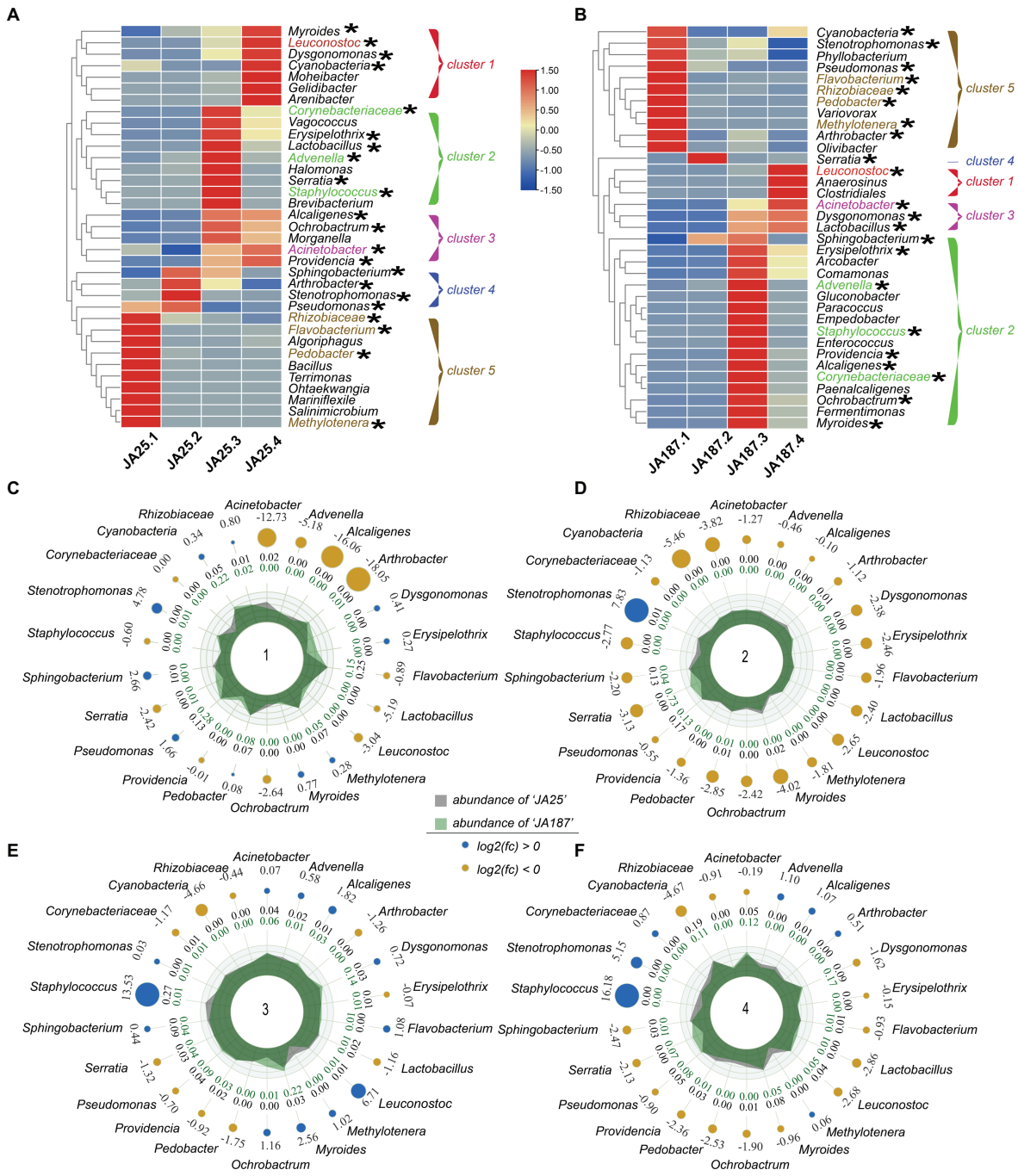

FIGURE 4
Dynamics of high-abundance bacteria in two Jerusalem artichoke resources during storage. (**A;** 'JA25') and (**B;** 'JA187') are the top 34 bacterial genus level Heatmap maps from the two resources, Cluster 1–5 indicates 5 bacterial clusters, with red and blue indicating high and low correlation, respectively. Radar plots show the abundance of a total of 22 bacteria from two chrysanthemum resources, with (**C–F**) representing four storage periods.

Relationship between bacterial taxa and carbohydrates

RDA was used to analyze the correlation between bacterial communities and carbohydrate factors, with the first two coordinate axes cumulatively explaining 60.93% of the variation in the microbial community structure. Based on the length of the arrow for each carbohydrate factor, inulin, sucrose, fructose, DP2–5, and DP6–10 were finally identified as key factors influencing the distribution of microbial communities in that order, whereas glucose, DP11–15, DP16–20, and DP > 20 had a little effect on species distribution

(Figure 6). Specifically, Cyanobacteria, *Sphingobacterium*, *Staphylococcus*, and *Serratia* correlated positively with inulin; *Acinetobacter*, *Myroides*, and *Dysgonomonas* correlated positively with sucrose. The RDA revealed a relative aggregation of the positions of *Myroides* and *Dysgonomonas*. A positive correlation between the two with glucose and fructose was observed. Cyanobacteria correlated positively with all four sugars. *Seudomonas* and *Flavobacterium* correlated negatively with glucose and fructose. DP2–5 and DP6–10 correlated positively with the distribution of *Acinetobacter*, *Myroides*, and *Dysgonomonas*; *Myroides* correlated positively with all five DPs.

Carbohydrate drivers of bacterial community composition

Carbohydrates exert a strong impact on the microbial community on the surface of JA tubers. Therefore, correlations between the carbohydrate variable matrix and the species abundance matrix were visualized by Mantel test statistics (Figure 7) to identify the main carbohydrate drivers in the dataset, to facilitate the understanding of their contribution to community formation. Overall, fructose and inulin were the strongest drivers of the community formation on the tuber surface. The positive correlation between degree of polymerization (DP) of inulin-fructans and decay gradually increased with increasing DP values. Fructans with a high degree of polymerization accelerated the decay of JA tubers. In the 'JA187' variety, *Dysgonomonas* and *Acinetobacter* showed a strong correlation with decay, thus suggesting that bacteria associated with decay rates may be directly involved in the degradation of highly polymerized fructans. Additionally, a significant negative correlation between decay and inulin was observed, whereas *Serratia* showed a highly significant positive correlation with inulin, suggesting its antagonistic role against pathogenic bacteria on the surface of stored JA tubers. Furthermore, a strong positive correlation between decay and fructose was observed in the 'JA25' variety. Nevertheless, there was also a strong positive correlation between *Sphingobacterium* and fructose, indicating its inhibitory effect on the decomposition of fructose during storage. In addition, the positive correlation with inulin gradually increased with the increase in fructan within DP < 20, reaching a maximum between16-20, indicating that the fructans present in the tubers of the 'JA25' variety generally showed a high degree of polymerization. In the 'JA187' variety, the

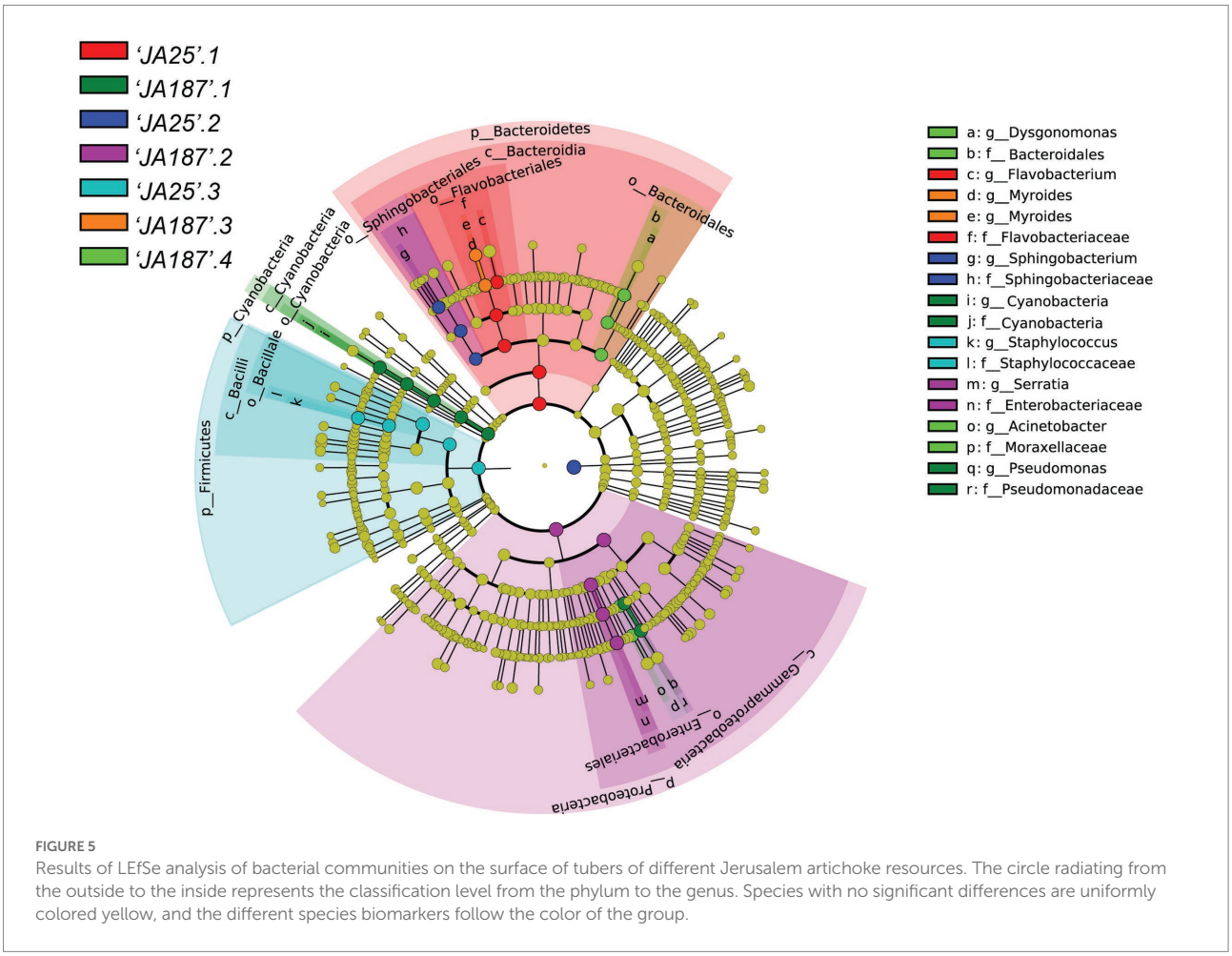

FIGURE 5
Results of LEfSe analysis of bacterial communities on the surface of tubers of different Jerusalem artichoke resources. The circle radiating from the outside to the inside represents the classification level from the phylum to the genus. Species with no significant differences are uniformly colored yellow, and the different species biomarkers follow the color of the group.

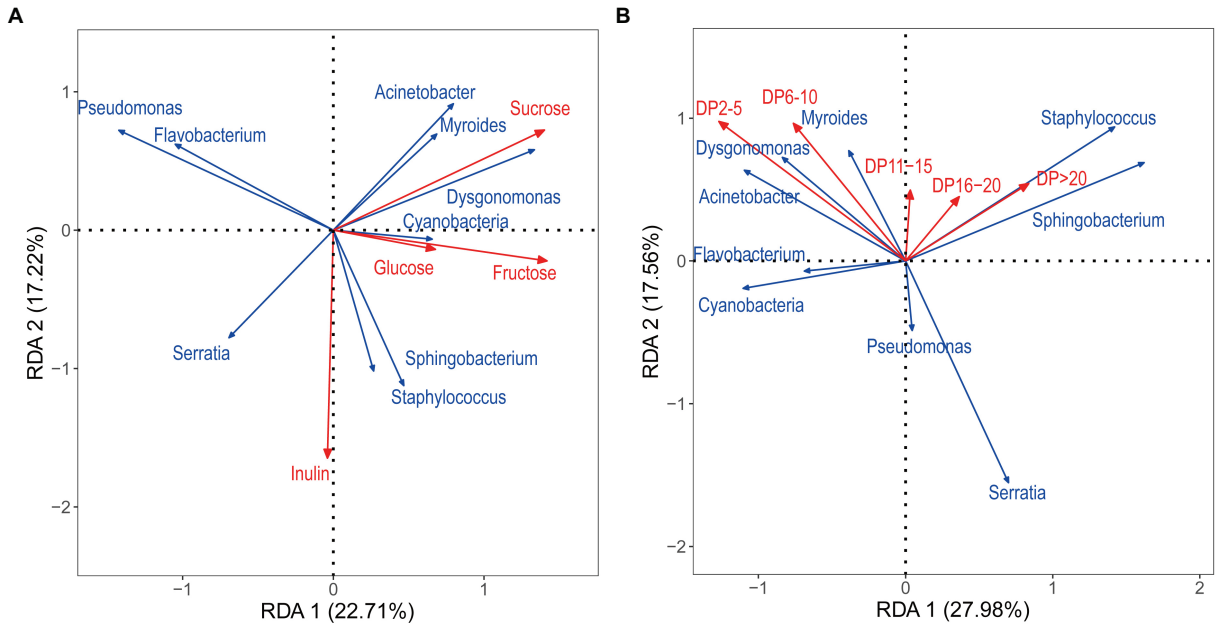

FIGURE 6
Redundancy analysis (RDA) based on bacteria OTU data with chemical parameters. (**A**): RDA between carbohydrate and bacterial communities, (**B**): RDA between the DP of inulin and bacterial communities. The correlation between carbohydrate factors and RDA axes is represented by the length and angle of arrows.

negative correlation with inulin gradually increased with decreasing DP values and reached a maximum between 2 and 5, indicating that fructans in the tubers were mainly present in a state of low polymerization. Therefore, the differences in the carbohydrate metabolite patterns may lead to the differential storage characteristics among different genotypes of JA varieties.

Discussion

The expansion of stolons in JA forms tubers, wherein carbohydrates are stored in the form of an inulin (Li et al., 2017). Similar to rhizospheric microbes, those attached to the tuber surface are influenced to some extent by plant genetics (Walters et al., 2018). Herein, we demonstrated that selection for crop genotypes drives changes in the recruitment of the plant microbiome using two differential storage-tolerant JA varieties. At the beginning of storage, microbial communities on the tuber surface differed only in their abundance, suggesting homogeneity of the rhizospheric microbiome during the recruitment process. However, the two JA genotypes remained highly heterogeneous for carbohydrates and metabolites. Consequently, the microbial community on the tuber surface changed dramatically during storage. Several studies have confirmed that heterogeneity of crop genotypes and selection effects exert a significant impact on the assembly of the microbial community (Schmidt et al., 2020; Favela et al., 2021). Therefore, further studies are needed to determine changes in pre-harvest bacterial communities on the tuber surface to validate the effects of plant genotype on the recruitment behavior of bacteria on the surface of post-harvest tubers.

JA needs to be stored for commercial processing, especially in the Qinghai–Tibet Plateau region, where the harvesting period is concentrated in early October. Early harvesting results in insufficient tuber yield and fructan content for commercialization. However, harvesting at ground temperatures below 0°C causes the tubers to freeze, and re-thawing during intensive processing results in significant sugar loss and increased decay rates. This challenge is not confined to the alpine regions. In hot areas of Thailand, the environmental factors pose challenges in the processing of JA (Jirayucharoensak et al., 2018). Therefore, storage is the only solution to relieve the processing pressure and the most convenient and easy way to preserve germplasm resources for asexually propagated crops. Research on microbial disease infestation during JA storage has focused on fungi, including *Botrytis*, *Aspergillus*, *Fusarium*, *Rhizopus*, and *Pennicillum,* which cause the decay of JA tubers, premature germination, and decrease the fructan quality during the storage (Kosaric et al., 1984; Jin et al., 2013; Yang et al., 2020). The surface of harvested and stored crops enriches with a large population of microorganisms, including bacteria, filamentous fungi, and yeasts, either as epiphytes or endophytes (Droby et al., 2016). At present, there is a lack of knowledge on the microbial variability and diversity of tuber crops, including JA that is stored for overwintering. The residual soil attached to the tuber surfaces after harvesting is the main contributor to the bacterial community diversity during storage, as evidenced by the phylum-level observations between the two stored varieties' tubers during

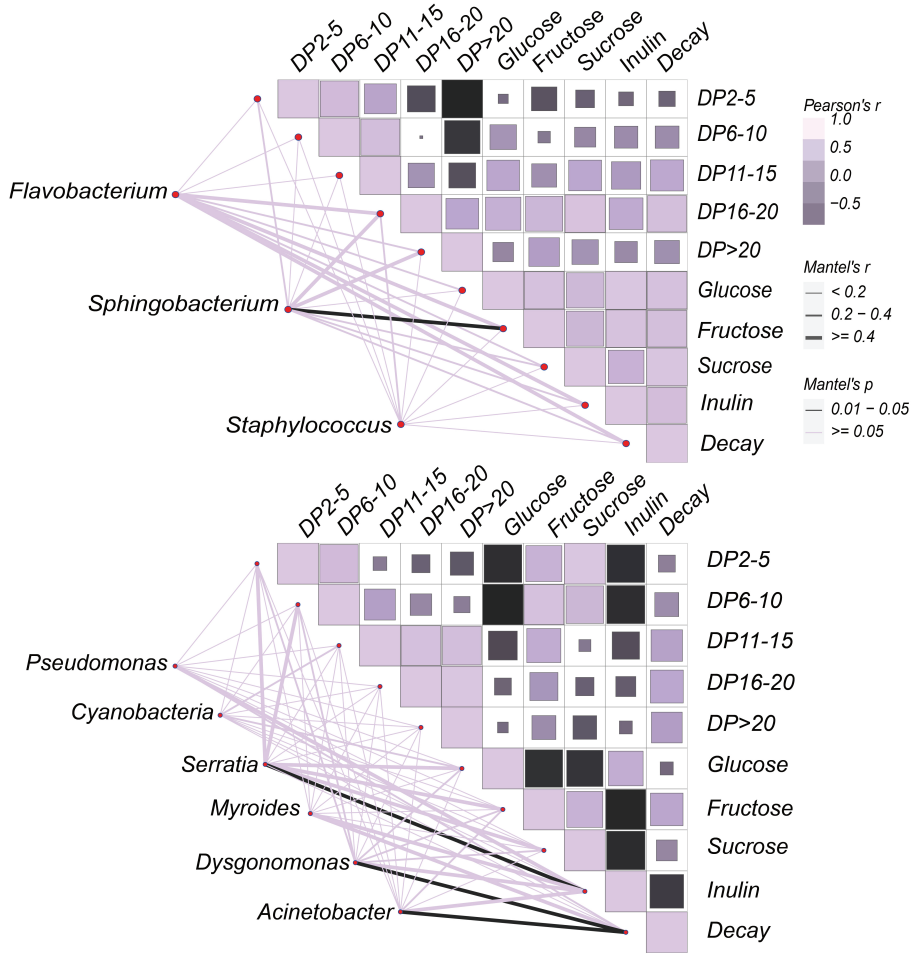

FIGURE 7
Correlation between bacterial communities and carbohydrates on the surface of Jerusalem artichoke tubers during storage. The horizontal and vertical axes of the heat map on the right side represent the various types of carbohydrate factors that respond to or interact with the community, respectively. The color of the block in each square of the heat map indicates a positive or negative correlation with carbohydrate factors, and its size indicates the absolute value of the correlation coefficient. The shading from dark purple to light purple indicates a positive correlation gradient from low to high, and the shading from dark purple to black represents a negative correlation gradient from low to high. On the left side is the bacterial data obtained from LEfSe analysis, which are linked to each carbohydrate factor data one by one through connecting lines. The edge width corresponds to the R value and edge color denotes the statistical significance.

the initial period of storage. Apart from some differences in abundance, the degree of differences at the species level was not high. Indicators of microbial diversity of 'JA187' were significantly lower in the first two storage periods as compared to the storage-tolerant variety. Disease outbreaks in plants are often correlated with shifts in the microbiome composition, resulting in microbial dysbiosis (Berg et al., 2017). The abundance of *Serratia* in the perishable variety, 'JA187', changed dramatically especially during the second storage period, leading to a decrease in the abundance of bacterial communities. *Serratia rubidaea* and *Serratia plymuthica* isolated from onion corms are the main causal agent of tulip bulbs (Kowalska et al., 2011; Stoyanova et al., 2012). In contrast, *Serratia plymuthica* plays an antagonistic role against fungal diseases during the storage of potato tubers (Gould et al., 2008; Czajkowski et al., 2012; Maciag et al., 2020). Most of the potential biocontrol agents are screened by *in vitro* antagonism activity against the pathogen. However, there is a long and intense debate on the screening assay (Berg et al., 2017). The artificial environment leads to no or only a very low *in vitro* antagonism (Adesina et al., 2009). However, bacteria that exhibit antagonistic effects in the *in vitro* experiments exert opposite effects due to the lack of community support (Rybakova et al., 2016). Pathogen infestation and spoilage may often not be caused by a single organism but is likely to result from the interplay of individual members of the microbial community in crops. Microbes enriched in unrotten samples primarily belong to Cyanobacteria, *Staphylococcus*, and *Staphylococcaceae*, which could act as potential biocontrol agents against rot (Prasanna et al., 2015; Cebrián et al., 2020; Lorenzini and Zapparoli, 2020; Shah et al., 2021). We speculated that this effect could originate directly from the impact of the biocontrol agents on the composition of the microbiota or indirectly from their impact on a pathogen. Treatment of ginger (*Zingiber officinale* Roscoe) with biological

control agents using *Bacillus* and *Trichoderma*, significantly alter the structure and diversity of bacterial communities on its surface (Huang et al., 2021).

In the plant taxa, there is a close association between seeds and bacteria. Tuber crops develop and mature in the soil, and microorganisms on the surface of the tuber during this process have a distinct relationship with the environment. In particular, microorganisms attached to the surface of root crops have been observed, including *Staphylococcus*, *Pseudomonas*, and *Actinobacteria* (Buchholz et al., 2019, 2021; Shi et al., 2019). This finding is consistent with the microbial species on the surface of the JA tubers during storage herein, which may be attributed to the wide distribution of these bacteria that genera-level in soils worldwide (Fierer et al., 2012), and thus, is the genus of the most likely taxa that encounter tubers during the developmental stages and beyond (Nelson, 2018). In addition, a significant difference in tuber bacterial communities was observed between the two genotypes during dormancy (the second and third storage periods), indicating the continuous dynamics of bacterial communities during dormancy. Interestingly, changes in microbial communities observed during the storage of potatoes and sugar beets are independent of crop genotypes (Kusstatscher et al., 2019; Buchholz et al., 2021). This result is not quite consistent with our findings, which may be attributed to the differences in carbohydrates or a selective relationship between bacterial communities and carbohydrates due to the chemical specificity of fructans. The Baas Becking hypothesis propounds that 'everything is everywhere but the environment selects.' Therefore, environmental selection is the primary evolutionary driver in a gradient-differentiated environment, regardless of the size of the community. Indeed, natural selection has dominated changes in communities. Many microbial community studies have correspondingly only attempted to evaluate the role of selection in community assemblage. Overall, there has been less focus on evaluating whether microbial communities may differentiate as a consequence of various neutral processes (Hanson et al., 2012; Morrison-Whittle and Goddard, 2015).

The human gut microbiota encodes a huge diversity of enzymes for the digestion of all components of plant polysaccharides including inulin. A study on inulin and arabinoxylan-oligosaccharides as carbon sources for simulation experiments shows that the complexity of the carbon source structure maintains a greater microbial diversity (Chung et al., 2019). The relationships between carbohydrate structural complexity and sustained diversity may be a fundamental property underlying the carbohydrate-microbiome interactions (Yao et al., 2020). The results of the correlational analysis revealed significant associations between continuous changes in carbohydrate and bacterial communities, with positive or negative correlations between decay and several carbohydrates. These data suggested that changes in carbohydrate structure could alter the microbial communities that consume specific carbohydrates. In a continuously changing environment, decay consistently shows a positive correlation with degree of polymerization (DP) of inulin-fructans, and high-DP inulin accelerates the decay of JA tubers. Therefore, decay-related bacteria may be directly involved in the decomposition of degree of polymerization (DP) of inulin-fructans, as evidenced b a significant correlation of *Dysgonomonas* and *Acinetobacter* in storage-intolerant JA varieties, 'JA187', with decay. *Dysgonomonas* is found in the gut of many insects (McManus et al., 2018; Jang and Kikuchi, 2020) and are commonly cultured on complex media containing blood, peptone, tryptone, yeast, or plants under anaerobic conditions (Bridges and Gage, 2021). We hypothesized that bacteria belonging to the genus, *Dysgonomonas,* play a driving role in the decay of JA tubers. This is one of the few studies on plants wherein the function of *Dysgonomonas* has been elucidated, and there may be an unknown important role in the degradation and utilization of inulin. *Acinetobacter* is capable of producing high amounts of inulinase (Muslim et al., 2015), and inulin is an excellent substrate. Therefore, *Acinetobacter* can spearhead the catabolic conversion of inulin during storage of JA tubers, as monosaccharides produced by the degradation of inulin are the best culture substrates for several microorganisms. *Serratia* was mainly enriched in 'JA187' but it cannot directly ferment inulin (Gavini et al., 1979). In addition, 10% inulin content has a good inhibitory effect on multiple bacteria including *Serratia* (Salman, 2009). Results of the correlational analysis revealed a highly significant positive correlation of *Serratia* with inulin during storage; an opposite trend was observed with decay rate, confirming that *Serratia* played an antagonistic role against pathogenic bacteria on the surface of stored JA tubers. However, we did not observe the aforementioned association between bacteria and carbohydrates in storage-tolerant varieties, and decay exhibited a positive correlation with inulin. These findings suggested that crop genotypes cause differential microbial community-related selection effects, as environmental conditions for tuber storage and pre-harvest planting soil conditions were consistent. *Sphingobacterium* showed a positive correlation with fructose in storage-tolerant varieties, which may be attributed to the inhibition of fructose catabolite utilization. *Sphingobacterium* aerobic bacterium is capable of suppressing *Fusarium graminearum*, *Exserohilum turcicum*, *Pythium aphanidermatum*, and *Cochliobolus sativus.* The strain of *Sphingobacterium* harbors sets of genes responsible for the production of 2,3-butanediol and salicylic acid, which can elicit induced systemic resistance in the host plant (Xu et al., 2020; Sahu et al., 2021). Information on the dynamics and diversity of microbiota in stored JA may be useful for developing a new paradigm in postharvest biocontrol based on the construction of synthetic microbial communities that provide superior pathogen control strategiess.

Conclusion

In Jerusalem artichoke tuber, the inulin-type fructans serve as carbohydrate reserve, inulin are one source of soluble dietary

fibers. Currently, very few studies have been reported on the association of inulin with bacterial communities during JA storage, especially in fructane-based tuber crops. The analysis of the results in this study proved that *Flavobacterium*, *Sphingobacterium*, *Staphylococcus*, *Dysgonomonas*, *Acinetobacter* and *Serratia* assumed an important role in the storage process. Both crop genotype and carbohydrate structure affected the bacterial community composition.

Data availability statement

The data presented in the study are deposited in the https://www.ncbi.nlm.nih.gov/ repository, accession number PRJNA822494.

Author contributions

GD: conceptualization, methodology, formal analysis, investigation, data curation, writing–original draft, and visualization. ZS: visualization and writing–review and editing. SB: investigation, methodology, and data curation. QZ: resources, data curation, and funding acquisition. SY: conceptualization, methodology, resources, data curation, writing–review and editing, supervision, funding acquisition, and project administration. All authors contributed to the article and approved the submitted version.

Funding

This study was financially supported by Key Laboratory Project of Qinghai Science & Technology Department (Grant reference: 2020-ZJ-Y02), Qinghai key research and development conversion project (Grant reference: 2022-NK-117), and National Natural Science Foundation of China (31760600).

Acknowledgments

We thank Bullet Edits Limited for linguistic editing and proofreading of the manuscript.

Conflict of interest

The authors declare that the research was conducted in the absence of any commercial or financial relationships that could be construed as a potential conflict of interest.

Publisher's note

All claims expressed in this article are solely those of the authors and do not necessarily represent those of their affiliated organizations, or those of the publisher, the editors and the reviewers. Any product that may be evaluated in this article, or claim that may be made by its manufacturer, is not guaranteed or endorsed by the publisher.

Supplementary material

The Supplementary material for this article can be found online at: https://www.frontiersin.org/articles/10.3389/fmicb.2022.986659/full#supplementary-material

References

Adesina, M. F., Grosch, R., Lembke, A., Vatchev, T. D., and Smalla, K. (2009). In vitro antagonists of Rhizoctonia solani tested on lettuce: rhizosphere competence, biocontrol efficiency and rhizosphere microbial community response. *FEMS Microbiol. Ecol.* 69, 62–74. doi: 10.1111/j.1574-6941.2009.00685.x

Amann, R. I., Ludwig, W., and Schleifer, K.-H. (1995). Phylogenetic identification and in situ detection of individual microbial cells without cultivation. *Microbiol. Rev.* 59, 143–169. doi: 10.1128/mr.59.1.143-169.1995

Berg, G., Köberl, M., Rybakova, D., Müller, H., Grosch, R., and Smalla, K. (2017). Plant microbial diversity is suggested as the key to future biocontrol and health trends. *FEMS Microbiol. Ecol.* 93:050. doi: 10.1093/femsec/fix050

Bridges, C. M., and Gage, D. J. (2021). Development and application of aerobic, chemically defined media for *Dysgonomonas*. *Anaerobe* 67:102302. doi: 10.1016/j.anaerobe.2020.102302

Brunson, J. C. (2018). Ggalluvial: alluvial diagrams in'ggplot2'. *R pack. ver.* 1.

Buchholz, F., Antonielli, L., Kostić, T., Sessitsch, A., and Mitter, B. (2019). The bacterial community in potato is recruited from soil and partly inherited across generations. *PLoS One* 14:e0223691. doi: 10.1371/journal.pone.0223691

Buchholz, F., Junker, R., Samad, A., Antonielli, L., Sarić, N., Kostić, T., et al. (2021). 16S rRNA gene-based microbiome analysis identifies candidate bacterial strains that increase the storage time of potato tubers. *Sci. Rep.* 11:3146. doi: 10.1038/s41598-021-82181-9

Caporaso, J. G., Kuczynski, J., Stombaugh, J., Bittinger, K., Bushman, F. D., Costello, E. K., et al. (2010). QIIME allows analysis of high-throughput community sequencing data. *Nat. Methods* 7, 335–336. doi: 10.1038/nmeth.f.303

Cebrián, E., Núñez, F., Gálvez, F. J., Delgado, J., Bermúdez, E., and Rodríguez, M. (2020). Selection and evaluation of *staphylococcus xylosus* as a biocontrol agent against toxigenic moulds in a dry-cured ham model system. *Microorganisms* 8:793. doi: 10.3390/microorganisms8060793

Chatellard, L., Trably, E., and Carrère, H. (2016). The type of carbohydrates specifically selects microbial community structures and fermentation patterns. *Bioresour. Technol.* 221, 541–549. doi: 10.1016/j.biortech.2016.09.084

Chung, W. S. F., Walker, A. W., Vermeiren, J., Sheridan, P. O., Bosscher, D., Garcia-Campayo, V., et al. (2019). Impact of carbohydrate substrate complexity on the diversity of the human colonic microbiota. *FEMS Microbiol. Ecol.* 95:fiy201. doi: 10.1093/femsec/fiy201

Czajkowski, R., de Boer, W. J., van Veen, J. A., and van der Wolf, J. M. (2012). Characterization of bacterial isolates from rotting potato tuber tissue showing antagonism to *Dickeya* sp. biovar 3 in vitro and in planta. *Plant Pathol.* 61, 169–182. doi: 10.1111/j.1365-3059.2011.02486.x

DeSantis, T. Z., Hugenholtz, P., Larsen, N., Rojas, M., Brodie, E. L., Keller, K., et al. (2006). Greengenes, a chimera-checked 16S rRNA gene database and workbench compatible with ARB. *Appl. Environ. Microbiol.* 72, 5069–5072. doi: 10.1128/AEM.03006-05

Droby, S., and Wisniewski, M. (2018). The fruit microbiome: A new frontier for postharvest biocontrol and postharvest biology. *Postharvest Biol. Technol.* 140, 107–112. doi: 10.1016/j.postharvbio.2018.03.004

Droby, S., Wisniewski, M., Teixidó, N., Spadaro, D., and Jijakli, M. H. (2016). The science, development, and commercialization of postharvest biocontrol

products. *Postharvest Biol. Technol.* 122, 22–29. doi: 10.1016/j.postharvbio.2016.04.006

Edgar, R. C. (2013). UPARSE: highly accurate OTU sequences from microbial amplicon reads. *Nat. Methods* 10, 996–998. doi: 10.1038/nmeth.2604

Favela, A. O., Bohn, M., and Kent, A. (2021). Maize germplasm chronosequence shows crop breeding history impacts recruitment of the rhizosphere microbiome. *ISME J.* 15, 2454–2464. doi: 10.1038/s41396-021-00923-z

Fierer, N., Leff, J. W., Adams, B. J., Nielsen, U. N., Bates, S. T., Lauber, C. L., et al. (2012). Cross-biome metagenomic analyses of soil microbial communities and their functional attributes. *Proc. Natl. Acad. Sci.* 109, 21390–21395. doi: 10.1073/pnas.1215210110

Gavini, F., Ferragut, C., Izard, D., Trinel, P., Leclerc, H., Lefebvre, B., et al. (1979). *Serratia fonticola*, a new species from water. *Int. J. Syst. Evol. Microbiol.* 29, 92–101.

Gould, M., Nelson, L. M., Waterer, D., and Hynes, R. K. (2008). Biocontrol of *Fusarium sambucinum*, dry rot of potato, by *Serratia plymuthica* 5–6. *Biocontrol Sci. Tech.* 18, 1005–1016. doi: 10.1080/09583150802478189

Gunina, A., and Kuzyakov, Y. (2015). Sugars in soil and sweets for microorganisms: review of origin, content, composition and fate. *Soil Biol. Biochem.* 90, 87–100. doi: 10.1016/j.soilbio.2015.07.021

Haas, B. J., Gevers, D., Earl, A. M., Feldgarden, M., Ward, D. V., Giannoukos, G., et al. (2011). Chimeric 16S rRNA sequence formation and detection in sanger and 454-pyrosequenced PCR amplicons. *Genome Res.* 21, 494–504. doi: 10.1101/gr.112730.110

Hanson, C. A., Fuhrman, J. A., Horner-Devine, M. C., and Martiny, J. B. (2012). Beyond biogeographic patterns: processes shaping the microbial landscape. *Nat. Rev. Microbiol.* 10, 497–506. doi: 10.1038/nrmicro2795

Huang, Z., Liu, B., Yin, Y., Liang, F., Xie, D., Han, T., et al. (2021). Impact of biocontrol microbes on soil microbial diversity in ginger (Zingiber officinale roscoe). *Pest Manag. Sci.* 77, 5537–5546. doi: 10.1002/ps.6595

Huang, H., Zhou, L., Chen, J., and Wei, T. (2020). Ggcor: extended tools for correlation analysis and visualization. *R pack. ver.*, 7.

Jang, S., and Kikuchi, Y. (2020). Impact of the insect gut microbiota on ecology, evolution, and industry. *Curr. Opin. Insect Sci.* 41, 33–39. doi: 10.1016/j.cois.2020.06.004

Jin, S., Liu, L., Liu, Z., Long, X., Shao, H., and Chen, J. (2013). Characterization of marine *pseudomonas* spp. antagonist towards three tuber-rotting fungi from Jerusalem artichoke, a new industrial crop. *Ind. Crop. Prod.* 43, 556–561. doi: 10.1016/j.indcrop.2012.07.038

Jirayucharoensak, R., Khuenpet, K., Jittanit, W., and Sirisansaneeyakul, S. (2018). Physical and chemical properties of powder produced from spray drying of inulin component extracted from Jerusalem artichoke tuber powder. *Dry. Technol.* doi: 10.1080/07373937.2018.1492934

Kosaric, N., Cosentino, G., Wieczorek, A., and Duvnjak, Z. (1984). The Jerusalem artichoke as an agricultural crop. *Biomass* 5, 1–36. doi: 10.1016/0144-4565(84)90066-0

Kowalska, B., Smolińska, U., and Oskiera, M. (2011). First report of *Serratia plymuthica* causing onion bulb rot in Poland. *Pol. J. Microbiol.* 60, 85–87. doi: 10.33073/pjm-2011-012

Kusstatscher, P., Cernava, T., Abdelfattah, A., Gokul, J., Korsten, L., and Berg, G. (2020). Microbiome approaches provide the key to biologically control postharvest pathogens and storability of fruits and vegetables. *FEMS Microbiol. Ecol.* 96:fiaa119. doi: 10.1093/femsec/fiaa119

Kusstatscher, P., Zachow, C., Harms, K., Maier, J., Eigner, H., Berg, G., et al. (2019). Microbiome-driven identification of microbial indicators for postharvest diseases of sugar beets. *Microbiome* 7:112. doi: 10.1186/s40168-019-0728-0

Li, L., Shao, T., Yang, H., Chen, M., Gao, X., Long, X., et al. (2017). The endogenous plant hormones and ratios regulate sugar and dry matter accumulation in Jerusalem artichoke in salt-soil. *Sci. Total Environ.* 578, 40–46. doi: 10.1016/j.scitotenv.2016.06.075

Li, H.-Y., Wang, H., Wang, H.-T., Xin, P.-Y., Xu, X.-H., Ma, Y., et al. (2018). The chemodiversity of paddy soil dissolved organic matter correlates with microbial community at continental scales. *Microbiome* 6, 1–16. doi: 10.1186/s40168-018-0561-x

Liu, X., Gao, Y., Yang, H., Li, L., Jiang, Y., Li, Y., et al. (2020). *Pichia kudriavzevii* retards fungal decay by influencing the fungal community succession during cherry tomato fruit storage. *Food Microbiol.* 88:103404. doi: 10.1016/j.fm.2019.103404

Lorenzini, M., and Zapparoli, G. (2020). Epiphytic bacteria from withered grapes and their antagonistic effects on grape-rotting fungi. *Int. J. Food Microbiol.* 319:108505. doi: 10.1016/j.ijfoodmicro.2019.108505

Lovegrove, A., Edwards, C., De Noni, I., Patel, H., El, S., Grassby, T., et al. (2017). Role of polysaccharides in food, digestion, and health. *Crit. Rev. Food Sci. Nutr.* 57, 237–253. doi: 10.1080/10408398.2014.939263

Maciag, T., Krzyzanowska, D. M., Jafra, S., Siwinska, J., and Czajkowski, R. (2020). The great five—an artificial bacterial consortium with antagonistic activity towards *Pectobacterium* spp. and *Dickeya* spp.: formulation, shelf life, and the ability to prevent soft rot of potato in storage. *Appl. Microbiol. Biotechnol.* 104, 4547–4561. doi: 10.1007/s00253-020-10550-x

Magerl, M., Lammel, V., Siebenhaar, F., Zuberbier, T., Metz, M., and Maurer, M. (2008). Non-pathogenic commensal *Escherichia coli bacteria* can inhibit degranulation of mast cells. *Exp. Dermatol.* 17, 427–435. doi: 10.1111/j.1600-0625.2008.00704.x

Magoč, T., and Salzberg, S. L. (2011). FLASH: fast length adjustment of short reads to improve genome assemblies. *Bioinformatics* 27, 2957–2963. doi: 10.1093/bioinformatics/btr507

Man, S., Liu, T., Yao, Y., Lu, Y., Ma, L., and Lu, F. (2020). Friend or foe? The roles of inulin-type fructans. *Carbohydr. Polym.* 252:117155. doi: 10.1016/j.carbpol.2020.117155

McManus, R., Ravenscraft, A., and Moore, W. (2018). Bacterial Associates of a Gregarious Riparian Beetle With Explosive Defensive Chemistry. *Front. Microbiol.* 9:2361. doi: 10.3389/fmicb.2018.02361

Morrison-Whittle, P., and Goddard, M. R. (2015). Quantifying the relative roles of selective and neutral processes in defining eukaryotic microbial communities. *ISME J.* 9, 2003–2011. doi: 10.1038/ismej.2015.18

Muslim, S. N., Ali, A. N. M., Salman, I. M. A., AL Kadmy, I. M., and Muslim, S. N. (2015). Detection of the optimal conditions for inulinase productivity and activity by *Acinetobacter baumannii* isolated from agricultural rhizosphere soil. *Biolog. Sci. (IJACEBS)* 2, 1–7. doi: 10.15242/IJACEBS.C0315004

Nelson, E. B. (2018). The seed microbiome: origins, interactions, and impacts. *Plant Soil* 422, 7–34. doi: 10.1007/s11104-017-3289-7

Prasanna, R., Babu, S., Bidyarani, N., Kumar, A., Triveni, S., Monga, D., et al. (2015). Prospecting cyanobacteria-fortified composts as plant growth promoting and biocontrol agents in cotton. *Exp. Agric.* 51, 42–65. doi: 10.1017/S0014479714000143

Rognes, T., Flouri, T., Nichols, B., Quince, C., and Mahé, F. (2016). VSEARCH: a versatile open source tool for metagenomics. *PeerJ* 4:e2584. doi: 10.7717/peerj.2584

Rybakova, D., Schmuck, M., Wetzlinger, U., Varo-Suarez, A., Murgu, O., Müller, H., et al. (2016). Kill or cure? The interaction between endophytic *Paenibacillus* and *Serratia* strains and the host plant is shaped by plant growth conditions. *Plant Soil* 405, 65–79. doi: 10.1007/s11104-015-2572-8

Sahu, K. P., Kumar, A., Patel, A., Kumar, M., Gopalakrishnan, S., Prakash, G., et al. (2021). Rice blast lesions: an unexplored Phyllosphere microhabitat for novel antagonistic bacterial species Against *Magnaporthe oryzae*. *Microb. Ecol.* 81, 731–745. doi: 10.1007/s00248-020-01617-3

Salman, J. A. (2009). Synbiotic effect of probiotic (*Bifidobacterium* sp) and prebiotics (chicory and inulin) aganist some pathogenic bacteria. *Baghdad Sci. J.* 6, 354–360.

Schmidt, J. E., Rodrigues, J. L. M., Brisson, V. L., Kent, A., and Gaudin, A. C. (2020). Impacts of directed evolution and soil management legacy on the maize rhizobiome. *Soil Biol. Biochem.* 145:107794. doi: 10.1016/j.soilbio.2020.107794

Shah, S. T., Basit, A., Ullah, I., and Mohamed, H. I. (2021). Cyanobacteria and algae as biocontrol agents Against fungal and bacterial plant pathogens. *Plant Growth-Promot. Microb. Sustain. Biotic. Abiotic Stress Manage.* 1–23. doi: 10.1007/978-3-030-66587-6_1

Shen, Y., Nie, J., Dong, Y., Kuang, L., Li, Y., and Zhang, J. (2018). Compositional shifts in the surface fungal communities of apple fruits during cold storage. *Postharvest Biol. Technol.* 144, 55–62. doi: 10.1016/j.postharvbio.2018.05.005

Shi, W., Li, M., Wei, G., Tian, R., Li, C., Wang, B., et al. (2019). The occurrence of potato common scab correlates with the community composition and function of the geocaulosphere soil microbiome. *Microbiome* 7:14. doi: 10.1186/s40168-019-0629-2

Spang, E. S., Moreno, L. C., Pace, S. A., Achmon, Y., Donis-Gonzalez, I., Gosliner, W. A., et al. (2019). Food loss and waste: measurement, drivers, and solutions. *Annu. Rev. Environ. Resour.* 44, 117–156. doi: 10.1146/annurev-environ-101718-033228

Stoyanova, M., Georgieva, L., Petrov, N., Badjakov, I., and Bogatzevska, N. (2012). Bacterial bulb decay of summer snowflake/Leucojum Aestivum L. *Biotechnol. Biotechnol. Equip.* 26, 3338–3344. doi: 10.5504/BBEQ.2012.0096

Tholozan, J. L., Cappelier, J. M., Tissier, J. P., Delattre, G., and Federighi, M. (1999). Physiological characterization of viable-but-Nonculturable *campylobacter jejuniCells*. *Appl. Environ. Microbiol.* 65, 1110–1116. doi: 10.1128/AEM.65.3.1110-1116.1999

Walters, W. A., Jin, Z., Youngblut, N., Wallace, J. G., Sutter, J., Zhang, W., et al. (2018). Large-scale replicated field study of maize rhizosphere identifies heritable microbes. *Proc. Natl. Acad. Sci.* 115, 7368–7373. doi: 10.1073/pnas.1800918115

Wang, Q., Garrity, G. M., Tiedje, J. M., and Cole, J. R. (2007). Naive Bayesian classifier for rapid assignment of rRNA sequences into the new bacterial taxonomy. *Appl. Environ. Microbiol.* 73, 5261–5267. doi: 10.1128/AEM.00062-07

Wenneker, M., and Thomma, B. P. (2020). Latent postharvest pathogens of pome fruit and their management: from single measures to a systems intervention approach. *Eur. J. Plant Pathol.* 156, 663–681. doi: 10.1007/s10658-020-01935-9

Xu, L., Zhang, H., Xing, Y.-T., Li, N., Wang, S., and Sun, J.-Q. (2020). Complete genome sequence of *Sphingobacterium psychroaquaticum* strain SJ-25, an aerobic bacterium capable of suppressing fungal pathogens. *Curr. Microbiol.* 77, 115–122. doi: 10.1007/s00284-019-01789-3

Yang, S., Du, G., Tian, J., Jiang, X., Sun, X., Li, Y., et al. (2020). First report of tuber soft rot of Jerusalem artichoke (Helianthus tuberosus) caused by *Rhizopus arrhizus* in Qinghai Province of China. *Plant Dis.* 104:3265. doi: 10.1094/PDIS-02-20-0280-PDN

Yao, T., Chen, M.-H., and Lindemann, S. R. (2020). Structurally complex carbohydrates maintain diversity in gut-derived microbial consortia under high dilution pressure. *FEMS Microbiol. Ecol.* 96:158. doi: 10.1093/femsec/fiaa158

Zhang, C., Li, S., Yang, L., Huang, P., Li, W., Wang, S., et al. (2013). Structural modulation of gut microbiota in life-long calorie-restricted mice. *Nat. Commun.* 4, 1–10. doi: 10.1038/ncomms3163

Zhang, Q., Shi, W., Zhou, B., Du, H., Xi, L., Zou, M., et al. (2021). Variable characteristics of microbial communities on the surface of sweet cherries under different storage conditions. *Postharvest Biol. Technol.* 173:111408. doi: 10.1016/j.postharvbio.2020.111408

Zheng, X.-W., Yan, Z., Robert Nout, M. J., Boekhout, T., Han, B.-Z., Zwietering, M. H., et al. (2015). Characterization of the microbial community in different types of Daqu samples as revealed by 16S rRNA and 26S rRNA gene clone libraries. *World J. Microbiol. Biotechnol.* 31, 199–208. doi: 10.1007/s11274-014-1776-z

frontiers | Frontiers in Microbiology

TYPE Original Research
PUBLISHED 29 September 2022
DOI 10.3389/fmicb.2022.1008817

OPEN ACCESS

EDITED BY
Khamis Youssef,
Agricultural Research Center, Egypt

REVIEWED BY
Khaled A. El-Tarabily,
United Arab Emirates University,
United Arab Emirates
Hoda S. El-Sayed,
National Research Centre, Egypt
Shukho Kim,
Kyungpook National University,
South Korea

*CORRESPONDENCE
Ratthaphol Charlermroj
ratthaphol.cha@biotec.or.th

SPECIALTY SECTION
This article was submitted to Food Microbiology, a section of the journal Frontiers in Microbiology

RECEIVED 01 August 2022
ACCEPTED 15 September 2022
PUBLISHED 29 September 2022

CITATION
Charlermroj R, Makornwattana M, Phuengwas S and Karoonuthaisiri N (2022) A rapid colorimetric lateral flow test strip for detection of live *Salmonella* Enteritidis using whole phage as a specific binder. *Front. Microbiol.* 13:1008817. doi: 10.3389/fmicb.2022.1008817

A rapid colorimetric lateral flow test strip for detection of live *Salmonella* Enteritidis using whole phage as a specific binder

Ratthaphol Charlermroj[1]*, Manlika Makornwattana[1], Sudtida Phuengwas[1] and Nitsara Karoonuthaisiri[1,2,3]

[1]National Center for Genetic Engineering and Biotechnology (BIOTEC), National Science and Technology Development Agency (NSTDA), Pathum Thani, Thailand, [2]International Joint Research Center on Food Security, Pathum Thani, Thailand, [3]Institute for Global Food Security, Queen's University Belfast, Belfast, United Kingdom

Specific antibodies are essential components of immunoassay, which can be applied for the detection of pathogens. However, producing an antibody specific to live bacterial pathogens by the classical method of immunizing animals with live pathogens can be impractical. Phage display technology is an effective alternative method to obtain antibodies with the desired specificity against selected antigenic molecules. In this study, we demonstrated the power of a microarray-based technique for obtaining specific phage-derived antibody fragments against *Salmonella*, an important foodborne pathogen. The selected phage-displayed antibody fragments were subsequently employed to develop a lateral flow test strip assay for the detection of live *Salmonella*. The test strips showed specificity to *Salmonella* Enteritidis without cross-reactivity to eight serovars of *Salmonella* or other bacteria strains. The test strip assay requires 15 min, whereas the conventional biochemical and serological confirmation test requires at least 24 h. The microarray screening technique for specific phage-based binders and the test strip method can be further applied to other foodborne pathogens.

KEYWORDS

phage-derived antibody fragment, foodborne pathogen, *Salmonella* Enteritidis, lateral flow assay, colorimetric assay

Introduction

Salmonella bacterial species are causative agents of foodborne illness in humans and animals, which are commonly found in many types of food such as pork, eggs, poultry, seafood, unpasteurized dairy products, and vegetables (Jackson et al., 2013; Gu et al., 2018). The standard methods for detecting *Salmonella* are based on culturing techniques including pre-enrichment, selective-enrichment, and confirmation with biochemical tests, following procedures outlined by the International Organization for Standardization (ISO 6579) or Bacteriological Analytical Manual (BAM). These

methods can detect low numbers or injured viable *Salmonella*; however, they are time-consuming and laborious. Thus, rapid and accurate methods are required for detecting foodborne pathogens (Law et al., 2015).

Methods have been developed to detect viable bacterial cells using fluorescent dyes such as SYTO 9 and propidium iodide (Ou et al., 2019), and mammalian cell-based immunoassay (Xu et al., 2020). Although they can detect or differentiate live cells from dead cells, these methods require many steps and special equipment. These shortcomings could be addressed by immuno-based lateral flow assays, which are more rapid, simple, and affordable. However, to our knowledge, there is no report of an immuno-based lateral flow method capable of discriminating viable from dead bacteria cells. The major challenge for applying lateral flow assays for detecting viable bacteria is the requirement for an antibody that binds specifically to viable bacterial cells of interest, but not to injured or non-viable cells.

The traditional method of producing an antibody for immunoassay relies on an *in vivo* immune response from an antigen. The success of antibody production depends on the antigen characteristics such as types of immunogens, antigenicity, and antigen dosing. Alternatively, antibodies can be produced by phage display technology, which can identify binders to antigens regardless of their immunogenic properties, thus allowing the selection of binders against self-antigens, toxic, unstable, and non-immunogenic antigens (Frenzel et al., 2016). This technology also facilitates genetic engineering of the binding sites to improve affinity and specificity. Its advantages over the traditional *in vivo* antibody production method have fostered applications ranging from epitope mapping (Spillner et al., 2003; Youn et al., 2004), the detection of bacteria and viruses (Ferrer and Harrison, 1999; Yang et al., 2003; Morton et al., 2013b; Karoonuthaisiri et al., 2014; Wang et al., 2014; Niyomdecha et al., 2018), protein domains (Christ and Winter, 2006), and small molecules (Zhao et al., 2005; Qi et al., 2008).

Given the power of phage technology, this study aimed to (1) develop a bacterial microarray method to speed up the process of screening and selecting phage clones expressing specific antibody fragments and (2) utilize the selected phage clones for developing a rapid lateral flow detection method for live *Salmonella* Enteritidis.

Materials and methods

Bacteria, antibodies, and phage clones

All bacteria in **Table 1**, except for *Campylobacter* spp., were inoculated from a single colony grown in a LB agar plate and cultured in 10 mL of 2xYT medium (16 g/L tryptone, 10 g/L yeast extract, and 5 g/L NaCl) at 37°C, 250 rpm for 16–18 h. *Campylobacter* spp. were cultured in 10 mL of Campylobacter Enrichment Broth (CEB) supplemented with 20 mg/L cefoperazone, 20 mg/L vancomycin, 20 mg/L trimethoprim, and 25 mg/L natamycin (#X132, Lab M, UK) at 41.5°C, in microaerophilic conditions (5% CO_2 and 10% O_2) for 48 h.

The sources and reactivity of all antibodies and phage clones used in this study were reported in **Supplementary Table 1**.

Biopanning and individual phage clone amplification

A phage-displayed human domain antibody library displaying a single human VH framework (V3-23/D47) with diversity introduced in the antigen-binding site and short complementarity-determining region 3 (CDR3) of the heavy chains was used in this study (Lee et al., 2007) (Source Bioscience). Biopanning steps were performed according to the library instructions and modified with a suspension method previously employed (Paoli et al., 2004; Morton et al., 2013a; **Figure 1A**). Briefly, sterilized protein low binding tubes were blocked with 1 mL of 5% skimmed milk in phosphate buffered saline (PBS, pH 7.4 containing 1 mM KH_2PO_4, 0.15 mM Na_2HPO_4, 3 mM NaCl) overnight at 4°C. The blocked tubes were washed twice with PBS. For the first round of biopanning, a cocktail of nine serovars (Choleraesuis, Dublin, Enteritidis, Hadar, Infantis, Mbandaka, Senftenberg, Typhimurium, and Virchow) of *Salmonella* (5×10^9 colony forming units

TABLE 1 Bacteria strains used in this project.

Bacterial strain	Serotype	Source
Salmonella Choleraesuis	1, 6,7:c:1,5	DMST 5580
Salmonella Dublin	1, 9,12:g,p	DMST 30404
Salmonella Enteritidis	1, 9,12:g,m	ATCC 13076
Salmonella Hadar	1, 8,z10:e,n,x	DMST 10634
Salmonella Infantis	1, 6,7:r:1,5	DMST 26426
Salmonella Mbandaka	1, 6,7:z10:e,n,z15	DMST 17377
Salmonella Senftenberg	1, 1,3,19:g,s,t	DMST 17013
Salmonella Typhimurium	1, 4,12:i:1,2	ATCC 13311
Salmonella Virchow	1, 6,7:r:1,2	DMST 32758
Listeria innocua	–	DMST 9011
Listeria ivanovii	–	ATCC 700402
Listeria monocytogenes	–	ATCC 19115
Listeria welshimeri	–	DMST 20559
Escherichia coli	–	ATCC 25922
Escherichia coli O157:H7	–	DMST 12743
Campylobacter coli	–	DMST 11353
Campylobacter jejuni	–	ATCC 33291
Staphylococcus aureus	–	ATCC 25923
Vibrio parahaemolyticus	–	ATCC 17802

ATCC, American Type Culture Collection (Manassas, VA); DMST, Department of Medical Sciences, Thailand.

(CFU)/mL for each *Salmonella* serovar) and the phage library (5×10^{11} plaque forming unit, pfu/mL) were mixed in PBS (total volume 1 mL) in the blocked tube, 20 rpm at RT for 1 h. Unbound phages were removed by centrifuging at 3,200 × g for 10 min. The pellet of phage-bound bacterial cells was washed five times by resuspending in PBS containing 0.1% Tween 20 and separation of phage-bound bacterial cell pellet by centrifugation at 3 200 × g for 10 min. To elute phages from the bacterial target, a trypsin solution (1 mL of 100 μg/mL Trypsin in Tris-buffered saline calcium chloride) was added, and the suspension was incubated at RT for 1 h. The eluted phages were used to infect a mid-log phase culture of *E. coli* TG1 TR strain (OD_{600} = 0.5) at 37°C for 1 h. The non-infecting phages were separated by centrifugation at 3,200 × g for 5 min. To enumerate the phage-infected *E. coli* TG1, the pellet was resuspended in 1 mL of 2xYT medium, and the bacterial cell suspension was serially diluted and plated on TYE ampicillin glucose agar plates (10 g/L bacto-tryptone, 5 g/L yeast extract, 8 g/L NaCl, 100 mg/L ampicillin and 40 g/L glucose).

To amplify and purify phages for the next rounds of biopanning, the phagemid-carrying *E. coli* TG1 bacterial cells (phage clones) from the TYE agar plates were scraped from plates using 5 mL of 2xYT medium per plate. The bacterial suspension was diluted to an OD_{600} value of 0.1 in 500 mL of 2xYT medium supplemented with 100 μg/mL ampicillin and 4% glucose. Bacteria were cultured at 37°C and 250 rpm to an OD_{600} value of 0.5. The bacterial culture was then infected with KM13 helper phages (2×10^{12} pfu) and incubated at 37°C for 1 h. The supernatant was removed by centrifuging at 3,200 × g for 10 min, and the cell pellets were resuspended in 500 mL of 2xYT medium supplemented with 0.1% glucose, 100 μg/mL ampicillin and 50 μg/mL kanamycin, and incubated at 25°C, 250 rpm for 16-20 h. Phages in the supernatant were precipitated with 20% polyethylene glycol 6,000 (20% PEG6000, 2.5 M NaCl) and reconstituted in 1 mL PBS. The phage titer was estimated using the following equation (Lee et al., 2007).

$$\text{phage titer(phage/mL)} = OD_{260} \times \text{dilution factor} \times 22.14 \times 10^{10}$$

From a phage clone collection, 188 individual colonies of phage-infected cells from each biopanning round were picked from 10-fold serial dilution plates of 2xYT agar supplemented with 100 μg/mL ampicillin and 4% glucose (**Figure 1B**). Each colony was transferred into a well of 96-well plates (Costar) containing 200 μL of 2xYT medium supplemented with 100 μg/mL ampicillin and 4% glucose, covered with a breathable sealing film (Axygen) and incubated at 37°C, 250 rpm overnight. These phage clones were kept at 4°C until use.

To screen for specific phage and to test cross-reactivity against other relevant bacteria, 600 μL of 2xYT supplemented with 100 μg/mL ampicillin and 4% glucose was inoculated with 30 μL of a suspension of individual phage clone stock and cultured at 37°C, 250 rpm for 3 h. After 3 h of incubation, KM13 helper phages (150 μL of 8×10^9 pfu/mL) were added to infect the cells in the culture, which was then incubated at 37°C without shaking for 1 h. To remove the helper phage, the bacterial cells were collected by centrifuging at 2,000 rpm for 30 min. The cell pellets were resuspended in 600 μL of 2xYT supplemented with 100 μg/mL ampicillin, 50 μg/mL kanamycin, and 0.1% glucose and cultured at 25°C, 250 rpm for 16-24 h. The phages were separated from bacterial cells by centrifugation at 2,000 rpm for 30 min. The phage supernatants were screened by the optimized bacterial microarray method described below.

Bacterial microarray development in a multi-well plate

To develop a bacterial microarray method in a multi-well plate (**Figures 1C,D**), bacterial cells (1×10^{11} CFU/mL) were suspended in carbonate buffer (44 mM $NaHCO_3$ and 6 mM Na_2CO_3, pH 9.6) with Tween 20 (0.05%) and glycerol (0.5%) for Gram-negative bacteria, and in a carbonate buffer with glycerol (0.5%) for Gram-positive bacteria. The bacteria suspension was spotted (5 replicates) onto microplate wells (Corning) using a NanoPrint 210 microarrayer equipped with 946NS pins (TeleChem). Relevant spotting buffers were used as negative controls, and an anti-mouse antibody was used as a positive control and to indicate spot positions. The bacterial microarrays were kept at 4°C until use.

Screening of phage-displayed antibody fragments using a bacterial microarray technique

To identify phage clones specific to *Salmonella* spp., bacterial microarrays were used to screen the phage clones (**Figure 1D**). The bacterial microarray plates were blocked with 5% skimmed milk in PBST (300 μL/well) for 1 h at RT, then washed with PBST three times by an automatic microplate washer (BIO-RAD). Phage supernatant (100 μL) was added to each well and incubated for 1 h at RT before being washed again as before. An antibody specific to bacteriophage M13 (100 μL/well, 5 μg/mL) was added and the plates were incubated for 1 h at RT. After washing again, a Cy3 labeled anti-mouse antibody (100 μL/well, 5 μg/mL) was added and incubated in the dark for 1 h at RT. The microplates were washed as before and dried by centrifuging at 200 rpm for 5 min. The plates were then scanned using a fluorescence scanner (TECAN), and the fluorescent intensities of spots were determined using the Array-Pro Analyzer software version 4.5.1.73 (TECAN). Background noise in each experiment was determined as the

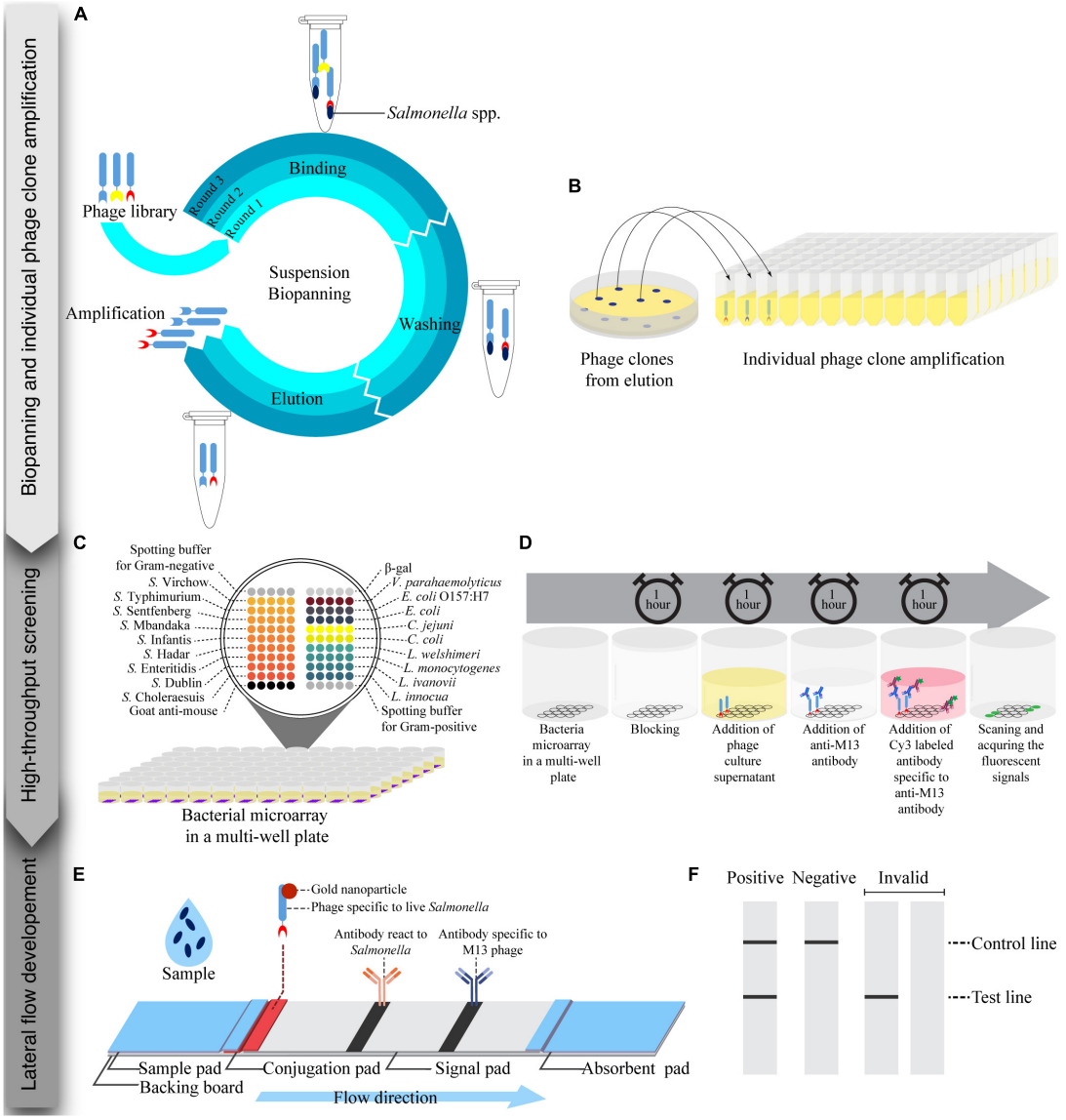

FIGURE 1
Schematic of the process for the development of a lateral flow strip test assay for live *Salmonella* detection consisting of three steps: biopanning and individual phage clones amplification, high-throughput screening, and lateral flow development. **(A)** Suspension biopanning was performed against a mixture of nine *Salmonella* serovars adapted from Lee et al. (2007). **(B)** Phage clones were amplified in a 96-well plate and screened by a bacterial microarray method. **(C)** A bacterial microarray in a 96-well plate format was developed and constructed. Each well was spotted with target and non-target bacteria. **(D)** Phage supernatant was tested with a bacterial microarray. **(E)** Lateral flow strip test was developed using a gold nanoparticle-labeled phage as a biorecognition element and signal reporter. Anti-*Salmonella* and anti-M13 phage antibodies were printed at the test line and control line, respectively. **(F)** Readouts of lateral flow strip test were visualized by the naked eye and images of the strip were captured by a smartphone.

mean value taken from wells containing spotting buffer with no phage added. Normalized signals were determined as the ratio of mean fluorescent intensity of bacterial spots (5 technical replicates/bacterial strain) to background. Mean normalized signals from 5 spots greater than or equal to two were considered positive. To visualize microarray data, a heat map was created from the mean normalized signals with the GraphPad Prism software version 9.4.1 (681).

Plate-trapped antigen-ELISA

A plate-trapped antigen (PTA)-ELISA method was used to validate the microarray results of the selected phage clones. Bacterial cells (10^9 CFU/mL) were heat inactivated at 100°C for 15 min. Each of the 18 inactivated bacterial strains was diluted in carbonate buffer pH 9.6 (1×10^8 CFU/mL, 100 μL/well) and coated onto plate wells overnight at 4°C. The plates were

then washed by an automatic washer machine (BIO-RAD) with 300 μL/well PBS containing 0.1% Tween 20 (PBST) three times before being blocked with 5% skimmed milk (300 μL/well, Difco laboratory) in PBST for 1 h at RT. The washing step was repeated before 100 μL of phage suspension was added into each well. Plates with phage added were incubated for 1 h at RT. After washing as before, a horseradish peroxidase (HRP)-labeled anti-M13 antibody (diluted 5,000-fold in 5% skimmed in PBST; GE Healthcare) was added and the plate incubated for 1 h at RT. The plate was washed as before and a substrate solution for HRP (TMB: 3,3',5,5'-Tetramethylbenzidine; Invitrogen) was added (100 μL/well). The plate was then incubated for 5–30 min at RT. The reaction was stopped by adding 0.5 M H_2SO_4 (50 μL/well) and the signal was measured at 450 nm absorbance using a SpectraMax M5 microplate reader (Molecular device). Each experiment was repeated three times. A signal three times above the value of background reading was considered positive.

Limit of detection of phage clones by plate-trapped antigen-ELISA

Twelve different bacteria titers (0, 1×10^4, 5×10^4, 1×10^5, 5×10^5, 1×10^6, 5×10^6, 1×10^7, 5×10^7, 1×10^8, 5×10^8, and 1×10^9 CFU/mL) were prepared by dilution of bacterial culture in carbonate buffer. The bacteria were coated onto plate wells. The assay was performed in triplicate using the same steps as described above in the PTA-ELISA method. Limit of detection (LOD) values were calculated as the minimal titer with a signal greater than three times background (negative control). The ELISA signal data were fitted to the following dose-response equation with three parameters and confidence level at 95% (Iturria, 2005; Charlermroj et al., 2014).

$$\%B/B_0 = [B_0 + (B - B_0)/(1 + 10^{\mathrm{LogEC50}-x})] \times 100,$$

where B and B_0 were absorbance values at 450 nm of a phage clone binding in the presence (B) or absence (B_0) of bacterial cells, respectively, in which% B/B_0 response was measured at varying titers of bacteria (X), and EC_{50} is the bacterial titer that produced a 50% response between B and B_0.

Preparation of whole phage-gold nanoparticles (phage-AuNPs) conjugates

To prepare phage-AuNPs, AuNPs solution (1 mL, 40 nm, #KP-05120003, Kestrel Bioscience, Thailand) was adjusted to pH 8.0 with 100 mM K_2CO_3 before purified whole phage (100 μL of 10^{12} pfu/mL) suspension was added. The mixture was incubated at RT for 10 min. The unconjugated AuNPs were subsequently blocked with bovine serum albumin (BSA, 110 μL of 10% (w/v) in distilled water adjusted to pH 7.0) at 4°C overnight. The excess of phage was removed by centrifugation at 12,000 rpm at 4°C for 30 min. The pellet was resuspended in 50 μL of conjugate buffer (PBS containing 10% sucrose, and 5% trehalose, pH 7.4). The phage-AuNPs suspension was kept at 4°C until use.

Preparation of lateral flow test strips

The composition of lateral flow test strips is shown in **Figure 1E**. A sample pad (CF3, GE Healthcare, USA) was impregnated with PBS containing 0.4% Tween 20, and 2% (w/v) BSA, pH 7.4, before drying overnight at 37°C. The suspension of whole phage-AuNPs conjugates (10 μL) was applied on a conjugated pad (4 mm × 1 cm., GF33, Kestrel Bioscience, Thailand), and dried at 37°C for 30 min. An antibody specific to *Salmonella* (1 mg/mL, ab35156, AbCAM, UK) and an antibody specific to M13 phage (0.5 mg/mL) were prepared in carbonate buffer, pH 9.6. The antibodies were dispensed (0.8 μL/cm) on the signal pad (CN95, Kestrel Bioscience, Thailand) at a test line (TL) for *Salmonella* detection and a control line (CL) for positive control, respectively, using a non-contact microarray dispenser equipped with Biojet Elite dispenser (AD1520, BioDot, USA). The signal pad was then dried at RT for 30 min before blocking with treating buffer (10 mM di-sodium tetraborate containing 1% (w/v) BSA, 0.5% (w/v) polyvinyl pyrrolidone (PVP40), and 0.15% (v/v) Triton X-100, pH 8.0) and dried at 37°C overnight. The sample pad, conjugate pad, and absorbent pad (CF5, GE Healthcare, USA) were assembled onto a backing board, and cut into 4 mm wide strips with a guillotine cutter (CM5000, BioDot, USA).

Lateral flow assay procedure

The lateral flow test strips were tested as follows. Bacteria were cultured in Luria-Bertani broth (LB, Difco, USA) at 37°C, 250 rpm for 16-18 h. Test sample (100 μL) was applied onto the sample pad, and incubated for 15 min at RT. Signals were captured at 11 cm above the strip by a smart phone (Samsung Note 20) under the white light condition for qualitative assessment of the result (**Figure 1F**). To test the specificity of the lateral flow test strips, nine serovars of *Salmonella,* heat-killed *Salmonella* Enteritidis, and three other bacteria strains (*E. coli* O157:H7, *L. monocytogenes*, and *S. aureus*) were tested at 10^8 CFU/mL with three replications. For sensitivity of detection, ten different titers of *Salmonella* Enteritidis (0, 1×10^6, 5×10^6, 1×10^7, 5×10^7, 1×10^8, 5×10^8, 1×10^9, 5×10^9, 1×10^{10} CFU/mL were tested with three replications. To analyze optical density of test line (TL) and control line (CL), the images were converted to grayscale using the Adobe Photoshop Software version 23.5.0, and band intensities were subsequently

measured using the Quantity One Software version 4.6.8. The TL/CL ratio values were calculated and used for a statistical analysis.

Statistical analysis

All data are express as the mean values ± standard deviations (mean ± *SD*) of three replicates, except a specificity test by an ELISA method. All analyses were conducted using the GraphPad Prism 9 (681) software. The experiments were compared using an analysis of variance (ANOVA) and Tukey's post-test. *P*-value of < 0.05 was considered to indicate a significant difference.

Results

Phage high-throughput screening and characterization

To facilitate the screening of phage binders specific to bacteria of interest, a bacterial microarray was developed. Microarray spotting buffers were first optimized using *Salmonella* Typhimurium and *Listeria monocytogenes* as model cells. We found that a carbonate buffer containing Tween 20 and glycerol (CBTG) and a carbonate buffer containing glycerol (CBG) was suitable for Gram-negative (**Supplementary Figure 1A**) and Gram-positive bacteria, respectively (**Supplementary Figure 1B**). These spotting buffers were validated with 18 different bacterial strains using antibodies and a phage with known specificities (**Supplementary Table 1**). The antibodies and phage showed accurate detection of their corresponding bacterial targets when the bacterial cells were prepared in the selected spotting buffers, except in case of SalKPL and ListKPL antibodies (**Supplementary Figure 1C**). SalKPL antibody reacted strongly with *Salmonella* spp. with some cross reactivity with *E. coli* in the bacterial microarray. This result is in agreement with cross reactivity to related Enterobacteriaceae reported by the antibody's supplier. ListKPL showed minor cross reactivity to *Salmonella* Infantis on the microarray, which agrees with the cross-reactivity information from the antibody supplier. The results showed that they were suitable for the production of bacterial microarray.

The bacterial microarray was used to screen a total of 564 phage clones (188 from each round of biopanning, 3 rounds in total) and to test the specificity of the phage-displayed antibody against 18 different bacterial strains. The number of *Salmonella*-specific phage clones increased after three rounds of biopanning (20.2, 20.2, and 35.6% for the 1st–3rd biopanning rounds, respectively), while the number of phage clones that could bind to *Salmonella* and cross-react with other bacteria dramatically increased (8.5, 22.3, and 57.4% for the 1st–3rd biopanning rounds, respectively) (**Figure 2**). We sought phage clones that can detect the nine serovars of *Salmonella* with no cross-reactivity to other bacterial species. Unfortunately, no phage clones were isolated that bound to all nine serovars of *Salmonella* after the third round of biopanning. Moreover, most of the phage clones detecting one or more serovars of *Salmonella* also cross-reacted with *Vibrio parahaemolyticus*. However, we were able to identify phage clones specific to *Salmonella* Enteritidis. Thus, we randomly selected four phage clones from the third round of biopanning for further characterization using a PTA-ELISA method against 18 different bacterial strains (**Figure 3A**). All randomly selected phage clones could specifically bind to *Salmonella* Enteritidis, except for clone 03P1D05 that showed some cross-reactivity to *V. parahaemolyticus* (**Figure 3A**). Of the remaining three *Salmonella*-specific phage clones, clone 03P2H03 exhibited the highest signal (**Figure 3A**) and was selected for its ability to discriminate between live and dead *Salmonella*. 03P2H03 was able to distinguish between live and dead (heat-killed) *Salmonella* Enteritidis cells, while the commercial antibodies could not (**Figure 3B**). The limit of detection (LOD) of the 03P2H03 phage clone in detecting *Salmonella* was found to be within the same order of magnitude (3.0×10^6 CFU/mL) as that of the *Salmonella*-specific antibody (4.1×10^6 CFU/mL) (**Figure 3C**).

Lateral flow test strip for detection of live *Salmonella* Enteritidis

To test the specificity and sensitivity of the constructed lateral flow test strip using whole phage-AuNPs as a detecting molecule, different bacterial strains and varying titers of live *Salmonella* Enteritidis were tested. The lateral flow test strip could specifically detect *Salmonella* Enteritidis but showed no reaction to eight *Salmonella* serovars and other relevant bacterial strains (**Figures 4A,B**). For sensitivity, the test line signal indicating the presence of *Salmonella* Enteritidis was apparent to the naked eye for cell titers 1×10^7–1×10^{10} CFU/mL, indicating a LOD of 1×10^7 CFU/mL for the test strip. At the highest titer tested (1×10^{10} CFU/mL), the test line showed slightly lower intensity than lower titers (**Figures 4C,D**). The assay time of the lateral flow test strip was only 15 min. These results demonstrated the usefulness of whole phage as a biorecognition element for a lateral flow detection method of live *Salmonella* Enteritidis.

Discussion

While phage technology can be applied for pathogen detection, its full potential has yet to be realized owing to the difficulty in obtaining specific phage clones for downstream

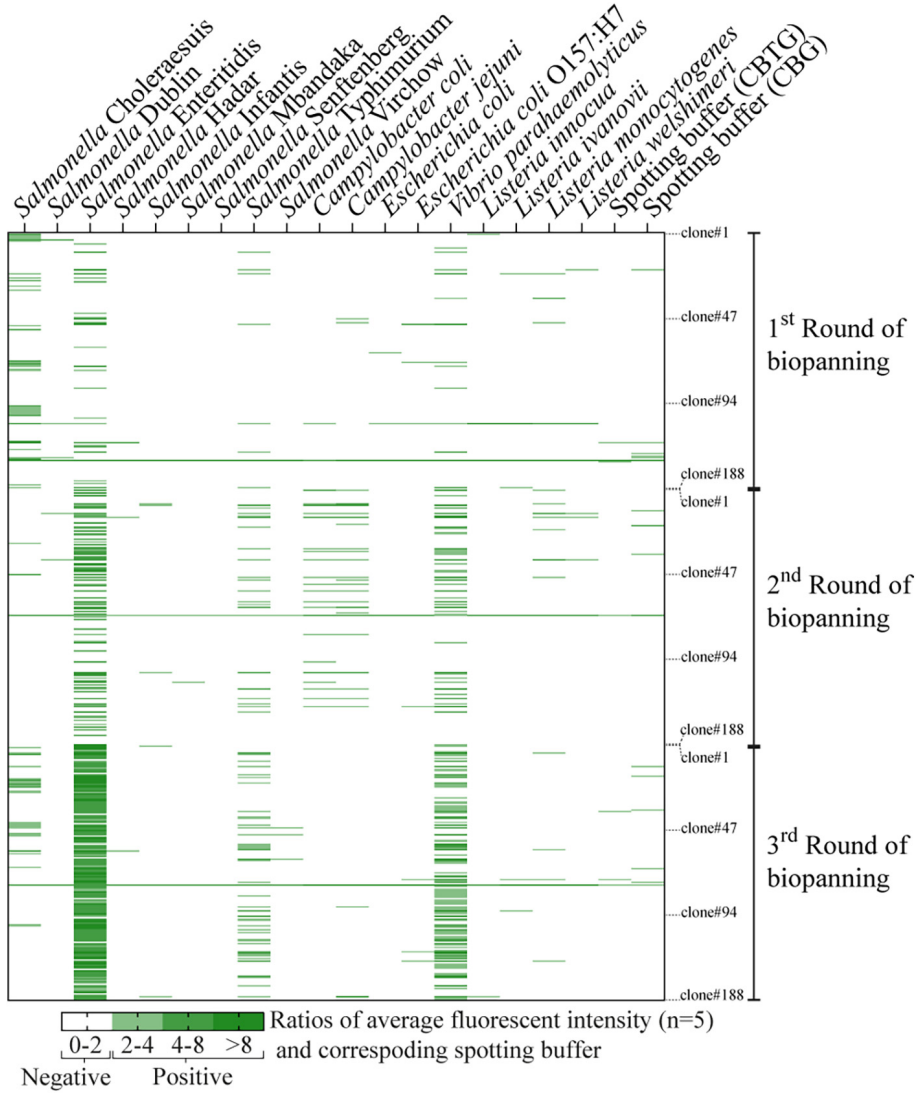

FIGURE 2
Heat map of individual phage clones (rows) tested against 18 different bacteria strains (columns). A total of 564 phage clones (188 clones for each round of biopanning, 3 rounds total) were tested for their binding specificity using bacterial microarray. Fluorescent intensity values were averaged from five spots and normalized with the signal from their corresponding spotting buffers (CBTG for Gram-negative bacteria, and CBG for Gram-positive bacteria). Normalized fluorescent signals greater than or equal to two were considered as positive results and are indicated by the green color gradient. Normalized signals (negative results) below the threshold are indicated in white.

applications. In this study, a high-throughput microarray method was developed to screen and characterize the binding specificity of phage clones. From prior experience, we found that selection of appropriate spotting buffers was the key factor for success. For instance, we found that a carbonate-based buffer was suitable for producing an antibody array (Charlermroj et al., 2014). Unlike the antibody array, the bacterial microarray in this study is more complicated because the major components of the bacterial cell wall for each Gram stain reactive group are different, i.e., lipopolysaccharide for Gram-negative bacteria and peptidoglycan for Gram-positive bacteria. Thus, spotting buffers needed to be optimized for each type of bacterial cell.

The bacterial microarray in multi-well plate format provides several advantages. First and foremost, the microarray was able to identify phages specific to *Salmonella* from the first round of biopanning. Generally, most protocols recommend 3–5 rounds of biopanning to obtain specific phage clones (Song et al., 2011; Hamzeh-Mivehroud et al., 2013). However, when a phage-antibody library is selected against highly complex targets such as whole cells, a strong bias for binders against abundant proteins has been reported. Therefore, the ability to characterize binders early in the biopanning process will result in a wider diversity of binders that can be used for diagnostics development (de Wildt et al., 2000).

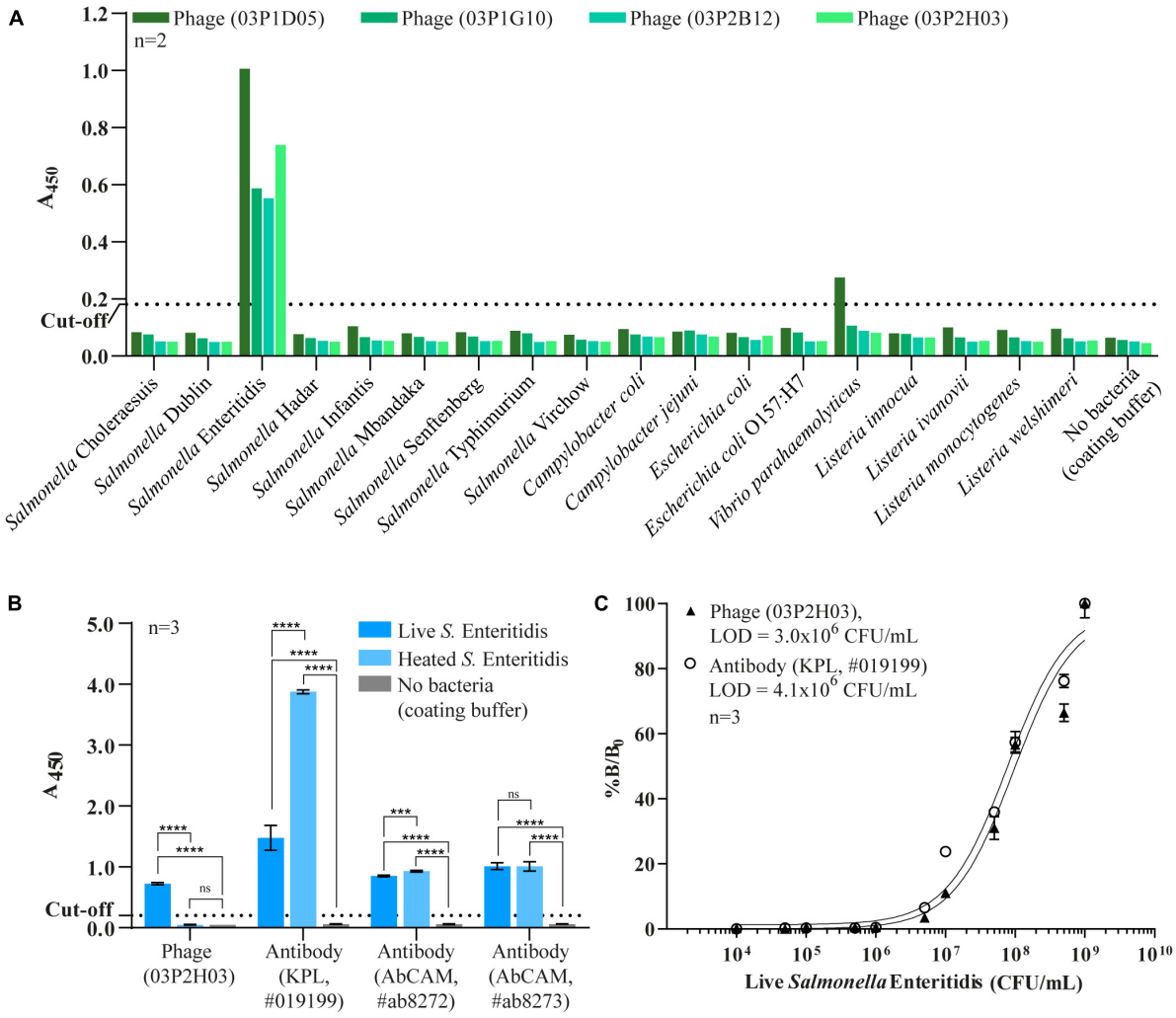

FIGURE 3
Characterization of randomly selected phage clones by a PTA-ELISA method against 18 different strains of bacteria. **(A)** Specificity of the four phage clones previously selected from bacterial microarray data. **(B)** Comparison of specificity against live/dead cells of the selected phage clone 03P2H03 and the three commercial antibodies specific to *Salmonella*. Each bar is represented and mean ± standard derivation (*SD*) which was compared to no bacteria (one-way ANOVA for indicate comparison, Tukey's multiple comparison test, ***$p < 0.005$, ****$p < 0.0001$, and *ns* = no significance). **(C)** Limit of detection (LOD) for live *Salmonella* Enteritidis of phage clone (03P2H03) and a commercial *Salmonella* antibody by PTA-ELISA. The dotted line represents the cut-off value three times that of the background (LB medium) used to determine the limit of detection. Error bars indicate standard derivation (SD) ($n = 3$). Solid lines indicate curve fits to the data using a three-parameter dose-response model.

The selected phage clone reacts to *Salmonella* Enteritidis, but did not react to eight serovars of *Salmonella*. While *Salmonella* Enteritidis and *Salmonella* Dublin belong to the same group of O antigen (D1 group), these two serovars have different H antigens: g and m for *Salmonella* Enteritidis, and g and p for *Salmonella* Dublin (Grimont and Weill, 2007). It might be that this phage clone bind to flagella "m" antigen of *S.* Enteritidis, resulting in specificity to only *Salmonella* Enteritidis among the nine *Salmonella* serovars, which should be investigated further in the next research.

The phage-derived antibody fragments identified by the microarray method showed similar characteristics (LODs and specificity) to those of the commercial antibodies. Moreover, the selected phage clone was able to distinguish between live and dead cells, whereas commercial antibodies cannot. Many publications reported the use of phages as biorecognition elements for the diagnosis of *Salmonella* (Morton et al., 2013b; Karoonuthaisiri et al., 2014); however, to our knowledge, there is no report on phages that can discriminate live from dead *Salmonella* Enteritidis.

The fact that our phage-derived antibody fragments were able to discriminate between viable and dead cells can be instrumental for many applications, especially for food safety. Molecular techniques have been developed to discriminate

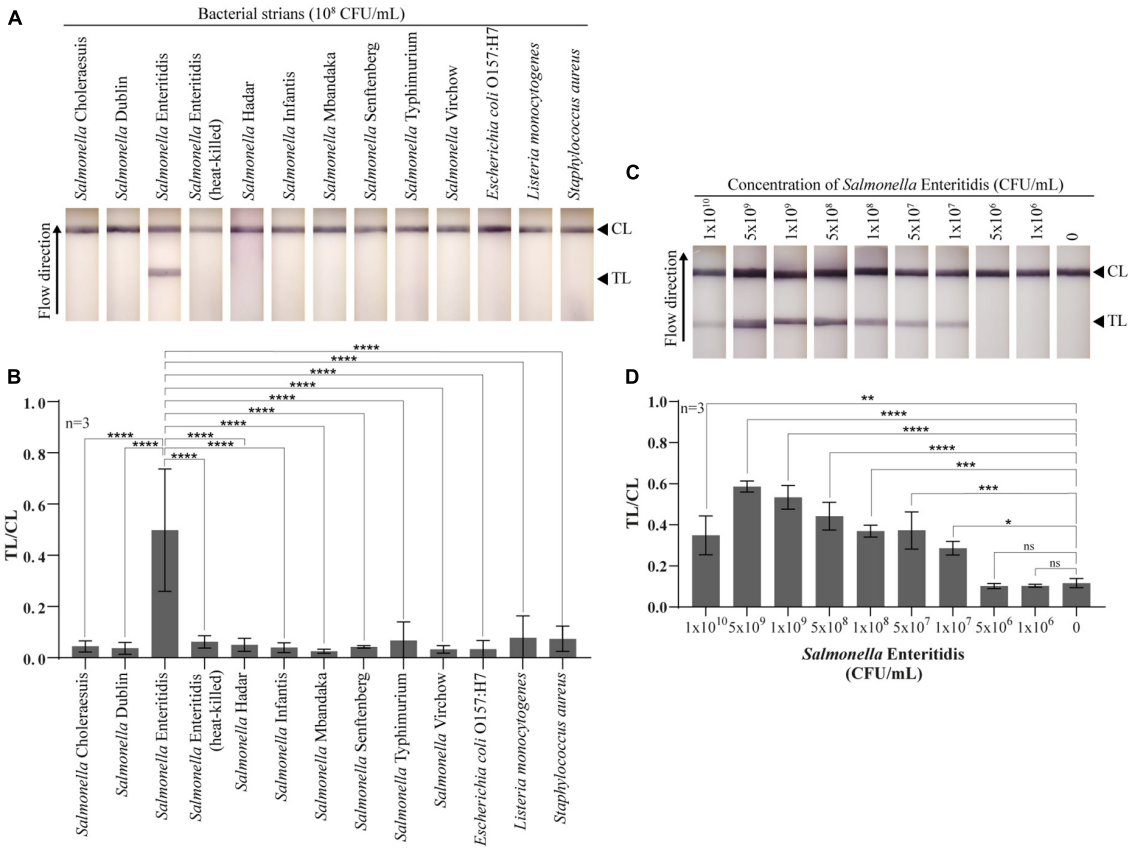

FIGURE 4
Specificity and sensitivity of the developed lateral flow test strip for *Salmonella* Enteritidis detection. **(A)** Photographs of the lateral flow test strips with different 12 bacterial strains and heat-killed *Salmonella* Enteritidis at 10^8 CFU/mL in LB medium. **(B)** Quantitative of lateral flow test strips for specificity test. Test line (TL) and control line (CL) ratios were compared with *Salmonella* Enteritidis using a statistical analysis. **(C)** Photographs of the lateral flow test with ten different titers of *Salmonella* Enteritidis. **(D)** Quantitative of lateral flow test strips for sensitivity test. Test line (TL) and control line (CL) ratios were compared with no bacteria using a statistical analysis. All experiments were tested with three independent test strips (one-way ANOVA for indicate comparison, Tukey's multiple comparison test, $*p < 0.05$, $**p < 0.001$, $***p < 0.005$, $****p < 0.0001$, and *ns* = no significance).

between viable and dead cells, including PCR-based methods such as reverse transcription (RT)-PCR and nucleic acid sequence-based amplification (NASBA) (Morin et al., 2004), and viability dyes coupled with DNA amplification (Elizaquivel et al., 2013). These molecular techniques are often more tedious and laborious than immunoassay-based methods and are typically only employed in a laboratory. Therefore, the phage-derived antibody fragments that can distinguish viable from dead foodborne pathogens can open a new horizon for more rapid and simpler diagnostics for food safety, which can be applied in different settings outside of the laboratory.

We developed a lateral flow test strip using the selected phage as a biorecognition element for the detection of live *Salmonella* Enteritidis and proved the specificity of the assay for detecting *Salmonella* Enteritidis. In addition, although this phage clone was not previously screened against *Staphylococcus aureus* during the screening process, the test strips using this phage showed no cross-reactivity with *S. aureus*. The low intensity observed at the highest titer of *Salmonella* (1×10^{10} CFU/mL) could be explained by the hook effect from excessively high antigen concentration in lateral flow immunoassays (Ross et al., 2020). Although sensitivities of the phage clone and antibody were around 10^6 CFU/mL by the PTA-ELISA method, the sensitivity for the phage-based lateral flow test strip was found to be 10^7 CFU/mL. The greater sensitivity of the ELISA method compared with that of the lateral flow method has previously been reported (Serrano et al., 2020). However, the sensitivity of the phage-based lateral flow test strip in this study is lower than that of a previous report of an immuno-lateral flow assay for *Salmonella* Enteritidis and Typhimurium at 10^6 and 10^4 CFU/mL in culture media, respectively (Moongkarndi et al., 2011). The sensitivity of the test strip can be further improved by exploring other reporting molecules such as luminescent nanoparticles (Xie et al., 2014), carbon nanoparticles (Noguera et al., 2011), and streptavidin-labeled AuNPs (Chen et al., 2022).

In summary, a lateral flow test strip assay developed using phage from microarray screening was able to distinguish live from dead *Salmonella* Enteritidis. The assay time of 15 min is much shorter than that of any culture-based method which usually requires at least 24 h. The microarray-based screening method presented here is not limited to the selection of *Salmonella*-specific phage-derived binders, but it can also be readily adapted for phage-based binder selection against other to other pathogen targets, obviating the need for animal immunization. In addition, phage-based lateral flow test strip assay is not limited to foodborne pathogens and could be applied to other targets of interest, e.g., viruses.

Data availability statement

The original contributions presented in this study are included in the article/**Supplementary material**, further inquiries can be directed to the corresponding author/s.

Author contributions

RC and NK conceived the idea, designed the experiments, and wrote the manuscript. RC, MM, and SP carried out the experiments. All authors contributed to the data analysis and reviewed the manuscript.

Funding

This project was financially supported by the National Center for Genetic Engineering and Biotechnology (BIOTEC, Thailand) (grant agreement nos. P1450542 and P1950903) and the Thailand Science Research and Innovation (grant agreement nos. TRG5780014 and RSA6280033).

Acknowledgments

Antibodies specific to *Salmonella* spp. and *Listeria monocytogenes* were kindly supplied by Oraprapai Gajanandana, Orawan Himananto, and Mallika Kumposiri, Monoclonal Antibody Production and Application Research Team, BIOTEC, Thailand. We are also grateful to David Brandon, USDA, for supplying the antibodies specific to *Campylobacter* (C818Ab), and Linda Stewart for her invaluable comments and suggestions to improve the manuscript. We thank Philip J. Shaw for manuscript editing.

Conflict of interest

The authors declare that the research was conducted in the absence of any commercial or financial relationships that could be construed as a potential conflict of interest.

Publisher's note

All claims expressed in this article are solely those of the authors and do not necessarily represent those of their affiliated organizations, or those of the publisher, the editors and the reviewers. Any product that may be evaluated in this article, or claim that may be made by its manufacturer, is not guaranteed or endorsed by the publisher.

Supplementary material

The Supplementary Material for this article can be found online at: https://www.frontiersin.org/articles/10.3389/fmicb.2022.1008817/full#supplementary-material

References

Charlermroj, R., Himananto, O., Seepiban, C., Kumpoosiri, M., Warin, N., Gajanandana, O., et al. (2014). Antibody array in a multiwell plate format for the sensitive and multiplexed detection of important plant pathogens. *Anal. Chem.* 86, 7049–7056. doi: 10.1021/ac501424k

Chen, X., Zhou, Q., Tan, Y., Wang, R., Wu, X., Liu, J., et al. (2022). Nanoparticle-based lateral flow biosensor integrated with loop-mediated isothermal amplification for rapid and visual identification of *Chlamydia trachomatis* for point-of-care use. *Front. Microbiol.* 13:914620. doi: 10.3389/fmicb.2022.914620

Christ, D., and Winter, G. (2006). Identification of protein domains by shotgun proteolysis. *J. Mol. Biol.* 358, 364–371. doi: 10.1016/j.jmb.2006.01.057

de Wildt, R. M., Mundy, C. R., Gorick, B. D., and Tomlinson, I. M. (2000). Antibody arrays for high-throughput screening of antibody-antigen interactions. *Nat. Biotechnol.* 18, 989–994. doi: 10.1038/79494

Elizaquivel, P., Azizkhani, M., Sanchez, G., and Aznar, R. (2013). Evaluation of *Zataria multiflora* Boiss. essential oil activity against *Escherichia coli* O157:H7, *Salmonella enterica* and *Listeria monocytogenes* by propidium monoazide quantitative PCR in vegetables. *Food Control* 34, 770–776. doi: 10.1016/j.foodcont.2013.06.036

Ferrer, M., and Harrison, S. C. (1999). Peptide ligands to human immunodeficiency virus type 1 gp120 identified from phage display libraries. *J. Virol.* 73, 5795–5802. doi: 10.1128/JVI.73.7.5795-5802.1999

Frenzel, A., Schirrmann, T., and Hust, M. (2016). Phage display-derived human antibodies in clinical development and therapy. *MAbs* 8, 1177–1194. doi: 10.1080/19420862.2016.1212149

Grimont, P. A. D., and Weill, F.-X. (2007). *Antigenic Formulae of the Salmonella Serovars*. Paris: WHO.

Gu, G., Strawn, L. K., Oryang, D. O., Zheng, J., Reed, E. A., Ottesen, A. R., et al. (2018). Agricultural practices influence *Salmonella* contamination and survival in pre-harvest tomato production. *Front. Microbiol.* 9:2451. doi: 10.3389/fmicb.2018.02451

Hamzeh-Mivehroud, M., Alizadeh, A. A., Morris, M. B., Bret Church, W., and Dastmalchi, S. (2013). Phage display as a technology delivering on the promise of peptide drug discovery. *Drug Discov. Today* 18, 1144–1157. doi: 10.1016/j.drudis.2013.09.001

Iturria, S. J. (2005). Statistical inference for relative potency in bivariate dose-response assays with correlated responses. *J. Biopharm. Stat.* 15, 343–351. doi: 10.1081/Bip-200048798

Jackson, B. R., Griffin, P. M., Cole, D., Walsh, K. A., and Chai, S. J. (2013). Outbreak-associated *Salmonella enterica* serotypes and food commodities, United States, 1998-2008. *Emerg. Infect. Dis.* 19, 1239–1244. doi: 10.3201/eid1908.121511

Karoonuthaisiri, N., Charlermroj, R., Morton, M. J., Oplatowska-Stachowiak, M., Grant, I. R., and Elliott, C. T. (2014). Development of a M13 bacteriophage-based SPR detection using *Salmonella* as a case study. *Sens. Actuators B Chem.* 190, 214–220. doi: 10.1016/j.snb.2013.08.068

Law, J. W.-F., Ab Mutalib, N.-S., Chan, K.-G., and Lee, L.-H. (2015). Rapid methods for the detection of foodborne bacterial pathogens: principles, applications, advantages and limitations. *Front. Microbiol.* 5:770. doi: 10.3389/fmicb.2014.00770

Lee, C. M., Iorno, N., Sierro, F., and Christ, D. (2007). Selection of human antibody fragments by phage display. *Nat. Protoc.* 2, 3001–3008. doi: 10.1038/nprot.2007.448

Moongkarndi, P., Rodpai, E., and Kanarat, S. (2011). Evaluation of an immunochromatographic assay for rapid detection of *Salmonella enterica* serovars Typhimurium and Enteritidis. *J. Vet. Diagn. Invest.* 23, 797–801. doi: 10.1177/1040638711408063

Morin, N. J., Gong, Z. L., and Li, X. F. (2004). Reverse transcription-multiplex PCR assay for simultaneous detection of *Escherichia coli* O157 : H7, *Vibrio cholerae* OI, and *Salmonella typhi*. *Clin. Chem.* 50, 2037–2044. doi: 10.1373/clinchem.2004.036814

Morton, J., Karoonuthaisiri, N., Charlermroj, R., Stewart, L. D., Elliott, C. T., and Grant, I. R. (2013a). Phage display-derived binders able to distinguish *Listeria monocytogenes* from other *Listeria* species. *PLoS One* 8:e74312. doi: 10.1371/journal.pone.0074312

Morton, J., Karoonuthaisiri, N., Stewart, L. D., Oplatowska, M., Elliott, C. T., and Grant, I. R. (2013b). Production and evaluation of the utility of novel phage display-derived peptide ligands to *Salmonella* spp. for magnetic separation. *J. Appl. Microbiol.* 115, 271–281. doi: 10.1111/jam.12207

Niyomdecha, S., Limbut, W., Numnuam, A., Kanatharana, P., Charlermroj, R., Karoonuthaisiri, N., et al. (2018). Phage-based capacitive biosensor for *Salmonella* detection. *Talanta* 188, 658–664. doi: 10.1016/j.talanta.2018.06.033

Noguera, P., Posthuma-Trumpie, G. A., van Tuil, M., van der Wal, F. J., de Boer, A., Moers, A. P., et al. (2011). Carbon nanoparticles in lateral flow methods to detect genes encoding virulence factors of Shiga toxin-producing *Escherichia coli*. *Anal. Bioanal. Chem.* 399, 831–838. doi: 10.1007/s00216-010-4334-z

Ou, F., McGoverin, C., Swift, S., and Vanholsbeeck, F. (2019). Near real-time enumeration of live and dead bacteria using a fibre-based spectroscopic device. *Sci. Rep.* 9:4807. doi: 10.1038/s41598-019-41221-1

Paoli, G. C., Chen, C.-Y., and Brewster, J. D. (2004). Single-chain Fv antibody with specificity for *Listeria monocytogenes*. *J. Immunol. Methods* 289, 147–155. doi: 10.1016/j.jim.2004.04.001

Qi, M., O'Brien, J. P., and Yang, J. (2008). A recombinant triblock protein polymer with dispersant and binding properties for digital printing. *Biopolymers* 90, 28–36. doi: 10.1002/bip.20878

Ross, G. M. S., Filippini, D., Nielen, M. W. F., and Salentijn, G. I. J. (2020). Unraveling the hook effect: a comprehensive study of high antigen concentration effects in sandwich lateral flow immunoassays. *Anal. Chem.* 92, 15587–15595. doi: 10.1021/acs.analchem.0c03740

Serrano, M. M., Rodríguez, D. N., Palop, N. T., Arenas, R. O., Córdoba, M. M., Mochón, M. D. O., et al. (2020). Comparison of commercial lateral flow immunoassays and ELISA for SARS-CoV-2 antibody detection. *J. Clin. Virol.* 129:104529. doi: 10.1016/j.jcv.2020.104529

Song, J., Matthews, A. Y., Reboul, C. F., Kaiserman, D., Pike, R. N., Bird, P. I., et al. (2011). "Chapter twelve - Predicting serpin/protease interactions," in *Methods in Enzymology*, eds J. C. Whisstock and P. I. Bird (Cambridge, MA: Academic Press), 237–273. doi: 10.1016/B978-0-12-385950-1.00012-2

Spillner, E., Deckers, S., Grunwald, T., and Bredehorst, R. (2003). Paratope-based protein identification by antibody and peptide phage display. *Anal. Biochem.* 321, 96–104. doi: 10.1016/s0003-2697(03)00439-1

Wang, J., Morton, M. J., Elliott, C. T., Karoonuthaisiri, N., Segatori, L., and Biswal, S. L. (2014). Rapid detection of pathogenic bacteria and screening of phage-derived peptides using microcantilevers. *Anal. Chem.* 86, 1671–1678. doi: 10.1021/ac403437x

Xie, Q. Y., Wu, Y. H., Xiong, Q. R., Xu, H. Y., Xiong, Y. H., Liu, K., et al. (2014). Advantages of fluorescent microspheres compared with colloidal gold as a label in immunochromatographic lateral flow assays. *Biosens. Bioelectron.* 54, 262–265. doi: 10.1016/j.bios.2013.11.002

Xu, L., Bai, X., Tenguria, S., Liu, Y., Drolia, R., and Bhunia, A. K. (2020). Mammalian cell-Based immunoassay for detection of viable bacterial pathogens. *Front. Microbiol.* 11:575615. doi: 10.3389/fmicb.2020.575615

Yang, B., Gao, L., Li, L., Lu, Z., Fan, X., Patel, C. A., et al. (2003). Potent suppression of viral infectivity by the peptides that inhibit multimerization of human immunodeficiency virus type 1 (HIV-1) Vif proteins. *J. Biol. Chem.* 278, 6596–6602. doi: 10.1074/jbc.M210164200

Youn, J. H., Myung, H.-J., Liav, A., Chatterjee, D., Brennan, P. J., Choi, I.-H., et al. (2004). Production and characterization of peptide mimotopes of phenolic glycolipid-I of *Mycobacterium leprae*. *FEMS Immunol. Med. Microbiol.* 41, 51–57. doi: 10.1016/j.femsim.2004.01.001

Zhao, S. W., Shen, P. P., Zhou, Y., Wei, Y., Xin, X. B., and Hua, Z. C. (2005). Selecting peptide ligands of microcystin-LR from phage displayed random libraries. *Environ. Int.* 31, 535–541. doi: 10.1016/j.envint.2004.09.002

frontiers | Frontiers in Microbiology

TYPE Original Research
PUBLISHED 12 January 2023
DOI 10.3389/fmicb.2022.1075033

OPEN ACCESS

EDITED BY
Antonio Ippolito,
University of Bari Aldo Moro, Italy

REVIEWED BY
Chuying Chen,
Jiangxi Agricultural University, China
Loris Pinto,
Institute of Sciences of Food Production (CNR), Italy

*CORRESPONDENCE
Yi-Wei Mo
✉ ywmo@163.com

SPECIALTY SECTION
This article was submitted to Food Microbiology, a section of the journal Frontiers in Microbiology

RECEIVED 20 October 2022
ACCEPTED 19 December 2022
PUBLISHED 12 January 2023

CITATION
Guo T-R, Zeng Q, Yang G, Ye S-S, Chen Z-Y, Xie S-Y, Wang H and Mo Y-W (2023) Isolation, identification, biological characteristics, and antifungal efficacy of sodium bicarbonate combined with natamycin on *Aspergillus niger* from Shengzhou nane (*Prunus salicina* var. taoxingli) fruit.
Front. Microbiol. 13:1075033.
doi: 10.3389/fmicb.2022.1075033

Isolation, identification, biological characteristics, and antifungal efficacy of sodium bicarbonate combined with natamycin on *Aspergillus niger* from Shengzhou nane (*Prunus salicina* var. taoxingli) fruit

Tian-Rong Guo, Qing Zeng, Guo Yang, Si-Si Ye, Zi-Yi Chen, Shi-Ying Xie, Hai Wang and Yi-Wei Mo*

College of Life Science, Shaoxing University, Shaoxing, China

The fungi causing fruit rot were isolated from symptomatic Shengzhou nane (*Prunus salicina* var. taoxingli) fruit and were identified as *Aspergillus niger* by biological characteristics and molecular analysis of the internal transcribed spacer region (rDNA-ITS) and translation elongation factor-1α (TEF-1α) sequences. Optimal growth conditions for *A. niger* were 30°C, pH 5.0–6.0, and fructose and peptone as carbon and nitrogen sources. The effects of sodium bicarbonate (SBC), natamycin (NT), and combined treatments on *A. niger* inhibition were investigated. Treatment with 4.0g/L sodium bicarbonate (SBC)+5.0mg/L natamycin (NT) inhibited mycelial growth and spore germination as completely as 12.0mg/L SBC or 25.0mg/L NT. SBC and NT treatments disrupted the structural integrity of cell and mitochondria membranes and decreased enzyme activities involved in the tricarboxylic acid (TCA) cycle, mitochondrial membrane potential (MMP), ATP production in mitochondria, and ergosterol content in the plasma membrane, thus leading to the inhibition of *A. niger* growth. Moreover, experimental results *in vivo* showed that the rot lesion diameter and decay rate of Shengzhou nane fruit treated with SBC and NT were significantly reduced compared with the control. The results suggest that the combination treatment of SBC and NT could be an alternative to synthetic fungicides for controlling postharvest Shengzhou nane decay caused by *A. niger*.

KEYWORDS

***Prunus salicina* var. taoxingli, *Aspergillus niger*, sodium bicarbonate, natamycin, antifungal mechanism**

1. Introduction

Fruit suffers from rapid spoilage as a result of infection with many fungal pathogens, such as *Penicillium digitatum*, *Botritis cinerea*, *Aspergillus*, *Richoderma viridescens*, and *Monilinia fructigena*, that cause decay during storage and marketing and reduce fruit quality (Zhou et al., 2018; Cui et al., 2021; Huang et al., 2021; Xu et al., 2021). Postharvest decay is the most serious disease affecting peach fruit quality and causing a great loss for farmers (Liu et al., 2017; Hashem et al., 2019). Recent investigations have shown that more than one-third of harvested fruit is lost due to pathogen infection. Meanwhile, many fungal pathogens that cause postharvest fruit rot produce toxins that are harmful and potentially carcinogenic to humans (Baggio et al., 2016). Several postharvest synthetic fungicides, including benzoxystrobin, iprodione, prohydantoin, and dysenine, which usually have wide target spectra, are available to control fruit rot (Knight et al., 1997). However, in response to scientific and consumer concerns about human health and environmental safety caused by synthetic fungicides due to possible toxicological risks, as well as the increasing regulatory restrictions on the postharvest use of synthetic chemicals (Dezman et al., 1986), synthetic fungicides are being withdrawn from the market. Therefore, the need for an alternative strategy to control postharvest fruit diseases has been the focus of considerable research.

Shengzhou nane (*Prunus salicina* var. taoxingli), a main cultivated plum with high nutrition and pleasant flavor, is native to Zhejiang, China (Xu et al., 2020). Shengzhou nane usually ripens in mid-July in summer, and the high ambient temperature makes it susceptible to microbial infection during harvest (Mo et al., 2017; Yan et al., 2021). In particular, fungi infections result in significant postharvest losses in the market. To lower disease occurrence in Shengzhou nane fruit and increase farmers' incomes, the disease occurrence needs to be monitored, and preventative measures should be taken to avoid its spread. However, to the best of our knowledge, till present, there have been no verified reports focusing on pathogen identification and cheap, safe, and eco-friendly alternatives to synthetic fungicides for the control of postharvest decay of Shengzhou nane fruit.

Sodium bicarbonate (SBC) is a general food additive, has less risk of phytotoxicity at the low concentrations at which it is used (1–4%; Karabulut et al., 2001; Palou et al., 2001; Usall et al., 2008), and is generally regarded as safe by the United States Food and Drug Administration (FDA) (Lai et al., 2015). Several previous studies have demonstrated that SBC plays an important role in the inhibition of postharvest diseases in several fruits. For example, SBC controls postharvest diseases caused by *P. digitatum* (Zhu et al., 2012), *Penicillium italicum*, *Geotrichum citri-aurantii* (Hong et al., 2014), and *Monilinia fructigena* (Lyousfi et al., 2022). Nonetheless, similar to other alternative treatments, its application alone shows much lower effectiveness compared to synthetic fungicides. Thus, the antibacterial effect of the combined treatments of SBC with other bactericides has been reported (Ippolito et al., 2005; Casals et al., 2010; Lyousfi et al., 2022). Natamycin (NT), a natural antifungal substance, is a polyene macrolide produced by *Streptomyces* spp. during fermentation (Aparicio et al., 2016). NT is effective against fungal pathogens regardless of their fungicide-resistance phenotypes. Accordingly, NT has been widely used as a preservative in certain foods, such as strawberry, mandarin, and lemon (Haack et al., 2018; Saito et al., 2020; Fernández et al., 2022). However, no study has been performed on SB or NT applications for controlling fungal diseases of Shengzhou nane fruit. Therefore, the objectives of this study were (i) to identify the major pathogen infecting Shengzhou nane using morphological features and rDNA-ITS analysis; (ii) to understand the epidemic properties of the pathogen by determining its biological characteristics, including the optimum culture pH, temperature, and sources of carbon and nitrogen for pathogen growth; and (iii) to evaluate the antifungal efficacy of SBC and NT against pathogens and the possible mechanism. The results will provide novel insights into exploring the potential of SBC and NT in controlling pathogen infection of Shengzhou nane fruit.

2. Materials and methods

2.1. Isolation and identification of fungal strains

Pathogens were isolated from naturally infected Shengzhou nane fruit obtained from an orchard in Shengzhou city, Zhejiang Province, China, and were immediately transported to the laboratory for experiments. The naturally infected tissues were collected at the junction of the diseased and healthy parts of the fruit when they decayed with typical diseases. The samples were sterilized with 75% alcohol for 1 min, soaked with 1.0% NaClO for 5 min, and rinsed with sterile water 3 times. Subsequently, the tissues were transferred to potato dextrose agar (PDA) medium and cultured at 30°C in the dark until mycelia appeared. Morphological traits, namely, color, shape, growth rate of the colony, and size of the spore, were measured using a microscope, and a total of more than 50 conidia were randomly selected for further length and width measurement.

The nuclear ribosomal internal transcribed spacer region (ITS) gene was amplified using the following universal primers: ITS1-F (CTTGGTCATTTAGAGGAAGTAA) and ITS4 R (TCCTCCGCTTAT TGATATGC) (Hashem et al., 2019). The translation elongation factor-1 (EF-1) gene was amplified with EF1-728F and EF1-986R primers (Carbone and Kohn, 1999). Using tweezers, 0.10 g of mycelium was collected from *A. niger* colonies cultured in PDA for 5 days. Samples were rapidly frozen in liquid nitrogen and homogenized to a powder, and the total genomic DNA was extracted using a DNeasy Kit (Beijing Solarbio Science and Technology Co., Ltd., China) following the manufacturer's instructions. PCR was performed in a 25 μl volume containing a 1.0 μl DNA template, 1.0 μl of each primer (10 μmol/L), 12.5 μl

2×PCR Taq Master Mix (Tiangen Biotech, China), and 10.5 μl ddH_2O. The amplification conditions were performed in a thermal cycle as follows: 95°C for 4 min, followed by 34 cycles of 95°C for 30 s, 56.5°C for 30 s, 72°C for 1 min, and 72°C for 10 min. The PCR products were sequenced by Sangon Biotech, Shanghai, China. The ITS and EF-1 sequences were used for BLAST searches in the GenBank database, and the obtained results were compared with those of similar sequences deposited in the National Center for Biotechnology Information (NCBI)[1] databank. A phylogenetic tree was constructed using MEGA7.0 software. To fulfill Koch's postulates, 10 healthy Shengzhou nane fruits were inoculated with a pathogen spore suspension (15 μL, 1×10^5 spores/mL) from isolates collected from rotted fruit after surface sterilization, and sterilized water injection was used as the control. All samples were kept in sealed plastic boxes at 30°C with 90% relative humidity for 4 days.

2.2. Pathogenicity test

A pathogenicity test was carried out according to the methods described by Hashem et al. (2019) and Huang et al. (2021). Healthy fruit including Shengzhou nane, yellow peach (*Prunus persica*), flat peach (*Prunus persica* "Compressa"), nectarine (*Prunus persica* var. nectarine), snow pear (*Pyrus* spp.), sand pear (*Pyrus pyrifolia*), apple (*Malus domestica*), carmine plum (*Prunus salicina*), red plum (*Prunus persica*), black plum (*Prunus persica*), cherry (*Prunus avium* L.), jujube (*Ziziphus jujuba* Mill.), tomato (*Solanum lycopersicum*), and grape (*Vitis vinifera* L.), which are the main fruits cultivated in the local area and easily decayed by fungi, were obtained from local orchards without apparent damage or disease on the surface. Six fruits were soaked in 1.0% NaClO for 2 min, washed with sterile water, air dried, and wounded using a sterilized steel rod. Fifteen microliters of the spore suspension (1×10^5 spores/mL) was used to inoculate each healthy fruit (three replicates), while another three healthy fruits were inoculated with sterilized water as the control. All inoculated fruit was kept in sealed plastic boxes at 25°C with 90% relative humidity. The results were observed after 3 days of incubation.

2.3. Biological characteristics of the pathogen

To understand its epidemic properties, the biological characteristics of the pathogen, including optimal temperature, pH, carbon (C) source, and nitrogen (N) source for pathogen growth, were evaluated. The isolate was incubated on the PDA medium at 15, 20, 25, 30, 35, and 40°C and at pH 6.0 in the dark for 4 days. Furthermore, four lethal temperatures of 50–75°C were evaluated in a hot water bath for mycelia growth. Meanwhile, the isolate was inoculated on PDA at a pH of 4, 5, 6, 7, 8, 9, 10, and 11 at 30°C in the dark for 4 days. The pH of the medium was adjusted to 1.0 mol/L HCl or NaOH.

To determine the optimal C and N source, according to the formula of Czapek-Dox agar medium (3.0 g/L $NaNO_3$, 1.0 g/L KH_2PO_4, 0.5 g/L $MgSO_4{\cdot}7H_2O$, 0.5 g/L KCl, 0.01 g $FeSO_4$, 30.0 g/L sucrose, 20 g/L agar, 1,000 mL H_2O, pH 7.0), 31.58 g/L glucose, 31.93 g/L sorbitol, 31.93 g/L maltose, 31.58 g/L fructose, 28.42 g/L starch, 31.58 g/L galactose or 28.42 g/L xylose instead of 30.0 g/L sucrose as a C source, and 10.58 g/L beef extract, 8.08 g/L peptone, 2.65 g/L glycine, 5.82 g/L phenylalanine, 1.54 g/L arginine, 1.41 g/L N_aNO_3, or 1.06 g/L urea instead of 3.0 g/L $NaNO_3$ as an N source were used. A control without a C or N source was used for each experiment. The isolate was incubated at pH 6.0 and 30°C in the dark for 4 days. The colony diameter was measured daily in all treatments using the decussation method.

2.4. Antifungal efficacy of SBC and NT against mycelia growth

Based on the antifungal activities of SBC and NT (Sigma Aldrich), the effect of SBC and NT on the mycelia growth of the pathogen was measured following protocols described by Zhou et al. (2018) and Xu et al. (2021). In brief, SBC was added to sterilized PDA to generate media with final concentrations of 0.0, 2.0, 4.0, 6.0, 8.0, 10.0, and 12.0 g/L; meanwhile, NT was added to sterilized PDA to generate media with final concentrations of 0.0, 2.5, 5.0, 10.0, 15.0, 20.0, and 25.0 mg/L. In addition, SBC and NT were both added to sterilized PDA to generate media with final concentrations of 6.0 g/L SBC + 2.5 mg/L NT and 6.0 g/L SBC + 5.0 mg/L NT according to the pretest results. The medium was poured into glass Petri dishes, and a 10 μL spore suspension (1×10^5 spores/mL) of the pathogen was used to inoculate the PDA at 4 different points. Then, the Petri dishes were incubated at 30°C for 4 days, and the colony diameter was measured daily using the decussation method. The antifungal effect of the chemistry was evaluated according to Fadda et al. (2021). In brief, the antifungal effect of the plant extract was evaluated when the control colonies completely covered the plate surface. The results were expressed as a percentage of growth inhibition, calculated as follows:

$$GI = 100 * (G - g) / G,$$

where GI is the growth inhibition, G is the growth (cm) of the control without extract, and g is the growth of the colony in the media with extracts. The experiment was repeated three times.

2.5. Antifungal efficacy of SBC and NT against spore germination

Spore germination was very sensitive to chemistry culture; thus, several lower concentrations of SBC and NT were applied to

1 http://www.ncbi.nlm.nih.gov

evaluate the antifungal efficacy of SBC and NT against spore germination, based on our pretest results. The effects of SBC and NT on the spore germination of *A. niger in vitro* were assessed according to Jiao et al. (2020). Briefly, the solutions of 6.0 g/L SBC, 2.5 mg/L NT, 5.0 mg/L NT, and the combinations of 6.0 g/L SBC + 2.5 mg/L NT and 6.0 g/L SBC + 5.0 mg/L NT were prepared in 20 mL sterile potato dextrose broth (PDB) medium containing an *A. niger* suspension (1×10^5 spores/mL). The samples in cotton-plugged glass tubes were cultivated at 30°C. After incubation for 24 h, the conidia were washed at least two times with phosphate-buffered saline (PBS, pH 7.0) and resuspended with sterile water. Subsequently, 20 μL of the spore suspension was added to a concave slide with a sterile pipette. From each slide, 200 spores were counted at random using an optical microscope. A spore was considered germinated when the length of the germinal tubule reached two times that of the total spore diameter. The inhibition percentage of spore germination was determined with respect to the control. The percentage of germinating spores among all spores detected was determined using a light microscope at a magnification of 1,000×. The average of the data obtained from the three replications is presented (Figures 1, 2).

2.6. Plasma membrane integrity of the pathogen

Propidium iodide (PI) staining, following the methods described by Zhou et al. (2018) and Kong et al. (2019) with some modifications, was used to test the membrane integrity of the pathogen mycelia and spores. According to our pretest results, 6.0 g/L or higher SBC, 10.0 mg/L or higher NT, and lower concentrations of the combined SBC and NT treatments destroyed the cell structure. Mycelia and spores treated with 6.0 g/L SBC, 10.0 mg/L NT, and 4.0 g/L SBC + 2.5 mg/L NT were cultured for 4 days. Mycelia were collected from *A. niger* colonies cultured in PDA for 5 days using tweezers. Spores were collected from 5-day-old cultures of fungi growing in a PDA medium. The spores were collected from the plates, rinsed with 5 mL sterile distilled water containing 0.1% Tween-80, filtered through five layers of sterile cheesecloth to remove hyphae, counted by a hemocytometer, and used in the next test. The collected mycelia and spores were incubated with PI at a final concentration of 10.0 μg/mL and kept in the dark at 37°C for 30 min. The mycelia

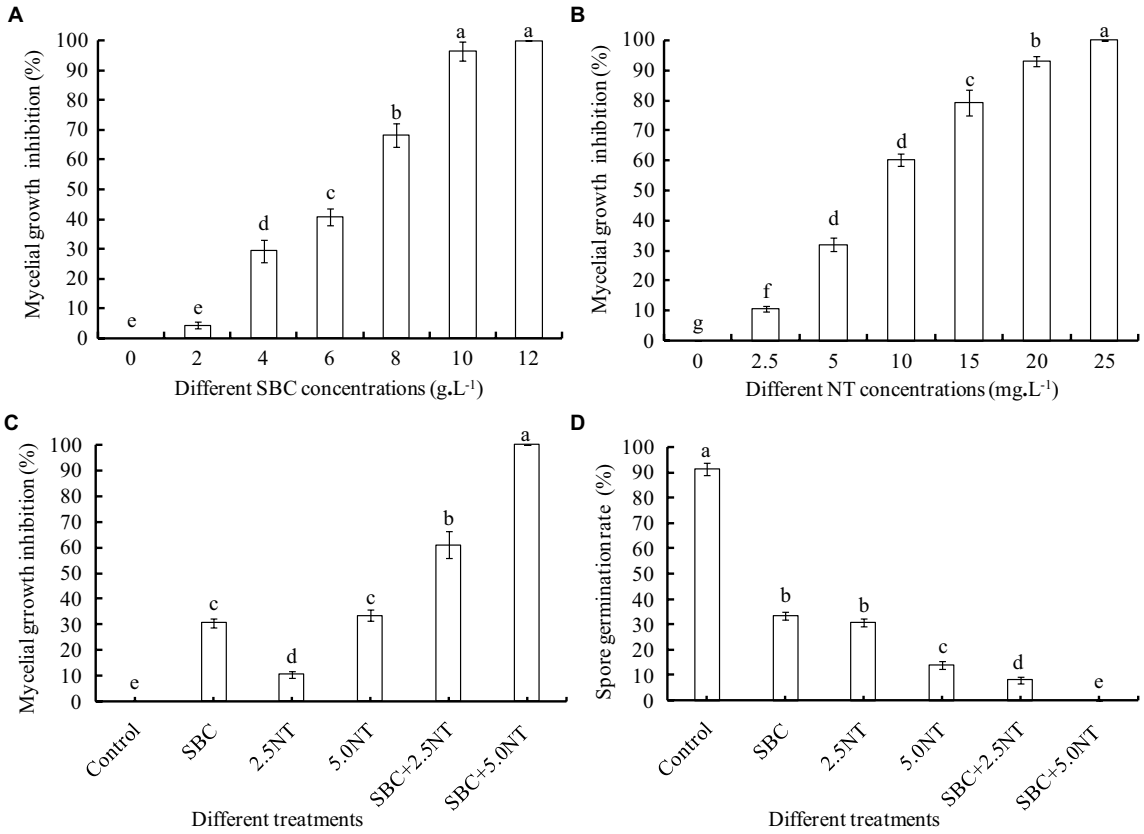

FIGURE 1
Effect of SBC, NT, and combination treatments on the mycelial growth and spore germination of *Aspergillus niger*. **(A)** Effect of SBC on colony growth. **(B)** Effect of NT on colony growth. **(C)** Effect of SBC and NT combinations on colony growth. **(D)** Effect of SBC and NT combination on spore germination rate. SBC means 6.0g/L $NaHCO_3$; 2.5NT means 2.5mg/L natamycin; 5.0NT means 5.0mg/L natamycin; SBC+2.5NT means 4.0g/L $NaHCO_3$+2.5mg/L natamycin; and SBC+5.0NT means 4.0g/L $NaHCO_3$+5.0mg/L natamycin. ANOVA was used to compare the mean values of analysis parameters (p<0.05). The results are shown as the mean±standard deviation (n=3). Different superscript letters in the same column indicate significant differences (p<0.05).

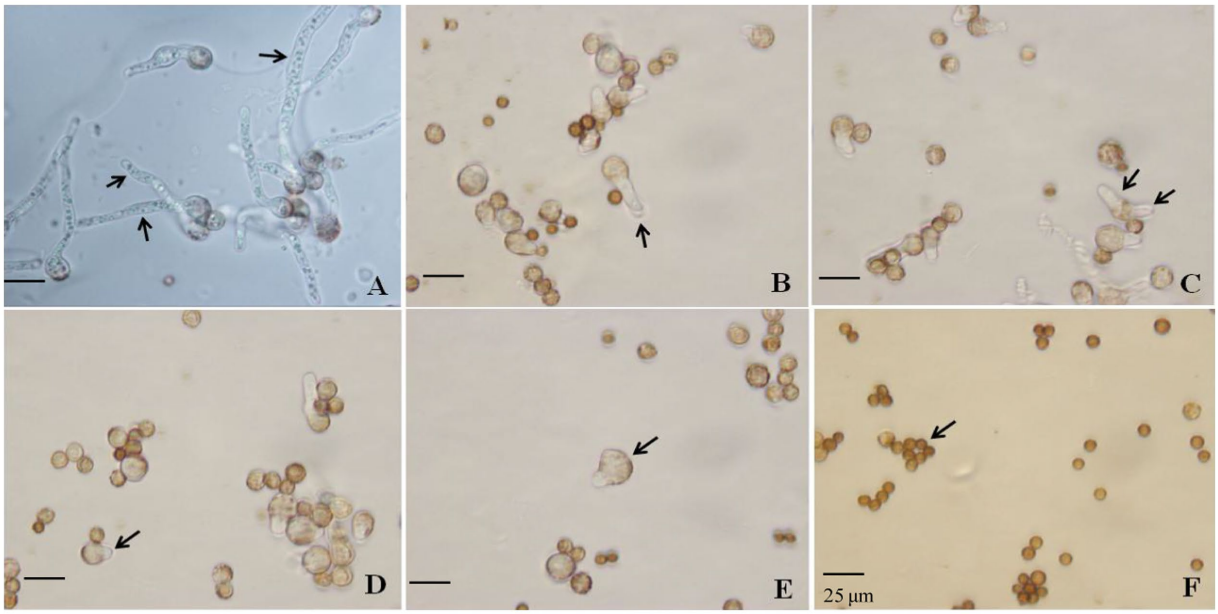

FIGURE 2
Effect of SBC, NT, and the combination treatment on spore germination of *Aspergillus niger*. **(A)** Control; **(B)** 6.0g/L SBC; **(C)** 2.5mg/L NT; **(D)** 5.0mg/L NT; **(E)** 4.0g/L SBC+2.5mg/L NT; **(F)** 4.0g/L SBC+5.0mg/L NT, 24h after inoculation. Images were obtained by microscopy at 1,000× magnification, bar=25μm.

and spores were then collected and washed three times with 50 mmol/L PBS (pH 7.2). Samples were observed with a fluorescence microscope.

Membrane integrity was also assayed using a flow cytometer, following the method described by Wang et al. (2015) and Li et al. (2017), with some modifications. In brief, a 100 μL spore suspension of *A. niger* (1×10^5 spores/mL) was added to 5 mL of 50 mmol/L PBS (pH 7.2) with 2% (w/v) D-glucose containing 0 (control), 6.0 g/L SBC, 10.0 mg/L NT, or 4.0 g/L SBC + 2.5 mg/L NT. They were incubated on a rotary shaker (120 r/min) for 24 h at 30°C. The spore suspension was then centrifuged at 5,000 × *g* for 10 min at 4°C, washed two times with PBS, and filtered two times through a 400 mesh screen to remove cell debris and aggregates. Subsequently, the spores were resuspended in 500 μL of 100 mmol/L PBS (pH 7.2) and stained with PI (10.0 μg/mL) for 30 min at 30°C in the dark. The mixture was centrifuged at 5,000 × *g* for 5 min at 4°C; the precipitate was washed two times with PBS to remove the residual dye, and then resuspended in 500 μL of PBS. Unstained spore suspension was used as an auto-fluorescence control. The spores were detected using a CytoFLEX flow cytometer (BD Biosciences). Fluorescence intensity upon stimulation with an argon-ion laser at 488 nm was measured using the PMT4 channel (625DL filter) and plotted against the cell number. From each sample, 20,000 spores were sorted and analyzed. The percentage of fluorescent spores in the population was calculated. Three replicates of each treatment were performed, and the entire experiment was performed three times.

2.7. Mitochondrial activities of the pathogen

Aspergillus niger treated with 6.0 g/L SBC, 10.0 mg/L NT, and 4.0 g/L SBC + 2.5 mg/L NT were cultured for 4 days. Collected mycelia and spores were used to determine the mitochondrial activity, the enzyme activities involved in the tricarboxylic acid (TCA) cycle, MMP, ATP, and ergosterol contents, as shown below.

Rhodamine 123 and a mitochondrial red fluorescence probe were used to test the mitochondrial activity. Mycelia and spores were incubated with Rhodamine 123 (50.0 μg/L) for 30 min and the mitochondrial red fluorescence probe (1.0 μg L^{-1}) for 1.0 h in the dark at 37°C. Mycelia and spores were collected and washed three times with 50 mmol/L PBS (pH 7.2). Samples with different stained proportions were observed with a fluorescence microscope to evaluate the mitochondrial activity.

2.8. Enzyme activities involved in the TCA cycle and mitochondrial membrane potential (MMP)

To prepare mitochondria, 2.0 g of mycelia was added to a mortar with a small amount of liquid nitrogen and ground to break up whole cells. Broken cells were suspended with a five-fold volume of mitochondrial extract buffer. The mitochondrial extract buffer was composed of 50 mM potassium phosphate buffer (pH 8.0), 0.3 M mannitol, 0.5% (w/v) bovine serum

albumin (BSA), 0.5% (w/v) polyvinylpyrrolidone-40 (PVP-40), 2 mM EGTA, and 20 mM cysteine. The homogenate was squeezed through a 40 × 40 μm mesh nylon cloth and centrifuged at 2,000 × *g* for 15 min. The supernatant was centrifuged at 12,000 × *g* for 15 min. The precipitate was suspended in wash medium buffer [0.3 M mannitol, 0.1% (w/v) BSA and 10 mM TES (pH 7.5)] and centrifuged again at 12,000 × *g* for 15 min. The final precipitate was washed once with wash medium and suspended in a small volume of the washing medium (mitochondrial fraction). The precipitate was used to determine enzyme activity and MMP.

Citrate synthetase (CS), isocitrate dehydrogenase (IDH), α-ketoglutarate dehydrogenase (α-KGDH), succinate dehydrogenase (SDH), and malate dehydrogenase (MDH) reagent kits were purchased from the Nanjing Jiancheng Bioengineering Institute (Nanjing, China). CS, MDH, SDH, IDH, and α-KGDH activities in the mitochondria of the pathogen were determined spectrophotometrically. The reagent kits were used following the manufacturer's instructions. MDH, SDH, and IDH activities were estimated at 340 nm in terms of redox reactions. α-KGDH and CS activities were determined at 600 and 412 nm, respectively (Kong et al., 2021).

Mitochondrial membrane potential, as a key indicator of mitochondrial function, can reflect the cellular health status (Li et al., 2020). The MMP Detection Kit (JC-1; Jiancheng Bioengineering Institute, Nanjing, China) was used as a fluorescent probe, as it is a rapid and sensitive kit for assessing changes in MMP in cells. It can be used for the early detection of cell apoptosis. First, a working solution of JC-1 was prepared. A positive control was then set up, and the experiment was carried out. Staining was observed using laser confocal microscopy. The JC-1 monomer (green fluorescence) was determined at an excitation wavelength of 490 nm and an emission wavelength of 530 nm. The JC-1 polymer (red fluorescence) was determined at an excitation wavelength of 525 nm and an emission wavelength of 590 nm.

2.9. ATP and ergosterol content in mycelia

ATP extraction from mycelia was carried out according to the methods reported by Mo et al. (2013). Typically, fresh mycelia (1.5 g) were rapidly frozen in liquid nitrogen and homogenized to powder. ATP was extracted from the powder with 6.0 mL of 0.6 mol/L perchloric acid in an ice bath for 5 min. The extraction mixture was centrifuged at 8,000 *g* (Heraeus Multifuge X1R, United States) for 15 min at 4°C. The supernatant was then collected and quickly neutralized to pH 6.5–6.8 with 1.0 mol/L NaOH solution. The neutralized supernatant was placed in an ice bath for 40 min to precipitate most of the potassium perchlorate and subjected to filtration paper to remove potassium perchlorate. The filtrate solution was filtered through a 0.45 μm filter. The samples were analyzed with an LC-20 AD HPLC system (Japan) equipped with an LC-20 AD pump system and an SPD-20 AD diode array detector. The column effluent was monitored by absorbance at 259 nm. Ten microliter samples were applied to an Ultrasphere ODS EC 250 × 4.60 mm column (CTO-10AS VP Japan). The materials were eluted with the mobile phase (pH 6.8, 50.0 mmol/L NaH_2PO_4) at 1.0 mL/min. The entire running time was about 20 min for the full separation and determination of ATP. ATP in mycelium samples was identified by comparison with the retention time of the standards. Standard ATP (Sigma, United States) was used for quantitative detection, and its concentration was determined using the external standard method.

Ergosterol was extracted as described by Wang et al. (2018). Mycelia were centrifuged at 8,000 × *g* for 10 min and washed two times with distilled water. Then, mycelia (1.5 g) were rapidly frozen in liquid nitrogen and homogenized to powder. A quantity of 15 ml KOH-C_2H_5OH solution (30%, w/w) was added to each pellet and vortexed. The mixture was incubated at 85°C for 4 h. After the tubes were cooled to room temperature, 10 mL of ether was added and vortexed. The ergosterol of the upper phase was sampled and quantified using the LC-20 AD HPLC system (Japan). Sterol extracts were separated on a C-18 packed column (245 × 4.6 mm) with methanol at a flow rate of 1 mL/min, and the eluate was continuously monitored using a UV spectrophotometer at 280 nm. Standard ergosterol (Sigma, United States) was used for quantitative detection. The ergosterol content was quantified as milligrams of ergosterol per gram of dry weight (mg/g).

2.10. SBC and NT against Shengzhou nane fruit rot *in vivo*

The effects of SBC and NT on controlling postharvest disease *in vivo* were determined following the method described by He et al. (2019). Shengzhou nane was wounded with a sterile nail at the equator before inoculation. Then, the fruit was inoculated with a 10 μl spore suspension (1 × 10^5 spores/mL) on each wound. After the fruit was air dried for 3 h, 10 μl SBC_1 (2.0 g/L SBC), SBC_2 (4.0 g/L SBC), SBC_3 (6.0 g/L SBC), NT_1 (25.0 mg/L NT), NT_2 (50.0 mg/L NT), NT_3 (100.0 mg/L NT), NT_4 (200.0 mg/L NT), NT_5 (400.0 mg/L NT), $(SBC+NT)_1$ (4.0 g/L SBC + 25.0 mg/L NT), $(SBC+NT)_2$ (4.0 g/L SBC + 50.0 mg/L NT), $(SBC+NT)_3$ (4.0 g/L SBC + 100.0 mg/L NT), or $(SBC+NT)_4$ (4.0 g/L SBC + 150.0 mg/L NT) were added to the wound sites. In addition, water-treated fruit was used as the control. Treated fruit was placed in a plastic box, and each tray was enclosed with a polyethylene bag to maintain high humidity (95%). The lesion diameter and decay rate of the fruit were used to determine disease severity 4 and 6 days after treatment. Each treatment contained three replicates, with 18 fruits per replicate.

2.11. Statistical analysis

All experiments were carried out with at least three replicates. Data were analyzed using one-way ANOVA in SPSS 23 software (SPSS Inc., Chicago, IL, United States). Statistical significance was followed by Tukey's HSD test at $p < 0.05$ to examine differences between treatments.

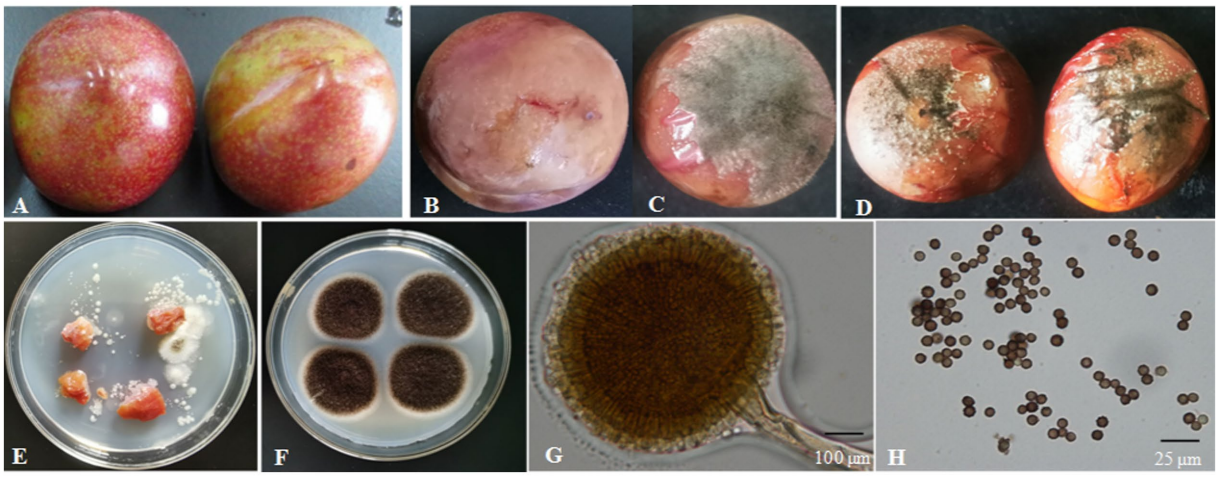

FIGURE 3
Isolation of the fungal strain from naturally infected fruit. **(A)** Healthy fruit; **(B,C)** naturally infected fruit; **(D)** fruit 4days after inoculation with fungi for 4days; **(E)** fungi isolated from naturally infected fruit; **(F)** fungi colony cultured for 4days on PDA; **(G)** conidium and sporangium, 200×, bar=100μm; **(H)** spore, 1,000×, bar=25μm.

3. Results

3.1. Isolation and identification of fungal strains

The surface of the healthy Shengzhou nane fruit was smooth, with bright skin (Figure 3A). However, the peel became pale, and the fruit started to go rotten after being infected by the pathogen; then, black mold appeared (Figures 3B, C). The pathogen from a typical decay Shengzhou nane fruit was isolated and purified by growth on PDA (Figure 3E). After culturing at 30°C in the dark for 4 days, round and aerial hyphae were observed from the colony appearance (Figure 3F). Furthermore, the colony was white in the initial stage, then became dark and extended outward in a strip with no marginal or adherent growth (Figure 3F). Colonies grew with a mean hyphae growth rate of 9.42 ± 0.28 mm per day on PDA in the dark at 30°C. Mycelia were characterized by transverse septa and branches. The spore shape was round, and the size was 3.27 ± 0.13 μm ($n = 50$). The outside surface was uneven due to its sporulation with a single bottle-stem type, while many irregular protrusions were observed on the spore surface (Figures 3G, H).

A DNA-ITS sequence of about 681 bp was extracted from the isolated DNA (Figure 4A). The ITS regions of the fungal genes were sequenced and aligned to entries in the NCBI sequence database. The Blastn results indicated that ITS sequences shared 99% similarity with *A. niger*. Phylogenetic analysis was conducted using MEGA7.0 software, and the results showed that the isolated colony was clustered with the MT 430878.1 *A. niger* clade (Figure 4B).

The translation elongation factor-1 (EF-1) gene sequence was also amplified with EF1-728F and EF1-986R primer pairs (Figure 5A). The representative sequence was submitted to GenBank. The Blastn results indicated that the EF-1 sequence shared 100% similarity with a strain of *A. niger* (Accession Nos. MT318312.1 and MT318310.1). The isolated colony was clustered with the *A. niger* clade (Figure 5B). Therefore, the isolate was identified as *A. niger* (TXL-1).

In Koch's postulate experiment, 10 healthy Shengzhou nane fruits were inoculated with isolated *A. niger*. The inoculated fruit became infected, and the same symptoms were found in naturally infected fruits, while those in the control group remained symptomless after 4 days of culture (Figure 3D).

3.2. Pathogenicity tests

The pathogenicity test of *A. niger* was determined on the fruits of yellow peach, flat peach, nectarine, snow pear, sand pear, apple, carmine plum, red plum, black plum, cherry, jujube, tomato, and grape. The typical round lesions appeared on all fruit surfaces 3 days after inoculation with *A. niger,* which was consistent with the symptoms in those of naturally infected Shengzhou nane fruit. The pathogen was re-isolated from symptomatic rotten fruit. As a result, it was identified as *A. niger* based on its morphological characteristics and gene sequences. Moreover, the pathogenicity of *A. niger* varied in different fruits. For example, mycelium was observed in peach and tomato, but the decay in grapes was not serious (Figure 6).

3.3. Biological characteristics of *Aspergillus niger*

The biochemical tests showed that *A. niger* grew in a temperature range of 15–40°C. The greatest colony diameter was

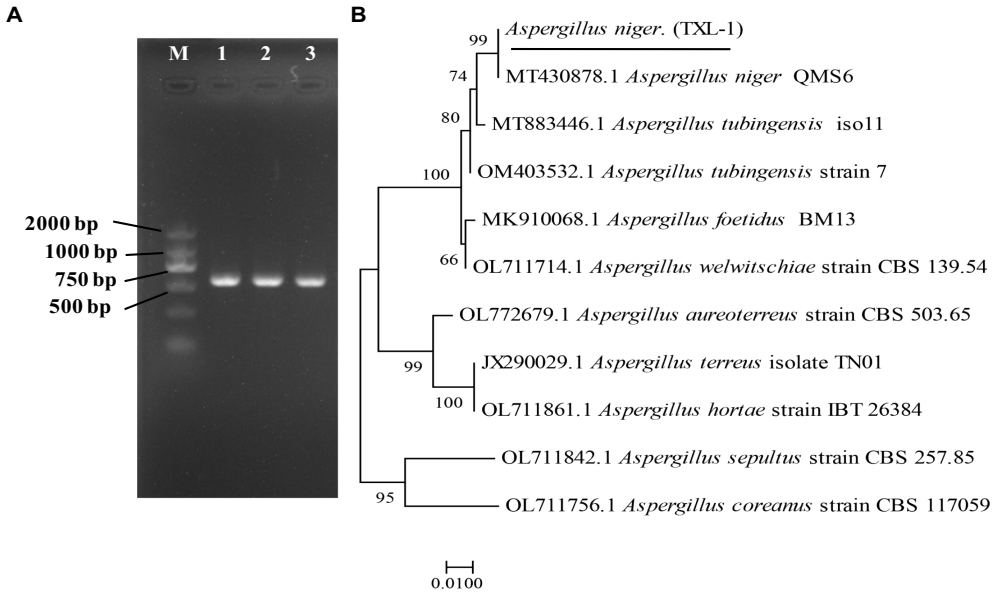

FIGURE 4
Molecular identification of fungal strains. **(A)** PCR results of the pathogen using DNA-ITS; **(B)** phylogenetic tree based on ITS sequences; (M) marker DL2000; (1, 2, 3) three replications.

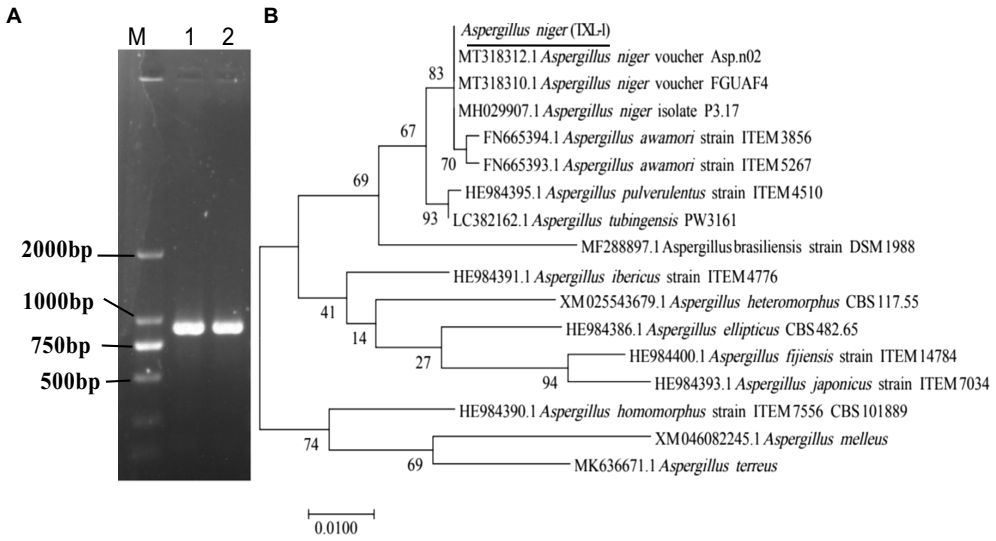

FIGURE 5
Molecular identification of fungal strains. **(A)** PCR results of the pathogen using EF-1 sequences; **(B)** phylogenetic tree based on EF-1 sequences; (M) marker DL2000; (1, 2) two replications.

observed at 30°C (40.83 mm), followed by 25°C (32.93 mm) after 4 days of culture. However, mycelial growth was significantly inhibited at 40°C (Figure 7A). Thus, the optimal culture temperature for *A. niger* growth was 30°C.

To clarify the endurance temperature, the spores were treated with a hot water bath from 50 to 75°C for 10 min. Complete inactivation of the spore occurred at 75°C. However, there was no significant difference in colony diameter between treatments below 75°C (Figure 7B). These results suggest that the lethal temperature for *A. niger* is 75°C for 10 min.

Aspergillus niger grew in a pH range of 4.0–11.0. The greatest colony diameter was observed at pH 5.0 and 6.0 but decreased at pH values higher than 8.0 (Figure 7C).

Fructose as a C source in the medium produced the greatest colony diameter, recorded as 33.88 mm after 4 days of culture, followed by sucrose, maltobiose, xylose, and glucose. However, a

very thin mycelial density and lower diameter were observed in the galactose media (Figure 7D). Mycelia did not grow in a starch- or carbon-free medium. The results indicated that the optimal C source for *A. niger* growth was fructose.

Peptone and beef paste as N sources in the medium produced the largest colony diameters, recorded as 41.94 and 40.98 mm, respectively, after 4 days of culture, followed by glycine, phenylalanine, sodium nitrate, and arginine. The smallest colony diameters were observed in the urea medium and the control (Figure 7E). The optimal N sources for *A. niger* growth were peptone and beef paste. Interestingly, unlike the C-free medium, the colony grew slowly in the N-free culture, indicating that some other substances could replace the N sources needed for *A. niger* growth.

3.4. Antifungal efficacy of SBC and NT against *Aspergillus niger*

Sodium bicarbonate or natamycin caused a significant decrease in the mycelial growth rate in proportion to the concentration (Figures 1A, B). Compared to the control, 6.0 g/L SBC induced mycelial growth inhibition by 40.73% ($p < 0.05$) after inoculation for 4 days, while it increased to 96.48 and 100% at 10.0 and 12.0 g/L SBC, respectively. Mycelial growth was significantly inhibited by all concentrations of NT tested in this experiment, and 25.0 mg/L NT inhibited mycelial growth by 100.0%. Moreover, the combination of SBC and NT induced a higher inhibition efficacy compared with the single chemistry treatments. For example, 4.0 g/L SBC, 2.5 mg/L NT, and 5.0 mg/L NT induced mycelial growth inhibition by 30.55, 10.56, and 33.58%, respectively, whereas the mycelial growth inhibition was 60.93 and 100% under treatments of 4.0 g/L SBC + 2.5 mg/L NT and 4.0 g/L SBC + 5.0 mg/L NT, respectively (Figure 1C).

Spore germination is the key process required to initiate vegetative growth. The germination rate of the spores, as well as the germination time of *A. niger,* differed by treatment. After 24 h incubation in control conditions, 91.28% of spores germinated, whereas the germination rates decreased and were recorded as 35.55, 30.72, 14.23, 5.22, and 0.0% in 6.0 g/L SBC, 2.5 mg/L NT, 5.0 mg/L NT, 4.0 g/L SBC + 2.5 mg/L NT, and 4.0 g/L SBC + 5.0 mg/L NT treatments, respectively (Figure 1D). The spores swelled and were enlarged, and the mycelia grew quickly with many granular inclusions formed in the mycelium after 24 h of culture in the control group during germination. However, only a few spores swelled, but no germination was observed in the SBC or NT treatments. Therefore, spore swelling may be the premise of spore germination. In addition, the 4.0 g/L SBC + 5.0 mg/L NT treatment completely inhibited spore germination (Figure 2).

3.5. SBC and NT destroyed the plasma membrane integrity of *Aspergillus niger*

Propidium iodide (PI), a fluorescent molecule, is membrane impermeable and can bind to DNA by intercalating between the bases with less or no sequence preference, which causes the nucleus to be stained with red fluorescence. Therefore, cells stained by PI can be used to identify the extent of cell damage (Jiao et al., 2020). In this study, the PI staining results showed that the mycelia and spores treated with 6.0 g/L SBC, 10.0 mg/L NT, or

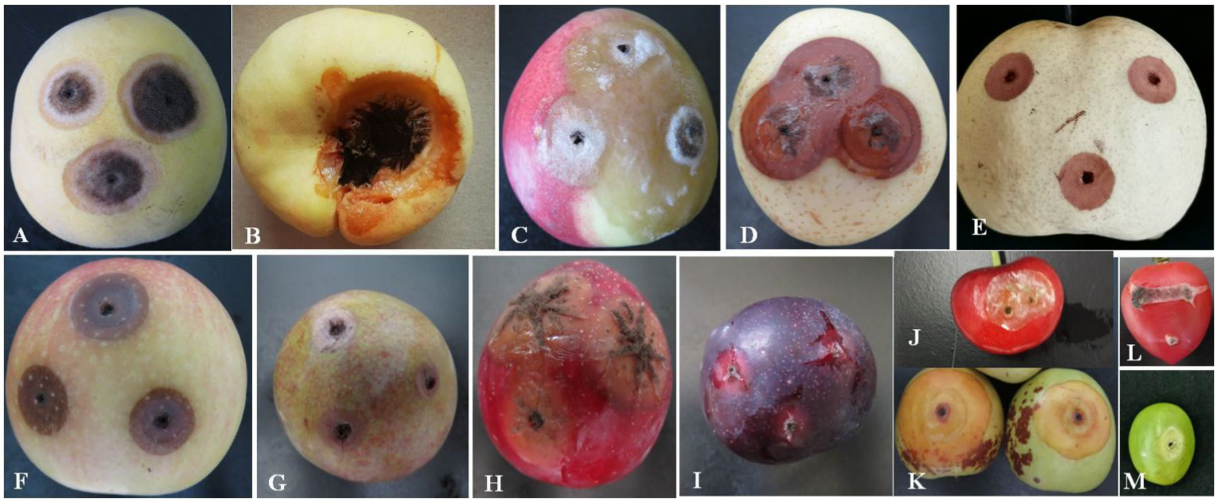

FIGURE 6
Pathogenicity of *A. niger* to different local fruits. **(A)** Yellow peach; **(B)** flat peach; **(C)** nectarine; **(D)** snow pear; **(E)** sand pear; **(F)** apple; **(G)** carmine plum; **(H)** red plum; **(I)** black plum; **(J)** cherry; **(K)** jujube; **(L)** tomato; and **(M)** grape.

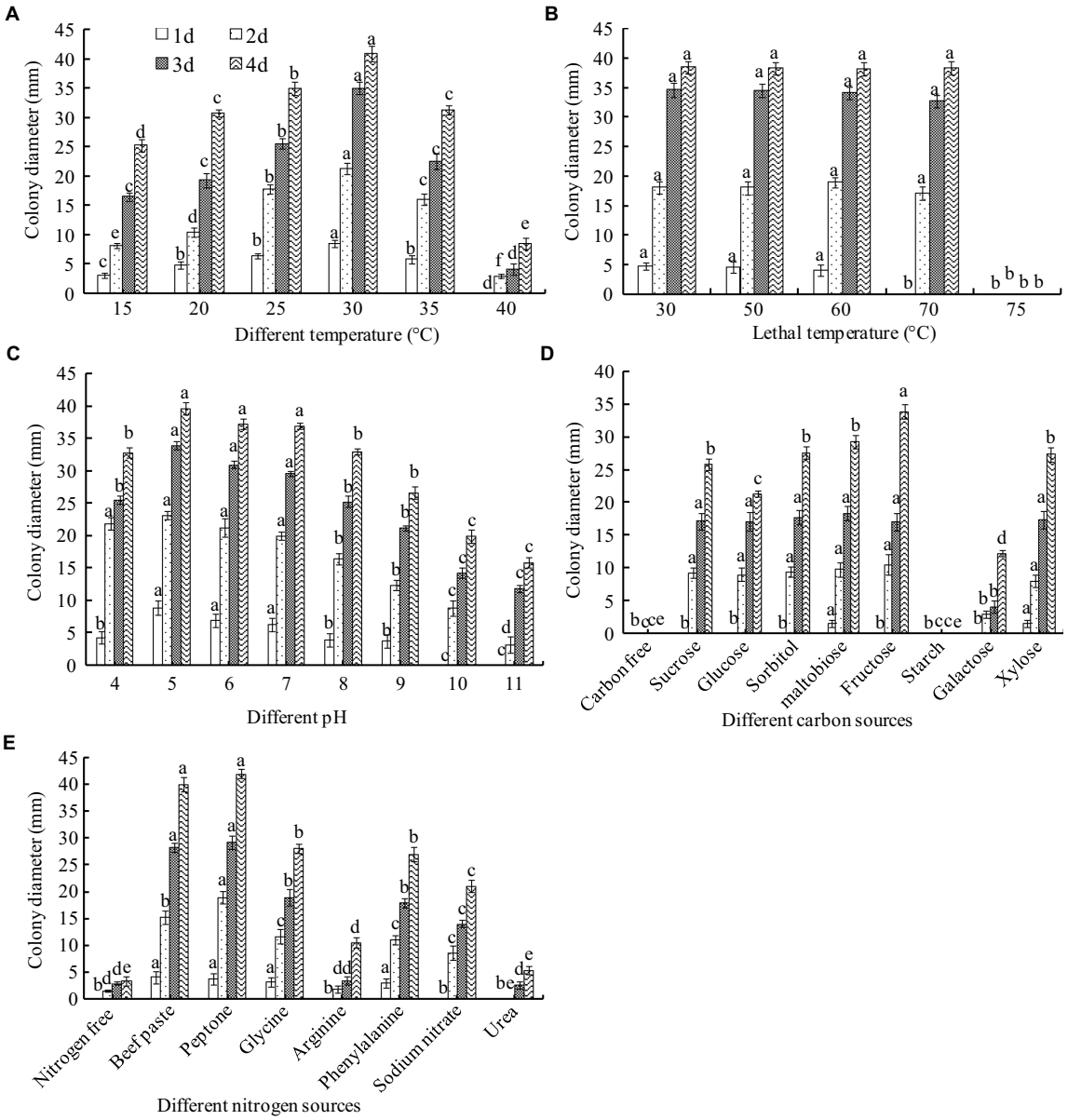

FIGURE 7
Biological characteristics of *A. niger*. **(A)** Temperature; **(B)** lethal temperature; **(C)** pH; **(D)** carbon sources; **(E)** nitrogen sources. ANOVA was employed to compare the mean values of analysis parameters ($p<0.05$). The results are shown as the mean±standard deviation ($n=5$). Different superscript letters in the same column indicate significant differences ($p<0.05$).

4.0 g/L SBC + 2.5 mg/L NT were stained deeply compared to the control (Figure 8), indicating that SBC and NT destroyed the cell membrane integrity of *A. niger* cells and induced mycelia and spore death.

The membrane integrity of *A. niger* was also determined using flow cytometry after being stained with PI and was presented in two-dimensional dot plots. As shown in Figure 9, a homogenous population of undamaged cells was dominant in the control, while various cell sizes (forward scatter, FSC) and variations in complexity (side scatter, SSC) were observed on a scattergram of *A. niger* spores after 24 h of incubation in SBC and NT. Furthermore, a histogram plot was obtained by counting PI-labeled spores. In the control, the PI-stained spores accounted for only 3.39% of total spores (Figures 9B, b). In treatments of 6.0 g/L SBC (Figures 9C, c), 10.0 mg/L NT (Figures 9D, d), and 4.0 g/L SBC + 2.5 mg/L NT (Figures 9E, e), the percentage of PI-stained spores increased to 53.75, 63.65, and 75.03% (Figure 9F) ($p < 0.05$), respectively, indicating a loss in integrity and heavy damage to the cell membrane of the pathogen.

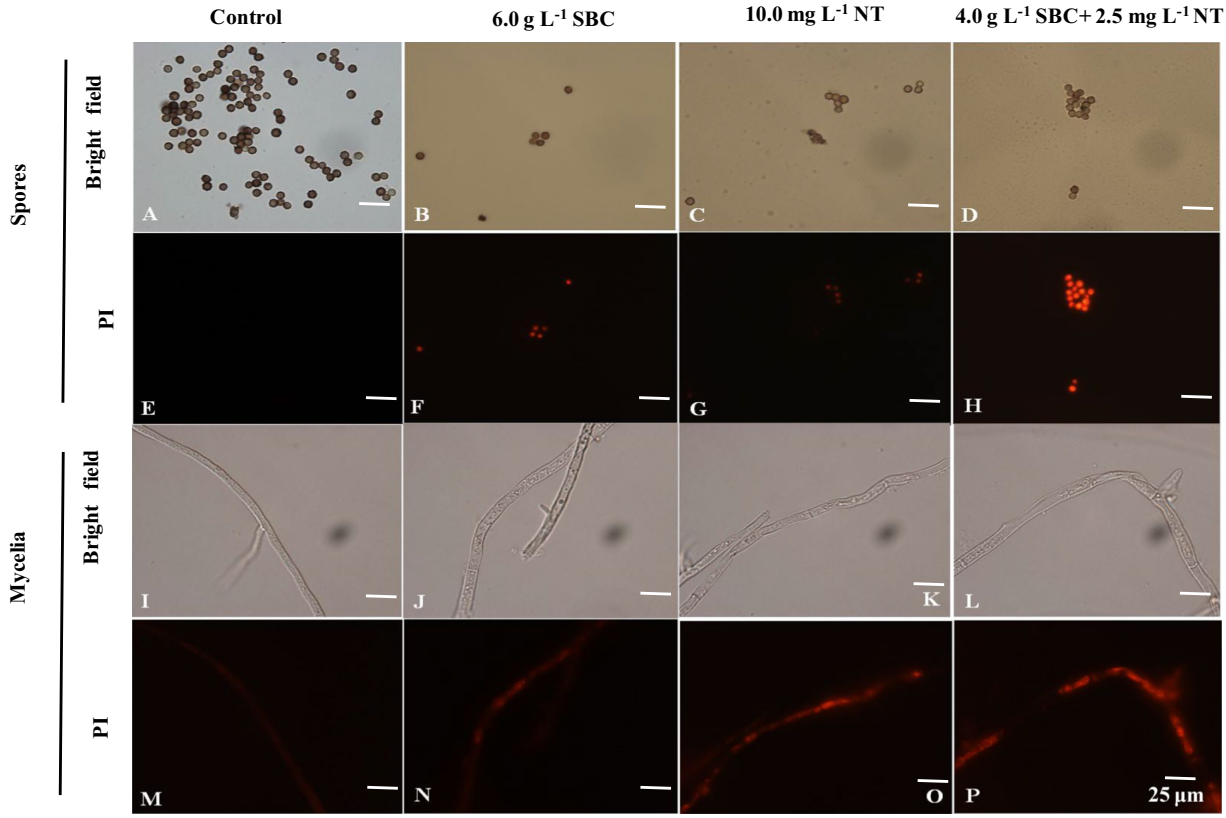

FIGURE 8
Effect of SBC, NT, and combination treatment on the plasma membrane integrity of *Aspergillus niger*. **(A,E)** Spores in control; **(B,F)** spores treated with 6.0g/L SBC; **(C,G)** spores treated with 10.0mg/L NT; **(D,H)** spores treated with 4.0g/L SBC+2.5mg/L NT; **(I,M)** mycelia in control; **(J,N)** mycelia treated with 6.0g/L SBC; **(K,O)** mycelia treated with 10.0mg/L NT; **(L,P)** mycelia treated with 4.0g/L SBC+2.5mg/L NT mycelia. Images were obtained by microscopy at 1,000× magnification, bar=25μm.

3.6. SBC and NT damage the mitochondrial activity of *Aspergillus niger*

The mitochondrial red fluorescence probe bound the active mitochondria and emitted red fluorescence at different intensities, according to the MMP of living cells. The spores and mycelia of *A. niger* treated with 6.0 g/L SBC, 10.0 mg/L NT, and 4.0 g/L SBC + 2.5 mg/L NT showed a less stained proportion by mitochondrial red fluorescence compared with the control group (Figure 10).

Rhodamine 123 (Rh-123) is a specific probe used for evaluating changes in MMP since it can accumulate in normal mitochondria and be released to the outside of the mitochondria with a loss of MMP, leading to a stronger green fluorescence signal (Su et al., 2014). As shown in Figure 11, the fluorescence intensity of Rh-123 in the groups treated with 6.0 g/L SBC, 10.0 mg/L NT, and 4.0 g/L SBC + 2.5 mg/L NT was higher than that of the control group. Combined with the fluorescence staining results, it revealed that suitable concentrations of SBC and NT could destroy the cell structure, leading to the hyperpolarization of MMP and causing mitochondrial dysfunction in *A. niger* cells.

3.7. SBC and NT decreased the activity of enzymes involved in the TCA cycle

Compared with the control, the activity of the key enzymes involved in the TCA cycle, such as CS, IDH, α-KGDH, SDH, and MDH, in the mitochondria of *A. niger* cells decreased significantly ($p < 0.05$) under the treatments of 6.0 g/L SBC, 10.0 mg/L NT, and 4.0 g/L SBC + 2.5 mg/L NT (Figures 12A–E), especially α-KGDH activity. The significant decreases in the activities of these key enzymes indicated that mitochondrial function was destroyed by SBC and NT treatments.

3.8. SBC and NT decreased the ATP content and MMP

The effects of the SBC and NT treatments on the ATP content of *A. niger* are presented in Figure 13A. Compared with the control,

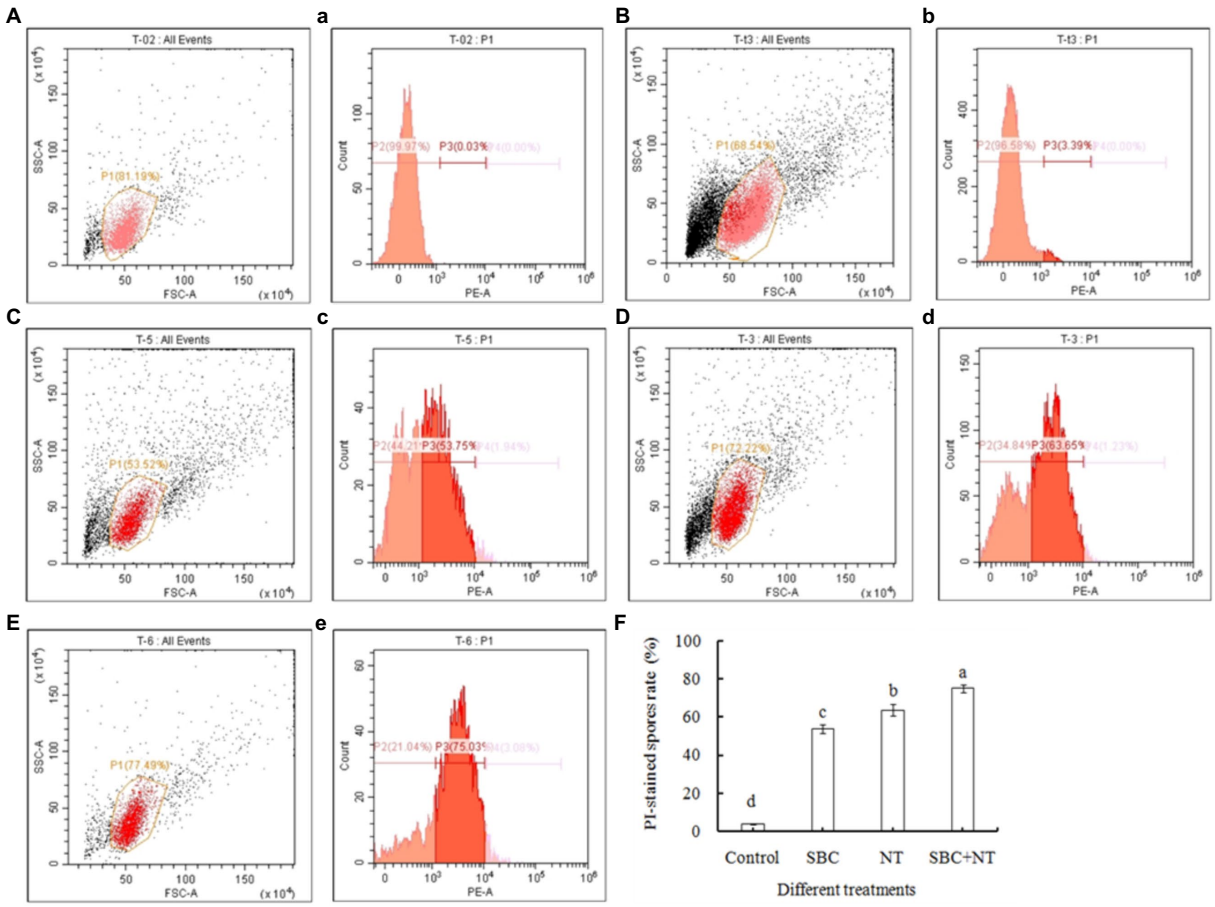

FIGURE 9
Flow cytometry analysis of the plasma membrane integrity of *Aspergillus niger* spores treated with SBC or NT. **(A–E)** Scattergram showing cell complexity (side scatter, SSC) vs. cell size (forward scatter, FSC); **(a–e)** the corresponding percentage of PI-stained spores compared with the control. **(A,a)** Autofluorescence of non-treated cells; **(B,b)** fluorescence of non-treated cells for PI staining; **(C–E)** cells treated with the varying treatments of SBC **(c)**, NT **(d)**, and SBC+NT **(e)**; **(F)** the percentage of PI-stained spores rate after different treatments. ANOVA was employed to compare the mean values of analysis parameters (p<0.05). The results are shown as the mean±standard deviation (n=3). Different superscript letters in the same column indicate significant differences (p<0.05).

6.0 g/L SBC, 10.0 mg/L NT, and 4.0 g/L SBC + 2.5 mg/L NT decreased the ATP content by 31.50, 50.51, and 63.68%, respectively ($p < 0.05$). Meanwhile, MMP decreased significantly in *A. niger* cells under the treatments of 6.0 g/L SBC, 10.0 mg/L NT, and 4.0 g/L SBC + 2.5 mg/L NT and was recorded as 30.03, 41.51, and 59.51% of the control, respectively ($p < 0.05$) (Figure 13B).

3.9. SBC and NT decreased the ergosterol content in mycelia

The effects of SBC and NT on the ergosterol content in the plasma membranes of *A. niger* mycelia are shown in Figure 14. After incubating with SBC or NT, the total ergosterol content decreased significantly. In detail, the ergosterol content decreased by 18.17, 39.42, and 58.09% ($p < 0.05$) of the control under the treatments of 6.0 g/L SBC, 10.0 mg/L NT, and 4.0 g/L SBC + 2.5 mg/L NT, respectively.

3.10. SBC and NT against Shengzhou nane fruit rot caused by *Aspergillus niger*

Rot lesions were significantly alleviated in Shenzhou nane fruit treated with different concentrations of SBC and NT 4 days after inoculation with *A. niger* spores (Figures 15A–C). The rot lesion diameter in the control fruit reached 13.67 mm. In contrast, it was reduced by 29.33, 43.76, 57.57, 34.79, 52.69, 61.96, 83.02, 100.00, 63.42, 68.30, 100.00, and 100.00% of the control ($p < 0.05$) in fruit treated with SBC_1 (2.0 g/L SBC), SBC_2 (4.0 g/L SBC), SBC_3 (6.0 g/L SBC), NT_1 (25.0 mg/L NT), NT_2 (50.0 mg/L NT), NT_3 (100.0 mg/L NT), NT_4 (200.0 mg/L NT), NT_5 (400.0 mg/L NT), $(SBC + NT)_1$ (4.0 g/L SBC + 25.0 mg/L NT), $(SBC + NT)_2$ (4.0 g/L SBC + 50.0 mg/L NT), $(SBC + NT)_3$ (4.0 g/L SBC + 100.0 mg/L NT), or $(SBC + NT)_4$ (4.0 g/L SBC + 150.0 mg/L NT), respectively (Figure 15D). Disease occurrence was completely restricted by the treatments NT_5, $(SBC + NT)_3$, and $(SBC + NT)_4$ (Figures 15B, C). Six days after inoculation, the fruit became soft,

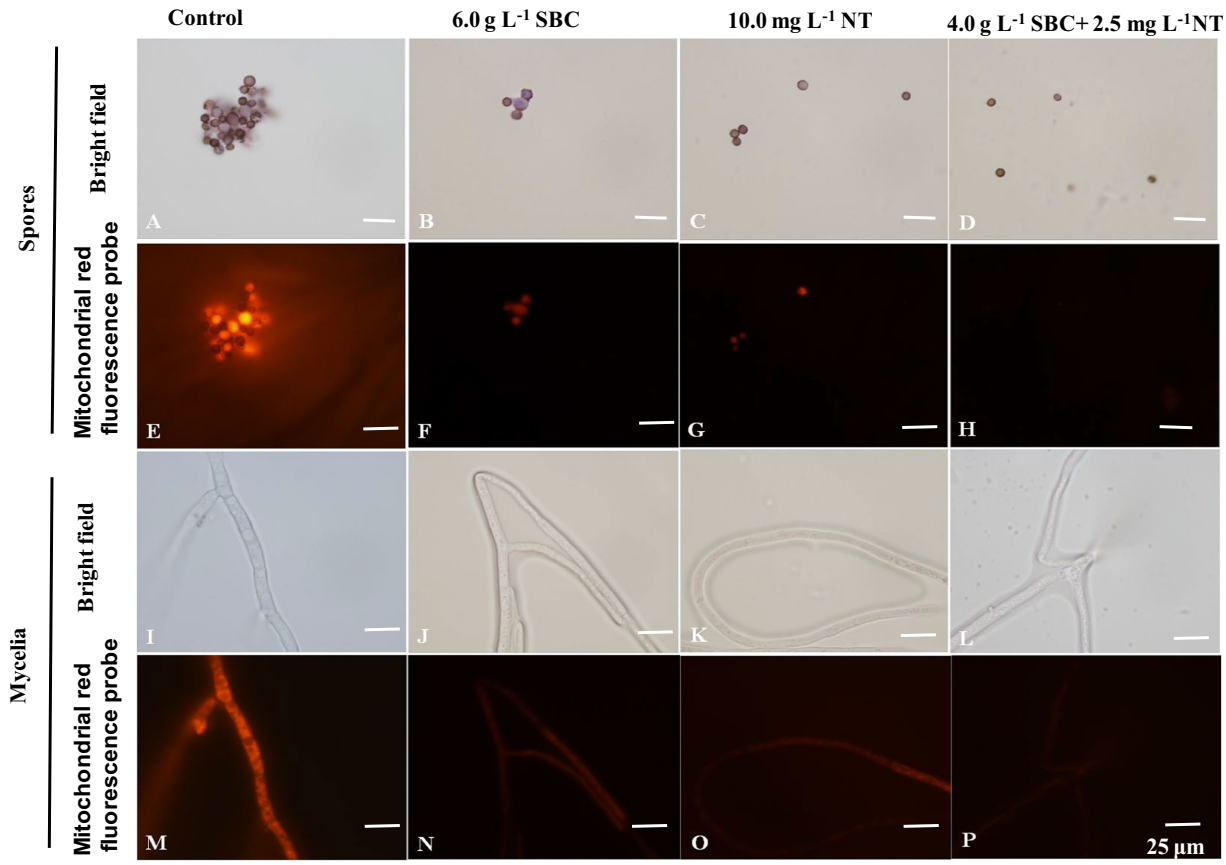

FIGURE 10
Aspergillus niger stained with the mitochondrial red fluorescence probe after treatment with SBC or NT. **(A,E)** Spores in the control; **(B,F)** spores treated with 6.0g/L SBC; **(C,G)** spores treated with 10.0mg/L NT; **(D,H)** spores treated with 4.0g/L SBC+2.5mg/L NT; **(I,M)** mycelia in control; **(J,N)** mycelia treated with 6.0g/L SBC; **(K,O)** mycelia treated with 10.0mg/L NT; **(L,P)** mycelia treated with 4.0g/L SBC+2.5mg/L NT mycelia. Images were obtained by microscopy at 1,000× magnification, bar=25μm.

and the rot lesion diameters increased in all treatments. Moreover, the difference in the rot lesion diameters between the control and treatments SBC, NT, and SBC + NT was more marked. For instance, the rot lesion diameter was only 9.17% of the control in the fruit treated with $(SBC + NT)_4$. Meanwhile, after inoculation with *A. niger* spores, the decay rate of the fruit treated with NT_5 and SBC + NT was significantly reduced during storage compared with the control. The decay rate of the control group was 97.0%, while it was 2.66, 9.33, 3.67, 0.0, and 0.0% in the fruit treated with NT_5, $(SBC + NT)_1$, $(SBC + NT)_2$, $(SBC + NT)_3$, and $(SBC + NT)_4$, respectively, on the 6th day of storage (Figure 15E). The results indicated that SBC + NT was effective against *A. niger* in Shengzhou nane fruit.

4. Discussion

In this study, *A. niger* isolated from the naturally infected Shengzhou nane fruit was identified by morphological features, rDNA-ITS analysis, and EF-1 analysis. The biochemical tests indicated that the optimal incubation temperature for pathogen growth was 30°C, which was consistent with the temperature at the time of disease outbreak since the daily mean temperature was about 30°C in the Shenzhou nane mature period in the local orchard. However, temperatures below 15°C or above 40°C significantly inhibited mycelial growth. The lethal temperature showed complete inactivation of the spores at 75°C for 10 min, indicating that the spores have excellent resistance to heat stress. The optimal C sources for *A. niger* growth were sucrose and fructose, which corresponded to a marked increase in fructose and glucose content in fruit during maturity (Xu et al., 2021). Compared with a single organic or inorganic N source, peptone and beef paste were optimal N sources, indicating that the nutritious compound N source was more suitable for *A. niger* growth. Coincidentally, a large amount of protein accumulated in the fruit of Shengzhou nane during maturity (Mo et al., 2017), which could provide the best N source for pathogen growth. Moreover, the isolates infected several local fruits, indicating that they had a broad host range. Therefore, it was suggested

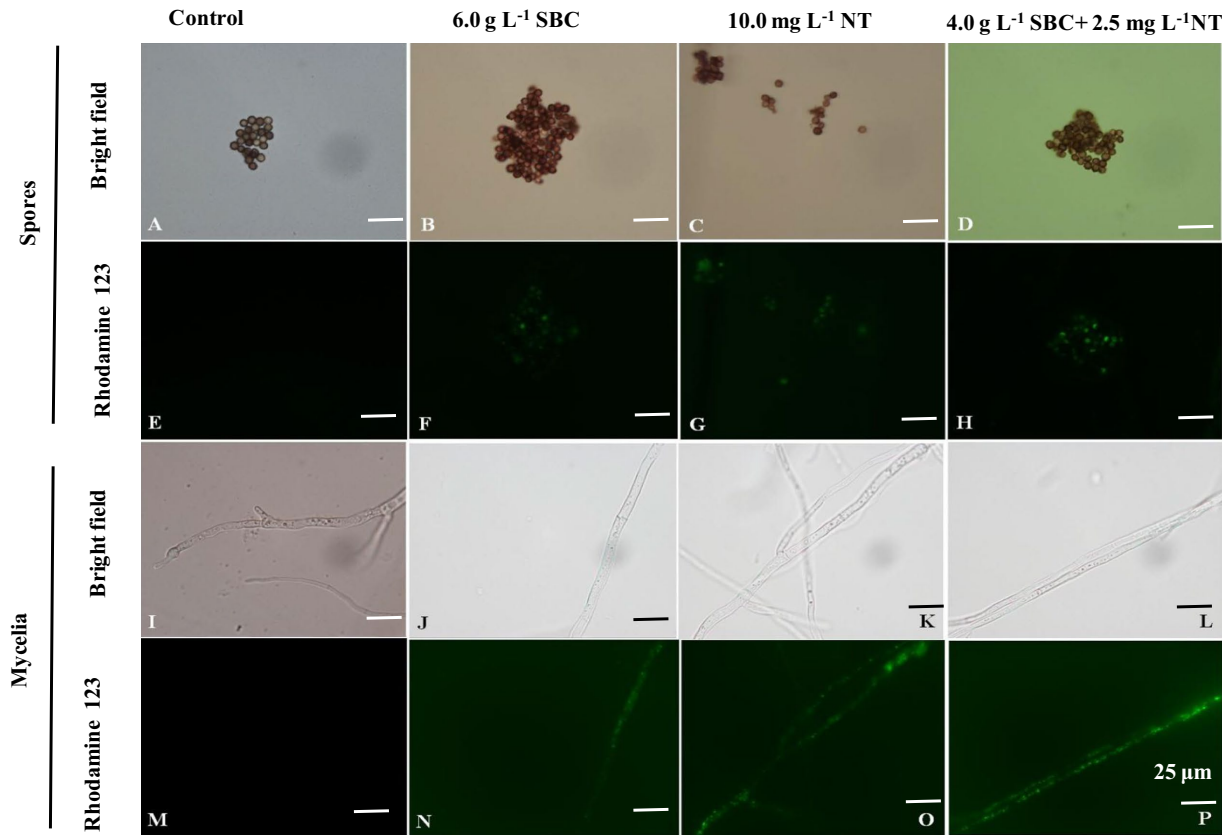

FIGURE 11
Aspergillus niger stained with Rhodamine 123 after treatment with SBC or NT. **(A,E)** Spores in the control; **(B,F)** spores treated with 6.0g/L SBC; **(C,G)** spores treated with 10.0mg/L NT; **(D,H)** spores treated with 4.0g/L SBC+2.5mg/L NT; **(I,M)** mycelia in control; **(J,N)** mycelia treated with 6.0g/L SBC; **(K,O)** mycelia treated with 10.0mg/L NT; **(L,P)** mycelia treated with 4.0g/L SBC+2.5mg/L NT mycelia. Images were obtained by microscopy at 1,000× magnification, bar=25μm.

that Shengzhou nane fruit should be kept away from those fruits that are susceptible to *A. niger* during the storage and marketing process.

In Shenzhou nane production, there is an urgent need for new residue-free and safer strategies to replace conventional fungicides for the control of postharvest pathogens. This study focused on evaluating new alternatives (SBC and NT) for *A. niger* rot control in Shenzhou nane fruit, addressing both laboratory and commercial conditions. The present results indicated that 6.0 g/L or higher SBC distinctly inhibited spore germination and the colonial expansion of *A. niger*. Similarly, SBC also showed a good ability to inhibit germ tube elongation, mycelial expansion, and hypha production of *Penicillium expansum,* thus affecting the survival of microbial cells (Lai et al., 2015). Castro-Ríos et al. (2021) reported that 3.0 g/L SBC presented a significant reduction in *A. niger* growth 72 h after inoculation. Some researchers speculated that pH may be involved in the inhibitory activity of SBC since SBC could change the pH of the growth environment of microbes (Lyousfi et al., 2022). Lai et al. (2015) found that pH could induce different expressions of some genes, resulting in the inhibition of the growth of *P. expansum*. Moreover, previous studies showed that bicarbonate (HCO_3^-) also could dissipate the transmembrane pH gradient and dissipate $\Delta\psi m$ and ΔpH, indicating that it was a selective dissipater of the pH gradient of the proton motive force across the cytoplasmic membrane of bacteria (Farha et al., 2017). Additionally, SBC can inactivate fungal extracellular enzymes since they can act directly on cell membranes and lead to an alteration of cellular physiology Castro-Ríos et al., 2021. In addition, bicarbonate salts could reduce the intense pressure of fungal cells by increasing osmotic stress and causing the collapse and contraction of hyphae and spores (Alvindia, 2013).

Moreover, NT, a biofungicide, has been demonstrated to be effective against fungal pathogens regardless of their fungicide resistance phenotypes (Haack et al., 2018; Saito et al., 2020). It has been widely accepted that NT mainly inhibits fungal growth *via* specific binding to ergosterol, which is a necessary component of fungal membranes (Aparicio et al., 2016). In this study, 5.0 mg/L or higher NT distinctly inhibited the colonial expansion of *A. niger*, and complete inhibition of colony growth occurred at 25.0 mg/L. Moreover, 2.5 mg/L NT inhibited spore germination, indicating that spore germination was more sensitive to NT. This finding coincides with the results that a lower concentration of NT decreased the spore germination of *Alternaria* spp. and *B. cinerea*

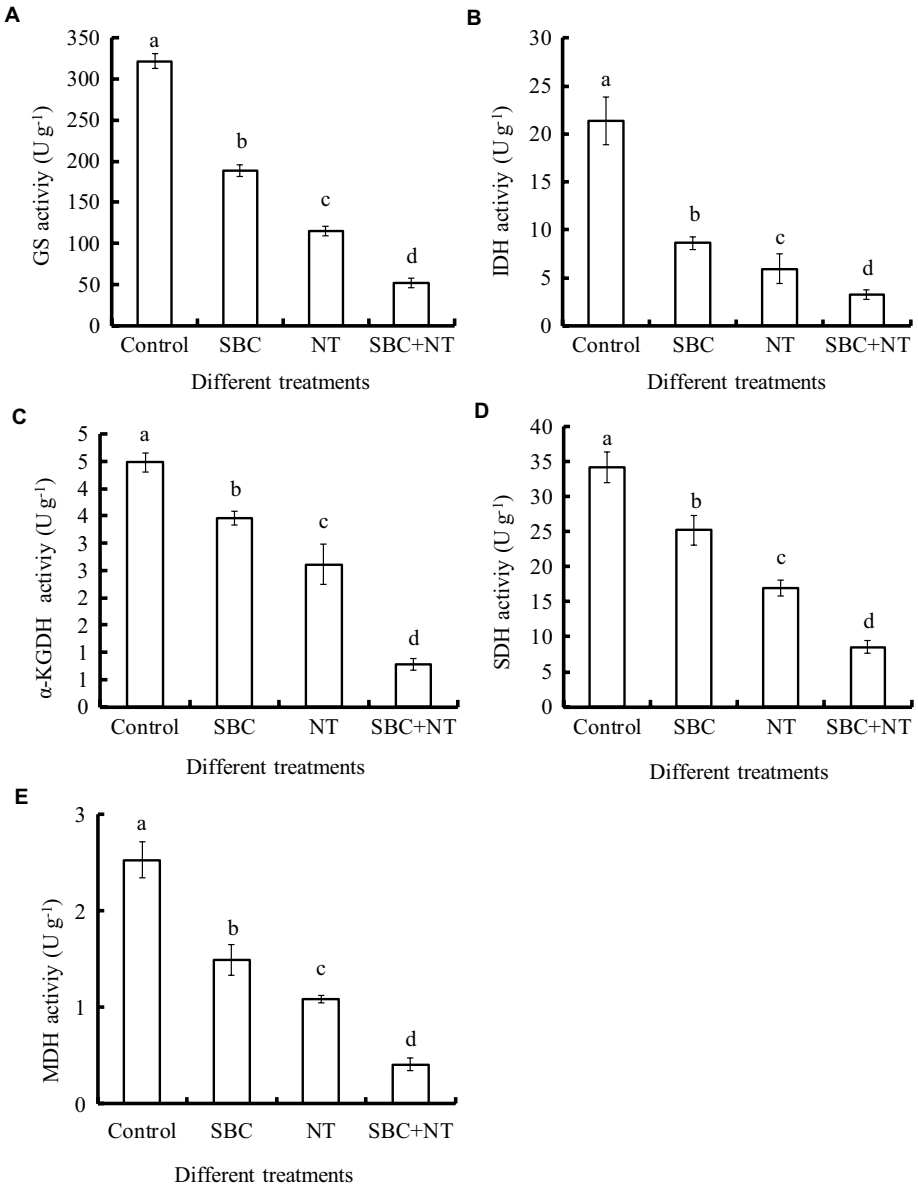

FIGURE 12
Effect of SBC, NT, and combined SBC and NT on enzyme activities involved in the TCA cycle. **(A)** GS activity; **(B)** IDH activity; **(C)** a-KGDH activity; **(D)** SDH activity; **(E)** MDH activity. ANOVA was employed to compare the mean values of analysis parameters ($p<0.05$). The results are shown as the mean±standard deviation ($n=3$). Different superscript letters in the same column indicate significant differences ($p<0.05$).

(Saito et al., 2020; Wang et al., 2021). Similarly, NT application has been reported to protect grapes from fungal rot during storage (Chang et al., 2021) and showed high antifungal efficacy on *P. expansum*, *Sclerotinia sclerotiorum,* and *Geotrichum citri-aurantii* (He et al., 2019; Seyedmohammadreza et al., 2020; Fernández et al., 2022). The elucidated mechanism of action of NT involves damage to the plasma membrane (Te Welscher et al., 2008; He et al., 2019), disturbance of nutrient transportation (Te Welscher et al., 2012), and mitochondrial dysfunction (Awasthi and Mitra, 2018). Since NT has a different mode of action from other chemical fungicides, it can be an alternative tool for controlling fungal rot in packing houses, particularly those caused by fungicide-resistant strains.

Furthermore, antimicrobial agents with synergistic effects showed more antimicrobial activities in a lower concentration than a single compound, which reduced its application cost and was more resource friendly (Kong et al., 2019). In this study, complete inhibition of colony growth occurred at 12.0 g/L SBC or 25 mg/L NT. D'Aquino et al. (2022) suggested that rinsing in a higher concentration of SBC solution could be phytotoxic to peel tissues. Therefore, the SBC concentration needs to decrease to a level that may be harmless to fruit tissues while retaining

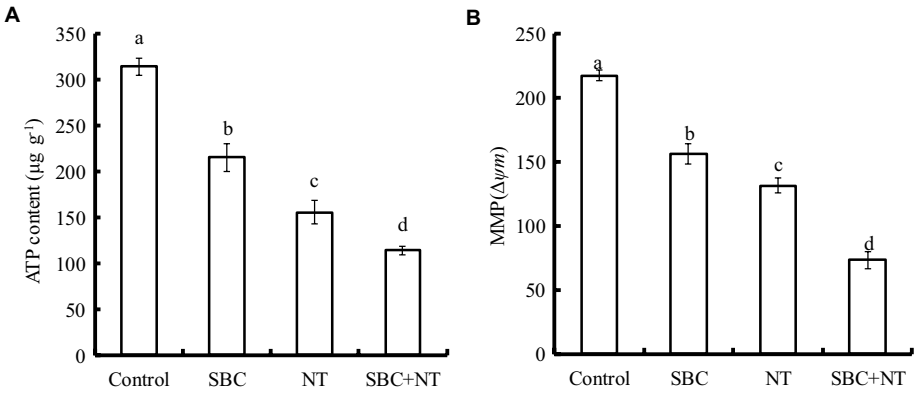

FIGURE 13
Effect of SBC or NT on ATP content **(A)** and MMP **(B)**. ANOVA was employed to compare the mean values of the analysis parameters (p<0.05). The results are shown as the mean±standard deviation (n=3). Different superscript letters in the same column indicate significant differences (p<0.05).

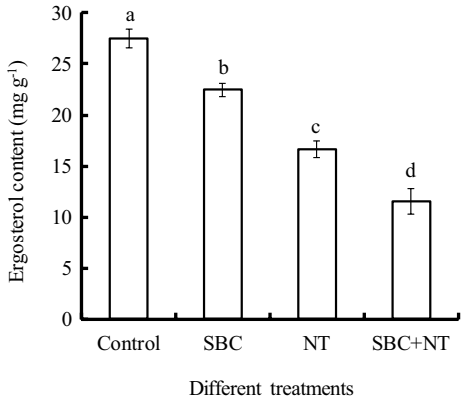

FIGURE 14
Effect of SBC or NT on ergosterol content in mycelia. ANOVA was used to compare the mean values of analysis parameters (p<0.05). The results are shown as the mean±standard deviation (n=3). Different superscript letters in the same column indicate significant differences (p<0.05).

antibacterial activity by combined application. Therefore, a combination of 4.0 g/L SBC + 5.0 mg/L NT was assayed, and the results showed that SBC + NT had excellent efficacy in inhibiting spore germination and colony expansion of *A. niger* in the PDA medium. Rather than acting independently of SBC or NT, it is more likely that the different eco-friendly methods worked together synergistically.

The cell membrane plays an important role in maintaining a homeostatic environment, exchanging materials, and transferring energy and information in the cell to keep the cell healthy. The destroyed cell membrane may lead to the efflux of cellular contents, affect the membrane structure, and result in mycelial growth, eventually leading to cell death. In this study, the results of PI staining confirmed that SBC and NT could change the membrane integrity of *A. niger*. Moreover, ergosterol is an essential component of the fungal cell membrane in fungi. Ergosterol content can affect the permeability and fluidity of the membrane, which is of considerable significance for cell survival. The PI staining results, coupled with the reduction in ergosterol content in this study, indicated that the cell membrane was an important target of SBC and NT. A similar result was found by He et al. (2019), who pointed out that NT may affect membrane function by reducing ergosterol synthesis because ergosterols are important in maintaining cell function in the transport of cellular material and physiology. Reductions in total lipid and ergosterol levels usually reflect irreversible damage to cell membranes (Niu et al., 2022). However, Te Welscher et al. (2010) suggested that the antifungal mechanism of NT was that it could combine with ergosterol on the cell membrane of fungi to change the permeability of the cell membrane. Kong et al. (2021) demonstrated that SBC can directly influence the membranes of fungi by affecting the proteins that make up about 70% of most cell membranes.

In addition to acting on the cell membrane, in this study, SBC and NT treatments damaged the mitochondrial membrane integrity of *A. niger*, as shown by the results of mitochondrial red fluorescence probe staining and the fluorescence intensity of Rh-123. Mitochondria are very important organelles in eukaryotic cells and are the center of metabolism and energy conversion. Maintaining the structural integrity of mitochondria is key to maintaining cellular energy status, as well as membrane-coupled and energy-dependent processes. Therefore, in this study, coupled with the structural damage of the mitochondrial membrane, SBC and NT also caused the reduction of MMP; decreased the key enzyme activities of CS, IDH, α-KGDH, SDH, and MDH involved in the TCA cycle; and reduced the intracellular ATP content. Meanwhile, the TCA cycle is the primary metabolic and transformed pathway for generating ATP from three major nutrients: carbohydrates, lipids, and amino acids (Fernie et al., 2004). ATP content is related to the energy metabolism,

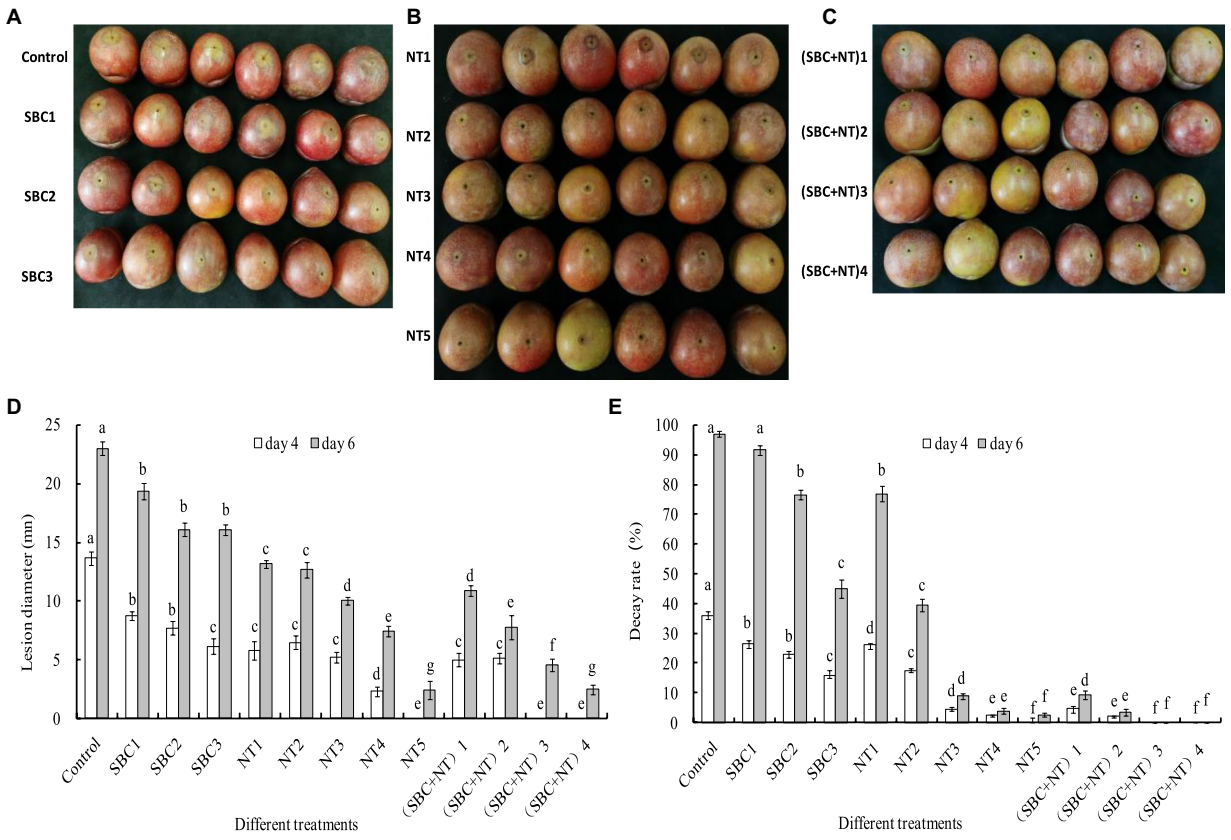

FIGURE 15
SBC or NT inhibits *Aspergillus niger* virulence on harvested Shengzhou nane fruit. **(A)** Control and SBC treatments; **(B)** NT treatments; **(C)** SBC and NT combined treatments; **(D)** corresponding histograms for statistical data on lesions on harvested fruit; **(E)** fruit decay rate. SBC_1: 2.0g/L, SBC_2: 4.0g/L, SBC_3: 6.0g/L, NT_1: 25.0mg/L, NT_2: 50.0mg/L, NT_3: 100.0mg/L, NT_4: 200.0mg/L, NT_5: 400.0mg/L, $(SBC+NT)_1$: 4.0g/L SBC+25.0mg/L NT, $(SBC+NT)_2$: 4.0g/L SBC+50.0mg/L NT, $(SBC+NT)_3$: 4.0g/L SBC+100.0mg/L NT, $(SBC+NT)_4$: (4.0g/L SBC+150.0mg/L NT). ANOVA was employed to compare the mean values of the analysis parameters (p<0.05). The results are shown as the mean±standard deviation (n=3). Different superscript letters in the same column indicate significant differences (p<0.05).

release, storage, and utilization of microorganisms. The rapid reduction of key enzyme activities involved in the TCA cycle or the loss of ATP content in microorganisms leads to a lack of energy for cells for transcription and translation, cell membrane component synthesis, and so on, and eventually results in growth inhibition and cell death. The decreased MMP further proved that mitochondria were a physiological target for SBC and NT to inhibit fungal growth. The results of this study were similar to the findings in *Fusarium solani* cells with synergistic treatment by thymol and salicylic acid (Kong et al., 2021) and in *A. niger* after treatment with cinnamaldehyde in the vapor phase (Niu et al., 2022). Similarly, Tan et al. (2022) found sodium dehydroacetate interference with cell membrane metabolism and energy metabolism in the antifungal mechanism against *P. digitatum*. Cinnamon essential oil resulted in a significant decrease ($p < 0.05$) in the ATP content of *P. expansum*, suggesting that the antifungal mechanism of cinnamon essential oil against *P. expansum* might be related to the carbohydrate metabolism of fungi (Lai et al., 2021). Taken together, these findings elucidate that the damage to cell and mitochondria membrane integrity and the disruption of energy metabolism might be closely involved in the antifungal mechanism of SBC and NT against *A. niger*. However, microbial energy metabolism is a very complicated process. Further studies are necessary to investigate the TCA pathways, including the levels of TCA cycle intermediates, such as pyruvic acid, acetyl-CoA, succinate, malate, and α-ketoglutarate, and the key action sites of SBC and NT in microbial energy metabolism.

Finally, the results of this study showed the effect of SBC, NT, and their combination on postharvest disease in Shengzhou nane fruit, which was consistent with the *in vitro* test on PDA plates. In general, the combination of SBC and NT was more effective in controlling rot than individual treatments. However, it showed that the effective concentrations in the *in vivo* assay were much higher than those the *in vitro* assay. For example, 4.0 g/L SBC + 150 mg/L NT was required to control the disease caused by *A. niger* in Shengzhou nane fruit, while 4.0 g/L

SBC + 2.5 mg/L NT inhibited mycelial growth completely. The effective dose of SBC and NT for the control of *A. niger* rot in inoculated fruit was higher than that derived from *in vitro* assays, possibly because the fruit provides a better environment for pathogen development and represents a hurdle for the product (He et al., 2019; Fernández et al., 2022). Our results were similar to those of Cui et al. (2021), who found that higher concentrations of magnolol were required to reduce virulence on harvested apple fruit and grapes than to suppress *in vitro B. cinerea* mycelial growth. Similarly, He et al. (2019) found that 80 mg/L NT inhibited the occurrence of gray mold disease in grapefruit, while 3.0 mg/L NT was enough to completely stunt colony growth in the PDA medium.

5. Conclusion

The pathogen causing fruit rot was isolated from symptomatic Shengzhou nane fruit and identified as *A. niger* by biological characteristics and molecular analysis. Optimal growth conditions for *A. niger* were 30°C, pH 5.0–6.0, and fructose and peptone as carbon and nitrogen sources. SBC, NT, and combined treatments against *A. niger* showed that the combined treatment of SBC and NT had a higher antifungal efficacy against *A. niger*. The damage to cell and mitochondrial membrane integrity and the disruption of energy metabolism might be closely involved in the antifungal mechanisms of SBC and NT. Moreover, the results of the *in vivo* experiment showed that SBC and NT reduced the rot lesion diameter and decay rate of Shengzhou nane fruit. In conclusion, the combination treatment of SBC and NT could be an alternative to synthetic fungicides for controlling postharvest Shengzhou nane decay caused by *A. niger*.

Data availability statement

The original contributions presented in this study are included in the article material; further inquiries can be directed to the corresponding authors.

Author contributions

T-RG performed the experiments and prepared the original draft. QZ and GY performed the experiments. S-SY and Z-YC contributed to the methodology. S-YX contributed to the resources. HW contributed to the review and editing. Y-WM contributed to the supervision, review, and editing. All authors contributed to the article and approved the submitted version.

Funding

This study was supported by the basic public welfare research projects of Zhejiang Province, China (Nos. LGN20C150004 and LGN22C150002).

Acknowledgments

We thank LetPub (www.letpub.com) for its linguistic assistance during the preparation of this manuscript.

Conflict of interest

The authors declare that the research was conducted in the absence of any commercial or financial relationships that could be construed as a potential conflict of interest.

Publisher's note

References

Alvindia, D. G. (2013). An integrated approach with hot water treatment and salt in the control of crown rot disease and preservation of quality in banana. *Int. J. Pest Manage.* 59, 271–278. doi: 10.1080/09670874.2013.845927

Aparicio, J. F., Barreales, E. G., Payero, T. D., Vicente, C. M., de Pedro, A., and Santos Aberturas, J. (2016). Biotechnological production and application of the antibiotic pimaricin: biosynthesis and its regulation. *Appl. Microbiol. Biotechnol.* 100, 61–78. doi: 10.1007/s00253-015-7077-0

Awasthi, B. P., and Mitra, K. (2018). In vitro leishmanicidal effects of the antifungal drug natamycin are mediated through disruption of calcium homeostasis and mitochondrial dysfunction. *Apoptosis* 23, 420–435. doi: 10.1007/s10495-018-1468-5

Baggio, J., Gonçalves, F., Lourenço, S., Tanaka, F., Pascholati, S., and Amorim, L. (2016). Direct penetration of *f* into stone fruits causing rhizopus rot. *Plant Pathol.* 65, 633–642. doi: 10.1111/ppa.12434

Carbone, I., and Kohn, L. M. (1999). A method for designing primer sets for speciation studies in filamentous ascomycetes. *Mycologia* 91, 553–556. doi: 10.1080/00275514.1999.12061051

Casals, C., Teixido, N., Vinas, I., Silvera, E., Lamarca, N., and Usall, J. (2010). Combination of hot water, Bacillus subtilis CPA-8 and sodium bicarbonate treatments to control postharvest brown rot on peaches and nectarines. *Eur. J. Plant Pathol.* 128, 51–63. doi: 10.1007/s10658-010-9628-7

Castro-Ríos, K., Montoya-Estrada, C. N., Martínez-Miranda, M. M., Cortés, S. H., and Taborda-Ocampo, G. (2021). Physicochemical treatments for the reduction of aflatoxins and *Aspergillus niger* in corn grains (*Zea mays*). *J. Sci. Food Agric.* 101, 3707–3713. doi: 10.1002/jsfa.11001

Chang, P., Tai, B., Zheng, M., Yang, Q., and Xing, F. (2021). Inhibition of *Aspergillus flavus* growth and aflatoxin B1 production by natamycin. *World Mycotoxin J.* 15, 269–283. doi: 10.3920/WMJ2020.2620

Cui, X., Ma, D., Liu, X., Zhang, Z., Li, B., Xu, Y., et al. (2021). Magnolol inhibits gray mold on postharvest fruit by inducing autophagic activity of *Botrytis cinerea*. *Postharvest Biol. Technol.* 180:111596. doi: 10.1016/j.postharvbio.2021.111596

D'Aquino, S., Strano, M. C., Gentile, A., and Palma, A. (2022). Decay incidence and quality changes of film packaged 'Simeto' mandarins treated with sodium bicarbonate. *Horticulturae* 8:354. doi: 10.3390/horticulturae8050354

Dezman, D. J., Nagy, S., and Brown, G. E. (1986). Postharvest fungal decay control chemicals: treatments and residues in citrus fruits. *Residue Rev.* 159, 407–411. doi: 10.1007/s11046-004-8401-x

Fadda, A., Sarais, G., Lai, C., Sale, L., and Mulas, M. (2021). Control of postharvest diseases caused by *Penicillium spp*. with myrtle leaf phenolic extracts: in vitro and in vivo study on mandarin fruit during storage. *J. Sci. Food Agric.* 101, 4229–4240. doi: 10.1002/jsfa.11062

Farha, M. A., French, S., Stokes, J., and Brown, E. D. (2017). Bicarbonate alters bacterial susceptibility to antibiotics by targeting the proton motive force. *ACS Infect. Dis.* 4, 382–390. doi: 10.1021/acsinfecdis.7b00194

Fernández, G., Sbres, M., Lado, J., and Pérez-Faggiani, E. (2022). Postharvest sour rot control in lemon fruit by natamycin and an Allium extract. *Int. J. Food Microbiol.* 368:109605. doi: 10.1016/j.ijfoodmicro.2022.109605

Fernie, A. R., Carrari, F., and Sweetlove, L. J. (2004). Respiratory metabolism: glycolysis, the TCA cycle and mitochondrial electron transport. *Curr. Opin. Plant Biol.* 7, 254–261. doi: 10.1016/j.pbi.2004.03.007

Haack, S. E., Ivors, K. L., Holmes, G. J., Forster, H., and Adaskaveg, J. E. (2018). Natamycin, a new biofungicide for managing crown rot of strawberry caused by QoI-resistant *Colletotrichum acutatum*. *Plant Dis.* 102, 1687–1695. doi: 10.1094/PDIS-12-17-2033-RE

Hashem, M., Alamri, S. A. M., Alqahtani, M. S. A., and Alshehri, S. R. Z. (2019). A multiple volatile oil blend prolongs the shelf life of peach fruit and suppresses postharvest spoilage. *Sci. Hortic.* 251, 48–58. doi: 10.1016/j.scienta.2019.03.020

He, C., Zhang, Z., Li, B., Xu, Y., and Tian, S. (2019). Effect of natamycin on *Botrytis cinerea* and *Penicillium expansum*-postharvest pathogens of grape berries and jujube fruit. *Postharvest Biol. Technol.* 151, 134–141. doi: 10.1016/j.postharvbio.2019.02.009

Hong, P., Hao, W., Luo, J., Chen, S., Hu, M., and Zhong, G. (2014). Combination of hot water, Bacillus amyloliquefaciens HF-01 and sodium bicarbonate treatments to control postharvest decay of mandarin fruit. *Postharvest Biol. Technol.* 88, 96–102. doi: 10.1016/j.postharvbio.2013.10.004

Huang, Y., Fan, Z., Cai, Y., Jin, L., and Yu, T. (2021). The influence of N-acetyl glucosamine: inducing *Rhodosporidium paludigenum* to enhance the inhibition of *Penicillium expansum* on pears. *Postharvest Biol. Technol.* 176:111486. doi: 10.1016/j.postharvbio.2021.111486

Ippolito, A., Schena, L., Pentimone, I., and Nigro, F. (2005). Control of postharvest rots of sweet cherries by pre- and postharvest applications of *Aureobasidium pullulans* in combination with calcium chloride or sodium bicarbonate. *Postharvest Biol. Technol.* 36, 245–252. doi: 10.1016/j.postharvbio.2005.02.007

Jiao, W., Liu, X., Chen, Q., Du, Y., Li, Y., Yue, F., et al. (2020). Epsilon-poly-L-lysine (ε-PL) exhibits antifungal activity in vivo and in vitro against *Botrytis cinerea* and mechanism involved. *Postharvest Biol. Technol.* 168:111270. doi: 10.1016/j.postharvbio.2020.111270

Karabulut, O. A., Lurie, S., and Droby, S. (2001). Evaluation of the use of sodium bicarbonate, potassium sorbate and yeast antagonists for decreasing postharvest decay of sweet cherries. *Postharvest Biol. Technol.* 23, 233–236. doi: 10.1016/S0925-5214(01)00151-X

Knight, S. C., Anthony, V. M., Brady, A. M., Greenland, A. J., Heaney, S. P., Murray, D. C., et al. (1997). Rationale and perspectives in the development of fungicides. *Annu. Rev. Phytopathol.* 35, 349–372. doi: 10.1146/annurev.phyto.35.1.349

Kong, J., Xie, Y., Yu, H., Guo, Y., Cheng, Y., Qian, H., et al. (2021). Synergistic antifungal mechanism of thymol and salicylic acid on *Fusarium solani*. *LWT Food Sci. Technol.* 140:110787. doi: 10.1016/j.lwt.2020.110787

Kong, J., Zhang, Y., Ju, J., Xie, Y., Guo, Y., Cheng, Y., et al. (2019). Antifungal effects of thymol and salicylic acid on cell membrane and mitochondria of *Rhizopus stolonifer* and their application in postharvest preservation of tomatoes. *Food Chem.* 285, 380–388. doi: 10.1016/j.foodchem.2019.01.099

Lai, T., Bai, X., Wang, Y., Zhou, J., Shi, N., and Zhou, T. (2015). Inhibitory effect of exogenous sodium bicarbonate on development and pathogenicity of postharvest disease *Penicillium expansum*. *Sci. Hortic.* 187, 108–114. doi: 10.1016/j.scienta.2015.03.010

Lai, T., Sun, Y., Liu, Y., Li, R., Chen, Y., and Zhou, T. (2021). Cinnamon oil inhibits *Penicillium expansum* growth by disturbing the carbohydrate metabolic process. *J. Fungi* 7, 123–139. doi: 10.3390/jof7020123

Li, Y., Shao, X., Xu, J., Wei, Y., Xu, F., and Wang, H. (2017). Tea tree oil exhibits antifungal activity against *Botrytis cinerea* by affecting mitochondria. *Food Chem.* 234, 62–67. doi: 10.1016/j.foodchem.2017.04.172

Li, X., Zhao, Y., Yin, J., and Lin, W. (2020). Organic fluorescent probes for detecting mitochondrial membrane potential. *Coord. Chem. Rev.* 420:213419. doi: 10.1016/j.ccr.2020.213419

Liu, K., Zhou, X., and Fu, M. (2017). Inhibiting effects of epsilon-poly-lysine (ε-PL) on *Pencillium digitatum* and its involved mechanism. *Postharvest Biol. Technol.* 123, 94–101. doi: 10.1016/j.postharvbio.2016.08.015

Lyousfi, N., Letrib, C., Legrifi, I., Blenzar, A., Khetabi, A. E., Hamss, H. E., et al. (2022). Combination of sodium bicarbonate (SBC) with bacterial antagonists for the control of brown rot disease of fruit. *J. Fungi.* 8:636. doi: 10.3390/jof8060636

Mo, Y., Jin, W., and Liu, K. (2013). Determination of ATP, ADP, and AMP concentrations in several tropical fruits by high performance liquid chromatography. *J. Fruit Sci.* 30, 1077–1082. doi: 10.13925/j.cnki.gsxb.2013.06.028

Mo, Y., Zhang, F., Yang, G., Lv, Y., Wang, Q., Hu, H., et al. (2017). Effects of combined treatment of 1-MCP and chitosan coating on the storability of Shengzhou Nane (*Prunus salicina* var. taoxingli) fruit. *J. Fruit Sci.* 34, 75–83. doi: 10.13925/j.cnki.gsxb.20160198

Niu, A., Wu, H., Ma, F., Tan, S., Wang, G., and Qiu, W. (2022). The antifungal activity of cinnamaldehyde in vapor phase against *Aspergillus niger* isolated from spoiled paddy. *LWT Food Sci. Technol.* 159:113181. doi: 10.1016/j.lwt.2022.113181

Palou, L., Smilanick, J. L., Usall, J., and Viñas, I. (2001). Control of postharvest blue and green molds of oranges by hot water, sodium carbonate, and sodium bicarbonate. *Plant Dis.* 85, 371–376. doi: 10.1094/PDIS.2001.85.4.371

Saito, S., Wang, F., and Xiao, C. L. (2020). Efficacy of natamycin against gray mold of stored mandarin fruit caused by isolates of *Botrytis cinerea* with multiple fungicide resistance. *Plant Dis.* 104, 787–792. doi: 10.1094/pdis-04-19-0844-re

Seyedmohammadreza, O., Zhang, L., and Wang, L. (2020). Inhibitory effect of natamycin against carrot white mold caused by *Sclerotinia sclerotiorum*. *Trop. Plant Pathol.* 45, 425–433. doi: 10.1007/s40858-020-00369-2

Su, X. M., Chen, Y., Wang, X. B., Wang, Y., Wang, P., Li, L., et al. (2014). PpIX induces mitochondria-related apoptosis in murine leukemia L1210 cells. *Drug Chem. Toxicol.* 37, 348–356. doi: 10.3109/01480545.2013.866135

Tan, X., Long, C., Meng, K., Shen, X., Wang, Z., Li, L., et al. (2022). Transcriptome sequencing reveals an inhibitory mechanism of *Penicillium digitatum* by sodium dehydroacetate on citrus fruit. *Postharvest Biol. Technol.* 188:111898. doi: 10.1016/j.postharvbio.2022.111898

Te Welscher, Y. M., Jones, L., van Leeuwen, M. R., Dijksterhuis, J., de Kruijffff, B., Eitzen, G., et al. (2010). Natamycin inhibits vacuole fusion at the priming phase via a specific interaction with ergosterol. *Antimicrob. Agents Chem.* 54, 2618–2625. doi: 10.1128/AAC.01794-09

Te Welscher, Y. M., ten Napel, H. H., Balague, M. M., Souza, C. M., Riezman, H., de Kruijff, B., et al. (2008). Natamycin blocks fungal growth by binding specifically to ergosterol without permeabilizing the membrane. *J. Biol. Chem.* 283, 6393–6401. doi: 10.1074/jbc.M707821200

te Welscher, Y. M., van Leeuwen, M. R., de Kruijff, B., Dijksterhuis, J., and Breukink, E. (2012). Polyene antibiotic that inhibits membrane transport proteins. *Proc. Natl. Acad. Sci. U. S. A.* 109, 11156–11159. doi: 10.1073/pnas.1203375109

Usall, J., Smilanick, J., Palou, L., Denis-Arrue, N., Teixidó, N., Torres, R., et al. (2008). Preventive and curative activity of combined treatments of sodium carbonates and Pantoea agglomerans CPA-2 to control postharvest green mold of citrus fruit. *Postharvest Biol. Technol.* 50, 1–7. doi: 10.1016/j.postharvbio.2008.03.001

Wang, F., Saito, S., Michailides, T. J., and Xiao, C. L. (2021). Postharvest use of natamycin to control *Alternaria* rot on blueberry fruit caused by *Alternaria alternata* and *A. arborescens*. *Postharvest Biol. Technol.* 172:111383. doi: 10.1016/j.postharvbio.2020.111383

Wang, S. Q., Wang, T., Liu, J. F., Deng, L., and Wan, F. (2018). Overexpression of Ecm 22 improves ergosterol biosynthesis in *Saccharomyces cerevisiae*. *Lett. Appl. Microbiol.* 67, 484–490. doi: 10.1111/lam.1306

Wang, Y., Zhang, X., Zhou, J., Li, X., Min, J., Lai, T., et al. (2015). Inhibitory effects of five antifungal substances on development of postharvest pathogen *Rhizopus oryzae*. *J. Agric. Biotech.* 23, 107–117. doi: 10.3969/j.issn.1674-7968.2015.01.012

Xu, Y., Li, S., Huan, C., Jiang, T., Zheng, X., and Brecht, J. K. (2020). Effects of 1-methylcyclopropene treatment on quality and anthocyanin biosynthesis in plum (*Prunus salicina* cv. Taoxingli) fruit during storage at a non-chilling temperature. *Postharvest Biol. Technol.* 169:111291. doi: 10.1016/j.postharvbio.2020.111291

Xu, Y., Wei, J., Wei, Y., Han, P., Dai, K., Zou, X., et al. (2021). Tea tree oil controls brown rot in peaches by damaging the cell membrane of *Monilinia fructicola*. *Postharvest Biol. Technol.* 175:111474. doi: 10.1016/j.postharvbio.2021.111474

Yan, R., Xu, Q., Dong, J., Kebbeh, M., Shen, S., Huan, C., et al. (2021). Effects of exogenous melatonin on ripening and decay incidence in plums (*Prunus salicina L.* cv. Taoxingli) during storage at room temperature. *Sci. Hortic.* 292:110655. doi: 10.1016/j.scienta.2021.110655

Zhou, D., Wang, Z., Li, M., Xing, M., Xian, T., and Tu, K. (2018). Carvacrol and eugenol effectively inhibit *Rhizopus stolonifer* and control postharvest soft rot decay in peaches. *J. Appl. Microbiol.* 124, 166–178. doi: 10.1111/jam.13612

Zhu, R., Lu, L., Guo, J., Lu, H., Abudureheman, N., Yu, T., et al. (2012). Postharvest control of green mold decay of citrus fruit using combined treatment with sodium bicarbonate and rhodosporidium paludigenum. *Food Bioproc. Tech.* 6, 2925–2930. doi: 10.1007/s11947-012-0863-0

frontiers | Frontiers in Microbiology

TYPE Correction
PUBLISHED 28 March 2023
DOI 10.3389/fmicb.2023.1172964

OPEN ACCESS

APPROVED BY
Frontiers Editorial Office,
Frontiers Media SA, Switzerland

*CORRESPONDENCE
Yi-Wei Mo
ywmo@163.com

SPECIALTY SECTION
This article was submitted to Food Microbiology, a section of the journal Frontiers in Microbiology

RECEIVED 24 February 2023
ACCEPTED 06 March 2023
PUBLISHED 28 March 2023

CITATION
Guo T-R, Zeng Q, Yang G, Ye S-S, Chen Z-Y, Xie S-Y, Wang H and Mo Y-W (2023) Corrigendum: Isolation, identification, biological characteristics, and antifungal efficacy of sodium bicarbonate combined with natamycin on *Aspergillus niger* from Shengzhou nane (*Prunus salicina* var. taoxingli) fruit. *Front. Microbiol.* 14:1172964. doi: 10.3389/fmicb.2023.1172964

Corrigendum: Isolation, identification, biological characteristics, and antifungal efficacy of sodium bicarbonate combined with natamycin on *Aspergillus niger* from Shengzhou nane (*Prunus salicina* var. taoxingli) fruit

Tian-Rong Guo, Qing Zeng, Guo Yang, Si-Si Ye, Zi-Yi Chen, Shi-Ying Xie, Hai Wang and Yi-Wei Mo*

College of Life Science, Shaoxing University, Shaoxing, China

KEYWORDS

***Prunus salicina* var. taoxingli, *Aspergillus niger*, sodium bicarbonate, natamycin, antifungal mechanism**

A corrigendum on

Isolation, identification, biological characteristics, and antifungal efficacy of sodium bicarbonate combined with natamycin on *Aspergillus niger* from Shengzhou nane (*Prunus salicina* var. taoxingli) fruit

by Guo, T.-R., Zeng, Q., Yang, G., Ye, S.-S., Chen, Z.-Y., Xie, S.-Y., Wang, H., and Mo, Y.-W. (2023). *Front. Microbiol.* 13:1075033. doi: 10.3389/fmicb.2022.1075033

In the published article, there was an error in Equation 1. Instead of "$GI = 100 * (G \times g)/G$", it should be "$GI = 100 * (G - g)/G$".

The authors apologize for this error and state that this does not change the scientific conclusions of the article in any way. The original article has been updated.

Publisher's note

All claims expressed in this article are solely those of the authors and do not necessarily represent those of their affiliated organizations, or those of the publisher, the editors and the reviewers. Any product that may be evaluated in this article, or claim that may be made by its manufacturer, is not guaranteed or endorsed by the publisher.

frontiers | Frontiers in Microbiology

TYPE Original Research
PUBLISHED 20 February 2023
DOI 10.3389/fmicb.2023.1139749

OPEN ACCESS

EDITED BY
Antonio Ippolito,
University of Bari Aldo Moro,
Italy

REVIEWED BY
Elsherbiny A. Elsherbiny,
Mansoura University,
Egypt
Ugo De Corato,
Energy and Sustainable Economic Development (ENEA), Italy

*CORRESPONDENCE
Junjie Wang
✉ smkxwjj@163.com
Huaiyu Zhang
✉ domybest-001@163.com

SPECIALTY SECTION
This article was submitted to Food Microbiology, a section of the journal Frontiers in Microbiology

RECEIVED 07 January 2023
ACCEPTED 01 February 2023
PUBLISHED 20 February 2023

CITATION
Zhao L, Wang J, Zhang H, Wang P, Wang C, Zhou Y, Li H, Yu S and Wu R (2023) Inhibitory effect of carvacrol against *Alternaria alternata* causing goji fruit rot by disrupting the integrity and composition of cell wall. *Front. Microbiol.* 14:1139749. doi: 10.3389/fmicb.2023.1139749

Inhibitory effect of carvacrol against *Alternaria alternata* causing goji fruit rot by disrupting the integrity and composition of cell wall

Lunaike Zhao, Junjie Wang*, Huaiyu Zhang*, Peng Wang, Cong Wang, Yueli Zhou, Huanhuan Li, Shukun Yu and Rina Wu

Key Laboratory of Storage and Processing of Plant Agro-Products, School of Biological Science and Engineering, North Minzu University, Yinchuan, China

Goji (*Lycium barbarum* L.) is a widely planted crop in China that is easily infected by the pathogenic fungus *Alternaria alternata*, which causes rot after harvest. Previous studies showed that carvacrol (CVR) significantly inhibited the mycelial growth of *A. alternata in vitro* and reduced Alternaria rot in goji fruits *in vivo*. The present study aimed to explore the antifungal mechanism of CVR against *A. alternata*. Optical microscopy and calcofluor white (CFW) fluorescence observations showed that CVR affected the cell wall of *A. alternata*. CVR treatment affected the integrity of the cell wall and the content of substances in the cell wall as measured by alkaline phosphatase (AKP) activity, Fourier transform-infrared spectroscopy (FT-IR), and X-ray photoelectron spectroscopy (XPS). Chitin and β-1,3-glucan contents in cells decreased after CVR treatment, and the activities of β-glucan synthase and chitin synthase decreased. Transcriptome analysis revealed that CVR treatment affected cell wall-related genes in *A. alternata*, thereby affecting cell wall growth. Cell wall resistance also decreased with CVR treatment. Collectively, these results suggest that CVR may exert antifungal activity by interfering with cell wall construction, leading to impairment of cell wall permeability and integrity.

KEYWORDS

carvacrol, *Alternaria alternata*, cell wall, antifungal mechanism, transcriptome

1. Introduction

Goji (*Lycium barbarum* L.) berry is one of the most widely cultivated and economically important fruit crops in northwest China (Wang et al., 2021). It is also a traditional Chinese herbal medicine, possessing vital biological activities such as anti-oxidation, anti-aging, and cancer prevention activities (Wang et al., 2010; Ma et al., 2022). However, goji berries are easily infected by *Alternaria alternata*, a pathogenic fungus that is responsible for black mold rot (Wang et al., 2018; Zhao et al., 2021; Supplementary Figure S1). The infected fruits not only cause important economic losses through postharvest decay, but also lead to health problems through contamination with various toxins produced by the pathogen (Wei et al., 2017; Xing et al., 2020). Fungicidal chemicals such as iprodione, tebuconazole, and mancozeb can effectively control postharvest rot caused by *A. alternata* (Yuan et al., 2019). However, the persistent application of synthetic fungicides has led to

the emergence of drug resistance, environmental contamination, and health hazards for consumers caused by chemical residues (Fu et al., 2017; Zhou et al., 2018). Therefore, it is necessary to explore new alternatives to reduce the use of these traditional synthetic fungicides.

In recent years, single or blended compounds from plant essential oils have been widely considered to be a promising alternative to chemical fungicides owing to their potential antimicrobial activities and natural and environmentally friendly properties. Carvacrol (2-methyl-5-(1-methylethyl)-phenol, CVR), a significant component of oregano essential oil (Suntres et al., 2015), has been approved as a Generally Recognized As Safe (GRAS) food additive by the Food and Drug Administration (FDA) and the European Commission, and can therefore be used in a variety of foods and beverages (Ultee et al., 1999; De Vincenzi et al., 2022). Many studies have shown that CVR exhibits significant antifungal effects against a range of postharvest decay pathogens, such as *Pilidiella granati* (Thomidis and Filotheou, 2016), *Botrytis cinerea* (Zhang et al., 2019), *Fusarium verticillioides,* and *Aspergillus westerdijkiae* (Schloesser and Prange, 2019), *Penicillium verrucosum* (Ochoa-Velasco et al., 2017), and *Geotrichum citri-aurantii* (Serna-Escolano et al., 2019). Our previous study suggested that CVR can effectively suppress black mold rot caused by *A. alternata* and maintain the postharvest quality of goji berries (Wang et al., 2019). Meanwhile, Abbaszadeh et al. (2014) demonstrated that CVR can inhibit the growth of *A. alternata in vitro*. However, the mechanisms of CVR against *A. alternata* have yet to be elucidated.

The antifungal mechanism of CVR has been extensively studied. CVR treatment can disrupt the cell morphology of *Botrytis cinerea* and alter the permeability of the cell membrane (De Souza et al., 2015). Kim et al. (2019) found that reactive oxygen species (ROS) generated by CVR damaged the cell membrane and even caused cell death of *Raffaelea quercus-mongolicae* and *Rhizoctonia solani*. Furthermore, Li J. et al. (2021) reported that CVR treatment could result in the death of *Botryosphaeria dothidea*-like cells by significantly inhibiting mitochondrial activity and respiration rates. However, to date, no studies have shown whether CVR affects the cell wall of *A. alternata*, and its mechanism of action against this pathogenic fungus has not been reported. Therefore, the impact of CVR on the cell wall of *A. alternata* requires further examination.

Accordingly, the objective of the present research was to investigate the effect of CVR treatment on the morphology and integrity of the cell wall of *A. alternata in vitro*. Meanwhile, the functional groups and surface chemical composition of the mycelia of the cell wall were measured by FT-IR and XPS, respectively. Furthermore, the major polysaccharide content of chitin and β-1,3-glucan and the enzyme's activity related to these polycarbohydrates metabolism were determined. Further study was conducted to evaluate the effect of the CVR treatment on transcriptome and gene expressions using RNA-seq and qRT-PCR techniques. In addition, the growth of *A. alternata* in different environments was studied to explore the stress resistance response. The study verified the inhibition mechanism of CVR on the cell wall of *A. alternata*, and laid the groundwork for the application of CVR to control other fruit fungal diseases.

2. Materials and methods

2.1. Fungal strain

According to the method of Jiang et al. (2019), a strain isolated from goji berries showing black mold rot symptoms was identified as *A. alternata* causing goji postharvest rot by analyzing morphological characteristics (Supplementary Figure S1) and nucleotide sequences containing the internal transcribed spacer rDNA region (*ITS*) (Supplementary Figure S2), β-tubulin (*tub2*) (Supplementary Figure S3), endopolygalacturonase (*endoPG*) (Supplementary Figure S4), and Alternaria major allergen (*Alta1*) (Supplementary Figure S5). The gene sequences of the isolated pathogen were submitted to GenBank (accession nos. MN653245.1, MN702782.1, MN698284.1, and MN702781.1 for *ITS*, *tub2*, *endoPG*, and *Alta1*, respectively). The strain of *A. alternata* was cultured on potato dextrose agar (PDA) for 8 days at 28 ± 1°C (Zhao et al., 2021).

2.2. Preparation of CVR treatments

Alternaria alternata was treated with CVR (purity ≥98.0%, Tokyo Kasei Kogyo Co., Ltd., Japan) by using the fumigation method (Cardiet et al., 2012). Briefly, 6-mm inoculum disks of *A. alternata* were cut from the leading edge of the fungal culture on PDA plates using a hole punch, placed in the center of new plates, and incubated at 28°C and 90% relative humidity (RH) for 2 days. Next, a 60-mm filter paper sheet was placed on the lid of each plate and 1 ml dissolved CVR (containing 5% Tween-80) was added to the filter paper so that the concentration of volatile CVR in the sealed plates was 0, 0.06, 0.12, and 0.24 μl/ml, respectively. The edge of each plate was sealed with parafilm and the plates were incubated upside down at 28°C and 90%RH for 3 days. The colony was divided into inside and outside parts, as shown in Supplementary Figure S6, simulating the effect of CVR on the formed mycelia (inside) and on the newly grown mycelia (outside), respectively. The outside and inside mycelia were scraped and weighed to 1 g portions, then wrapped in tin foil, rapidly frozen in liquid nitrogen, and stored at −80°C for later use.

2.3. Effect of CVR on cell wall integrity of *A. alternata*

2.3.1. Microscopy observations

Changes in mycelial morphology of *A. alternata* after CVR treatment were observed by optical microscopy. The effects of CVR on the integrity of the cell wall of *A. alternata* were analyzed by calcofluor white (CFW) staining coupled with fluorescence microscopy (Ouyang et al., 2019). The original mycelia and newly formed mycelia treated with different concentrations of CVR were picked and stained with 10 μl of 10% KOH and 10 μl CFW.

2.3.2. Extracellular alkaline phosphatase activity assay

The extracellular AKP activity of *A. alternata* mycelia treated with different concentrations of CVR was assayed using an AKP kit (Beijing Solarbio Science and Technology Co., Ltd., China) according to the

manufacturer's instructions. Enzyme activity was expressed as U/mg protein.

2.3.3. Fourier transform-infrared spectroscopy

The FT-IR of the *A. alternata* mycelia treated with different concentrations of CVR was determined according to the method of Li Q. et al. (2021). Briefly, the mycelia were lyophilized and ground to a powder. The samples and KBr were mixed at 1:100 (M:M) and placed in an agate mortar. After fine grinding and drying, the mixture was pressed into thin slices and the surface functional groups were determined by FT-IR spectrophotometer. The FT-IR wavelength range was 400–4,000 cm^{-1} and the background was determined using pure KBr.

2.3.4. X-ray photoelectron spectroscopy

The relative substance content of *A. alternata* mycelia treated with different concentrations of CVR was determined according to method of Dague et al. (2008). Samples were lyophilized and ground into a powder. The powder was pressed into thin slices and etched with argon gas for 30 s. The test parameters were set as follows: energy, 1486.8 eV; test spot area, 400 μm; tube voltage, 15 kV; tube current, 10 mA; and background vacuum, 2×10^{-9} mbar. The binding energy range for the collection measurement scan was 1,100 eV to 0. The analyzer pass energy was 50 eV with a step of 1.00 eV.

2.4. Effect of CVR on polysaccharides in the cell wall of *A. alternata*

2.4.1. Determination of β-1,3-glucan content

Referring to the method of Fortwendel et al. (2008), the content of β-1,3-glucan was determined by aniline blue fluorescence. A total of 50 mg of mycelia was harvested, washed with 0.1 mol/l NaOH, and lyophilized to powder. Next, 5 mg lyophilized mycelia powder was resuspended in 250 μl of 1 mol/l NaOH and reacted at 52°C for 30 min. Subsequently, 50 μl sample extract was transferred to a 96-well microtiter plate, and 210 μl aniline blue mixture was added to each well. After incubation at 52°C for 30 min, the plate was cooled at room temperature for 30 min to decolorize the unbound dye. The fluorescence of the bound dye complexes was detected with a microplate reader at an excitation wavelength of 450 nm and an emission wavelength of 460 nm. A β-1,3-glucan standard curve was created with a concentration range of 10 to 50 μg/ml and was used quantify the amount of β-1,3-glucan present in each sample.

2.4.2. Measurement of β-1,3-glucan synthase activity

β-1,3-glucan synthase activity was measured referring to the method of Belewa et al. (2017). Microsomal proteins were obtained by crushing mycelia and pulverizing by ultracentrifugation. The microsomal proteins were resuspended in 500 μl buffer (1 mmol/l EDTA; 1 mmol/l DTT; 33% (v/v) glycerol; 50 mmol/l Tris–HCl, pH 7.5) and stored at −80°C until use. A 50 μl reaction system was established consisting of 50 mmol/l Tris–HCl (pH 7.5), 20 μmol/l GTP, 4 mmol/l EDTA, 0.5% Brij-35, 6.6% glycerol, 2 mmol/l UDP-Glc, and 100 μg microsomal protein. After incubation at 25°C for 30 min, the reaction was stopped by adding 10 μl of 6 mol/l NaOH. The dextran produced by the previous process was dissolved at 80°C for 30 min. The glucan content was measured by the aniline blue method. One unit of enzymatic activity (U/mg protein) is defined as 1 mg protein catalyzed to produce 1 μg of glucan.

2.4.3. Determination of chitin content

Chitin content was determined by the method of Belewa et al. (2017). A total of 5 mg lyophilized mycelia was mixed with 3 ml of 1 mol/l KOH and incubated at 130°C for 1 h. Then, 8 ml of 70% ethanol was added to the mixture and the mixture was washed with 13.3% (w/v) cellulose acetate, 10 ml of 40% ethanol, and distilled water. The mixture was centrifuged at 1500 *g* for 5 min at 2°C. The resulting precipitate was added into a buffer containing 0.5 ml sterile double-distilled water mixed with 0.5 ml of 5% (w/v) sodium nitrite and potassium bisulfate, and then, the reaction system was centrifuged at 1500 *g* for 2 min. The 3-methyl-2-benzothiazolinone hydrochloride (MBTH) method was used to determine the glucosamine in the supernatant. The concentration of chitin in mycelia was determined by measuring the concentration of glucosamine produced by decomposition. Standard curves were constructed using various concentrations (5–25 μg/ml) of glucosamine.

2.4.4. Measurement of chitin synthase

Chitin synthase activity was measured according to the method of Mellado et al. (2003). Microsomal proteins were obtained as described by the method in section 2.4.2. The microsomal proteins were resuspended in 400 μl Tris–HCl buffer (pH 7.5, 50 mmol/l, containing 30% (v/v) glycerol) and stored at −80°C until use. Subsequently, 100 μl of 2× buffer (32 mmol/l Tris–HCl, pH 7.5; 4.3 mmol/l magnesium acetate; 32 mmol/l GlcNAc; 1.1 mmol/l UDP-GlcNAc; and 4 μg trypsin) and 100 μg microsomal protein were added to a 96-well plate pretreated by 100 μl of a solution of 50 μg/ml WGA. The plates were incubated at 25°C for 90 min to synthesize chitin. Next, 20 μl of 50 mmol/l EDTA and 100 μl of 1 μg/ml WGA horseradish peroxidase conjugate were added to each well. The plate was shaken vigorously for 15 min, washed five times with double-distilled water, and then 100 μl TMB peroxidase reagent (1 ml 20% H_2O_2; 9 ml sterile distilled water; and 1 mg TMB dissolved in sterile water containing 20% H_2O_2) was added to the wells. The reaction was stopped by adding 100 μl of 1 mol/l sulfuric acid and the absorbance was measured at 450 nm. One unit of enzymatic activity (U/mg protein) is defined as 1 mg protein catalyzing the production of 1 μg chitin.

2.4.5. Assays for chitinase and β-1,3-glucanase

Chitinase and β-1,3-glucanase activities of *A. alternata* mycelia were assayed according to the instructions of the chitinase kit and the β-1,3-glucanase kit (Suzhou Comin Biotechnology Co., Ltd., Jiangsu, China), respectively. Enzyme activity is expressed as U/mg protein.

2.5. Transcriptomic and quantitative real-time PCR analyses

Alternaria alternata were cultured on PDA for 3 days and then fumigated with or without 0.06 μl/ml CVR for 48 h. Referring to the method described in section 2.2, the external mycelia were rapidly frozen in liquid nitrogen and stored at −80°C for transcriptome analysis. The transcriptome information had been deposited at the

GenBank Sequence Read Archive (SRA) database, with accession numbers SRR23083390, SRR23083389, SRR23083388, SRR23083387, SRR23083386, and SRR23083385. Total RNA was extracted with a TRIzol kit (Invitrogen, Carlsbad, CA, United States). cDNA library construction and Illumina RNA sequencing were performed by Microeco Technology Co., Ltd., Shenzhen, China (Parkhomchuk et al., 2009). Differentially expressed genes (DEGs) were screened by fold change (FC) >2 and p-value <0.05. Gene Ontology (GO) classification was conducted using clusterProfiler. Kyoto Encyclopedia of Genes and Genomes (KEGG) pathway annotation was performed by KOBAS 2.1 (Xie et al., 2011).

For qRT-PCR, total RNA was extracted by a fungal RNA kit (Omega Bio-Tek, Inc.) and reverse transcribed using the ABScript III rt. master mix kit (ABclonal Technology Co., Ltd). qRT-PCR was performed using the Genious 2× SYBR Green rapid qPCR mix kit (ABclonal Technology Co., Ltd). The β-tubulin gene was used as an internal control and relative gene expression was calculated using the $2^{-\Delta\Delta CT}$ method. Primer sequences are listed in Supplementary Table S1.

2.6. Analysis of the effects of CVR on stress resistance in *A. alternata*

For stress resistance assays, the inner and outer mycelia of *A. alternata* treated with CVR (0, 0.06, 0.12, and 0.24 μl/ml) were made into 6-mm inoculum disks, respectively, and applied to plates of PDA without or with each stress substance (Zhang et al., 2020): (i) 0.2 mg/ml Congo red or 0.005% SDS for cell wall-perturbing stress, (ii) 0.5 mol/l NaCl for osmotic stress, (iii) 0.01 mol/l H_2O_2 for oxidative stress, and (iv) 32°C for high-temperature stress. Plates were incubated at 28°C for 5 days, except for high-temperature stress plates, which were incubated at 32°C for 5 days. The colony diameter was measured vertically and inhibition rates were calculated; samples without treatment were used as controls.

2.7. Statistical analysis

All data were expressed as the mean ± standard deviation of three independent replicates. SPSS software version 16.0 was used for one-way analysis of variance (ANOVA) and a p-value <0.05 was deemed significant.

3. Results

3.1. Effect of CVR on cell wall integrity of *A. alternata*

Microscopy observations showed that CVR treatment affected the morphology of internal and external mycelia of *A. alternata* (Supplementary Figure S7). The inner and outer mycelia without treatment were straight and thick. However, the mycelia treated with CVR gradually became thinner, the cell contents gradually clouded, the mycelia broke, and the cell wall collapsed (Supplementary Figures S7H,P). The integrity of the cell wall was detected by CFW staining using a fluorescence microscope. As shown in Figure 1A, the surface of *A. alternata* mycelia in the control sample had uniform fluorescence with bright cell spacing. In contrast, the fluorescence distribution on the surface of the mycelia treated with CVR was not uniform, and the brightness of the treated mycelia interval was decreased. With increasing concentrations of CVR, the degree of uneven fluorescence on the mycelia surface deepened. Furthermore, deformities occurred in the mycelia treated with 0.24 μl/ml CVR. These results indicated that CVR may cause damage and alterations to the integrity of the mycelial cell wall of *A. alternata*.

Determination of AKP activity in *A. alternata* treated with CVR can reflect the damage to the cell wall. The AKP activity of the treatment group was always higher than that of the control group (Figure 1B). After treatment with 0.06, 0.12, and 0.24 μl/ml CVR, the AKP activity of the inside mycelia increased by 3.69, 16.23, and 67.45%, respectively (Figure 1B1), while that of the outside part increased by 4.23, 30.21, and 90.26%, respectively (Figure 1B2).

3.2. FT-IR analysis of CVR-treated mycelia

To determine the structural differences in the mycelial cell wall between the control and CVR-treated groups, FT-IR was used to analyze the functional groups of these samples. Each site in the figure represented different hanging energy groups; 3396.5 cm^{-1} was O-H, 2924.5 cm^{-1} was C-H, 1653.6 cm^{-1} was amide I, 1552.9 cm^{-1} was amide II, and 1078.5 cm^{-1} was the C-C bond in glucose (Figure 1C). The bonds of amide I and amide II are characteristic protein bonds. After CVR treatment, external peak deflections were observed at sites a, c, and d in both inside and outside parts of the mycelia of *A. alternata*. This indicated that CVR caused changes in the OH functional group and proteins in the mycelia of *A. alternata*.

3.3. CVR treatment decreased the polysaccharide content of the cell wall surface

C, N, and O are the three main elements in the cell wall. XPS analyses were performed to determine the changes in these elements following CVR treatment. Typical XPS spectra between treated and control groups are presented in Supplementary Figure S8. The C_{1s} peak on the surface of *A. alternata* can be decomposed into C-(C,H) at 284.4 eV, C-(O,N) at 286.3 eV, and C=O bond at 288.0 eV. The O_{1s} peak had two components—one belonged to the O-C bond at 532.7 eV and the other belonged to the O=C bond at 531.4 eV. The N_{1s} peak was composed of two components: one component at 399.9 eV was attributed to amine or amide function, and the other component at 401.4 eV was attributed to protonated nitrogen. According to the formula, $[N/C]_{obs} = 0.279(C_{Pr}/C)$; $[N/C]_{obs} = 0.279(C_{Pr}/C)$; $[C/C]_{obs} = (C_{Pr}/C) + (C_{Ps}/C) + (C_{Lp}/C) = 1$, the values of C_{Pr}, C_{Lp}, and C_{Ps} can be calculated (Table 1). C_{Ps} is the relative content of polysaccharide substance. The content of C_{Ps} in *A. alternata* was decreased after CVR treatment, indicating that the content of polysaccharide substances in the *A. alternata* cell wall decreased after CVR treatment.

10.3389/fmicb.2023.1139749

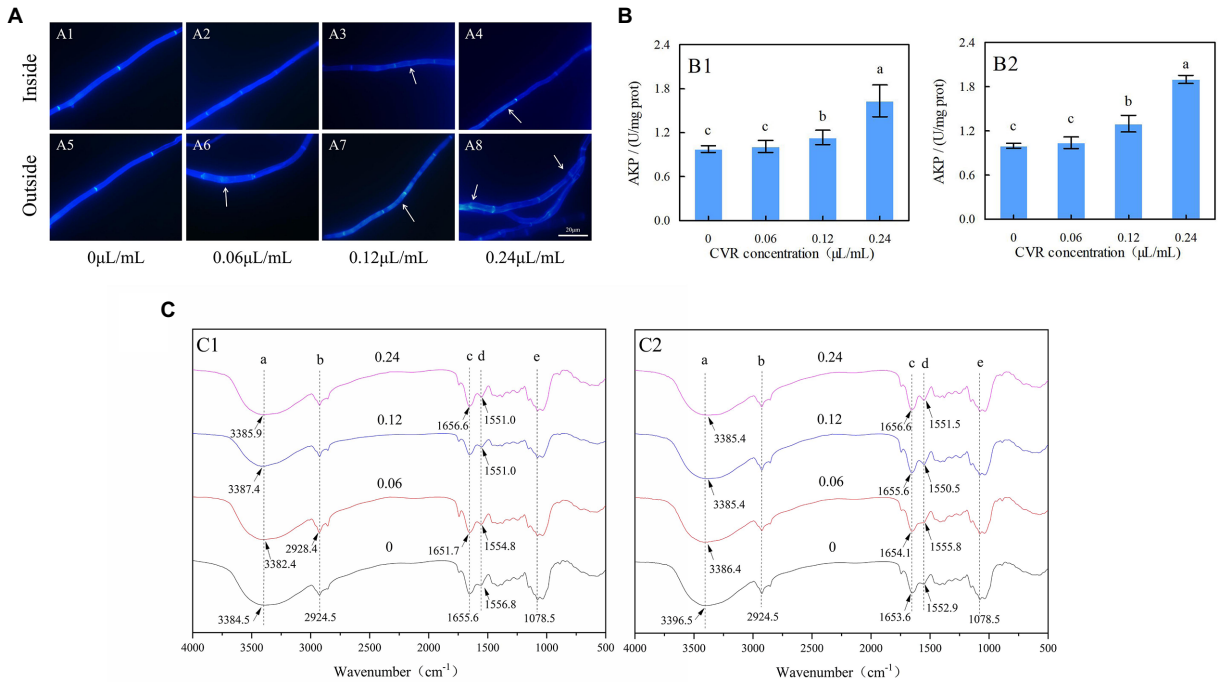

FIGURE 1
Alternaria alternata treated with CVR and observed under a fluorescence microscope after CWF staining (×100 magnification). **(A)** CK treatment of inside **(A1)** and outside **(A5)** parts of mycelia; 0.06μl/ml CVR treatment of inside **(A2)** and outside **(A6)** parts of mycelia; 0.12μl/ml CVR treatment of inside **(A3)** and outside **(A7)** parts of mycelia; 0.24μl/ml CVR treatment of inside **(A4)** and outside **(A8)** parts of mycelia, respectively, **(B)** The effect of AKP enzyme activity after CVR treatment of inside **(B1)** and outside **(B2)** parts of mycelia, and **(C)** Influence of CVR on cell walls of *A. alternata*. Different letters represent significant differences at the level of $p<0.05$. FT-IR spectra of mycelia treated with CVR at 0, 0.06, 0.12, and 0.24μl/ml of outside **(C1)** and inside **(C2)** parts of mycelia.

TABLE 1 Surface chemical composition of mycelia of *A. alternata* treated with CVR at 0, 0.06, 0.12, and 0.24μl/ml, measured by XPS.

Mycelia	CVR concentration (μg/mL)	%C	%N	%O	N/C	O/C	N/O	C_{Pr}	C_{Ps}	C_{Lp}
Inside	0	69.08	2.95	27.97	0.04	0.40	0.11	10.57	29.45	29.05
	0.06	69.19	3.24	27.57	0.05	0.40	0.12	11.61	28.57	29.01
	0.12	69.85	3.31	27.84	0.05	0.40	0.12	11.86	28.79	28.19
	0.24	70.34	3.19	26.46	0.05	0.38	0.12	11.43	27.30	31.60
Outside	0	70.76	2.50	26.74	0.04	0.38	0.09	8.96	28.60	33.19
	0.06	70.31	2.97	26.72	0.04	0.38	0.11	10.65	27.92	31.74
	0.12	70.65	3.78	25.57	0.05	0.36	0.15	13.55	25.41	31.69
	0.24	70.37	4.16	25.47	0.06	0.36	0.16	14.91	24.76	30.70

3.4. Effects of CVR on β-1,3-glucan and chitin contents

The contents of β-1,3-glucan and chitin in *A. alternata* were significantly reduced after CVR treatment (Figures 2A,B). After treatment with 0.06, 0.12, and 0.24 μl/ml CVR, the β-1,3-glucan content in the inner mycelia decreased by 54.01%, 53.03, and 71.43%, respectively, compared with the control, while that in the outer mycelia decreased by 65.43, 75.05, and 83.50%, respectively, compared with the control. The content of chitin in the inner mycelia decreased by 4.81, 53.66, and 60.49%, respectively, after treatment with 0.06, 0.12, and 0.24 μl/ml CVR, while chitin content in the outer mycelia decreased by 29.86, 54.05, and 61.08%, respectively. This indicated that CVR treatment can destroy the cell wall structure of *A. alternata* by reducing the contents of β-1,3-glucan and chitin.

3.5. Effects of CVR on β-glucan synthase and chitin synthase

The ability of *A. alternata* to synthesize β-1,3-glucan and chitin was reduced after CVR treatment (Figures 2C,D). After

10.3389/fmicb.2023.1139749

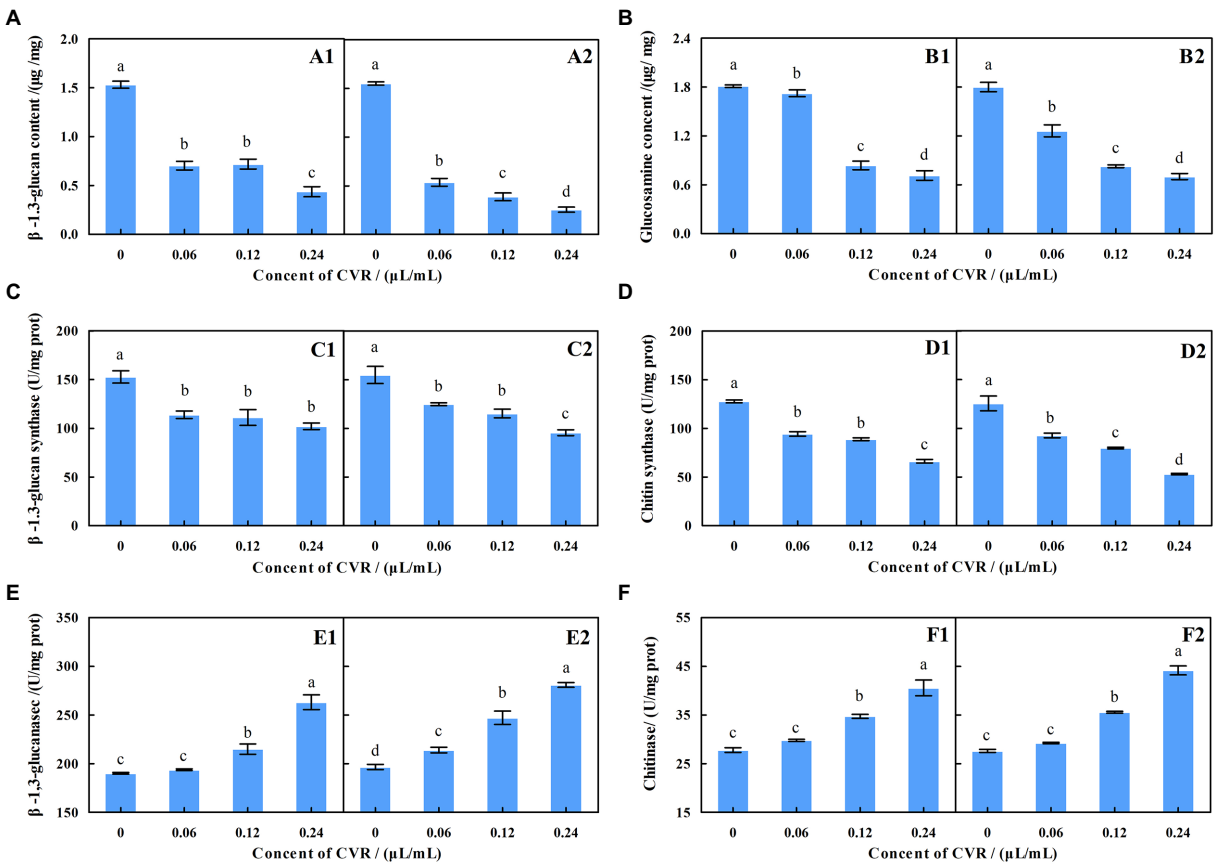

FIGURE 2
Effect of CVR on the content of β-1,3-glucan **(A)** in inside **(A1)** and outside **(A2)**, parts of mycelia, respectively; the content of chitin **(B)** in inside **(B1)** and outside **(B2)** parts of mycelia, respectively; the β-glucan synthase **(C)** activity in inside **(C1)** and outside **(C2)** parts of mycelia, respectively; the production of chitin synthase activity **(D)** in inside **(D1)** and outside **(D2)** parts of mycelia, respectively; the production of β-1,3-glucanase activity **(E)** in inside **(E1)** and outside **(E2)** parts of mycelia, respectively; and the production of chitinase activity **(F)** in inside **(F1)** and outside **(F2)** parts of mycelia, respectively. Different letters represent significant differences at the level of $p<0.05$.

treatment with 0.06, 0.12, and 0.24 μl/ml CVR, the amount of β-glucan produced by the internal mycelia was 74.61, 72.86, and 66.91% of the control group, respectively, while that of the external mycelia was 80.59, 74.42, and 61.67% of the control group, respectively. The content of glucan produced by the inner mycelia was 73.93, 69.65, and 51.88% of the control group, respectively, and that of the outer mycelia was 73.86, 63.59, and 42.36% of the control group, respectively. This demonstrated that CVR can reduce the content of β-1,3-glucan and chitin by reducing the activity of β-glucan synthase and chitin synthase in the mycelia of *A. alternata*.

3.6. Effects of CVR on β-1,3-glucanase and chitinase

Figures 2E,F show the effect of CVR treatment on β-1,3-glucanase and chitinase activities in the mycelia of *A. alternata*. The higher the concentration of CVR, the larger the increased effect on the activities of β-1,3-glucanase and chitinase. In general, CVR treatment accelerated the degradation of chitin and β-1,3-glucan in the cell wall of *A. alternata*.

3.7. Transcriptome sequencing and analysis of DEGs

Sequencing data statistics showed Q20 > 97.25% and Q30 > 92.58%, which indicated that the sequencing quality was good. After eliminating primer and adapter sequences and filtering out poor-quality reads, 23.79 and 22.30 million clean reads were obtained in the CVR-treated and control samples, respectively (Figure 3A). Based on the clean reads of CVR-treated samples, approximately 76.91% were mapped to the *A. alternata* unique genes, 0.12% were mapped to multiple genes, and 22.97% did not map to known genes (defined as unmapped), respectively. Similar results were obtained in the control group samples (Figure 3B). The transcriptomes of *A. alternata* with CVR treatment and the control treatment were analyzed and a total of 1,492 DEGs were found (FC ≥2, $p<0.05$), which included 504 upregulated DEGs and 988 downregulated DEGs (Figure 3C).

10.3389/fmicb.2023.1139749

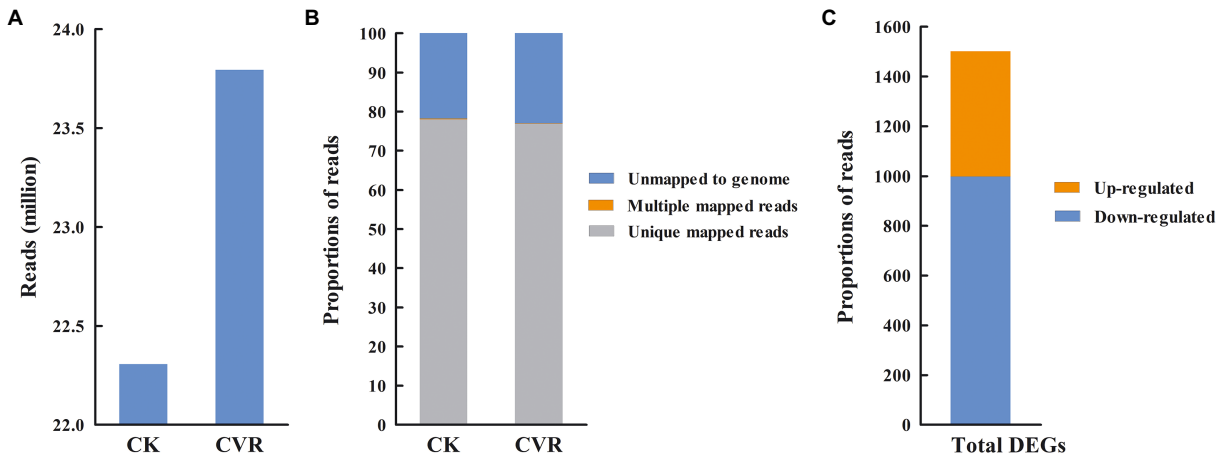

FIGURE 3
Summary information for transcriptome data. **(A)** High-quality clean reads, **(B)** The proportion of high-quality clean reads of mapped to unique genes, multiple genes, and unmapped genes, and **(C)** The number of differentially expressed genes (DEGs).

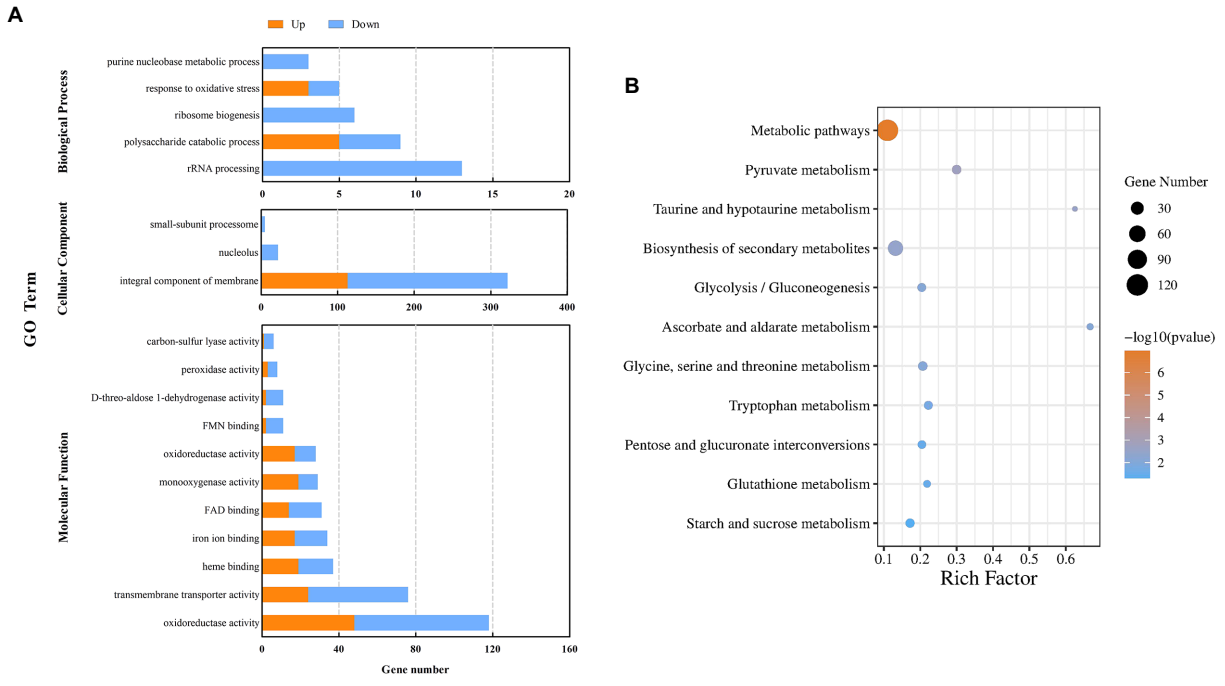

FIGURE 4
GO analysis of DEGs in the control sample and after treatment with CVR **(A)**. KEGG pathways and DEGs after treatment with CVR **(B)**.

3.8. Go term enrichment and KEGG pathway analysis of DEGs

GO enrichment analysis was performed on all DEGs ($p < 0.05$), and the DEGs were classified from three aspects: biological process, molecular function, and cellular component (Figure 4A). The DEGs in biological process were enriched in the terms of rRNA processing (13 DEGs), polysaccharide catabolic process (9), ribosome biogenesis (6), response to oxidative stress (5), and purine nucleobase metabolic process (3). The DEGs in molecular functions included oxidoreductase activity (118), transmembrane transporter activity (76), heme binding (37), iron ion binding (34), FAD binding (31), monooxygenase activity (29), oxidoreductase activity (28), FMN binding (11), D-threo-aldose 1-dehydrogenase activity (11), peroxidase activity (8), and carbon-sulfur lyase activity (6). It was also observed that DEGs classified in cellular component were enriched in the terms of integral component of membrane (322) and nucleolus (22).

The DEGs were further annotated against the KEGG database (Figure 4B) and were grouped into 84 KEGG pathways, including 5 in cell process, 2 in environmental information processing, 10 in genetic information processing, and 67 in metabolic pathways. Among them, 13 KEGG pathways were considered to be significantly enriched

($p < 0.05$). The significantly enriched KEGG pathways and the number of DEGs in each were metabolic pathways (120 DEGs), pyruvate metabolism (12), taurine and hypotaurine metabolism (5), biosynthesis of secondary metabolites (49), glycolysis/gluconeogenesis (10), ascorbate and aldarate metabolism (6), glycine, serine, and threonine metabolism (12), tryptophan metabolism (10), pentose and glucuronate interconversions (9), glutathione metabolism (7), and starch and sucrose metabolism (11). These results showed that CVR altered the overall metabolic process(es) of *A. alternata*.

3.9. Changes in gene expression of starch and sucrose metabolism signaling pathways

The starch and sucrose metabolism pathway is related to the changes of polysaccharides in the cell wall of *A. alternata* treated with CVR. There were 7 upregulated genes and 4 downregulated genes in the starch and sucrose metabolism pathway after CVR treatment (Figure 5A). Among these DEGs, the gene *CC77DRAFT_1029827* (hypothetical protein) regulating β-fructofuranosidase was markedly upregulated. Two downregulated genes—*CC77DRAFT_1067874* (family 17 glycoside hydrolase) and *CC77DRAFT_237249* (GPI-anchored cell wall beta-1,3-endoglucanase EglC)—and an upregulated gene, *CC77DRAFT_598231* (glucan 1,3-beta-glucoside-like protein), are involved in the regulation of glucan endo-1,3-β-D-glucosidase. Meanwhile, the upregulated gene *CC77DRAFT_933414* (Pectin lyase-like protein) and the downregulated gene *CC77DRAFT_983002* (glycoside hydrolase) jointly regulate glucan-1,3-β-glucosidase. The gene *CC77DRAFT_991870* (glycoside hydrolase) regulating cellulase was markedly downregulated and the gene *CC77DRAFT_1021571* (glycosyltransferase) regulating glycogen phosphorylase was clearly upregulated. All 10 genes except *CC77DRAFT_1021571* were related to the degradation of cell wall polysaccharides, which indicated that CVR treatment significantly affects the metabolism of polysaccharides in *A. alternata* (Figures 5A,B).

3.10. Changes in genes that may regulate the metabolism of cell wall growth and verification of the expression of candidate genes

Through the analysis of DEGs, 14 genes that may be related to cell wall integrity and substance content of *A. alternata* (Supplementary Table S1) were screened by qRT-PCR. The qRT-PCR data (Figure 5C) were consistent with the RNA-seq data, and the correlation coefficient $R^2 = 0.9998$ (Figure 5D) verified the expression of the 14 candidate genes. These results indicated that the transcriptome data were reliable.

3.11. Effects of CVR on stress resistance

The inside and outside parts of the mycelia of *A. alternata* after treatment with CVR were applied to culture media containing different stress substances. The antifungal effect was observed to determine the resistance of the *A. alternata* cell wall to external stimuli after CVR treatment (Figure 6A). The resistance of *A. alternata* mycelia to NaCl, CR, and SDS was weakened (Figure 6B). In response to H_2O_2, inhibition of the inside part of the mycelia was not significant but inhibition of the outside part of the mycelia was more significant after CVR treatment. This indicates that there were differences in the ability of the internal and external mycelia of *A. alternata* to respond to oxidative stress after CVR.

4. Discussion

Postharvest black mold rot infected by *A. alternata* is one of the most critical fungal decays encountered in goji berries during storage, resulting in tremendous economic losses (Wang et al., 2018, 2021). The defects of harmful to human health and environmental pollution in controlling Alternaria rot by using chemical fungicides promote the need to explore environmentally friendly acceptable sources of antifungal compounds. Essential oils are a promising alternative to synthetic fungicides for controlling postharvest fungal disease (Gonçalves et al., 2021). Previous studies have demonstrated that CVR can effectively inhibit the growth of *A. alternata in vitro* and control the black mold of goji berries after harvest (Abbaszadeh et al., 2014; Wang et al., 2019; Zhang et al., 2019). This study is to further explore the possible antifungal mechanism of CVR against the mycelial growth of *A. alternata*. Microscopy observations showed that CVR disrupted the cell wall of *A. alternata* by thinning, fracturing, and collapsing the mycelia (Supplementary Figure S7). This is consistent with the results of CVR treatment disrupting the cell wall of *Botryosphaeria dothidea* (Li J. et al., 2021; Li Q. et al., 2021). CWF can specifically bind chitin in the cell wall, which can be observed by fluorescence microscopy under blue fluorescence. After CVR treatment, the mycelial surface fluorescence was uneven, the mycelial interval was shortened, the mycelial septum was damaged, and the cell wall was obviously damaged. This showed that CVR can inhibit *A. alternata* by destroying the cell wall (Figure 1A). This phenomenon is consistent with the effect of cinnamaldehyde on *Geotrichum citri-aurantii* (a postharvest pathogen of citrus) reported by Ouyang et al. (2019). AKP is an enzyme that is produced in the cytoplasm and leaks into the periplasmic space. Generally, AKP releases from the fungal cells through the cell wall in which permeability is impaired (Yang et al., 2016). The cell wall permeability was significantly increased and the integrity of the cell wall of *A. alternata* was destroyed after CVR treatment (Figure 1B). CVR treatment of *A. alternata* resulted in the inability to maintain normal hypha morphology and affected normal growth of the hypha. FT-IR revealed that the -OH groups and protein-specific functional groups (amide I and amide II) in the mycelia of *A. alternata* were changed after CVR treatment (Figure 1C). Serrano et al. (2010) reported that the deflection of the -OH group was due to the substitution of some of the -H. In summary, the structural material on the surface of *A. alternata* was changed after CVR treatment, and this affected mycelial growth.

The fungal cell wall determines the complex shapes of fungi, and changes in cell shape underpin morphogenesis and cellular differentiation (Gow et al., 2017). Meanwhile, the cell wall is also the natural interface between the fungus and its environment, and plays a key role in the infection of hosts by fungi (Kou and Naqvi, 2016). Therefore, the integrity and construction of the cell wall are

10.3389/fmicb.2023.1139749

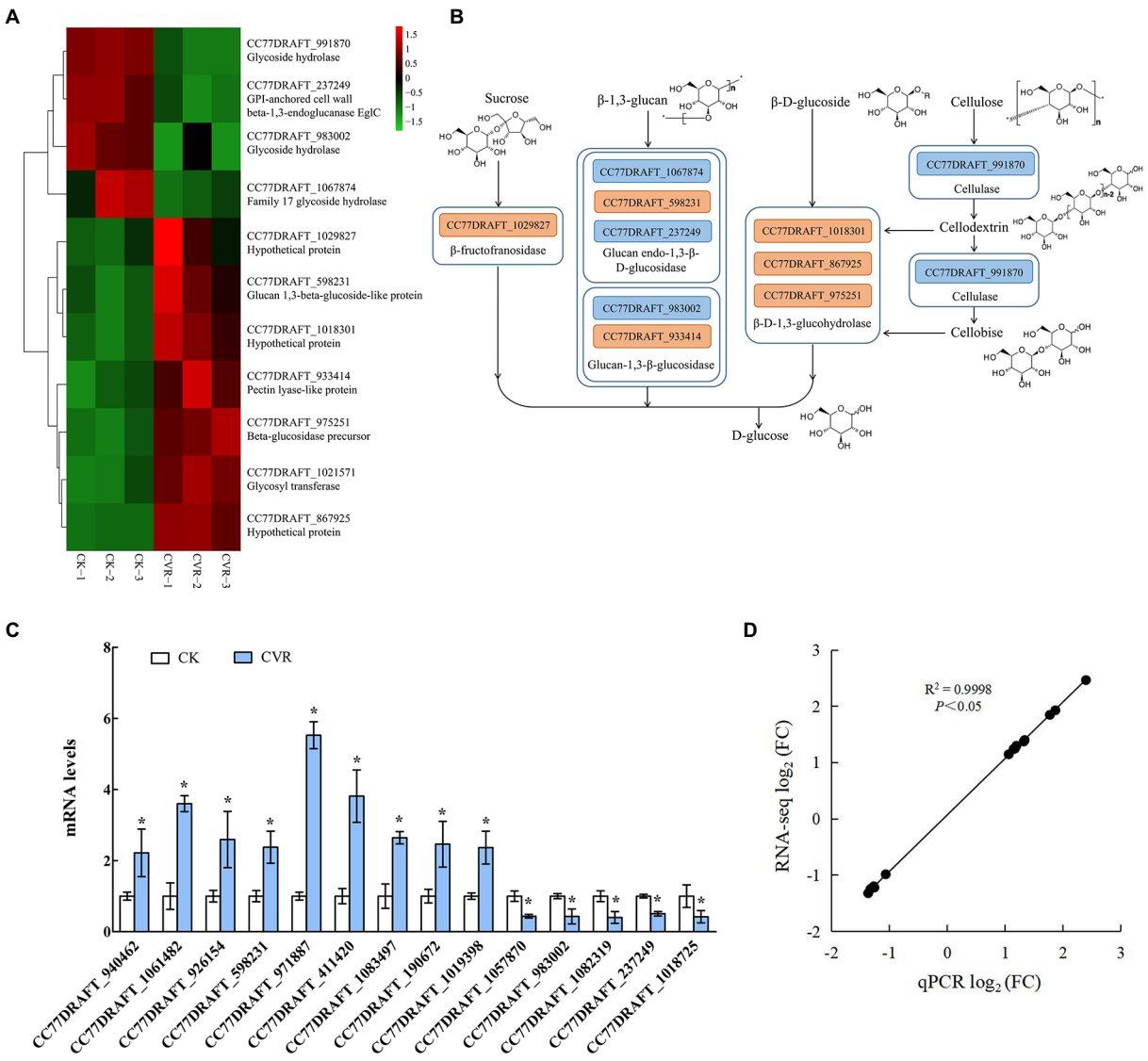

FIGURE 5
RNA-Seq influence of CVR treatment on metabolism of polysaccharide substances. **(A)** DEGs in sucrose metabolism signaling pathway, **(B)** Possible mechanism of CVR treatment regulating sucrose metabolism signaling pathway, **(C)** Relative expression levels of candidate genes by qRT-PCR. The data were analyzed by *t*-test; * represents significant difference ($p<0.05$), and **(D)** Correlation between results of qRT-PCR and results of RNA-seq.

instrumental in the success of fungi. The cell wall has been extensively studied and is an antifungal target. Polysaccharides, which are the main component of the fungal cell wall, maintain the structure of the cell wall. Structural characterization of the cell wall showed that it comprised an outer layer of mannose and proteins, and an inner layer of β-glucan and chitin, close to the cytoplasmic membrane (Rappleye et al., 2007). In fungal cell walls, β-1,3-glucan and chitin are both indispensable predominant components; the cross-linked product of the two can improve the stability of the cell wall and protect the fungus from being effect during the infection process. Simultaneously, β-1,3-glucan and chitin were also found to be the main substances supporting the cell wall structure (Gow et al., 2017). Relative changes of polysaccharides in mycelia can be calculated by XPS (Dague et al., 2008). In this study, XPS showed that the content of C_{Ps} in the hyphal cell wall of *A. alternata* was significantly decreased after CVR treatment (Table 1). CVR reduced the content of polysaccharides in the cell wall and thus damaged the integrity of cell wall. The contents of chitin and β-1,3-glucan in *A. alternata* were decreased significantly after CVR treatment (Figures 2A,B). Meanwhile, CVR treatment reduced the activities of β-1,3-glucan synthase and chitin synthase (Figures 2C,D), while the activity of β-1,3-glucanase and chitinase was increased in *A. alternata* after CVR treatment (Figures 2E,F). Hopke et al. (2018) showed that fungal responses to stresses include altering their cell surfaces to enhance or limit immune recognition and responses, linking the two disparate fields of cell wall integrity and immunity. The fungal cell wall can escape host immunity by increasing the content of chitin, while the β-glucan content increases the strength of cell wall. CVR inhibited the production of β-1,3-glucan and chitin by inhibiting the activities of β-1,3-glucan synthase and chitin synthase and promoted the degradation of the two polysaccharides by increasing the activities of β-1,3-glucanase and chitinase. This result was consistent with the report of *Tulbaghia violacea* Harv. plant

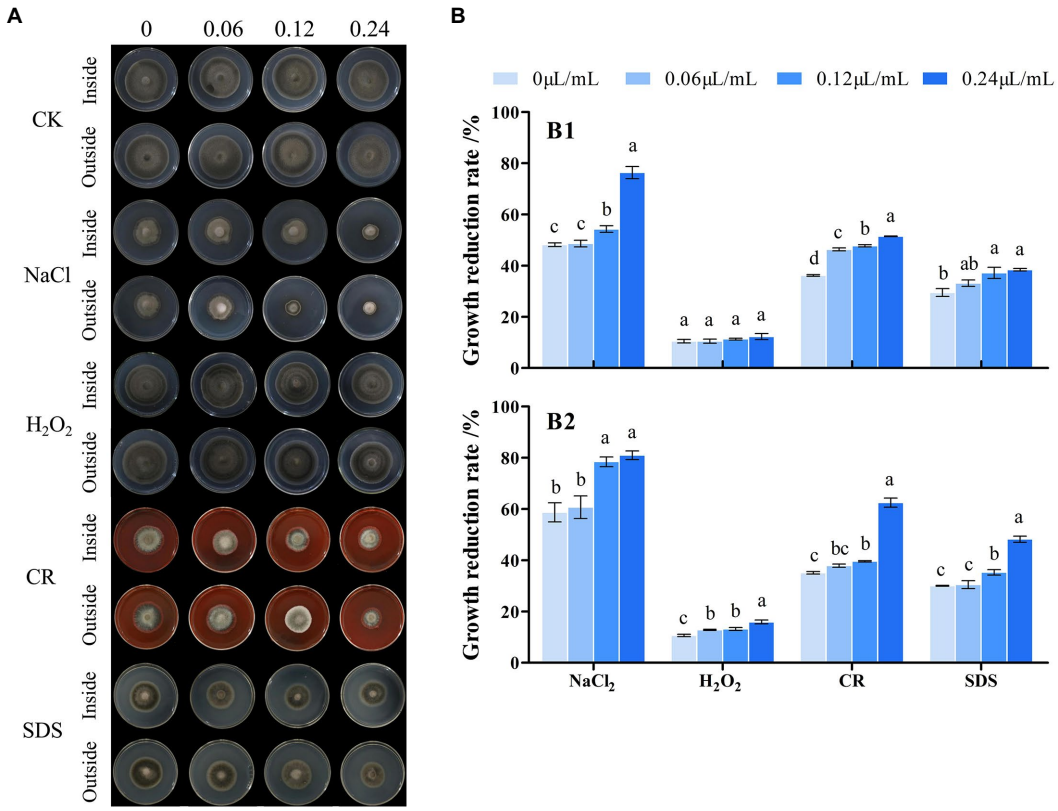

FIGURE 6
Influence of CVR treatment on stress resistance. Image of cultured under different conditions **(A)**. Growth reduction rate (%), **(B)** of inside **(B1)** and outside **(B2)** fungal colonies grown at 25°C for 8days on PDA plates supplemented with NaCl (0.5M), CR (Congo red 5μg/ml), H_2O_2 (1.5mM), and SDS (0.1mg/ml), respectively. Different letters represent significant differences at the level of $p<0.05$.

extract decreasing the chitin and β-1,3-glucan contents in *Aspergillus flavus* (Belewa et al., 2017). CVR treatment affected the integrity and stability of the cell wall of *A. alternata* by affecting the synthesis and metabolism of β-1,3-glucan and chitin in the cell wall. Comparison of the inside and outside parts of the mycelia revealed that CVR treatment had a more significant effect on the outer part of the mycelia. At sites of cell wall expansion, chitin synthases constitute a family of membrane-embedded enzymes that catalyze the synthesis of chitin, while β-1,3-glucan synthase catalyzes synthesis of β-1,3-glucan and transports it to the cell wall in the form of vesicles (Riquelme et al., 2018). Owing to different growth states, polysaccharide construction of the formed mycelia and at sites of cell wall expansion is different. Therefore, the effect of CVR treatment on the construction of chitin and β-1,3-glucan in the outside part of the mycelia was more intense.

To reveal the effect of CVR on polysaccharide metabolism and transportation, the outer mycelia treated with 0.06 μl/ml CVR were selected for transcriptomic analyses. The results showed the regulation of a large number of gene expression levels and metabolic processes by CVR-treated. Polysaccharides were the main substances constituting the cell wall, and the transcriptome data showed that CVR treatment had a significant effect on starch and sucrose metabolic pathways in *A. alternata*. There were eight DEGs involved in the decomposition of β-1,3-glucan and β-D-glucoside (Figures 5A,B). Glucan endo-1,3-β-D-glucosidase, glucan-1,3-β-glucosidase, and β-D-1,3-glucohydrolase can regulate the degradation of β-1,3-glucan (Donzelli et al., 2001; Belewa et al., 2017). GPI-anchored cell wall beta-1,3-endoglucanase EglC is the main gene that regulates the growth cycle of fungi and insufficient expression of this gene can cause defects in cell growth (Ramirez-Garcia et al., 2017). CVR treatment significantly affected the expression of regulatory genes related to glucan endo-1,3-β-D-glucosidase and glucan-1,3-β-glucosidase and significantly increased the expression of β-D-1,3-glucohydrolase regulatory genes, which accelerated the conversion of β-1,3-glucan and β-D-glucoside from polysaccharide to D-glucose (Henrissat and Bairoch, 1993). The upregulated expression of glucan endo-1,3-β-D-glucosidase and glucan-1,3-β-glucosidase was consistent with the increase in activity of β-1,3-glucanase. In addition, genes related to chitin anabolism were affected by CVR treatment. Chitin deacetylase-like protein can catalyze the hydrolysis of acetamido groups of *N*-acetylglucosamine units of chitin, producing glucosamine units and acetic acid (Mukherjee et al., 2019). The expression of the gene encoding this chitin deacetylase-like protein was increased in the CVR-treated samples, indicating that accelerated breakdown of chitin occurred in the hyphal cell wall after CVR treatment. The upregulated expression of this gene was also consistent with the increase in activity of chitinase. Chitin-binding protein can promote the synthesis of chitin, and the chitin-binding protein has an important role in the growth and development of infectious mycelia which has diverse functions in morphogenesis, pathogenesis, parasitism, nutrition, and immune regulation (Kuranda and Robbins, 1991). The upregulation of the gene encoding this enzyme indicates that CVR treatment affects

the growth cycle of mycelia. The downregulated expression of the chitin synthase gene indicated that CVR treatment inhibited chitin synthesis. The gene expression data were consistent with the activity of chitin synthase. Therefore, CVR treatment affected the integrity of the cell wall of *A. alternata* by regulating the genes related to polysaccharide biosynthesis and metabolism of the cell wall.

Recent studies have begun to reveal the extraordinary influence of the fungal cell wall on many aspects of fungal physiology, particularly in the interaction of fungi with the environment and during the colonization of host tissues (Geoghegan et al., 2017). Mycelia treated with different concentrations of CVR showed growth inhibition in the media containing different stress substances. The results of these assays indicated that the function of the cell wall was weakened to resist perturbing stress, osmotic stress, and high-temperature stress after CVR treatment (Figure 6). This was congruent with the findings of Zhang et al. (2020). Concurrently, CVR treatment affected the infection function of *A. alternata* cell wall. Covalently linked cell wall protein was covalently cross-linked to the cell wall and was an important site for hyphal cell wall adhesion and recognition. The upregulation of this gene of covalently linked cell wall protein indicates that CVR treatment affects the infection and stress resistance of *A. alternata* mycelia. However, the inside part of the mycelia did not exhibit a significant inhibitory effect in the medium containing H_2O_2. The reason(s) underlying the differing response of different parts of the mycelia to oxidative stress requires further investigation.

5. Conclusion

In summary, CVR has a destructive effect on the cell wall of *A. alternata* by damaging and altering the integrity of the mycelial cell wall. Meanwhile, both the contents of cell wall polycarbohydrates containing chitin and β-1,3-glucan and the activities of the enzymes related to the biosynthesis of these polycarbohydrates were significantly decreased by CVR treatment, while the activities of chitinase and β-1,3-glucanase response of degrading the two polycarbohydrates were increased by CVR treatment. The transcriptomic analysis further revealed that CVR influenced the polycarbohydrate metabolism pathways, especially starch and sucrose metabolism signaling pathways. In addition, CVR treatment inhibited the stress resistance of *A. alternata in vitro*. These findings implicated that CVR might exhibit its antifungal activity against *A. alternata* by interfering with the construction of the cell wall and therefore lead to the destruction of cell wall integrity and function. However, the inhibition mechanism of CVR treatment on the cell wall of *A. alternata* needs to be further studied by combining proteomics or metabolomics.

Data availability statement

The datasets presented in this study can be found in online repositories. The names of the repository/repositories and accession number(s) can be found below: BioProject: accession number: PRJNA923470.

Author contributions

LZ, JW, and HZ contributed in conceptualization, methodology, formal analysis, investigation, writing original draft, writing review and editing, and supervision. JW contributed in validation, resources, funding acquisition, and experimental materials. PW, CW, YZ, LH, and RW contributed in investigation. All authors contributed to the article and approved the submitted version.

Funding

This work was supported by Natural Science Foundation of Ningxia Province (2020AAC03255) and Natural Science Foundation of China (32060565).

Conflict of interest

The authors declare that the research was conducted in the absence of any commercial or financial relationships that could be construed as a potential conflict of interest.

Publisher's note

All claims expressed in this article are solely those of the authors and do not necessarily represent those of their affiliated organizations, or those of the publisher, the editors and the reviewers. Any product that may be evaluated in this article, or claim that may be made by its manufacturer, is not guaranteed or endorsed by the publisher.

Supplementary material

The Supplementary material for this article can be found online at: https://www.frontiersin.org/articles/10.3389/fmicb.2023.1139749/full#supplementary-material

References

Abbaszadeh, S., Sharifzadeh, A., Shokri, H., Khosravi, A. R., and Abbaszadeh, A. (2014). Antifungal efficacy of thymol, carvacrol, eugenol and menthol as alternative agents to control the growth of food-relevant fungi. *J. Mycol. Med.* 24, e51–e56. doi: 10.1016/j.mycmed.2014.01.063

Belewa, V., Baijnath, H., Frost, C., and Somai, B. M. (2017). *Tulbaghia violacea* Harv. Plant extract affects cell wall synthesis in *aspergillus flavus*. *J. Appl. Microbiol.* 122, 921–931. doi: 10.1111/jam.13405

Cardiet, G., Fuzeau, B., Barreau, C., and Fleurat-Lessard, F. (2012). Contact and fumigant toxicity of some essential oil constituents against a grain insect pest *Sitophilus oryzae* and two fungi, *aspergillus westerdijkiae* and *fusarium graminearum*. *J. Pest. Sci.* 85, 351–358. doi: 10.1007/s10340-011-0400-3

Dague, E., Delcorte, A., Latgé, J. P., and Dufrêne, Y. S. (2008). Combined use of atomic force microscopy, X-ray photoelectron spectroscopy, and secondary ion mass spectrometry for cell surface analysis. *Langmuir* 24, 2955–2959. doi: 10.1021/la703741y

De Souza, E. L., Sales, C. V., De Oliveira, C. E. V., Lopes, L. A. A., De Conceição, M. L., Berger, L. R. R., et al. (2015). Efficacy of a coating composed of chitosan from Mucor circinelloides and carvacrol to control *aspergillus flavus* and the quality of cherry tomato fruits. *Front. Microbiol.* 6:732. doi: 10.3389/fmicb.2015.00732

De Vincenzi, M., Stammati, A., De Vincenzi, A., Maialetti, F., and Scazzocchio, B. (2022). Constituents of aromatic plants: carvacrol. *Fitoterapia* 73, 269–275. doi: 10.1016/S0367-326X(02)00062-X

Donzelli, B. G. G., Lorito, M., Scala, F., and Harman, G. E. (2001). Cloning, sequence and structure of a gene encoding an antifungal glucan 1,3-β-glucosidase from *Trichoderma atroviride* (*T. harzianum*). *Gene* 277, 199–208. doi: 10.1016/S0378-1119(01)00681-3

Fortwendel, J. R., Juvvadi, P. R., Pinchai, N., Perfect, B. Z., Alspaugh, J. A., Perfect, J. R., et al. (2008). Differential effects of inhibiting chitin and 1,3-β-D-glucan synthesis in ras and calcineurin mutants of *aspergillus fumigatus*. *Antimicrob. Agents Chemother.* 53, 476–482. doi: 10.1128/AAC.01154-08

Fu, Y., Yang, T., Zhao, J., Zhang, L., Chen, R. X., and Wu, Y. L. (2017). Determination of eight pesticides in *Lycium barbarum* by LC-MS/MS and dietary risk assessment. *Food Chem.* 218, 192–198. doi: 10.1016/j.foodchem.2016.09.014

Geoghegan, I., Steinberg, G., and Gurr, S. (2017). The role of the fungal cell wall in the infection of plants. *Trends Microbiol.* 25, 957–967. doi: 10.1016/j.tim.2017.05.015

Gonçalves, D. C., Ribeiro, W. R., Gonçalves, D. C., Luciano, M., and Costa, H. (2021). Recent advances and future perspective of essential oils in control *Colletotrichum* spp.: a sustainable alternative in postharvest treatment of fruits. *Food Res. Int.* 150:110758. doi: 10.1016/j.foodres.2021.110758

Gow, N. A. R., Latge, J. P., and Munro, C. A. (2017). The fungal cell wall: structure, biosynthesis, and function. *Microbiol. Spectrum* 5:funk-0035. doi: 10.1128/microbiolspec.FUNK-0035-2016

Henrissat, B., and Bairoch, A. (1993). New families in the classification of glycosil hydrolases based on aminoacid sequence similarities. *Biochemist* 293, 781–788. doi: 10.1042/bj2930781

Hopke, A., Brown, A. J. P., Hall, R. A., and Wheeler, R. T. (2018). Dynamic fungal cell wall architecture in stress adaptation and immune evasion. *Trends Microbiol.* 26, 284–295. doi: 10.1016/j.tim.2018.01.007

Jiang, N., Li, Z. L., Wang, L. Q., Li, H., Zhu, X., Feng, X. Y., et al. (2019). Effects of ultraviolet-c treatment on growth and mycotoxin production by *Alternaria* strains isolated from tomato fruits. *Int. J. Food Microbiol.* 311:108333. doi: 10.1016/j.ijfoodmicro.2019.108333

Kim, J. E., Lee, J. E., Huh, M. J., Lee, S. C., Seo, S. M., Kwon, J. H., et al. (2019). Fumigant antifungal activity via reactive oxygen species of *Thymus vulgaris* and *Satureja hortensis* essential oils and constituents against *Raffaelea quercus-mongolicae* and *Rhizoctonia solani*. *Biomol. Ther.* 9:561. doi: 10.3390/biom9100561

Kou, Y. J., and Naqvi, N. I. (2016). Surface sensing and signaling networks in plant pathogenic fungi. *Semin. Cell Dev. Biol.* 57, 84–92. doi: 10.1016/j.semcdb.2016.04.019

Kuranda, M. J., and Robbins, P. W. (1991). Chitinase is required for cell separation during growth of *Saccharomyces cerevisiae*. *Biol. Chem.* 266, 19758–19767. doi: 10.1016/S0021-9258(18)55057-2

Li, J., Fu, S., Fan, G., Li, D. M., Yang, S. Z., Peng, S. Y., et al. (2021). Active compound identification by screening 33 essential oil monomers against *Botryosphaeria dothidea* from postharvest kiwifruit and its potential action mode. *Pestic. Biochem. Physiol.* 179:104957. doi: 10.1016/j.pestbp.2021.104957

Li, Q., Zhu, X. M., Xie, Y. L., and Zhong, Y. (2021). *O*-vanillin, a promising antifungal agent, inhibits A*spergillus flavus* by disrupting the integrity of cell walls and cell membranes. *Appl. Microbiol. Biotechnol.* 105, 5147–5158. doi: 10.1007/s00253-021-11371-2

Ma, R. H., Zhang, X. X., Thakur, K., Zhang, J. G., and Wei, Z. J. (2022). Research progress of *Lycium barbarum* L. as functional food: phytochemical composition and health benefits. *Curr. Opin. Food Sci.* 47:100871. doi: 10.1016/j.cofs.2022.100871

Mellado, E., Dubreucq, G., Mol, P., Sarfati, J., Paris, S., Diaquin, M., et al. (2003). Cell wall biogenesis in a double chitin synthase mutant (*chs*G$^-$/*chs*E$^-$) of *aspergillus fumigatus*. *Fungal Genet. Biol.* 38, 98–109. doi: 10.1016/S1087-1845(02)00516-9

Mukherjee, A., Sarkar, S., Gupta, S., Banerjee, S., Senapati, S., Chakrabarty, R., et al. (2019). DMSO strengthens chitin deacetylase-chitin interaction: physicochemical, kinetic, structural and catalytic insights. *Carbohydr. Polym.* 223:115032. doi: 10.1016/j.carbpol.2019.115032

Ochoa-Velasco, C. E., Navarro-Cruz, A. R., Vera-López, O., Palou, E., and Avila-Sosa, R. (2017). Growth modeling to control (in vitro) *fusarium verticillioides* and *Rhizopus stolonifer* with thymol and carvacrol. *Rev. Argent. Microbiol.* 50, 70–74. doi: 10.1016/j.ram.2016.11.010

Ouyang, Q. L., Duan, X. F., Li, L., and Tao, N. G. (2019). Cinnamaldehyde exerts its antifungal activity by disrupting the cell wall integrity of *Geotrichum citri-aurantii*. *Front. Microbiol.* 10:55. doi: 10.3389/fmicb.2019.00055

Parkhomchuk, D., Borodina, T., Amstislavskiy, V., Banaru, M., Hallen, L., Krobitsch, S., et al. (2009). Transcriptome analysis by strand-specific sequencing of complementary DNA. *Nucleic Acids Res.* 37:e123. doi: 10.1093/nar/gkp596

Ramirez-Garcia, A., Pellon, A., Buldain, I., Antoran, A., Arbizu-Delgado, A., Guruceaga, X., et al. (2017). Proteomics as a tool to identify new targets against *aspergillus* and *Scedosporium* in the context of cystic fibrosis. *Mycopathologia* 183, 273–289. doi: 10.1007/s11046-017-0139-3

Rappleye, C. A., Eissenberg, L. G., and Goldman, W. E. (2007). *Histoplasma capsulatum* α-(1,3)-glucan blocks innate immune recognition by the betaglucan receptor. *Proc. Natl. Acad. Sci. U. S. A.* 104, 1366–1370. doi: 10.1073/pnas.0609848104

Riquelme, M., Aguirre, J., Bartnicki-García, S., Braus, G. H., Feldbrügge, M., Fleig, U., et al. (2018). Fungal morphogenesis, from the polarized growth of hyphae to complex reproduction and infection structures. *Microbiol. Mol. Biol. Rev.* 82, e00068–e00017. doi: 10.1128/MMBR.00068-17

Schloesser, I., and Prange, A. (2019). Effects of selected natural preservatives on the mycelial growth and ochratoxin a production of the food-related moulds *aspergillus westerdijkiae* and *Penicillium verrucosum*. *Food Addit. Contam. Part A Chem. Anal. Control Expo Risk Assess* 36, 1411–1418. doi: 10.1080/19440049.2019.1640397

Serna-Escolano, V., Serrano, M., Valero, D., Rodríguez-Lopez, M. I., Gabaldon, J. A., Castillo, S., et al. (2019). Effect of thymol and carvacrol encapsulated in Hp-B-cyclodextrin by two inclusion methods against *Geotrichum citri-aurantii*. *J. Food Sci.* 84, 1513–1521. doi: 10.1111/1750-3841.14670

Serrano, L., Egüés, I., Alriols, M. G., Llano-Ponte, R., and Labidi, J. (2010). Miscanthus sinensis fractionation by different reagents. *Chem. Eng.* 156, 49–55. doi: 10.1016/j.cej.2009.09.032

Suntres, Z. E., Coccimiglio, J., and Alipour, M. (2015). The bioactivity and toxicological actions of carvacrol. *Crit. Rev. Food Sci. Nutr.* 55, 304–318. doi: 10.1080/10408398.2011.653458

Thomidis, T., and Filotheou, A. (2016). Evaluation of five essential oils as bio-fungicides on the control of *Pilidiella granati* rot in pomegranate. *Crop Prot.* 89, 66–71. doi: 10.1016/j.cropro.2016.07.002

Ultee, A., Kets, E. P. W., and Smid, E. J. (1999). Mechanisms of action of carvacrol on the food-borne pathogen *Bacillus cereus*. *Appl. Environ. Microbiol.* 65, 4606–4610. doi: 10.1128/AEM.65.10.4606-4610.1999

Wang, C. C., Chang, S. C., Inbaraj, B. S., and Chen, B. H. (2010). Isolation of carotenoids, flavonoids and polysaccharides from *Lycium barbarum* L. and evaluation of antioxidant activity. *Food Chem.* 120, 184–192. doi: 10.1016/j.foodchem.2009.10.005

Wang, J. J., Li, Z. B., Zhang, H. Y., Wang, P., Fan, C. X., Chen, S. G., et al. (2019). Control of carvacrol treatment on black mold of postharvest goji berry. *Sci. Technol. Food Ind.* 40, 229–240. doi: 10.13386/j.issn1002-0306.2019.08.03, (in Chinese with English abstract)

Wang, P., Wang, J. J., Zhang, H. Y., Wang, C., Zhao, L. N. K., Huang, T., et al. (2021). Chemical composition, crystal morphology, and key gene expression of the cuticular waxes of goji (*Lycium barbarum* L.) berries. *J. Agric. Food Chem.* 69, 7874–7883. doi: 10.1021/acs.jafc.1c02009

Wang, X., Xu, X. D., Chen, Y., Zhou, R. L., Tian, S. P., and Li, B. Q. (2018). Isolation and identification of postharvest pathogens in fresh wolfberry from Ningxia and the inhibitory effect of salicylic acid. *J. Food Saf. Qual.* 22, 5837–5842. doi: 10.3969/j.issn.2095-0381.2018.22.008 (in Chinese with English abstract)

Wei, D. Z., Wang, Y., Jiang, D. M., Feng, X. Y., Li, J., and Wang, M. (2017). Survey of *Alternaria* toxins and other *mycotoxins* in dried fruits in China. *Toxins* 9:200. doi: 10.3390/toxins9070200

Xie, C., Mao, X., Huang, J., Ding, Y., Wu, J., Dong, S., et al. (2011). KOBAS 2.0: a web server for annotation and identification of enriched pathways and diseases. *Nucleic Acids Res.* 39, W316–W322. doi: 10.1093/nar/gkr483

Xing, L. J., Zou, L. J., Luo, R. F., and Wang, Y. (2020). Determination of five *Alternaria* toxins in wolfberry using modified QuEChERS and ultra-high performance liquid chromatography-tandem mass spectrometry. *Food Chem.* 311:125975. doi: 10.1016/j.foodchem.2019.125975

Yang, S. Z., Liu, L. M., Li, D. M., Xia, H., Su, X. J., Peng, L. T., et al. (2016). Use of active extracts of poplar buds against *Penicillium italicum* and possible modes of action. *Food Chem.* 196, 610–618. doi: 10.1016/j.foodchem.2015.09.101

Yuan, S. Z., Li, W. S., Li, Q. Q., Wang, L. M., Cao, J. K., and Jiang, W. B. (2019). Defense responses, induced by *p*-Coumaric cid and methyl *p*-Coumarate, of jujube (*Ziziphus jujuba* mill.) fruit against black spot rot caused by Alternaria alternata. *J. Agric. Food Chem.* 67, 2801–2810. doi: 10.1021/acs.jafc.9b00087

Zhang, J. H., Ma, S., Du, S. L., Chen, S. Y., and Sun, H. L. (2019). Antifungal activity of thymol and carvacrol against postharvest pathogens *Botrytis cinerea*. *J. Food Sci. Technol.* 56, 2611–2620. doi: 10.1007/s13197-019-03747-0

Zhang, L. B., Tang, L., Guan, Y., and Feng, M. G. (2020). Subcellular localization of Sur7 and its pleiotropic effect on cell wall integrity, multiple stress responses, and virulence of *Beauveria bassiana*. *Appl. Microbiol. Biotechnol.* 104, 6669–6678. doi: 10.1007/s00253-020-10736-3

Zhao, L. N. K., Wang, P., Chen, S. G., Aizez, A., Wang, C., and Wang, J. J. (2021). Biological characterization of black mold pathogen in *Lycium barbarum* L. fruits and antifungal chemicals screening. *China Plant Protect.* 41:11-19+24. doi: 10.3969/j.issn.1672-6820.2021.03.002, (in Chinese with English abstract)

Zhou, R. W., Zhou, R. S., Yu, F., Xi, D. K., Wang, P. Y., Li, J. W., et al. (2018). Removal of organophosphorus pesticide residues from *Lycium barbarum* by gas phase surface discharge plasma. *Chem. Eng. J.* 342, 401–409. doi: 10.1016/j.cej.2018.02.107

frontiers | Frontiers in Microbiology

TYPE Original Research
PUBLISHED 27 February 2023
DOI 10.3389/fmicb.2023.1109028

OPEN ACCESS

EDITED BY
Khamis Youssef,
Agricultural Research Center, Egypt

REVIEWED BY
Abhay K. Pandey,
Tea Research Association, India
Mohamed A. Mohamed,
Agricultural Research Center, Egypt

*CORRESPONDENCE
Hao Zhai
✉ zhaihao688@163.com
Xiaomin Xue
✉ xuexiaomin79@126.com

SPECIALTY SECTION
This article was submitted to Food Microbiology, a section of the journal Frontiers in Microbiology

RECEIVED 27 November 2022
ACCEPTED 06 February 2023
PUBLISHED 27 February 2023

CITATION
Wang D, Wang G, Wang J, Zhai H and Xue X (2023) Inhibitory effect and underlying mechanism of cinnamon and clove essential oils on *Botryosphaeria dothidea* and *Colletotrichum gloeosporioides* causing rots in postharvest bagging-free apple fruits. *Front. Microbiol.* 14:1109028. doi: 10.3389/fmicb.2023.1109028

Inhibitory effect and underlying mechanism of cinnamon and clove essential oils on *Botryosphaeria dothidea* and *Colletotrichum gloeosporioides* causing rots in postharvest bagging-free apple fruits

Dan Wang, Guiping Wang, Jinzheng Wang, Hao Zhai* and Xiaomin Xue*

Shandong Institute of Pomology, Shandong Academy of Agricultural Sciences, Tai'an, China

Bagging-free apple is more vulnerable to postharvest disease, which severely limits the cultivation pattern transformation of the apple industry in China. This study aimed to ascertain the dominant pathogens in postharvest bagging-free apples, to evaluate the efficacy of essential oil (EO) on inhibition of fungal growth, and to further clarify the molecular mechanism of this action. By morphological characteristics and rDNA sequence analyses, *Botryosphaeria dothidea* (*B. dothidea*) and *Colletotrichum gloeosporioides* (*C. gloeosporioides*) were identified as the main pathogens isolated from decayed bagging-free apples. Cinnamon and clove EO exhibited high inhibitory activities against mycelial growth both in vapor and contact phases under *in vitro* conditions. EO vapor at a concentration of 60 μL L^{-1} significantly reduced the incidence and lesion diameter of inoculated decay *in vivo*. Observations using a scanning electron microscope (SEM) and transmission electron microscope (TEM) revealed that EO changed the mycelial morphology and cellular ultrastructure and destroyed the integrity and structure of cell membranes and major organelles. Using RNA sequencing and bioinformatics, it was demonstrated that clove EO treatment impaired the cell membrane integrity and biological function *via* downregulating the genes involved in the membrane component and transmembrane transport. Simultaneously, a stronger binding affinity of *trans*-cinnamaldehyde and eugenol with CYP51 was assessed by *in silico* analysis, attenuating the activity of this ergosterol synthesis enzyme. Moreover, pronounced alternations in the oxidation/reduction reaction and critical materials metabolism of clove EO-treated *C. gloeosporioides* were also observed from transcriptomic data. Altogether, these findings contributed novel antimicrobial cellular and molecular mechanisms of EO, suggesting its potential use as a natural and useful preservative for controlling postharvest spoilage in bagging-free apples.

KEYWORDS

bagging-free apple, post-harvest pathogens, essential oil, cell membrane, transcriptome

Introduction

Apple is one of the most important temperate tree fruits in the world. China is the leader in apple production and accounts for more than 50% of the total yield. Pre-harvest bagging has been conventionally practiced for apple cultivation in China, Japan, and Australia in order to improve fruit appearance and increase market value (Fallahi et al., 2001), but such treatment alters the microenvironment for apple development, leading to multiple effects on internal quality such as reduced phenolic compounds and faded flavor (Arakawa et al., 1994; Chen et al., 2012; Feng et al., 2014). In recent years, there has been growing interests in examining the potential of non-bagging patterns due to the decline of fruit inner quality and the increase in labor force cost and ecological pollution. It has been recognized that the bagging-free cultivation pattern is an inevitable trend in the apple industry development in China.

Nevertheless, under the bagging-free cultivation mode, apples are more vulnerable to insect pests and diseases resulting from the lack of bag protection. Although through monitoring and forecasting, combined with biological management and precise pesticide application, the incidence of pre-harvest pests and diseases is controlled below 1% (Zhai et al., 2019), bagging-free apples show higher susceptibility to postharvest disease damage mainly caused by latent fungal pathogens infection in the field or cold chain handling process, which limits good fruit quality and shortens the shelf life of fresh apple fruit during storage, resulting in significant economic losses. At present, relevant studies on pathological research during the conservation period, especially fungal decay that occurred in bagging-free apples, have seldom been reported.

Chemically synthetic fungicides, like difenoconazole, are commonly used for the postharvest control of apple spoilage and pathogenic fungus. In the last decade, there is strong public and scientific controversy about the application of pesticides because of their hazardous side impacts on the environment and human health such as residual toxicity and fungicide-resistance development (Holmes et al., 2016; Hofer, 2019). In this case, consumer demands for organically produced fruit led to the extensive use of naturally derived preservatives. Essential oils (EOs) are secondary metabolites directly extracted from aromatic and medicinal plants, containing a variety of substances called "phytochemicals" and having a natural or avirulent image. Due to the abundant bioactive chemical components, EOs are endowed with remarkable antimicrobial and antioxidative activities, which enable them to effectively defend against foodborne pathogens and extend the storage life of fresh products (Kwon et al., 2017; Alanazi et al., 2018; Ju et al., 2018; Almeida et al., 2019). In general, two application methods may be used for the inhibition of postharvest mold: (i) fumigation solution in which less EO is used due to its high volatility, and (ii) directly contact solution by agar or broth diffusion (Sivakumar and Bautista-Baños, 2014; Wang et al., 2019).

Essential oils exhibited a great variety of the microbial inhibitory spectrum due to their complex chemical composition and diverse mode of action. Cinnamon and clove EO are promising natural fungicides widely used for the control of foodborne pathogens and spoilage microorganisms, and cinnamaldehyde and eugenol are the major active ingredients of them, respectively (Tu et al., 2018; Dávila-Rodríguez et al., 2019; El amrani et al., 2019). Recently, the antimicrobial effect of cinnamon and clove EO has been widely researched. Duduk et al. (2015) found that cinnamon EO had good inhibitory effects against *Colletotrichum acutatum* isolated from strawberry anthracnose. Castellanos et al. (2020) demonstrated that clove EO could reduce the growth of *Aspergillus niger* from 50 to 70% and *Fusarium oxysporum* to 40% and provide an alternative solution to the use of hazardous chemical fungicides for the postharvest treatment of tomato during storage and transportation. Khaleque et al. (2016) reported that high concentrations of cinnamon and clove EOs could inhibit *Listeria monocytogenes* in ground beef meat and improve the safety of ground beef products. *Botryosphaeria dothidea* (*B. dothidea*) and *Colletotrichum gloeosporioides* (*C. gloeosporioides*) can infect apple fruit before and after picking, thus, resulting in reduced apple yield (Moreira et al., 2019; Yu et al., 2022). EOs or components have been demonstrated as useful effective antifungal agents against postharvest *B. dothidea* and *C. gloeosporioides*. Carvacrol appeared to evidently inhibit the mitochondrial activity and respiration rate of *B. dothidea* and could be a very useful EO compound for controlling postharvest rot soft in kiwifruit (Li J. et al., 2021). Rabari et al. (2018) tested the inhibitory activities of 75 EOs against *C. gloeosporioides* isolated from the infected mango, and four EOs showed remarkably higher antifungal efficacy.

Although many studies reported EO's antimicrobial action, very few have focused on the mechanism underlying these effects and the investigation at the cellular or molecular level is yet to be explored. The fungal cell membrane was the main target for the fungistatic action of EOs due to their lipophilicity (Burt, 2004). In the previous study, it was suggested that an increase in membrane permeability and subsequent release of cellular material might be responsible for EO's antifungal ability (Shao et al., 2013). Lanosterol 14α-demethylase (also known as CYP51) served as a rate-limiting enzyme that can regulate the rate and quantity of ergosterol produced in the fungal cell membrane (Monk et al., 2020). Azole class of antifungal drugs inhibited CYP51, and subsequently, researchers considered CYP51 as the most attractive protein target to develop antifungal drugs (Sun et al., 2019; Dong et al., 2020). However, there is a piece of scattered information where phytochemicals could inhibit CYP51. Several phytochemicals were reported to inhibit various CYPs, for instance, a natural product of *Curcuma longa* can inhibit CYP1A2, CYP3A4, CYP21A2, and CYP17A1 (Schwarz et al., 2011). Now an intriguing question arises: can cinnamon and clove EOs also restrict identical protein CYP51 and impede the production of ergosterol in pathogenic fungi?

Hence, in the present study, the dominant pathogens, which caused postharvest decay in bagging-free apples, were first isolated and identified. In addition, the inhibitory activities of cinnamon and clove EO as well as their application methods against the pathogens were examined both *in vitro* and *in vivo;* meanwhile, a combination of approaches including microscopic (SEM and TEM) and molecular (transcriptomic and docking analysis) investigations was further carried out to provide insights into their antifungal mechanism. The aim of this study was to provide theoretical reference on the potential use of EOs as a natural and

efficient preservative for the control of postharvest diseases in the cultivation mode transformation of the apple industry.

Materials and methods

Materials and chemicals

Fresh apple fruits under the bagging-free cultivation pattern were harvested at commercial maturity and were transferred to the laboratory within 6 h. Uniform fruits free of defects and mechanical damage were selected and stored at 0 ± 0.5°C, 90% RH.

Pure-grade cinnamon EO (bark steam distillation; origin: China) and clove EO (bud distillation; origin: China) were purchased from Guangzhou Hengxin Spice Co., Ltd., Guangzhou, China, and stored in the dark, at room temperature. The cinnamon and clove EO were analyzed on an Agilent gas chromatography–mass spectrometry (GC-MS) 7890 column (30 m × 0.25 mm × 0.25 μm). Helium was used as carrier gas. The injection volume was 1 μL, and the injector temperature was set at 250°C. The oven temperature was programmed at 50°C for 2 min, raised to 260°C at a rate of 5°C/min, and maintained for 10 min. In the full-scan mode, electron ionization mass spectra were recorded at 70 eV electron energy with a mass range of 10–550 Da. The temperatures of the interface, ion source, and quadrupole were held at 280, 230, and 150°C, respectively. The main components of EOs were assigned by comparing their relative retention time and matching their mass spectra characteristic features with the mass spectral library (Wiley Register TM of Mass Spectral Data). The main composition of cinnamon and clove EO is given in Table 1.

TABLE 1 Chemical compositions of cinnamon and clove EO.

No.	Components	RT[a] (s)	Percentage (%)
Cinnamon EO			
1	*Trans*-cinnamaldehyde	553.74	82.228
2	Benzaldehyde	274.62	7.907
3	2,4-decadienal	587.52	3.174
4	Phenethyl acetate	532.32	1.387
5	Camphorene	265.56	0.714
6	4-isopropyltoluene	328.56	0.706
7	2-carbitol	464.16	0.688
8	Salicylaldehyde	347.82	0.612
9	O-methoxybenzaldehyde	521.10	0.506
10	O-methoxycinnamaldehyde	755.64	0.387
11	*Trans*-2-decenal	539.34	0.385
12	Nonanal	398.28	0.350
13	Eugenol	617.10	0.301
14	α-ylangene	733.14	0.228
15	2-undecenal	624.30	0.221
16	Limonene	332.94	0.175
17	Eucalyptol	336.36	0.031
Clove EO			
1	Eugenol	615.66	78.952
2	Eugenol acetate	740.16	17.892
3	β-caryophyllene	674.76	2.059
4	α-caryophyllene	702.78	0.726
5	Oxetene	798.66	0.281
6	α-Humulene	756.21	0.068
7	Methyleugenol	718.92	0.022

RT[a], retention time.

Survey of postharvest diseases

Apples were stored at 25°C after picking, and disease incidence was measured at 20, 40, and 60 days. Each treatment included three replicates, and each replicate consisted of 40 apples.

Isolation, purification, and identification of pathogens

Isolation of the pathogens was carried out based on our previous method (Wang et al., 2020). Diseased fruits were surface-sterilized with 75% ethanol for the 30 s and 1% sodium hypochlorite (NaOCl) for 1 min. The sterilized tissues were rinsed three times with sterilized water, placed on potato dextrose agar (PDA) medium containing 0.02% streptomycin sulfate, and incubated in the dark at 25°C. Isolated fungal colonies were subcultured by the hyphal tip transferring technique until the pure culture was obtained. The two mold strains were obtained and marked as DH1 and HF2. After incubation for 7–10 days, the morphology of colonies and conidia of the two strains was observed and recorded. The isolated pathogens were assayed its pathogenicity in healthy apples. Furthermore, the pathogens were isolated again from diseased fruit using the earlier tissue separation method. Finally, the pathogen was subcultivated on PDA and stored at 4°C for consequent identification.

The genomic DNA of mycelia was extracted using CTAB (cetyltrimethylammonium bromide) method (Wang et al., 2020). The internal transcribed spacer (ITS) sequence of the rDNA was amplified using the primer ITS1 (5′-TCCGTAGGTGAACCTGCGG-3′) and ITS4 (5′-TCCTCCGCTTATTGATATGC−3′), and thermal cycling was set a predenaturation step at 94°C for 5 min, denaturation at 94°C for 40 s, annealing at 58°C for 40 s, following by 35 cycles of extension at 72°C for 1 min, and a final elongation step at 72°C for 10 min.

Polymerase chain reaction (PCR) products were purified and sequenced by Shanghai Boshang Biological Technology Co., Ltd. (Shanghai, China). To assess similarity, multiple related sequences were aligned by BLAST in the NCBI database. A phylogenetic tree was constructed using the neighbor-joining method in MEGA 5.2 software. *Torreya grandis* (AF259277.1) and *Pestalotiopsis microspora* (KF941280.1) were used as the out-group for DH1 and HF2, respectively. Bootstrapping was performed with 1,000 replicates to evaluate the significant internal branches in the tree.

Mycelial growth inhibition testing *in vitro*

Gas diffusion test

A mycelial plug with a size of 7 mm from 7 days of actively growing culture was priorly inoculated onto the center of the bottom of the Petri dishes with 12.5 mL of PDA. Subsequently, a sterilized filter paper was attached to the center of the inner side of the plate lid with different amounts of EOs (1.5, 2.25, 3, and 3.75 μL) added; then, the plate lid was quickly covered, and 37.5 mL air space was offered to obtain final concentrations of 40, 60, 80, and 100 μL L^{-1} of air (v/v). PDA plates without EO were used as controls. All plates were sealed with laboratory parafilm to prevent leakage of EO vapor, kept in an inverted position, and incubated at 26°C for 4 days. The radical growth diameters of each treatment were measured using a digital vernier caliper in triplicate.

Solid diffusion test

Following our previous procedures with some minor modifications (Wang et al., 2019), 9.6, 19.2, 28.8, and 38.4 μL of pure EO were dispersed using 8 mL Tween 80 (0.2% v/v) while mixing with a high-speed homogenizer (IKA-ULTRATURRAX T25 basic, IKA Works, Inc., Wilmington, NC, USA) at 14,000 rpm for 4 min. Then, 40 mL PDA was added (48 mL total) immediately before it was poured into the glass Petri dishes (15 mL/plate, in triplicate) to obtain a final concentration of 200, 400, 600, and 800 μL L^{-1}. The control was prepared similarly with Tween 80 alone. Afterward, mycelia was inoculated in the center of each plate. All plates were sealed with laboratory parafilm to avoid EO evaporation, kept in an inverted position, and incubated at 26°C for 4 days. The radical growth diameters of each treatment were measured using a digital vernier caliper in triplicate.

The lowest concentration of the EOs at which there was no strain growth for 48 h was defined as the minimum inhibitory concentration (MIC).

Antifungal assays *in vivo*

The fungal inoculation was performed according to the previous research (Zhou et al., 2018). Apple fruits were sterilized with 2% sodium hypochlorite for 2 min and air-dried at room temperature. Each fruit was wounded (3 mm deep and 3 mm wide) at its equator using a sterile nail. Then, 10 μL of the spore suspension at 1.0×10^8 spores L^{-1} were evenly inoculated into the puncture wounds ("Fuji" and "Orin" apples were inoculated with *B. dothidea* and *C. gloeosporioides*, respectively). The volume ratio of the EO and the container (μL L^{-1}) was used to represent the vapor concentration. Based on our preliminary experiments, 60 μL L^{-1} EO were placed on filter paper. During EO vapor treatments, apple fruits were placed in a container of 6.5 L volume sealed with PVC cling film to make it evaporate naturally and stored in a 95% relative humidity incubator at 25°C. Samples for lesion diameter assay were recorded daily. Each treatment contained three replicates, and the whole experiment was performed twice.

SEM and TEM assays

The scanning electron microscopy (SEM) and transmission electron microscopy (TEM) assays were carried out based on some previous studies (Li et al., 2014; Zhang et al., 2016). In brief, the spore suspension of *B. dothidea* and *C. gloeosporioides* was obtained from 4-day-old cultures by adding 10 mL 0.9% NaCl solution to each Petri dish and gently scraping the mycelial surface three times with a sterile L-shaped spreader to free the spores. A 1 mL spore suspension (1×10^7 CFU mL^{-1}) was added to 150 mL PDB medium and incubated at 26°C shaking for 2 days. The fully emulsified cinnamon and clove EO by Tween 80 solution (0.2% v/v) were added to the shake flask of *B. dothidea* and *C. gloeosporioides* to achieve the concentrations of their MIC, respectively. No EO added was set as the control. After that, all of the samples were incubated at 26°C for 12 h and collected by centrifugation at 4,000 rpm for 10 min. Then mycelial cells were washed three times with phosphate buffer solution (PBS). Each treatment was performed in triplicate.

For SEM assay, the cells were fixed with 2.5% glutaraldehyde and 4% formaldehyde for 4 h and were dehydrated with ethanol at gradient concentrations (15 min at 30, 50, 70, 80, and 90% and 20 min twice at 100%). Subsequently, the cells were freeze-dried, spray-gold, and visualized in an SEM (Sigma 300, ZEISS).

For the TEM assay, the mycelial cells were treated by ultra-thin sectioning and negatively stained (1% phosphotungstic acid, 5 min) and then directly examined in a TEM (MORADA-G2, Olympus, Japan).

RNA-sequencing and bioinformatics analysis

Total RNA was extracted using TRIzol reagent (Invitrogen), and RNA quality and purity were assessed by Nanodrop spectrophotometer. In brief, rRNA was removed and mRNAs were fragmented, then transcribed mRNA fragments into first-strand cDNA, and followed by second-strand cDNA synthesis. After that, sequencing libraries were constructed and sequenced at Biomarker Technologies (Beijing, China) with an Illumina platform. Raw reads were filtered into high-quality clean reads used for subsequent bioinformatics analysis.

The gene expression levels were normalized by FPKM (fragments per kilobase of transcript per million fragments mapped). Genes with a p-value <0.05 and $|\log_2 FC| \geq 1$ were considered to be differentially expressed genes (DEGs). GO and KEGG enrichment analysis was performed on the identified DEGs. Only GO terms and KEGG pathways with FDR < 0.05 were statistically considered to be significantly enriched.

Docking analysis

The CYP51 protein sequences of *Botryosphaeria dothidea* (KAF4313409.1) and *Colletotrichum gloeosporioides* (KAF4925022.1) were downloaded from the NCBI. The models of these proteins were built by the online tools SWISS-MODEL

and assessed by using the program "PROCHECK" on the website of SAVES (https://nihserver.mbi.ucla.edu/SAVES/) for docking studies (Waterhouse et al., 2018). The 3D structures of the ligands including *trans*-cinnamaldehyde (CAS14371-10-9) and eugenol (CAS97-53-0) were downloaded from Pubmed. Molecular docking was performed using Autodock 4.2 software (Morris et al., 2009), and PyMOL (Delano, 2002) and LIGPLOT (Laskowski and Swindells, 2011) software were used to visualize and analyze the modes with the lowest binding score from the docking results.

Statistical analysis

Data were listed as mean value ± standard deviation (SD) of three independent repeated experiments, as the interaction between treatment and experimental variables was not significant. All statistical analyses were performed using SPSS 16.0 software (IBM, Inc., NY, USA). One-way analysis of variance (ANOVA) was used to compare the three mean values. Mean separations were analyzed using Tukey's test correction. Differences at $p < 0.05$ were considered statistically significant.

Results

Occurrence of postharvest diseases

We sampled apple fruits in Weihai, Yantai, and Taian, the main apple-producing areas in Shandong Province, and surveyed postharvest rot. As shown in Table 2 and Figure 1, regardless of the production area, the decay rate of apple fruits under the bagging-free cultivation mode was significantly higher than that under the bagging cultivation mode at the same time point ($p < 0.05$). Ring rot and anthracnose were the most important fungi-associated postharvest diseases of bagging-free apples (Table 3).

Isolation and identification of pathogens

Two strains of fungi were isolated from rotten non-bagging apples and were coded as DH1 and HF2. The colonial morphology and microscopic features of the isolated pathogens are shown in Figures 2A–F. The colony of the first pathogen DH1 was circular on PDA after 4-day incubation, and its color on the front of the plates was white to become dark gray. The aerial mycelia grew radically from the center to the surrounding area, and its texture was loose and cotton-like. Mycelia were hyaline and septate. The germinal spores were the single, colorless, rod-shaped, diameter of (15.0 – 29.5) × (5.1 – 7.6) μm ($n = 40$). The morphology of colonies and conidia was identical with *Botryosphaeria dothidea* (Wang et al., 2020). On the PDA medium of the second pathogen HF2, the colony was circular with regular edges. Mycelia were initially grayish white, and their texture was soft and villous. After 4–7 days, they turned dark gray with orange conidial masses. Under the microscope, we determined that conidia were hyaline and cylindrical to oblong, with 13.0–22.2 μm of length and 5.0–7.2 μm of width ($n = 40$). Morphological characteristics were in accordance with *Colletotrichum gloeosporioides* (Riera et al., 2019).

To further identify the two isolated pathogens, internal transcribed spacer (ITS) regions were sequenced. DNA sequences of these genes were deposited in GenBank with Accession Nos. MT734023 (DH1) and MN594823 (HF2), respectively. The homology sequences were analyzed with MEGA 5.02 software to construct a phylogenetic tree by the neighbor-joining method. Bootstrap values from the neighbor-joining method were determined. *Torreya grandis* (AF259277.1) and *Pestalotiopsis microspora* (KF941280.1) were used as the out-group for DH1 and HF2, respectively. In the phylogenetic tree, DH1 and other reference strain *B. dothidea* (KF766151.1) formed a clade with 100% bootstrap support (Figure 2G), while HF2 and two other reference strain *C. gloeosporioides* (NR160754.1, GQ485605.1) formed a clade with 100% bootstrap support (Figure 2H). Based on morphological features and molecular analysis, DH1 and HF2 were identified as *Botryosphaeria dothidea* (*B. dothidea*) and *Colletotrichum gloeosporioides* (*C. gloeosporioides*), respectively.

Antifungal activity of EOs against *B. dothidea* and *C. gloeosporioides*

We further evaluated the inhibition of mycelial radical growth *in vitro* by fumigation and contact treatments. As presented in Figure 3, the inhibition zone diameter in all treatment exposure to EO was smaller than that in control at 25°C for 96 h. Lower concentrations were needed to inhibit the development of colony diameter by gaseous contact than by solution contact ($p < 0.05$). Both of the two EOs had stronger inhibitory effectiveness on *C. gloeosporioides* than that of *B. dothidea* by both solid and gas diffusion tests ($p < 0.05$), which indicated that *C. gloeosporioides* was more sensitive, while *B. dothidea* was more resistant to EO. In addition, the two EOs showed variable degrees of antifungal activity against the tested pathogens, which was verified by both fumigation and direct contact treatments. For *B. dothidea*, cinnamon EO exhibited an obviously stronger inhibition effect compared with clove EO; however, for *C. gloeosporioides*, cinnamon EO had poorer fungitoxic ability than clove EO. The MIC value of cinnamon and clove EO on *B. dothidea* and *C. gloeosporioides* by contact and vapor diffusion tests as presented in Table 4 confirmed the earlier statement.

Effects of EOs on rot development in inoculated bagging-free apple

Further investigation of the inhibition effects of EOs on the lesion diameter of fruit rot caused by *B. dothidea* and *C. gloeosporioides* demonstrated alleviated severity of corruption after treatment with cinnamon and clove EO fumigation, respectively. As shown in Figure 4, EO groups indicated significant decreases in bagging-free apple rot as compared to the control during the same period of storage after inoculation ($P < 0.05$).

TABLE 2 Infection incidence of postharvest apple fruit.

Treatments	Storage time (d)	Bagging-free cultivation mode			Bagging cultivation mode		
		Weihai	Yantai	Taian	Weihai	Yantai	Taian
Decay rate (%)	20	2.8b	3.5b	7.5a	0c	0c	0c
	40	31.4b	34.3b	45.0a	3.0c	2.0c	2.5c
	60	40.0c	57.1b	66.0a	11.0d	8.0d	12.3d

Different lowercase letters indicate significant differences in the same row ($p < 0.05$).

FIGURE 1
Different levels of fruit decay between bagging-free apple **(A)** and bagging apple **(B)** after 60 days of storage at 25°C.

TABLE 3 Occurrence of different diseases in bagging-free apple.

Treatments	Disease incidence (%)				
	Anthracnose	Bitter pit	Black spot	Ring rot	Rust
Weihai	1.11a	0c	0c	0.97a	0.4b
Yantai	0.88b	0c	0.05c	1.32a	0.72b
Taian	1.39b	0d	0d	1.53a	0.66c

Different lowercase letters indicate significant differences in the same row ($p < 0.05$).

Effects of EOs on hyphal morphology and cellular ultrastructure

From the SEM images in Figure 5, we could intuitively observe the hyphal morphological alterations of *B. dothidea* and *C. gloeosporioides*. In the control groups, the mycelia were smooth, flat, and uniform, presenting a flourishing growth period. After 48 h EO treatment, the hyphae became folded, winding, rough, and even collapsed, indicating the destruction of the mycelium wall.

The effects of EOs on the cellular ultrastructure were observed by TEM. The control samples revealed uniform shapes in which all organelles had a normal and regular appearance and were clearly identified, while in the treated fungi, most organelles were indistinct and unidentifiable with deformed and disorganized mitochondria. Meanwhile, the cell wall was gradually becoming rough and villous, and the cell membrane was partially detached from the cell wall (Figure 5). SEM and TEM analyses partly manifested the mechanism of antimicrobial activity, but further investigation is required to reveal more gene-based changes during treatment with EO.

Transcriptome analysis of *C. gloeosporioides* exposed to clove EO

The overall profile of gene transcription

Based on the results of antifungal activity analysis, we selected clove EO against *C. gloeosporioides* cells to further explore the potential antifungal mechanisms underlying the molecular

10.3389/fmicb.2023.1109028

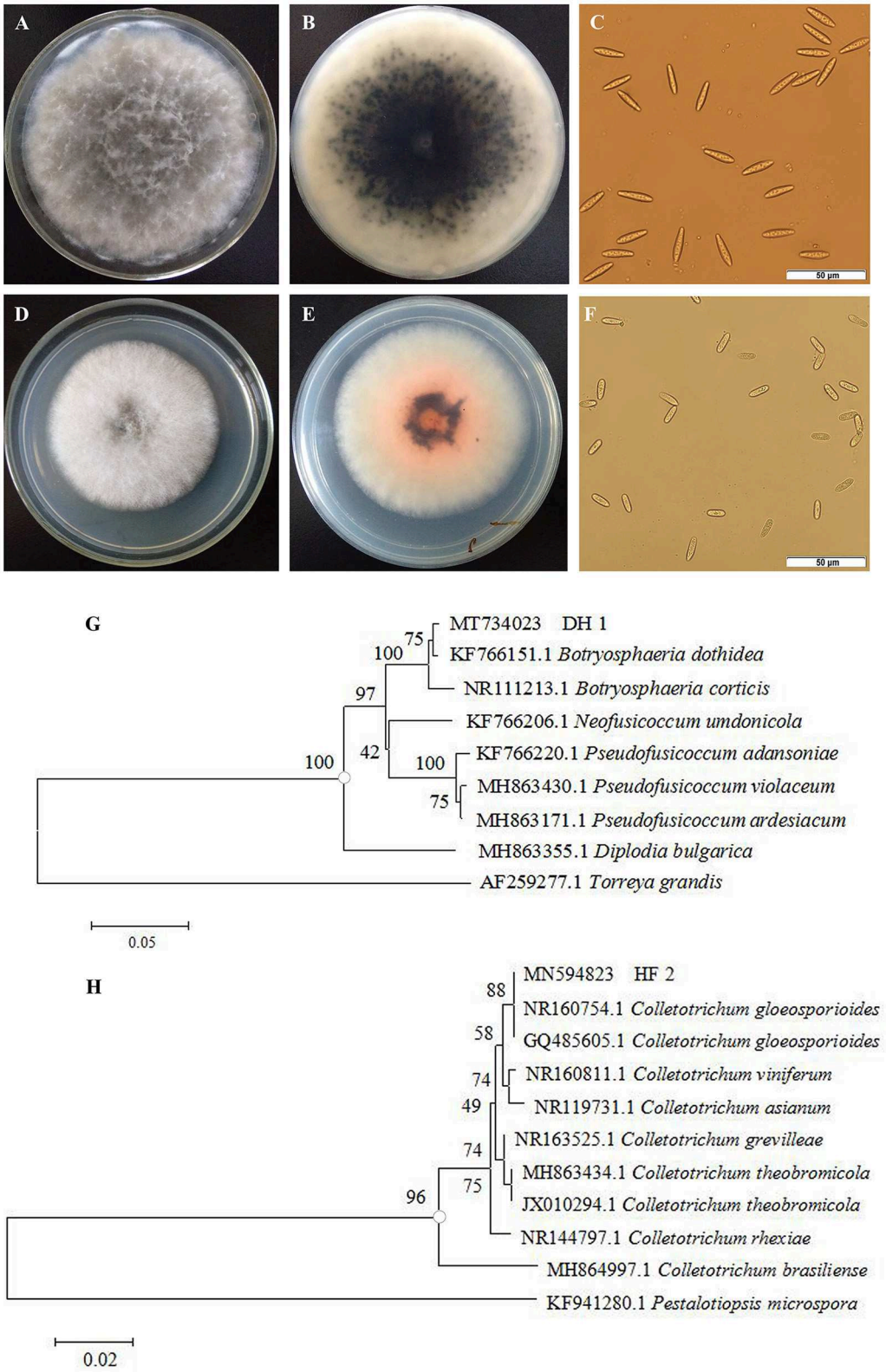

FIGURE 2
Morphological characteristics and phylogenetic tree of isolated pathogens. Colonies of pathogen DH1 **(A, B)** and HF2 **(D, E)**. Spores of pathogen DH1 **(C)** and HF2 **(F)**. Phylogenetic analysis of rDNA-ITS sequences obtained from the isolate DH1 **(G)** and HF2 **(H)** along with the reference sequences from NCBI.

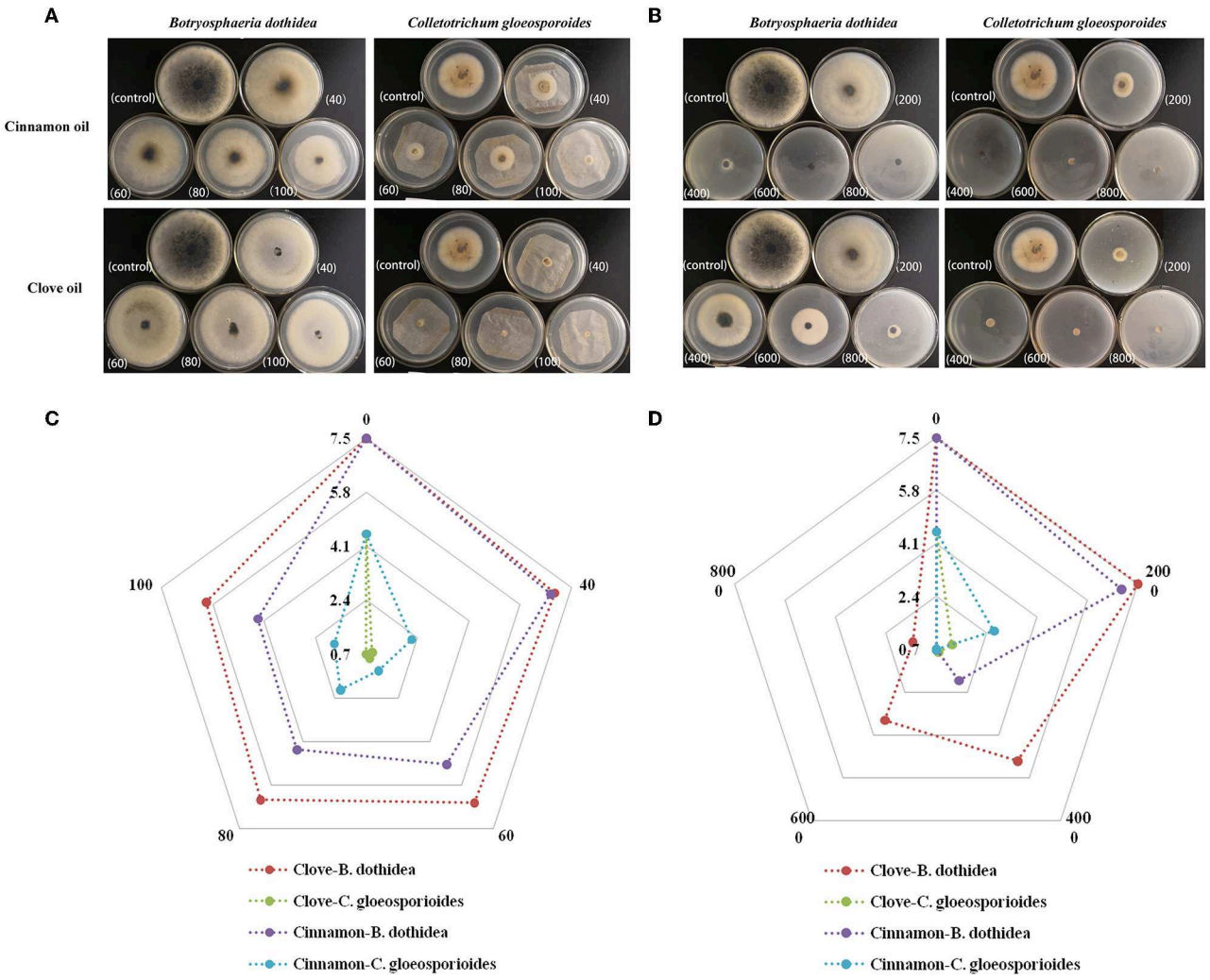

FIGURE 3
Mycelial growth inhibition of cinnamon and clove EOs against *B. dothidea* and *C. gloeosporioides*. **(A)** Morphological images of medium in EO vapor phase. **(B)** Morphological images of medium in EO contact phase. **(C)** Radar map of the radical growth diameters in EO vapor phase. **(D)** Radar map of the radical growth diameters in EO contact phase.

response. High-throughput sequencing of the transcriptome was performed to screen the global gene expression profile changes of *C. gloeosporioides* with or without clove EO fumigation treatment (for 6 h at 1×MIC concentration).

A total of 1,662 genes were identified as significantly differentially expressed genes (DEGs) ($p < 0.05$, $|\mathrm{Log_2FC}| \geq 1$), with 857 genes upregulated and 805 genes downregulated. As shown in Figure 5, all the DEGs were displayed in Heatmap (Figure 6A), volcano plot (Figure 6B), and MA plot (Figure 6C) to be illustrated in a macroscopic view.

Furthermore, all the DEGs were subjected to Gene Ontology (GO) annotation and KEGG enrichment analysis. As shown in Figure 7A, the DEGs were assigned to 19 biological processes, 15 cellular components, and 10 molecular functions. The top three categories of the biological process were the metabolic process (GO0008152), the ingle-organism process (GO0044699), and the cellular process (GO0009987). In the cellular component classification, the most represented categories were membrane (GO0016020), cell (GO0005623), and organelle (GO0043226). These results demonstrated that many DEGs were involved in the changes in cell membrane components, which was consistent with our observation of SEM and TEM. Catalytic activity (GO0003824), binding (GO0005488), and transporter activity (GO0005215) occupied the most variable categories of the molecular function classification.

Biological functions are vital to recognizing the antimicrobial mechanisms of EOs. Then, KEGG enrichment was performed to further explore the DEGs associated with the biological response pathways. In total, the DEGs were assigned to 49 KEGG annotation pathways, and the highly ranked terms were tryptophan metabolism (ko00380), peroxisome (ko04146), ABC transporters (ko02010), fatty acid degradation (ko00071), pantothenate and CoA biosynthesis (ko00770), lysine degradation (ko00310), and phenylalanine metabolism (ko00360), respectively (Figure 8A). From these data, most of the enrichment pathways were relevant to metabolism. Based on both GO annotation and KEGG enrichment,

TABLE 4 MIC values of cinnamon and clove EO on *B. dothidea* and *C. gloeosporioides*.

Treatment	MIC ($\mu L \cdot L^{-1}$)
Vapor phase	
Cinnamon EO-*B. dothidea*	120
Cinnamon EO-*C. gloeosporioides*	80
Clove EO-*B. dothidea*	150
Clove EO-*C. gloeosporioides*	40
Contact phase	
Cinnamon EO-*B. dothidea*	400
Cinnamon EO-*C. gloeosporioides*	300
Clove EO-*B. dothidea*	600
Clove EO-*C. gloeosporioides*	200

some crucial genes or pathways were screened out for further investigation as below.

Regulation of genes related to the cell membrane and cytoplasmic components

The GO enrichment analyses of the cellular component category manifested that membrane-associated items were mainly enriched (Figure 7B), and more genes were downregulated in these GO terms (Supplementary Figure 1D). Furthermore, other terms related to critical cytoplasmic components such as vacuole, Golgi apparatus, and spindle were also enriched (Figure 7B).

Regulation of genes related to cell transmembrane transport

A total of 18 items were involved in transport under the biological process and molecular function category in the GO enrichment analysis (Figures 7C, D). It could be seen that items related to transmembrane transport accounted for the greatest proportion in molecular function classification (Figure 7D), and most of the genes were downregulated (Supplementary Figure 1F), which was consistent with the response of cell membrane mentioned in the previous paragraph.

Meanwhile, as shown in the KEGG database, ATP-binding cassette (ABC) transport (ko02010), the most enriched pathway assigned to the environment information processing category (Figure 8B), was selected for further analysis. There were 18 DEGs in the ABC transport pathway with both upregulated and downregulated (Figure 8A). For example, POU3F3 (encoding POU domain, class 3, transcription factor 3, $\log_2$ FC = 9.84), *CH25H* (encoding cholesterol 25-hydroxylase, $\log_2$ FC = 1.76), and *TMEM258* (encoding transmembrane protein 258, $\log_2$ FC = 3.35) of ABCG2 subfamily (involved in the export of toxic compounds, organic anionic, and the translocation of various lipid molecules) were all upregulated. *Prdm1* (encoding PR domain zinc finger protein 1, $\log_2$ FC = −1.38), *CSH2* (encoding somatotropin family of hormones, $\log_2$ FC = −1.25), *AGA* (encoding aspartylglucosaminidase, $\log_2$ FC = −4.22) of ABCB1 subfamily (involved in the export of mitochondrial peptides, pheromone, and xenobiotics), and *ASIC2* (encoding decentering/epithelial sodium channel, $\log_2$ FC = −3.15), *RLF* (encoding Zn-15 related zinc finger protein, $\log_2$ FC = −2.74), and *ZNF137P* (encoding zinc finger protein 137, $\log_2$ FC = −4.73) of ABCG2 were all downregulated.

Regulation of genes related to the oxidation/reduction reaction

Gene Ontology enrichment analysis illustrated that the oxidation/reduction reaction of *C. gloeosporioides* cells was remarkably affected by clove EO treatment. As demonstrated in Figures 7C, D, oxidation–reduction process was enriched in the biological process and molecular function category. The expressions of about two-thirds of the DEGs involved in the oxidation/reduction reaction process were upregulated (Supplementary Figures S1B, C).

Docking analysis of EOs constituents with CYP51 of pathogenic fungi

According to the TEM observation and the transcriptome analysis, it could be deduced that the presence of the EOs led to the alterations of the cell membrane composition and transmembrane transport function in the pathogenic fungi. To characterize the EO's antifungal mechanism more specifically and completely, molecular docking was used to explore the potential binding site of the inhibitory interaction. From the results of GC-MS analysis shown in Table 1, the main chemical components of cinnamon and clove EO were *trans*-cinnamaldehyde and eugenol, which have been reported as effective antimicrobial agents for foodborne pathogenic microorganisms in many studies. Here, *in silico* analysis studies could provide insight into the potential binding affinity of *trans*-cinnamaldehyde and eugenol with the key transmembrane protein CYP51.

Homology modeling

The 3D structures of CYP51 of *C. gloeosporioides* and *B. dothidea* have not yet been analyzed; therefore, based on their amino acid sequences, homology modeling was utilized to obtain the best models of the two CYP51 proteins. Then, model qualities were assessed by the online tool SAVES. As shown in Ramachandran plots, CYP51 of *C. gloeosporioides* had 88.2% of the amino acid residues in the most favored regions (red areas) and 9.6% in the additional allowed regions (yellow areas) (Figure 9A); CYP51 of *B. dothidea* had 88.9% of the amino acid residues in the most favored regions (red areas), and 9.9% are in additional allowed regions (yellow areas) (Figure 9B); the proportion of total amino acids in the reasonable range is 97.8 and 98.8%, respectively (Figures 9A, B), which were indications of high quality for a model.

In silico analysis

The optimal binding conformations of eugenol with CYP51 of *C. gloeosporioides* and *trans*-cinnamaldehyde with CYP51 of

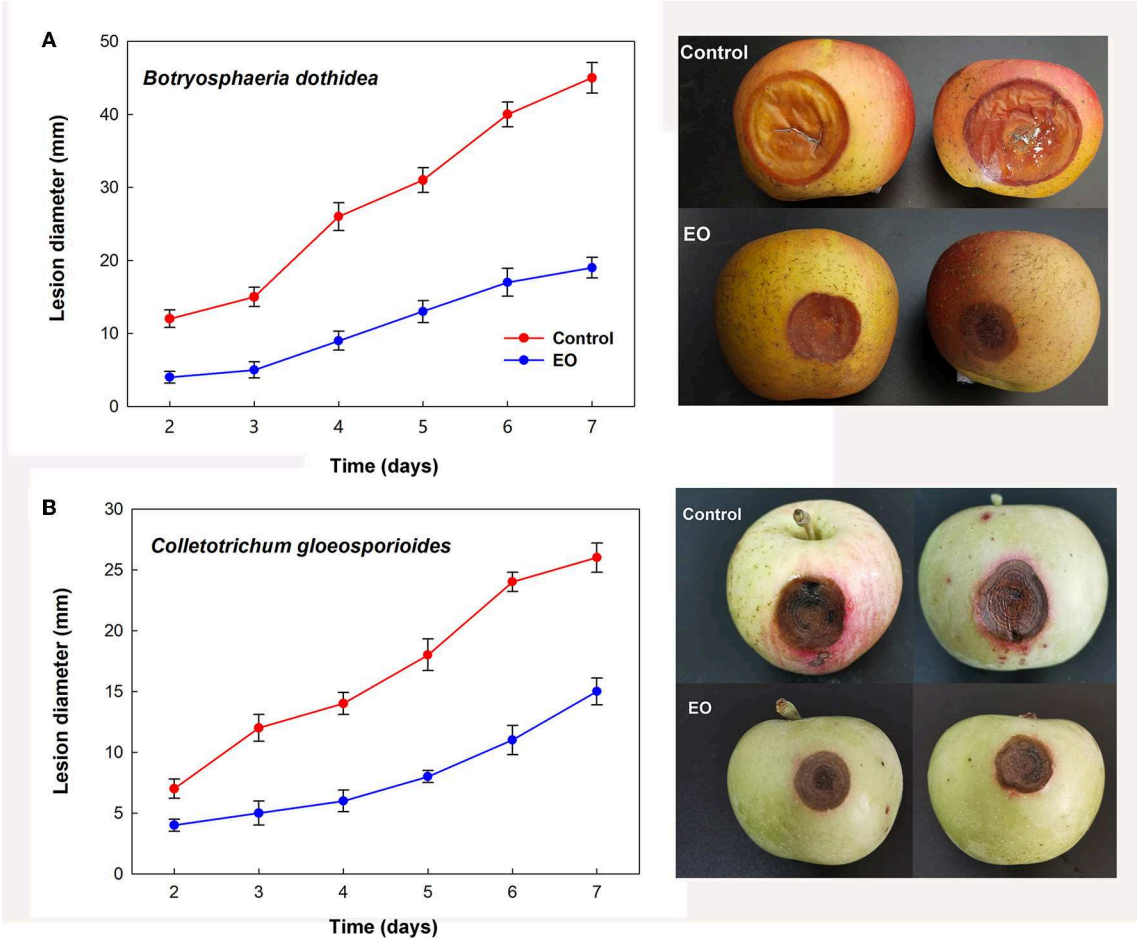

FIGURE 4
Controlling effect of cinnamon and clove EO on mold rot caused by *B. dothidea* **(A)** and *C. gloeosporioides* **(B)** in bagging-free apple. Bar represents the standard deviation of the means of three independent experiments. Lesions in apple fruit are also shown after 7 days of storage at 25°C.

B. dothidea were shown in Figures 9C, D, with a binding score of −4.45 and −4.69 kJ mol^{-1}, respectively. Eugenol was well-embedded into a cavity in the vicinity of the active site, showing a hydrophobic behavior with the key amino acid residues which included Leu116, Ala292, Ile295, Asn296, Thr369, Gly370, and Ala494 (Figure 9C). *Trans*-cinnamaldehyde formed one hydrogen bond with Arg122 and interacted with other residues (Phe117, Ile143, Gly288, Ala289, Ala292, and Leu447) *via* the hydrophobic effect (Figure 9D). It was suggested that *trans*-cinnamaldehyde showed a better *in silico* affinity toward CYP51 than eugenol because of a higher binding score and additional hydrogen bond.

Discussion

Because of the relatively low rot rate of bagging apples under low temperatures and controlled atmosphere conditions, a previous study has been largely focused on postharvest physiological diseases, for instance, superficial scald and bitter pit (Susan and Watkins, 2012; Jarolmasjed et al., 2016). In this study, a higher rot degree was found in apple fruit under bagging-free cultivation mode (Figure 1; Table 2); thus, pathological research related to the control of fungal decay during the conservation period is vital to raise the commercial value of bagging-free fresh fruit.

The advantage of EOs is their bioactivity in the vapor phase, making postharvest sterilization processing more convenient for the stored commodity (Tzortzakis, 2009). It was found that EOs of the volatile phase were effective at a very low concentration and were beneficial in limiting the spread of the pathogen by lowering the spore load (Chutia et al., 2009). The results of the present study indicated that cinnamon and clove EO in vapor and contact phases both showed antifungal activity on the mycelial growth of *B. dothidea* and *C. gloeosporioides* in a concentration-dependent manner *in vitro* condition, and the volatile phase exhibited more toxic than the contact (Figure 3). SEM also demonstrated large and abnormal alterations in hyphal morphology, indicating the degeneration of fungal hyphae (Figure 5). Furthermore, *B. dothidea* and *C. gloeosporioides* had variable resistance against cinnamon and clove EO, which could be related with distinct sensitivity of pathogenic cells to the different types and amounts of EO components. Cinnamon and clove EO are classified as "generally regarded as safe" (GRAS) by the United State Food and Drug

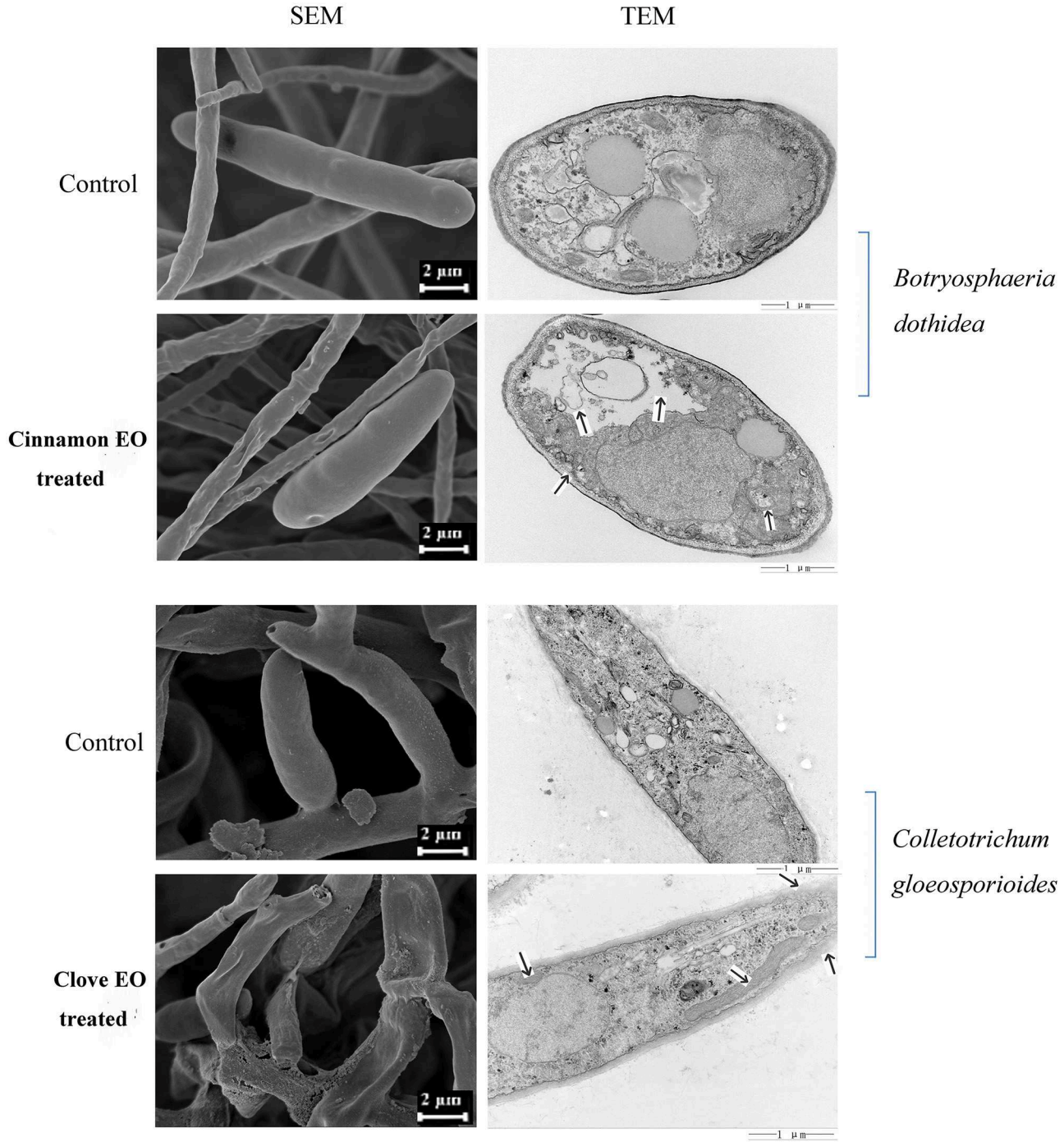

FIGURE 5
SEM and TEM micrograph of pathogen cells treated and untreated with EOs.

Administration (Hammer et al., 2006). For the *in vivo* test, the EOs vapor treatment also alleviated the severity of fruit rot in artificially infected bagging-free apples (Figure 4). In the future, the synergistic or additive effects between the two EOs could be further investigated to reduce the active doses needed to control postharvest rot for bagging-free apple.

The fungal cell membrane consists of a semi-permeable lipid bilayer that protects the integrity of the cell along with maintaining the cell shape and regulates the transport of materials entering and exiting the cell. It is the main target for the fungistatic action of EOs due to their lipophilicity (Burt, 2004; Paul et al., 2011). For example, tea tree EO destroyed membrane integrity and increases the permeability of *Botrytis cinerea*, resulting in ion leakage and membrane dysfunction (Yu et al., 2015). Bayer et al. (2000) and Pasqua et al. (2007) demonstrated a strong decrease in the unsaturated fatty acids and a high degree of

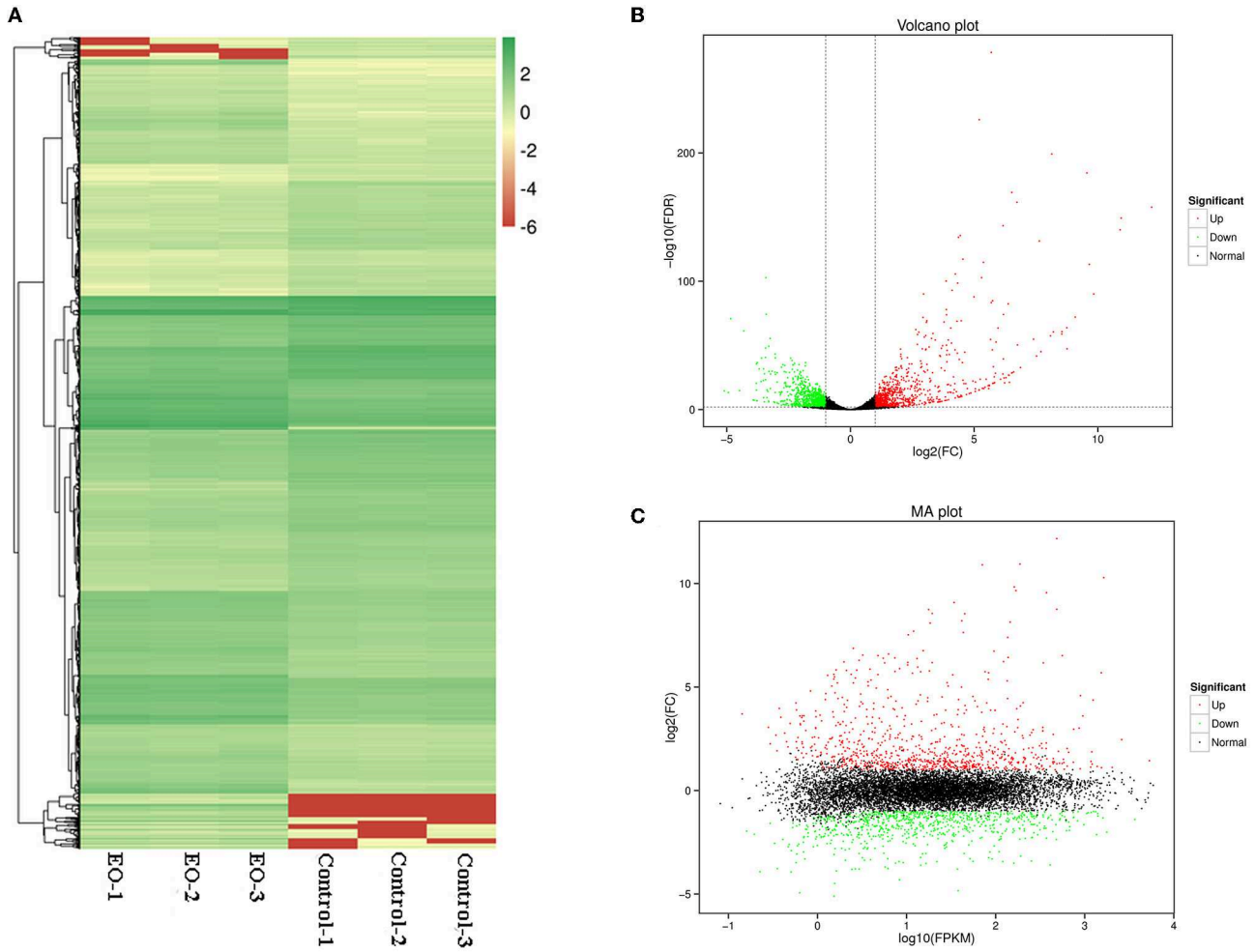

FIGURE 6
Differentially expressed genes (DEGs) analyzed in *C. gloeosporioides* cells for global comparison of transcription profiles (clove EO treatment vs. control). **(A)** Heatmap. **(B)** Volcano plot. **(C)** MA plot.

saturated fatty acids in the fungal membrane in essential oil-treated bacteria, causing a decrease in membrane fluidity and a consequent increase in its rigidity. In our previous study, clove EO exposure to *C. gloeosporioides* caused leakage of intracellular proteins and nucleic acids and ultimately cell lysis (Wang et al., 2019). Our TEM observation found the shriveled, ruptured, or disappeared plasmalemma, the loss or disappearance of cytoplasm, and the extrusion of abundant material from the outside of the cell wall (Figure 5). Transcriptome had been widely used to conduct a preliminary analysis of the gene-based mechanisms by which active substances inhibit pathogens, such as thymol against *Fusarium oxysporum* (Liu et al., 2022) and nerol against *Ceratocystis fimbriata* (Li X. Z. et al., 2021). The GO terms assigned by DEGs related to membrane occupied the most represented categories of the cellular component classification (Figure 7B), and the majority of genes were downregulated (Supplementary Figure S1D), inferring that these genes might be the target of clove EO to destroy the cellular membrane. The membrane undertakes the function of transmembrane transport of various substances; after treatment of clove EO, the genes coding the structure and component of the cell membrane were downregulated, which may decrease the overall capacity of cellular molecules transport. ABC proteins, which were exclusively found in both prokaryotes and eukaryotes, form a large subfamily of ATP-dependent transporters that participate in mediating cellular import and export processes and play vital physiological roles (Wilkens, 2015). Approximately 18 DEGs associated with ABC transporters were detected (Figure 8A), implying that the regulation of materials transport (such as lipids, toxins, minerals, and organic ions) altered significantly after clove EO treatment. Ergosterol is the major sterol component of the fungal cell membrane, helping to maintain cell function and integrity, and is considered the fundamental target of antifungal drugs (Pinto et al., 2013). As mentioned earlier, dill EO could cause a considerable reduction in ergosterol quantity (Tian et al., 2012). CYP51 belongs to a main transmembrane protein and serves as the key enzyme in the fungi ergosterol biosynthesis pathway (Zhang et al., 2019). The suitability of CYP51 as an antifungal azole target has been discussed in many previous studies (Song et al., 2018); however, there is still limited information about the relationship between the antifungal action of EOs and CYP51. To

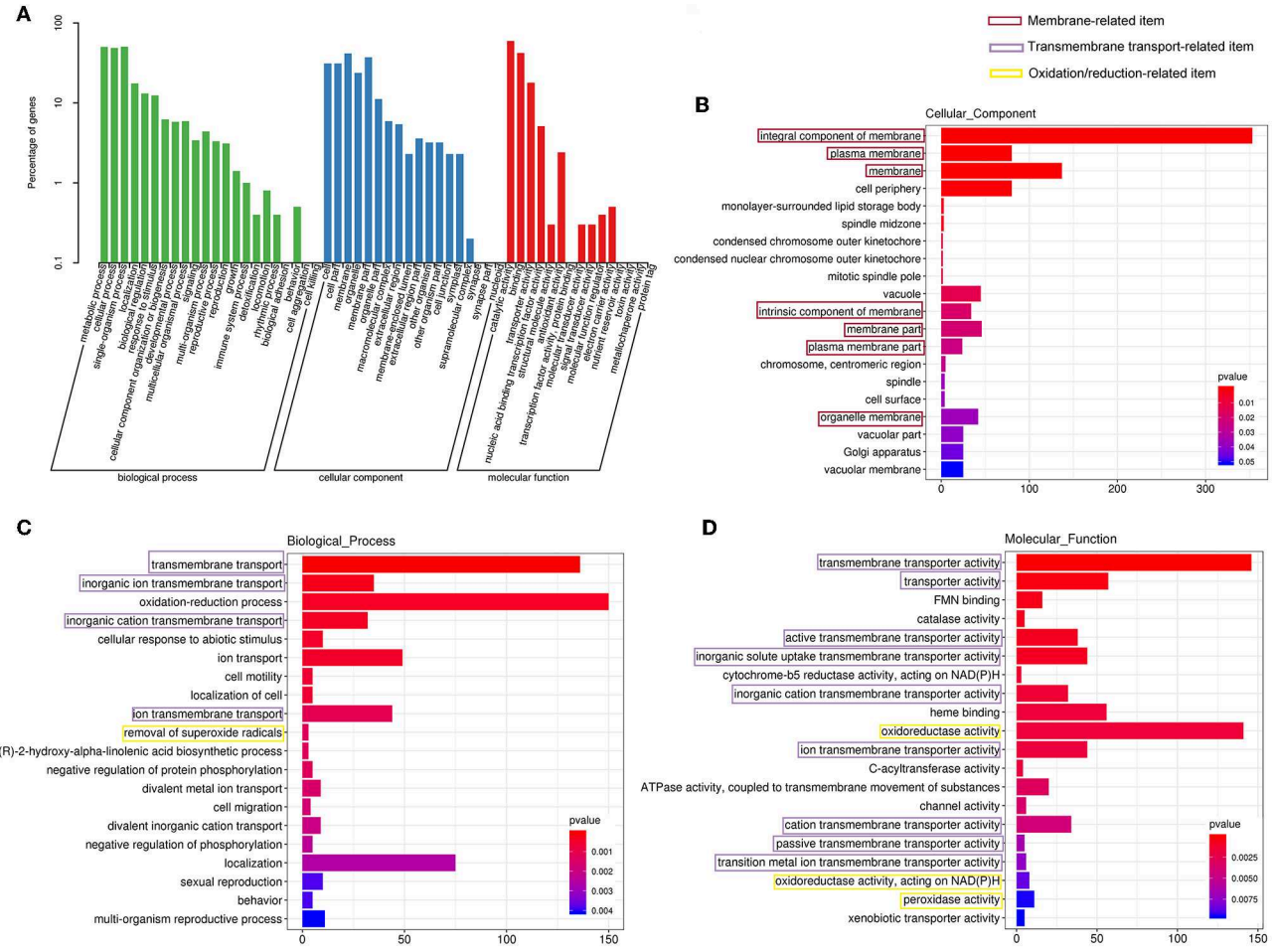

FIGURE 7
Gene Ontology (GO) analysis of the differentially expressed genes. **(A)** The GO classification. GO enrichment for cellular component **(B)**, biological process **(C)**, and molecular function **(D)** category, respectively.

investigate the inhibitory mechanism of cinnamon and clove EO on *B. dothidea* and *C. gloeosporioides*, relevant protein-molecular interactions were first evaluated by *in silico* analysis. According to the molecular docking results, we noticed high binding scores of *trans*-cinnamaldehyde and eugenol with the protein CYP51 of the two identified pathogenic fungi. *Trans*-cinnamaldehyde and eugenol entered the active pocket of the protein and led to instability of the catalytic region, which further attenuated CYP51 activity and decreased ergosterol content. In CYP51 of *C. gloeosporioides*, eugenol was well-embedded into a cavity in the vicinity of the active site, the key residues of which included Leu116, Ala292, Ile295, Asn296, Thr369, Gly370, and Ala494 (Figure 9C). In CYP51 of *B. dothidea*, *trans*-cinnamaldehyde formed one hydrogen bond with Arg122 and showed a hydrophobic behavior with other residues (Phe117, Ile143, Gly288, Ala289, Ala292, and Leu447) (Figure 9D). The hydrogen bonding is considered to play a major role in the protein-molecular interactions (Gerdt et al., 2015). In this study, *trans*-cinnamaldehyde showed a better *in silico* affinity toward CYP51 than eugenol because of a higher binding score and additional hydrogen bond. Our data confirmed that the inhibitory mechanism of EOs on the cell membrane of pathogens might involve the interaction of antifungal components with the CYP51 protein and subsequent interference of ergosterol biosynthesis. These findings strongly supported EOs inhibited the pathogen microorganism through loss of cytoplasmic membrane integrity and function.

One of the earliest and most prominent fungi defense responses is an oxidative burst. Our transcriptome data also showed that the oxidation/reduction reaction of *C. gloeosporioides* cells was remarkably affected by clove EO treatment (Figures 7C, D), and the expression of the majority of the DEGs involved was upregulated (Supplementary Figures S1B, C), which corresponds to the findings of Guo et al. (2019) and Wu et al. (2022). This indicated that clove EO caused some degree of oxidative stress and activated defensive function against stress response to enhance the antioxidant capacity of *C. gloeosporioides*, but some other antifungal agents, such as iturin A and acriflavine, downregulated most genes involved in oxidation–reduction reaction of fungi (Persinoti et al., 2014; Jiang et al., 2020). This discrepancy suggested that the oxidation/reduction process might respond distinctly under various stimuli or stress.

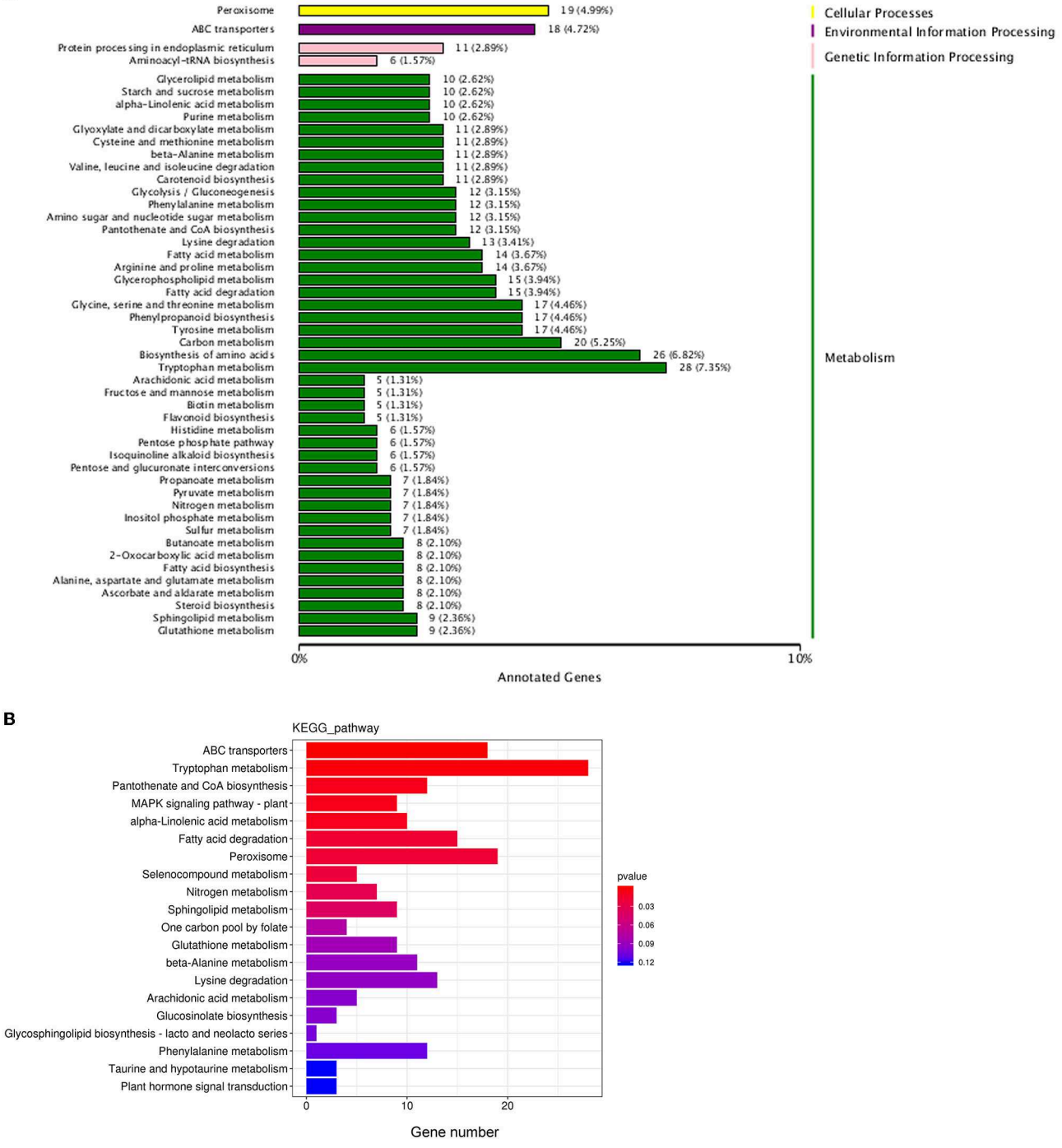

FIGURE 8
Statistical analysis of the differentially expressed genes in KEGG pathways. **(A)** The KEGG pathways annotation; **(B)** the enrichment of the differentially expressed genes in KEGG pathways.

In addition, the clove EO showed a marked disruption of the cell wall and major organelles such as mitochondria, Golgi apparatus, vacuole, and disorder of biological functions including metabolism of crucial materials (Figures 7, 8). Overall, EOs contribute to antimicrobial activity through diverse modes of action, which need further investigation.

Despite the prominent preservative potency of EOs in the food system, some limitations have been recognized in their practical application, such as negative effect on organoleptic properties, volatility, low water solubility, and low stability, which prevent their large-scale practical utilization (Akash et al., 2021). Hence, specific delivery systems are required for a gradual release of EO aroma compatible with food-based applications. Nanoencapsulation (Das

10.3389/fmicb.2023.1109028

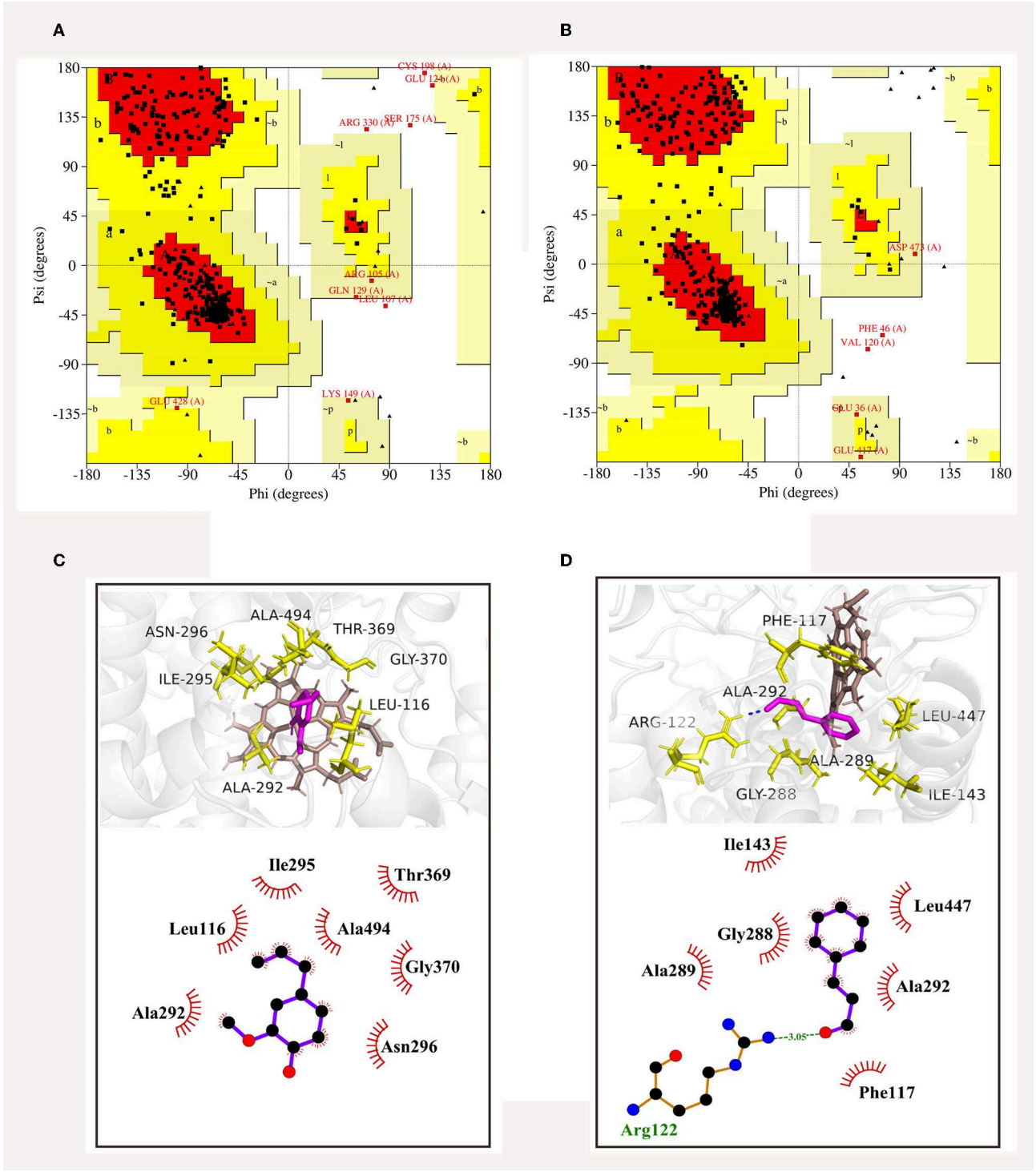

FIGURE 9
Ramachandran plots of CYP51 of *C. gloeosporioides* **(A)** and *B. dothidea* **(B)**, as well as the 3D and 2D diagrams of docked modes of CYP51 with *trans*-cinnamaldehyde **(C)** and eugenol **(D)**.

et al., 2021), active packaging (Li et al., 2018), and polymer-based coating (Guerra et al., 2016) are promising delivery strategies of EOs that help ease dispersion with consistent antimicrobial action and enhancement in food shelf life. Furthermore, controlled release behavior minimizes EO's impact on food organoleptic attributes and showed better diffusion kinetics.

The increased use of EOs has also raised serious concerns with respect to their eventual adverse health and environmental

effects, though this is still waiting to be confirmed (Woolf, 1999). In the national standards for food safety of China, EO is the designation for ingredients approved as food additives. In America, EO is considered "Generally Recognized as Safe" (GRAS) by the Food and Drug Administration (FDA), but the documents do not include dosages that are considered safe. In fact, there was evidence that when EOs are inappropriately used, they can give adverse effects in humans, such as skin irritation, headache, and nausea (Fandohan et al., 2008). Burdock and Carabin (2009) reported a non-observed adverse effect level (NOAEL) for *Coriandrum sativum* L. essential oil of ∼160 mg/kg/day in rats, being considered safe at the present concentration used in food. Consumption of horticultural commodities treated with these oils is likely to be safe for humans if the recommended oil concentration is respected. Current information indicates that EOs are safe for the consumer and the environment with a few qualifications (Isman, 2000; Antunes and Cavaco, 2010). Considering the food-based industrial relevance of EOs, possible toxicological studies in a mammalian system and the market value of EOs need to be further investigated for their potential application as eco-friendly smart green preservatives in the food and agriculture industries.

Conclusion

In the current study, the results demonstrated that the main pathogens causing postharvest decay of bagging-free apples were *B. dothidea* and *C. gloeosporioides*. *In vitro* and *in vivo* trials indicated that cinnamon and clove EOs fumigation effectively limited fungal growth and reduced rot. The two identified organisms had variable resistance against the tested Eos; consequently, cinnamon and clove EOs will be further studied for their synergistic effects on the control of postharvest spoilage in bagging-free apples. Morphological, transcriptomic, and docking analyses suggested that EOs reduced the component synthesis and activity of fungal cell membranes and disturbed the biological function of cytoplasmic components as a whole. In a word, cinnamon and clove EOs are potential biocontrol agent candidates for preventing and controlling diseases of bagging-free apples, but detailed examinations of the biological activity and undesirable effects on the postharvest fruit or on human health and the environment require further investigations.

Data availability statement

The datasets presented in this study can be found in online repositories. The names of the repository/repositories and accession number(s) can be found in the article/Supplementary material.

Author contributions

DW: methodology, writing—original draft, and visualization. GW: investigation and formal analysis. JW: resources, investigation, and writing—reviewing and editing. HZ: conceptualization, methodology, resources, and writing—reviewing and editing. XX: supervision, project administration, and funding acquisition. All authors contributed to the article and approved the submitted version.

Funding

This study was supported by the China Agriculture Research System of MOF and MARA (CARS-27).

Conflict of interest

The authors declare that the research was conducted in the absence of any commercial or financial relationships that could be construed as a potential conflict of interest.

Publisher's note

Supplementary material

The Supplementary Material for this article can be found online at: https://www.frontiersin.org/articles/10.3389/fmicb.2023.1109028/full#supplementary-material

SUPPLEMENTARY FIGURE S1
GO enrichment of up- **(A–C)** and down- **(D–F)** regulated genes for cellular component, biological process, and molecular function category.

References

Akash, M., Jitendra, P., Somenath, D., and Kumar, D. A. (2021). Essential oils and their application in food safety. *Front. Sustain. Food Syst.* 5, 653420. doi: 10.3389/fsufs.2021.653420

Alanazi, S., Alnoman, M., Banawas, S., Saito, R., and Sarker, M. R. (2018). The inhibitory effects of essential oil constituents against germination, outgrowth and vegetative growth of spores of *Clostridium perfringens* type A in laboratory medium and chicken meat. *Food Microbiol.* 73, 311–318. doi: 10.1016/j.fm.2018.02.003

Almeida, E. T. D. C., de Souza, G. T., de Sousa Guedes, J. P., Barbosa, I. M., de Sousa, C. P., Castellano, L. R. C., et al. (2019). Menthapiperita L. essential oil inactivates spoilage yeasts in fruit juices through the perturbation of different physiological functions in yeast cells. *Food Microbiol.* 82, 20–29. doi: 10.1016/j.fm.2019.01.023

Antunes, M. D. C., and Cavaco, A. M. (2010). The use of essential oils for postharvest decay control. A review. *Flavour Fragr. J.* 25, 351–366. doi: 10.1002/ffj.1986

Arakawa, O., Uematsu, N., and Nakajima, H. (1994). Effect of bagging on fruit quality in apples [*Malus pumila*]. *Bull. Faculty Agric. Hirosaki Univ.* 57, 25–32.

Bayer, A. S., Presad, R., Chandra, J., Koul, A., Smirti, A. M., Varma, A., et al. (2000). *In vitro* resistance of *Staphylococcus aureus* to thrombin induced platelet microbicidal protein is associated with alterations in cytoplasmic membrane fluidity. *Infect. Immun.* 68, 3548–3553. doi: 10.1128/IAI.68.6.3548-3553.2000

Burdock, G. A., and Carabin, I. G. (2009). Safety assessment of coriander (*Coriandrum sativum* L.) essential oil as a food ingredient. *Food Chem. Toxicol.* 47, 22–34. doi: 10.1016/j.fct.2008.11.006

Burt, S. (2004). Essential oils: their antibacterial properties and potential applications in foods-a review. *Int. J. Food Microbiol.* 94, 223–253. doi: 10.1016/j.ijfoodmicro.2004.03.022

Castellanos, L. M., Olivas, N. A., Ayala-Soto, J., De La O Contreras, C. M., Ortega, M. Z., Salas, F. S., et al. (2020). *In vitro* and *in vivo* antifungal activity of clove (*Eugenia caryophyllata*) and pepper (*Piper nigrum* L.) essential oils and functional extracts against *Fusarium oxysporum* and *Aspergillus niger* in tomato (*Solanum lycopersicum* L.). *Int. J. Microbiol.* 30, 1702037. doi: 10.1155/2020/1702037

Chen, C. S., Zhang, D., Wang, Y. Q., Li, P. M., and Ma, F. W. (2012). Effects of fruit bagging on the contents of phenolic compounds in the peel and flesh of 'Golden Delicious', 'Red Delicious', and 'Royal Gala' apples. *Sci. Hortic.* 142, 68–73. doi: 10.1016/j.scienta.2012.05.001

Chutia, M., Deka Bhuyan, P., Pathak, M. G., Sarma, T. C., and Boruah, P. (2009). Antifungal activity and chemical composition of *Citrus reticulata* Blanco essential oil against phytopathogens from North East India. *LWT* 42, 777–780. doi: 10.1016/j.lwt.2008.09.015

Das, S., Singh, V. K., Dwivedy, A. K., Chaudhari, A. K., and Dubey, N. K. (2021). *Anethum graveolens* essential oil encapsulation in chitosan nanomatrix: investigations on *in vitro* release behavior, organoleptic attributes, and efficacy as potential delivery vehicles against biodeterioration of rice (*Oryza sativa* L.). *Food Bioprocess. Technol.* 14, 1–23. doi: 10.1007/s11947-021-02589-z

Dávila-Rodríguez, M., López-Malo, A., Palou, E., Ramírez-Corona, N., and Jiménez-Munguía, M. T. (2019). Antimicrobial activity of nanoemulsions of cinnamon, rosemary, and oregano essential oils on fresh celery. *LWT* 112, 108247. doi: 10.1016/j.lwt.2019.06.014

Delano, W. (2002). *The PyMOL Molecular Graphics System*. San Carlos, CA: Delano Scientific.

Dong, Y., Liu, X., An, Y., Liu, M., Han, J., and Sun, B. (2020). Potent arylamide derivatives as dual-target antifungal agents: design, synthesis, biological evaluation, and molecular docking studies. *Bioorg. Chem.* 99, 103749. doi: 10.1016/j.bioorg.2020.103749

Duduk, N., Markovic, T., Vasic, M., Duduk, B., Vico, I., and Obradovic, A. (2015). Antifungal activity of three essential oils against *Colletotrichum acutatum*, the causal agent of strawberry anthracnose. *J. Essent. Oil Bear Plants* 18, 529–537. doi: 10.1080/0972060X.2015.1004120

El amrani, S., El OualiLalami, A., Ezzoubi, Y., Moukhafi, K., Bouslamti, R., and Lairini, S. (2019). Evaluation of antibacterial and antioxidant effects of cinnamon and clove essential oils from Madagascar. *Mater. Today* 13, 762–770. doi: 10.1016/j.matpr.2019.04.038

Fallahi, E., Colt, W. M., Baird, C. R., Fallahi, B., and Chun, I. J. (2001). Influence of nitrogen and bagging on fruit quality and mineral concentrations of 'BC-2 Fuji' apple. *Horttechnology* 11, 462–466. doi: 10.21273/HORTTECH.11.3.462

Fandohan, P., Gnonlonfin, B., Laleye, A., Gbenou, J. D., Darboux, R., and Moudachirou, M. (2008). Toxicity and gastric tolerance of essential oils from *Cymbopogon citratus*, *Ocimum gratissimum* and *Ocimum basilicum* in Wistar rats. *Food Chem. Toxicol.* 46, 2493–2497. doi: 10.1016/j.fct.2008.04.006

Feng, F. J., Li, M. J., Ma, F. W., and Cheng, L. L. (2014). The effects of bagging and debagging on external fruit quality, metabolites, and the expression of anthocyanin biosynthetic genes in 'Jonagold' apple (Malus domestica Borkh). *Sci. Hortic.* 165, 123–131. doi: 10.1016/j.scienta.2013.11.008

Gerdt, J. P., Mcinnis, C. E., Schell, T. L., and Blackwell, H. E. (2015). Unraveling the contributions of hydrogen-bonding interactions to the activity of native and non-native ligands in the quorum-sensing receptor LasR. *Org. Biomol. Chem.* 13, 1453–1462. doi: 10.1039/C4OB02252A

Guerra, I. C. D., de Oliveira, P. D. L., Santos, M. M. F., Lúcio, A. S. S. C., Tavares, J. F., and Barbosa-Filho, J. M. (2016). The effects of composite coatings containing chitosan and *Mentha* (piperita L. or x villosa Huds) essential oil on postharvest mold occurrence and quality of table grape cv. Isabella. *Innovat. Food Sci. Emerg. Technol.* 34, 112–121. doi: 10.1016/j.ifset.2016.01.008

Guo, J. J., Gao, Z. P., Li, G. Y., Fu, F. H., Liang, Z. N., Zhu, H., et al. (2019). Antimicrobial and antibiofilm efficacy and mechanism of essential oil from *Citrus Changshan-huyou* Y. B. chang against Listeria monocytogenes. *Food Control* 105, 256–264. doi: 10.1016/j.foodcont.2019.06.014

Hammer, K. A., Carson, C. F., Riley, T. V., and Nielsen, J. B. (2006). A review of the toxicity of *Melaleuca alternifolia* (tea tree) oil. *Food Chem. Toxicol.* 44, 616–625. doi: 10.1016/j.fct.2005.09.001

Hofer, U. (2019). The cost of antimicrobial resistance. *Nat. Rev. Microbiol.* 17, 3. doi: 10.1038/s41579-019-0152-2

Holmes, A. H., Moore, L. S., Sundsfjord, A., Steinbakk, M., Regmi, S., Karkey, A., et al. (2016). Understanding the mechanisms and drivers of antimicrobial resistance. *Lancet* 387, 176–187. doi: 10.1016/S0140-6736(15)00473-0

Isman, M. B. (2000). Plant essential oils for pest and disease management. *Crop Prot.* 19, 603–608. doi: 10.1016/S0261-2194(00)00079-X

Jarolmasjed, S., Espinoza, C. Z., Sankaran, S., and Khot, L. R. (2016). Postharvest bitter pit detection and progression evaluation in 'Honeycrisp' apples using computed tomography images. *Postharvest Biol. Technol.* 118, 35–42. doi: 10.1016/j.postharvbio.2016.03.014

Jiang, C. M., Li, Z. Z., Shi, Y. H., Guo, D., Pang, B., Chen, X. Q., et al. (2020). *Bacillus subtilis* inhibits *Aspergillus carbonarius* by producing iturinA, which disturbs the transport, energy metabolism, and osmotic pressure of fungal cells as revealed by transcriptomics analysis. *Int. J. Food Microbiol.* 330, 108783. doi: 10.1016/j.ijfoodmicro.2020.108783

Ju, J., Xu, X. M., Xie, Y. F., Guo, Y. H., Cheng, Y. L., Qian, H., et al. (2018). Inhibitory effects of cinnamon and clove essential oils on mold growth on baked foods. *Food Chem.* 240, 850–855. doi: 10.1016/j.foodchem.2017.07.120

Khaleque, M. A., Keya, C. A., Hasan, K. N., Hoque, M. M., Inatsu, Y., and Bari, M. L. (2016). Use of cloves and cinnamon essential oil to inactivate *Listeria monocytogenes* in ground beef at freezing and refrigeration temperatures. *LWT* 74, 219–223. doi: 10.1016/j.lwt.2016.07.042

Kwon, S. J., Chang, Y., and Han, J. (2017). Oregano essential oil-based natural antimicrobial packaging film to inactivate *Salmonella enterica* and yeasts/molds in the atmosphere surrounding cherry tomatoes. *Food Microbiol.* 65, 114–121. doi: 10.1016/j.fm.2017.02.004

Laskowski, R. A., and Swindells, M. B. (2011). LigPlot+: multiple ligand-protein interaction diagrams for drug discovery. *J. Chem. Inf. Model.* 51, 2778–2786. doi: 10.1021/ci200227u

Li, J., Fu, S., Fan, G., Li, D. M., Yang, S. Z., Peng, L. T., et al. (2021). Active compound identification by screening 33 essential oil monomers against *Botryosphaeria dothidea* from postharvest kiwifruit and its potential action mode. *Pest. Biochem. Physiol.* 179, 104957. doi: 10.1016/j.pestbp.2021.104957

Li, J., Ye, F., Lei, L., and Zhao, G. (2018). Combined effects of octenylsuccination and oregano essential oil on sweet potato starch films with an emphasis on water resistance. *Int. J. Biol. Macromol.* 115, 547–553. doi: 10.1016/j.ijbiomac.2018.04.093

Li, W. R., Shi, Q. S., Liang, Q., Xie, X. B., Huang, X. M., and Chen, Y. B. (2014). Antibacterial activity and kinetics of Litseacubeba oil on *Escherichia coli*. *PLoS ONE* 9, e110983. doi: 10.1371/journal.pone.0110983

Li, X. Z., Liu, M., Huang, T. G., Yang, K. L., Zhou, S. H., Li, Y. X., et al. (2021). Antifungal effect of nerol via transcriptome analysis and cell growth repression in sweet potato spoilage fungi *Ceratocystis fimbriata*. *Postharvest Biol. Technol.* 171, 111343. doi: 10.1016/j.postharvbio.2020.111343

Liu, Y. L., Liu, S. H., Luo, X. G., Wu, X., Ren, J., Huang, X. Q., et al. (2022). Antifungal activity and mechanism of thymol against *Fusarium oxysporum*, a pathogen of potato dry rot, and its potential application. *Postharvest Biol. Technol.* 192, 112025. doi: 10.1016/j.postharvbio.2022.112025

Monk, B. C., Sagatova, A. A., Hosseini, P., Ruma, Y. N., Wilson, R. K., and Keniya, M. V. (2020). Fungal Lanosterol 14α-demethylase: a target for next-generation antifungal design. *Biochim Biophys Acta Prot. Proteom.* 1868, 140206. doi: 10.1016/j.bbapap.2019.02.008

Moreira, R. R., Peres, N. A., and May De Mio,. L. L. (2019). *Colletotrichum acutatum* and *C. gloeosporioides* species complexes associated with apple in Brazil. *Plant Dis.* 103, 268–275. doi: 10.1094/PDIS-07-18-1187-RE

Morris, G. M., Huey, R., Lindstrom, W., Sanner, M. F., Belew, R. K., Goodsell, D. S., et al. (2009). AutoDock 4 and AutoDockTools 4: automated docking with selective receptor flexibility. *J. Comput. Chem.* 30, 2785–2791. doi: 10.1002/jcc.21256

Pasqua, R. D., Betts, G., Hoskins, N., Edwards, M., Ercolini, D., and Mauriello, G. (2007). Membrane toxicity of antimicrobial compounds from essential oils. *J. Agric. Food Chem.* 55, 4863–4870. doi: 10.1021/jf0636465

Paul, S., Dubey, R. C., Maheswari, D. K., and Kang, S. C. (2011). *Trachyspermum ammi* (L.) fruit essential oil influencing on membrane permeability and surface characteristics in inhibiting food-borne pathogens. *Food Control* 22, 725–731. doi: 10.1016/j.foodcont.2010.11.003

Persinoti, G. F., de Aguiar Peres, N. T., Jacob, T. R., Rossi, A., Vêncio, R. Z., and Martinez-Rossi, N. M. (2014). RNA-sequencing analysis of *Trichophyton rubrum* transcriptome in response to sublethal doses of acriflavine. *BMC Genomics* 15, S1. doi: 10.1186/1471-2164-15-S7-S1

Pinto, E., Goncalves, M. J., Hrimpeng, K., Pinto, J., Vaz, S., Vale-Silva, L. A., et al. (2013). Antifungal activity of the essential oil of *Thymus villosus* subsp. lusitanicus against Candida, Cryptococcus, Aspergillus and dermatophyte species. *Ind. Crops Prod.* 51, 93–99. doi: 10.1016/j.indcrop.2013.08.033

Rabari, V. P., Chudashama, K. S., and Thaker, V. S. (2018). *In vitro* screening of 75 essential oils against *Colletotrichum gloeosporioides*: a causal agent of anthracnose disease of mango. *Int. J. Fruit Sci.* 18, 1–13. doi: 10.1080/15538362.2017.1377666

Riera, N., Ramirez-Villacis, D., Barriga-Medina, N., Alvarez-Santana, J., Herrera, K., Ruales, C., et al. (2019). First report of banana anthracnose caused by *Colletotrichum gloeosporioides* in Ecuador. *Plant Dis.* 103, 763. doi: 10.1094/PDIS-01-18-0069-PDN

Schwarz, D., Kisselev, P., Schunck, W. H., and Roots, I. (2011). Inhibition of 17β-estradiol activation by CYP1A1: genotype- and regioselective inhibition by St. John's Wort and several natural polyphenols. *Biochim. Biophys. Acta* 1814, 168–174. doi: 10.1016/j.bbapap.2010.09.014

Shao, X., Cheng, S., Wang, H., Yu, D., and Mungai, C. (2013). The possible mechanism of antifungal action of tea tree oil on *Botrytis cinerea*. *J. Appl. Microbiol.* 114, 1642–1649. doi: 10.1111/jam.12193

Sivakumar, D., and Bautista-Baños, S. (2014). A review on the use of essential oils for postharvest decay control and maintenance of fruit quality during storage. *Crop Prot.* 64, 27–37. doi: 10.1016/j.cropro.2014.05.012

Song, J. X., Zhang, S. Z., and Lu, L. (2018). Fungal cytochrome P450 protein Cyp51: what we can learn from its evolution, regulons and Cyp51-based azole resistance. *Fungal Biol. Rev.* 32, 131–142. doi: 10.1016/j.fbr.2018.05.001

Sun, B., Dong, Y., Lei, K., Wang, J., Zhao, L., and Liu, M. (2019). Design, synthesis and biological evaluation of amide-pyridine derivatives as novel dual-target (SE, CYP51) antifungal inhibitors. *Bioorg. Med. Chem.* 27, 2427–2437. doi: 10.1016/j.bmc.2019.02.009

Susan, L., and Watkins, C. B. (2012). Superficial scald, its etiology and control. *Postharvest Biol. Technol.* 65, 44–60. doi: 10.1016/j.postharvbio.2011.11.001

Tian, J., Ban, X., Zeng, H., He, J., Chen, Y., and Wang, Y. (2012). The mechanism of antifungal action of essential oil from dill (*Anethum graveolens* l.) on *Aspergillus flavus*. *PLoS ONE* 7, e30147. doi: 10.1371/journal.pone.0030147

Tu, X. F., Hu, F., Thakur, K., Li, X. L., Zhang, Y. S., and Wei, Z. J. (2018). Comparison of antibacterial effects and fumigant toxicity of essential oils extracted from different plants. *Ind. Crops Prod.* 124, 192–200. doi: 10.1016/j.indcrop.2018.07.065

Tzortzakis, N. G. (2009). Impact of cinnamon oil-enrichment on microbial spoilage of fresh produce. *Innov. Food Sci. Emerg.* 10, 97–102. doi: 10.1016/j.ifset.2008.09.002

Wang, D., Zhang, J., Jia, X. M., Xin, L., and Zhai, H. (2019). Antifungal effects and potential mechanism of essential oils on *Collelotrichum gloeosporioides in vitro* and *in vivo*. *Molecules* 24, 3386. doi: 10.3390/molecules24183386

Wang, X., Zhang, X., Li, M., Ji, X., Feng, C., and Wang, F. (2020). First report of ficuscarica bot rot caused by *Botryosphaeria dothidea* in China. *Plant Dis.* 104, 1869. doi: 10.1094/PDIS-09-19-2039-PDN

Waterhouse, A., Bertoni, M., Bienert, S., Studer, G., Tauriello, G., Gumienny, R., et al. (2018). SWISS-MODEL: homology modelling of protein structures and complexes. *Nucleic Acids Res.* 46, W296–W303. doi: 10.1093/nar/gky427

Wilkens, S. (2015). Structure and mechanism of ABC transporters. *F1000Prime Rep.* 7, 14. doi: 10.12703/P7-14

Woolf, A. (1999). Essential oil poisoning. *J. Toxicol. Clin. Toxicol.* 37, 721–727. doi: 10.1081/CLT-100102450

Wu, Y. X., Zhang, Y. D., Li, N., Wu, D. D., Li, Q. M., Chen, Y. Z., et al. (2022). Inhibitory effect and mechanism of action of juniper essential oil on gray mold in cherry tomatoes. *Front. Microbiol.* 13, 1000526. doi: 10.3389/fmicb.2022.1000526

Yu, D., Wang, J., Shao, X., Xu, F., and Wang, H. (2015). Antifungal modes of action of tea tree oil and its two characteristic components against *Botrytis cinerea*. *J. Appl. Microbiol.* 119, 1253–1262. doi: 10.1111/jam.12939

Yu, X., Hou, Y., Cao, L., Zhou, T., Wang, S., Hu, K., et al. (2022). MicroRNA candidate miRcand137 in apple is induced by *Botryosphaeria dothidea* for impairing host defense. *Plant Physiol.* 189, 1814–1832. doi: 10.1093/plphys/kiac171

Zhai, H., Wang, J. Z., Xue, X. M., Wang, L. P., Chen, R., Nie, P. X., et al. (2019). Population dynamics of *grapholitha molesta* (Lepidoptera: Tortrididae) and control effects by sexual pheromone in apple orchards with non-bagged-fruit cultivation pattern. *Sci. Silvae Sinicae* 55, 111–118. doi: 10.11707/j.1001-7488.20190712

Zhang, J. X., Li, L. P., LV, Q.Z., Yan, L., Wang, Y., and Jiang, Y. Y. (2019). The fungal CYP51s: their functions, structures, related drug resistance, and inhibitors. *Front. Microbiol.* 10, 691. doi: 10.3389/fmicb.2019.00691

Zhang, Y. B., Liu, X. Y., Wang, Y. F., Jiang, P. P., and Quek, S. Y. (2016). Antibacterial activity and mechanism of cinnamon essential oil against *Escherichia coli* and *Staphylococcus aureus*. *Food Control* 59, 282–289. doi: 10.1016/j.foodcont.2015.05.032

Zhou, T., Wang, X. H., Ye, B. S., Shi, L., Bai, X. L., and Lai, T. F. (2018). Effects of essential oil decanal on growth and transcriptome of the postharvest fungal pathogen *Penicillium expansum*. *Postharvest Biol. Technol.* 145, 203–212. doi: 10.1016/j.postharvbio.2018.07.015

frontiers | Frontiers in Microbiology

TYPE Original Research
PUBLISHED 02 March 2023
DOI 10.3389/fmicb.2023.1131737

OPEN ACCESS

EDITED BY
Khamis Youssef,
Agricultural Research Center, Egypt

REVIEWED BY
Yasmeen Siddiqui,
Universiti Putra Malaysia, Malaysia
Ayat F. Hashim,
National Research Centre, Egypt
Elhanan Tzipilevich,
MIGAL - Galilee Research Institute, Israel

*CORRESPONDENCE
Caixia Wang
✉ cxwang@qau.edu.cn

†These authors have contributed equally to this work and share first authorship

SPECIALTY SECTION
This article was submitted to Food Microbiology, a section of the journal Frontiers in Microbiology

RECEIVED 26 December 2022
ACCEPTED 30 January 2023
PUBLISHED 02 March 2023

CITATION
Sun Z, Hao B, Wang C, Li S, Xu Y, Li B and Wang C (2023) Biocontrol features of *Pseudomonas syringae* B-1 against *Botryosphaeria dothidea* in apple fruit. *Front. Microbiol.* 14:1131737. doi: 10.3389/fmicb.2023.1131737

Biocontrol features of *Pseudomonas syringae* B-1 against *Botryosphaeria dothidea* in apple fruit

Zihao Sun[1†], Baihui Hao[1†], Cuicui Wang[2], Shiyu Li[1], Yuxin Xu[1], Baohua Li[1] and Caixia Wang[1*]

[1]Shandong Engineering Research Center for Environment-Friendly Agricultural Pest Management, Shandong Province Key Laboratory of Applied Mycology, College of Plant Health and Medicine, Qingdao Agricultural University, Qingdao, Shandong, China, [2]Shandong Provincial University Laboratory for Protected Horticulture, Shandong Facility Horticulture Bioengineering Research Center, Weifang University of Science and Technology, Weifang, Shandong, China

Apple ring rot caused by *Botryosphaeria dothidea* is an important disease that leads to severe quality deterioration and yield loss at pre-harvest and postharvest stages. Therefore, it is urgent to develop safe and efficient measures to control this disease. The objective of the present study was to investigate the biocontrol features of *Pseudomonas syringae* B-1 against *B. dothidea* and explore its mechanism of action utilizing *in vitro* and *in vivo* assays. The results showed that *P. syringae* B-1 strongly reduced the incidence of apple ring rot and lesion diameter by 41.2 and 90.2%, respectively, in comparison to the control fruit. In addition, the control efficiency of strain B-1 against *B. dothidea* infection depended on its concentration and the interval time. *P. syringae* B-1 cells showed higher inhibitory activities than its culture filtrates on the mycelial growth and spore germination of *B. dothidea*. Moreover, *P. syringae* B-1 treatment alleviated electrolyte leakage, lipid peroxidation, and H_2O_2 accumulation in *B. dothidea*-infected apple fruit by increasing antioxidant enzyme activities, including peroxidase, catalase, superoxide dismutase, and ascorbate peroxidase. We also found that strain B-1 treatment enhanced four defense-related enzyme activities and stimulated the accumulation of three disease-resistant substances including phenolics, lignin, and salicylic acid (SA) in apple fruit. In addition, strain B-1 triggered the upregulated expression of defense-related genes such as PR genes (*PR1*, *PR5*, *GLU*, and *CHI*) and two genes involved in the biosynthesis of SA (*SID2* and *PAD4*) to promote the resistance potential in apple fruit. Hence, our results suggest that *P. syringae* B-1 is a promising strategy against *B. dothidea*, mainly through reducing oxidative damage, activating defense-related enzymes, accumulating disease-resistant substances, and triggering the expression of resistance-correlated genes in apple fruit.

KEYWORDS

***Pseudomonas syringae* B-1, *Botryosphaeria dothidea*, apple fruit, oxidative damage, antioxidant and defense system, salicylic acid signaling**

1. Introduction

Botryosphaeria dothidea, the most destructive pathogen of apples, is responsible for preharvest and postharvest ring rot, leading to huge economic losses in apple production. In detail, the fungal pathogen infects twigs, stems, and branches in the field and could survive several years on diseased apple trees (Tang et al., 2012; Zhao et al., 2016). According to the survey by Guo et al. (2009), the incidence of apple trees with ring rot symptoms was more than 77% in the main apple-producing areas of China. Apple fruit infected by *B. dothidea* is usually 10–20% each year, though it can reach 70% under favorable conditions for fungal growth, such as wet and humid weather (Wang and Hou, 2001).

Currently, the prevention and control of apple diseases caused by fungi are implemented by eliminating the inoculum, spraying the chemical fungicides, and bagging fruit (Zhao et al., 2016; Huang et al., 2021a). As the cost of bagging is increasing yearly, the bagless cultivation of apples has become an inevitable trend in China. Nevertheless, *B. dothidea* rot on apple fruit is the main disease that needs to be overcome under the condition of bagless cultivation. Once the apple tissues were infected by *B. dothidea*, the effects of therapeutic fungicides are low, for example, the control efficiency of difenoconazole was only 55%, which is one of the most effective fungicides (Zhang et al., 2010). Moreover, these chemical fungicides can cause adverse health effects and severe environmental pollution, in addition to fungicide resistance (Ma et al., 2002; Fan et al., 2016). Thus far, many chemical fungicides have been regulated or banned for use in postharvest fruit (Casals et al., 2010). Thus, it is pressing to seek eco-friendly, effective, and safe products to control *B. dothidea* rot on apple fruit.

Numerous studies and global programs have focused on biological control products as promising alternatives to the traditional fungicides for managing plant diseases in agricultural production (Droby et al., 2016). In Europe, biological control has been advocated since 2009, and in China, a "National research program on reduction in chemical pesticides and fertilizers" was launched in 2016. Until now, many microbial antagonists have been developed and commercialized to control plant diseases (Sharma et al., 2009; Spadaro and Droby, 2016). For apple fruit, biological control products have also been applied to reduce postharvest decay, mainly by biocontrol bacteria and yeast. For example, many biocontrol bacteria, including *Bacillus* spp., *Pseudomonas* spp., and *Streptomyces* spp., were able to reduce fruit postharvest decay (Chen et al., 2016; Zhang Q. M. et al., 2016; Calvo et al., 2017). In addition, a large number of biocontrol yeasts, such as *Meyerozyma guilliermondii*, *Rhodotorula mucilaginosa*, and *Pichia membranifaciens*, were used to control fruit decay caused by fungi during postharvest storage (Li et al., 2011; Yan et al., 2018; Zhang et al., 2020; Huang et al., 2021b).

The bacterial species belonging to *Pseudomonas* genera are widely found in nature, which include species causing plant diseases, as well as biocontrol microorganisms, already registered for agricultural biocontrol (van Lenteren et al., 2017; Aiello et al., 2019). It was reported that *P. syringae* strains were effective to control fruit postharvest decays caused by various fungal pathogens, including *Penicillium digitatum* (Smilanick, 1996; Cirvilleri et al., 2005; Panebianco et al., 2015), *Monilinia fructicola*, *Rhizopus stolonifer* (Zhou et al., 1999), *Botrytis cinerea*, and *P. expansum* (Zhou et al., 2001; Errampalli and Brubacher, 2006). It is noteworthy that the strains of *P. syringae*, for example, ESC-10, ESC-11, and 742RS, were developed and commercialized by EcoScience Corporation as biocontrol agents to manage postharvest decays on multiple fruits and even tubers (Williamson et al., 2008; Al-Mughrabi et al., 2013; van Lenteren et al., 2017). However, whether *P. syringae* could effectively protect apple fruit against *B. dothidea* infection is unknown, and the possible biocontrol mechanisms need to be further explored.

The present study explored the biocontrol bacterial strain *P. syringae* B-1, which was isolated from the apple fruit collected from a commercial orchard. The strain B-1 did neither induce necrotic lesions on the fruit of apple, orange, peach, and grape nor did it have effects on the internal fruit appearance. Hence, the aims of the present study were to first investigate the antifungal potential and the efficiency of *P. syringae* B-1 against *B. dothidea in vitro* and *in vivo*. Another purpose was to explore the underlying mechanisms of strain B-1 against *B. dothidea*, such as reducing oxidative damage, activating defense-related enzymes, accumulating disease-resistant substances, and triggering the expression of resistance-correlated genes in apple fruit. These results will further enrich our understanding of the action mechanisms of *P. syringae* and provide alternatives for postharvest apple decay caused by *B. dothidea*.

2. Materials and methods

2.1. Fruit, *Pseudomonas syringae* B-1, and *Botryosphaeria dothidea*

Apple (cv. 'Fuji') fruit used in this study was collected from the local orchards in Shandong, China. The fruit at a commercial mature stage has not received any postharvest treatment and was kept at 4°C before being used. The apples were disinfected and washed according to the method of Sun et al. (2021). *P. syringae* B-1, isolated from the healthy apple fruit, was preserved in China Center for Culture Collection (M2015813). The bacteria were cultured in nutrient broth (NB) on a shaker at 28°C for 48 h. *B. dothidea* LXS030101, isolated from apple fruit with ring rot symptoms, was characterized by our research team based on morphological observation and molecular identification. The strain was cultured on potato dextrose agar (PDA) for routine use (Zhang Q. M. et al., 2016). The conidia of strain LXS030101 was induced with the modified method of Leng et al. (2009). The wounded young apple fruit was inoculated with mycelial plugs of *B. dothidea* and incubated under UV light (365 nm) at 25°C. After about 2 weeks, the conidia was produced and collected from the lesion around the inoculation sites.

2.2. Efficiency of *Pseudomonas syringae* B-1 *in vivo*

Each apple fruit was punctured with a borer to make three wounds (5 mm wide and 3 mm deep) at the equatorial region. Then,

the strain B-1 suspension at different concentrations (1×10^5, 1×10^6, 1×10^7, 1×10^8, and 1×10^9 CFU mL^{-1}) was dripped into the wounds. Following 48 h of incubation at 25°C, the conidia suspension of *B. dothidea* (5×10^5 spores mL^{-1}) was added to the treated wounds with the pipette (Lu et al., 2013; Huang et al., 2021a). All fruits were placed into enclosed plastic boxes and stored at 25°C in a relative humidity of about 95%. Thirty fruits were selected as controls and were treated with sterile water and inoculated only with the pathogen suspension. For each treatment, there were three replicates with 10 apple fruits in each replicate. Disease incidence was calculated as the percentage of infected wounds, and the lesion size around the wounds was recorded at 3 and 5 days post-inoculation (dpi).

2.3. Effect of interval time on the efficiency *in vivo*

The effect of interval time after *P. syringae* B-1 treatment on control efficiency was determined according to the assay mentioned in Section "2.2. Efficiency of *Pseudomonas syringae* B-1 *in vivo*" A volume of 30 μL of strain B-1 suspension at 1×10^8 CFU mL^{-1} was added into each wound using a pipette. After 0, 6, 12, 24, 48, and 96 h of incubation at 25°C, respectively, 30 μL of *B. dothidea* spore suspension at 5×10^5 spores mL^{-1} was inoculated to the treated wound. The fruits were incubated at a relative humidity of about 95% at 25°C for 5 days. The diseased symptoms were observed; the disease incidence and lesion diameter were recorded at 5 dpi. The assay was conducted two times, and there were three replicates with 10 apple fruit in each replicate.

2.4. *In vitro* inhibitory effect of *Pseudomonas syringae* B-1 cells and culture filtrates

Strain B-1 cells were obtained from 2-day-old cultures in NB by centrifuging at 12,000 × *g* for 15 min and re-suspended in distilled water. The culture filtrates were prepared by a 0.22-μm polycarbonate membrane filter (Sangon Biotech, Shanghai, China). For the inhibiting mycelium growth assay, PDA plates were prepared, which contained 10% (v/v) culture filtrates or different concentrations of strain B-1 cells (1×10^5, 1×10^6, 1×10^7, 1×10^8, and 1×10^9 CFU mL^{-1}). The mycelial plugs (5 mm in diameter) containing *B. dothidea* grown on medium for 3 days were transferred to the PDA plates. After incubating for 5 days at 25°C, the colony diameter of *B. dothidea* was determined and the inhibition rate was calculated. For the spore germination assay, the culture filtrates or different concentrations of strain B-1 cells and the pathogen suspension were dripped into the concavity slides (Zhang Q. M. et al., 2016). Following 12 h of incubation at 25°C, the spore germination was observed using the microscope (DM2500, Leica, German). Conidia were considered germinated when the length of the germ tube was longer than the length of the conidia. For each treatment, sterile distilled water was used as the control. The assays were carried out two times with four replicates.

2.5. Estimation of oxidative damage

Four treatments were performed in apple fruit including control and sterile water; B-1, *P. syringae* B-1 suspension at 1×10^8 CFU mL^{-1}; pathogen, *B. dothidea* suspension at 5×10^5 spores mL^{-1}; B-1 + pathogen, strain B-1 treatment, followed by *B. dothidea* inoculation. Fruit tissues were collected in different treatments at 0, 12, 24, 48, 72, 96, and 120 h. To reveal the oxidative damage in apple fruit, electrolyte leakage, malondialdehyde (MDA), and hydrogen peroxide (H_2O_2) contents were analyzed. For electrolyte leakage, it was measured according to the modified method of Ji et al. (2020). A total of 0.5 g of fresh tissues were cut into small pieces and dropped into 10 mL of deionized water. After 1 h incubation at room temperature, the conductivity (C1) was determined by a conductivity meter (DDBJ-350, Inesa, China). The tissue samples were then boiled for 15 min and the conductivity (C2) was measured. The formula (C1/C2) × 100% was used to calculate the electrolyte leakage.

For MDA content, it was conducted with the assay kit (#A003) from Nanjing Jiancheng Bioengineering Institute (Nanjing, China). For the analysis of H_2O_2 content, 1 g fresh tissues were homogenized with 3 mL of chilled 0.2% trichloroacetic acid (≥99.0%, Sangon Biotech, Shanghai, China), and then centrifuged at 12,000 × *g* for 15 min at 4°C. According to the report of Wang et al. (2015), the supernatant was mixed with 0.1 mmol L^{-1} phosphate buffer and 1 mol L^{-1} potassium iodide (≥99.0%, Sangon Biotech, Shanghai, China), then the absorbance of the reaction system was measured at 390 nm with a spectrophotometer (Philes, T6, China). The units of MDA and H_2O_2 contents were expressed as mmol in 1 kg of fresh weight (mmol kg^{-1}).

2.6. Determination of antioxidant and defense-related enzyme activities

Apple fruit was treated with *P. syringae* B-1 or sterile water according to the method described in Section "2.5. Estimation of oxidative damage" Fruit tissues were collected near the wound at different time points and were ground to powder with liquid nitrogen. For the antioxidant enzymes, activities of catalase (CAT, #A007), peroxidase (POD, #A084), superoxide dismutase (SOD, #A001), and ascorbate peroxidase (APX, #A123) were measured with the assay kits from Nanjing Jiancheng Bioengineering Institute (Nanjing, China). For the defense-related enzymes, the activities of phenylalanine ammonialyase (PAL), polyphenoloxidase (PPO), β-1,3-glucanase (GLU), and chitinase (CHI) were assayed referring to the report of Zhang Q. M. et al. (2016). The enzyme activity units are expressed on the fresh weight basis as U g^{-1}.

2.7. Qualification of total phenolics, lignin, and hormone contents

The total phenolics content was measured with the assay kit (#A143) from Nanjing Jiancheng Bioengineering Institute (Nanjing, China). The lignin content was assayed as described by Li et al. (2019), and the absorbance of the reaction mixture was detected at 280 nm. The lignin content was expressed as A_{280}

TABLE 1 Specific primers used for quantitative real-time PCR (qPCR) to analyze gene expression.

Primer name	Forward primer 5′→3′	Reverse primer 5′→3′	Annealing temperature (°C)
MdEF1α	ACATTGCCCTGTGGAAGTT	GTCTGACCATCCTTGGAAA	53/56/58
MdPR1	GCAGCAGTAGGCGTTGGTCCCT	CCAGTGCTCATGGCAAGGTTTT	58
MdPR5	AGCAGCTTCCCTCCTCGGC	CCCAGAAGCGACCAGACC	58
MdCHI	TGGAGGATGGGAAAGTGC	GGGTGAGTTGGATGGGTC	58
MdGLU	TGCCGTAGGAAACGAAAT	TGATGGAGGAAAGGAATT	53
MdSID2	TTATACTTCATTCCGCTGCT	GCCTCTAATTTTCTTTGTATGCT	56
MdPAD4	GCTTCACCGTAAGTTACTCG	CAAGAAACTCGCAACTGTC	58

g^{-1} on a fresh weight basis. Quantification of hormones including salicylic acid (SA) and jasmonic acid (JA) in apple fruit was analyzed using the enzyme-linked immunosorbent assay (ELISA) kit from Jingmei Biotechnology (Yancheng, China). SA and JA contents were expressed as μg kg^{-1} and ng kg^{-1} on the fresh weight basis, respectively.

2.8. Analysis of gene expression

Fruit tissues were collected near the wounds after being treated with *P. syringae* B-1 or sterile water at 0, 12, 24, and 48 h. Total RNA was extracted from different tissue samples and the cDNA synthesis was performed using the HiScript 1st Strand cDNA Synthesis kit (Vazyme, Nanjing, China). Quantitative real-time PCR (qPCR) was conducted as reported by Huang et al. (2021a), using a Light Cycler® 96 PCR Detection System (Roche, Germany). Each reaction consists of at least three biological replicates, with a 25 μL reaction volume. The transcript levels of six genes involved in the defense response and the SA pathway (*MdPR1*, *MdPR5*, *MdGLU*, *MdCHI*, *MdSIT2*, and *MdPAD4*) were analyzed with the $2^{-\Delta\Delta CT}$ method (Zhang Q. M. et al., 2016; Huang et al., 2021a). Referenced gene *MdEF1a* (elongation factor 1-a) was used to normalize the expression levels of target genes. The primers for the qPCR assay are shown in Table 1.

2.9. Statistical analysis

Data analysis was performed using the software SPSS Version 19.0. All the data consisted of at least three replicates and were represented as mean ± standard deviation (SD). Statistical differences were conducted by analysis of variance using Duncan's multiple range test at a significance level of 0.05.

3. Results

3.1. Efficiency of *Pseudomonas syringae* B-1 against *Botryosphaeria dothidea* in apple fruit

The biocontrol efficiency of *P. syringae* B-1 to control *B. dothidea* rot in apple fruit was influenced by its concentrations (Figure 1). As shown in Figure 1A, the control fruit showed rapidly developing brown lesions around the inoculation sites. In contrast, although strain B-1 at 1×10^5 CFU mL^{-1} did not inhibit fruit decay caused by *B. dothidea* in fruit (Figures 1B, C), strain B-1 at 1×10^6 CFU mL^{-1} to 1×10^9 CFU mL^{-1} all resulted in a decrease in disease incidence (Figure 1B) and lesion diameter (Figure 1C). When the concentrations of strain B-1 were higher ($>10^8$ CFU mL^{-1}), their efficiency against *B. dothidea in vivo* had no significant difference. Following storage for 5 days at 25°C, strain B-1 at 1×10^8 CFU mL^{-1} reduced the incidence of apple ring rot and lesion diameter by 41.2 and 90.2%, respectively, compared with the control fruit.

3.2. Effect of *Pseudomonas syringae* B-1 with different treatment intervals against *Botryosphaeria dothidea in vivo*

In comparison to the 0 h treatment, the diameter and incidence of *B. dothidea* rot reduced when the interval time between *P. syringae* B-1 treatment and the pathogen inoculation was 6 h or longer (Figure 2). The efficiency of strain B-1 was improved with the extension of interval time from 6 to 24 h. The expansion of decay symptoms was inhibited at the interval time of 24 h, as the incidence of apple ring rot and lesion diameter in strain B-1 treated fruit were reduced by 30.8 and 85.6%, respectively, compared with the 0 h treatment (Figure 2). There was no obvious difference in the incidence and lesion size of apple ring rot at the interval time from 24 to 96 h (Figures 2B, C).

3.3. *Pseudomonas syringae* B-1 inhibited *B. dothidea in vitro*

Pseudomonas syringae B-1 cells ranging from 1×10^6 CFU mL^{-1} to 1×10^9 CFU mL^{-1} and culture filtrates all exhibited inhibitory effects on the mycelial growth of the fungal pathogen at 25°C. When the concentration of strain B-1 cells reached 1×10^8 CFU mL^{-1}, the mycelial growth of *B. dothidea* was almost completely inhibited. Moreover, strain B-1 culture filtrates showed lower antifungal activity against *B. dothidea* than the bacterial cells at 1×10^6 CFU mL^{-1}, with 18.28 and 49.64% mycelial growth inhibition, respectively (Figure 3A).

The effect of *P. syringae* B-1 on *B. dothidea* spore germination was also determined by mixing strain B-1 cells or culture filtrates

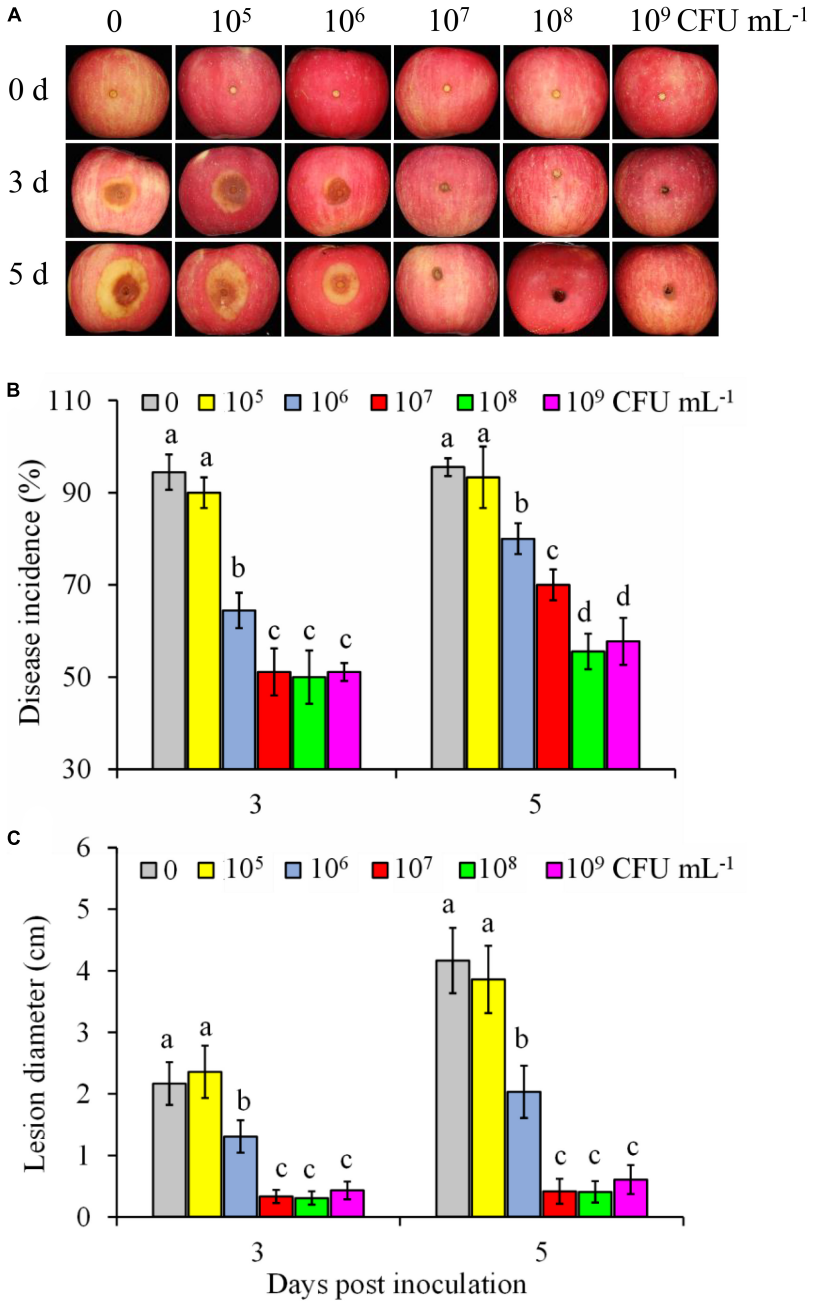

FIGURE 1
Efficiency of *P. syringae* B-1 against *B. dothidea* in apple fruit. Disease symptoms **(A)** in control and strain B-1 treated fruit at 3 and 5 days post-inoculation (dpi) with *B. dothidea*. Effect of strain B-1 on disease incidence **(B)** and lesion diameter **(C)** in inoculated apple fruit at 3 and 5 dpi. Error bars represent the SD of three replicates. Different letters above the bars indicate significant differences ($p < 0.05$) within the same panel at the same time point.

with *B. dothidea* conidia. As shown in Figure 3B, the spore germination rate decreased as the concentration of strain B-1 cells increased, which indicated that the inhibitory efficiency of strain B-1 cells against the spore germination of *B. dothidea* depended on its concentration. At 12 h of incubation, the germination rate of control reached 88.07%; however, the bacterial cells at 1×10^9 CFU mL^{-1} showed the lowest germination rate with only 1.23%. Similarly, *P. syringae* B-1 culture filtrate showed less inhibition on spore germination than its cells ranging from 1×10^6 CFU mL^{-1} to 1×10^9 CFU mL^{-1} (Figure 3B).

3.4. *Pseudomonas syringae* B-1 reduced the oxidative damage in apple fruit

To analyze the effect of *P. syringae* B-1 on oxidative damage in apple fruit, the electrolyte leakage, MDA, and H_2O_2 contents were determined in four different treatments (Figure 4). During the storage, no statistical differences in the three factors were detected between strain B-1 treated fruit and the control. The level of electrolyte leakage rose in the fruit inoculated with *B. dothidea* from

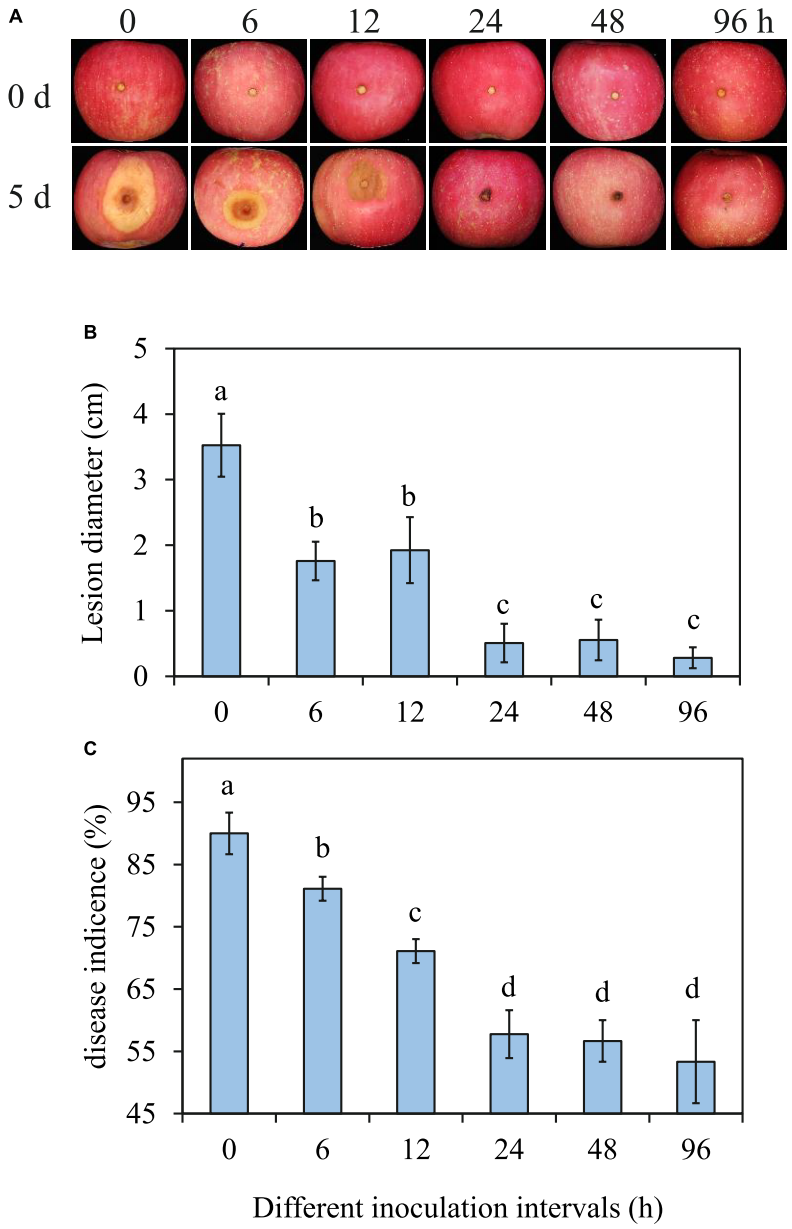

FIGURE 2
Effects of *P. syringae* B-1 with different inoculation intervals at 1 × 10^8 CFU mL–^{1} on the disease symptoms **(A)**, lesion diameter **(B)**, and disease incidence **(C)** in inoculated apple fruit at 5 dpi. Error bars represent the SD of three replicates. Different letters above the bars indicate significant differences ($p < 0.05$) between the different inoculation intervals.

24 h post-inoculation (hpi) and attained the maximum leakage of 97.3% at 120 hpi. However, the level of leakage in strain B-1 plus *B. dothidea*-treated fruit was only 45.7% at 120 hpi, which had no difference compared with the control fruit (Figure 4A).

In the fruit only inoculated with *B. dothidea*, MDA content increased from 24 hpi, which was up to 164.9 and 173.1% more than the control at 96 and 120 hpi, respectively (Figure 4B). In strain B-1 plus *B. dothidea*-treated fruit, although the MDA content rose from 96 hpi, it was only 16.4 and 31.6% more than the control at 96 and 120 hpi, respectively. Consistent with the level of electrolyte leakage and MDA content, the H_2O_2 level sharply increased in *B. dothidea*-inoculated fruit from 48 hpi and reached the highest value of 14.08 mmol kg^{-1} at 120 hpi. Nevertheless, in the fruit treated with strain B-1 plus pathogen, the level of H_2O_2 enhanced slowly and showed no difference compared with the control until 96 hpi, with only 0.90 mmol kg^{-1} at 120 hpi (Figure 4C).

3.5. *Pseudomonas syringae* B-1 affected the antioxidant enzyme activities in apple fruit

To reveal the effect of *P. syringae* B-1 on the apple fruit, the activities of the four antioxidant enzymes were analyzed (Figure 5). During storage, POD activity in apple fruit varied as time progressed (Figure 5A). An ascending tendency of POD

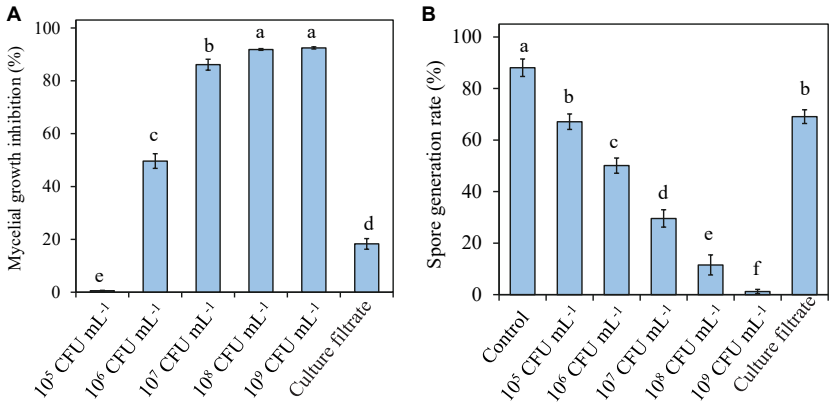

FIGURE 3
Effects of *P. syringae* B-1 cells and culture filtrate on mycelial growth inhibition **(A)** and spore generation **(B)** of *B. dothidea in vitro*. Strain B-1 cells were used at 1×10^5 CFU mL^{-1} to 1×10^9 CFU mL^{-1}, and sterile distilled water was used as the control. Each column represents the mean and vertical bars represent the SD of four replicates. Different letters above the bars indicate significant differences ($p < 0.05$) between the control and the different treatments of strain B-1.

activity was observed in fruit treated with *P. syringae* B-1 from 24 h and the peaked was at 48 h with 2.21-fold higher than the control. POD activity in strain B-1 treated fruit decreased from 72 h; however, it remained higher than the control during the whole storage. The result of Figure 5B showed that CAT activity was affected by *P. syringae* B-1 treatment. In strain B-1 treated fruit, the activity of CAT began to rapidly increase from 24 h and reached the peak at 48 h of storage, which was more than 2.85-fold higher compared with the control. Then, the enzyme activity in strain B-1 treated fruit decreased until 72 h, but CAT activity quickly rosed again and the second peak was at 96 h, which was 2.41-fold higher than the control.

In contrast to the control, *P. syringae* B-1 treatment also increased the activities of SOD and APX in apple fruit during storage (Figures 5C, D). The activity of SOD in fruit treated with strain B-1 rose steadily from 12 h and reached the peak at 72 h with 5.79 U g^{-1}. Although the enzyme activity declined from 96 h, SOD activity induced by strain B-1 was still higher than the control throughout the storage period (Figure 5C). As shown in Figure 5D, APX activity was induced by stain B-1 from 12 h and peaked at 48 h, which was 2.09-fold higher than the control. Then, the enzyme activity declined rapidly and it even reduced to the control level at 120 h.

3.6. *Pseudomonas syringae* B-1 induced the defense-related enzyme activities in apple fruit

In addition to an enhancement of antioxidant enzyme activities by *P. syringae* B-1 treatment, Figure 6 shows that the four defense-related enzyme activities were induced by *P. syringae* B-1 in apple fruit. For PAL and PPO, the activities increased from 12 h in the fruit treated with strain B-1 and they reached the highest values, 1.57-fold and 2.47-fold higher than the control, respectively. After that, the two enzymes' activities induced by strain B-1 decreased quickly, and they were not different from the control at 96 h for PAL and 120 h for PPO, respectively (Figures 6A, B).

Figures 6C, D show that GLU and CHI activities were affected by *P. syringae* B-1 treatment in apple fruit. The GLU activity in fruit treated with strain B-1 showed a sharp increase and peaked at 48 h. Thereafter, the enzyme activity decreased from 72 to 120 h; however, it remained higher than the control during the storage phase (Figure 6C). The change of CHI activity induced by strain B-1 was similar to GLU activity. The enzyme activity rose within 24 h after strain B-1 treatment and reached the highest level at 72 h. Then, CHI activity declined from 96 h after treatment, and it was still 2.19-fold higher than the control at 120 h (Figure 6D).

3.7. *Pseudomonas syringae* B-1 promoted the total phenolics, lignin, and hormone content in apple fruit

To get a better insight into the impact of *P. syringae* B-1 on apple fruit and the mechanisms of induced protection against *B. dothidea*, several metabolites and hormones involved in pathogen resistance were measured. Generally, the contents of total phenolics and lignin contents changed slowly in the control fruit, whereas they were greatly induced in strain B-1 treated fruit. As indicated in Figure 7A, strain B-1 enhanced the accumulation of total phenolics from 24 h (1.31-fold) after treatment during the storage period, and reached the maximum level at 72 h with 1.52-fold higher than the control. In addition, strain B-1 promoted the lignin content from 24 h after treatment compared with the control. Then, the lignin content in strain B-1 treated fruit peaked at 48, with 1.71-fold higher than the control. After that, it decreased only slightly and maintained a higher level throughout the storage (Figure 7B).

Regarding plant hormones, the contents of SA and JA were determined, with or without strain B-1 treatment. During the storage, SA and JA levels had no obvious changes in the control fruit (Figure 8). Strain B-1 treatment slightly enhanced the accumulation of JA at 48 h in apple fruit, with a 1.20-fold higher compared with the control. Nevertheless, the result of

10.3389/fmicb.2023.1131737

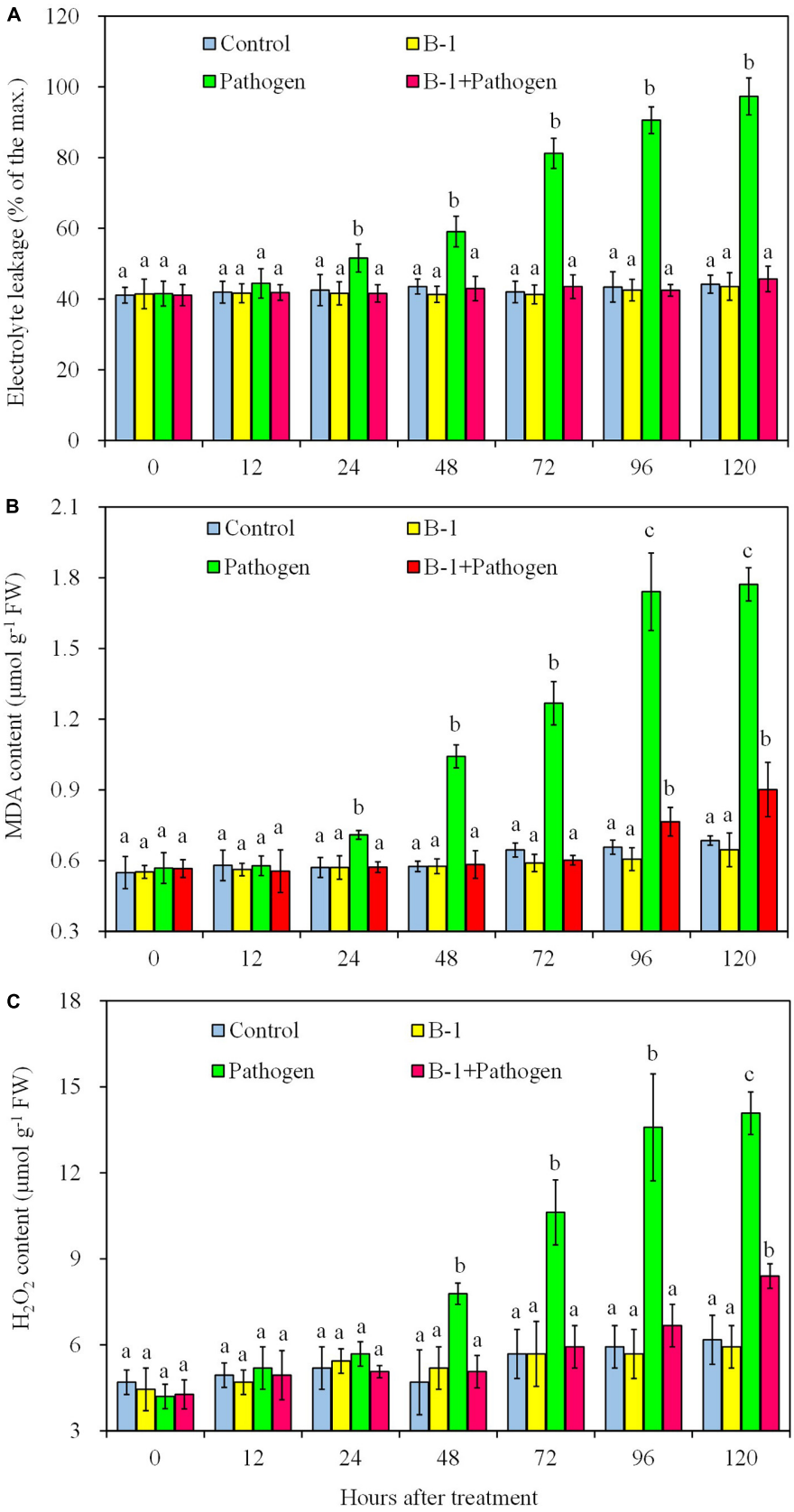

FIGURE 4
The electrolyte leakage **(A)**, MDA content **(B)**, and H_2O_2 content **(C)** in apple fruit with four treatments stored at 25°C. Each data represents the mean ± SD of three replicates. Different letters above the bars indicate significant differences ($p < 0.05$) at the same time point.

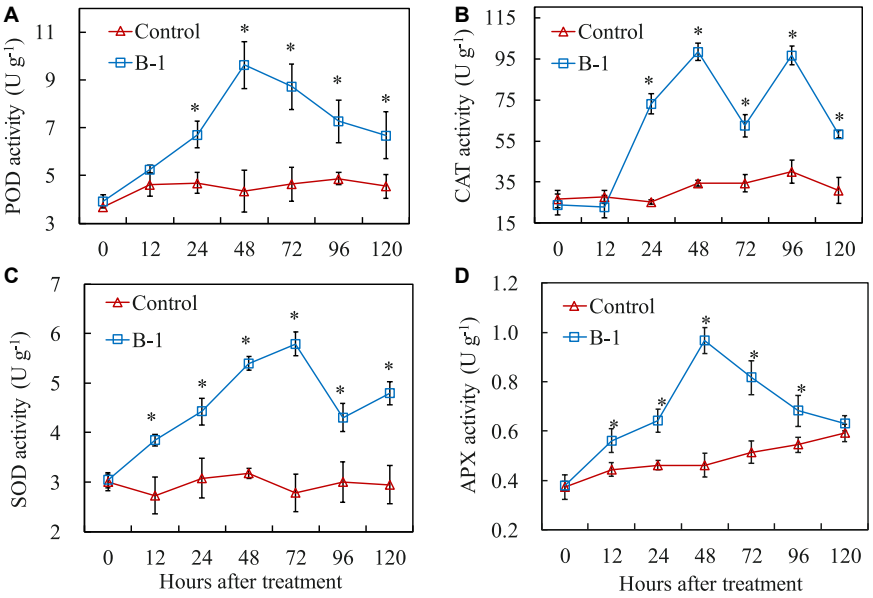

FIGURE 5
The activities of POD **(A)**, CAT **(B)**, SOD **(C)**, and APX **(D)** in apple fruit treated with *P. syringae* B-1 at 1×10^8 CFU mL^{-1} stored at 25°C. Each data represents the mean ± SD of three replicates. Asterisks (*) denote a significant difference ($p < 0.05$) between the strain B-1 treatment and the control apple fruit at the same time point.

Figure 8B illustrated that strain B-1 treatment enhanced the SA levels compared with the control. The content of SA increased from 12 h and continued to accumulate, which was 4.24-fold higher than the control.

3.8. *Pseudomonas syringae* B-1 activated the upregulated expression of PR genes and SA biosynthesis-related genes in apple fruit

Given the increased SA content in strain B-1-treated fruit, we next determined the expressions of genes involved in defense response (*MdGLU* and *MdCHI*) and SA pathway (*MdPR1*, *MdPR5*, *MdSID2*, and *MdPAD4*) by quantitative PCR to reveal the biocontrol mechanism of *P. syringae* B-1. *PR1* and *PR5* are widely used molecular markers that correlate with SA signaling activation (Zhang Q. M. et al., 2016). Meanwhile, *SID2* (SA induction deficient 2) and *PAD4* (phytoalexin deficient 4) are the genes related to SA biosynthesis (Huang et al., 2021b).

Compared with the control, the transcript level of *MdPR1* in strain B-1 treated fruit upregulated significantly at 12 h, and then reached the maximum at 48 h, which was 27.50-fold higher than that in the control fruit (Figure 9A). As shown in Figure 9B, the transcript level of *MdPR5* in fruit treated with strain B-1 peaked the highest at 24 h, with 9.60-fold higher than the control. Similarly, strain B-1 treatment upregulated the expression of *MdSID2* and *MdGLU* at 12–48 h, which exhibited similar trends with *MdPR5* (Figures 9C, E). The result of Figure 9F indicated that the expression of *MdPAD4* was triggered by strain B-1, and its transcript level was 7.63-fold higher than the control at 48 h. For *MdCHI*, compared with the control, the transcript level was activated by strain B-1 and showed 5.15- and 8.28-fold increases at 24 and 48 h, respectively (Figure 9D).

4. Discussion

Biological control is a possible and safe strategy for chemical fungicides to manage the postharvest decay in fruit and tuber (Droby et al., 2009). Previous studies indicated that many strains of the *Pseudomonas* genus, including *P. syringae*, are effective in controlling multiple postharvest decays caused by *B. cinerea*, *M. fructigena*, and *P. digitatum* rot (Zhou et al., 2001; Panebianco et al., 2015; Aiello et al., 2019). In this research, we demonstrated for the first time that *P. syringae* B-1 could effectively control postharvest apple ring rot by reducing the disease incidence and lesion size in fruit during the whole storage. The pretreatment of strain B-1 alone showed no effect on the surface color, weight loss, firmness, or total soluble solids content of apple fruit (data not shown). Given these promising results, we further investigated the possible mechanisms of *P. syringae* B-1-induced biocontrol against *B. dothidea*.

Our findings revealed that the ability of *P. syringae* B-1 to control apple ring rot depended on its concentration, and 1×10^6 CFU mL^{-1} strain B-1 was its threshold concentration to control *B. dothidea* effectively. This also exists in other antagonists for their control efficiency. For example, *M. guilliermondii* at high concentration has better efficiency against blue mold decay in pear fruit (Yan et al., 2018). Moreover, we found the time interval between *P. syringae* B-1 pretreatment and *B. dothidea* infection was another important element for its efficiency *in vivo*. Previous studies also showed that the biocontrol efficiency was closely related to the interval time after antagonist treatment (Lu et al., 2013; Huang et al., 2021b), which aligned with our current finding.

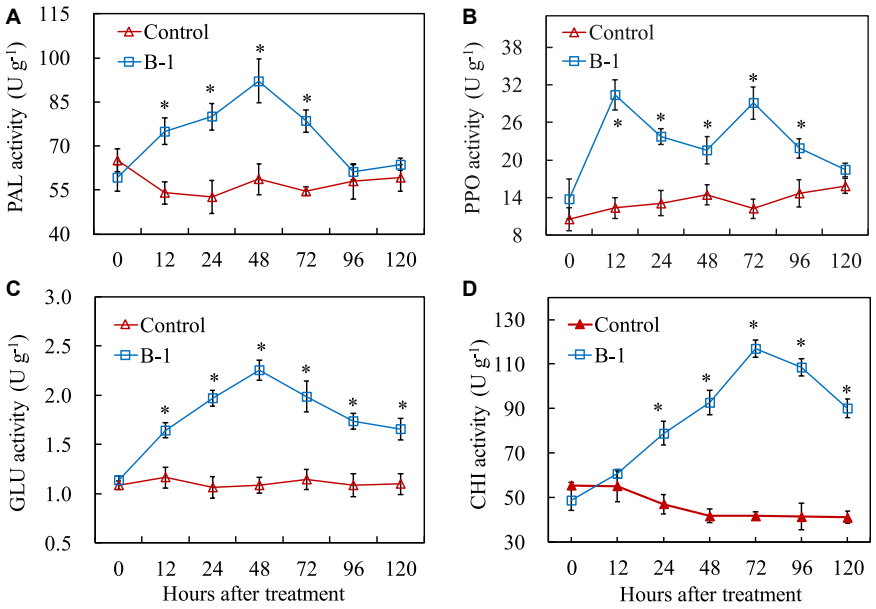

FIGURE 6
The activities of PAL **(A)**, PPO **(B)**, GLU **(C)**, and CHI **(D)** in apple fruit treated with *P. syringae* B-1 at 1 × 10^8 CFU mL^{-1} stored at 25°C. Each data represents the mean ± SD of three replicates. Asterisks (*) denote a significant difference ($p < 0.05$) between the strain B-1 treatment and the control apple fruit at the same time point.

Furthermore, *P. syringae* B-1 showed a protective rather than curative effect to manage apple ring rot, which agreed with the biocontrol effect of *Clavispora lusitaniae* 146 and *Streptomyces* sp. H4, two agents against postharvest green mold and anthracnose, respectively (Perez et al., 2019; Li et al., 2021).

The action mechanisms of biocontrol bacteria to manage postharvest decays are complicated (Rocío et al., 2021), the understanding of which, however, is pivotal to registering and commercializing a biocontrol product (Droby et al., 2016). In this research, we analyzed the antagonist effects of *P. syringae* B-1 using live cells and culture filtrates. Overall, strain B-1 culture filtrates showed lower but notably inhibitory activity on *B. dothidea* compared with the bacterial cells (≥10^6 CFU mL^{-1}). Similarly, Aiello et al. (2019) found that *P. synxantha* cells exhibited the best effects to inhibit *M. fructigena* and *M. fructicola* compared to culture filtrates. These data clearly indicated that *Pseudomonas* spp. functioned by other mechanisms involving the presence of living cells, but not antibiosis. For example, competing for nutrients and space with pathogens is the principal mode of *P. syringae*, an availably commercial agent Bio-Save (Bull et al., 1998). This mechanism is also true for other antagonistic bacteria *P. fluorescens* and *B. amyloliquefaciens* B4 (Wallace et al., 2017; Ye et al., 2021).

The pathogen's infection could cause oxidative damage, which has a negative impact on the cytomembrane and can be illustrated by the changes in electrolyte leakage and MDA contents (Zhang et al., 2012). Previous studies demonstrated that the levels of electrolyte leakage or MDA enhanced in plant tissues infected with pathogens, such as in peach fruit infected with *M. fructicola*, and in apple leaves inoculated with *Glomerella cingulata* (Zhang Q. M. et al., 2016; Ji et al., 2020). Our present research also showed that the levels of electrolyte leakage and MDA increased greatly in apple fruit with only *B. dothidea* infection from 24 to 120 hpi, whereas *P. syringae* B-1 treatment reduced the electrolyte leakage and MDA contents in fruit after *B. dothidea* inoculation. Therefore, these results indicated antagonists were effective in delaying MDA accumulation and mitigating electrolyte leakage in fruit (Zhang Q. M. et al., 2016; Ji et al., 2020).

In addition, oxidative damage also can be induced by the excessive production of ROS in cells (Glazebrook, 2005). It has been reported that ROS is a harmful substance produced during pathogens infection and that the levels of ROS correlate with the severity of disease symptoms (Mittler et al., 2004). In this research, our data indicated that strain B-1 treatment effectively reduced H_2O_2 aggregation in response to *B. dothidea* infection. Thus, we speculated that strain B-1 played the antioxidant function, hence alleviating subsequence oxidative damage to apple fruit and conferring resistance to *B. dothidea*. This result agrees with the report of Ji et al. (2020) where the authors reported that *B. licheniformis* W10 treatment reduced disease severity and ROS aggregation in nectarine fruit caused by *M. fructicola*.

Various antioxidant enzymes have vital functions in balancing ROS levels and inducing plant resistance responses (Mittler et al., 2004). Numerous studies have demonstrated that the activation of POD, CAT, SOD, and APX participated in the reaction of plant defense (Zhang Q. M. et al., 2016; Ji et al., 2020; Huang et al., 2021a). For example, in loquat fruit, *B. amyloliquefaciens* B4 increased the defense reaction against various pathogens, and the activity of POD was greatly higher than the control (Ye et al., 2021). In apple fruit, *M. guilliermondii* Y-1 improved three antioxidant enzyme activities and the total antioxidant capacity, thereby correspondingly increasing the fruit resistance to apple ring rot (Huang et al., 2021b). This finding revealed that strain B-1 treatment could trigger the activation of the fruit defense response and mitigate its oxidative damage against *B. dothidea* infection.

In addition to the antioxidant enzymes, the defense-related enzymes, secondary metabolites, and host-resistance proteins are

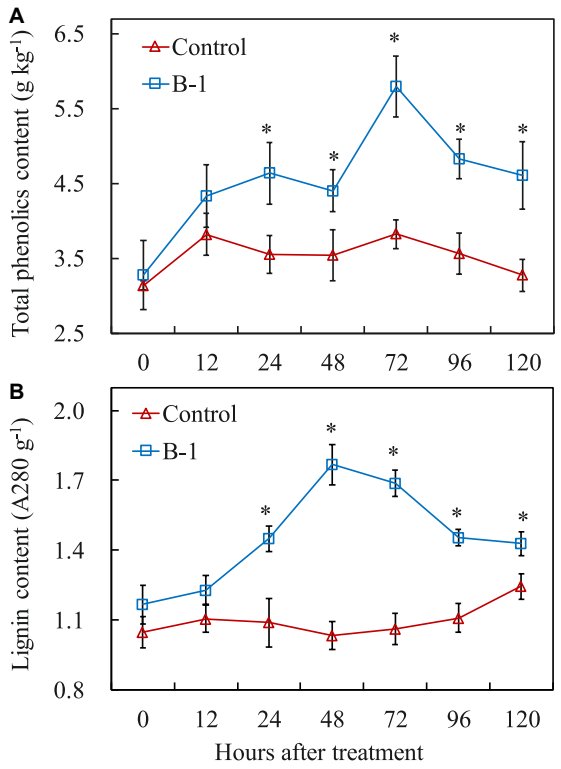

FIGURE 7
The content of total phenolics **(A)** and lignin **(B)** in apple fruit treated with *P. syringae* B-1 at 1 × 10^8 CFU mL^{-1} stored at 25°C. Each data represents the mean ± SD of three replicates. Asterisks (*) denote a significant difference ($p < 0.05$) between the strain B-1 treatment and the control apple fruit at the same time point.

all involved in plant disease resistance (Huang et al., 2021b; Zhang et al., 2021). PAL participates in the biosynthesis of phenolics and lignin in plant tissues, and PPO produces quinines that can inhibit or kill invading pathogens (Mayer, 2006; Romanazzi et al., 2016). Our results also indicated that *P. syringae* B-1 treatment activated those two enzymes, which is consistent with Zhang Q. M. et al. (2016) who reported that PAL and PPO were potentially induced by the antagonist *S. rochei* A-1 in apple fruit. Similarly, those two enzyme activities were also promoted by *Pichia membranifaciens*, which was related to enhancing peach resistance to Rhizopus rot (Zhang et al., 2020). In addition, CHI and GLU are other key enzymes involved in plant defense response by disrupting the cell wall structure of pathogens (Romanazzi et al., 2016). Liu et al. (2021) stated that the activities and gene expression of both GLU and CHI were upregulated to decrease the lesion diameter of Alternaria rot in pear fruit. In this study, we also indicated here that GLU and CHI were markers of plant defense response, due to their activities and gene expression levels being enhanced and could persist in strain B-1 treated fruit. These data in our research demonstrate that the induced resistance against *B. dothidea* may be the main action mechanism of strain B-1.

Phenolics and lignin are the pivotal metabolic products in the phenylpropanoid metabolic pathway, which can strengthen the structure of wound tissues and effectively prevent the invasion of pathogens (Jiang et al., 2019). Our results indicated that *P. syringae* B-1treatment induced the increase of total phenolics and lignin contents in apple fruit throughout the storage. Our results are also consistent with Li et al. (2019), where they found that β-Aminobutyric acid could stimulate total phenolics and lignin contents against *Gilbertella persicaria* infection in red pitaya fruit. Moreover, MeJA could promote wound healing by activating total phenolics and lignin contents in harvested kiwifruit (Wei et al., 2021).

In the plant defense system, SA is a critical regulatory signal molecule, and recent research indicated that it participated in the resistance response against *B. dothidea* in apple fruit (Zhao et al., 2020). In our study, MeJA contents changed slightly after *P. syringae* B-1 treatment in apple fruit; however, SA contents were induced by stain B-1. These results suggested that the SA pathway may play an important role in apple fruit resistance induced by strain B-1. Based on our data, we also found strain B-1 treatment upregulated the transcript levels of *MdPR1* and *MdPR5*, which are the key molecular markers correlating with SA signaling activation

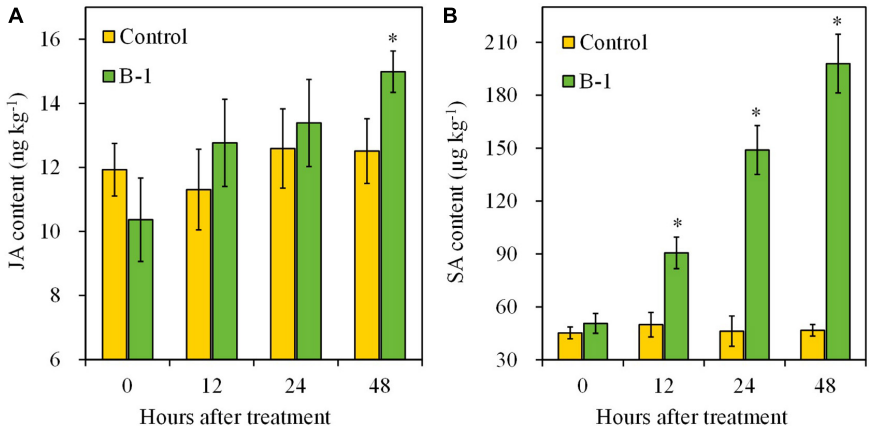

FIGURE 8
The content of JA **(A)** and SA **(B)** in apple fruit treated with *P. syringae* B-1 at 1 × 10^8 CFU mL^{-1} stored at 25°C. Each data represents the mean ± SD of three replicates. Asterisks (*) denote a significant difference ($p < 0.05$) between the strain B-1 treatment and the control apple fruit at the same time point.

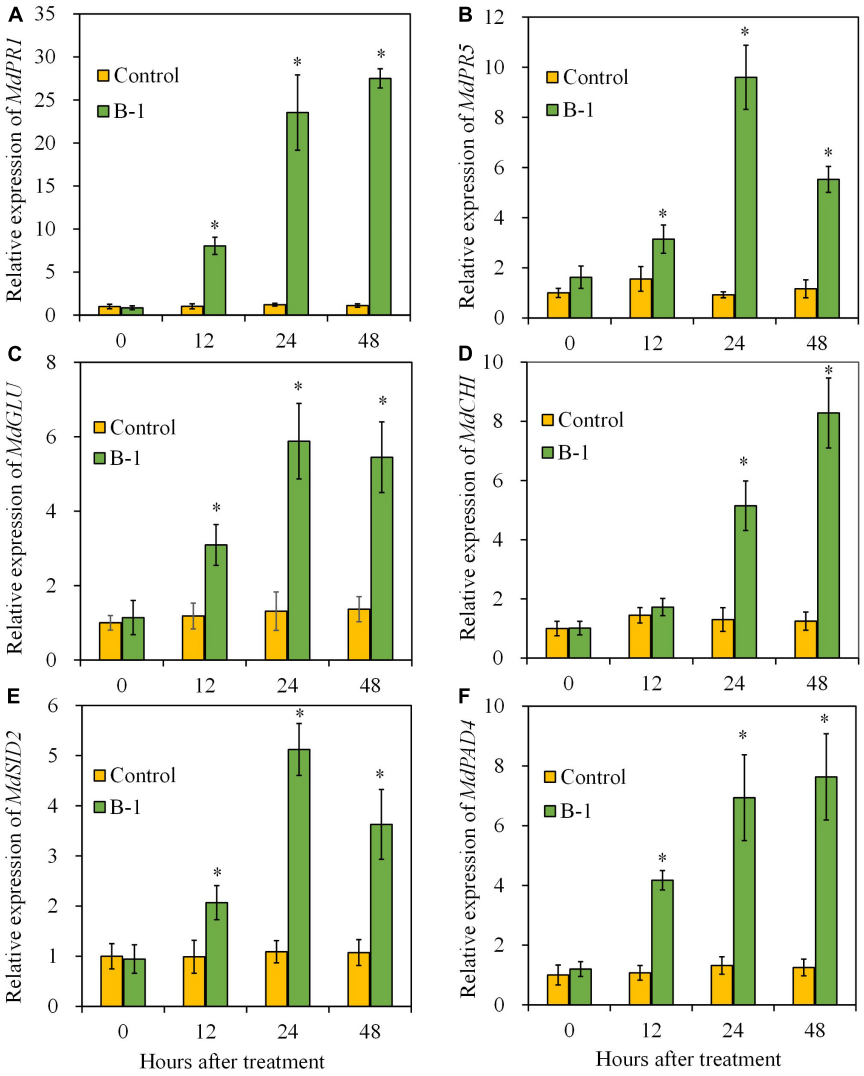

FIGURE 9
The gene expressions of *MdPR1* **(A)**, *MdPR5* **(B)**, *MdGLU* **(C)**, *MdCHI* **(D)**, *MdSID2* **(E)**, and *MdPAD4* **(F)** in apple fruit treated with *P. syringae* B-1 at 1×10^8 CFU mL^{-1} stored at 25°C. Each data represents the mean ± SD of three biological replicates. Asterisks (*) denote a significant difference ($p < 0.05$) between the strain B-1 treatment and the control apple fruit at the same time point.

(Zhang Q. M. et al., 2016; Huang et al., 2021a). Furthermore, strain B-1 also activated *MdSID2* and *MdPAD4* expression in apple fruit. *MdSID2* performs a vital role in the aggregation of SA signal, and *MdPAD4* contributes to regulating plant defense against pathogen infection (Wiermer et al., 2005; Zhao et al., 2020). These findings further exhibited that SA is involved in apple fruit resistance induced by strain B-1, and similar results were also reported by Huang et al. (2021a). Their research showed that butylated hydroxytoluene effectively controls apple ring rot mainly by activating the SA signaling pathway.

5. Conclusion

In our research, a newly isolated *P. syringae* strain B-1 exhibited a strong efficiency against postharvest apple ring rot. Application of strain B-1 suspension at 1×10^8 CFU mL^{-1} reduced the incidence and lesion diameter of apple ring rot *in vivo*. The investigation of the mode of action demonstrated that strain B-1 not only shows the antifungal ability and activates the defense enzymes but also promotes the accumulation of disease-resistant substances and upregulates the transcript levels of PR genes by activating the SA signaling pathway. These results indicate that *P. syringae* strain B-1 has an enormous potential in controlling *B. dothidea* rot during the storage of apple fruit. Further exploration of the application technologies of strain B-1 is under investigation by our team, such as evaluating the tolerance of strain B-1 to fungicides used on apple fruit and the control efficiency of their combined treatments against *B. dothidea*.

Data availability statement

The original contributions presented in this study are included in the article/supplementary material, further inquiries can be directed to the corresponding author.

Author contributions

ZS: conceptualization, data curation, and writing—original draft. BH: methodology, investigation, and writing—original draft. CuW: formal analysis and data curation. SL: methodology and data curation. YX: methodology and investigation. BL: funding acquisition and writing—review and editing. CaW: supervision, funding acquisition, and writing—review and editing. All authors contributed to the article and approved the submitted version.

Funding

This work was supported by the Chinese Modern Agricultural Industry Technology System (No. CARS-27), the National College Student Innovation and Entrepreneurship Training Program (No. 202210435017), the Graduate Student Innovation Program of Qingdao Agricultural University (No. QNYCX21093), and the Student Innovation Training of Qingdao Agricultural University.

Acknowledgments

We thank Dr. Xiangnan Guan at Oregon Health and Science University for their helpful suggestions and for revising the manuscript.

Conflict of interest

The authors declare that the research was conducted in the absence of any commercial or financial relationships that could be construed as a potential conflict of interest.

Publisher's note

All claims expressed in this article are solely those of the authors and do not necessarily represent those of their affiliated organizations, or those of the publisher, the editors and the reviewers. Any product that may be evaluated in this article, or claim that may be made by its manufacturer, is not guaranteed or endorsed by the publisher.

References

Aiello, D., Restuccia, C., Stefani, E., Vitale, A., and Cirvilleri, G. (2019). Postharvest biocontrol ability of *Pseudomonas* synxantha against *Monilinia fructicola* and *Monilinia fructigena* on stone fruit. *Postharvest Biol. Technol.* 149, 83–89. doi: 10.1016/j.postharvbio.2018.11.020

Al-Mughrabi, K., Vikram, A., Peters, R. D., Howard, R. J., Grant, L., Barasubiye, T., et al. (2013). Efficacy of *Pseudomonas syringae* in the management of potato tuber diseases in storage. *Biol. Control* 64:315. doi: 10.1016/j.biocontrol.2012.11.011

Bull, C. T., Wadsworth, M. L., Sorensen, K. N., Takemoto, Y. J., Austin, R. K., and Smilanick, J. L. (1998). Syringomycin E produced by biological control agents controls green mold on lemons. *Biol. Control* 12, 89–95. 0622 doi: 10.1006/bcon.1998

Calvo, H., Marco, P., Blanco, D., Oria, R., and Venturini, M. E. (2017). Potential of a new strain of *Bacillus amyloliquefaciens* BUZ-14 as a biocontrol agent of postharvest fruit diseases. *Food Microbiol.* 63, 101–110. doi: 10.1016/j.fm.2016.11.004

Casals, C., Teixidó, N., Viñas, I., Cambray, J., and Usall, J. (2010). Control of *Monilinia* spp. on stone fruit by curing treatments. Part II: The effect of host and *Monilinia* spp. variables on curing efficacy. *Postharvest Biol. Technol.* 56, 26–30. doi: 10.1016/j.postharvbio.2009.11.009

Chen, X. Y., Zhang, Y. Y., Fu, X. C., Li, Y., and Wang, Q. (2016). Isolation and characterization of Bacillus amyloliquefaciens PG12 for the biological control of apple ring rot. *Postharvest Biol. Technol.* 115, 113–121. doi: 10.1016/j.postharvbio.2015.12.021

Cirvilleri, G., Bonaccorsi, A., Scuderi, G., and Scortichini, M. (2005). Potential biological control activity and genetic diversity of *Pseudomonas syringae* pv. *syringae* strains. *J. Phytopathol.* 153, 654–666. doi: 10.1111/j.1439-0434.2005.01033.x

Droby, S., Wisniewski, M. E., Macarisin, D., and Wilson, C. (2009). Twenty years of postharvest biocontrol research: Is it time for a new paradigm. *Postharvest Biol. Technol.* 52, 137–145. doi: 10.1016/j.postharvbio.2008.11.009

Droby, S., Wisniewski, M., Teixidó, N., Spadaro, D., and Jijakli, M. H. (2016). The science, development, and commercialization of postharvest biocontrol products. *Postharvest Biol. Technol.* 122, 22–29. doi: 10.1016/j.postharvbio.2016.04.006

Errampalli, D., and Brubacher, N. (2006). Biological and integrated control of postharvest blue mold (*Penicillium expansum*) of apples by *Pseudomonas syringae* and cyprodinil. *Biol. Control* 36, 49–56. doi: 10.1016/j.biocontrol.2005.07.011

Fan, K., Wang, J., Fu, L., Li, X., Zhang, Y., Zhang, X., et al. (2016). Sensitivity of *Botryosphaeria dothidea* from apple to tebuconazole in China. *Crop Prot.* 87, 1–5. doi: 10.1016/j.cropro.2016.04.018

Glazebrook, J. (2005). Contrasting mechanisms of defense against biotrophic and necrotrophic pathogens. *Annu. Rev. Phytopathol.* 43, 205–227. doi: 10.1146/annurev.phyto.43.040204.135923

Guo, L. Y., Li, J. Y., Li, B. H., Zhang, X. Z., Zhou, Z. Q., Li, G. X., et al. (2009). Investigations on the occurrence and chemical control of *Botryosphaeria* canker of apple in China. *Plant Protect.* 35, 120–123. doi: 10.3969/j.issn.0529-1542.2009.04.027

Huang, Y., Sun, C. C., Guan, X. N., Lian, S., Li, B., and Wang, C. (2021a). Butylated hydroxytoluene induced resistance against *Botryosphaeria dothidea* in apple fruit. *Front. Microbiol.* 11:599062. doi: 10.3389/FMICB.2020.599062

Huang, Y., Sun, C. C., Guan, X. N., Lian, S., Li, B., and Wang, C. (2021b). Biocontrol efficiency of *Meyerozyma guilliermondii* Y-1 against apple postharvest decay caused by *Botryosphaeria dothidea* and the possible mechanisms of action. *Int. J. Food Microbiol.* 338:108957. doi: 10.1016/J.IJFOODMICRO.2020.108957

Ji, Z. L., Peng, S., Zhu, W., Dong, J. P., and Zhu, F. (2020). Induced resistance in nectarine fruit by *Bacillus licheniformis* W10 for the control of brown rot caused by *Monilinia fructicola*. *Food Microbiol.* 92:103558. doi: 10.1016/j.fm.2020.103558

Jiang, H., Wang, B., Ma, L., Zheng, X. Y., Gong, D., Xue, H. L., et al. (2019). Benzo-(1, 2, 3)-thiadiazole-7-carbothioic acid s-methylester (BTH) promotes tuber wound healing of potato by elevation of phenylpropanoid metabolism. *Postharvest Biol. Technol.* 153, 125–132. doi: 10.1016/j.postharvbio.2019.03

Leng, W. F., Li, B. H., Guo, L. Y., Dong, J. H., Wang, C. X., Li, G. F., et al. (2009). Method to promote sporulation of *Botryosphaeria berengeriana* f. sp. piricola. *Acta Phytopathol. Sinica* 39 536–539. doi: 10.13926/j.cnki.apps.2009.05.017

Li, G. L., Meng, F. B., Wei, X. P., and Lin, M. (2019). Postharvest dipping treatment with BABA induced resistance against rot caused by *Gilbertella persicaria* in red pitaya fruit. *Sci. Hortic.* 257:108713. doi: 10.1016/j.scienta.2019.108713

Li, R., Zhang, H., Liu, W., and Zheng, X. (2011). Biocontrol of postharvest gray and blue mold decay of apples with *Rhodotorula mucilaginosa* and possible mechanisms of action. *Int. J. Food Microbiol.* 146, 151–156. doi: 10.1016/j.ijfoodmicro.2011.02.015

Li, X. J., Jing, T., Zhou, D. B., Zhang, M. Y., Qi, D. F., Zang, X. P., et al. (2021). Biocontrol efficacy and possible mechanism of *Streptomyces* sp. H4 against postharvest anthracnose caused by *Colletotrichum fragariae* on strawberry fruit. *Postharvest Biol. Technol.* 175:111401. doi: 10.1016/J.POSTHARVBIO.2020.111401

Liu, Y. X., Li, Y. C., Bi, Y., Jiang, Q. Q., Mao, R. Y., Liu, Z. T., et al. (2021). Induction of defense response against Alternaria rot in Zaosu pear fruit by exogenous L-lysine through regulating ROS metabolism and activating defense-related proteins. *Postharvest Biol. Technol.* 179:111567. doi: 10.1016/J.POSTHARVBIO.2021.111567

Lu, L., Lu, H., Wu, C., Fang, W., Yu, C., Ye, C., et al. (2013). *Rhodosporidium paludigenum* induces resistance and defense-related responses against *Penicillium digitatum* in citrus fruit. *Postharvest Biol. Technol.* 85, 196–202. doi: 10.1016/j.postharvbio.2013.06.014

Ma, Z. H., Morgan, D. P., Felts, D., and Michailides, T. J. (2002). Sensitivity of *Botryosphaeria dothidea* from California pistachio to tebuconazole. *Crop Prot.* 21, 829–835. doi: 10.1016/S0261-2194(02)00046-7

Mayer, A. M. (2006). Polyphenol oxidases in plants and fungi: Going places? A review. *Phytochemisry* 67, 2318–2331. doi: 10.1016/j.phytochem.2006.08.006

Mittler, R., Vanderauwera, S., Gollery, M., and Breusegem, F. V. (2004). Reactive oxygen gene network of plants. *Trends Plant Sci.* 9, 490–498. doi: 10.1016/j.tplants.2004.08.009

Panebianco, S., Vitale, A., Polizzi, G., Scala, F., and Cirvilleri, G. (2015). Enhanced control of postharvest citrus fruit decay by means of the combined use of compatible biocontrol agents. *Biol. Control* 84, 19–27. doi: 10.1016/j.biocontrol.2015.02.001

Perez, M. F., Díaz, M. A., Pereyra, M. M., Córdoba, J. M., Isas, A. S., Sepúlveda, M., et al. (2019). Biocontrol features of *Clavispora lusitaniae* against *Penicillium digitatum* on lemons. *Postharvest Biol. Technol.* 155, 57–64. doi: 10.1016/j.postharvbio.2019.05.012

Rocío, R. C., David, F. F. J., and Raúl, R. (2021). Mechanisms of action of microbial biocontrol agents against Botrytis cinerea. *J. Fungi* 7:1045. doi: 10.3390/JOF7121045

Romanazzi, G., Sanzani, S. M., Bi, Y., Tian, S. P., Martínez, P. G., and Alkan, N. (2016). Induced resistance to control postharvest decay of fruit and vegetables. *Postharvest Biol. Technol.* 122, 82–94. doi: 10.1016/j.postharvbio.2016.08.003

Sharma, R., Singh, D., and Singh, R. (2009). Biological control of postharvest diseases of fruits and vegetables by microbial antagonists: A review. *Biol. Control* 50, 205–221. doi: 10.1016/j.biocontrol.2009.05.001

Smilanick, J. (1996). Virulence on citrus of *Pseudomonas syringae* strains that control postharvest green mold of citrus fruit. *Plant Dis.* 80:1123. doi: 10.1094/PD-80-1123

Spadaro, D., and Droby, S. (2016). Development of biocontrol products for postharvest diseases of fruit: The importance of elucidating the mechanisms of action of yeast antagonists. *Trends Food Sci. Technol.* 47, 39–49. doi: 10.1016/j.tifs.2015.11.003

Sun, C. C., Huang, Y., Lian, S., Saleem, M., Li, B. H., and Wang, C. X. (2021). Improving the biocontrol efficacy of *Meyerozyma guilliermondii* Y-1 with melatonin against postharvest gray mold in apple fruit. *Postharvest Biol. Technol.* 171:111351. doi: 10.1016/j.postharvbio.2020.111351

Tang, W., Ding, Z., Zhou, Z. Q., Wang, Y. Z., and Guo, L. Y. (2012). Phylogenetic and pathogenic analyses show that the causal agent of apple ring rot in China is *Botryosphaeria dothidea*. *Plant Dis.* 96, 486–496. doi: 10.1094/PDIS-08-11-0635

van Lenteren, J., Bolckmans, K., Köhl, J., Ravensberg, W., and Urbaneja, A. (2017). Biological control using invertebrates and microorganisms: Plenty of new opportunities. *BioControl* 63, 39–59. doi: 10.1007/s10526-017-9801-4

Wallace, R. L., Hirkala, D. L., and Nelson, L. M. (2017). Postharvest biological control of blue mold of apple by *Pseudomonas* fluorescens during commercial storage and potential modes of action. *Postharvest Biol. Technol.* 133, 1–11. doi: 10.1016/j.postharvbio.2017.07.003

Wang, J. Z., and Hou, B. L. (2001). Causes of serious occurrence of apple fruit ring rot in 2000 and its control countermeasures (in Chinese). *Hebei Fruits* 1, 22–23. doi: 10.19440/j.cnki.1006-9402.2001.01.015

Wang, Z., Ma, L., Zhang, X. F., Xu, L. M., Cao, J. K., and Jiang, W. B. (2015). The effect of exogenous salicylic acid on antioxidant activity, bioactive compounds and antioxidant system in apricot fruit. *Sci. Hortic.* 181, 113–120. doi: 10.1016/j.scienta.2014.10.055

Wei, X. B., Guan, W. L., Yang, Y., Shao, Y. J., and Mao, L. C. (2021). Methyl jasmonate promotes wound healing by activation of phenylpropanoid metabolism in harvested kiwifruit. *Postharvest Biol. Technol.* 175:111472. doi: 10.1016/J.POSTHARVBIO.2021.111472

Wiermer, M., Feys, B. J., and Parker, J. E. (2005). Plant immunity: The EDS1 regulatory node. *Curr. Opin. Plant Biol.* 8, 383–389. doi: 10.1016/j.pbi.2005.05.010

Williamson, S. M., Guzmán, M., Marin, D., Anas, O., Xu, J.-J., and Sutton, T. B. (2008). Evaluation of *Pseudomonas syringae* strain ESC-11 for biocontrol of crown rot and anthracnose of banana. *Biol. Control* 46, 279–286. doi: 10.1016/j.biocontrol.2008.05.016

Yan, Y., Zhang, X., Zheng, X., Apaliya, M. T., Yang, Q., Zhao, L., et al. (2018). Control of postharvest blue mold decay in pears by *Meyerozyma guilliermondii* and it's effects on the protein expression profile of pears. *Postharvest Biol. Technol.* 136, 124–131. doi: 10.1016/j.postharvbio.2017.10.016

Ye, W. Q., Sun, Y. F., Tang, Y. J., and Zhou, W. W. (2021). Biocontrol potential of a broad-spectrum antifungal strain Bacillus amyloliquefaciens B4 for postharvest loquat fruit storage. *Postharvest Biol. Technol.* 174:111439. doi: 10.1016/J.POSTHARVBIO.2020.111439

Zhang, G. L., Li, B. H., Wang, C. X., Dong, X. L., and He, X. J. (2010). Curative effects of six systemic fungicides on tumor development on apple branches caused by *Botryosphaeria dothidea* (in Chinese). *J. Fruit Sci.* 27, 1029–1031. doi: 10.13925/j.cnki.gsxb.2010.06.012

Zhang, H. Y., Liu, F. R., Wang, J. J., Yang, Q. R., Wang, P., Zhao, H. J., et al. (2021). Salicylic acid inhibits the postharvest decay of goji berry (*Lycium barbarum* L.) by modulating the antioxidant system and phenylpropanoid metabolites. *Postharvest Biol. Technol.* 178:111558. doi: 10.1016/J.POSTHARVBIO.2021.111558

Zhang, L., Oh, Y., Li, H. Y., Baldwin, I. T., and Galis, I. (2012). Alternative oxidase in resistance to biotic stresses: Nicotiana attenuate AOX contributes to resistance to a pathogen and a piercing-sucking insect but not *Manduca sexta* larvae. *Plant Physiol.* 160, 1453–1467. doi: 10.2307/41694006

Zhang, Q. M., Yong, D. J., Zhang, Y., Shi, X. P., Li, B. H., Li, G. F., et al. (2016). *Streptomyces rochei* A-1 induces resistance and defense-related responses against *Botryosphaeria dothidea* in apple fruit during storage. *Postharvest Biol. Technol.* 115, 30–37. doi: 10.1016/j.postharvbio.2015.12.013

Zhang, X., Wu, F., Gu, N., Yan, X., Wang, K., Dhanasekaran, S., et al. (2020). Postharvest biological control of Rhizopus rot and the mechanisms involved in induced disease resistance of peaches by *Pichia membranefaciens*. *Postharvest Biol. Technol.* 163:111146. doi: 10.1016/j.postharvbio.2020.111146

Zhang, Y., Shi, X. P., Li, B. H., Zhang, Q. M., Liang, W. X., and Wang, C. C. (2016). Salicylic acid confers enhanced resistance to *Glomerella* leaf spot in apple. *Plant Physiol. Biochem.* 106, 64–72. doi: 10.1016/j.plaphy.2016.04.047

Zhao, L. J., Peng, S., Zhu, W., Dong, J., and Zhu, F. (2020). Induced resistance in nectarine fruit by *Bacillus licheniformis* W10 for the control of brown rot caused by *Monilinia fructicola*. *Food Microbiol.* 92:103558.

Zhao, X., Zhang, G. L., Li, B. H., Xu, X. M., Dong, X. L., Wang, C. X., et al. (2016). Seasonal dynamics of *Botryosphaeria dothidea* infections and symptom development on apple fruits and shoots in China. *Eur. J. Plant Pathol.* 146, 507–518. doi: 10.1007/s10658-016-0935-5

Zhou, T., Chu, C. L., Liu, W. T., and Schaneider, K. E. (2001). Postharvest control of blue mold and gray mold on apples using isolates of *Pseudomonas syringae*. *Can. J. Plant Pathol.* 23, 246–252. doi: 10.1080/07060660109506937

Zhou, T., Northover, J., and Schneider, K. E. (1999). Biological control of postharvest diseases of peach with phyllosphere isolates of *Pseudomonas syringae*. *Can. J. Plant Pathol.* 21, 375–381. doi: 10.1080/07060669909501174

frontiers | Frontiers in Microbiology

TYPE Original Research
PUBLISHED 07 March 2023
DOI 10.3389/fmicb.2023.1146065

OPEN ACCESS

EDITED BY
Antonio Ippolito,
University of Bari Aldo Moro,
Italy

REVIEWED BY
Mathabatha Evodia Setati,
Stellenbosch University,
South Africa
Severino Zara,
University of Sassari,
Italy

*CORRESPONDENCE
Ana Mendes-Ferreira
✉ anamf@utad.pt

SPECIALTY SECTION
This article was submitted to Food Microbiology, a section of the journal Frontiers in Microbiology

RECEIVED 16 January 2023
ACCEPTED 17 February 2023
PUBLISHED 07 March 2023

CITATION
Esteves M, Lage P, Sousa J, Centeno F, Teixeira MdF, Tenreiro R and Mendes-Ferreira A (2023) Biocontrol potential of wine yeasts against four grape phytopathogenic fungi disclosed by time-course monitoring of inhibitory activities. *Front. Microbiol.* 14:1146065. doi: 10.3389/fmicb.2023.1146065

Biocontrol potential of wine yeasts against four grape phytopathogenic fungi disclosed by time-course monitoring of inhibitory activities

Marcos Esteves[1,2], Patrícia Lage[1,2], João Sousa[1,2], Filipe Centeno[3], Maria de Fátima Teixeira[3], Rogério Tenreiro[2] and Ana Mendes-Ferreira[1,2]*

[1]WM&B—Laboratory of Wine Microbiology and Biotechnology, Department of Biology and Environment, University of Trás-os-Montes and Alto Douro, Vila Real, Portugal, [2]BioISI—Biosystems & Integrative Sciences Institute, Faculty of Sciences, University of Lisbon, Lisbon, Portugal, [3]PROENOL—Indústria Biotecnológica, Lda, Canelas, Portugal

Grapes' infection by phytopathogenic fungi may often lead to rot and impair the quality and safety of the final product. Due to the concerns associated with the extensive use of chemicals to control these fungi, including their toxicity for environment and human health, bio-based products are being highly preferred, as eco-friendlier and safer alternatives. Specifically, yeasts have shown to possess antagonistic activity against fungi, being promising for the formulation of new biocontrol products.In this work 397 wine yeasts, isolated from Portuguese wine regions, were studied for their biocontrol potential against common grapes phytopathogenic fungal genera: *Aspergillus*, *Botrytis*, *Mucor* and *Penicillium*. This set comprised strains affiliated to 32 species distributed among 20 genera. Time-course monitoring of mold growth was performed to assess the inhibitory activity resulting from either diffusible or volatile compounds produced by each yeast strain. All yeasts displayed antagonistic activity against at least one of the mold targets. *Mucor* was the most affected being strongly inhibited by 68% of the tested strains, followed by *Botrytis* (20%), *Aspergillus* (19%) and *Penicillium* (7%). More notably, the approach used allowed the detection of a wide array of yeast-induced mold response profiles encompassing, besides the decrease of mold growth, the inhibition or delay of spore germination and the complete arrest of mycelial extension, and even its stimulation at different phases. Each factor considered (taxonomic affiliation, mode of action and fungal target) as well as their interactions significantly affected the antagonistic activity of the yeast isolates. The highest inhibitions were mediated by volatile compounds. Total inhibition of *Penicillium* was achieved by a strain of *Metschnikowia pulcherrima*, while the best performing yeasts against *Mucor*, *Aspergillus* and *Botrytis*, belong to *Lachancea thermotolerans*, *Hanseniaspora uvarum* and *Starmerella bacillaris*, respectively. Notwithstanding the wide diversity of yeasts tested, only three strains were found to possess a broad spectrum of antagonistic activity, displaying strong or very strong inhibition against the four fungal targets tested. Our results confirm the potential of wine yeasts as biocontrol agents, while highlighting the need for the establishment of fit-for-purpose selection programs depending on the mold target, the timing, and the mode of application.

KEYWORDS

biocontrol, wine yeasts, phytopathogenic fungi, antagonism, *Aspergillus niger*, *Botrytis cinerea*, *Penicillium* sp., *Mucor* sp.

1. Introduction

Phytopathogenic fungi are one of the major concerns in several agricultural crops, being responsible for significant losses in production and associated economy. Grapes are a particularly rich nutrient source for pathogenic agents, whose action can affect not only grape health and productivity, but also the quality of the final product, whether they are intended for fresh human consumption or for processed products such as raisins, juices and wines. Necrotrophic filamentous fungi are the group of microorganisms presenting most of the concerns in the pre- and post-harvested grapes. If not timely controlled, several species mainly belonging to the genera *Alternaria*, *Aspergillus*, *Botrytis*, *Fusarium*, *Mucor*, *Penicillium* and *Rhizopus* are capable of causing major grape diseases involving the decay of fruit, production of mycotoxins and/or off-flavors (Kassemeyer, 2017; Solairaj et al., 2021). In wine industry, grapes infected with molds are more prone to rot and harbor much higher loads of microorganisms, particularly yeasts and bacteria, that may lead to microbial wine spoilage (Barata et al., 2012). To avoid fungal infections, table grape-growers and winemakers mostly rely on the application of synthetic fungicides on-field, during the different phenological growth stages of the grapes, and at postharvest. However, the increasing concerns about on the harmful side-effects of these compounds on environment and human health, along with the discover of multi-drug resistant biotypes of fungal pathogens, has encouraged scientific community to find efficient, less toxic and more sustainable resources (Wilson and Wisniewski, 1989; Pertot et al., 2017a). In this context, the concept of biocontrol emerged and currently is restricted to the use of living agents (including viruses), with the ability of preventing or at least reduce the growth of the pathogen or the disease producing activity (Ward, 2016; Stenberg et al., 2021).

Among these biocontrol agents, several yeasts have demonstrated antagonistic activity against different fungal phytopathogens of fruits and vegetables (reviewed in Ferraz et al., 2019; Freimoser et al., 2019; Di Canito et al., 2021). Competition for nutrients and space, antibiosis (production of diffusible or volatile compounds), mycoparasitism, and induction of host resistance have been pointed out as the main modes of action underlying their antagonistic activity (reviewed in Bélanger et al., 2012; Spadaro and Droby, 2016). Therefore, it is likely that the best sources of antagonistic strains are their own natural environments in which they have developed strategies to colonize, access nutrients and space and, to inhibit other coexisting microorganisms (including epiphytic pathogens), thus ensuring their survival (Parafati et al., 2015; Pretscher et al., 2018; Pereyra et al., 2021).

In this line, the wine ecosystem (grapes and leaves surfaces, grape-juices, wines and winery equipment) constitutes a valuable source of strains with potential to be used in the biocontrol of grape phytopathogens as it harbors a large diversity of yeast species. The most frequently reported yeasts associated with wine-related ecosystems either belong to oligotrophic and oxidative species affiliated to genera such as *Aureobasidium*, *Cryptococcus*, *Filobasidium*, *Naganishia*, *Rhodotorula* and *Sporidiobolus* as well as to copiotrophic and/or fermentative species of genera such as *Candida*, *Hanseniaspora*, *Metschnikowia*, *Meyerozyma*, *Pichia*, *Saccharomyces*, *Starmerella*, *Torulaspora* and *Wickerhamomyces* (Barata et al., 2012; Bokulich et al., 2014; Sirén et al., 2019).

The prospect of using these so-called "wine yeasts" as antagonists of grape fungal pathogens led to a variety of *in vitro* screenings using dual-culture assays (Suzzi et al., 1995; Bleve et al., 2006; Raspor et al., 2010; Nally et al., 2012; Pantelides et al., 2015; Lemos Junior et al., 2016; Cordero-Bueso et al., 2017; Pretscher et al., 2018; Reyes-bravo et al., 2019). In addition to the assessment of their inhibitory activity, and according to the experimental setup used, this screening methodology also gave insights on the potential modes of action associated, typically the production of antimicrobial compounds (Köhl et al., 2019). In one of the first reports (Suzzi et al., 1995), natural wine yeast strains of the genera *Saccharomyces* and *Zygosaccharomyces* were found to be antagonists of 10 species of soil-borne fungal plant pathogens. Later, *Aspergillus carbonarius* and *A. niger* were found to be inhibited by strains of *Pic. kudriavzevii*, *Met. pulcherrima*, *L. thermotolerans*, *Pic. terricola* and *Can. incommunis* (Bleve et al., 2006). Studies targeting the biocontrol of *Botrytis cinerea* have identified strains of *Aur. pullulans*, *Met. pulcherrima* and *Mey. guilliermondii* (Raspor et al., 2010); of *Schizosaccharomyces pombe* and *Sac. cerevisiae* (Nally et al., 2012); and *Sta. bacillaris* (Lemos Junior et al., 2016) with antagonistic activity. Cordero-Bueso et al. (2017) also identified strains of *H. uvarum*, *Mey. guilliermondii*, *Pic. kluyveri*, *Sac. cerevisiae*, *Han. clermontiae*, *Met. pulcherrima*, and *Can. californica* with a strong antagonistic action against *B. cinerea*, *A. carbonarius* and *P. expansum*. More recently, Reyes-bravo et al. (2019) reported strains of *Aur. pullulans, Cry. antarcticus*, *Cry. terrestris* and *Cry. oeirensis* capable of inhibit the growth of both *B. cinerea* and *P. expansum*. The biocontrol activity of several of the wine yeast strains above enumerated have also been validated *in vivo*, using wounded grapes (Bleve et al., 2006; Raspor et al., 2010; Nally et al., 2012; Lemos Junior et al., 2016; Cordero-Bueso et al., 2017).

In this context, the present work aimed to evaluate the antagonistic activity of a wide-range of yeast strains, previously isolated from grapes, grape-juices and wines, against fungi belonging to *Aspergillus*, *Botrytis*, *Mucor* and *Penicillium* genera. A time-course assessment of the yeasts' effects on the growth of the targeted fungi, associated with the production of diffusible and volatile compounds, was conducted in order to get insights into the yeast-mold target interaction and the mode of action, to ultimately uncover more suitable biocontrol agents for application in the vineyards and/or at postharvest.

2. Materials and methods

2.1. Microorganisms and culture conditions

Three hundred and ninety-seven yeast isolates, randomly selected from a wider yeast culture collection available at WMB LAB at UTAD assembled over the last 20 years and comprising more than 3,000 microbial isolates collected from wine-related environments from different wine-producing regions across Portugal, were used. Yeast isolates were stored in stocks at −80°C in YPD medium (5 g/L of yeast extract, 10 g/L of peptone, 20 g/L of glucose) added with 20% (v/v) glycerol. The selected isolates were transferred to YPD agar (5 g/L of yeast extract, 10 g/L of peptone, 20 g/L of glucose, 20 g/L of agar), grown at 28°C and maintained at 4°C.

Four strains of phytopathogenic fungal genera were used, namely *Aspergillus niger* strain AN1 (isolated from wine bottle cork), *Botrytis cinerea* strain BO1 (isolated from table grapes), *Mucor* sp. strain MU3 (isolated from wine grapes) and *Penicillium* sp. strain

PE3 (isolated from wine grapes). Stocks of mold cultures were prepared in Potato Dextrose Agar (PDA) slants flooded in liquid paraffin and maintained at room temperature. Prior to their use, mold cultures were transferred to PDA plates and grown at 25°C. Spore suspensions of each fungal strain were obtained by harvesting spore mass at the surface of 15 days old colonies with glass beads using PBS buffer 1X with 0.01% Tween 20 and 50% (v/v) glycerol, to assist in spore dispersal and ultra-freezing preservation. After filtration through sterile glass wool, spore concentration was determined using a hemocytometer, adjusted to 1×10^6 or 1×10^4 spores/mL for the ascomycetous phytopathogens and *Mucor* sp., respectively. Spore suspensions were divided into aliquots and stored at −80°C.

2.2. Yeast molecular identification and characterization

Genomic DNA extraction of the autochthonous isolates was performed by phenol-chloroform-isoamyl alcohol method from single-strain pure cultures (Seixas et al., 2019). The identification was achieved by 26S rDNA D1/D2 sequencing using primers NL-1 (5′-GCA TAT CAA TAA GCG GAG GAA AAG-3′) and NL-4 (5′-GGT CCG TGT TTC AAG ACG G-3′), and subsequent BLAST comparison with the deposited 26S rRNA gene sequences in the GenBank data library. Species identification was attributed to an isolate if its 26S rDNA D1/D2 sequence diverged by no more than 2–3 base substitutions (i.e., ≥99.0% sequence identity) to that of a taxonomically accepted species type strain. All isolates matching to *Metschnikowia pulcherrima*-clade species were affiliated to *Met. pulcherrima* as proposed by Sipiczki, (2022). Differentiation of *Han. opuntiae* and *Han. guilliermondii* was achieved by 5.8S-ITS-RFLP analysis, in which ITS1/ITS4 amplification products were digested with restriction enzyme DraI, and separated on 2% agarose gel on 1 × TBE buffer as previously described by Nisiotou and Nychas, (2007).

The molecular diversity of yeast isolates belonging to the most prevalent genera was also evaluated through PCR-fingerprinting, using minisatellite csM13 (5′GAGGGTGGCGGTTCT3′) and microsatellite $(GTG)_5$ (5′GTGGTGGTGGTGGTG3′), as single primers, following the methodology described previously by Barbosa et al. (2018). DNA banding patterns were analyzed using the BioNumerics software (version 5.0, Applied Maths, Sint-Martens-Laterat, Belgium). Similarities among isolates, using the combined $(GTG)_5$ and csM13 genomic fingerprinting patterns, were estimated using the Pearson coefficient and clustering was based on the UPGMA method. A cut-off value of 80% similarity was used to define the number of clusters inside each genus.

2.3. Extracellular enzymatic activities of yeasts

The ability of the set of yeast strains to secrete lytic enzymes (protease, pectinase, chitinase, glucanase, cellulase, mannanase, and amylase) eventually associated with the suppression of growth of fungal pathogens was evaluated by spotting 3 µL of freshly grown yeast culture suspensions (~10^7 cells/mL) onto solid media containing the specific enzyme substrates.

For proteolytic activity, Skim Milk agar was used. The formation of a light halo around the colonies after incubation at 28°C for 5 days indicated the enzymatic activity (Strauss et al., 2001).

Pectinolytic activity was tested by using a selective medium containing 12.5 g/L polygalacturonic acid, 6.8 g/L potassium phosphate (pH 3.5), 6.7 g/L yeast nitrogen base without ammonium sulfate, 10 g/L glucose, and 20 g/L agar. After incubation at 28°C for 5 days, the plates were stained with 0.1% (w/v) ruthenium red after the colonies being rinsed off with distilled water. Colonies showing a purple halo were considered positive (Strauss et al., 2001).

For glucanase, chitinase and cellulase activities YPD plates containing 0.2% β-D-glucan from barley or 0.2% chitin from shrimp shells or carboxymethyl cellulose (CMC) sodium salt were used, respectively. After incubation, at 28°C for 5 days, the plates were rinsed with distilled water and stained with 0.03% (w/v) Congo red. A clear zone around the colony was indicative of the presence of glucanase or chitinase activity (Strauss et al., 2001). For the cellulase assay, after incubation, the plates for were stained with 0.1% (w/v) Congo red solution for 30 min and then washed with 1 M NaCl solution for 15 min. The detection of a degradation halo around the colonies was indicative of a positive result (Chen et al., 2018).

The endo-1,4-β-mannanase activity was determined using a medium containing 9.0 g/L peptone, 1.0 g/L yeast extract, 1.0 g/L KH_2PO_4, 0.5 g/L $MgSO_4.7H_2O$, 15 g/L agar and a carbon source of commercial mannan, azo-carob-galactomannan (2 g/L). The pH of the medium was adjusted to 5.5. Positive mannanase producers were detected based on the clear zone formed on the medium around the colony after 5 days of incubation at 28°C (Asfamawi et al., 2013).

Amylase activity was assessed using a selective medium containing 10 g/L of yeast extract, 20 g/L of peptone from meat, 20 g/L of starch, and 20 g/L of agar. The pH of the medium was adjusted to 5.0. The amylase plates were overlaid with Lugol's solution (iodine–potassium iodide solution) and amylase activity was detected by the presence of a bright lysis zone around the colonies, while the rest of the medium remained violet, as the dye solution stained the non-hydrolyzed starch (Pretscher et al., 2018).

2.4. *In vitro* antagonistic activity assays

The antagonistic activity of the set of 397 yeast strains against four common phytopathogenic fungal agents was evaluated using two *in vitro* assays approaches related to distinct modes of action underlying their inhibition. For all the assays, yeast strains were pre-cultivated in YPD medium and incubated overnight at 28°C. Prior to inoculation of each mold target, the suspensions of spores, prepared as described above, were removed from the freezer, and allowed to attain room temperature. The incubation period and the measuring points were previously established by performing mock trials in which the time taken for each mold target to extend from the point of inoculation to the edge of the Petri dish was observed. Based on these experiments it was established, a total incubation period of 40 h and 4, 5, and 7 days for *Mucor* sp., *B. cinerea*, *A. niger* and *Penicillium* sp., respectively, and daily measurements of radial mycelial extension. Due to the rapid growth of *Mucor* sp. additional measurements, at 16 h, were performed.

2.4.1. Confrontation assay (CY)

A dual screening assay in which the mold target is confronted with each yeast strain (CY assay) was used to investigate the potential inhibitory effect, mainly resulting from diffusible compounds, of the yeast strains against the four phytopathogenic fungi. Briefly, 3 µL of seven fresh yeast cultures were equidistantly positioned at 3 cm or 1.5 cm (in the case of *Penicillium* sp.) distance from the center of a YPD agar plate (ø = 90 mm), and allowed to grow during 48 h at 25° C. Then, 3 µL of a mold spore suspension were inoculated in the center of each Petri plate and again incubated at 25°C. The radial mycelial extension of the phytopathogens in the direction of each yeast was recorded. For each mold target, and each round of assays, plates without yeast inoculation were used as external controls.

2.4.2. Volatile organic compounds assay (VOCs)

All yeast strains were also screened for the potential production of volatile organic compounds (VOCs assay) with inhibitory activity against the four phytopathogenic fungi. To avoid yeast-mold target contact, Petri dishes with four compartments, containing 4 mL of YPD agar in each sector were used. In two compartments, 50 µL of pre-grown fresh yeast culture were spread plated, while in the other two, 3 µL of a mold spore suspension were inoculated in central corner of the plate. For each mold target, and each round of assays, plates without yeast inoculation were used as external controls. The plates were sealed with Parafilm® to prevent the outflow of volatile compounds and incubated at 25°C. Radial mycelial extension of the phytopathogen was daily recorded.

A schematic overview of the two *in vitro* antagonistic activity assays is presented in the Supplementary Figure S1.

2.5. Data analysis

The inhibition of radial growth-IRG (%), which considers the radial growth-RG (mm)-of the mold target in the absence ($RG_{control}$) and in the presence of a yeast strain (RG_{tested}) at the end of the incubation period, was calculated as described by Lemos Junior et al. (2016):

$$IRG(\%) = \left(1 - \frac{RG_{tested}}{RG_{control}}\right) * 100$$

The effect of each yeast strain on mold growth profiles was also quantified considering the daily measurements of radial mycelial extension during the overall established period of incubation. The area under the mycelial extension/time curve (AUC, mm.day) was calculated applying the linear trapezoid rule using GraphPad Prism software 9.3.1 (2021 GraphPad Software, San Diego, CA, United States). The obtained data were used to determine an additional parameter to assess yeast antagonistic ability (IAC; %) which relates the AUC (mm.day) of growth of the mold target in the absence ($AUC_{control}$) and in the presence of a yeast strain (AUC_{tested}) during the incubation period, calculated as follows:

$$IAC(\%) = \left(1 - \frac{AUC_{tested}}{AUC_{control}}\right) * 100$$

The reproducibility of antagonistic assays was assessed performing at least 20% of duplicate assays (CY and VOCs) using randomly selected yeast strains against the four targeted strains and evaluating the coefficient of variation (CV%) and respective confidence intervals obtained for the RG (mm) and AUC (mm.day) measurements.

Principal-component analysis (PCA) was carried out to represent yeast strains correlated to the inhibition of the four mold targets by diffusible and volatile compounds as response variables using JMP 11.0 software (SAS Inc., 2013).

As the data of the inhibitory activities (IRG and IAC) against the four targets by the two modes of action did not meet the assumptions of a normal distribution (Shapiro–Wilk test), prior to ANOVA analysis, data was transformed using the Aligned Rank Tool (ARTool) (Wobbrock et al., 2011). Pair-comparison of means was obtained by either *t*-test or Tukey's procedure at $p < 0.05$, using JMP 11.0 software (SAS Inc., 2013).

The data set consisting of time-series measurements of mold growth in each dual-assay was analyzed using MiniTab software (2022 Minitab LLC). The similarity of the 397 yeast-induced mold target responses was calculated using the Pearson coefficient and UPGMA clustering. A cut-off value of 80% was applied for the definition of distinct response profile types. To facilitate comparisons among taxonomic groups (yeast genera and mold target), Pielou's (J') evenness index was calculated (Pielou, 1966) for the most prevalent genera ($n > 20$ isolates), as a quantitative estimate of the genomic and antagonistic distribution of the strains based on the number of profiles types of PCR-fingerprinting and of the mold responses. In other words, this evenness index expresses how evenly the strains are distributed among the different profiles obtained for each taxonomic group. If all yeast strains are represented in equal numbers in the obtained profiles, meaning great diversity, then $J' = 1$, if one profile strongly dominates, meaning less diversity, J' is close to zero (Zar, 1996).

3. Results

3.1. Molecular identification of the yeast collection

From a wider collection of autochthonous yeasts collected from different Portuguese wine regions, a subset of 397 isolates were randomly selected for this study. This set was considered to represent the regional diversity of our collection, which includes mostly isolates of samples from the Douro Demarcated Region (grapes, musts, and wines), so that most of them were expected to be originated from this region (Figure 1A). Among the set, a few isolates had been previously identified (Seixas et al., 2019); the remaining isolates, whose identity was still unknown, were herein disclosed.

Thirty-three species belonging to 20 different genera of yeasts were represented in the yeast set (Figure 1B; Supplementary Table S1). The six most prevalent genera were *Metschnikowia* (105 isolates) represented by *Met. pulcherrima*, *Starmerella* (84 isolates) represented by *Sta. bacillaris* (83) and *Sta. stellata* (1), *Hanseniaspora* (62 isolates) represented by *Han. uvarum* (48), *Han. guilliermondii* (11) and *Han. opuntiae* (3), *Saccharomyces* (53 isolates) represented by *Sac. cerevisiae*, *Lachancea* (28 isolates) represented by *L. thermotolerans* and *Aureobasidium* (21 isolates) represented by *Aur. pullulans* only.

All together these genera represented approximately 89% of the isolates.

In lower numbers, we found the genera *Pichia* (9 isolates), *Candida*, *Meyerozyma, Torulaspora* and *Zygosaccharomyces* with 5 isolates each, *Rhodotorula* (4 isolates) *Naganishia* (3 isolates) and *Wickerhamomyces* (2 isolates). The genera *Filobasidium*, *Hyphopichia, Nakazawaea*, *Saccharomycodes, Yamadazyma* and *Zygoascus* were represented by a single isolate.

The sequence data of D1/D2 domains of all strains used in this study have been deposited in GenBank under the accession numbers MG832576 to MG832583, MG877743 and MG87744 (Seixas et al., 2019) and OQ304691-OQ305072.

3.2. Extracellular enzymatic activities of yeasts

The production of fungal cell wall-degrading enzymes is considered to be one of the important characteristics associated with the activity of biocontrol agents (Spadaro and Droby, 2016). Thus, herein, all yeasts were evaluated for extracellular enzymatic activities (amylase, glucanase, cellulase, chitinase, mannanase, protease, and pectinase).

Only 12 out of the 20 genera included strains displaying at least one enzymatic activity, and any isolate exhibited all the enzymatic activities (Table 1). Besides this intra-genus diversity, also interspecific variability was observed among strains of the same species. Six of the seven enzymatic activities tested were detected in *Aur. pullulans* strains, being the only species displaying mannanase and pectinolytic activities. In contrast, none of the *Aur. pullulans* strains exhibited glucanase activity while, notably, 21 out of 28 L. *thermotolerans* strains produced this enzyme. Protease release was found in a higher number of isolates (37), while cellulase activity was found to be the most common hydrolytic activity detected among different yeast species (7).

3.3. *In vitro* antagonistic assays

3.3.1. Mold growth inhibition induced by yeasts

All 397 yeast strains were screened for their ability to inhibit four important fungal pathogens using two dual-culture growth inhibition tests. A very good intra-plate reproducibility of the assays (CY and VOCs) was found, with the average coefficient of variation for RG (mm) measurements at the end of incubation period being minor, homogeneous and similar in both types of assays (5.52% ± 1.25 and 5.73% ± 1.22% in the CY and VOCs assays, respectively).

In general, all yeasts exhibited an antagonistic phenotype, with an IRG > 5%, against at least one of the mold targets tested, through the production of diffusible (CY) and/or volatile compounds (VOCs) (Supplementary Table S1). The strains of *Pic. membranifaciens* and *R. nothofagi* exhibited the worst overall performance, not reaching 25% inhibition against any of the targets either in the CY or VOCs assays. Considering all the assays performed against all targets, the IRG (%) induced by yeasts volatile compounds production ranged from −19%, consistent with a stimulant effect by an *Aur. pullulans* strain, to 100%, corresponding to the total inhibition of *Penicillium* sp. PE3 by a *Met. pulcherrima* strain. The greatest inhibition activity against *A. niger* AN1 (81%), *B. cinerea* BO1 (94%) and *Mucor* sp. MU3 (94%) were also attained in the VOCs assays by a *Han. uvarum*, a *Sta. bacillaris* and a *L. thermotolerans* strain, respectively.

A stimulant effect of yeasts on mold growth was also observed in the CY assays, but only against *B. cinerea* BO1 and *Mucor* sp. MU3. On the other hand, the maximum inhibition levels against all targets in this assay were lower than those induced by volatile compounds:

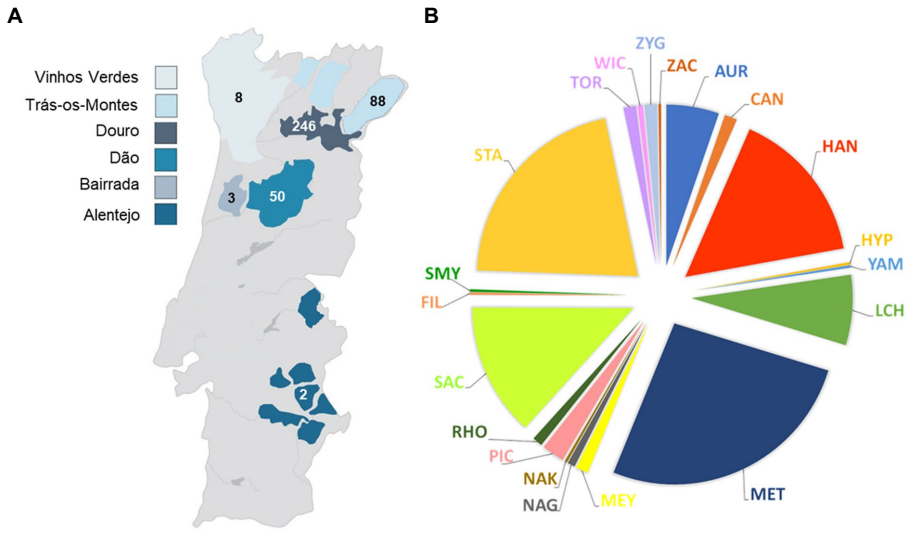

FIGURE 1
Geographical **(A)** and taxonomic distribution at the genus level **(B)** of the isolates examined in this study. The numbers of yeast isolates from the different wine regions are indicated and the colors represent the different genera. AUR, *Aureobasidium*; CAN, *Candida*; HAN, *Hanseniaspora*; HYP, *Hyphopichia*; YAM, *Yamadazyma*; LCH, *Lachancea*; MET, *Metschnikowia*; MEY, *Meyerozyma*; NAG, *Naganishia*; NAK, *Nakazawaea*; PIC, *Pichia*; RHO, *Rhodotorula*; SAC, *Saccharomyces*; FIL, *Filobasidium*; SMY, *Saccharomycodes*; STA, *Starmerella*; TOR, *Torulaspora*; WIC, *Wickerhamomyces*; ZAC, *Zygoascus*; ZYG, *Zygosaccharomyces*.

TABLE 1 Yeast species comprising strains with positive results in the screening performed for enzymatic activities.

Yeast species	Man	Pec	Pro	Cel	Glu	Amy	Chi
Aureobasidium pullulans ($n = 21$)	13	15	21	19	–	16	2
Candida glabrata ($n = 4$)	–	–	–	1	–	–	–
Hanseniaspora guilliermondii ($n = 11$)	–	–	4	–	–	–	–
Hanseniaspora uvarum ($n = 48$)	–	–	10	–	2	–	–
Hyphopichia burtonii ($n = 1$)	–	–	–	–		1	–
Lachancea thermotolerans ($n = 28$)	–	–	–	–	21	1	2
Metschnikowia pulcherrima ($n = 105$)	–	–	–	–	2	–	6
Nakazawaea ishiwadae ($n = 1$)	–	–	1	–	–	–	–
Pichia kluyveri ($n = 2$)	–	–	–	1	–	–	–
Rhodotorula nothofagi ($n = 2$)	–	–	–	2	–	–	–
Saccharomyces cerevisiae ($n = 53$)	–	–	–	1	1	–	1
Starmerella bacillaris ($n = 83$)	–	–	1	1	2	–	9
Wickerhamomyces anomalus ($n = 2$)	–	–	–	1	–	–	–
Total	13	15	37	26	28	18	20

The number of isolates tested of each species is given in parenthesis. Man, Mannanase; Pec, Pectinase; Pro, Protease; Cel, Cellulase; Glu, Glucanase; Amy, Amylase; Chi, Chitinase.

two *Han. uvarum* strains were the most effective in inhibiting the growth of *A. niger* AN1 (56%) and *Mucor* sp. MU3 (49%) while strains of *Sta. bacillaris* and *Sac. cerevisiae* were able to reduce 60 and 66% of the growth of *B. cinerea* BO1 and *Penicillium* sp. PE3, respectively.

In general, the IRG (%) values obtained in the different assays for the isolates belonging to the same genus were broadly distributed and showed several outliers, as this behavior was highly variable with the target and/or the mode of action (Supplementary Table S1; Supplementary Figure S2). Indeed, the ART-ANOVA analysis showed that the antagonistic activity of this set of yeasts was significantly dependent ($p < 0.05$) on their taxonomic affiliation, the mode of action, the mold target and the interactions between all factors (Supplementary Table S2). To evaluate the overall similarity of yeast strains Principal Component Analysis (PCA) was performed, based on their combined inhibitory traits, measured in CY and VOCs assays, against the four targets (Figure 2). The results showed that only 44.6% of the total variation could be explained by the first two components of the PCA, with no clear separation of the yeast strains according to either the mold target or the mode of action. Nevertheless, a tendency for a genus-based clustering of the isolates affiliated to *Hanseniaspora* and *Starmerella,* which displayed on average significantly higher antagonistic activity ($p < 0.05$), could be noticed, with the majority of the strains grouping together away from the remaining genera according to PC1 and being separated in the first and second quadrant, respectively, according to PC2.

3.3.2. Time-course mold growth responses induced by yeasts

Since that, in addition to the final growth during the incubation period, the daily extension of the mycelium was also recorded, we then sought to analyze the temporal response of each of the four mold targets to the 397 wine yeast strains. In this line, the overall time series data of *A. niger* AN1, *B. cinerea* BO1, *Mucor* sp. MU3 and *Penicillium* sp. PE3, obtained in the control and in the presence of each yeast strain were analyzed by hierarchical clustering with Pearson correlation coefficient and UPGMA (Supplementary Figure S3). This analysis allowed the distinction of yeasts strains based on their differential effect on the growth of each of the four mold targets, while identifying groups of strains inducing similar mold responses. For all targets, a higher number of responsive growth profiles were obtained for the CY (8–19 clusters) than for VOCs assay (4–9 clusters). Both mold target and mode of action were identified as factors driving the number and yeast genera distribution among each mold target response profile.

The high diversity of mold response profiles induced by the different yeast strains was further highlighted by the analysis of Pielou's (J') evenness index of diversity, calculated for the most representative genera/species ($n > 20$ isolates), using a cut-off value of 80% similarity for each dendrogram (Supplementary Figure S3) as well as in the UPGMA dendrogram of the combined $(GTG)_5$ and csM13 genomic fingerprinting patterns (Supplementary Figure S4). The radar charts presented in Figure 3 illustrate the yeast inter and intra-genera diversity of induced inhibitory responses, highly dependent on both the mold target and the mode of action. Additionally, the results show that no association could be established between the genotypic diversity within a taxonomic group and the number of antagonistic responses induced by yeasts. Accordingly, despite the low genotypic diversity found among the strains of *L. thermotolerans* ($J' = 0.37$), the 28 isolates induced a wide diversity of responses on *A. niger* AN1 ($J' = 0.97$) and *Mucor* sp. MU3 ($J' = 0.83$) in the VOCs and CY assays, respectively. Conversely, notwithstanding the high genotypic diversity found for *Aur. pullulans* ($J' = 0.86$), the volatile compounds produced by the 21 isolates induced the same response profile on *A. niger* AN1 and highly similar ones on *Penicillium* sp. PE3 ($J' = 0.28$).

The average profiles (Supplementary Figure S3) were subsequently visually inspected and, in some cases, those displaying similar trends were merged, producing more congruent and manageable number of profiles. The ultimate distinctive growth response patterns of each mold target, as well as the number and taxonomic affiliation of the associated yeast strains, are presented in Figure 4.

The impact of yeast metabolite production could be more clearly seen in the reshaping of the growth profile of each of the four targets, with some yeast strains displaying marked effects on the germination of spores, growth rate and/or final radial mycelia extension, these being dependent on the yeast mode of action (Figure 4A). All yeast

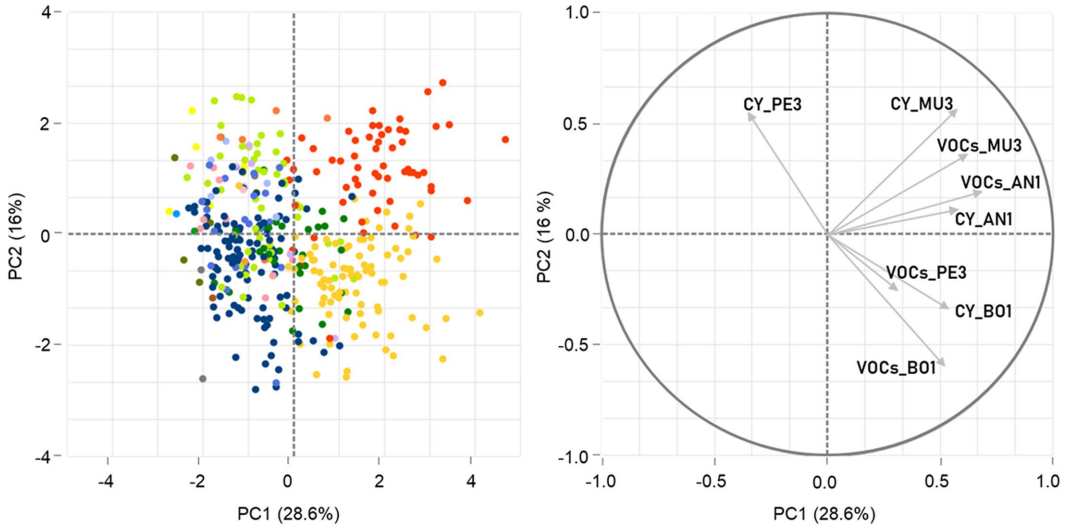

FIGURE 2
Principal component analysis (PCA) of yeast antagonistic activity against the four mold targets. The spatial representation of the 397 yeast strains according to the two first principal components (PC1 and PC2) is built on their inhibitory activity against *Aspergillus niger* AN1, *Botrytis cinerea* BO1, *Mucor* sp. MU3 and *Penicillium* sp. PE3, mediated by diffusible (CY) and volatile compounds (VOCs) and determined by IRG. The data points, corresponding to the yeast strains tested, were colored by genera affiliation following the color scheme used in Figure 1.

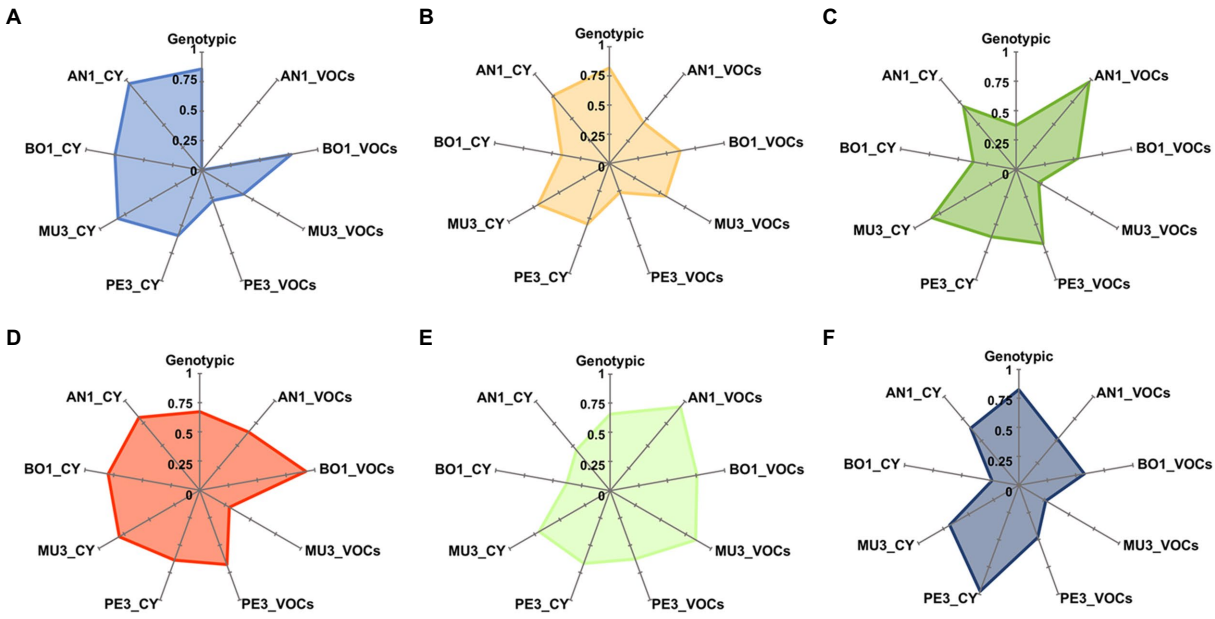

FIGURE 3
Radar plots of genotypic and antagonistic activity diversity indexes. For the most representative yeast genera, *Aureobasidium* **(A)**, *Starmerella* **(B)**, *Lachancea* **(C)**, *Hanseniaspora* **(D)**, *Saccharomyces* **(E)** and *Metschnikowia* **(F)**, Pielou's J' evenness index was calculated based on groups defined at 80% similarity level on dendrograms constructed, using Pearson correlation coefficient and UPGMA of the PCR fingerprinting profiles (Supplementary Figure S4) and of the mold response profiles (Supplementary Figure S3). AN1, *Aspergillus niger*; BO1, *Botrytis cinerea*; MU3, *Mucor* sp.; PE3, *Penicillium* sp.; CY, diffusible compounds assay; VOCs, volatile compounds assay.

strains were found to affect the growth kinetics of *A. niger* AN1 by the production of volatile compounds and the growth of *Penicillium* sp. PE3 by either one of the type of compounds, as no response patterns clustered to the respective controls (patterns E in Figure 4A). A stimulatory effect of different yeast genera (patterns A in Figures 4A,C) on spore germination and/or on growth of all mold targets could also be observed, this being more evident in the VOCs assays for *A. niger* AN1 (146 isolates in Figure 4B). Still, the majority of the response patterns denoted antagonistic effects, at different extents, induced by yeasts against all mold targets (patterns B and D in Figure 4A).

Overall, the most prevalent response pattern prompted by yeasts, detected in the CY assays, was characterized by a decrease of mold

mycelia extension rate (patterns D in Figures 4A,B). The particular average response patterns A1 and D2 of *A. niger* AN1 and D2 and D3 of *Penicillium* sp. PE3 (patterns in Figure 4A) should be highlighted as they denote yeast-induced effects characterized by a significant reduction or even the early complete arrest of mycelial extension, after an initial regular mold growth.

Volatile compounds had a more marked effect on the timing of the onset of spore germination, inducing more or less longer lag growth phases of all targets, except *B. cinerea* BO1 (patterns B in Figures 4A,B). These plateaus are disregarded by the commonly used IRG (%) metric that only considers the final RG (mm) and thus may underestimate the categorization of yeast antagonistic potential. Indeed, while the IRG (%) value seems to adequately reflect the antagonistic activity of yeasts when the mycelial extension rate is steady across the incubation period, this may not be the case when either the onset of spore germination or mycelial extension rate is differentially affected. An illustrative example is the similar average IRG (%) of the yeast strains assigned to patterns B1 and D2 for *A. niger* AN1 or assigned to patterns B2 and D2 for *Penicillium* sp. PE3, despite the marked differences between the mold growth patterns.

Collectively, those observations prompt us to propose a new metric (IAC, %), with a higher discriminating power, for the categorization of yeasts based on the determination of the area under the curves (AUC, mm.day) of mold growth in the absence and in the presence of the different yeast strains, during the incubation period (Supplementary Table S1). As seen for RG (mm) measurements the average variance of the determined AUC (mm.day) values was low and homogeneous in both assays, although higher in the VOCs assay (8.67% ± 1.95%) than in the CY (4.68% ± 0.6%). The two metrics were highly correlated, particularly in the VOCs assays (> 90%) irrespective of the mold target (Supplementary Figure S5). With the exception of *B. cinerea* BO1, lower correlations were found between the metrics determined for the CY assays, this being associated with the higher number of yeast strains inducing more pronounced variations or the abrupt arrest in the mycelial extension rate during the incubation period in these assays (Figures 4A,B).

Principal component analysis was also performed to assess the distribution of the 397 yeast strains based on IAC (%) (Supplementary Figure S5). Although the amount of total variation

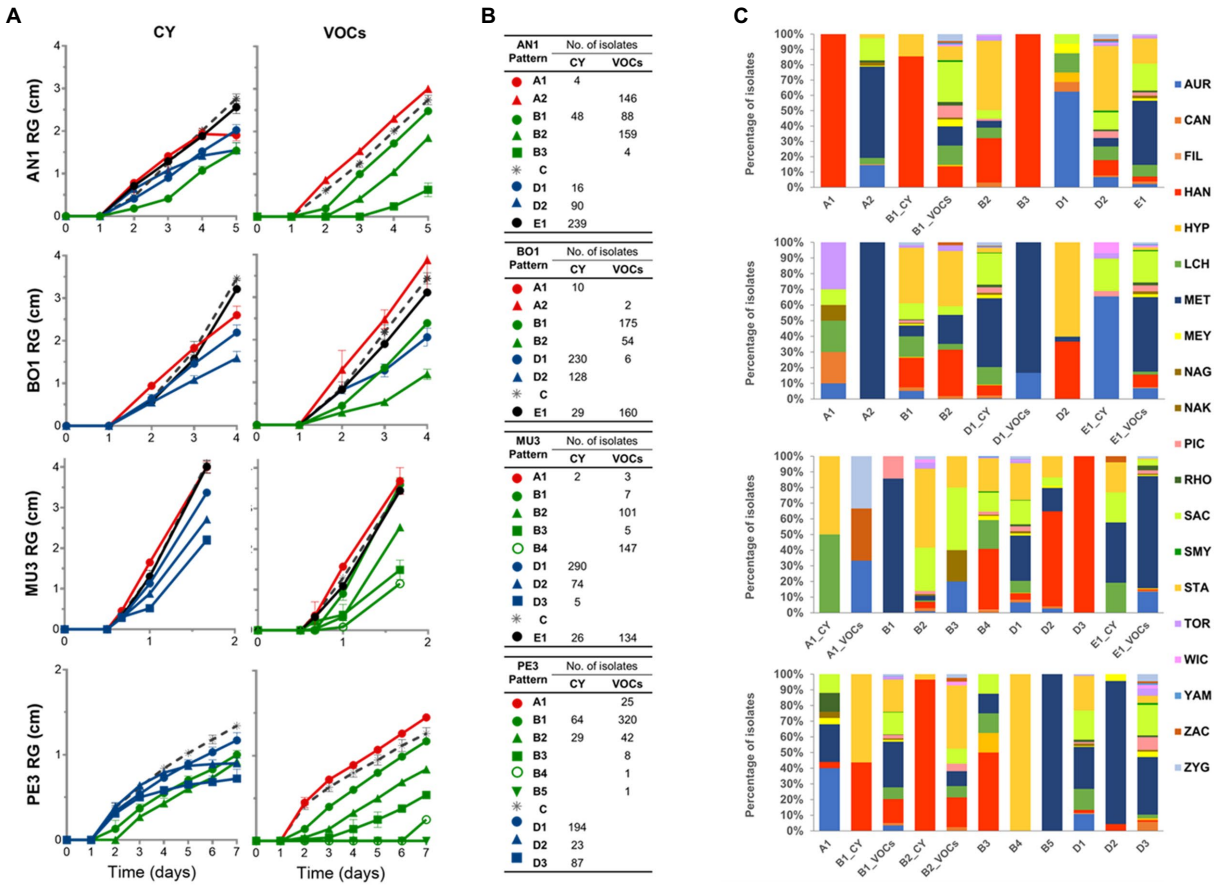

FIGURE 4
Representative growth patterns of the mold targets in response to yeast activity mediated by diffusible (CY) and volatile compounds (VOCs). Representative growth patterns of *Aspergillus niger* AN1, *Botrytis cinerea* BO1, *Mucor* sp. MU3 and *Penicillium* sp. PE3 in response to yeast activity were defined based on hierarchical clustering with Pearson correlation coefficient and UPGMA of time-course measurements **(A)**. Different colors were assigned to highlight the different mold growth patterns induced by yeasts: stimulatory effect (patterns A, in red); inhibition or delaying of the germination of mold spores (patterns B, in green); delayed effect on the growth rate (patterns D, in blue); no effect (pattern E, in black). For each target, mold growth pattern in the absence of yeast (control) is represented by the gray dashed line. The symbols represent mean values, with the bars indicating the standard error. The total number of isolates **(B)** and the prevalence of the yeast species **(C)** allocated to each profile are presented.

explained (46.6%) was not markedly higher than that obtained using the IRG (%) metric (Figure 2), the use of the IAC (%) values led to a better genus-based distribution of the yeast strains built on the antagonistic activity (PC1) and a higher effectiveness of PC2 in distinguishing the mode of action of yeast strains within each genus, as demonstrated by the direction and magnitude of the respective PCA score plots. These results are more in agreement with the significant differences found in ART-ANOVA analysis of the inhibitory activity among genera and within each genus according to the different types of metabolites produced by yeasts (Supplementary Table S3).

3.3.3. Diversity of yeasts with antagonistic activity against the mold targets

For a biological interpretation of the data, the yeast strains were classified in different categories based on their inhibitory activity using the IAC (%) metric: class 0 (no effect: $-5 < IAC < 5\%$), class 1 (weak effect: $5\% \leq IAC < 25\%$), class 2 (moderate effect: $25\% \leq IAC < 50\%$), class 3 (strong effect: $50\% \leq IAC < 75\%$) and class 4 (very strong effect: $IAC \geq 75\%$). Strains with stimulatory activity, identified by a negative IAC ($< -5\%$) effect of mold growth were included in class S. Figure 5 summarizes the distribution of the yeast strains for each species on those classes. In accordance with the above description of yeast-induced diversity of mold responses (Figure 3), the distribution of the IAC values amongs yeast strains was found to be heterogeneous, and none of the yeast genus/species represented by more than one strain comprised only one class of strains against all targets. Furthermore, the data presented in Figure 5, underscores the variability in the biocontrol potential found among yeasts of the same taxonomic group. For example, the 105 Met. *pulcherrima* strains were considered for all the six classes, from S through 4, according to their VOCs-induced effect on *Penicillium* sp. while the three strains of *Han. opuntiae* tested were placed in classes 1,2, and 3, based to their VOCs-induced antagonistic activity (22, 44, and 59%, respectively) against *B. cinerea* BO1.

In order to identify the most promising candidates to be used as biocontrol agents we restrained our subsequent analysis to those isolates exhibiting a more prominent inhibitory activity by selecting strains only included in classes 3–4 by both type of assays (CY and VOCs). Interestingly, no isolate was found in those classes for *Mucor* sp. MU3 in the CY assay and thus a less stringent criterion was applied, and isolates included in class 2 for this target were considered instead in the following analysis.

In a first approach we aimed to identify the most effective strains against each mold target, irrespective of the mode of action. The Venn diagrams presented in Figures 6A–D present the number of shared strains included in these categories for each target. Irrespective of the type of assay, the percentage of yeast isolates with strong and or very strong antifungal activity was the highest against *Mucor* sp. MU3 (68%) followed by *B. cinerea* BO1 (20%), *A. niger* AN1(19%) and *Penicillium* sp. PE3 (7%).

Twelve isolates were found to be highly effective by both modes of action against *A. niger* AN1 and comprise strains of *Sta. bacillaris* (1), *Han. uvarum* (9) and *Han. opuntiae* (2) (Figure 6A). These yeasts were all associated with the response patterns B1_CY and B2, except one *Han. uvarum* that was assigned to the pattern B3 (Figure 4). The average IAC in both assays ranged from 71 to 51.8% induced by two *Han. uvarum* strains.

Three isolates of *Han. uvarum*, one of *Met. pulcherrima* and the only representative of *Zygoascus meyerae* showed a strong inhibitory activity against *B. cinerea* BO1 by both modes of action (Figure 6B). The latter displayed the highest average IAC (65.7%) and was part of the strains inducing a D1 and B2 response patterns in *B. cinerea* (Figure 4).

As for *Mucor* sp. MU3, 80 isolates, belonging to eight different genera, were considered as potentially interesting biocontrol strains with an average IAC (%) in both assays ranging from 39.1% by one *Sac. cerevisiae* strain, assigned to patterns D1 and B2 (Figure 4), to 71.8% by one *Han. uvarum* allocated to patterns D3 and B4 (Figure 3).

The single strong inhibitor of *Penicillium* sp. PE3, with an average IAC of 58.3%, was the only representative of *Hyphopichia burtonii* in our set of yeasts. This yeast was included in the group of strains inducing a D3 and B3 response patterns in this mold target (Figure 4), being able to completely inhibit *Penicillium* sp. PE3 proliferation since day 5 in the CY assay.

Additionally, the strains affiliated to *Pic. terricola* (2) and *Mey. guilliermondii* (2), which inhibited *Penicillium* sp. PE3 growth since day 3 until de end of the experiment (patterns D3, Figures 4A,B), and the strains of *Aur. pullulans* (2), *Can. glabrata*, *Han. uvarum*, *Hyp. burtoni, L. thermotolerans*, which effectively led to an early arrest of *A. niger* AN1 growth (patterns A1 and D2, Figures 4A,B), warrants them being considered in a future selection program due their remarkable effects.

We then aimed to identify strains with broad spectrum of antagonistic activity (Figures 6E–F). No yeast strain was found to be highly effective against all four mold targets through the production of diffusible compounds. Nevertheless, we have identified five *Han. uvarum* strains that are strong inhibitors of three of the four targets. While four strains were effective against *A. niger* AN1, *B. cinerea* BO1 and *Mucor* sp. MU3, one other strain was effective against *A. niger* AN1, *Mucor* sp. MU3 and *Penicillium* sp. PE3. On the other hand, three strains affiliated to different species – *H. uvarum, L. thermotolerans* and *Sta. bacillaris* were identified as having strong or very strong antagonistic activity through the production volatile compounds against all the targets tested, with average IAC (%) values of 73, 67, and 68%, respectively.

4. Discussion

Vitis vinifera L. grapevine is one of the most cultivated (in an estimated surface area of 7.3 million hectares) and valued fruit crops, given the many applications of grape production, from its fresh consumption (table grapes and raisins) to its use in the production of juices and wines (FAO-OIV, 2016; OIV, 2022). Accordingly, a great wealth of technology investment is devoted to control the development of fungal rots that may occur during grape maturation and postharvest, and reduce the quality and safety of the final product. These phytopathogenic fungi include *B. cinerea,* which is responsible for severe gray rot, during pre- and post- harvest (Kassemeyer, 2017); several species belonging to *Aspergillus* and *Penicillium,* that besides being responsible for black and green/blue rots, respectively, are recognized as producers of mycotoxins that can cause a risk for human health (Serra et al., 2005); and *Mucor* spp. which are mainly known as post-harvest disease causing agents that can develop even at cool storage conditions (Kassemeyer, 2017).

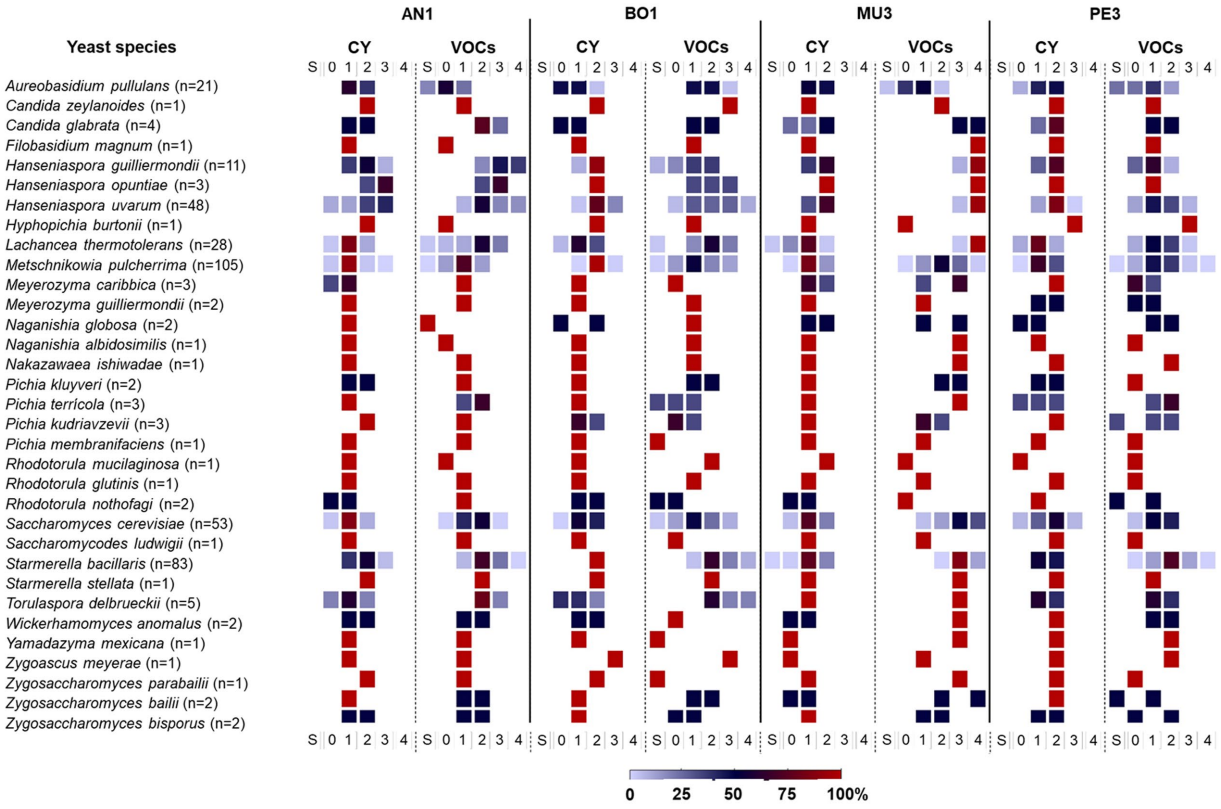

FIGURE 5
Frequency distribution of yeast strains for each species based on their antagonistic activity against the four mold targets. Classes of yeast strains were defined based on IAC values: class 0 (no effect: IAC<5%), class 1 (weak effect: 5%≤IAC<25%), class 2 (moderate effect: 25%≤IAC<50%), class 3 (strong effect: 50%≤IAC<75%) and class 4 (very strong effect: IAC ≥75%). Strains with stimulatory effect of mold growth were included in class S. The color gradient refers to the percentage of strains in each class. AN1 – *Aspergillus niger*; BO1 – *Botrytis cinerea*; MU3 – *Mucor* sp.; PE3 – *Penicillium* sp.; CY – diffusible compounds assay; VOCs – volatile compounds assay. The number of isolates tested of each species is given in parenthesis.

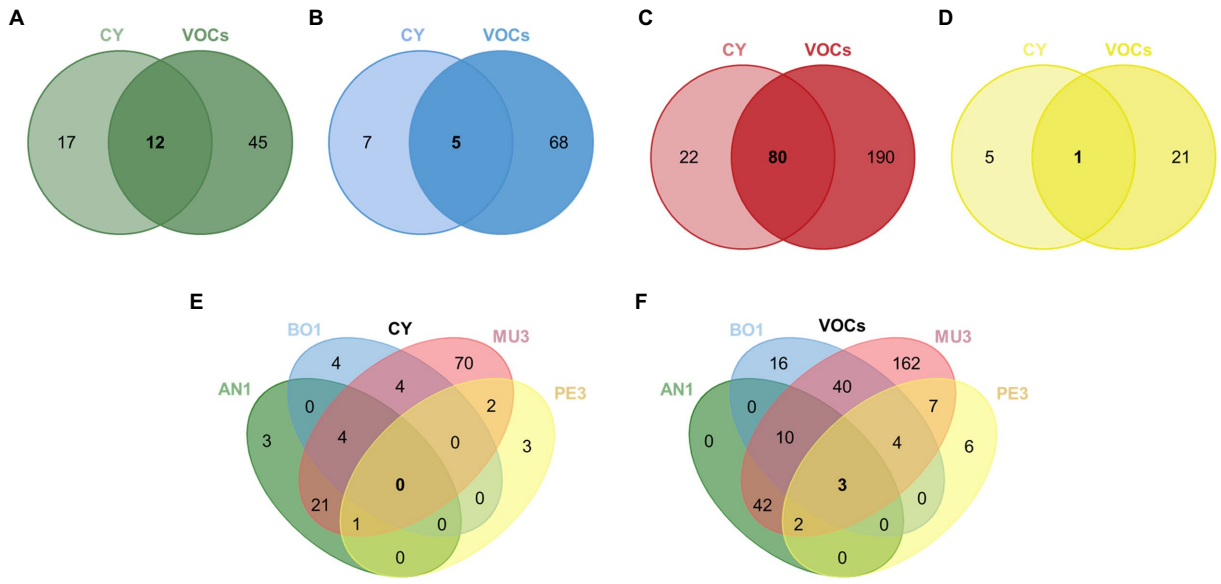

FIGURE 6
Venn diagrams illustrating the number of yeast strains with inhibitory activity against each target individually, *Aspergillus niger* AN1 **(A)**, *Botrytis cinerea* BO1 **(B)**, *Mucor* sp. MU3 **(C)** and *Penicillium* sp. PE3 **(D)**, or against all targets **(E,F)** mediated by diffusible (CY) and volatile compounds (VOCs). The number of strains classified on class 3 (strong effect: 50%≤IAC<75%) or class 4 (very strong effect: IAC≥75%) for each mold target were included, except for MU3 in the CY assay, where only strains classified on class 2 were included (moderate effect: 25%≤IAC<50%).

Presently, there is an increasing demand for more sustainable and eco-friendly practices in the agricultural ecosystems aiming the replacement, or at least the reduction, of the chemical products that are currently being used (Wilson and Wisniewski, 1989; Pertot et al., 2017b). A considerable number of reports have demonstrated the antagonistic behavior of several strains of different yeast species against phytopathogenic fungi, pointing out their potential for biocontrol applications (Zhang et al., 2020; Di Canito et al., 2021). Despite the demonstrated efficiency, the number of yeasts available at the market for using as biofungicides in grapes against phytopathogenic fungi in the pre- and/or postharvest stages remains limited (Palmieri et al., 2022). According to the data available on EU pesticide database, accessed on 13 January 2023, there are only two yeast-based products being commercialized or submitted for approval, with different active substances (yeasts), Julieta® (*Sac. cerevisiae* LAS02) and Shemer® (*Met. fructicola* NRRL Y-27328), both targeting only *B. cinerea*. Thus, the quest for new yeasts with reliable biocontrol prospects against grape phytopathogenic fungi continues.

In this study 397 wine yeast strains were tested for their biocontrol potential against four major grapes fungal pathogens, *A. niger*, *B. cinerea*, *Mucor* sp. and *Penicillium* sp. This set of yeast strains, isolated from grapes/grape-juices and spontaneous grape-juice fermentations derived from different Portuguese wine-regions, was found to be highly diverse in their taxonomic groups, encompasses mostly non-*Saccharomyces* species (approximately 87%) and 53 *Sac. cerevisiae* strains and thus represents the broad biodiversity common in the targeted niche (Fleet and Heard, 1993; Bokulich et al., 2014; Pinto et al., 2015). The exploration of these epiphytic yeasts as biocontrol agents arises as a valuable option as they have the advantage of not disrupting the local ecological makeup. In addition, while being in their natural ecosystem they can evolve better and easily adjust to the associated environmental conditions, thus being more prone to demonstrate effective and consistent biocontrol activity against grapes phytopathogens (Parafati et al., 2015; Pretscher et al., 2018; Pereyra et al., 2021). In fact, most of the species represented in our collection include previously reported antagonists of grape phytopathogenic fungi (Suzzi et al., 1995; Bleve et al., 2006; Raspor et al., 2010; Nally et al., 2012; Pantelides et al., 2015; Lemos Junior et al., 2016; Cordero-Bueso et al., 2017; Pretscher et al., 2018; Reyes-bravo et al., 2019) while the antagonistic potential of *Nakazawaea ishiwadae* and *Yamadazyma mexicana* are herein reported for the first time.

However, the lack of standardized protocols for *in vitro* dual culture assays is a major drawback for the direct comparison of the results obtained in the different studies and the accomplishment of definitive classification of antagonistic yeasts. Indeed, the level of yeast inhibition has been distinctly evaluated, either by arbitrary scales (Suzzi et al., 1995; Bleve et al., 2006), inhibition halos (Nally et al., 2012; Cordero-Bueso et al., 2017; Reyes-bravo et al., 2019) or percentages (Raspor et al., 2010; Pantelides et al., 2015; Lemos Junior et al., 2016; Pretscher et al., 2018; Reyes-bravo et al., 2019)(Lemos Junior et al., 2016; Reyes-bravo et al., 2019) obtained by comparing the mold colony sizes in the presence of the yeasts with that for its single culture at a defined end time point. In addition, the use of a panoply of distinct methodologies related with the yeast inoculation technique (incorporation, spot, streak or spread plating), type of mold inoculum (spore suspension or mycelial plug), nature of interaction (direct or indirect contact), period of incubation and the culture medium used, introduce even more entropy in the data comparison.

In this work, yeast strains with strong inhibitory activity (> 50%) against all the phytopathogenic fungi tested were found. Overall, the strains affiliated to species of *Hanseniaspora*, *Lachancea* and *Starmerella* tested in our study were the most effective against *A. niger*, *B. cinerea* and *Mucor* sp. Previous studies have already reported wine strains of *Han. uvarum* and *Sta. bacillaris* with strong inhibitory activity against *Aspergillus* spp. and *B. cinerea* (Lemos Junior et al., 2016; Cordero-Bueso et al., 2017; Fernandez-San Millan et al., 2021) and of *L. thermotolerans* against *Aspergillus* spp. (Bleve et al., 2006). Although *L. thermotolerans* have already been tested against *B. cinerea* (Nally et al., 2012; Fernandez-San Millan et al., 2021), our report is the first to demonstrate the antagonism of a wine yeast strain of this species against this grape phytopathogen. Also, to our knowledge, our study is the first showing the potential of wine yeasts to control *Mucor* sp. development. We were only able to find one study on the biocontrol activity of yeasts against Mucor rot of pears, by a pear-isolated strain of *Cryptococcus infirmo-miniatus* (Chand-Goyal and Spotts, 1996). Strains of *Sac. cerevisiae*, *Sta. bacillaris* and the single strain of *Hyp. burtonii* were found as strong inhibitors of *Penicillium* sp. growth. While wine strains of *Sac. cerevisiae* and *Sta. bacillaris* have already shown antagonistic behavior against *P. expansum* (Cordero-Bueso et al., 2017; Fernandez-San Millan et al., 2021) the biocontrol potential of *Hyp. burtonii* against *Penicillium* spp. is herein reported for the first time. However, despite being poorly studied, this species has previously shown biocontrol potential against other phytopathogenic fungal targets such as *Alternaria alternata*, *Aspergillus niger* and *B. cinerea*, either by strains isolated from green coffee beans (Poitevin et al., 2020) or grape-must (Maluleke et al., 2022).

Biocontrol activity of yeasts by direct mold antagonism is mainly mediated by the competition for nutrients and space, secretion of non-volatile compounds (including cell wall degrading enzymes) and production of volatile compounds (Freimoser et al., 2019). In this work, besides the search for secreted hydrolytic enzymes, the yeast antagonistic activity was evaluated using two designs of dual-culture assays, directed to either the production of diffusible (CY assay) or volatile compounds (VOCs assay). The evaluation of the different putative modes of action already points toward different prospective applications, in pre- and/or postharvest grapes. Accordingly, the prior inoculation of fast colonizer strains aided by production of antagonistic diffusible compounds (CY assays), could be envisaged for both pre- and postharvest applications, as a preventive intervention to control development. Yet the safety of the direct application of such biocontrol agents on the grape surface must be assured as there are reported cases of infections caused by yeasts in humans (Nally et al., 2013). On the other hand volatile compounds (VOCs assays), which may have a limited activity in the open field (Song and Ryu, 2013), but present reduced hazard for both environment and human beings (Tilocca et al., 2020) would be more likely indicated for post-harvest applications, under more controlled environments.

In addition, the original time-course mold growth monitoring approach, performed in the present study, allowed the detection of a high diversity of mold growth effects induced by yeasts. Indeed, it has been demonstrated that the comparison based on time series analysis enables a more thorough and objective comparison of the influence of environmental conditions on mold growth dynamics (De Ligne et al., 2019). All the aforementioned studies that evaluated the

antagonistic effect of yeasts on phytopathogenic mold growth, neglect time, measuring mold growth inhibition after a predetermined number of days. Additionally, since the yeast effects on the inhibition of spore germination may differ from those involved in the inhibition of mycelial extension, the use of spore suspensions coupled with daily monitoring of mold growth allowed us to identify potentially effective new strains that could not be revealed by using mycelial plugs. Taken together, our approach further uncovered important yeast-mediated effects throughout the experiments besides the commonly measure of reduction of mold growth, including the inhibition or delay of spore germination and the complete arrest of mycelial extension, and even their stimulation at different mold growth stages, this being highly dependent on yeast species/genus, mode of action and mold target.

Herein we uncover a remarkable intra and interspecific diversity in the yeast inhibition levels against mold targets, which is in line with previous works (Suzzi et al., 1995; Raspor et al., 2010; Lemos Junior et al., 2016). Besides, our approach also emphasizes the wide range of yeast-induced antagonistic profiles across different yeast species and strains. Yet, no association could be established between the genotypic diversity within a species and the respective diversity of antagonistic responses, nor with the intensity of the inhibition induced by strains, demonstrating that taxonomic affiliation is not a reliable predictor for biocontrol potential.

The diversity of yeast-mediated mold growth responses led us to propose another parameter, IAC (%), based on the area under the mycelial extension/time curve (AUC; mm.s), which integrates the different effects over time. The AUC measure is also preferred in other fields of study such as pharmacology where, for example, it is used to accurately estimate the extent of a body's exposure to a particular drug over time (Scheff et al., 2011). The use of IAC (%) allows ascribing greater prominence to antagonists that inhibit spore germination and that would be more suitable for preventive treatments, as their associated AUCs would be low. However, the IAC (%) underestimates the inhibitory effect of the strains that lead to the early cessation of mold growth, and would likely be excluded during the selection process, as the AUC (mm.day) will be accounted throughout. This highlights the importance of analyzing the mold growth profiles as an independent step, yet complementary to the calculated inhibition parameters, IRG (%) and IAC (%), during a selection program.

Overall, the response patterns prompted by yeast in the CY assays correspond to a decrease of mold mycelia extension rate, that ultimately led to the early complete arrest of mycelial extension, after a regular initial growth. Our CY assay setup does not allow distinguishing the production of diffusible metabolites (antibiosis), or competition for nutrients, or the secretion of extracellular enzymes as the underlying mechanism of inhibition (Freimoser et al., 2019). However according to our results, we could not find a direct link between the secretion of glucanases, chitinases, proteases and mannanases, that may degrade the cell wall constituents of the tested molds, and the antagonism observed in the CY assays. Indeed, our screening for hydrolytic enzymatic activities uncovered intra-genus and several intraspecific differences within the yeast isolates, with *Aur. pullulans* strains exhibiting the highest diversity of lytic enzymes released, in line with the recognized ability of this species (Bozoudi and Tsaltas, 2018). On the other hand, glucanase activity was highly frequent in our *L. thermotolerans* strains, a feature that has been previously identified for this species (Romo-Sánchez et al., 2010), although it is considered rare (Vicente et al., 2021). Nevertheless, the role of these hydrolytic enzymes on the inhibitory activity of these species was unclear, as no enhanced antagonism was detected in CY assays.

In the CY assays, a strong deceleration, or even the arrest, of mycelial extension of mold growth, induced mainly by *Met. pulcherrima* and *Sta. bacillaris* was detected against the most phylogenetically closer targets, *A. niger* and *Penicillium* sp. Also, a delay in spore germination of these mold targets by strains of *Hanseniaspora* spp. and *Sta. bacillaris* was found. These observations suggest the involvement of diffusible compounds on mold inhibition, with the distinct effects being dependent on their toxicity, and rates of production and diffusion (Swadling and Jeffries, 1996). In practice, yeasts strains with marked effects on mold mycelial extension, may be also important as protective agents to reduce disease severity and spread to other fruit clusters. Regardless, depending on the concentration of the active compound(s), these inhibitory effects are amenable to be optimized to achieve maximum effectiveness in practical applications.

The production of volatile compounds appeared to be a major mechanism of yeast-mediated inhibition of the four mold targets, with maximum IACs (%) surpassing 90%. Alcohols and their respective esters, have been associated with the antagonistic activity of yeasts against phytopathogenic fungi (Tilocca et al., 2020). The most reported inhibitory volatile compounds produced by yeasts include 2-phenylethanol and its respective ester 2-phenylethyl acetate and 1,3,5,7-cyclooctatetraene and 3-methyl-1-butanol, 2-ethyl-hexanol and ethyl acetate (Masoud et al., 2005; Huang et al., 2011, 2012; Hua et al., 2014; Di Francesco et al., 2015; Farbo et al., 2018; Oro et al., 2018). Wine yeasts have been described as large producers of several of these volatile compounds, mainly in the context of grape-juice fermentation where they are interesting for the development and complexity of wine aroma (reviewed in Petruzzi et al., 2017; Liu et al., 2022). A formulation of a product with a bi-functional role of application, as a biocontrol and bioflavoring agent could then be foreseen for the strains of these species that presented the best inhibitory performances in this work, as proposed by Lemos Junior et al. (2016).

A relevant effect induced on the mold targets by volatile compounds was the delay on spore germination, detected in *A. niger*, *Mucor* sp. and *Penicillium* sp. These compounds are known to be used by fungi as chemical signals to control physiological processes such as nutrient acquisition, sporulation, sexual development and spore germination (Leeder et al., 2011; Bennett et al., 2012). It is known that when too many spores exist in proximity, fungi may produce volatile compounds to act as self-inhibitors of spore germination (Bitas et al., 2013). The volatile compounds produced by the yeast strains may have a similar chemical constitution and be perceived as self-inhibitors or in turn, other compounds with different chemical structure may be produced that disturb mold chemical signaling. In the present study, *Mucor* sp. has been shown to be the most susceptible to the volatile compounds produced, with 68% of yeast strains being strong or very strong inhibitors, particularly strains of *Han. uvarum*, *L. thermotolerans*, *Sac. cerevisiae* and *Sta. bacillaris*. This result suggests that *Mucor* sp. sporangiospores might be more sensitive than the conidia of the ascomyceteous fungi, especially those of *B. cinerea*, to the volatile compounds produced by the wine yeasts strains. A

discrepant sensitivity between spores of *B. cinerea* and *Mucor racemosus* has been reported by Catskx et al. (1975) that studied the effects of volatile metabolites released by swelling seeds on spore germination of five genera of fungi.

Strikingly, a *Met. pulcherrima* strain was found in this work to completely inhibit the spore germination of *Penicillium* sp. through the production of volatile compounds. The antagonistic activity of *Met. pulcherrima* strains has been for long reported and is mainly associated with the iron depletion and diffusion of the pulcherrimin pigment (Sipiczki, 2006). Our findings may therefore be useful to further expand its range of applications. Several strains of other species, mainly of *Han. uvarum* and *Sta. bacillaris* showed a temporary inhibition of spore germination of all the mold targets, except *B. cinerea*. From the practical point of view, complete inhibition of spore germination is always the most desirable as a treatment, preventing fungal proliferation and associated diseases in fruits. These strains could be useful to achieve grapes protection during the timeframes more crucial to target pathogen proliferation in the vineyard. At postharvest, they could be as well advantageous during transportation and storage, to extend the fruit shelf-life.

5. Conclusion

The time-course analysis performed in this study provided a robust exploitation of the biocontrol potential of a large set of wine yeasts, enabling the identification of yeast effects on mold targets at different growth stages. The wide diversity of inhibitory effects found, highlighted the importance of establishing target-and application-oriented protocols for yeast strain selection. Herein, a catalog of potential biocontrol agents, including several with a large target-spectrum of activity and versatility of mode of action was established. Particularly, strains of *Han. uvarum*, *L. thermotolerans*, *Met. pulcherrima* and *Sta. bacillaris* stood out as the best candidates for application either in pre- or post-harvest grapes, being very interesting for further research. Yeast consortia, combining yeasts with distinct modes of action and effects on spore germination and mold growth, could be a promising strategy in the formulation of new ecosystem-based tools as environmentally friendly alternatives to chemical fungicides, supporting the development of a more sustainable vitiviniculture.

Data availability statement

The datasets presented in this study can be found in online repositories. The names of the repository/repositories and accession number(s) can be found in the article/Supplementary material.

Author contributions

AM-F, FC, and MT were responsible for funding acquisition, AM-F and RT conceived and designed the experiments. ME, PL, and JS performed the experiments. ME prepared the original draft. ME, PL, FC, RT, and AM-F organized and analyzed the data. ME, RT, and AM-F wrote the manuscript. AM-F supervised the study. All authors contributed to the article and approved the submitted version.

Funding

This work was financially supported by ABCyeasts project no. NORTE-01-0247-FEDER-039793, co-financed by FEDER through NORTE 2020. ME is a recipient of a PhD grant with the reference PD/BD/150587/2020 from the FCT Doctoral Program in Applied and Environmental Microbiology (DP_AEM).

Acknowledgments

Support by Fundação para a Ciência e Tecnologia to Biosystems and Integrative Sciences Institute, through contract FCT/UIDB/04046/2020 is acknowledged.

Conflict of interest

FC and MT was employed by Proenol.

The remaining authors declare that the research was conducted in the absence of any commercial or financial relationships that could be construed as a potential conflict of interest.

Publisher's note

Supplementary material

The Supplementary material for this article can be found online at: https://www.frontiersin.org/articles/10.3389/fmicb.2023.1146065/full#supplementary-material

References

Asfamawi, K. K., Noraini, S., and Darah, I. (2013). Isolation, screening and identification of mannanase producing microorganisms. *J. Trop. Agric. Fd. Sci.* 1, 169–177.

Barata, A., Malfeito-Ferreira, M., and Loureiro, V. (2012). The microbial ecology of wine grape berries. *Int. J. Food Microbiol.* 153, 243–259. doi: 10.1016/j.ijfoodmicro.2011.11.025

Barbosa, C., Lage, P., Esteves, M., Chambel, L., Mendes-Faia, A., and Mendes-Ferreira, A. (2018). Molecular and phenotypic characterization of *Metschnikowia pulcherrima* strains from Douro wine region. *Fermentation* 4:8. doi: 10.3390/fermentation4010008

Bélanger, R. R., Labbé, C., Lefebvre, F., and Teichmann, B. (2012). Mode of action of biocontrol agents: all that glitters is not gold. *Can. J. Plant Pathol.* 34, 469–478. doi: 10.1080/07060661.2012.726649

Bennett, J. W. B., Hung, R. H., Lee, S. L., and Padhi, S. P. (2012). "Fungal and bacterial volatile organic compounds: an overview and their role as ecological signaling agents" in *The Mycota IX Fungal Interactions*. ed. B. Hock (Berlin Heidelberg: Springer-Verlag), 373–393.

Bitas, V., Kim, H., Bennett, J. W., and Kang, S. (2013). Sniffing on microbes: diverse roles of microbial volatile organic compounds in plant health. *Mol. Plant-Microbe Interact.* 26, 835–843. doi: 10.1094/MPMI-10-12-0249-CR

Bleve, G., Grieco, F., Cozzi, G., Logrieco, A., and Visconti, A. (2006). Isolation of *Epiphytic yeasts* with potential for biocontrol of *Aspergillus carbonarius* and *Aspergillus niger* on grape. *Int. J. Food Microbiol.* 108, 204–209. doi: 10.1016/j.ijfoodmicro.2005.12.004

Bokulich, N. A., Thorngate, J. H., Richardson, P. M., and Mills, D. A. (2014). Microbial biogeography of wine grapes is conditioned by cultivar, vintage, and climate. *Proc. Natl. Acad. Sci.* 111, E139–E148. doi: 10.1073/pnas.1317377110

Bozoudi, D., and Tsaltas, D. (2018). The multiple and versatile roles of *Aureobasidium pullulans* in the vitivinicultural sector. *Fermentation* 4, 4–S5. doi: 10.3390/fermentation4040085

Catskx, V., Afifi, A. F., and Vancura, V. (1975). The effect of volatile and gaseous metabolites of swelling seeds on germination of fungal spores. *Folia Microbiol.* 20, 152–156. doi: 10.1007/BF02876772

Chand-Goyal, T., and Spotts, R. A. (1996). Control of postharvest pear diseases using natural *Saprophytic yeast* colonists and their combination with a low dosage of thiabendazole. *Postharvest Biol. Technol.* 7, 51–64. doi: 10.1016/0925-5214(95)00031-3

Chen, P.-H., Chen, R.-Y., and Chou, J.-Y. (2018). Screening and evaluation of yeast antagonists for biological control of *Botrytis cinerea* on strawberry fruits. *Mycobiology* 46, 33–46. doi: 10.1080/12298093.2018.1454013

Cordero-Bueso, G., Mangieri, N., Maghradze, D., Foschino, R., Valdetara, F., Cantoral, J. M., et al. (2017). Wild grape-associated yeasts as promising biocontrol agents against *Vitis vinifera* fungal pathogens. *Front. Microbiol.* 8, 1–15. doi: 10.3389/fmicb.2017.02025

De Ligne, L., Vidal-Diez de Ulzurrun, G., Baetens, J. M., Van den Bulcke, J., Van Acker, J., and De Baets, B. (2019). Analysis of spatio-temporal fungal growth dynamics under different environmental conditions. *IMA Fungus* 10, 7–13. doi: 10.1186/s43008-019-0009-3

Di Canito, A., Mateo-vargas, M. A., Mazzieri, M., Cantoral, J., Foschino, R., Cordero-Bueso, G., et al. (2021). The role of yeasts as biocontrol agents for pathogenic fungi on postharvest grapes: a review. *Foods* 10, 1–15. doi: 10.3390/foods10071650

Di Francesco, A., Ugolini, L., Lazzeri, L., and Mari, M. (2015). Production of volatile organic compounds by *Aureobasidium pullulans* as a potential mechanism of action against postharvest fruit pathogens. *Biol. Control* 81, 8–14. doi: 10.1016/j.biocontrol.2014.10.004

FAO-OIV (2016). Food and Agriculture Organization, and Organisation Internationale de la Vine et du Vin focus 2016: table and dried grapes-non-alcoholic products of the vitivinicultural sector intended for human consumption, 1–64.

Farbo, M. G., Urgeghe, P. P., Fiori, S., Marcello, A., Oggiano, S., Balmas, V., et al. (2018). Effect of yeast volatile organic compounds on ochratoxin A-producing *Aspergillus carbonarius* and *Aspergillus ochraceus*. *Int. J. Food Microbiol.* 284, 1–10. doi: 10.1016/j.ijfoodmicro.2018.06.023

Fernandez-San Millan, A., Larraya, L., Farran, I., Ancin, M., and Veramendi, J. (2021). Successful biocontrol of major postharvest and soil-borne plant *Pathogenic fungi* by *Antagonistic yeasts*. *Biol. Control* 160:104683. doi: 10.1016/j.biocontrol.2021.104683

Ferraz, P., Cássio, F., and Lucas, C. (2019). Potential of yeasts as biocontrol agents of the Phytopathogen causing cacao witches' broom disease: is microbial warfare a solution? *Front. Microbiol.* 10, 1–13. doi: 10.3389/fmicb.2019.01766

Fleet, G. H., and Heard, G. M. (1993). "Yeast growth during fermentation" in *Wine Microbiology and Biotechnology*. ed. G. H. Fleet (Harwood Academic: Switzerland), 27–54.

Freimoser, F. M., Rueda-Mejia, M. P., Tilocca, B., and Migheli, Q. (2019). Biocontrol yeasts: mechanisms and applications. *World J. Microbiol. Biotechnol.* 35, 154–119. doi: 10.1007/s11274-019-2728-4

Hua, S. S. T., Beck, J. J., Sarreal, S. B. L., and Gee, W. (2014). The major volatile compound 2-phenylethanol from the biocontrol yeast, *Pichia anomala*, inhibits growth and expression of aflatoxin biosynthetic genes of *Aspergillus flavus*. *Mycotoxin Res.* 30, 71–78. doi: 10.1007/s12550-014-0189-z

Huang, R., Che, H. J., Zhang, J., Yang, L., Jiang, D. H., and Li, G. Q. (2012). Evaluation of *Sporidiobolus pararoseus* strain YCXT3 as biocontrol agent of *Botrytis cinerea* on post-harvest strawberry fruits. *Biol. Control* 62, 53–63. doi: 10.1016/J.BIOCONTROL.2012.02.010

Huang, R., Li, G. Q., Zhang, J., Yang, L., Che, H. J., Jiang, D. H., et al. (2011). Control of postharvest botrytis fruit rot of strawberry by volatile organic compounds of *Candida intermedia*. *Phytopathology* 101, 859–869. doi: 10.1094/PHYTO-09-10-0255

Kassemeyer, H.-H. (2017). "Fungi of grapes" in *Biology of Microorganisms on Grapes, in Must and in Wine*. eds. H. Konig, G. Unden and J. Frohlich (Heidelberg: Springer), 103–132.

Köhl, J., Kolnaar, R., and Ravensberg, W. J. (2019). Mode of action of microbial biological control agents against plant diseases: relevance beyond efficacy. *Front. Plant Sci.* 10, 1–19. doi: 10.3389/fpls.2019.00845

Leeder, A. C., Palma-guerrero, J., and Glass, N. L. (2011). The social network: deciphering fungal language. *Nat. Rev. Microbiol.* 9, 440–451. doi: 10.1038/nrmicro2580

Lemos Junior, W. J. F., Bovo, B., Nadai, C., Crosato, G., Carlot, M., Favaron, F., et al. (2016). Biocontrol ability and action mechanism of *Starmerella bacillaris* (synonym *Candida zemplinina*) isolated from wine musts against gray mold disease agent *Botrytis cinerea* on grape and their effects on alcoholic fermentation. *Front. Microbiol.* 7, 1–12. doi: 10.3389/fmicb.2016.01499

Liu, S., Laaksonen, O., Li, P., Gu, Q., and Yang, B. (2022). Use of non-saccharomyces yeasts in berry wine production: inspiration from their applications in winemaking. *J. Agric. Food Chem.* 70, 736–750. doi: 10.1021/acs.jafc.1c07302

Maluleke, E., Jolly, N. P., Patterton, H. G., and Setati, M. E. (2022). Antifungal activity of non-conventional yeasts against *Botrytis cinerea* and non-botrytis grape bunch rot fungi. *Front. Microbiol.* 13, 1–13. doi: 10.3389/fmicb.2022.986229

Masoud, W., Poll, L., and Jakobsen, M. (2005). Influence of volatile compounds produced by yeasts predominant during processing of *Coffea arabica* in East Africa on growth and ochratoxin a (OTA) production by *Aspergillus ochraceus*. *Yeast* 22, 1133–1142. doi: 10.1002/yea.1304

Nally, M. C., Pesce, V. M., Maturano, Y. P., Muñoz, C. J., Combina, M., Toro, M. E., et al. (2012). Biocontrol of *Botrytis cinerea* in table grapes by non-pathogenic indigenous *Saccharomyces cerevisiae* yeasts isolated from viticultural environments in Argentina. *Postharvest Biol. Technol.* 64, 40–48. doi: 10.1016/j.postharvbio.2011.09.009

Nally, M. C., Pesce, V. M., Maturano, Y. P., Toro, M. E., Combina, M., Castellanos de Figueroa, L. I., et al. (2013). Biocontrol of fungi isolated from sour rot infected table grapes by *Saccharomyces* and other yeast species. *Postharvest Biol. Technol.* 86, 456–462. doi: 10.1016/j.postharvbio.2013.07.022

Nisiotou, A. A., and Nychas, G. J. E. (2007). Yeast populations residing on healthy or botrytis-infected grapes from a vineyard in Attica, Greece. *Appl. Environ. Microbiol.* 73, 2765–2768. doi: 10.1128/AEM.01864-06

OIV (2022). Organisation Internationale de la Vine et du Vin: State of the world vine and wine Sector 2021. 1–19.

Oro, L., Feliziani, E., Ciani, M., Romanazzi, G., and Comitini, F. (2018). Volatile organic compounds from *Wickerhamomyces anomalus*, *Metschnikowia pulcherrima* and *Saccharomyces cerevisiae* inhibit growth of decay causing fungi and control postharvest diseases of strawberries. *Int. J. Food Microbiol.* 265, 18–22. doi: 10.1016/j.ijfoodmicro.2017.10.027

Palmieri, D., Ianiri, G., Del Grosso, C., Barone, G., De Curtis, F., Castoria, R., et al. (2022). Advances and perspectives in the use of biocontrol agents against fungal plant diseases. *Horticulturae* 8:577. doi: 10.3390/horticulturae8070577

Pantelides, I. S., Christou, O., Tsolakidou, M. D., Tsaltas, D., and Ioannou, N. (2015). Isolation, identification and in vitro screening of grapevine yeasts for the control of black aspergilli on grapes. *Biol. Control* 88, 46–53. doi: 10.1016/j.biocontrol.2015.04.021

Parafati, L., Vitale, A., Restuccia, C., and Cirvilleri, G. (2015). Biocontrol ability and action mechanism of food-isolated yeast strains against *Botrytis cinerea* causing post-harvest bunch rot of table grape. *Food Microbiol.* 47, 85–92. doi: 10.1016/j.fm.2014.11.013

Pereyra, M. M., Díaz, M. A., Soliz-Santander, F. F., Poehlein, A., Meinhardt, F., Daniel, R., et al. (2021). Screening methods for isolation of biocontrol *Epiphytic* yeasts against *Penicillium digitatum* in lemons. *J. Fungi* 7:166. doi: 10.3390/jof7030166

Pertot, I., Caffi, T., Rossi, V., Mugnai, L., Hoffmann, C., Grando, M. S., et al. (2017a). A critical review of plant protection tools for reducing pesticide use on grapevine and new perspectives for the implementation of IPM in viticulture. *Crop Prot.* 97, 70–84. doi: 10.1016/j.cropro.2016.11.025

Pertot, I., Giovannini, O., Benanchi, M., Caffi, T., Rossi, V., and Mugnai, L. (2017b). Combining biocontrol agents with different mechanisms of action in a strategy to control *Botrytis cinerea* on grapevine. *Crop Prot.* 97, 85–93. doi: 10.1016/j.cropro.2017.01.010

Petruzzi, L., Capozzi, V., Berbegal, C., Corbo, M. R., Bevilacqua, A., Spano, G., et al. (2017). Microbial resources and enological significance: opportunities and benefits. *Front. Microbiol.* 8, 1–13. doi: 10.3389/fmicb.2017.00995

Pielou, E. C. (1966). The measurement of diversity in different types of biological collections. *J. Theor. Biol.* 13, 131–144. doi: 10.1016/0022-5193(66)90013-0

Pinto, C., Pinho, D., Cardoso, R., Custódio, V., Fernandes, J., Sousa, S., et al. (2015). Wine fermentation microbiome: a landscape from different Portuguese wine appellations. *Front. Microbiol.* 6, 1–13. doi: 10.3389/fmicb.2015.00905

Poitevin, C. G., Veronesi, R. S., Pimentel, I. C., and Auer, C. G. (2020). Foliar application of endophytic *Wickerhamomyces anomalus* against grey mould in *Eucalyptus dunnii*. *Biocontrol Sci. Tech.* 30, 93–102. doi: 10.1080/09583157.2019.1687645

Pretscher, J., Fischkal, T., Branscheidt, S., Jäger, L., Kahl, S., Schlander, M., et al. (2018). Yeasts from different habitats and their potential as biocontrol agents. *Fermentation* 4:31. doi: 10.3390/fermentation4020031

Raspor, P., Miklič-Milek, D., Avbelj, M., and Čadež, N. (2010). Biocontrol of grey mould disease on grape caused by *Botrytis cinerea* with autochthonous wine yeasts. *Food Technol. Biotechnol.* 48, 336–343.

Reyes-bravo, P., Acuña-fontecilla, A., Rosales, I. M. I. M., and Godoy, L. (2019). Evaluation of native wine yeast as biocontrol agents against fungal pathogens related to postharvest diseases. *Agric. Sci. Agron.* doi: 10.20944/preprints201909.0113.v1

Romo-Sánchez, S., Alves-Baffi, M., Arévalo-Villena, M., Úbeda-Iranzo, J., and Briones-Pérez, A. (2010). Yeast biodiversity from oleic ecosystems: study of their biotechnological properties. *Food Microbiol.* 27, 487–492. doi: 10.1016/j.fm.2009.12.009

Scheff, J. D., Almon, R. R., Dubois, D. C., Jusko, W. J., and Androulakis, I. P. (2011). Assessment of pharmacologic area under the curve when baselines are variable. *Pharm. Res.* 28, 1081–1089. doi: 10.1007/s11095-010-0363-8

Seixas, I., Barbosa, C., Mendes-faia, A., Mendes-ferreira, A., and Mira, N. P. (2019). Genome sequence of the non-conventional wine yeast *Hanseniaspora guilliermondii* UTAD222 unveils relevant traits of this species and of the *Hanseniaspora genus* in the context of wine fermentation. *DNA Res.* 26, 67–83. doi: 10.1093/dnares/dsy039

Serra, R., Braga, A., and Venâncio, A. (2005). Mycotoxin-producing and other fungi isolated from grapes for wine production, with particular emphasis on ochratoxin a. *Res. Microbiol.* 156, 515–521. doi: 10.1016/j.resmic.2004.12.005

Sipiczki, M. (2006). *Metschnikowia* strains isolated from botrytized grapes antagonize fungal and bacterial growth by iron depletion. *Appl. Environ. Microbiol.* 72, 6716–6724. doi: 10.1128/AEM.01275-06

Sipiczki, M. (2022). Taxonomic revision of the pulcherrima clade of *Metschnikowia* (fungi): merger of species. *Taxon* 2, 107–123. doi: 10.3390/taxonomy2010009

Sirén, K., Mak, S. S. T., Melkonian, C., Carøe, C., Swiegers, J. H., Molenaar, D., et al. (2019). Taxonomic and functional characterization of the microbial community during spontaneous in vitro fermentation of Riesling must. *Front. Microbiol.* 10, 1–17. doi: 10.3389/fmicb.2019.00697

Solairaj, D., Yang, Q., Guillaume Legrand, N. N., Routledge, M. N., and Zhang, H. (2021). Molecular explication of grape berry-fungal infections and their potential application in recent postharvest infection control strategies. *Trends Food Sci. Technol.* 116, 903–917. doi: 10.1016/j.tifs.2021.08.037

Song, G. C., and Ryu, C. (2013). Two volatile organic compounds trigger plant self-defense against a bacterial pathogen and a sucking insect in cucumber under open field conditions. *Int. J. Mol. Sci.* 14, 9803–9819. doi: 10.3390/ijms14059803

Spadaro, D., and Droby, S. (2016). Development of biocontrol products for postharvest diseases of fruit: the importance of elucidating the mechanisms of action of yeast antagonists. *Trends Food Sci. Technol.* 47, 39–49. doi: 10.1016/j.tifs.2015.11.003

Stenberg, J. A., Sundh, I., Becher, P. G., Björkman, C., Dubey, M., Egan, P. A., et al. (2021). When is it biological control? A framework of definitions, mechanisms, and classifications. *J. Pest. Sci.* 94, 665–676. doi: 10.1007/s10340-021-01354-7

Strauss, M. L. A., Jolly, N. P., Lambrechts, M. G., and Van Rensburg, P. (2001). Screening for the production of extracellular hydrolytic enzymes by non-saccharomyces wine yeasts. *J. Appl. Microbiol.* 91, 182–190. doi: 10.1046/j.1365-2672.2001.01379.x

Suzzi, G., Romano, P., Ponti, I., and Montuschi, C. (1995). Natural wine yeasts as biocontrol agents. *J. Appl. Bacteriol.* 78, 304–308. doi: 10.1111/j.1365-2672.1995.tb05030.x

Swadling, I. R., and Jeffries, P. (1996). Isolation of microbial antagonists for biocontrol of grey mould disease of strawberries. *Biocontrol Sci. Tech.* 6, 125–136. doi: 10.1080/09583159650039584

Tilocca, B., Cao, A., and Migheli, Q. (2020). Scent of a killer: microbial Volatilome and its role in the biological control of plant pathogens. *Front. Microbiol.* 11:41. doi: 10.3389/fmicb.2020.00041

Vicente, J., Navascués, E., Calderón, F., Santos, A., Marquina, D., and Benito, S. (2021). An integrative view of the role of Lachancea thermotolerans in wine technology. *Foods* 10:2878. doi: 10.3390/foods10112878

Ward, M. G. (2016). The regulatory landscape for biological control agents. *Bull. OEPP/EPPO* 46, 249–253. doi: 10.1111/epp.12307

Wilson, C. L., and Wisniewski, M. (1989). Biological control of post harvest diseases offruit and vegetables: an emerging technology. *Annu. Rev. Phytopathol.* 27, 425–441. doi: 10.1146/annurev.py.27.090189.002233

Wobbrock, J. O., Findlater, L., Gergle, D., and Higgins, J. J. (2011). "The aligned rank transform for nonparametric factorial analyses using only ANOVA procedures" in *Proceedings of the SIGCHI Conference on Human Factors in Computing Systems*. New York: Association for Computer Machinery, 143–146.

Zar, J. H. (1996). *Biostatistical Analysis*. New Jersey, USA: Prentice Hall Inc.

Zhang, H., Godana, E. A., Sui, Y., Yang, Q., Zhang, X., and Zhao, L. (2020). Biological control as an alternative to synthetic fungicides for the management of grey and blue mould diseases of table grapes: a review. *Crit. Rev. Microbiol.* 46, 450–462. doi: 10.1080/1040841X.2020.1794793

Frontiers in Microbiology

Explores the habitable world and the potential of microbial life

The largest and most cited microbiology journal which advances our understanding of the role microbes play in addressing global challenges such as healthcare, food security, and climate change.

Discover the latest Research Topics

See more →

Frontiers

Avenue du Tribunal-Fédéral 34
1005 Lausanne, Switzerland
frontiersin.org

Contact us

+41 (0)21 510 17 00
frontiersin.org/about/contact